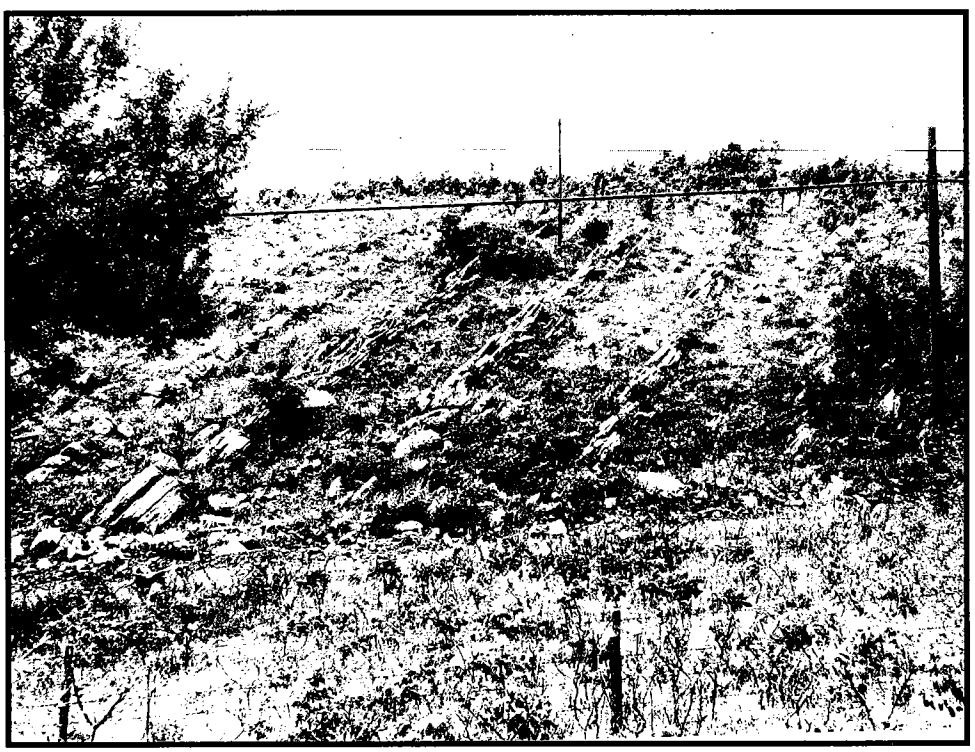
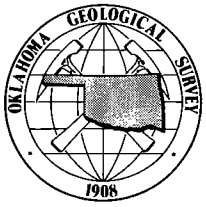
Oklahoma
Geological
Survey
1991

Special Publication 91-3

Arbuckle Group Core Workshop and Field Trip

Kenneth S. Johnson, *Editor*





Special Publication 91-3
ISSN 0275-0929

Arbuckle Group Core Workshop and Field Trip

Kenneth S. Johnson
Editor

Proceedings of a one-day core workshop (October 29, 1991) held in Norman, Oklahoma, and a two-day field trip (October 30–31, 1991) to the Arbuckle and Wichita Mountains of southern Oklahoma.

Co-sponsored by:
Oklahoma Geological Survey
and
Bartlesville Project Office,
U.S. Department of Energy

Oklahoma Geological Survey
Charles J. Mankin, *Director*
The University of Oklahoma
Norman, Oklahoma

1991

SPECIAL PUBLICATION SERIES

The Oklahoma Geological Survey's Special Publication series is designed to bring timely geologic information to the public quickly and economically. Review and editing of this material has been minimized in order to expedite publication, and author-prepared illustrations have been used throughout.

Front Cover

"Tombstone topography" of the Arbuckle Group, as seen on the south flank of the Arbuckle anticline in the Arbuckle Mountains. Differential weathering of steeply dipping alternating layers of resistant and nonresistant limestone have produced the parallel rows of furrows and "tombstones."

This publication, printed by the Oklahoma Geological Survey, is issued by the Oklahoma Geological Survey as authorized by Title 70, Oklahoma Statutes, 1981, Section 3310, and Title 74, Oklahoma Statutes,. 1981, Sections 231–238. 600 copies have been prepared at a cost of $4,347.45 to the taxpayers of the State of Oklahoma. Copies have been deposited with the Publications Clearinghouse of the Oklahoma Department of Libraries.

PREFACE

The Late Cambrian–Early Ordovician Arbuckle Group is a thick sequence of shallow-marine carbonates deposited on the south edge of the North American craton. This rock unit is a major target for petroleum exploration and reservoir development in the southern Midcontinent. The workshop was held to display cores and outcrop samples of the Arbuckle Group, along with cores of the equivalent Ellenburger Group of Texas and the Knox Group of Mississippi and Alabama.

The field trip was organized to compliment the workshop by allowing examination of excellent outcrops of the Arbuckle Group in both the Arbuckle and Wichita Mountains.

The core workshop and the field trip cover such topics as: petroleum-reservoir characterization; deposition, diagenesis, paleokarst, and structure of the Arbuckle Group as a carbonate reservoir; and interpretation of Arbuckle Group geology based upon petrologic, petrographic, and geochemical studies. To facilitate the exchange of information on these important topics, the Oklahoma Geological Survey (OGS) and the Bartlesville Project Office of the U.S. Department of Energy (BPO–DOE) co-sponsored this workshop and field trip. The ultimate goal of this program is to increase activity in the search for, and the production of, our oil and gas resources.

Special thanks are expressed to the workshop presenters and field-trip leaders who contributed to this volume. Each of them was successful in synthesizing years of work and many data into the report. Stratigraphic nomenclature and age determinations used by the various authors in this volume do not necessarily agree with those of the OGS.

Persons involved in the organization and planning of this workshop and field trip include: Kenneth Johnson and Charles Mankin of the OGS; Tom Wesson, Michael Ray, and Chandra Nautiyal of BPO–DOE; and R. Nowell Donovan, Texas Christian University, the Field-Trip Chair. Other OGS personnel who contributed include: Michelle Summers and Tammie Creel, Registration Co-Chairs; and Connie Smith, Publicity Chair.

Kenneth S. Johnson
General Chairman

CONTENTS

iii Preface

Part 1 — Core-Workshop Presentations

3 **Geologic Setting of the Arbuckle Group in Oklahoma**
Kenneth S. Johnson

9 **Sedimentology and Diagenesis of the Arbuckle Group in Outcrops of Southern Oklahoma**
Deborah A. Ragland and R. Nowell Donovan

31 **Paleokarstic Features and Thermal Overprints Observed in Some of the Arbuckle Cores in Oklahoma**
Mark Lynch and Zuhair Al-Shaieb

69 **Lithology, Stratigraphy, and Age of the Arbuckle Group in the Amoco SHADS No. 4, a Continuous Core from Grassroots into Basement, Rogers County, Oklahoma**
James R. Derby, Henry H. Hinch, and John R. Repetski

83 **Petrophysical Characteristics (Based on One Core) of the Cambro–Ordovician Arbuckle Dolostone, Arkoma Basin, Wilburton Field, Latimer County, Oklahoma**
Liang Chuanmao and Gerald M. Friedman

95 **Deformation Characteristics of the Arbuckle Group**
Bryan Tapp

103 **Diagenetic History of the Arbuckle Group, Slick Hills, Southwestern Oklahoma: A Petrographic and Geochemical Summary, and Comparison with the Ellenburger Group, Texas**
Lynton S. Land, Guoqiu Gao, and Julie A. Kupecz

111 **Comparison of the Arbuckle Group at Wilburton Field, Latimer County, with N.E. Alden Field, Caddo County, Oklahoma**
Bruce N. Carpenter and Michael C. Evans

133 **The Arbuckle Group—Relationship of Core and Outcrop Analyses to Cyclic Stratigraphy and Correlation**
James Lee Wilson, Richard D. Fritz, and Patrick L. Medlock

145 **Description and Interpretation of Karst-Related Breccia Fabrics, Ellenburger Group, West Texas**
Charles Kerans

157 **Results of a Deep Cambro–Ordovician Drilling Program, Northern Fort Worth Basin, Texas**
Joseph R. Whiteside and William E. McCommons

163 **Stratigraphy and Exploration of the Knox Group in the Appalachian Fold and Thrust Belt and Black Warrior Basin of Alabama**
Dorothy E. Raymond and W. Edward Osborne

181 **Hydrocarbon Potential and Subsurface Stratigraphy of the Cambro–Ordovician Sequence, Black Warrior Basin of Mississippi**
Kevin S. Henderson and S. Cragin Knox

185 **Karst Breccias of the Wade, Bray, and Brown Zones of the Upper Arbuckle Group in the Healdton Field, Carter County, Oklahoma**
R. Todd Waddell, Huaibo Liu, and J. M. Forgotson

Part 2 — Field Trip

193 **Field Trip Guide Introduction**
R. Nowell Donovan, Deborah A. Ragland, and Bryan Tapp

199 **The Arbuckle Group—An Aide de Memoire**
R. Nowell Donovan

DAY ONE

209 **STOP 1: Origin of the Kindblade, I-35 Megabreccia**
Bryan Tapp

213 **STOP 2: Flower Structure in the Lower Arbuckle**
Bryan Tapp

216 **STOP 3: Folding and Thrusting in the Lower Arbuckle**
Bryan Tapp

218 **STOP 4: The Cool Creek Formation at Turner Falls Park—A Platform Compendium**
Deborah A. Ragland and R. Nowell Donovan

223 **STOP 5: Turner Falls: Tufa, Travertine, and Bedding-Parallel Thrusts**
R. Nowell Donovan and Deborah A. Ragland

225 **STOP 6: Lateral Variations in the Upper Arbuckle Group Rocks—A Comparison Between Sections on I-35 and U.S. 77 in the Arbuckle Mountains**
R. Nowell Donovan, Matt Gallagher, Randy Hosey, Chai Phornprapha, Amy Smith, Sherman Smith, and Jeff Templeton

233 **STOP 7: Paleokarst Origin for Bedded Breccias in the Cool Creek Formation**
Bryan Tapp

236 **STOP 8: Parallel Folds and Shallowing-Upward Cycles in the Kindblade Formation, I-35**
R. Nowell Donovan

DAY TWO

239 **STOP 9: Permian Karst and Platform Carbonates, Cook Creek Road Cut**
R. Nowell Donovan and Deborah A. Ragland

244 **STOP 10: The Base of the Arbuckle Group at Bally Mountain**
R. Nowell Donovan and Deborah A. Ragland

247 **STOP 11: Three Types of Dolomite and the Transition from Fort Sill to Signal Mountain Formation at Raggedy Ridge, Bally Mountain**
R. Nowell Donovan and Deborah A. Ragland

250 **STOP 12: The Cool Creek and Lower Kindblade Formations on North Bally Mountain**
Deborah A. Ragland and R. Nowell Donovan

255 **STOP 13: Leatherbury's Quarry—The World's Smallest Oil Field**
R. Nowell Donovan and Arthur B. Busbey

259 **STOP 14: The Saddle Mountain Dolomite on Maukeen Hill**
R. Nowell Donovan and Debra L. Ross

263 **STOP 15: Parallel Folds and the Thatcher Creek Member in Blue Creek Canyon**
Deborah A. Ragland, Sherman S. Smith, and R. Nowell Donovan

PART 1

Core-Workshop Presentations

Geologic Setting of the Arbuckle Group in Oklahoma

Kenneth S. Johnson
Oklahoma Geological Survey

INTRODUCTION

The Arbuckle Group is a thick sequence of Late Cambrian and Early Ordovician carbonates that underlie most parts of Oklahoma and surrounding states. These strata are extremely important inasmuch as they are major sources of oil and gas, nonfuel minerals, and ground water; they also are used as disposal zones for oil-field brines and hazardous wastes (Johnson, 1991a).

The purpose of this paper is to describe briefly the geologic setting of the Arbuckle Group in Oklahoma and adjacent areas, in order to help set the stage for the other reports that are presented in this workshop volume. It is reprinted, with some revision, from Johnson (1991a), but is based largely upon summary reports and symposia by McHugh (1964), Ham and Wilson (1967), Ham (1969), Donovan (1986), Denison (in Johnson and others, 1988), Hatcher and others (1989), and Fay (1989). The reader also is referred to a recently published symposium on the Late Cambrian–Ordovician geology of the southern Midcontinent (Johnson, 1991b).

GEOLOGIC SETTING

Oklahoma is a geologically complex region with a number of major depositional and structural basins, separated by orogenic uplifts and mountain ranges created mainly during Pennsylvanian time (Fig. 1). However, the early Paleozoic history of the State is tectonically and sedimentologically much simpler. Late Cambrian and Early Ordovician strata in most parts of Oklahoma and the southern Midcontinent are characterized by 1,000–7,000 ft of shallow-marine carbonates (limestone and dolomite). These strata were deposited in a broad epicontinental sea, the Oklahoma basin (Fig. 2), which extended across all parts of Oklahoma (except the Ouachita trough in the southeast) during Late Cambrian through Mississippian time (Johnson and others, 1988). Stratigraphic units deposited in most parts of the Oklahoma basin are remarkably widespread and laterally persistent, reflecting the stability of this part of the craton and the importance of epeirogenic (rather than orogenic) movements during early Paleozoic time.

The depocenter for the Oklahoma basin was the southern Oklahoma aulacogen (SOA) (Fig. 2), a WNW-trending trough where subsidence and sediment accumulation were two to three times greater than on nearby shelf areas. The SOA comprised a region that now includes the Anadarko, Ardmore, and Marietta basins, along with the Arbuckle anticline, the Wichita Mountains uplift, and the Criner Hills.

Precambrian through Middle Cambrian basement rocks that underlie the Oklahoma basin consist mainly of igneous rocks, but some low-rank metasedimentary rocks are also present (Fig. 3) (Ham and others, 1964; Denison, 1981; Denison and others, 1984; Denison in Johnson and others, 1988). Precambrian rocks beneath most of Oklahoma are epizonal and mesozonal granites with comagmatic rhyolites. Early and Middle Cambrian basement rocks, limited to the aulacogen (Fig. 4), consist of granite, rhyolite, gabbro, and basalt. Basement rocks beneath the Ouachita trough have not been drilled and are unknown.

Late Cambrian seas transgressed to the north and west across Oklahoma, covering a basement-rock surface that

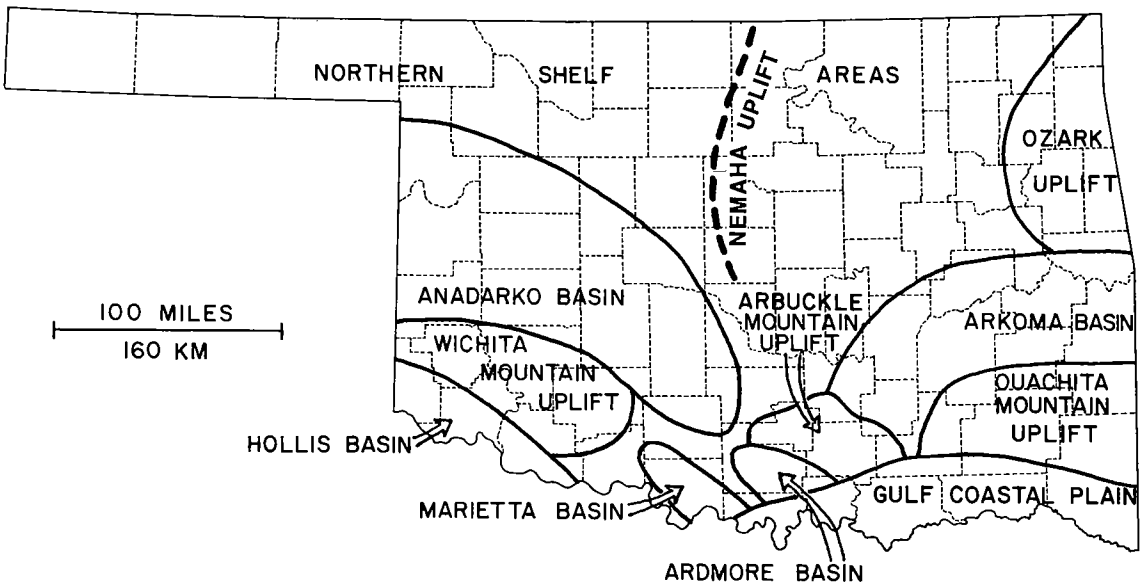


Figure 1. Major geologic provinces of Oklahoma (Johnson and others, 1980).

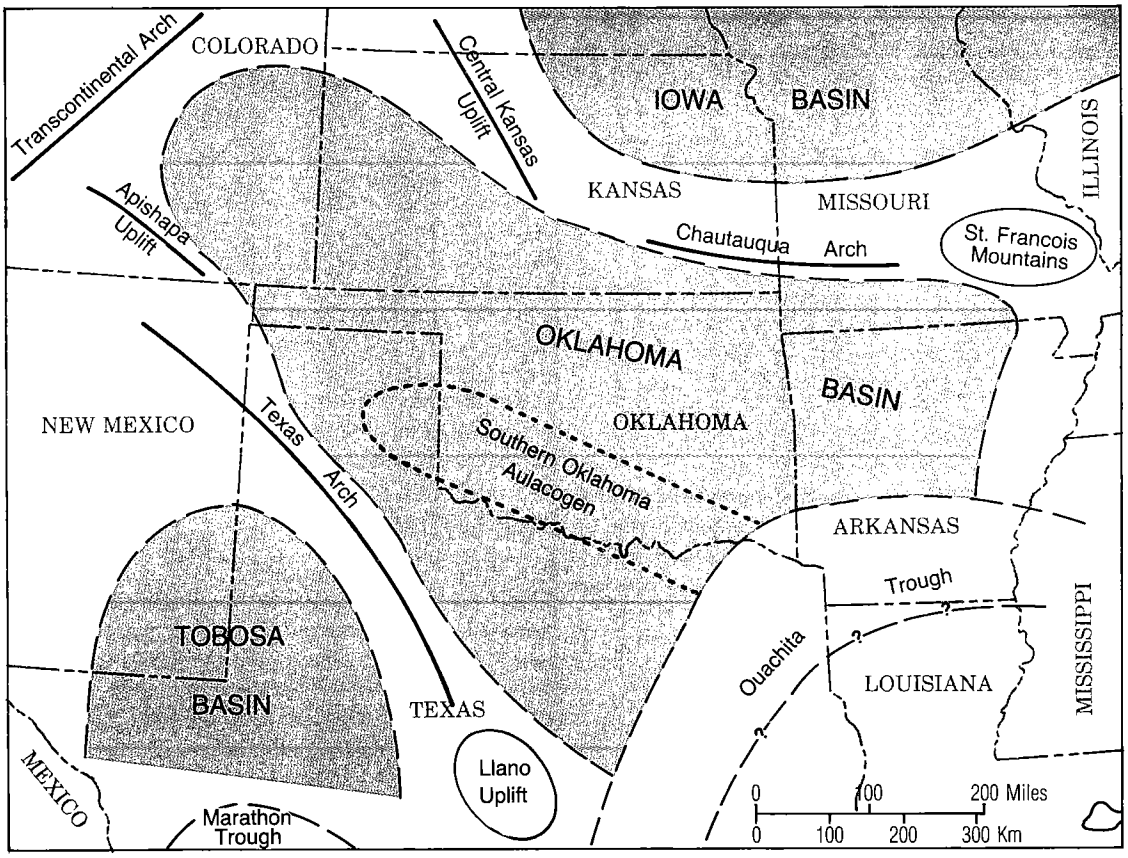


Figure 2. Map of southwestern United States, showing approximate outline of the Oklahoma basin and other major features that existed in early and middle Paleozoic time (Johnson and others, 1988).

AGE		FT. WORTH BASIN	ANAD. B. SW. OK.	ARBUCKLE MTS. ARDMORE B.		ARKOMA BASIN	W. ARKANSAS SW. MISSOURI	OUACHITA MTS.
SILUR.			Hunton Group	Hunton Group (Keel oolite)		Hunton Gp. (Pettit ool.)	Cason Shale	Blaylock Ss.
			Sylvan Sh.	Sylvan Shale		Sylvan Sh.		Polk Cr. Sh.
ORDOVICIAN	Up.	Viola Gp.	Viola Gp.	Viola Group		Viola Gp.	Fernvale Ls. Kimswick Ls.	Bigfork Cht.
	Mid.	Simpson Group	Simpson Group	Simpson	Bromide Fm. Tulip Creek McLish Fm. Oil Creek Fm. Joins Fm.	Fite Fm. Tyner Fm. Burgen Ss.	Plattin Ls. Joachim Dolo. St. Peter Ss. Everton Fm.	Womble Shale Blakely Ss.
	Low.	Ellenburger Group	Arbuckle Group	Arbuckle Group	West Spring Cr. Kindblade Fm. Cool Creek Fm. McKenzie Hill Butterly Dolo.	Arbuckle Group	Powell Cotter Jefferson City Roubidoux Gasconade Van Buren	Mazarn Sh. Crystal Mountain
CAMBRIAN	Up.	Moore Hollow Group	Timbered Hills Gp.		Signal Mtn. Royer Dolo. Fort Sill Ls.	Timbered Hills Gp.	Eminence Dolo. Potosi Dolo. Derby-Doerun	Collier Shale ?—?
				T. H. Gp.	Honey Cr. Ls. Reagan Ss.		Davis Fm.	
							Bonneterre Dolo. Lamott Ss.	
	Mid.		Gran., Rhy., Gab. ?	Rhyolite				
	Low.							
PRE-CAMB.		Granite, Gneiss, Schist	Granite, Rhyolite, Metaseds.	Granite and Gneiss		Granite and Rhyolite	Granite and Rhyolite	

Figure 3. Correlation chart for Cambrian and Ordovician rocks of Oklahoma and adjacent areas, based on COSUNA charts (Hills and Kottlowski, 1983; Mankin, 1987).

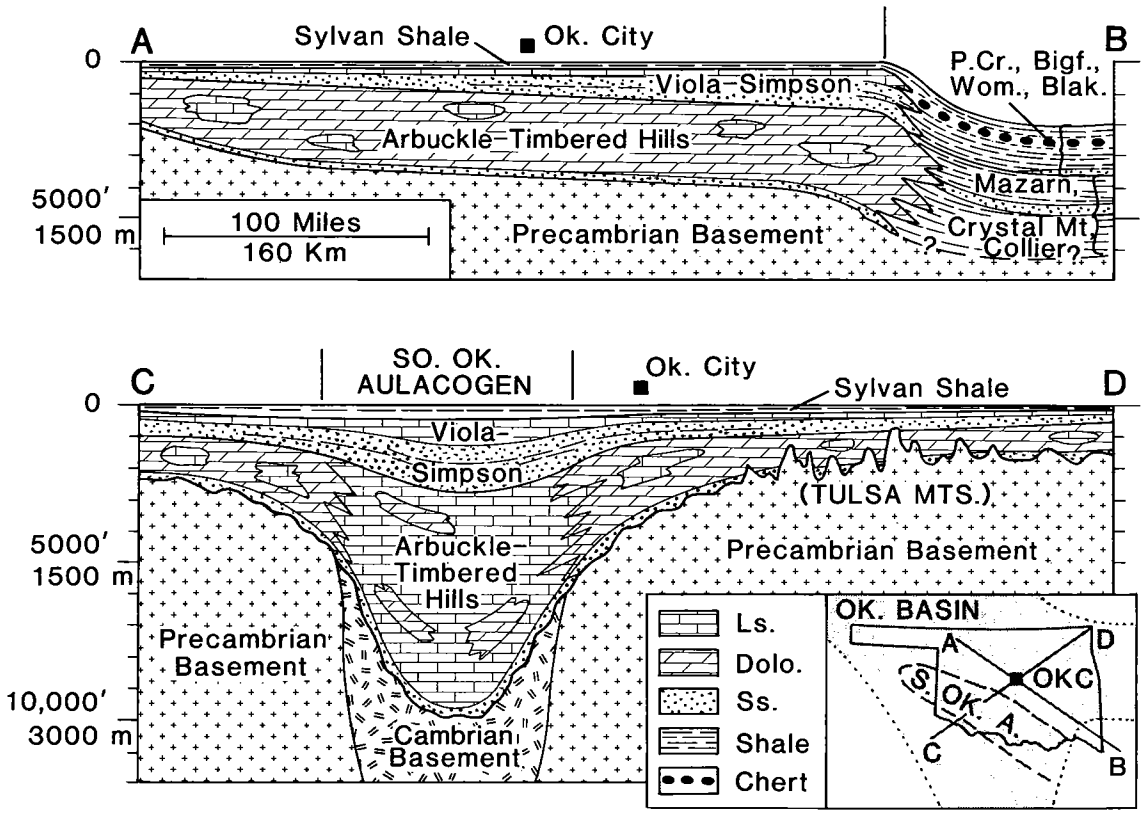


Figure 4. Schematic cross sections showing restored thickness of Late Cambrian and Ordovician strata in Oklahoma (Johnson, 1991a).

was of modest to locally rugged relief. A time-transgressive basal sand, the Reagan Sandstone, was deposited across most of the State; it grades upward into the succession of shallow-water carbonates and thin clastic units deposited more or less continuously until the end of Ordovician time. The term "Arbuckle facies" is used commonly for the sequence of thick carbonates and accompanying shales and sandstones, extending from the base of the Reagan Sandstone to the top of the Late Devonian–Early Mississippian Woodford Shale (Ham, 1959), and they are named for the excellent exposures in the Arbuckle Mountains: these strata were deposited mainly in shallow-marine environments ranging from the intertidal zone to water depths of several hundred feet. In contrast, the "Ouachita facies" consists mainly of black shales, cherts, and sandstones of equivalent age, deposited in several thousand feet of water in the Ouachita trough off the southern margin of the North American craton (Fig. 4).

The Reagan Sandstone and overlying Honey Creek Limestone constitute the Timbered Hills Group of Late Cambrian age (Fig. 3). The Reagan was deposited throughout the Oklahoma basin, except on topographic highs such as the "Tulsa Mountains" (basement highs in northeastern Oklahoma, as shown on Fig. 4) or the basement-rock hills buried in the Arbuckle Mountains (Ham, 1969) and the Wichita Mountains (Donovan, 1986). The Reagan is a feldspathic and glauconitic sandstone, consisting mainly of reworked detritus weathered from the basement complex. It commonly is 50–200 ft thick, but reaches 450 ft in the Arbuckle Mountains part of the SOA. The Honey Creek is a fossiliferous limestone in the aulacogen that grades into sandy dolomite on the shelf: the unit typically is 100–200 ft thick. Rocks equivalent to the Timbered Hills Group in the Ouachita province are neither exposed or encountered in drilling.

The Arbuckle Group, which overlies the Timbered Hills Group, is the thickest sequence of lower Paleozoic strata in Oklahoma; it is as much as 6,700 ft of limestone in the aulacogen, as exposed in the Arbuckle anticline (Fay, 1989), and it thins to ~4,000 ft of dolomite in the eastern Arbuckle Mountains, and about 1,000–4,000 ft of dolomite in most other shelf areas of the Oklahoma basin (Fig. 5) (Denison in Johnson and others, 1988). The lateral transition from mainly limestone to mainly dolomite occurs near the boundary of the SOA (Figs. 4,5), with the dolomite probably resulting from deposition of carbonates in an alternating shallow-marine and supratidal environment, as well as early exposure of carbonates to meteoric waters. Paleokarst features, such as dissolution cavities, collapse breccias, fractures enlarged by dissolution, and locally extensive vuggy porosity, probably result largely from intermittent exposure and subsidence of the vast carbonate shelf during Arbuckle deposition (Lynch and Al-Shaieb, 1991). Anhydrite has been encountered in Arbuckle Group boreholes in parts of south-central Oklahoma (Latham, 1970), but outcrop evidence is limited to anhydrite relics in chert, salt pseudomorphs, and karstic collapse features.

The Late Cambrian–Early Ordovician Arbuckle Group is divided into eight formations (six limestones and two secondary dolomites), based upon excellent exposures in

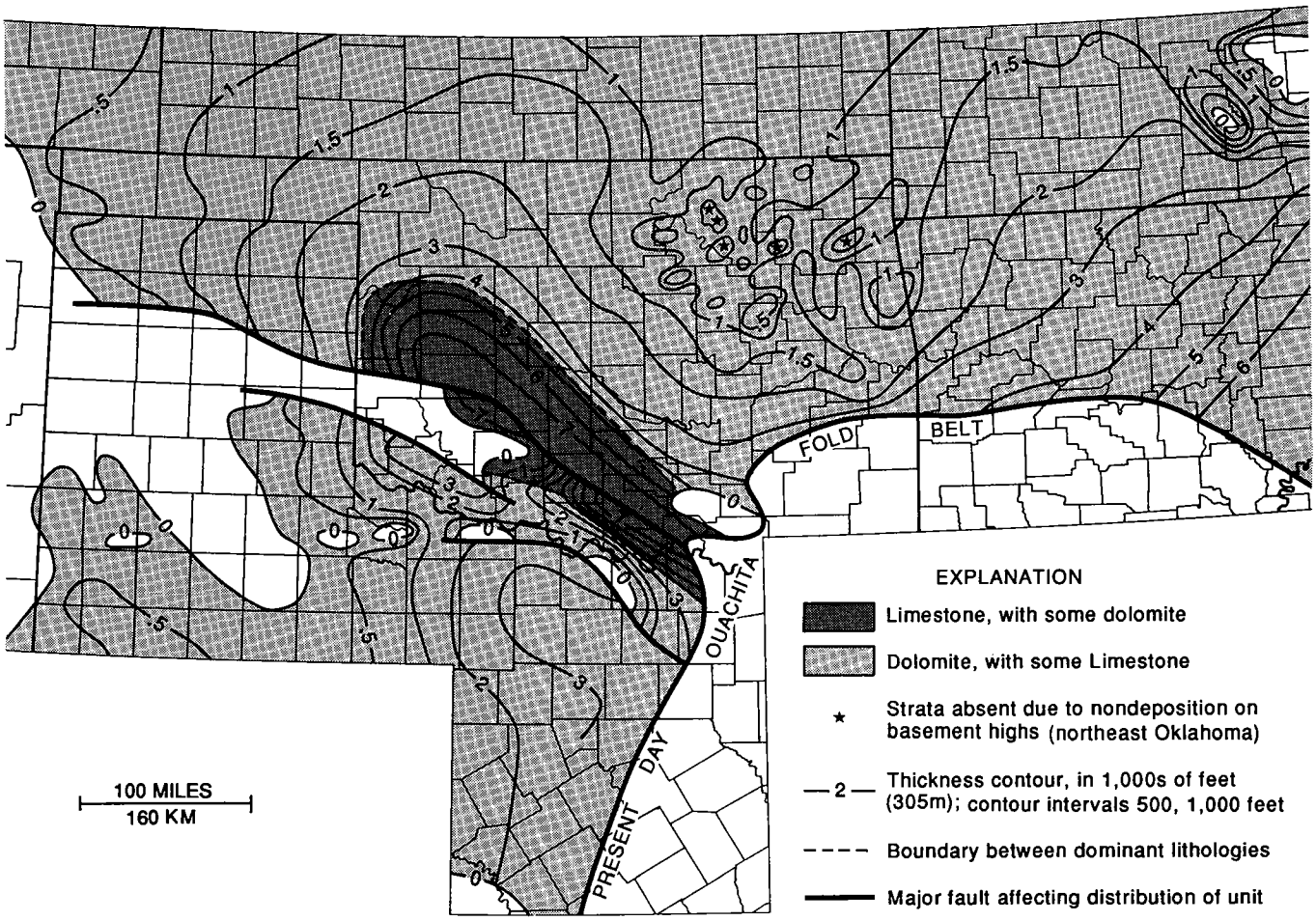


Figure 5. Thickness and dominant lithologies of the Timbered Hills and Arbuckle Groups in the southern Midcontinent (from Denison in Johnson and others, 1988).

the Arbuckle and Wichita Mountains (Fig. 3). The limestone units are readily correlated from the Arbuckle Mountains to outcrops in the Slick Hills, on the northeast side of the Wichita Mountains (Donovan, 1986), although zones of secondary dolomite in the Slick Hills are present at stratigraphic levels other than those in the Arbuckle Mountains. Limestones of these two major outcrop areas attest to shallow-water marine deposition. The strata consist mainly of cyclic arrangements of interbedded carbonate mudstones, intraclast calcarenites, oolitic calcarenites, stromatolites, and laminated dolomites or dolomitic limestones (Ham, 1969). They are highly fossiliferous, containing trilobites, brachiopods, mollusks, pelmatozoans, sponges, and stromatolites. In the shelf areas, equivalent strata consist of similar limestones that have been wholly or partly dolomitized.

Arbuckle Group shallow-water carbonates give way to the Ouachita facies of black shales, sandstones, and fine-grained dark limestones in the Ouachita trough (Fig. 4). The Collier, Crystal Mountain, and Mazarn Formations are sparingly fossiliferous, but graptolites and conodonts enable reasonable correlation of these units with the Arbuckle facies (Ethington and others, 1989). The base of the Collier Shale is not known in the Oklahoma Ouachitas, so the full thickness of these strata is uncertain. Estimated thicknesses in McCurtain County are 600 ft of Mazarn, 100 ft of Crystal Mountain, and at least 300 ft of Collier (Ham, 1959); the Viersen and Cochran No. 25-1 Weyerhaeuser well, drilled in the core of the Broken Bow uplift, penetrated ~10,000 ft of complexly folded and faulted black phyllites, quartzites, and dolomitic marble without reaching basement (Goldstein, 1975).

Epeirogenic subsidence continued in most of the Oklahoma basin from Middle Ordovician through Late Mississippian time, and 500–6,000 ft of relatively simple, marine-shelf carbonates, shales, and sandstones were deposited above the Arbuckle Group. A series of orogenic movements, mainly during the Pennsylvanian Period, subdivided the region into the various tectonic provinces that are so easily recognized today (Fig. 1). Thick sequences of Pennsylvanian marine and nonmarine sediments were deposited in the rapidly subsiding basins, and additional, moderately thick Permian strata were deposited in western Oklahoma and the Texas Panhandle. The maximum total thickness of Pennsylvanian and Permian strata in the various basins of the region ranges from about 8,000 to 25,000 ft.

As a result of Pennsylvanian tectonic activity, and thick accumulations of Middle Ordovician through Permian strata, the Arbuckle Group now is deeply buried in most parts of Oklahoma, but also it crops out in parts of the Arbuckle Mountains, Wichita Mountains, Criner Hills,

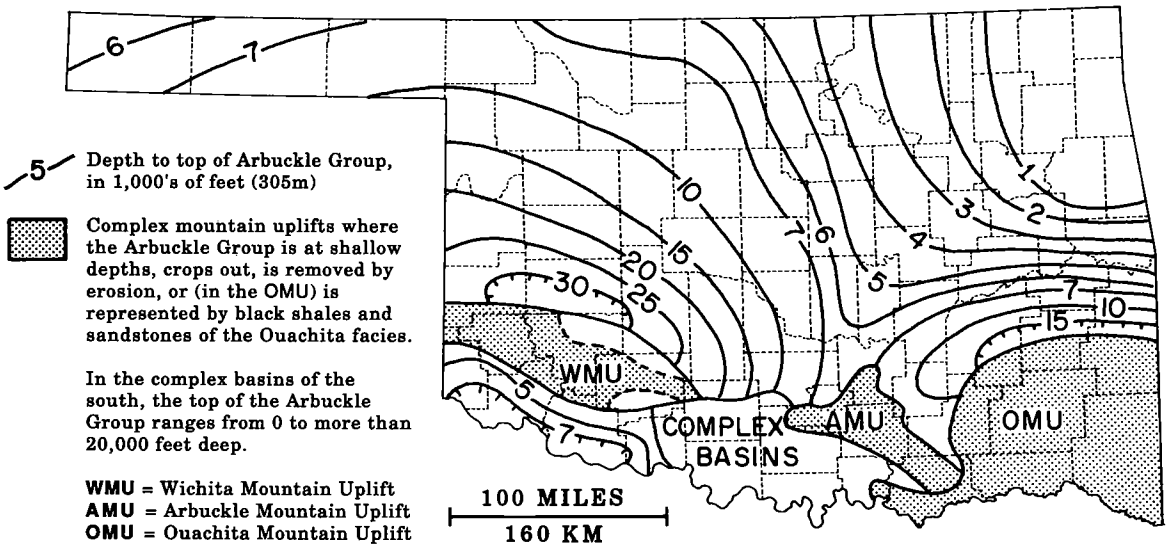


Figure 6. Generalized map showing depth to top of the Arbuckle Group in Oklahoma (modified from Johnson and others, 1980).

and Ozarks uplift: the depth to the top of the Arbuckle Group in subsurface is <1,000 ft in the Ozark region of northeast Oklahoma, and it increases to >15,000 ft in the Arkoma basin, and to >30,000 ft in the Anadarko basin (Fig. 6).

REFERENCES CITED

Denison, R. E., 1981, Basement rocks in northeast Oklahoma: Oklahoma Geological Survey Circular 84, 84 p.

Denison, R. E.; Lidiak, E. G.; Bickford, M. E.; and Kisvarsanyi, E. B., 1984, Geology and geochronology of Precambrian rocks in the central interior region of the United States: U.S. Geological Survey Professional Paper 1241-C, 20 p.

Donovan, R. N. (ed.), 1986, The Slick Hills of southwestern Oklahoma—fragments of an aulacogan?: Oklahoma Geological Survey Guidebook 24, 112 p.

Ethington, R. L.; Finney, S. C.; and Repetski, J. E., 1989, Biostratigraphy of the Paleozoic rocks of the Ouachita orogen, Arkansas, Oklahoma, and Texas, *in* Hatcher, R. D., Jr.; Thomas, W. A.; and Viele, G. W. (eds.), The Appalachian–Ouachita orogen in the United States: Geological Society of America, The Geology of North America, v. F-2, p. 563–574.

Fay, R. O., 1989, Geology of the Arbuckle Mountains along Interstate 35, Carter and Murray Counties, Oklahoma: Oklahoma Geological Survey Guidebook 26, 50 p.

Goldstein, A., Jr., 1975, Geologic interpretation of Viersen and Cochran's 25-1 Weyerhaeuser well, McCurtain County, Oklahoma: Oklahoma Geology Notes, v. 35, p. 167–181.

Ham, W. E., 1959, Correlation of pre-Stanley strata in the Arbuckle–Ouachita Mountains region, *in* Cline, L. M. (ed.), The geology of the Ouachita Mountains, a symposium: Dallas Geological Society and Ardmore Geological Society, p. 71–86. [Reprinted in Oklahoma Geology Notes, v. 21, p. 204–224.]

_____1969, Regional geology of the Arbuckle Mountains, Oklahoma: Oklahoma Geological Survey Guidebook 17, 52 p.

Ham, W. E.; and Wilson, J. L., 1967, Paleozoic epeirogeny and orogeny in the central United States: American Journal of Science, v. 265, p. 332–407.

Ham, W. E.; Denison, R. E.; and Merritt, C. A., 1964, Basement rocks and structural evolution of southern Oklahoma: Oklahoma Geological Survey Bulletin 95, 302 p.

Hatcher, R. D., Jr.; Thomas, W. A.; and Viele, G. W. (eds.), 1989, The Appalachian–Ouachita orogen in the United States: Geological Society of America, The Geology of North America, v. F-2, 767 p.

Hills, J. M.; and Kottlowski, F. E. (coordinators), 1983, Correlation of stratigraphic units in North America—southwest/southwest Mid-Continent correlation chart: American Association of Petroleum Geologists, Tulsa.

Johnson, K. S., 1991a, Geologic overview and economic importance of Late Cambrian and Ordovician rocks in Oklahoma, *in* Johnson, K. S. (ed.), Late Cambrian–Ordovician geology of the southern Midcontinent, 1989 symposium: Oklahoma Geological Survey Circular 92, p. 3–14.

_____(ed.), 1991b, Late Cambrian–Ordovician geology of the southern Midcontinent, 1989 symposium: Oklahoma Geological Survey Circular 92, 227 p.

Johnson, K. S.; Luza, K. V.; and Roberts, J. F., 1980, Disposal of industrial wastes in Oklahoma: Oklahoma Geological Survey Circular 80, 82 p.

Johnson, K. S.; Amsden, T. W.; Denison, R. E.; Dutton, S. P.; Goldstein, A. G.; Rascoe, B., Jr.; Sutherland, P. K.; and Thompson, D. M., 1988, Southern Midcontinent region, *in* Sloss, L. L. (ed.), Sedimentary cover—North American craton, U.S.: Geological Society of America, The Geology of North America, v. D-2, p. 307–359. [Reprinted as Oklahoma Geological Survey Special Publication 89-2, 53 p.]

Latham, J. W., 1970, Petroleum geology of the Healdton field, Carter County, Oklahoma: American Association of Petroleum Geologists Memoir 14, p. 255–276.

Lynch, M.; and Al-Shaieb, Z., 1991, Evidence of paleokarstic phenomena and burial diagenesis in the Ordovician Arbuckle Group of Oklahoma, *in* Johnson, K. S. (ed.), Late Cambrian–Ordovician geology of the southern Midcontinent, 1989 symposium: Oklahoma Geological Survey Circular 92, p. 42–60.

Mankin, C. J. (coordinator), 1987, Correlation of stratigraphic units in North America—Texas–Oklahoma tectonic region correlation chart: American Association of Petroleum Geologists, Tulsa.

McHugh, J. W. (ed.), 1964, Symposium on the Arbuckle: Tulsa Geological Society Digest, v. 32, 186 p.

Sedimentology and Diagenesis of the Arbuckle Group in Outcrops of Southern Oklahoma

Deborah A. Ragland
Conoco Inc., Ponca City, Oklahoma

R. Nowell Donovan
Texas Christian University

ABSTRACT.—Six formations comprise the Cambro–Ordovician Arbuckle Group of southern Oklahoma. The Fort Sill (base), Signal Mountain, McKenzie Hill, Cool Creek, Kindblade, and West Spring Creek (top) Formations are composed predominantly of limestones arranged in varying packages of facies, the most common of which are the micritic, peloidal, oolitic, fossiliferous, algal, and intraformational-conglomerate facies. Quartz detritus is an important admixture in the three upper formations. Three less common facies, intraformational breccias, evaporitic facies, and bedded cherts, are important in that they supply clues concerning the nature of the paleoenvironment during deposition of the sediments.

The six formations were deposited in the southern Oklahoma aulacogen under varying environmental conditions. All are dominated by lime-mud matrices, in contrast to the underlying Timbered Hills Group, thus signifying a reduction in overall energy of bottom currents. Differences in facies packages among formations may be representative of eustatic sea-level changes at formational boundaries. Intraformational variations are often the result of lateral migration of facies and rejuvenation of sequences following storm events. Isotope data from the Arbuckle Group and inclusion of evaporite traces indicate that the climate was warm to hot (+20°C) and, at least at times, arid to semi-arid. Storms were probably relatively frequent events supplying many of the intraformational clasts that are ubiquitous in the Arbuckle Group.

Diagenesis of the sediments is complicated not by a great variety of products, but by the overlapping of events and the immense amount of time in which alterations could take place. Cementation, dissolution, and replacement began penecontemporaneously with deposition, continuing through the post-depositional history of the sediments. Calcite, silica, and dolomite are the most common cements, whereas silica and dolomite are the most common replacement products. Although the cements and replacive dolomite are found throughout the group, replacive silica occurs mainly from the lower McKenzie Hill Formation upwards. Continuing diagenesis, i.e., weathering of the outcrops during the Holocene, has resulted in an unusual field morphology known locally as "tombstone topography."

INTRODUCTION

The Arbuckle Group crops out in two principal areas of southern Oklahoma: the Arbuckle Mountains and the Slick Hills on the north side of the Wichita Mountains (Fig. 1). In both areas, exposures are extraordinarily good for this part of the world, and the two areas complement each other in the variety and interest of the features that they display. Six formations comprise the group. All are exposed in the Arbuckle Mountains; all but the upper part of the West Spring Creek Formation are exposed in the Slick Hills (Fig. 2).

A study of the Arbuckle Group was initiated before the second world war in studies by Taff (1904), Decker and Merritt (1928), and Ulrich (1933). A great expansion of our understanding of the group was provided by the work of Ham (1955) and several students who worked under his direction, e.g., Barthelman (1969) and Brookby (1969). More recently, Stitt (1971,1977,1983) provided a firm paleontological basis to complement Ham's lithological appreciation of the subtleties of the group.

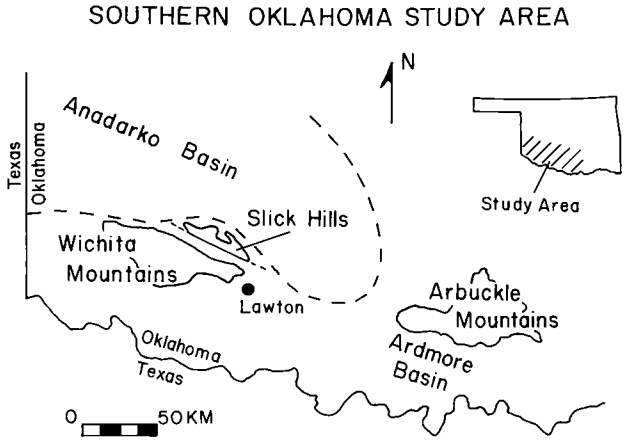


Figure 1. Location map of the study area, southern Oklahoma. The Arbuckle Group crops out in the Slick Hills and the Arbuckle Mountains. Modified from Johnson and others (1972).

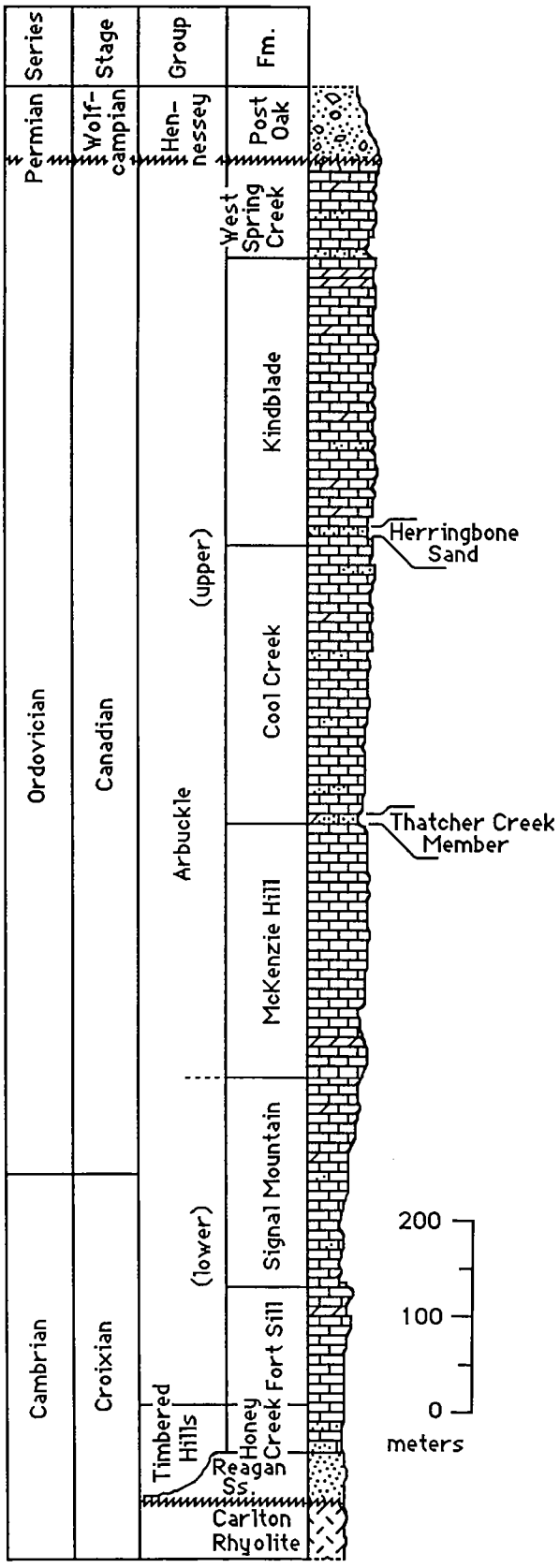


Figure 2. General stratigraphic log of outcrops in the Slick Hills. The top of the West Spring Creek Formation is covered in this area.

From the 1980s until the present, our own work, which is centered principally in the Slick Hills but also includes excursions into the Arbuckle Mountains, has focused on an understanding of the sedimentological problems raised by the Arbuckle Group (this work is to referred to where appropriate in the text that follows). Attention is drawn to a number of graduate theses that have come out of this phase of the study: Babaei (1980), Beauchamp (1983), McConnell (1983), Ragland (1983,1990), Rafalowski (1984), Ditzell (1984), Marchini (1986), Cloyd (1987), Shelby (1990), Stephenson (1990), White (1991), and Smith (1991).

The recent intense interest in the hydrocarbon potential of the Arbuckle Group has resulted in several important studies that pertain directly to that potential; for example, Lynch and Al-Shaieb (1989,1991) and Ragland and Matthews (1991). A number of important papers are also due to appear in publications by the Oklahoma Geological Survey, particularly those in the workshops on Late Cambrian–Ordovician geology of the southern Midcontinent (Circular 92), source rocks in the southern Midcontinent, and petroleum-reservoir geology in the southern Midcontinent.

In this paper we present an analysis of the sedimentology of the Arbuckle Group; our principal focus is on the primary depositional fabrics and facies of the group. Thus, we will restrict our discussion to those parameters that can be described as either primary or penecontemporaneous. A *caveat* is necessary at this stage; much of the modern study of the Arbuckle Group in the field has focused on the spectacular road cuts on Interstate 35 through the Arbuckle Mountains, where the upper part of the group is so splendidly exposed on the southern limb of the great Arbuckle anticline. We would emphasize, however, that much of the rest of the outcrop area of the group is poorly known. As an example of this, Donovan and Stephenson (1991) described a hitherto unknown basement-rock contact with the upper part of the Fort Sill Formation in the Slick Hills. It is our contention that much work still remains to be done before we can claim to have a true understanding of the Arbuckle Group.

GEOGRAPHICAL PARAMETERS

Where was Oklahoma in the Late Cambrian and Early Ordovician?

The Early Ordovician was a time of worldwide submergence when shallow seas increasingly transgressed vast areas of the globe (Fig. 3). Substantial relief existed only on the Siberian continent, Kazakhstania, and on the northern edge of Gondwana (Ross, 1976; Scotese and others, 1979; Frazier and Schwimmer, 1987). Most of the emergent cratons were lowlands, thus shallow seas dominated the proto-North American continent (Laurentia) with more than half of the craton under water (Kerans, 1990). Furthermore, Laurentia was, at this time, a free craton in the sense that none of its edges coincided with plate boundaries. It is the combination of an absence of relief and lack of tectonic dynamics that plays such an important part in a general understanding of the Arbuckle Group carbonate platform. Not only was the area tectonically quiescent throughout the Late Cambrian and Early Ordovician, but, as no substantial relief existed even when sea-level regressions (i.e., rejuvenations of ultimate

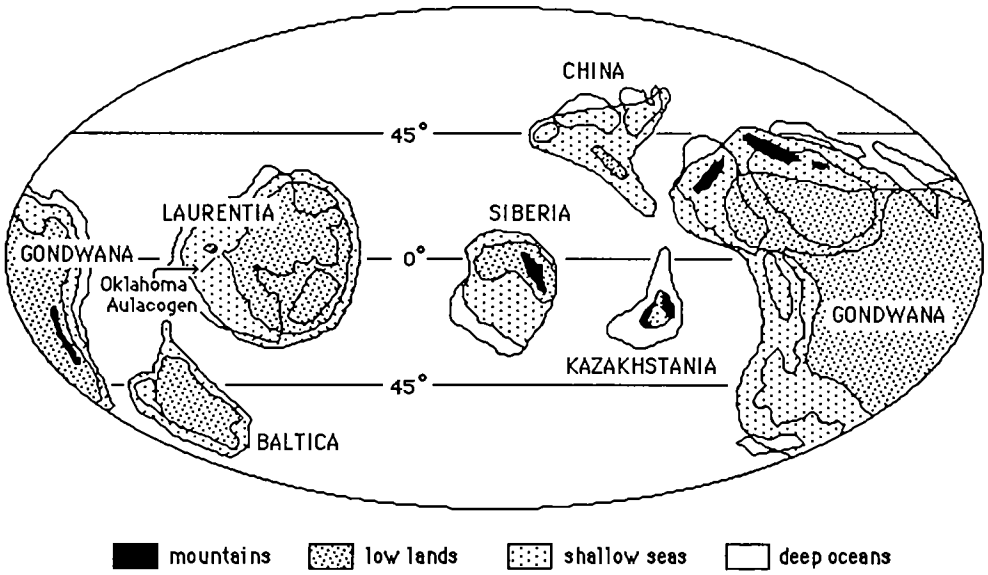


Figure 3. Global paleogeography during the Late Cambrian to Early Ordovician. Data from Termier and Termier (1960), Ross (1976), Scotese and others (1979), Windley (1977), and Frazier and Schwimmer (1987).

base level) took place, the siliciclastic detritus that was available was mineralogically mature because it had had such a long residence time on the cratonic regolith (Fig. 4). In essence, the lowland regions of Laurentia were composed of isolated flat land masses and islands (Chenoweth, 1968; Pratt and James, 1986).

Paleomagnetic studies suggest that the North American continent (Laurentia) lay between 20°N and 35°S latitude during the Early Ordovician (Ross, 1976; Habicht, 1979; Frazier and Schwimmer, 1987) (Fig. 3). There is some variance in the data presented by various authors, but generally it is thought that the continent was rotated approximately 30–45° clockwise to its present position. Although its longitudinal position is unknown, Laurentia seems to have been separated from the other continental masses by fairly substantial oceans. Within this geographical framework the southern Oklahoma aulacogen occupied a position between 800 and 1,600 km south of the equator. Because of the rotation of Laurentia, the shelf-platform boundary on this edge of the craton trended ~N70°W, while the axis of the aulacogen was oriented approximately N15° to 30°W. Thus, the area was within the southern tropics and would have been bathed by the warm waters of the eastward flowing southern equatorial current (Fig. 5). However, because the aulacogen was on the lee (westward) side of Laurentia, it is unlikely that this current packed very much punch in the area, even on the shelf edge.

What was the Climate Like at That Time?

Given the paleogeographic position of the southern Oklahoma aulacogen, an application of uniformitarian principal suggests that the ambient temperatures during Arbuckle deposition would have been warm to hot (St. John and Eby, 1978; Ragland and Donovan, 1986). Typically, temperatures in excess of 20°C would have prevailed throughout the area. Over the enormous extent of the Arbuckle platform, vast expanses of shallow water would have been heated throughout the entire water column. Hence, energy exchange would have been easy between water and atmosphere (Riehl, 1979). High water-vapor content in the air would have hindered the transmission of radiation through the atmosphere, keeping temperatures relatively high but preventing the extremes likely to have developed on the adjacent continent (which was essentially a biological desert devoid of vegetation).

In general, the climate across the platform might be expected to have been characterized by a humid climate. However, it is possible that if Milankovitch forcing of climatic belts took place, the southern Oklahoma aulacogen may well have been subjected to regular northward expansions of the southern semiarid belt. At such times, therefore, it is possible that the sediments may have been deposited in an environment where evaporation was great enough to cause local evaporite precipitation in areas of restricted circulation.

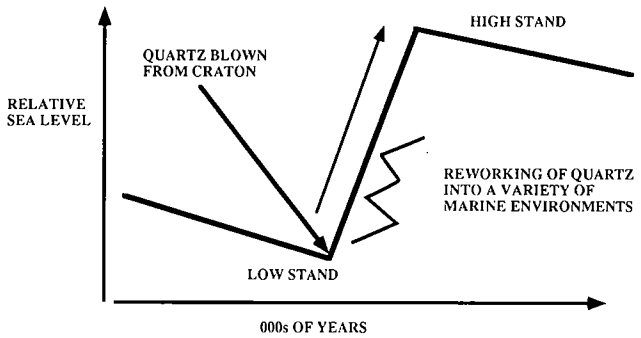


Figure 4. Origin of the finer-grained sands from the exposed cratons. Larger grain sizes would have washed in from the cratonic highs.

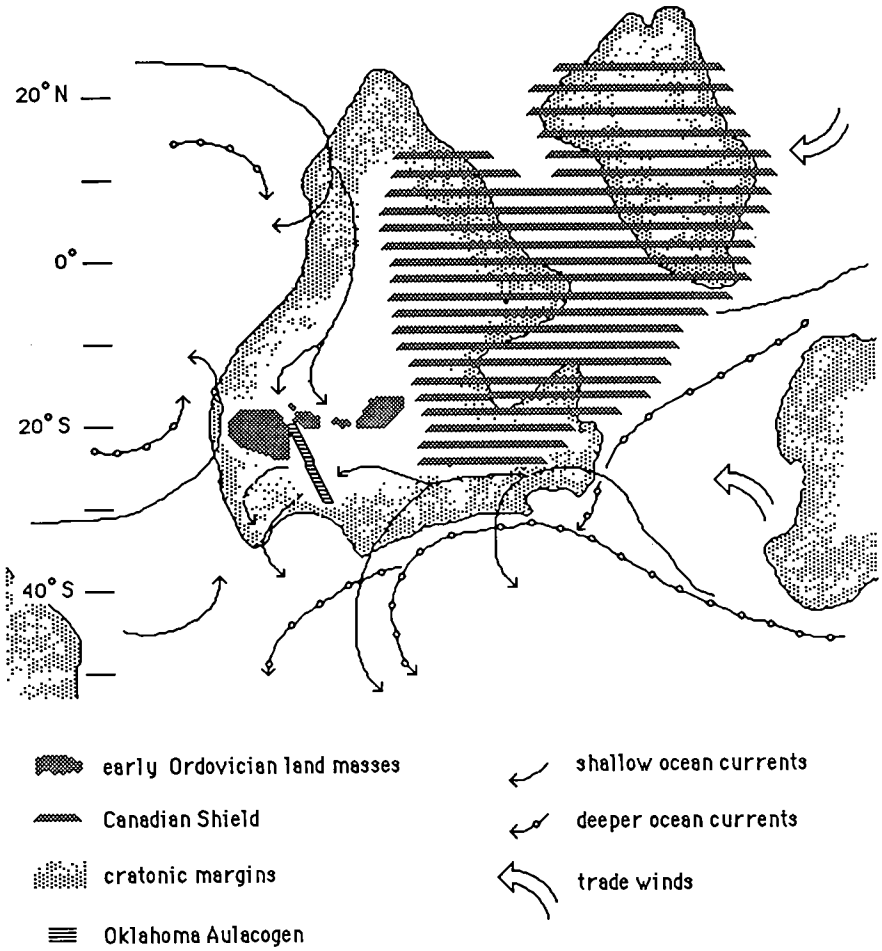


Figure 5. A hypothetical model of ocean-circulation patterns for the North American continent during the Early Ordovician. Modified and formulated from data in Ross (1976), Habicht (1979), Riehl (1979), Brewer and others (1983), Larson and others (1985), and Frazier and Schwimmer (1987).

FORMATIONAL ORGANIZATION IN THE ARBUCKLE GROUP

Within the southern Oklahoma aulacogen, the Arbuckle Group attains a maximum thickness of ~2,200 m. The principal distinctive feature shown by the group as a whole is that the rocks are thinly bedded, well-indurated carbonates dominated by lime-mud and mud-supported lithologies. The result is that the group generally has a rather monotonous appearance with few distinctive interbeds. Therefore, it has only been possible to divide the series into six primary formations (Fig. 2). Although dolomite "formations" have been recognized, these do not have lateral continuity throughout the aulacogen. The criteria that have been used to distinguish different formations are a combination of biostratigraphic and lithostratigraphic controls (see review in Donovan and Ragland, 1986).

The base of the Arbuckle Group is demarcated lithostratigraphically by the incoming of significant amounts of lime mud into the section. This provides a marked contrast to the underlying Honey Creek Limestone of the Timbered Hills Group, a formation that consists primarily of cross-bedded bioclastic grainstones. The incoming of major amounts of mud presupposes either that mud-producing organisms existed or that chemical conditions were appropriate for the production of the mud. In addition, it is probable that bottom currents were not strong enough to winnow mud away from the area. While the Timbered Hills Group was molded by strong tidal currents (Donovan, 1986), it seems likely that, as the Upper Cambrian transgression progressed across the Laurentian craton, tidal energy was progressively diminished in power, and, hence, the carbonate platform was able to retain most of the mud that its carbonate factory produced.

In the Slick Hills, three informal members can be recognized in the Fort Sill Formation (Donovan and Ragland, 1986). These are: a basal, thin-bedded limestone sequence dominated by mudstones, but with important detrital limestones and some stromatolites; a middle sequence consisting of an alternation of lime mudstones with thinly bedded dolomitic siltstones; and a topmost sequence of massive limestones containing abundant algal boundstones. In part, the top member of the Fort Sill Formation in the Slick Hills has been replaced by a thick, stratabound dolomite (the Bally dolomite). A similar dolomite, the Royer, has replaced not only the Fort Sill, but

also the lower part of the Signal Mountain Formation in the Arbuckle Mountains (Ham and others, 1964).

The stratigraphic contact between the Fort Sill and Signal Mountain Formations is perhaps the most distinctive contact in the Arbuckle Group. The massive algal boundstones of the Fort Sill give way abruptly to the thinly bedded, dark-colored carbonates of the Signal Mountain Formation. In fact, the latter is the most consistently thin-bedded formation in the group and it weathers to give the weakest topographic expression.

Typically, the Signal Mountain Formation contains a textural spectrum of clastic limestones ranging from intraformational conglomerates and grainstones, through packstones and wackestones, to mudstones (Ditzell, 1984). The formation is characterized by an abundant fauna, and, toward the base, contains significant amounts of glauconite (as much as 10%). It has been suggested that the abruptness of the formational boundary records the degree of tectonic adjustment at the margins of the developing southern Oklahoma aulacogen (Donovan, 1986). Certainly the environmental change is significant, for algal boundstones are not encountered in the group for >200 m above the top of the Fort Sill. Although the boundary between the Cambrian and Ordovician systems is located within the Signal Mountain (Stitt, 1977), no lithostratigraphic change takes place at the horizon in question.

While the lower boundary of the Signal Mountain is clear-cut, the upper boundary of the formation is the most difficult to place in the entire group. In general, the overlying McKenzie Hill Formation is characterized by relatively massive-bedded micritic limestones that form thick ledges. Unfortunately, "typical" lithologies of the two formations overlap in a zone that is ~60 m thick (Ditzell, 1984). It has been our practice in the field to take the lowest thickly bedded lime mudstone as the base of the McKenzie Hill Formation. (This method is of limited value in structurally complicated terrain.)

The lower part of the McKenzie Hill consists predominantly of lime mudstones, wackestones, and packstones that are quite fossiliferous (Stitt, 1977,1983). Toward the top of the formation a substantial number of grainstones and intraclastic deposits are present. In addition, the top part of the McKenzie Hill is characterized by a very thickly layered sequence in which algal boundstones are prominent. However, perhaps the most useful lithostratigraphic feature that permits placement within the formation is that the lower one-third contains practically no chert, whereas the upper two-thirds contain abundant chert in a variety of forms, including burrow fillings and lenticular varieties.

Although some detrital quartz silt is found near the top of the McKenzie Hill Formation, the base of the Cool Creek Formation is marked by a dramatic increase in the amount of quartz sand. This quartz-rich bed has been formally accorded member status by Ragland and Donovan (1985a) as the Thatcher Creek Member. It can be traced throughout the Slick Hills and is also seen in the Arbuckle Mountains (Ragland and Donovan, 1991).

The Cool Creek Formation consists of a number of sequential arrangements of carbonates which show a wide spectrum of lithologies. Thus, stromatolites, thrombolites, intraformational conglomerates, oolitic grainstones, packstones, wackestones, and mudstones are all abundant. These lithologies are interbedded with thinly laminated dolomitized beds that often contain abundant quartz detritus and traces of evaporites (Ragland and Donovan, 1986). The whole of the Cool Creek is characterized by abundant chert deposits occurring in an extravagant variety of forms (Ragland and Donovan, 1991). As a whole, Cool Creek outcrops are characterized by their lithological heterogeneity and their general thin-bedded characteristics, in comparison with adjoining formations.

The contact of the Cool Creek with the overlying Kindblade Formation is placed at the incoming of *Ceratopea* (a silicified gastropod operculum) (Ham, 1955; Yochelson and Bridge, 1957; Yochelson, 1973,1975), an unsatisfactory boundary when trying to demarcate the formations in the field. As Donovan and Ragland (1986) pointed out, this operculum is only visible in the field when it has been silicified, and thus the formational boundary is dependent upon a diagenetic modification for recognition. In general terms, the Kindblade Formation can be distinguished from the Cool Creek in that the Kindblade: (1) is usually thicker bedded; (2) contains a much more substantial biota; (3) contains less quartz detritus, less chert, and fewer intraformational conglomerates (however, see Ragland and Donovan, 1991); and (4) generally displays a cyclic arrangement of carbonates dominated by lithologies that show little evidence of emergence.

The upper contact between the Kindblade and West Spring Creek Formations is a quartz-rich, laminated sand that resembles the Thatcher Creek Member. The West Spring Creek resembles the Cool Creek Formation in that it displays sequential arrangements of great variability; however, quartz detritus is even more common in the uppermost formation. In addition, the West Spring Creek, particularly toward the top, contains a number of thin red beds that appear to be of primary origin.

The upper contact of the Arbuckle Group with the overlying Simpson Group is only clearly exposed in the Arbuckle Mountains. Here, within the original confines of the southern Oklahoma aulacogen, the West Spring Creek Formation is overlain by limestones of the Joins Formation, the basal member of the Simpson Group (Decker and Merritt, 1931). The Joins is characterized by thin limestones and interbedded shales with a basal conglomerate that varies from 8 to 40 cm thick. The Joins outcrop is limited to the middle, southern, and western part of the Arbuckle Mountains, and the northern end of the Criner Hills. Outside the boundaries of the aulacogen, the Arbuckle is overlain by the sandstones of the Oil Creek Formation in the Simpson Group, and thus the Joins is overlapped. The hiatus represented by this overlap appears to have been a widespread period of regression during which considerable karstification of the underlying carbonate platform took place (Kerans, 1990).

BEDDING, LAYERING, AND TOMBSTONES

As Donovan and others (1986) noted, in analyzing the Arbuckle Group a distinction must be made between empirically defined layers that are obvious at outcrop and genetically defined events (beds) that often can only be observed by close scrutiny of the rocks. Most people who have examined exposures of the Arbuckle Group will be familiar with the concept of "tombstone topography"

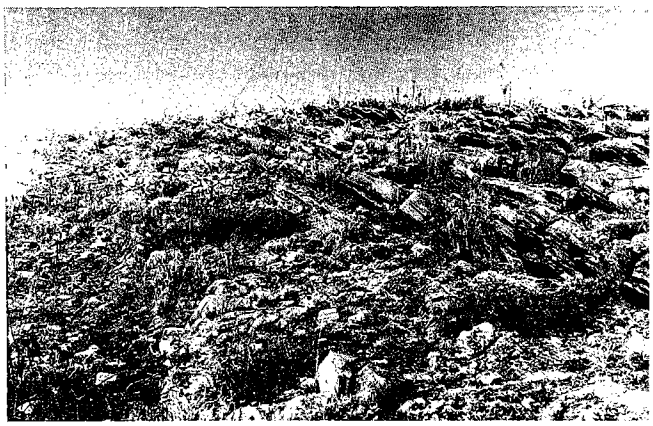


Figure 6. The Signal Mountain Formation, Slick Hills. Outcrop on the left is the typical, poorly exposed profile of the formation. The Signal Mountain exposure on the right is illustrative of the "tombstone topography" seen in the Arbuckle limestones.

(Fig. 6). This local geomorphologic term refers to dipping parallel layers of rock that protrude from the surface and are differentiated from each other by their varied resistance to weathering. Tombstones vary in thickness quite consistently throughout the group (Fig. 7) and, in general, reflect the subtle variations in the proportions of different facies that are related to formational subdivision. However, boundaries of tombstones are not necessarily the boundaries of genetic events (beds); in fact, many of the tombstones contain numerous genetic events (e.g., alternations of centimeter-thick, mud-supported lithologies defined by hardground surfaces [Donovan and others, 1986]). Thus, in a core where weathering has not had time to differentiate resistances to weathering, a rather different picture of stratum thickness may emerge from that which is seen at outcrop.

Differentiation of some tombstones that appear to be genuine bed boundaries (for example, where the sequence becomes more thinly laminated because siliciclastic detritus defines bedding) may be following bedding-parallel stylolites (Fig. 8). The stylolites may have wavelength magnitudes as great as 2.5 cm, although most are substantially less. Stylolites of this type are very common throughout the Arbuckle Group, and it is clear that substantial proportions of the original lithology have been removed by pressure solution generated by confining pressure. Donovan and others (1986) estimated that 23% of a 19-m-thick section of Kindblade in the Slick Hills had been removed in this way.

FACIES IN THE ARBUCKLE GROUP

The Arbuckle Group consists of a rather restricted range of facies; formational subdivision generally recognizes that the proportions of these facies in any given section may vary, although their general character does not. We recognize the following primary lithofacies in the group: micritic facies, peloidal facies, oolitic facies, algal boundstones, quartz sandstones and siltstones, intraformational conglomerates, and intraformational breccias. In addition, we will discuss two secondary lithotypes: chert and "penecontemporaneous" dolomite.

Sedimentary structures that are important in facies interpretation include: bedding, lamination, cross stratification, ripple marks, deformed bedding, burrows and bioturbation, hardgrounds, fenestrae, geopetal structures, graded bedding, subaerial mud cracks, and subaqueous shrinkage cracks.

In addition, a number of diagenetic imprints are important in facies attributions. These include cements (calcite, dolomite, silica, and minor feldspar), replacement products (silica, dolomite, and calcite, plus minor pyrite, hematite, and limonite), and pseudomorph casts and molds where either gypsum, anhydrite, or, less commonly, halite, have been replaced by one of the carbonate minerals or silica.

Micrite Facies

Within this facies we recognize a range that extends from the extremely bland, with little or no visible features, to extremely complex, wherein the rock is made up of several components. As noted previously, the overall distinguishing characteristic of the Arbuckle Group is that it contains copious amounts of lime mud. Thus the micritic facies, with or without additional components, is the most likely to be encountered in any given formation.

The micritic facies forms both massive, blocky units and platy, parallel-laminated units (Fig. 9). Laminations are usually smooth and of thicknesses varying from 1 to 10 mm. The color of the facies varies from light to medium gray, although some pink and red laminated micrites are found. Dolomicrite usually weathers to a tan color.

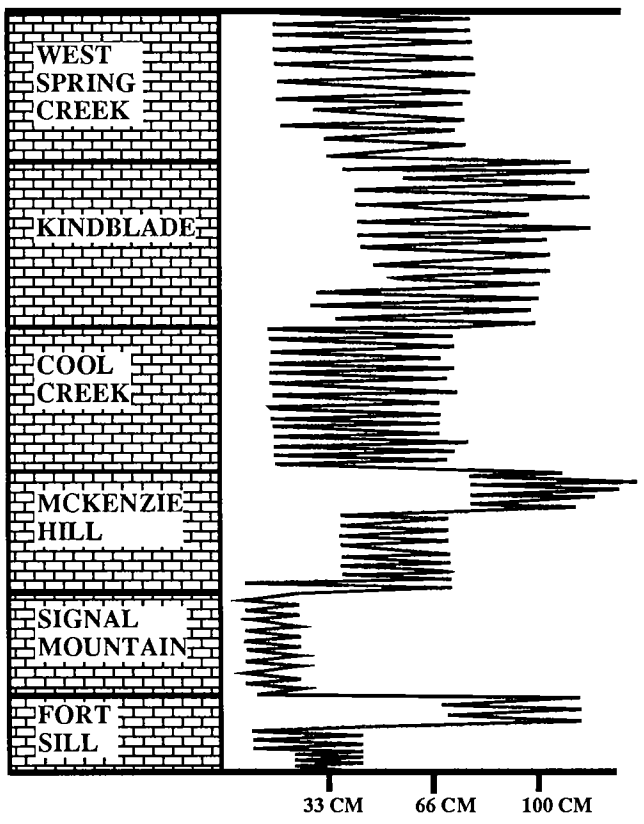


Figure 7. Diagram illustrating the differences in "tombstone" thickness for each formation in the group.

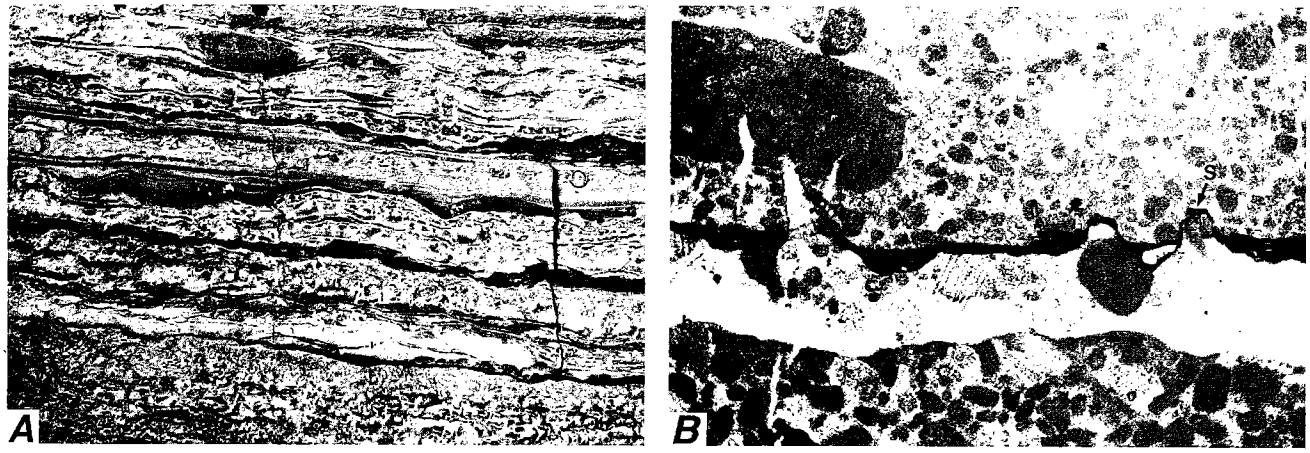


Figure 8. *A*—Stylolites (labeled "s," on the left) with relatively low amplitudes are parallel to bedding, but may not originally have formed along facies changes. This Kindblade outcrop photograph also illustrates the unusual "leopard skin" dolomite texture often found in the formation (lighter color is the dolomite; darker patches, the calcimicrite). Cook Creek road cut, Slick Hills. *B*—A high-relief stylolite (s) cuts an intrasparite sequence. A hardground (h) is evident below the stylolite. Ordinary light; field of view is 9 mm. Kindblade Formation, Arbuckle Mountains.

Microscopically, some micrites display aggradational neomorphism up to a maximum of 50 μ, but in most cases the micrite has a crystal size that is <4 μ.

The micritic facies often contains variable amounts of other components, resulting in a spectrum of rock types from mudstone to packstone. Particles commonly included are ooids, fossils, peloids, intraclasts, and detrital quartz. Micrite is also the major component of algal boundstones.

Sedimentary structures associated with the micritic facies include: parallel and (occasionally) cross lamination, mud cracks, subaqueous shrinkage cracks, deformed bedding, and, perhaps most common of all, various types of bioturbation (Figs. 9,10). Many burrows have formed permeability pathways for diagenetic modification and thus have been partially silicified or dolomitized. It is rarely possible to identify specific trace fossils; however, in one or two cases *Chondrites*? has been recognized (Fig. 10).

Peloidal Facies

Varying amounts of peloids are found throughout the Arbuckle Group limestones. While rarely forming homogeneous grain populations, peloids are a constant component of various types of grainstones, and, where they can be distinguished, are found in mud-supported textures.

It is likely that the peloids formed in two ways, either as faecal pellets or as small intraclasts of lime mud. True pellets are oval-shaped, whereas the detrital peloids often have irregular outlines.

Oolitic Facies

Ooids can be found throughout the group, particularly in the upper part and, especially, in the Cool Creek Formation. Ooids generally form sand shoals, some of which can be traced over lateral distances in excess of 500 m. Composite units composed of bedded ooids separated by hardgrounds have been noted up to 10 m thick. The most characteristic sedimentary structure found in these sand

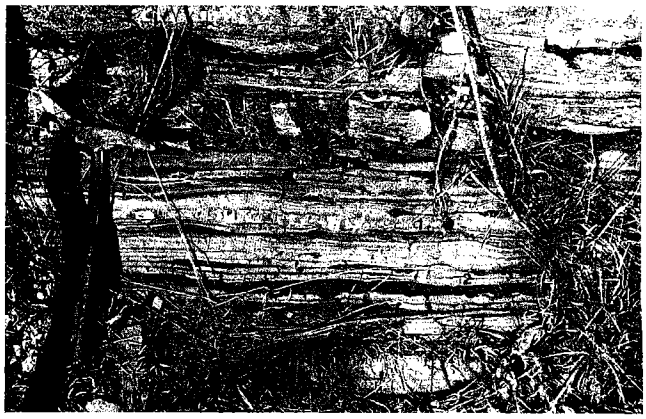


Figure 9. Parallel laminae and thin beds in the Cool Creek Formation, Slick Hills. The darkest, thin beds near the handle of the rock hammer are quartz rich. Shrinkage cracks are abundant, some filled with micrite (along horizon 1), others, with quartz detritus (along horizon 2).

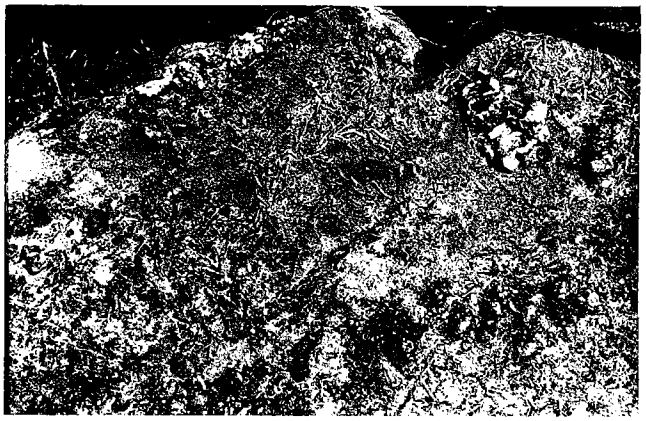


Figure 10. Trace fossils (*Chondrites*?) in the upper McKenzie Hill Formation, Slick Hills. Cauliflower chert nodules (C) may be related to former evaporites. Dark bar at top is 0.3 m long.

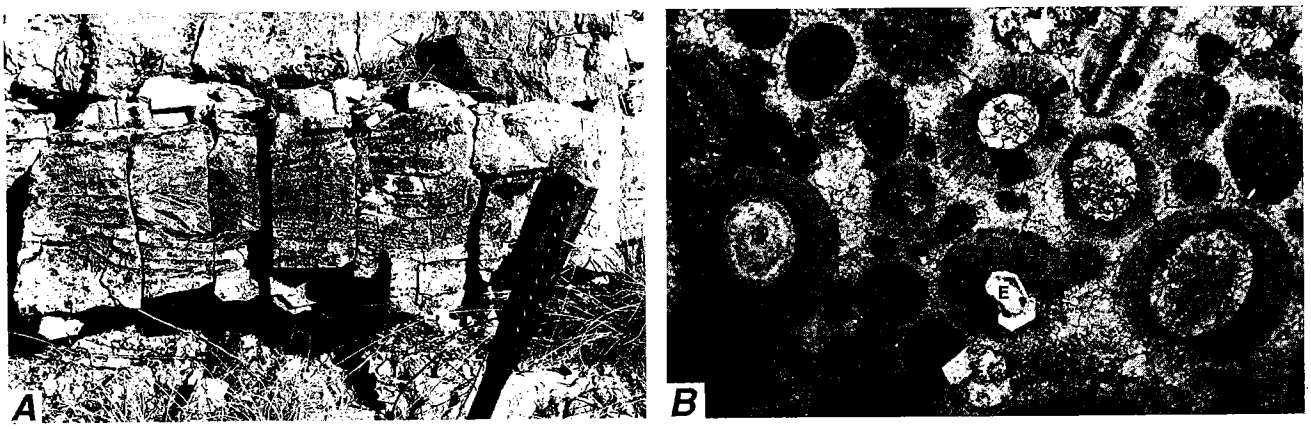


Figure 11. *A*—This 19-cm-thick oolitic bed is preserved by secondary silicification. Cross beds and penecontemporaneous soft-sediment deformational features stand out in relief because of preferential weathering. Cool Creek Formation, Slick Hills. *B*—An oosparite cemented by drusy sparite. Whereas all of the cortices of the ooids appear to be radial calcite, the nuclei show a great deal of variety. Some ooids have a nucleus that is a detrital fragment of lime mud and is presumably original (A, on right); Most of the others show various diagenetic modifications; e.g., one has a nucleus that is partly altered to idiotopic dolomite (B, at top); several are filled by drusy sparite (C, above center), suggesting that the original, aragonitic(?) nucleus has dissolved (and inferentially that the radial fabric of the cortex has always been calcite); yet another has its nucleus replaced by microcrystalline silica (D, on left); in addition, quartz grains with syntaxial overgrowths that replace the cortices of some nuclei are seen (E, below center). Ordinary light; field of view is 4.5 mm wide.

shoals is cross bedding, generally on a small scale, but occasionally as sets as much as 15 cm thick (Fig. 11).

A spectrum of textures from oosparite to oomicrite records the energy of the final depositional environment, but most ooids appear to have originated by the same processes as modern ooids; i.e., the oscillation of sand- and silt-sized grains in an energetic environment. In addition to their occurrence in homogeneous populations, ooids are also found mixed with various other allochems, particularly intraclasts.

Typically, the nucleus of an ooid is a piece of lime mud, such as a peloid or small intraclast; less frequently, quartz grains and bioclasts form nuclei (Fig. 11). Cortices are composed of either radial or concentric arrangements of calcite crystals, or combinations of the two patterns. Ooids display a wide variety of shapes that in most cases are related to the form of the nucleus. Many ooids have, however, undergone substantial diagenetic modification. Some show evidence of mechanical flattening and spalling, while in others the outer cortex has been biogenically altered by endolithic boring organisms. In the latter case, the ooids may possess the wavy outer rim that is typical of Carozzi's "cerebroid" texture (Carozzi, 1962) (Fig. 12).

Chemical modification of the ooids takes several forms. In some cases the ooids have been completely or partially silicified, thus preserving many of the details of their original form (Fig. 11). In other cases, ooids have been dolomitized and are recognizable only as ghosts. In rare cases, aggrading neomorphism has destroyed all but the vaguest outlines of the original oolitic-grain population.

Fossiliferous Facies

Because the limestones in the Arbuckle Group are very well indurated, fossils are rarely obvious in the field. Whole fossils are not abundant; fragments are the more common occurrence.

All of the formations contain some fossils, but the Signal Mountain, lower McKenzie Hill, and Kindblade Formations are the most fossiliferous (Chase and others, 1956; Stitt, 1977,1983; Toomey and Nitecki, 1979; Ethington and others, 1987). Gastropods appear to be the most common fossil; fragments of trilobites, brachiopods, echinoids, sponges, spicules, cephalopods, and conodonts are frequently seen in thin section. The fossil fragments are found in lithotypes that range from grainstones to mudstones. Ooids, peloids, and intraclasts are frequently intermixed with the fragments.

Algal Boundstones

Algal boundstones are the most dominant preserved biotic features in the group, occurring in all of the formations except the Signal Mountain (Donovan and Ragland, 1986; Ragland and Donovan, 1986; Donovan and others,

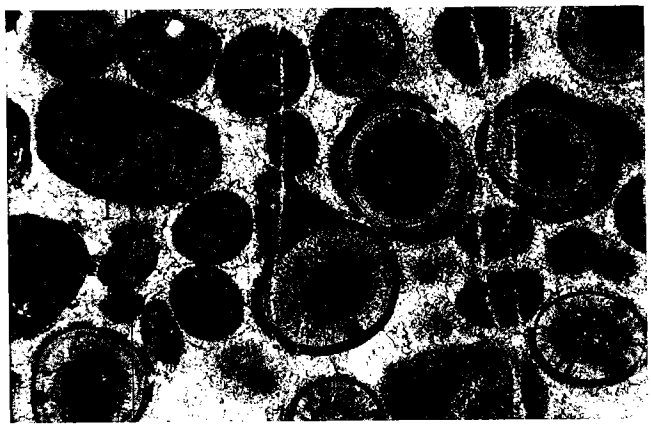


Figure 12. Cerebroid ooid with wavy cortical edge (now part of a grapestone texture) may be the result of endolithic boring (dark patches on outer cortices). Ordinary light; field of view is 2 mm high. Cool Creek Formation, Slick Hills.

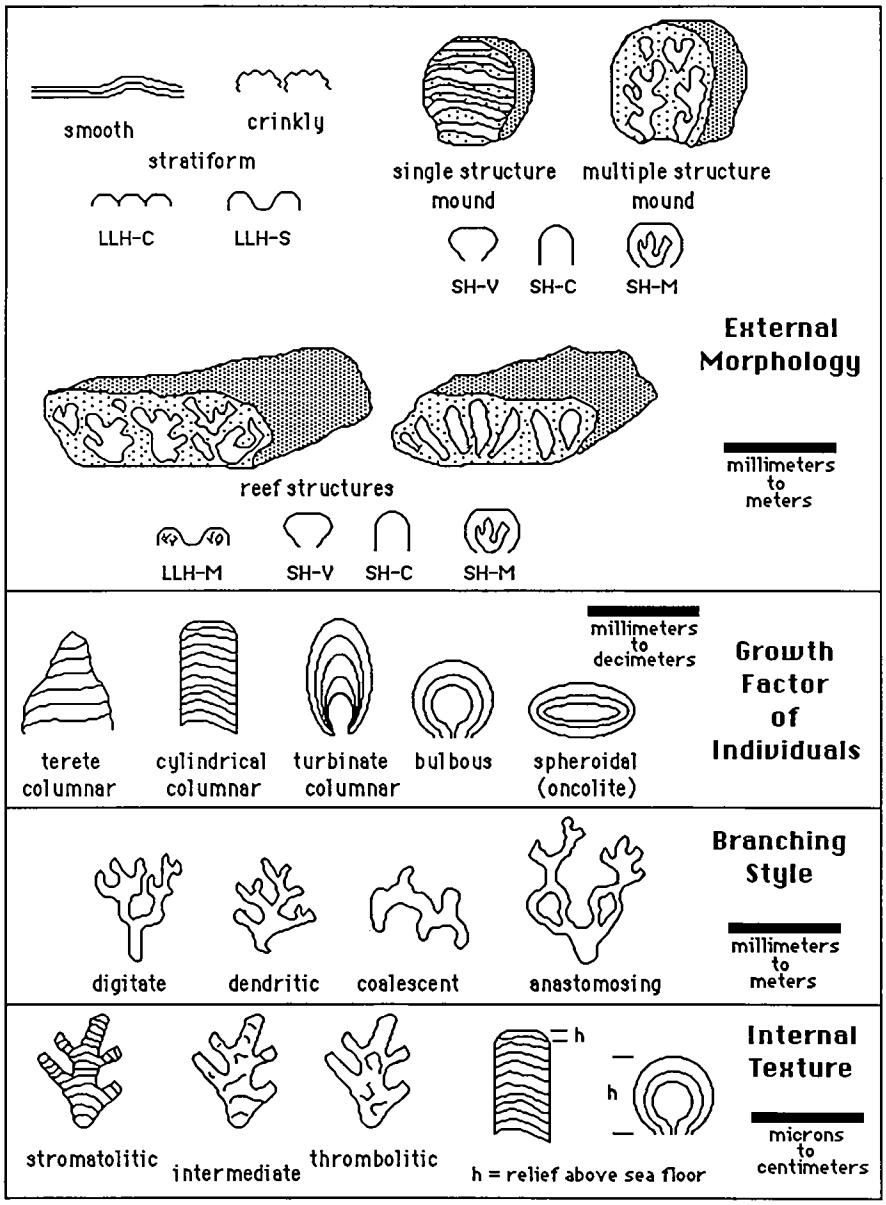


Figure 13. Morphologies and textures of algal boundstones found in the Arbuckle Group. Terminology and diagrams modified from Logan and others (1964), Aitken (1967), and Hofmann (1969).

1988). In this study we utilize a classification developed from the work of Nelson and others (1962), Dunham (1962,1970), Logan and others (1964), Aitken (1967), and Hofmann (1969,1973) (Fig. 13).

In the field, Arbuckle Group boundstones can usually be identified as encrusting, stratiform, or mound/reef structures. Assuming that all algal growths began as an initial patch of encrusting algae, the encrustations remained stratiform, grew at variable vertical and horizontal rates to form branches, or completely encased a fragment of the existing sediment to form a oncolite. Continued expansion of encrusting algae led to horizontally extensive but vertically limited buildups.

The cross profile of encrusting and stratiform boundstones is usually smoothly laminated; crinkly laminae characterized by small undulations superimposed on the larger undulations of stratiform algae are occasionally found. Mud cracks are often associated with the stratiform morphology. In addition, rare evaporite casts and/or salt pseudomorphs are seen in cases where the boundstone has been silicified.

Encrustations that had greater vertical than horizontal growth resulted in elongated individuals or groups of smaller elongated individuals. In the field, these vertically accentuated boundstones are seen as mounds or reefs. Individual mounds are composed of either single structures or colonies of smaller individuals of branching structures.

Colonies of large or small individuals can form reefs; i.e., aerially extensive buildups (Dunham, 1970) (Fig. 14). The internal components of such reefs in the group are the same as those seen in mounds, but the growth unit extends laterally over great distances until the reef eventually terminates against some other lithology. The terms



Figure 14. Algal mounds composed of cylindrical-columnar to slightly turbinate-columnar individuals. Some individuals are dendritically branched. Mounds coalesce laterally to form reefs; internal texture is intermediate between stromatolite and thrombolite. The mound-reef unit in the middle is ~0.3 m thick. Cool Creek Formation, Slick Hills.



Figure 15. Quartz detritus in the three uppermost formations occurs as discrete beds or as grains dispersed in carbonate facies. This unusually thick example is composed of cross-bedded sands with abundant micritic matrix. White bar on Jacob's staff is 0.3 m long. Kindblade Formation, Slick Hills.

bioherm and miniherm can be used with reference to Arbuckle boundstones (Toomey and Nitecki, 1979). Bioherms are multistoried boundstones that are 2 m or more in height, whereas miniherms are smaller equivalents. Sizes among the various morphologies range from microscopic to several meters in height, and from microscopic to several tens of meters in lateral extent.

Internal textures of boundstones grade from finely laminated stromatolitic to the disorganized thrombolitic texture (terminology from Aitken, 1967). Poorly to vaguely laminated textures comprise intermediate gradational textures.

In addition to the algae that are now preserved as the various types of boundstone, more definitive algal textures may be encountered in thin section. These include *Girvanella*, *Renalcis*, and *Calathium* (Toomey and Ham, 1967; Toomey and Nitecki, 1979). *Pulchrilamina*, *Renalcis*, and *Epiphyton* are some of the problematical organisms found in the group that may have blue-green algal affiliations.

Detrital Quartz Facies

Within the Arbuckle Group, detrital quartz has a somewhat erratic distribution (Donovan and Ragland, 1986). It is found in small amounts in the Fort Sill Formation and near the base of the Signal Mountain Formation. Quartz detritus is absent from much of the upper Signal Mountain and the McKenzie Hill Formations, but appears in small amounts toward the top of the latter. The Cool Creek Formation is characterized by a very prominent and visually distinctive development of quartz-rich sands (Ragland and Donovan, 1991). The overlying Kindblade, although containing several such sands, is rather quartz-poor in comparison with either the Cool Creek or the overlying West Spring Creek Formation. The uppermost formation contains perhaps the largest accumulation of detrital quartz sand.

While dispersed grains can be encountered within most of the various facies described above, detrital quartz is most often found in heterolithic units as much as 4 m thick, in which individual beds can be as thick as 1 m (Fig. 15). Grains associated with the quartz include intraformational clasts, recycled chert nodules, ooids, fossil fragments, peloids, and small amounts of feldspar and rock fragments.

Parallel laminae, cross laminae, and cross bedding are the sedimentary structures most commonly associated with the quartz sands. Rarely, ripple marks and climbing ripples are encountered. Quartz detritus is a common infill of mud cracks.

Quartz grains range in size from silt to granule, are angular to well rounded, and are slightly elongate to spheroidal in shape. Some grains contain boehm lamellae, vacuoles, and microfractures; however, most quartz grains are monocrystalline with simple straightforward extinction.

Intraformational Conglomerates

Intraclasts as much as 15 cm long are a very common grain type throughout the entire Arbuckle Group (Ragland and Donovan, 1985b) (Fig. 16). The clasts are usually composed of varieties of lime mud, but almost any of the sediments deposited in the carbonate environment were subject to recycling. The clasts form distinct beds ranging in thickness as much as 60 cm, or comprise a significant portion of the detritus filling the interareas between algal boundstones.

The intraclasts are elongate disc- and blade-shaped lime-mud pebbles and cobbles, often mixed with other detritus such as quartz grains, ooids, algal fragments, and fossil fragments. The clasts are usually found in a matrix of lime mud with accompanying detritus; occasionally, pebbles formed an open framework subsequently filled with cement. Variable packing arrangements (random, imbricate, edgewise, or horizontal) represent settling effects associated with the environmental processes which took place in the aulacogen (Ragland and Donovan, 1985b,1986, table 3).

Shinn and others (1969) and Shinn (1983) found that most intraclasts in the Bahamas originated in the dried, partially cemented, supratidal zone and were subsequently redeposited in channels or on the tidal flat. The

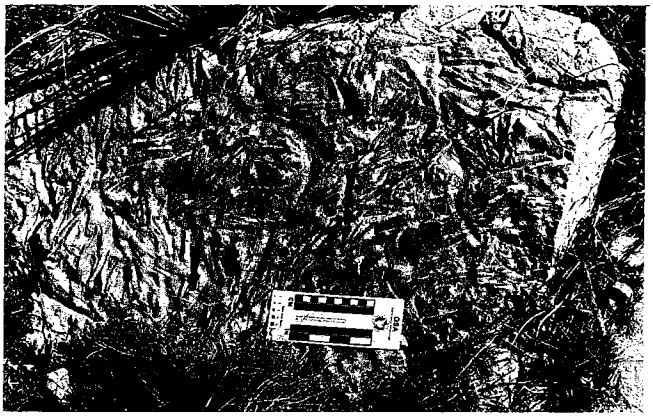


Figure 16. Intraformational conglomerates are very abundant throughout the Arbuckle Group. This view of the top of a bedded intraformational conglomerate shows clasts randomly oriented with respect to the movement of waters during the time of deposition. Cool Creek Formation, Slick Hills.

limited number of true supratidal facies in the Arbuckle Group, as well as the abundance of clasts in discrete beds and as admixtures, indicates origins other than strictly supratidal. Clasts composed of grains such as ooids or peloids suggest that the clasts can be derived from *in situ* sediments ranging from the supratidal zone to the subtidal zone (Whisonant, 1987) (Fig. 17). Minor storms, tides, channeling, and wave action probably accounted for formation of the majority of the clasts. Transgressions, regressions, and major storms may have been responsible for areally extensive intraformational conglomerate beds (Ragland and Donovan, 1986).

Intraformational Breccias

Intraformational breccias are not common in the group and are confined mostly to the Cool Creek Formation. Those existing units usually form lenses that range from 15 cm to 1 m thick. The breccias usually grade laterally into laminated micrites (Fig. 18).

Breccia clasts are angular to subangular micrite pebbles, cobbles, and boulders set in micritic matrices. Fragment sizes range from <2 cm to blocks as large as 40 cm (Ragland and Donovan, 1985b; Ragland, 1990).

Dissolution of pods of evaporites growing penecontemporaneously within the lime mud probably account for the generation of the breccias. Flushing of the evaporites led to collapse of overlying sediments, resulting in the agglomeration of large, angular blocks (Fig. 18).

Bedded Chert Facies

The bedded chert facies occurs rarely in the group; in fact only two such units have been identified. Both units, one in the Cool Creek, the other in the Kindblade, consist of interlaminated micrite and microquartz units 15–25 cm thick (Ragland and Donovan, 1991) (Fig. 19). The laminae range from 1 to 20 mm thick. Micrite laminae are usually thinner, medium gray in color, and of uniform texture, whereas silica laminae are usually slightly thicker and dark gray in color with a lighter colored rind (orange on a weathered surface). This facies has recently been interpreted as a primary deposit forming in restrictive lagoons subject to variations (probably annual) in alkalinity (Ragland and Donovan, 1991).

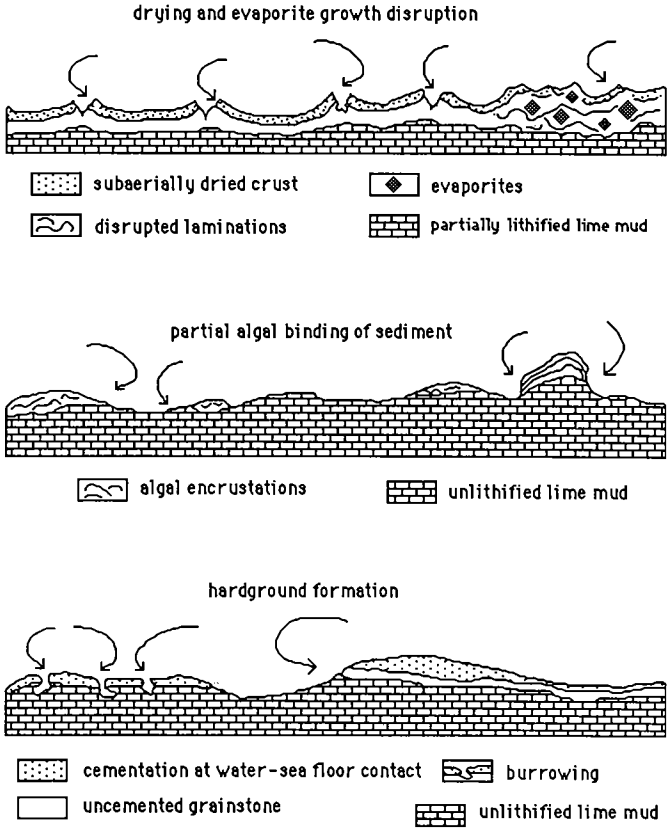


Figure 17. Diagram illustrating possible methods of intraclast formation in Arbuckle Group sediments.

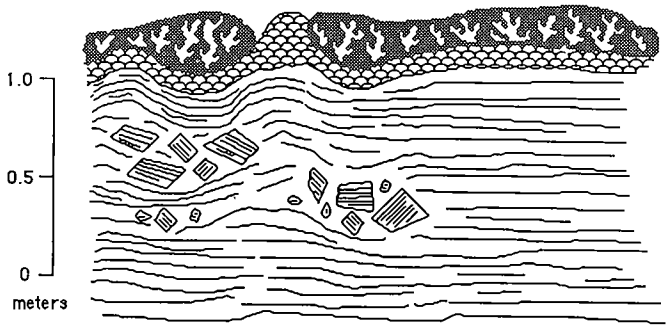


Figure 18. Collapse breccia in the Cool Creek Formation, Slick Hills. Large blocks of brecciated laminated micrite rest in swales of disrupted laminated micrite. The swales may have originated from the dissolution of pods of evaporites. Overlying algae have foundered into the underlying micrite; some algae have been squeezed between the mounds above. The disrupted unit is discontinuous laterally. Horizontal scale equals vertical scale.

Evaporite Facies

Only traces and pseudomorphs of evaporite minerals are preserved in the surface exposures of the Arbuckle Group (Ragland, 1984; Cloyd and others, 1986). Traces of

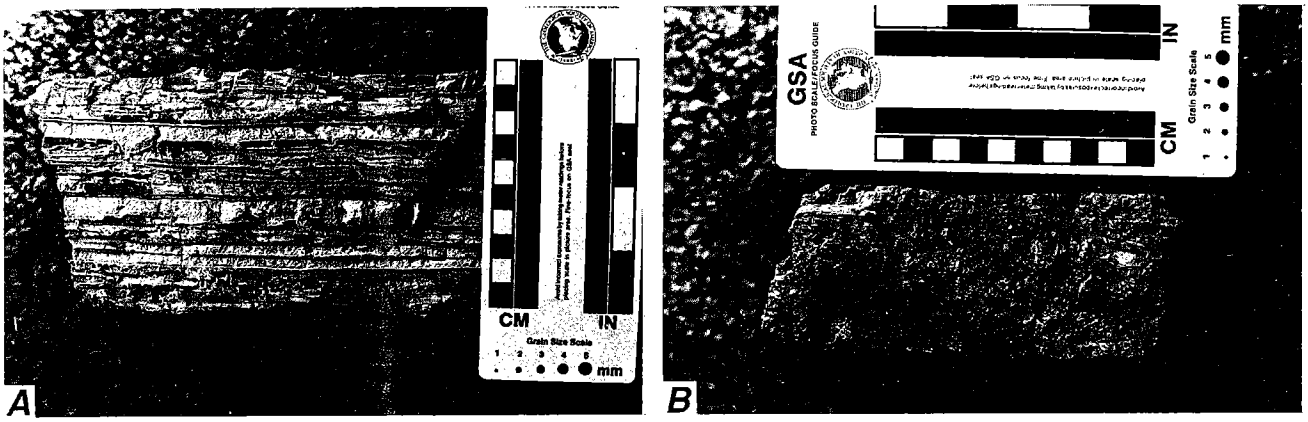


Figure 19. Bedded chert in the Kindblade Formation, Slick Hills. *A*—Light-colored laminae are calcimicrite and dolomicrite; dark laminae are chert. *B*—Top of the uppermost chert lamina in the sample seen in *A*. Molds in the chert layer may be after evaporites.

anhydrite and celestite within replacement silica have been identified with the aid of SEM and EDAX analysis. Molds and pseudomorphs are widely developed in the Cool Creek and West Spring Creek Formations. The most common pseudomorphing minerals are calcite, dolomite, and silica; shapes of the pseudomorphs suggest precursors of anhydrite and gypsum. "Cauliflower" nodules (terminology from Chowns and Elkins, 1974) containing shapes suggestive of evaporite minerals are often associated with penecontemporaneous dolomite strata (sabkha facies).

OVERVIEW OF THE CAMBRO–ORDOVICIAN DEPOSITIONAL ENVIRONMENT IN THE SOUTHERN OKLAHOMA AULACOGEN

Delineation of the Cambro–Ordovician depositional environments in the aulacogen can be refined by comparative study of the preserved sediments to modern settings. Isotope data from 24 samples from the McKenzie Hill, Cool Creek, and Kindblade Formations suggest that the sediments were deposited in hot conditions (Fig. 20). Although the $^{13/12}C$ is a relatively reliable indicator, the $^{18/16}O$, the indicator on which the paleotemperature is based, is subject to alteration with diagenesis (Hudson, 1977; Anderson and Arthur, 1983). However, even if the $\delta^{18}O$ has been depleted by as much as 75%, the data points would still lie within a temperature range of 20–30°C. If any reliability can be attached to the temperature scale, the sediments from the three formations were deposited in water temperatures that were in excess of 20°C.

On a regional scale, the physiography of the floor of the epicontinental sea was flat (Wilson, 1970,1974; Tucker, 1985). On a local scale, as in the aulacogen, the sea floor undulated gently in response to minor topographic differences and differential accumulation of concurrently existing facies. Slope sediments and slump structures are not found over large areas; occasional minor slump features are found associated with algal mounds or intraformational breccias.

Bathymetric conditions and sea-floor physiography varied among and within formations (Fig. 21). Normal-marine invertebrates dominated when deeper water (20 m deep, or more?) filled the aulacogen (e.g., the time of deposition of McKenzie Hill sediments). Hardgrounds attest to slow sedimentation rates (e.g., parts of the McKenzie Hill and Kindblade Formations). Lowstands are recorded in complex interweaving of facies such as algal boundstones, oolites, quartz-sandy facies, and evaporites (e.g., the Cool Creek Formation).

The local paleo-depositional environments in which specific algal morphologies were formed are very difficult to decipher, but some generalizations can be made. Various modern classifications and their applications to ancient settings are related to specific micro-environments, many of which result in conflicting interpretations. Whereas all of these classifications are legitimate, it is clear that comparison to one modern setting or one ancient interpretation is not adequate.

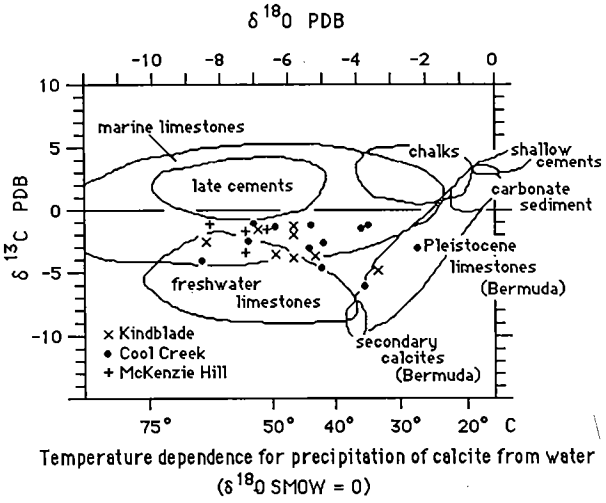


Figure 20. Isotope crossplot of 24 samples from the McKenzie Hill, Cool Creek, and Kindblade Formations plotted against Hudson's (1977) environments-of-precipitation fields. Modified from Hudson (1977) and Leeder (1982). Data kindly processed by R. E. Denison, Mobil Research.

Because the algae were located in an aulacogen within the body of a continent, the areal extent of the upper Arbuckle buildups was far greater than any modern setting. A somewhat evaporitic environment probably resulted in higher than normal salinities in the sea waters during the most active growth of the algae. These higher salinities probably extended at least into the upper subtidal zone, which resulted in exclusion of competing invertebrates and in widespread algal growth from the upper subtidal to the supratidal zones.

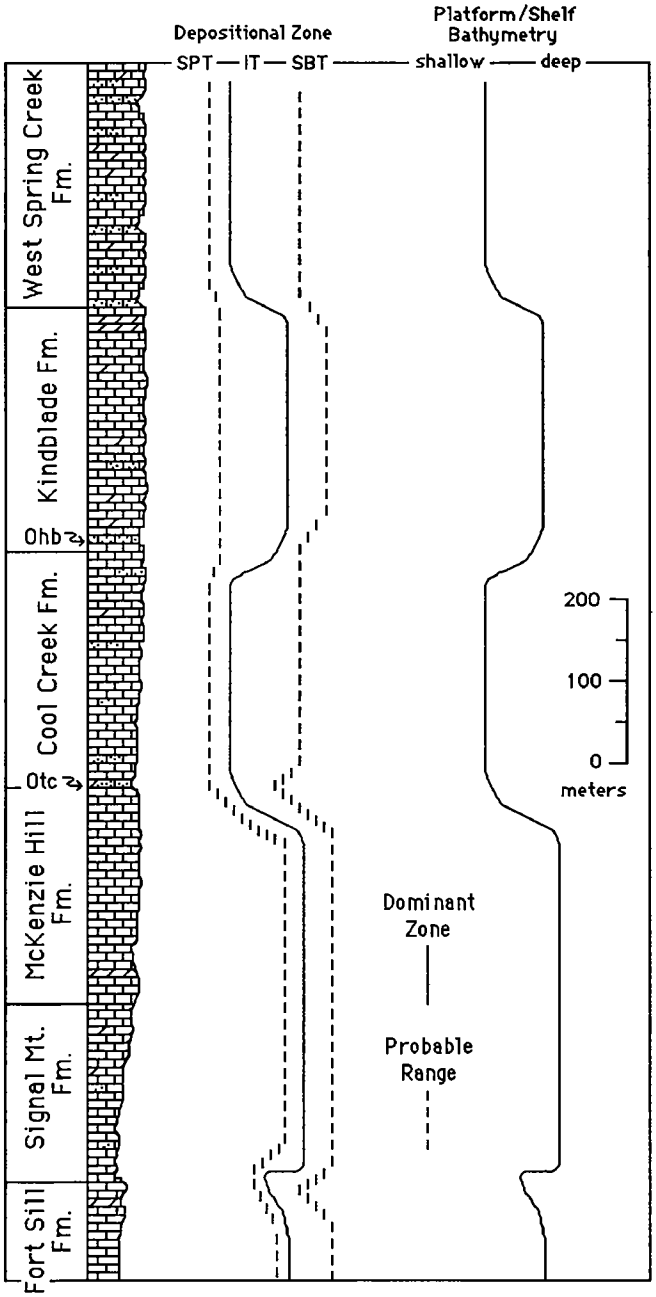


Figure 21. Generalized depositional environments for the Arbuckle Group based on facies analysis from field exposures. Large kicks in the general bathymetry curve near formation boundaries may reflect eustatic sea-level changes. SPT—supratidal zone; IT—intertidal zone; SBT—subtidal zone; Otc—Thatcher Creek Member (sandstone); Ohb—Herringbone sand.

TABLE 1. — ALGAL MORPHOLOGIES OF THE ARBUCKLE GROUP AND THEIR RELATION TO POSSIBLE DEPOSITIONAL ENVIRONMENTS

Zone	Algal structures	Associated structures and lithotypes
Supratidal	stratiform smooth LLH-C LLH-S crinkly	carbonates; mud cracks, clasts, evaporite casts and molds, minor quartz sand and silt, minor peloids and ooids from washover
Intertidal	all external morphologies all growth factors all branching styles all internal textures	carbonates; mud cracks, clasts, quartz sand and silt, fossils, peloids, ooids minor evaporite molds and casts
Subtidal	all external morphologies all growth factors all branching styles all internal textures	carbonates; clasts, quartz sand and silt, fossils, ooids, peloids

Associated sedimentary structures sometimes can be used to roughly estimate the zone in which algal buildups originated. The structures must be closely associated with the buildups (i.e., incorporated within) to be useful for interpretation. Unless specific structures can be found on the algal buildup, zonation is tentative at best. In the Arbuckle Group, most thicker stratiform laminates are associated with mud cracks or evaporites. Very thin encrustations (0.5–2.0 mm "mats" of Gebelein, 1969) are often not distinguishable in the rock record. The influence of algae in the group may be far greater than can ever be determined. As an example, thick-bedded micrites may have resulted in part from algal binding, but that influence was not preserved.

Because of the ambiguity of the zonations, the algal structures cannot be used to analyze cyclicity within formations. Different types of algae can inhabit the same bathymetric zone, and different facies can laterally interweave. For example, oolitic shoals may have resided in turbulent subtidal zones, thrombolites in less turbulent subtidal zones without regular sediment input, and stromatolites in subtidal zones with periodic sediment influx. At one horizon on Bally Mountain in the Slick Hills, stromatolitic miniherms alternate with quartz-sandy micrite and reefs of thrombolitic and intermediate-textured individuals over a lateral exposure of 160 m. These units obviously existed at the same time. As a consequence, vertical facies changes may not always reflect regional shallowing upward or deepening upward sequences, but local lateral facies migrations. Table 1 contains a summary of algal morphologies and the local environments in which they may have occurred.

The most definitive statements that can be made about the Cambrian–Ordovician environment in the aulacogen, based on comparison with modern environments, are:

1) Based on abundant algal boundstones in much of the group, and the large accumulation of carbonates in general, the paleoclimate was warm (e.g., one of the larg-

est modern algal accumulations is in Shark Bay, Australia [Logan, 1961]);

2) The water depth probably did not exceed 10–15 m when large algal buildups were present (based on diminution of sunlight intensity below 10 m [Blatt, 1982]), but may have exceeded 100 m in depth during high stands;

3) Currents may have varied from <100 cm/sec, and often <25 cm/sec, during algal accumulations (based on Scoffin's [1970] study of algae, offshore Bahamas), but may have been higher in deeper water, or when algae were not abundant;

4) Some physical or chemical factor, such as salinity, prevented the proliferation of normal-marine biota during periods of abundant algal growth (e.g., the largest Shark Bay buildups are in the hypersaline areas [Logan, 1961]), whereas normal salinities probably prevailed during highstands;

5) Tidal range may have been ~50 cm during times that algae proliferated (maximum height of the Arbuckle buildups is <50 cm [Ragland, 1990]);

6) Vast expanses of water, often shallow, plus the geographic location and warm climate, probably resulted in numerous storms yielding the abundance of intraformational clasts and redistribution of sediments (Ragland, 1990); and

7) The climate was hot and dry enough at times to allow the formation of small amounts of evaporites.

CYCLES VERSUS SEQUENCES

Repetition of the limited number of lithologies in the group is apparent. These lithologies do not, however, necessarily represent cyclicity in the context of innumerable eustatic sea-level changes. As was demonstrated by Pratt and James (1986) for the lower Ordovician St. George Group of western Newfoundland, "lithotype sequences" were formed by prograding and laterally migrating islands.

An ideal shallowing upward sequence, attributed to a transgressive event followed by prograding sediments, begins with a thin "high-energy deposit" (e.g., sands, intraclasts) (Wilson, 1975; James, 1984). This is overlain by subtidal, intertidal, and supratidal sediments. Most of the "high-energy deposits" in the Arbuckle Group can be attributed to storm processes rather than repeated transgressions and regressions. Following storms, less-energetic marine processes resumed. This may have resulted in similar or differing types of deposits at a given site. For example, if an island were destroyed during a particularly violent storm, the site may subsequently have fallen into the intertidal zone. The "basal" intraformational conglomerate may then have been overlain by lime muds, algal boundstones, or other intertidal facies. The repeated sequences noted in the group (Ragland and Donovan, 1985b) need not be attributed to constantly changing eustatic conditions.

Transgressions and regressions may have occurred on a larger scale, i.e., between formations, and perhaps at some levels within the formations (Fig. 21). For example, a regression is likely to have occurred at the transition zone between the McKenzie Hill and Cool Creek Formations. As a result, the carbonates began prograding, and this resulted in the shallow-water sediments of the upper McKenzie Hill and much of the Cool Creek. By the time of deposition of the upper Cool Creek, the aulacogen was subsiding more rapidly (or global sea level was rising), resulting in the slightly deeper-water facies at the transition zone between the Cool Creek and Kindblade Formations.

Within the formations, minor transgressions and regressions may have occurred, especially at those levels where abundant quartz sand was introduced. The carbonate sequences with apparent "basal" intraformational conglomerates, however, probably reflect the normal-marine processes of laterally migrating facies interrupted by storms. As was stated by Pratt and James (1986), "external forces of eustatic sea-level fluctuation or sporadic subsidence need not be invoked for causing most small-scale carbonate 'cycles'."

DIAGENETIC FEATURES IN THE ARBUCKLE OUTCROPS

Diagenesis in Arbuckle Group sediments is characterized by the same patterns as the sedimentology: horizontal and vertical variability. Although a limited number of diagenetic processes and products occur, complexities arise from the intertwining and repetition of the events in time.

The three most abundant diagenetic products are calcite, dolomite, and silica; each occurs as cement and replacement products. Pyrite (altered to hematite and limonite) is a minor replacement. The physical processes of compaction and tectonism combined with the chemical processes of dissolution, precipitation, and replacement left important imprints on the currently exposed rocks.

Cements

Calcium Carbonate

Calcium carbonate cements occur most commonly as isopachous rims or pore-filling crystals, sometimes arranged in a drusy texture; most are nonferroan (Figs. 11,22). Based on petrographic evidence, the majority of the cement appears to have been originally calcitic rather than aragonitic. Isopachous rims on grains are usually small, blocky crystals that often grade into large, pore-filling crystals.

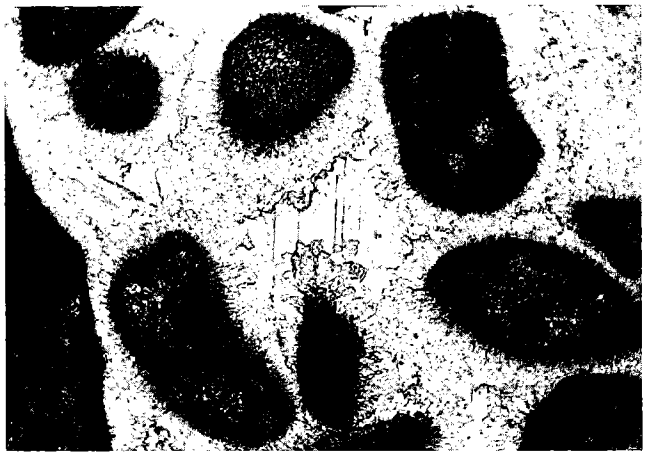


Figure 22. Intrasparite cemented by two stages of sparry calcite cement. The first is an isopachous rim, the second is drusy. Ordinary light; field of view is 2 mm. Kindblade Formation, Slick Hills.

The timing of calcite cementation is variable. In some cases, cemented grains may be widely dispersed, often as a result of thick, early isopachous rims. Most calcite cementation seems to postdate a considerable amount of grain-to-grain compaction, suggesting that for considerable periods of time, grain populations existed in contact with undersaturated floor waters.

Dolomite

Dolomite cements occur mainly in the later stages of diagenesis, filling or lining fractures and vugs (Fig. 23). Euhedral idiotopic-C crystals and baroque dolomite (xenotopic-C) (terminology from Gregg and Sibley, 1984) occur as the final rim or infill of vugs. Most dolomite cements are nonferroan, although some late vein-filling varieties are iron rich.

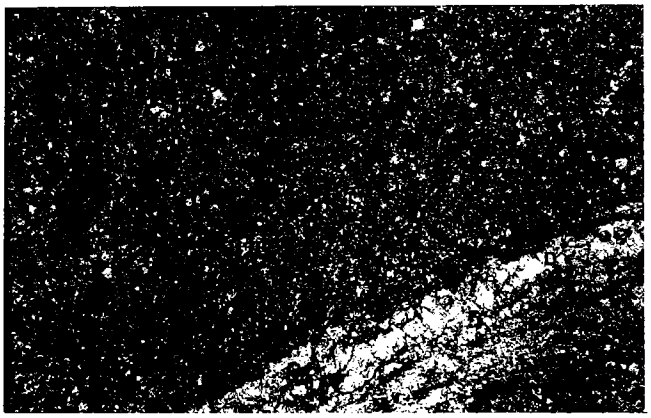


Figure 23. Penecontemporaneous (sabkha) dolomicrite containing a few scattered dolomite rhombs. The fracture (lower right) is filled with dolospar and baroque dolospar (D, white) which has been partially replaced with calcite (dedolomite) (C, gray, below dolospar). Small patches of the dolomicrite and some rhombs have also been dedolomitized. Ordinary light; field of view is 2 mm high. Kindblade Formation, Slick Hills.



Figure 24. Fibrous chalcedony of the zebraic variety filling in porosity after an initial dolomite cement. Crossed polars; field of view is 500 μ high. McKenzie Hill Formation, Slick Hills.

Silica

Silica cements occur in four basic forms: equicrystalline microquartz, equicrystalline megaquartz, fibrous quartz, and syntaxial overgrowths (Figs. 11,24). Syntaxial quartz overgrowths are the most common form. Equicrystalline megaquartz and fibrous quartz occur as minor cements and are often associated with replacement silica. Fibrous quartz occurs in length-slow, length-fast, lutecite, zebraic, and flamboyant varieties.

Replacement Products

Calcite

Calcite replacement of other mineralogies is not common in the Arbuckle Group, but minor amounts do preserve some textures. In some cases, when silica was not available, calcite replaced evaporites in sabkha facies. In rare instances, calcification (dedolomitization) that probably occurred during uplift of the sediments resulted in the preservation of dolomite textures (Fig. 23).

Dolomite

Dolomite may replace any of the facies in varying degrees. Thus, idiotopic-P dolomite is found throughout the group as isolated euhedral crystals partially replacing calcite. Idiotopic-E, -S, and xenotopic-A occur in patches which sometimes coalesce to form "leopard skin" mottling (Donovan and others, 1986) (Fig. 8).

Stratigraphic dolomicrite is found as a penecontemporaneous or very early diagenetic facies, probably the result of dorag-type dolomitization (Badiozamani, 1973) and evaporative dolomitization (Tucker, 1981; Longman, 1982), although modification of these dolomites is thought to have occurred during burial (Gao and Land, 1991) (Fig. 23). The light-brown to buff-weathered color distinguishes the facies from calcimicrites. Traces of evaporite minerals are often found associated with the dolomicrites.

Silica

Silica is an important replacement product from the mid-McKenzie Hill Formation upwards (Fig. 25). The silica often preserves textures originally present in the carbonates, replacing the host material on a one-to-one basis with equicrystalline microquartz (Figs. 11,26). Fibrous, pseudofibrous, and flamboyant quartz sometimes partially replace host sediments, especially those associated with evaporites. In rare cases, syntaxial quartz overgrowths grew beyond the boundaries of the pore spaces until the surrounding matrix, cement, and grains were partially replaced (Ragland and Matthews, 1991) (Figs. 11,24).

Distribution of chert in the Arbuckle Group.—As noted previously, chert occurs in a variety of forms in the Arbuckle Group (Fig. 25). However, the distribution of such chert requires comment. Minor amounts of chert are associated with the Fort Sill Formation, particularly the lowermost member. This chert consists of small nodules and burrow fills.

Throughout much of the Signal Mountain Formation, chert is rarely encountered and, as noted, its absence is one of the criteria for distinguishing the lower one-third of the McKenzie Hill Formation. Above this horizon, chert is common. In the upper part of the McKenzie Hill For-

CHERT TYPES	MICROSCOPIC TEXTURES
A. PRECIPITATIVE	MICROQUARTZ
1. BEDDED	FIBROUS CHALCEDONY a. length fast b. length slow c. lutecite
2. CEMENT a. intergranular b. intragranular	MEGAQUARTZ a. drusy b. flamboyant
B. REPLACIVE	
1. NODULAR, AFTER LIMESTONE	DESCRIPTIVE ADJECTIVES
2. NODULAR, AFTER EVAPORITES	1. BURROW-FILLING 2. CAULIFLOWER 3. VOID-FILLING 4. OOLITIC 5. OVATE NODULAR 6. LAMINATED

Figure 25. Types of chert seen in the Arbuckle Group, especially from the McKenzie Hill upwards.

mation, chert is seen as burrow fills, as irregular nodules, and, in some cases, as a crack-filling deposit (Fig. 10).

The Cool Creek Formation is noteworthy for the variety of its chert morphologies (Figs. 11,26B). Chert nodules range in size from a few millimeters to >30 cm in diameter. Nodules often coalesce to form bedding-parallel pseudolayers.

Chert is still common in the Kindblade Formation, although occurring less frequently than in the underlying formation. Chert abundance increases in the West Spring Creek Formation, in many respects mimicking many of the features seen in the Cool Creek.

Origin of the secondary silica.—Conventionally, chert deposits in shallow-water carbonates have been attributed to remobilization of siliceous sponge debris. Sponges are occasionally found in the Arbuckle Group, particularly in the McKenzie Hill and Kindblade Formations. However, they are very rare in the Cool Creek, the most chert-rich formation in the group. While it is possible that some of the secondary silica originated from the dissolution of sponge spicules, another source must be evoked to account for the immense amount of secondary silica that is seen in the Cool Creek Formation.

An approximate correspondence exists between the occurrence of detrital quartz and secondary silica in the Arbuckle Group. In addition, many quartz grains in thin section have corroded and embayed margins. It seems clear, therefore, that diagenetic conditions were often suitable for the mobilization of secondary silica from detrital quartz grains (Ragland and Donovan, 1991) (Fig. 27).

Uniformitarian analogy suggests that alkalinity of restricted carbonate platforms may, on a daily basis, achieve values of 9 or more. Epstein and Friedman (1982) demonstrated that maximum pH values reached 9.95 in modern carbonate reefs. When such elevated alkalinities occur, silica is readily dissolved. We suggest that when populations of quartz grains in the Arbuckle Group were subjected to these high alkalinities, the grains partially or completely dissolved. Small grains, because of their relatively greater surface area, would have preferentially dissolved, migrating in alkaline, near-surface ground waters of the platform. Upon encountering more acidic waters, the silica precipitated. This mechanism satisfactorily accounts for the commonly observed occurrence of chert in the center of algal-boundstone colonies (Fig. 26). Presumably, the centers of such boundstones were areas where slightly more acidic conditions developed due to decay of the algae.

A second mechanism of chert formation, a slight modification of Knauth and Epstein's (1976) mixing-zone model, may have resulted from the mixing of marginal-marine waters with meteoric waters, either at the edge of the craton or around islands that were emerging during low-stand conditions (Fig. 28). Large storms or packages of smaller storms may have produced sufficient amounts of rain to percolate into the sediments, freshening the ground water enough to initiate silica precipitation (Rag-

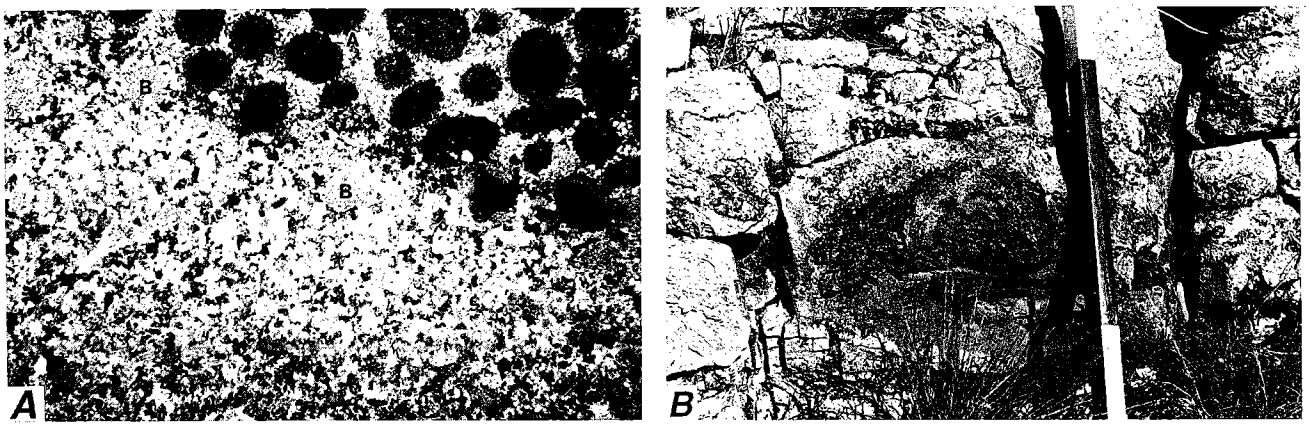


Figure 26. *A*—Silicification front in an oosparite. The silicified ooids are very clearly seen (A), but the calcareous oosparite has been almost completely neomorphosed so that only vague ghosts of the original ooids can be seen (B). Ordinary light; field of view is 9 mm wide. Kindblade Formation, Arbuckle Mountains. *B*—Partially silicified core of an algal mound. Dark bar is 0.3 m long; Cool Creek Formation, Slick Hills.

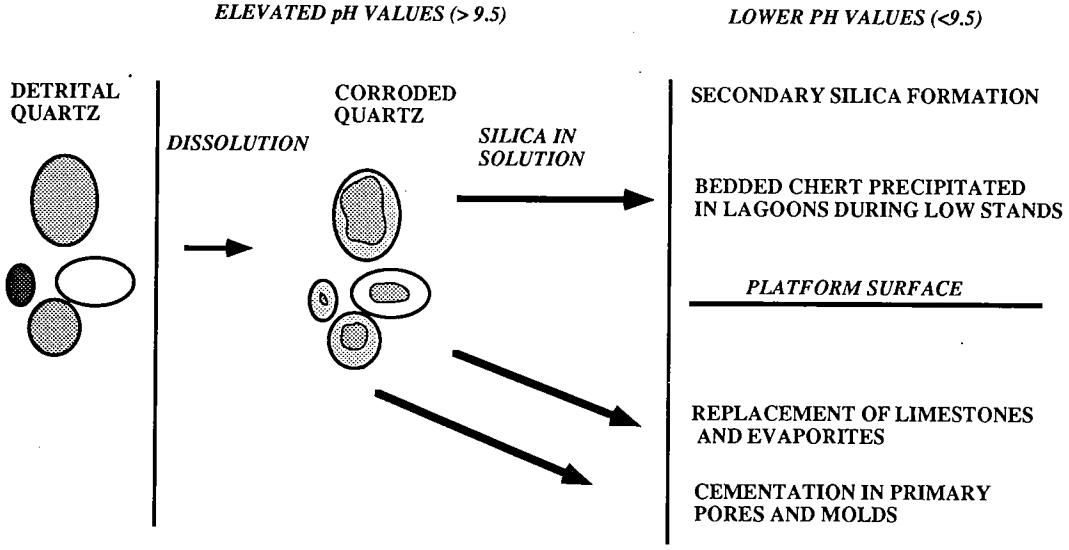


Figure 27. Method by which secondary silica is derived in most of the Arbuckle Group. In the general absence of siliceous sponge spicules, quartz sand and silt provide the source for secondary silica.

land and Donovan, 1991). A mechanism of this sort is attractive in that it accounts for great lateral continuity of many chert horizons (we have traced some for several miles) and explains those examples of stratification where there is no obvious nucleation point, e.g., the center of a stromatolite.

SUMMARY AND CONCLUSIONS

The Late Cambrian–Early Ordovician Arbuckle Group of southern and southwestern Oklahoma is composed of 2,200 m of carbonate sediments. Six formations comprise the group: the Fort Sill, Signal Mountain, McKenzie Hill, Cool Creek, Kindblade, and West Spring Creek Formations. In the field, the formations often weather into characteristic slab-like morphologies known locally as "tombstone topography."

The six formations of the group are composed of multi-textural carbonates. The most important facies include:

1. Micrite: The micritic facies is the most abundant lithotype, comprising massive, featureless beds to thinly laminated, texturally complex units. Close association with algae appears to have been an important factor in abundant micrite production in many cases.

2. Dolomicrite: Dolomicrites were often formed penecontemporaneously on supratidal flats. Recrystallization of intermixed carbonate grains by the early dolomites and later dolomites obscures many textural features. Quartz silts and sands occasionally delineate laminae; "cauliflower" chert nodules link the dolomicrites to subaerial evaporative conditions. Formation of the dolomites probably resulted from a combination of evaporation on the supratidal flats and ground-water mixing.

3. Peloidal facies: Peloids are a very common admixture throughout the formations, but are very difficult to see in field exposures. Many peloids may have originated as faecal pellets or as small intraclasts.

4. Oolitic facies: Ooids comprise a significant portion of the limestones either as admixtures with other detritus or as the dominant grain in the facies. The grains are encased in textures ranging from oomicrites to oosparites, and often occur as cross-stratified laminae and beds.

5. Fossiliferous facies: Most fossiliferous units are comprised of fragments of brachiopods, gastropods, trilobites, sponge spicules, and conodonts. Fossils are most abundant in the Fort Sill, McKenzie Hill, and Kindblade Formations.

6. Algal facies: Algal boundstones are a dominant lithotype in the uppermost Fort Sill, and from the uppermost McKenzie Hill through all of the Cool Creek, much of the Kindblade, and the West Spring Creek. At their height, boundstones covered vast areas and greatly influenced the morphology of the aulacogen. Algal structures alone cannot be used to analyze cyclicity within formations. Different morphologies of algae interwove laterally and alternated with other facies in the same depositional zones.

Environmentally, the most prolific buildups represent times when the paleoclimate was warm, water depth probably did not exceed 10–15 m, the substrate during algal initiation was neither mobile nor firmly cemented, current velocity was probably often <25 cm/sec, and abnormally high saline concentrations probably restricted normal-marine biota.

7. Quartz-sandy facies: Quartz sand is variable in its distribution in the group. Quartz is rarely found in the three lower formations but becomes an important admixture in the upper three. The grains are usually found dispersed in carbonate facies with admixtures of allochems. Discrete units of cross- and parallel-stratified quartz are more common in the Cool Creek and West Spring Creek Formations.

8. Intraformational conglomerates and intraformational breccias: All sediments deposited in the carbonate environments were subject to recycling and deposition as intraformational clasts. Clasts range in size from microscopic to >10 cm in length. Clast composition is diverse, ranging from pure micrite to multi-lithologic. Storms were probably the most important process in the redistri-

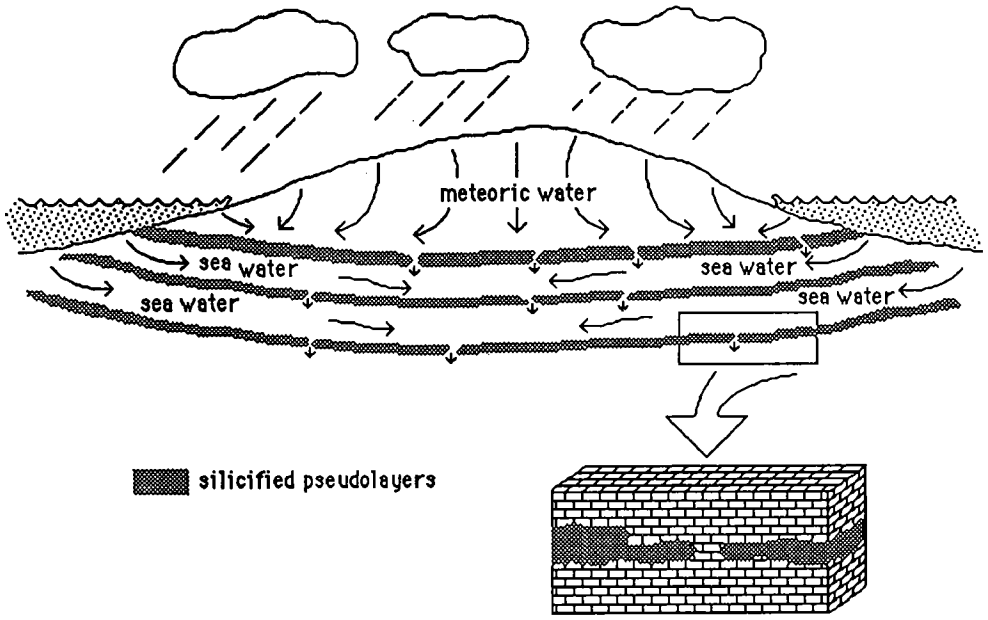


Figure 28. Hypothetical mixing of sea water and meteoric water within an island as a method of chert-nodule and pseudolayer formation. Pseudolayers of coalescing nodules may represent seasonal variations in rainfall or accumulations of silica over long periods. Modified from Knauth (1979).

bution of clasts, but normal events such as tides and channeling, and more infrequent events such as transgressions or regressions, also contributed to the clast supply. Subaerial drying, evaporite growth, disruption of bedding and hardgrounds, and disintegration of algal buildups were the sources of clasts.

9. Intraformational breccias: Intraformational breccias are usually associated with evaporite dissolution and collapse features. Large, angular clasts collapsed into underlying micrites as evaporites were flushed from the system.

10. Bedded cherts: Bedded cherts are a rarely occurring, but environmentally significant facies in the upper part of the group. Microcrystalline chert alternates in thin laminae with microcrystalline carbonate. The cherts represent shallow depositional sites similar to those of the modern Coorong. The chert-carbonate couplets may represent seasonal fluctuations in algal bloom and decay, associated with seasonal changes.

11. Evaporite facies: Evaporites are preserved in the upper part of the Arbuckle Group, mostly as molds and pseudomorphs. Gypsum and anhydrite crystals and nodules were pseudomorphed mostly by silica, preserving the shapes of evaporites and occasionally trapping remnant evaporite traces. Rare hopper-shaped halite crystals within stromatolite laminae were preserved by abundant micrite inclusions and silica. When silica sources were not available, calcite and dolomite sometimes acted as pseudomorphing agents.

The Fort Sill Formation is composed of three informal units: a basal muddy, thin-bedded limestone; an interbedded lime-mud and siltstone unit; and an upper massive unit with abundant algal boundstones.

The Signal Mountain is a thin-bedded formation containing abundant detritus, but it forms the weakest topographic expression of the group. The Cambrian–Ordovician boundary is contained within the Signal Mountain Formation.

The McKenzie Hill is composed of massive beds of fossiliferous mudstones, wackestones, and packstones. Algal boundstones become more prominent near the top of the formation. A significant change from a chert-free lower one-third to a chert-rich upper two-thirds signals the inclusion of abundant secondary chert throughout the upper part of the group. Minor inclusions of quartz detritus occur near the top of the formation.

The base of the Cool Creek is marked by a significant incoming of quartz sand, which thereafter forms prominent percentages of the rest of the group. The Cool Creek Formation is dominated by algal boundstones, probably deposited in shallower waters compared to most of the lower three formations.

The Kindblade is characterized by more abundant "normal-marine" fossil assemblages and fewer algal boundstones than the Cool Creek Formation. Quartz detritus is not as prominent as in the underlying formation.

The West Spring Creek is similar to the Cool Creek in composition, containing more abundant quartz detritus, but also containing red beds.

Diagenesis in the group is characterized by vertical and horizontal variability. Interweaving and repetitive diagenetic events complicate our understanding of the paragenesis. The most important diagenetic cements and replacement products are calcite, dolomite, and silica. All cements and replacements began very early in the diagenetic history, often penecontemporaneously with sedimentation.

Almost every morphology of secondary silica, from equant microcrystalline chert to fibrous chalcedony to megacrystalline quartz, is present in the sediments. Nodules of various sizes are found from the middle McKenzie Hill upward. Very early silica dissolution, precipitation,

and replacement may have been linked to the abundant algal growth as photosynthesis caused fluctuations in interstitial-fluid chemistry.

Preservation of traces of evaporites and pseudomorphs after evaporites by silica have facilitated interpretation of paleoenvironments. Early silicification occurred in mixing zones of islands, shoals, or algal buildups.

Calcium carbonate forms a substantial percentage of the cement in the formations, and, to a lesser degree, a localized replacement product. Carbonate cements and replacements began forming early and continued throughout the diagenetic history. Calcite occasionally preserved evaporite traces and textures when silica was not available. Calcification resulting in dedolomitization probably occurred during late Paleozoic uplift and subaerial exposure, and may be occurring during the current exposure.

Dolomitization began very early with the alteration of some sabkha sediments. Dorag and evaporative processes resulted in fine-grained crystalline and micritic fabrics. Expulsion of magnesium from decaying high-magnesium fossils or algae may have resulted in formation of scattered dolomite rhombohedra ubiquitous in the upper part of the group.

ACKNOWLEDGMENTS

We would like to acknowledge the financial support of Conoco, Inc., SOHIO, the Mobil Foundation, Sun Co., and the Moncrief Chair of Geology at Texas Christian University. Our thanks are extended to the many landowners who have given us access to their properties. We would like to thank R. E. Denison for his help in processing samples for isotope analysis. We are also indebted to the many graduate students at Oklahoma State University and Texas Christian University whose time and efforts in the completion of their theses contributed pertinent data to this paper.

REFERENCES CITED

Aitken, J. D., 1967, Classification and environmental significance of cryptalgal limestone and dolomite, with illustrations from the Cambrian and Ordovician of southwestern Alberta: Journal of Sedimentary Petrology, v. 37, p. 1163–1178.

Anderson, T. F.; and Arthur, M. A., 1983, Stable isotopes of oxygen and carbon and their application to sedimentologic and paleoenvironmental problems, *in* Arthur, M. A.; Anderson, T. F.; Kaplan, I. R.; Veizer, J.; and Land, L. S. (eds.), Stable isotopes in sedimentary geology: Society of Economic Paleontologists and Mineralogists Short Course No. 10, p. 1–151.

Babaei, A. ,1980, The structural geology of part of the Limestone Hills in the Wichita Mountains, Caddo and Comanche Counties, Oklahoma: Oklahoma State University unpublished M.S. thesis, 63 p.

Badiozamani, K., 1973, The dorag dolomitization model—application to the Middle Ordovician of Wisconsin: Journal of Sedimentary Petrology, v. 43, p. 965–984.

Barthelman, W. B., 1969, Upper Arbuckle (Ordovician) outcrops in the Unap Mountain–Saddle Mountain area, northeastern Wichita Mountains, Oklahoma: University of Oklahoma unpublished M.S. thesis, 67 p.

Beauchamp, W. H., 1983, The structural geology of the southern Slick Hills, Oklahoma: Oklahoma State University unpublished M.S. thesis, 119 p.

Blatt, H., 1982, Sedimentary petrology: W. H. Freeman and Co., San Francisco, 564 p.

Brewer, J. A.; Good, R.; Oliver, J. E.; Brown, L. D.; and Kaufman, S., 1983, COCORP profiling across the southern Oklahoma aulacogen: overthrusting of the Wichita Mountains and compression within the Anadarko basin: Geology, v. 11, p. 109–114.

Brookby, H. E., 1969, Upper Arbuckle (Ordovician) outcrops in Richards Spur–Kindblade Ranch area, northeastern Wichita Mountains, Oklahoma: University of Oklahoma unpublished M.S. thesis, 73 p.

Carozzi, A. V., 1962, Cerebroid oolites: Transactions of the Illinois State Academy of Science 55, p. 238–249.

Chafetz, H. S., 1973, Morphological evolution of Cambrian algal mounds in response to a change in depositional environment: Journal of Sedimentary Petrology, v. 43, p. 435–446.

Chase, G. W.; Frederickson, E. A.; and Ham, W. E., 1956, Resume of the geology of the Wichita Mountains, Oklahoma, *in* Petroleum geology of southern Oklahoma: American Association of Petroleum Geologists, p. 36–55.

Chenoweth, P. A., 1968, Early Paleozoic (Arbuckle) overlap, southern Mid-continent, United States: American Association of Petroleum Geologists Bulletin, v. 52, p. 1670–1688.

Chowns, J. M.; and Elkins, J. E., 1974, The origin of quartz geodes and cauliflower cherts through silicification of anhydrite nodules: Journal of Sedimentary Petrology, v. 44, p. 885–903.

Cloyd, K., 1987, Studies of dolomitization in selected units of the Cambro–Ordovician carbonates of southwestern Oklahoma: Oklahoma State University unpublished M.S. thesis.

Cloyd, K.; Ragland, D. A.; Jones, L.; and Donovan, R. N., 1986, Dolomite with evaporitic connections in the Ordovician Cool Creek Formation, southwestern Oklahoma, *in* Donovan, R. N. (ed.), The Slick Hills of southwestern Oklahoma—fragments of an aulacogen?: Oklahoma Geological Survey Guidebook 24, p. 29–34.

Decker, C. E.; and Merritt, C. A., 1928, Physical characteristics of the Arbuckle limestone: Oklahoma Geological Survey Circular 15, 56 p.

_____1931, The stratigraphy and physical characteristics of the Simpson Group: Oklahoma Geological Survey Bulletin 55, 112 p.

Ditzell, C., 1984, The sedimentary geology of the Cambro–Ordovician Signal Mountain Formation as exposed in the Wichita Mountains of southwestern Oklahoma: Oklahoma State University unpublished M.S. thesis, 165 p.

Donovan, R. N., 1986, Geology of the Slick Hills, *in* Donovan, R. N. (ed.), The Slick Hills of southwestern Oklahoma—fragments of an aulacogen?: Oklahoma Geological Survey Guidebook 24, p. 1–12.

Donovan, R. N.; and Ragland, D. A., 1986, Paleozoic stratigraphy of the Slick Hills, southwestern Oklahoma, *in* Donovan, R. N. (ed.), The Slick Hills of southwestern Oklahoma—fragments of an aulacogen?: Oklahoma Geological Survey Guidebook 24, p. 13–16.

Donovan, R. N.; and Stephenson, M. D., 1991, A new island in the southern Oklahoma archipelago, *in* Johnson, K. S. (ed.), Late Cambrian–Ordovician geology of the southern Mid-continent, 1989 symposium: Oklahoma Geological Survey Circular 92, p. 118–121.

Donovan, R. N.; Ragland, D. A.; and Schaefer, D., 1986, Stop 4: Geology of the Cool Creek road cut, *in* Donovan, R. N. (ed.), The Slick Hills of southwestern Oklahoma—fragments of an aulacogen?: Oklahoma Geological Survey Guidebook 24, p. 100–105.

Donovan, R. N.; Ragland, D. A.; Rafalowski, M.; McConnell, D.; Beauchamp, W.; Marcini, W. R.; and Sanderson, D. J., 1988, Pennsylvanian deformation and Cambro–Ordovician sedimentation in the Blue Creek Canyon, Slick Hills, southwestern Oklahoma, *in* Hayward, O. T. (ed.), Geological Society of America Centennial Field Guide, v. 4, South-Central Section, p. 127–134.

Dunham, R. J., 1962, Classification of carbonate rocks according

to depositional texture: American Association of Petroleum Geologists Memoir 1, p. 108–121.

_____1970, Stratigraphic reefs versus ecological reefs: American Association of Petroleum Geologists Bulletin, v. 54, p. 1931–1932.

Epstein, S. A.; and Friedman, G. M., 1982, Processes controlling precipitation of carbonate cement and dissolution of silica in reef and near-reef settings: Sedimentary Geology, v. 33, p. 157–172.

Ethington, R. L.; Engel, K. M.; and Elliott, K. L., 1987, An abrupt change in conodont faunas in the Lower Ordovician of the Midcontinent province, *in* Aldridge, R. J. (ed.), Paleobiology of conodonts: Ellis Horwood Limited, Chichester, p. 111–127.

Frazier, W. J.; and Schwimmer, D. R., 1987, Regional stratigraphy of North America: Plenum Press, New York, 719 p.

Gao, G.; and Land, L. S., 1991, Early Ordovician Cool Creek dolomite, middle Arbuckle Group, Slick Hills, SW Oklahoma, U.S.A.: origin and modification: Journal of Sedimentary Petrology, v. 61, p. 161–173.

Gebelein, C. D., 1969, Distribution, morphology, and accretion rate of recent subtidal algal stromatolites, Bermuda: Journal of Sedimentary Petrology, v. 39, p. 49–69.

Gregg, J. M.; and Sibley, D. F., 1984, Epigenetic dolomitization and the origin of xenotopic dolomite texture: Journal of Sedimentary Petrology, v. 54, p. 908–931.

Habicht, J. K. A., 1979, Paleoclimate, paleomagnetism, and continental drift: American Association of Petroleum Geologists Studies in Geology 9, 31 p.

Ham, W. E., 1955, Regional stratigraphy and structure of the Arbuckle Mountain region, *part 2 of* Geology of the Arbuckle Mountain region: Oklahoma Geological Survey Guidebook 3, 31 p.

Ham, W. E.; Denison, R. E.; and Merritt, C. A., 1964, Basement rocks and structural evolution of southern Oklahoma: Oklahoma Geological Survey Bulletin 95, 302 p.

Hofmann, H. J., 1969, Attributes of stromatolites: Geological Survey of Canada Paper 69–39, 58 p.

_____1973, Stromatolites: characteristics and utility: Earth Science Review, v. 9, p. 339–373.

Hudson, J. D., 1977, Stable isotopes and limestone lithification: Journal of the Geological Society of London, v. 133, p. 637–660.

James, N. P., 1984, Introduction to carbonate facies models, *in* Walker, R. G. (ed.), Facies models: Geological Association of Canada, Toronto, p. 209–211.

Johnson, K. S.; Branson, C. C.; Curtis, N. M., Jr.; Ham, W. E.; Marcher, M. V.; and Roberts, J. F., 1972, Geology and earth resources of Oklahoma—an atlas of maps and cross sections: Oklahoma Geological Survey Educational Publication 1, 8 p.

Kerans, C., 1990, Depositional systems and karst geology of the Ellenburger Group (Lower Ordovician), subsurface west Texas: Texas Bureau of Economic Geology Report of Investigations 193, 63 p.

Knauth, L. P., 1979, A model for the origin of chert in limestones: Geology, v. 7, p. 274–277.

Knauth, L. P.; and Epstein, S., 1976, Hydrogen and oxygen isotope ratios in nodular and bedded cherts: Geochimica et Cosmochimica Acta, v. 40, p. 1095–1108.

Larson, E. E.; Patterson, P. E.; Curtis, G.; Drake, R.; and Mutschler, F. E., 1985, Petrologic, paleomagnetic, and structural evidence of a Paleozoic rift system in Oklahoma, New Mexico, Colorado, and Utah: Geological Society of America Bulletin, v. 96, p. 1364–1372.

Leeder, M. R., 1982, Sedimentology: process and product: George Allen and Unwin, London, 344 p.

Logan, B. W., 1961, Cryptozoon and associate stromatolites from the Recent, Shark Bay, Western Australia: Journal of Geology, v. 69, p. 517–533.

Logan, B. W.; Rezak, R.; and Ginsburg, R. N., 1964, Classification and environmental significance of algal stromatolites: Journal of Geology, v. 72, p. 68–83.

Longman, M. W., 1982, Carbonate diagenesis as a control on stratigraphic traps: American Association of Petroleum Geologists Education Course Note Series No. 21, 159 p.

Lynch, M.; and Al-Shaieb, Z., 1989, Evidence of paleokarstic phenomena and burial diagenesis in the Ordovician Arbuckle Group of Oklahoma: Transactions of the 1989 American Association of Petroleum Geologists Mid-Continent Meeting, Oklahoma City, p. 1–55.

_____1991, Evidence of paleokarstic phenomena and burial diagenesis in the Ordovician Arbuckle Group of Oklahoma, *in* Johnson, K. S. (ed.), Late Cambrian–Ordovician geology of the southern Midcontinent, 1989 symposium: Oklahoma Geological Survey Circular 92, p. 42–60.

Marchini, W. R. D., 1986, Transpression: an application to the Slick Hills, southwest Oklahoma: Queen's University of Belfast, Northern Ireland, unpublished Ph.D. thesis, 286 p.

McConnell, D., 1983, The mapping and interpretation of the structure of the northern Slick Hills, southwest Oklahoma: Oklahoma State University unpublished M.S. thesis, 131 p.

Nelson, H. F.; Brown, C. W.; and Brineman, J. H., 1962, Skeletal limestone classification, *in* Classification of carbonate rocks—a symposium: American Association of Petroleum Geologists Memoir 1, p. 224–252.

Pratt, B. R.; and James, N. P., 1986, The St. George Group (Lower Ordovician) of western Newfoundland: tidal flat island model for carbonate sedimentation in shallow epeiric seas: Sedimentology, v. 33, p. 313–343.

Rafalowski, M. B., 1984, Sedimentary geology of the Late Cambrian Honey Creek and Fort Sill Formations as exposed in the Slick Hills of southwestern Oklahoma: Oklahoma State University unpublished M.S. thesis, 147 p.

Ragland, D. A., 1983, Sedimentary geology of the Ordovician Cool Creek Formation as it is exposed in the Wichita Mountains of southwestern Oklahoma: Oklahoma State University unpublished M.S. thesis, 170 p.

_____1984, Silica in the Ordovician Cool Creek Formation as seen in southwestern Oklahoma [abstract]: Oklahoma Geology Notes, v. 44, p. 103.

_____1990, Sedimentology, paleoenvironmental analysis and diagenesis of upper Arbuckle limestones in the Slick Hills, southwestern Oklahoma: Oklahoma State University unpublished Ph.D. thesis, 238 p.

Ragland, D. A.; and Donovan, R. N., 1985a, The Thatcher Creek Member: basal unit of the Cool Creek Formation in southern Oklahoma: Oklahoma Geology Notes, v. 45, p. 84–91.

_____1985b, The Cool Creek Formation (Ordovician) at Turner Falls in the Arbuckle Mountains of southern Oklahoma: Oklahoma Geology Notes, v. 45, p. 132–148.

_____1986, An environmental analysis of the Lower Ordovician Cool Creek Formation of southwestern Oklahoma, *in* Donovan, R. N. (ed.), The Slick Hills of southwestern Oklahoma—fragments of an aulacogen?: Oklahoma Geological Survey Guidebook 24, p. 21–28.

_____1991, Silica in the upper Arbuckle Group, Slick Hills, southwestern Oklahoma, *in* Johnson, K. S. (ed.), Late Cambrian–Ordovician geology of the southern Midcontinent, 1989 symposium: Oklahoma Geological Survey Circular 92, p. 127–142.

Ragland, D. A.; and Matthews, F. D., 1991, Porosity development in quartz-rich, oolitic limestones of the upper Arbuckle Group—a response to unloading, *in* Johnson, K. S. (ed.), Late Cambrian–Ordovician geology of the southern Midcontinent, 1989 symposium: Oklahoma Geological Survey Circular 92, p. 224–225.

Riehl, H., 1979, Climate and weather in the tropics: Academic Press, New York, 611 p.

Ross, R. J., Jr., 1976, Ordovician sedimentation in the western United States, *in* Bassett, M. G. (ed.), The Ordovician System: The University of Wales Press, Cardiff, p. 73–105.

St. John, J. W.; and Eby, D. E., 1978, Peritidal carbonates and evidence for vanished evaporites in the Lower Ordovician Cool Creek Formation, Arbuckle Mountains, Oklahoma: Gulf Coast Association of Geological Societies Transactions, v. 28, p. 589–599.

Scoffin, T. P., 1970, The trapping and binding of subtidal carbonate sediments by marine vegetation in Bimini Lagoon, Bahamas: Journal of Sedimentary Petrology, v. 40, p. 249–273.

Scotese, C. R.; and others, 1979, Paleozoic base maps: Journal of Geology, v. 87, p. 217–277.

Shelby, D. L., 1990, An occurrence of dolomite in the Lower Ordovician Arbuckle Group in the Slick Hills of southwestern Oklahoma: Texas Christian University unpublished M.S. thesis, 114 p.

Shinn, E. A., 1983, Tidal flat, *in* Scholle, P. A.; Bebout, D. G.; and Moore, C. H. (eds.), Carbonate depositional environments: American Association of Petroleum Geologists Memoir 33, p. 171–210.

Shinn, E. A.; Lloyd, R. M.; and Ginsburg, R. N., 1969, Anatomy of a modern carbonate tidal flat, Andros Island, Bahamas: Journal of Sedimentary Petrology, v. 39, p. 1202–1228.

Smith, S. S., 1991, Parallel Gold styles in the Blue Creek Canyon area of the Slick Hills, southwestern Oklahoma: Texas Christian University unpublished M.S. thesis.

Stephenson, M. D., 1990, Mapping and structural analysis of the southeastern eastern Slick Hills, Comanche County, Oklahoma: Texas Christian University unpublished M.S. thesis.

Stitt, J. H., 1971, Late Cambrian and earliest Ordovician trilobites, Timbered Hills and lower Arbuckle Groups, western Arbuckle Mountains, Murray County, Oklahoma: Oklahoma Geological Survey Bulletin 110, 83 p.

_____1977, Late Cambrian and earliest Ordovician trilobites, Wichita Mountains area, Oklahoma: Oklahoma Geological Survey Bulletin 124, 79 p.

_____1983, Trilobites, biostratigraphy, and lithostratigraphy of the McKenzie Hill Limestone (Lower Ordovician), Wichita and Arbuckle Mountains, Oklahoma: Oklahoma Geological Survey Bulletin 134, 54 p.

Taff, J. A., 1904, Preliminary report on the geology of the Arbuckle and Wichita Mountains in Indian Territory and Oklahoma: U.S. Geological Survey Professional Paper 31.

Termier, H.; and Termier, G., 1960, Atlas de Paleogeographis: Masson and Co., Paris, 99 p.

Toomey, D. F.; and Ham, W. E., 1967, *Pulchrilamina*, a new mound-building organism from Lower Ordovician rocks of west Texas and southern Oklahoma: Journal of Paleontology, v. 41, p. 981–987.

Toomey, D. F.; and Nitecki, M. H., 1979, Organic buildups in the Lower Ordovician (Canadian) of Texas and Oklahoma: Fieldiana Geology, New Series 2, Publication 1299, Field Museum of Natural History, Chicago, 181 p.

Tucker, M. E., 1981, Sedimentary petrology: an introduction: John Wiley and Sons, New York, 252 p.

_____1985, Shallow-marine carbonate facies and facies models, *in* Brenchley, P. J.; and Williams, B. P. J. (eds.), Sedimentology: recent developments and applied aspects: Blackwell Scientific Publications, Oxford, p. 147–169.

Ulrich, E. O., 1933, Simpson Group of Oklahoma: Geological Society of America Bulletin, v. 44, p. 105–106.

Whisonant, R. C., 1987, Paleocurrent and petrographic analysis of imbricate intraclasts in shallow marine carbonates, Upper Cambrian, southwestern Virginia: Journal of Sedimentary Petrology, v. 57, p. 983–994.

White, W. S., 1991, Analysis of fracture patterns in the Arbuckle anticline and Tishomingo Granite, Arbuckle Mountains, Oklahoma: Texas Christian University unpublished M.S. thesis.

Wilson, J. L., 1970, Depositional facies across carbonate shelf margins: Gulf Coast Association of Geological Societies Transactions, v. 20, p. 229–233.

_____1974, Characteristics of carbonate platform margins: American Association of Petroleum Geologists Bulletin, v. 58, p. 810–824.

_____1975, Carbonate facies in geologic history: Springer-Verlag, New York, 471 p.

Windley, B. F., 1977, The evolving continents: John Wiley and Sons, New York, 385 p.

Yochelson, E. L., 1973, The late Early Ordovician gastropod *Ceratopea* in the Arbuckle Mountains, Oklahoma: Oklahoma Geology Notes, v. 33, p. 67–78.

_____1975, Early Ordovician gastropod opercula and epicontinental seas: U.S. Geological Survey Journal of Research, v. 3, p. 447–450.

Yochelson, E. L.; and Bridge, J., 1957, The Lower Ordovician gastropod *Ceratopea*: U.S. Geological Survey Professional Paper 294-H, p. 281–304.

Paleokarstic Features and Thermal Overprints Observed in Some of the Arbuckle Cores in Oklahoma

Mark Lynch
Union Oil Company of California, Oklahoma City

Zuhair Al-Shaieb
Oklahoma State University

INTRODUCTION

This paper consists of two parts. Part I is a reprint of an earlier paper, "Evidence of Paleokarstic Phenomena and Burial Diagenesis in the Ordovician Arbuckle Group of Oklahoma," published as part of Circular 92, by the Oklahoma Geological Survey in 1991. It includes detailed descriptions and analyses of paleokarstic features observed in several Arbuckle reservoirs in Oklahoma. It also provides concise evidence concerning the thermal overprints as manifested by dolomitization and other diagenetic patterns.

Part II of this report includes a detailed description of eight cores examined in this study. The petrographic, sedimentological, isotopic, and fluid-inclusion data obtained from Part II were utilized to construct various models concerning the genesis of karstification phenomenon in the Arbuckle rocks, as well as to understand various diagenetic patterns which evolved during the burial of these rocks. These analyses and models were examined in Part I of this report.

PART I

ABSTRACT.— Cores of Ordovician-age Arbuckle Group carbonates from Oklahoma were examined for evidence of paleokarst. The depositional and diagenetic fabric of the rock was analyzed and compared with outcrop analogs to illustrate the nature of sedimentary, karstic, and diagenetic facies. Burial diagenesis and hydrothermal alteration have in many cases obscured the original fabric of these rocks.

Arbuckle rocks in different tectonic settings and stratigraphic intervals in the subsurface of south-central and north-central Oklahoma display surprisingly similar suites of karstic and diagenetic phenomena. Dissolution cavities, solution-enlarged fractures, collapse breccias, and vugular porosity are present in many cores and attest to the predominance of fabric-destructive processes in the development of Arbuckle paleokarst. Collapse breccias and sediment-filled solution features bear striking resemblance to outcropping analogs. Primary speleothemic precipitates were not readily observed; either they were not precipitated or were obscured by later dolomitization. Phreatic cements were more commonly encountered than vadose cements.

A complex history of exposure, subsidence, and diagenesis is recorded in these rocks. Although the actual physical manifestations of paleokarst are not difficult to identify, interpretation of the genesis and age of these features is decidedly problematic. Arbuckle carbonates have been exposed to surficial weathering for periods of variable intensity and duration numerous times in geologic history. Paleokarst horizons may have developed subjacent to disconformities within and between formations of the Arbuckle Group and where these rocks subcrop beneath regional unconformities. This complex hierarchy of unconformities can produce numerous porous horizons whose preservation potential may depend on subsidence rates rapid enough to prevent extensive low-temperature phreatic cementation, thereby preserving the open pore network of the karst profile.

Burial diagenesis is evidenced by the multi-event dolomitization of these rocks. Ferroan and nonferroan "growth-zoned" baroque and limpid phreatic dolomite cements commonly occlude vugular and fracture porosity. Host-rock carbonates have been extensively replaced or neomorphosed. Cathodoluminescent microscopy and chemical staining indicate that "growth-zoned" baroque dolomite is commonly uniform in composition and was precipitated under mildly reducing conditions. Dolomite cementation was arrested by the migration of oil into the remaining pore space.

INTRODUCTION

The limestones and dolomites of the Arbuckle Group have produced oil and gas from a wide variety of settings throughout the State of Oklahoma. While production is commonly structurally controlled, it can be demonstrated that porosity development is often due to modification of Arbuckle carbonates by (1) erosion at an unconformity surface, (2) fracturing and brecciation related to cavern collapse and/or tectonism, and (3) hydrothermal alteration of host rock in the subsurface. Recent unexpected and significant oil and gas production from Arbuckle paleokarst reservoirs (Shirley, 1988) in the Anadarko and Arkoma basins emphasizes the need for immediate, detailed inquiries into the nature of Arbuckle paleokarst.

Objectives

The primary objective of this study is to provide an inventory of paleokarstic features present in Arbuckle rocks from the subsurface in Oklahoma. The petrology, possible genesis, and subsequent diagenesis of these features are described; a complex set of dolomite types is presented and explained in relation to the burial history of these rocks.

This study is part of an on-going program at Oklahoma State University to investigate the geology of Arbuckle paleokarst in Oklahoma, both on the surface and in the subsurface.

Previous Investigations

It has long been recognized that fracturing and the establishment of vugular porosity play an important rôle in the productivity of Arbuckle reservoirs (Bartram and others, 1950; Walters, 1958; Gatewood, 1979). However, the study of these features in the context of karst facies is still in its infancy.

Paleokarstic sink holes and sand-filled caves have been identified in Cotter Dolomite outcrops in northeast Oklahoma by Gore (1952). Collapse breccias have been described in the Kindblade Formation in the Arbuckle Mountains by Tapp (1978) and in the Cool Creek Formation by Ragland and Donovan (1985). Post-Permian to recent karstification of Arbuckle rocks in southern Oklahoma has been documented by Decker and Merritt (1928) and Curtis (1959). Donovan (1987) described speleothems coeval with oil migration in a small Permian paleokarstic reservoir on Bally Mountain, in southwest Oklahoma.

Disconformities within and between the various formations of the Arbuckle Group have been recognized by Ireland (1955), Chenoweth (1968), Derby (1969), and Reeder (1974), although discussion of the role these events might play in karst formation has been lacking to date.

Arbuckle paleokarst in the subsurface of Kansas has been documented by Merriam and Atkinson (1956) and Walters (1958). Paleokarst features in the Arbuckle-equivalent Ellenburger Group carbonates in Texas have been described by Ijirigho and Schreiber (1986) and Kerans (1988).

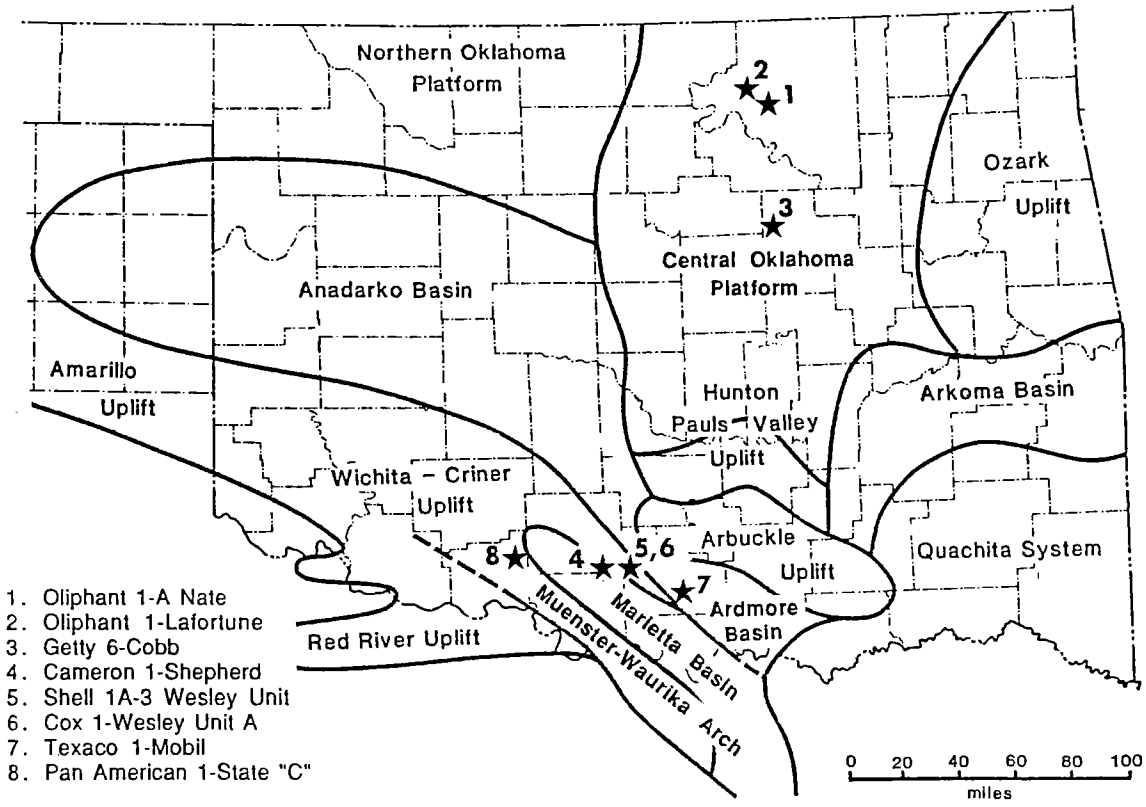


Figure 1. Locations of the cores (★) used in this study relative to the tectonic provinces of Oklahoma (after Al-Shaieb and Shelton, 1977; Arbenz, 1956).

TABLE 1. — CORE LOCATION AND INTERVAL INFORMATION

Core	Location	County/ field	Cored interval (depth, ft)	Cored formation	Depth below T/Arb. (ft)	Strata overlying Arbuckle
Oliphant 1-A Nate	15–T24N–R7E SW¼SW¼SE¼	Osage Naval Res.	–2,861 to –2,870	Cotter	0—at top	Burgen (Simpson)
Oliphant 1-Lafortune	8–T25N–R6E SE¼NW¼NE¼	Osage Burbank	–3,335 to –3,361	Cotter	0—at top	Burgen (Simpson)
Getty 6-Cobb	3–T17–R7E SE¼SE¼	Creek Cushing	–2,466 to –2,517	?	0—at top	Bartlesville
Cameron 1-Shepherd	20–T3S–R4W SE¼NW¼NE¼	Jefferson Dixie Area	–6,278 to –6,296 (poor recovery)	?	3,640	Deese
Shell 1A-3 Wesley Unit	3–T4S–R3W NW¼SW¼SE¼	Carter Healdton	–3,584 to –3,633	Kindblade[a]	1,050	Joins (Simpson)
E. L. Cox 1-Wesley Unit A	3–T4S–R3W NE¼SW¼SW¼	Carter Healdton	–3,806 to –3,983	West Spring Cr., Kindblade[ab]	870	Joins (Simpson)
Texaco 1-Mobil	1–T5S–R1W NE¼SE¼	Carter Wildcat	–6,300 to –6,310 –6,519 to –6,534	West Spring Cr., Kindblade[a]	420 640	Atoka
Pan American 1-State C	36–T2S–R10W N½NW¼NE¼	Cotton Wildcat	–7,475 to –7,500	Kindblade[b]	1,775	Joins (Simpson)

[a]Correlation based on well log signature.
[b]Correlation based on conodont biostratigraphy.

Methods and Procedures

Forty-two cores of Arbuckle Group rock housed at the Oklahoma Geological Survey Core and Sample Library in Norman, Oklahoma, were examined in a cursory manner to determine if the rock had in any way been affected by the physical or chemical processes that evidence karstification. Cores that exhibited unusual and possibly karstic features were procured for more detailed analysis. Those that did not exhibit these features were briefly described and cataloged for future reference. Seven cores from a variety of locations in Oklahoma were, on the basis of the initial macroscopic examination, selected for intensive study. Additionally, one other core was studied; it is the property of Oklahoma State University. Figure 1 shows the locations of the cores in relation to the tectonic provinces of Oklahoma. Pertinent data for each core is presented in Table 1. Each core was slabbed and described and data were recorded on a petrolog form that was specifically designed for description of both depositional and diagenetic (karstic) features. Thin sections were prepared for petrofabric analysis utilizing both polarizing and cathodoluminescence microscopes. Many thin sections were stained with alizarine red-S and potassium ferricyanide to distinguish ferroan and nonferroan varieties of dolomite and calcite (see Adams and others [1984] for procedure). A scanning electron microscope coupled with energy dispersive X-ray analyzer (SEM/EDXA) was used to investigate the crystallinity and chemical composition of individual crystals of each cement species. Preliminary analysis of stable carbon and oxygen isotopes was performed on 35 samples of host rock and dolomite and calcite cements by Paul Wagner, at Amoco Production Co. Research Center in Tulsa, Oklahoma. Conodont elements garnered from insoluble residues of selected intervals were identified by Scott Ritter of the Oklahoma State University School of Geology.

GENERAL GEOLOGY

Arbuckle Group Stratigraphy

Figure 2 depicts the stratigraphy of the Arbuckle Group in southern and northeastern Oklahoma. Note especially the locations and relative magnitudes of unconformities within the Arbuckle Group and between the Arbuckle Group and the overlying Simpson Group.

Arbuckle rocks have suffered exposure and erosion numerous times since their deposition. The possibility exists (and must be explored) that porosity and karst may have developed at any or all of these unconformities, given sufficient time of exposure and environmental conditions. The effects of pre-Simpson erosion on Arbuckle strata in northeastern Oklahoma are well documented (Walters, 1958; Reeder, 1974), but may be in question in southern Oklahoma where the Joins Formation of the Simpson Group overlies the West Spring Creek Formation with apparent conformity (Reed, 1957; Derby, 1969; Latham,

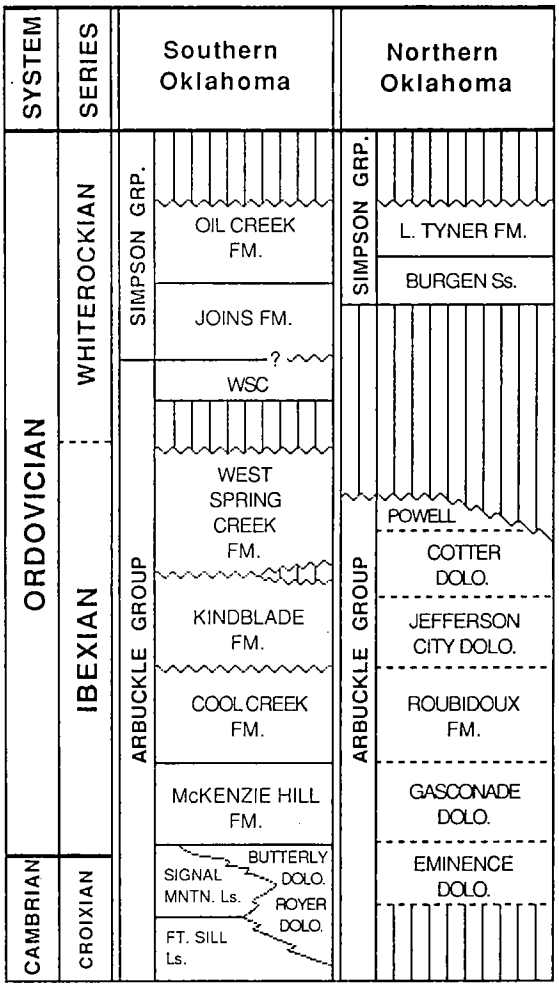


Figure 2. Stratigraphic column showing correlative formations of the Arbuckle Group in southern and northeastern Oklahoma (modified after Chenoweth, 1968; Ross and others, 1982).

1970). Due to the rapidly subsiding, more mobile, nature of the southern Oklahoma paleodeep, the "pre-Simpson unconformity" may not be represented by a single discrete surface at the top of the Arbuckle, but may instead be represented by subtle disconformities within the West Spring Creek Formation (see Derby, 1969).

Although they are lithologically similar, carbonates of the Arbuckle Group in southern Oklahoma are predominantly limestone, while those on the northern Oklahoma platform are dolomite (Ham, 1969). It is worth noting that all of the cores examined in this study were, regardless of location, extensively dolomitized.

Arbuckle Depositional Facies

Arbuckle rocks are characterized by numerous and recurring shallowing-upward, peritidal carbonate cycles. Subtidal mudstones and wackestones, intertidal bioclastic packstones and grainstones, and restricted, upper intertidal algal boundstones are commonly observed facies. Exquisite algal stromatolites and thrombolites occur in the Cool Creek Formation, and also in the Kindblade and West Spring Creek Formations more infrequently. Supratidal, evaporite-dominated sabkha facies are not well developed; either they were never deposited or were removed by erosion subsequent to deposition. In many instances a "typical" shallowing-upward cycle culminates with an intraformational conglomerate which probably represents a period of subaerial exposure, desiccation, erosion, and redeposition. Such erosive events may be correlative to hardgrounds and karst surfaces elsewhere in the Arbuckle environment (Donovan and others, 1983). Shallowing-upward sequences are seldom delimited above by supratidal facies such as interlaminated evaporites and dol-algal mats. Evaporites are encountered far more frequently in the literature (Reed, 1957; Latham, 1970; Gatewood, 1978; St. John and Eby, 1978; Beales and Hardy, 1980; Ragland and Donovan, 1985) than in either the outcrop or subsurface. Nodular and remobilized fracture-filling evaporites were noted in very few cores from southern Oklahoma; interestingly, these cores do not show signs of paleokarstification, nor do they exhibit the coarse dolomite textures found in the principle cores of this study. Evidence for evaporite presence in these cores is scant and equivocal, such as submillimeter-size anhydrite inclusions in chert nodules, and a few silicified salt hopper crystals recovered from insoluble residues from the Cox-Wesley core.

PALEOKARST FEATURES OBSERVED IN CORES OF ARBUCKLE ROCK

Breccias and Conglomerates

Breccias and conglomerates are lithotypes common to each of the Arbuckle Group cores studied. Where possible, the genesis of each conglomerate or breccia was inferred from the fabric of the rock and its relation to surrounding structures. Breccias were described with a combination of genetic terminology and textural modifiers, as proposed by Norton (1917) and Ijirigho and Schreiber (1986). Blount and Moore (1969) outlined certain criteria for differentiating between genetic breccia types.

Crackle Breccia

The term "crackle breccia" was introduced by Norton (1917) to describe incipient brecciation in extensively fractured rocks where the fragments have not been dislodged, rotated, or otherwise moved to any appreciable degree. This is a structural term that bears no genetic connotations. Ijirigho and Schreiber (1986) modified this term to describe crackle breccias with open or slightly dilated fractures, which they termed "microdil breccias." Kerans (1988) noted that these breccia-types, which he termed "fracture breccia" commonly occur in the "cave roof facies" of karstified Ellenburger Group carbonates in West Texas. Usually, this type of breccia is indistinguishable from—and indeed, may be nothing more than—intensely, and perhaps tectonically, fractured rock. It is only through its spatial relations to other karst features that this type of breccia has any use in karst-facies diagnosis.

Definitive crackle breccias were observed locally grading into mosaic or rubble collapse breccias in many of the study cores. Figure 3 shows crackle-brecciated rock subjacent to an intra-Arbuckle disconformity, in the Oliphant-Nate core. Early, crackle-breccia porosity is commonly occluded by infill sediment or cement.



Figure 3. Crackle-brecciated rock subjacent to an intra-Arbuckle disconformity. Many fractures are enlarged and filled with micritic sediment. (Oliphant-Lafortune core, –3,352 ft.)

Collapse Breccia

Collapse breccia is a term used to imply a genetic origin for breccia texture(s) that result from structural collapse of a previously open mega-pore or cavern network. The structural integrity of the host rock may be compromised by the dissolution of matrix carbonates and/or interbedded soluble evaporites. Foundering may be induced by gravity at the surface if the host rock is sufficiently eroded internally, or by the application of overburden subsequent to burial.

Collapse breccias are characterized by marked heterogeneity and angularity of clasts (which may be derived from numerous and lithologically dissimilar overlying stratigraphic units), poor sorting, with interstitial cement or matrix in a dominantly clast-supported fabric (Blount and Moore, 1969). Collapse breccias may exhibit the "mosaic," "random," and "rubble" textures of Norton (1917) and Ijirigho and Schreiber (1986).

Many of the breccias noted in this study exhibited fabrics suggestive of formation by solution and collapse. A few of the characteristic breccia fabrics observed in cores are described below.

The Pan American-State core from Cotton County (Fig. 4) is comprised nearly entirely of collapse breccia. The clast population—which ranges from granule to boulder size and is very poorly sorted—is comprised of at least six different lithologies, the most exotic of which is a silicified ooid grainstone that is not present as in-place host rock anywhere else in the core. The breccia exhibits a predominantly random fabric. Large, fractured clasts exhibit a mosaic fabric internally. The breccia matrix is a dark-brown, clayey, dolomitic mudstone.

Heterolithic, rubble collapse breccias as much as 4 ft thick were encountered in the Texaco-Mobil core (Fig. 5). These breccia immediately overlie crackle-brecciated host rock.

The Cox-Wesley core from Healdton field exhibits unique and complex "zebroid" brecciation (Beales and Hardy, 1980) and coarse dolomite cementation (Fig. 6A). This type of brecciation has been attributed to host-rock expansion due to displacive cementation subsequent to evaporite dissolution (Beales and Hardy, 1980). However, neither relict nor extant evaporites were noted in the brecciated interval. In places, the brecciated zone exhibits a random-fragment packing suggestive of collapse (Fig. 6B). The very angular breccia fragments are cemented with a 1-cm-thick rind of isopachous saddle dolomite.

Cavern-Fill Parabreccia

The term "cavern-fill parabreccia" was proposed by Lynch (1990) for poorly sorted, matrix-supported breccias that exhibit structures suggestive of subterranean deposition. (The precedent for this terminology is the paraconglomerate of Pettijohn [1975], which, with the exception of clast shape, this lithotype texturally resembles). The term is genetic, although structurally it is analogous to Norton's (1917) "pudding breccia," and also to the "pheno breccia" of Ijirigho and Schreiber (1986). Cavern-fill parabreccias are deposited by aqueous media flowing through an open mega-pore or cavern network within a karstified terrain. Phenoclasts may calve off the roof of the cavern in which they are deposited, or be transported from locations of collapse elsewhere in the cavern network (probably during periods of turbulent flow and rapid discharge after storm events). The fine matrix is composed of cave mud or infiltrated sediment. These breccias differ from true solution-collapse breccias in that they are comprised mostly of matrix that has filled an uncollapsed cavern. Analogous deposits have been observed by the authors in recent karst in the Lake of the Ozarks region of Missouri.

Figure 7A,B shows two interesting cavern-fill parabreccias in the Cox-Wesley core at depths of –3,939 and –3,972 ft. The parabreccias are lithologically similar; each is comprised of very angular phenoclasts of chert and light blue-gray limestone supported in a matrix of dark-brown, clayey, dolomitic mudstone. The parabreccia at –3,939 ft contains conspicuous limestone phenoclasts that are unlike any other lithology encountered in the cored interval. This breccia was deposited within an eviscerated chert bed, from whence the chert phenoclasts in both this deposit and the one at –3,972 ft appear to have been derived.

Thus it would appear that an open solution-tunnel network of at least 33 vertical feet (and of indeterminable lateral extent) was present within this sequence of rocks. There are no remnants of this pore network that are open currently as effective, channel porosity.

Sedimentary Breccias and Conglomerates

The terms "sedimentary conglomerate" and "sedimentary breccia" are used to describe carbonate rudstones having rounded or angular clasts, respectively, that are formed by erosion of an exposed carbonate terrain adjacent to, or possibly within, the environment of deposition. While perhaps not specifically related to karstification, these deposits do evince surficial erosion during the time of Arbuckle sedimentation. This type of breccia is analogous to the "depositional breccia" of Blount and Moore (1969).

A 1-ft-thick sedimentary conglomerate comprised of well-rounded pebbles of dark-gray mudstone within a light-gray, detrital quartz-sand-rich carbonate mudstone matrix was observed in the Oliphant-Lafortune core (Fig. 8A). The noncontemporaneity of clasts and matrix is indicated by the fact that some of the clasts are internally fractured, and none of them contain the quartz sand that is prevalent in the matrix. The clasts exhibit some rough im-



Figure 4. Heterolithic collapse breccia exhibiting random texture (RB) and mosaic texture (MB). (Pan American-State core.)



Figure 5. Rubble collapse breccia. (Texaco-Mobil core, –6,521 ft.)

brication which, together with the detrital quartz, suggests the possibility that this is a subaqueous channel-like deposit. The pre-burial formation of this conglomerate is indicated by the transection of both the clasts and the matrix by rather conspicuous stylolites.

The Getty-Cobb core from Cushing field exhibits a sedimentary breccia that contains phenoclasts of dolomudstone and silicified ooid grainstone(?) in a finely laminated, green shale matrix (Fig. 8B). The brecciated interval is delimited above and below by transitional contacts with the host rock.

Dissolution Features

The most commonly distinguishable type of dissolution observed in this study was that which was limited to the millimeter or centimeter scale, or those features that are small enough to be contained within the diameter of the core sample. Dissolution vugs, solution-enlarged fractures, and solution channels were observed in the study cores; more often than not the original pore space was occluded by infill sediment or cement.

The type of porosity created in karst terrains depends strongly upon the fabric and lithology of the host carbonate. In low-permeability carbonates such as Arbuckle rocks, vugular and solution-channel porosity (Choquette and Pray, 1970) may be created by the restriction of ground-water flow through high-permeability conduits such as fractures or bedding planes. Extensively karstified terrains may exhibit cavern porosity, which Choquette and Pray (1970) define as the smallest opening that an adult human can enter, or, if the rock is encountered in subsurface drilling, as any opening large enough to cause a noticeable drop in the drill bit.

The vugular porosity encountered in the rocks of this study typically range from 0.5 to 2 mm in diameter, and occasionally as large as 2 cm. The distinction between very large vugular porosity and channel porosity is often arbitrary, especially when determined from small-diameter core samples.

Striking examples of solution-induced channel porosity and matrix-vugular porosity were observed in the Oliphant-Nate core from Osage County. The fine (<1 mm in diameter) vugular porosity is notably concentrated in halos that extend a few centimeters outward from the eroded walls of the solution channels (Fig. 9A). Geopetal sediment, rhombic dolomite cement, and pyrobitumin (in order of emplacement) commonly fill the vugular and channel pore space.

A detailed view of a large vug in the Cox-Wesley core (Fig. 9B) shows clayey sediment geopetally filling the open pore. The orientation of the infill sediment relative to the dipping beds of the host rock suggests that the pore formed—or, was at least filled—after the Pennsylvanian tectonism that induced the folding.

Cements

The morphology of cementation in the karst environment is controlled largely by the amount of water present. In the unsaturated (vadose) zone, cements precipitate from water that gravitates toward the bottoms of grains or is bound by capillary pressure at grain contacts—hence, these cements often display characteristic pendant (also termed microstalactitic, or dripstone) and meniscoid fabrics. "Phreatic" cements precipitate in solution-filled cavities and tend to form isopachous coatings on pore walls and grains. Speleothemic precipitates (stalactites, stalagmites, dripstone curtains, etc.) composed of laminated calcium carbonate are typically formed in mature-stage karst close to the water table in the lower vadose zone (Esteban and Klappa, 1983).

Karst speleothems such as stalactites and stalagmites were not observed in any of the cores studied; either they were not precipitated or their presence was masked by later diagenetic events. Additionally, the tremendous improbability of actually coring one of these features cannot be discounted.

Cathodoluminescent microscopy revealed the presence of vadose-type microstalactitic calcite spar cementing breccia clasts in the Texaco-Mobil core (Fig. 10A,B).

The macro- and microscopically visible cements in all of the cores studied are principally subisopachous, pore-lining saddle and rhombic dolomite. Although these cements are not a product of low-temperature karst cementation (see discussion below), certainly their isopachous morphology suggests precipitation under predominantly phreatic conditions.

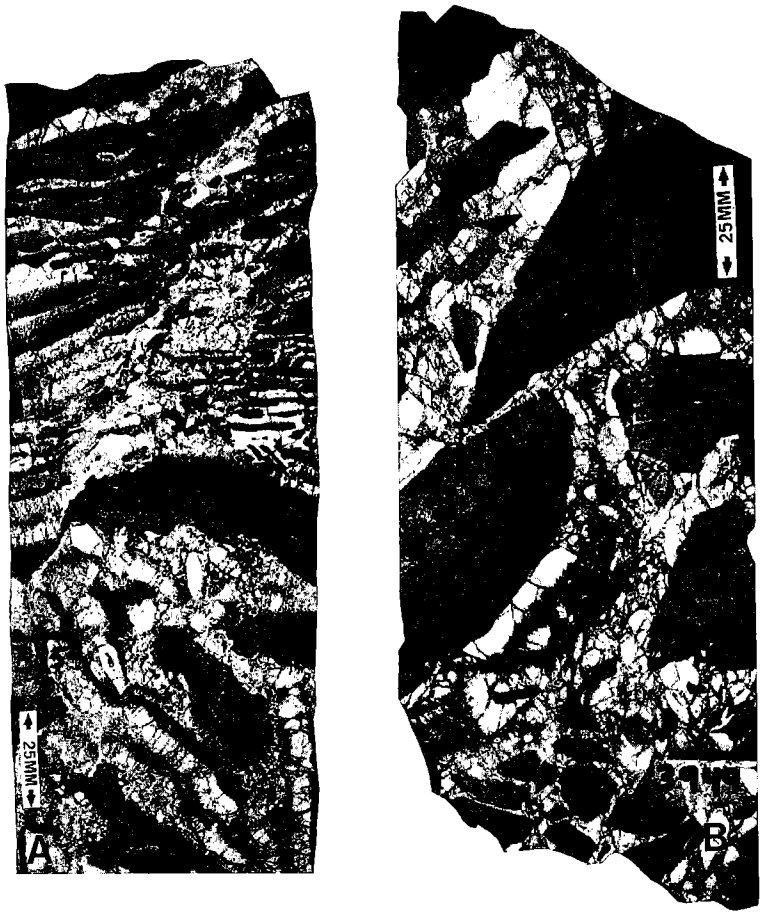


Figure 6. *A*—Zebroid breccia. Dark laminae are laths of host rock, white laminae are subisopachous crusts of columnar and saddle dolomite. (Cox-Wesley core, –3,954 ft.) *B*—Random collapse breccia cemented with isopachous saddle dolomite. (Cox-Wesley core, –3,949 ft.)

Infill Sediment

The phrase "infill sediment" refers to the sediments that are deposited anywhere within the karst profile, including breccia matrix and pore-filling sediments.

The lithology of the infilling sediment may reflect the origin of the sediment and, roughly, the timing of its deposition within the karst system. Arbuckle-age micrite was commonly observed filling solution-enlarged and crackle-breccia fractures (see Fig. 3). Additionally, some solution tubes were filled with what appears to be Simpson Group sand, below the eroded top of the Arbuckle (Fig. 11). It is perhaps significant that the detrital feldspars, polycrystalline quartz, and metamorphic rock fragments that are nearly ubiquitous in Pennsylvanian sandstones were not encountered in any infill sediment in the study cores. The parabreccia matrix described earlier is typically comprised of an admixture of terrigenous clastic clays, carbonate mud, and silty (possibly detrital?) dolomite.

DOLOMITE TYPES AND SEQUENCING

The dolomite in the study cores was differentiated into eight types on the basis of crystal habit and fabric, relation to host rock, and mineralogy as determined from energy dispersive X-ray analysis, cathodoluminescence, and staining. Five types of dolomite are considered matrix replacive, or recrystallized host rock, and include: (1) host matrix dolomicrite/dolomicrospar, (2) hypidiotopic-rhombic (sucrosic) dolomite, (3) clay-associated hypidiotopic-rhombic dolomite, (4) saddle-rhombic dolomite, and (5) xenotopic dolomite. Cements that were precipitated in open pore space include (1) saddle dolomite, (2) columnar dolomite, and (3) idiotopic-rhombic dolomite. The characteristics of each type of dolomite are discussed below. Many of the dolomite types described in this study are similar to those considered by Lee and Friedman (1987) as being indicative of deep burial-diagenesis in Ellenburger Group carbonates in Texas.

Matrix-Replacive Dolomites

The host rock or matrix carbonate in each of the cores studied is predominantly, if not entirely, composed of dolomite. The episodic and pervasive nature of the dolomitization has made it difficult in some instances to determine whether dolomite is syndepositional, neomorphic after a dolomitic precursor, or replaced calcitic matrix.

Host Rock Dolomicrite/Dolomicrospar

The peritidal carbonate mudstones in these Arbuckle rocks are composed principally of very finely crystalline dolomicrite and/or dolomicrospar. Individual crystals



Figure 7. Cavern-fill parabreccias from the Cox-Wesley core. *A*—Parabreccia within an eviscerated chert (CH) bed at –3,939 ft. Angular phenoclasts are blue-gray dolomicrite. *B*—Parabreccia within a tan dolomicrite host (HR) at –3,972 ft. Chert phenoclasts (CH) derived from chert bed at –3,939 ft exhibit early, internal fractures that are healed with dolomite cement. Late, open tectonic fractures transect host rock, parabreccia matrix, and chert clasts.

range from 0.01 to 0.05 mm in diameter and are usually anhedral in shape. These matrix dolomites exhibit dull red luminescence and a dirty appearance under plane polarized light (see Fig. 12A). The fine crystal size and pervasive nature of this dolomite suggest a primary, syndepositional or perhaps eogenetic origin. Petrographic evidence indicates that this type of dolomite formed prior to fracturing, brecciation, and stylolitization. This type of dolomite was observed in all of the study cores.

Hypidiotopic-Rhombic (Sucrosic) Dolomite

This type of dolomite is characterized by a porous fabric of loosely interlocking hypidiotopic to idiotopic rhomb-shaped crystals (Fig. 12B). The highest intercrystalline porosity values (7–13%) of any of the dolomite textures described in this study were encountered in this dolomite. This friable dolomite is what is commonly referred to as "sucrosic dolomite" in the subsurface vernacular. Individual euhedra range in size from 0.1 to 0.3 mm and are commonly comprised of a dirty, inclusion-rich core and a limpid outer rim. This dolomite is slightly ferroan, and has dull red luminescence. Crystals of this dolomite are noticeably larger than those of the clay-associated hypidiotopic dolomite described below, which they otherwise closely resemble.

Sucrosic dolomite is a common constituent in the fractured and brecciated host rock of the Getty-Cobb core. It is suggested that this dolomite is a product of eogenetic diagenesis.

Clay-Associated Hypidiotopic-Rhombic Dolomite

The presence of inclusions of clay in this matrix-replacive dolomite suggests that it was formed by replacement of a precursor lithology. This dolomite is limited in areal extent (on a millimeter or centimeter scale) to terrigenous clastic clay-rich seams in the carbonate host (Fig. 12C). This type of dolomite is typically fine crystalline, ranging in size from 0.05 to 0.20 mm. Individual crystals may be inclusion-free (clear throughout) or inclusion-rich (dirty throughout), or may exhibit fine growth zonation due to the inclusion of impurities imparted from the replaced host during crystal growth. Little or no mineralogical variance was observed across inclusion-rich and inclusion-free zones, and the dolomite tends to have an even, dull red luminescent quality. This type of dolomite was encountered in the Cox-Wesley and Shell-Wesley cores from Carter County.

Saddle-Rhombic Dolomite

This interesting dolomite texture was observed only in the Shell-Wesley core. This type of dolomite is characterized by medium to coarse (0.4– 1.0 mm) subhedral crystals that form a well-cemented, interlocking hypidiotopic fabric, with interstitial silty clay. The crystals are uniquely shaped, appearing rhombic in outline but with curved crystal faces reminiscent of pore-filling saddle dolomite cement (Fig. 12D). Radke and Mathis (1980) suggest that this type of dolomite is a matrix-replacive form of saddle dolomite, which is supported by the observation that the dolomite in this study contains inclusions of clay and quartz silt. Extinction is strongly undulose, often with opposing corners going extinct at the same time. This type of dolomite is characteristically growth zoned, although its luminescence is usually a non-zoned dull red.

Xenotopic Dolomite

The term "xenotopic" was proposed by Friedman (1965) for diagenetically altered carbonate rocks having a fabric comprised predominantly of anhedral crystals.

Fine- to medium-crystalline xenotopic dolomites were observed in the Texaco-Mobil, Cox-Wesley, and Shell-Wesley cores. Crystals range in size from 0.1 to 0.5 mm, and are usually arranged in a tightly interlocking fabric with little or no intercrystalline porosity. "Ghosts" of spherical and elliptical grains (perhaps ooids) were observed within the dolomite crystals, attesting to its replacement origin (Fig. 12E). In addition to replacing grainstones, the uniformly dirty appearance of some of this dolomite suggests that it also replaced wackestone mudstone (Fig. 12F). Individual anhedra tend to be smaller in the mudstone-replacive variety, although both varieties tend to appear dull red under cathodoluminescence.

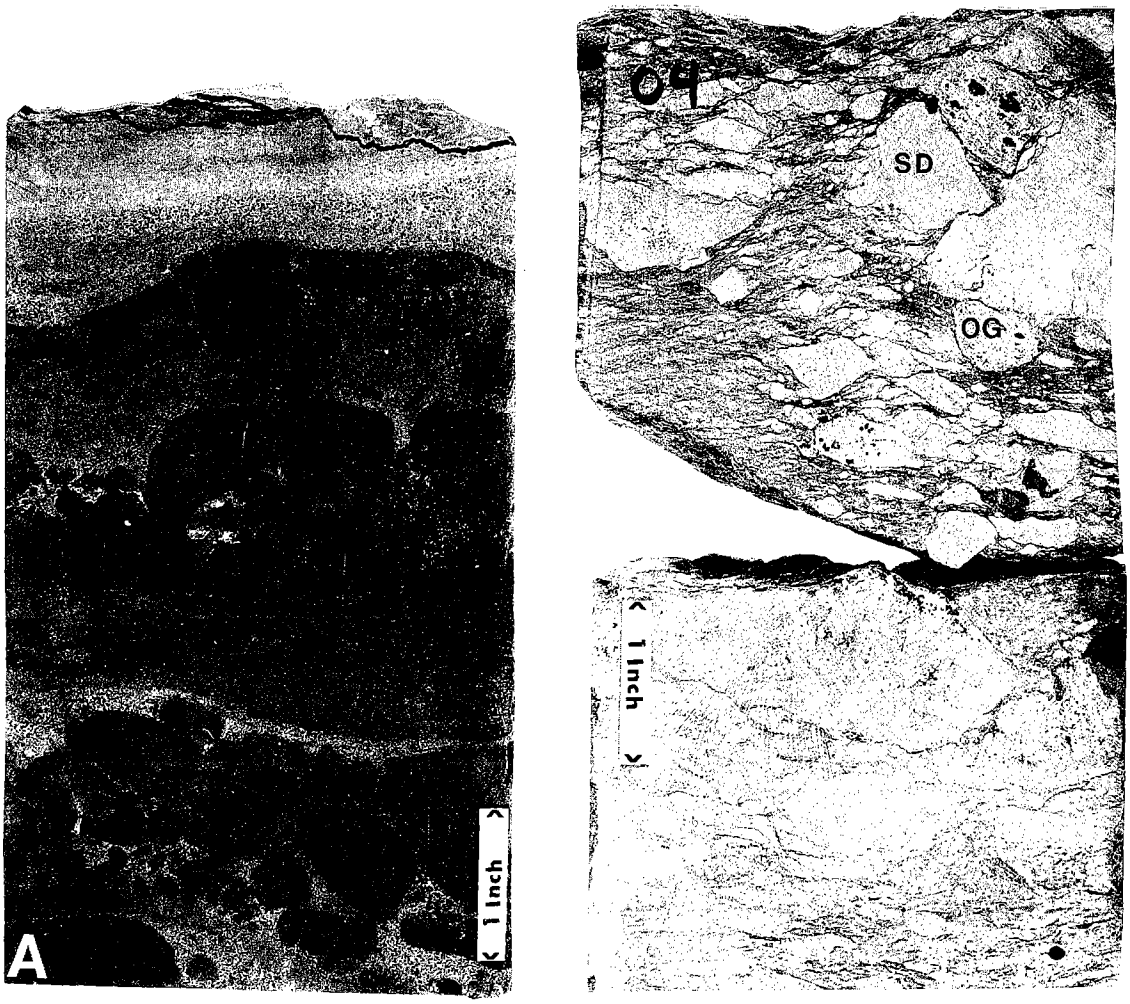


Figure 8. *A*—Sedimentary conglomerate comprised of dark-gray dolomicrite pebbles within a sandy, dolomicrite matrix. (Oliphant-Lafortune core, –3,349 ft.) *B*—Sedimentary breccia comprised of clasts of tan, sucrosic dolomite (SD) and silicified ooid grainstone (OG), within a green shale matrix. (Getty-Cobb core, –2,504 ft.)

Anhedral crystals that grow into pore space often exhibit subhedral to euhedral terminations. Additionally, some of the anhedra exhibit faint internal rhombic growth zonation, which suggests that crystallinity diminished as the dolomite crystals grew together in competition for the available pore space. This feature is more commonly observed in those xenotopic dolomites that replace grainstone than in the wackestone/mudstone-replacive variety. It would appear that the space available for crystal growth and the initial lithology of the replaced host carbonate exert some degree of control over the texture of the final dolomite.

Pore-Filling Dolomites

Three different morphologies of pore-filling dolomite cement were observed in the study cores. These dolomites exploit many different types of porosity, including vugular, channel and fracture porosity, and breccia-intergranular porosity.

Saddle Dolomite

Spear-type saddle dolomite (Radke and Mathis, 1980) occurs as a void-filling cement in the Cox-Wesley, Shell-Wesley, and Texaco-Mobil cores from Carter County, and in the Cameron-Shepherd core from Jefferson County. Typically, it occurs as subisopachous crusts of hypidiotopic to idiotopic crystals oriented normal to pore walls or grain boundaries (Fig. 13A). Saddle-dolomite crystals, which range in size from 0.5 to 5.0 mm, commonly exhibit pronounced undulose extinction. Individual crystals may be growth-zoned or, less commonly, clear or dirty throughout. Under cathodoluminescence, this type of dolomite exhibits subtle zonation comprised of dull red, bright red, yellow and non-luminescent laminae, attesting to the slight variance in chemical composition across each layer (Fig. 13B).

Radke and Mathis (1980) postulate that saddle dolomite forms at temperatures >80°C, and thus would imply a deep burial origin—or a hydrothermal origin at shallower depths—for this dolomite. It is interesting to note that the isotopic signature obtained for the saddle dolomites in this study (from rocks at –3,000 to –6,000 ft) is nearly identical to that observed by Lee and Friedman (1987) in saddle dolomite from Ellenburger carbonates at –15,000 to –20,000 ft.

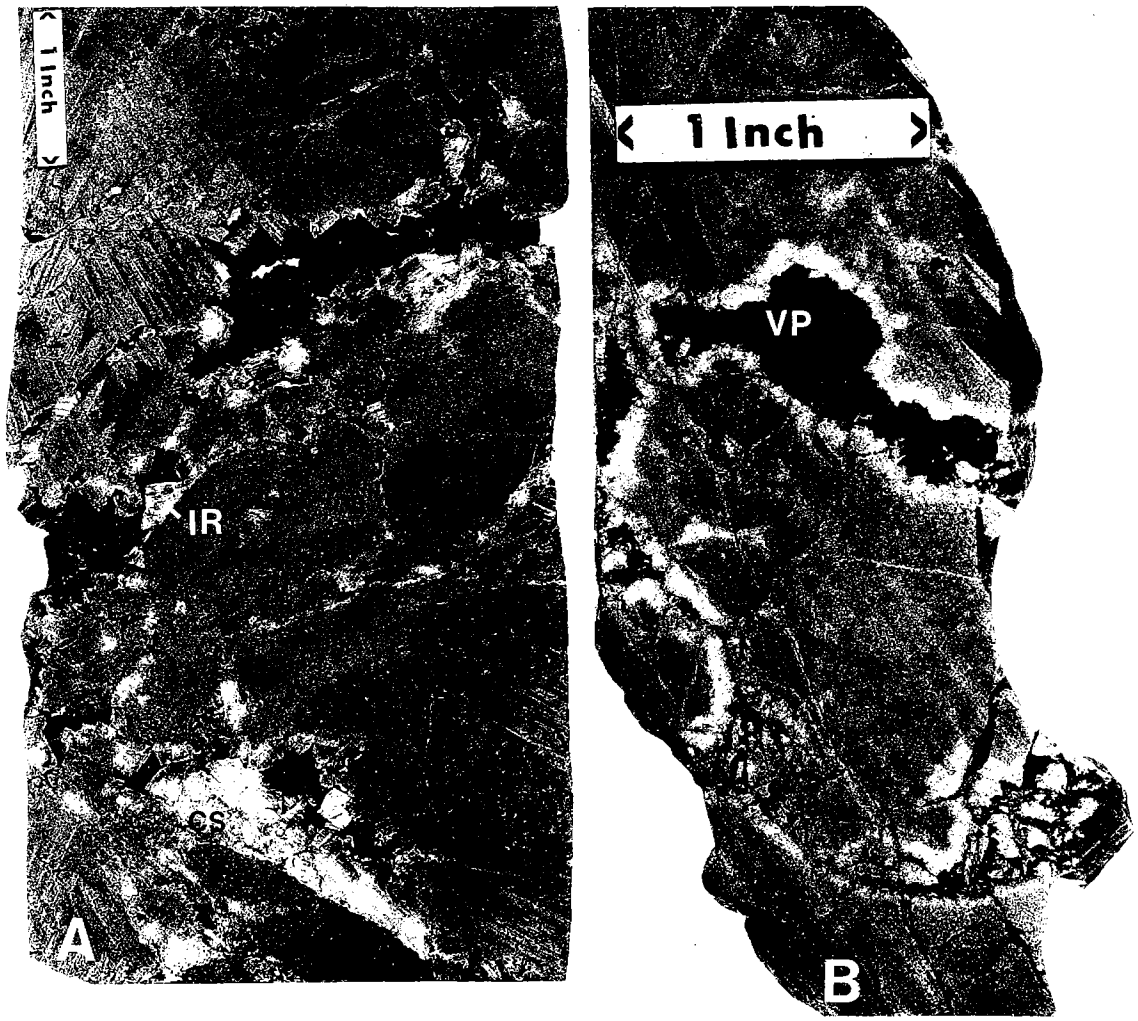


Figure 9. Examples of karstic porosity: *A*—Solution channels filled with clayey infill sediment (CS), idiotopic-rhombic dolomite cement (IR), and pyrobitumin (black, in pore space). Note vugular porosity halo (highlighted by black pyrobitumin mottling) surrounding the solution channels. (Oliphant-Nate core, –2,863 ft.) *B*—Enlarged vugular porosity (VP) with infilling sediment geopetally oriented with respect to present structural dip (indicated by black line). (Cox-Wesley core, –3,902 ft.)

Columnar Dolomite

This type of dolomite is similar in appearance to the saddle dolomite described above, except that the columnar variety has a greater length-to-width ratio than the saddle variety. Columnar dolomite also occurs as normal-to-substrate isopachous crusts (Fig. 14). Strong, sweeping undulose extinction characterizes this dolomite. This type of dolomite is predominantly inclusion-rich, appearing dirty throughout. This dolomite also exhibits dull red luminescence. Columnar dolomite was only encountered in the "zebroid" breccia interval in the Cox-Wesley core from Carter County.

Idiotopic-Rhombic Dolomite

Clear, equant rhombs of dolomite occur in the vugular pore space of the Oliphant-Nate, Cameron-Shepherd, and Pan American-State cores. Individual crystals range from 0.5 to 5 mm in diameter, have straight to slightly undulose extinction, and are typically nonluminescent. They occur as vug-lining, though not isopachous, cements (see Fig. 9A). Individual crystals are not interlocked to the extent observed in the saddle dolomites.

Dolomite Paragenesis

Paragenesis of the various dolomite types was inferred from the mutual cross-cutting relationships exhibited by types, by their occurrence relative to the structural fabric of the rock, and by consideration of certain crystal textures that are known to be temperature-dependent. Although dolomite-formation temperatures have not yet been verified by fluid-inclusion analyses, preliminary investigations into the stable-isotopic signature of these dolomites suggests that most of the dolomites formed at elevated temperatures. Additionally, the mineralogy of all dolomite types, as indicated by energy dispersive X-ray analysis, is slightly ferroan.

The first dolomite to form was the fine-crystalline dolomicrite/dolomicrospar, either as sedimentary dolomite

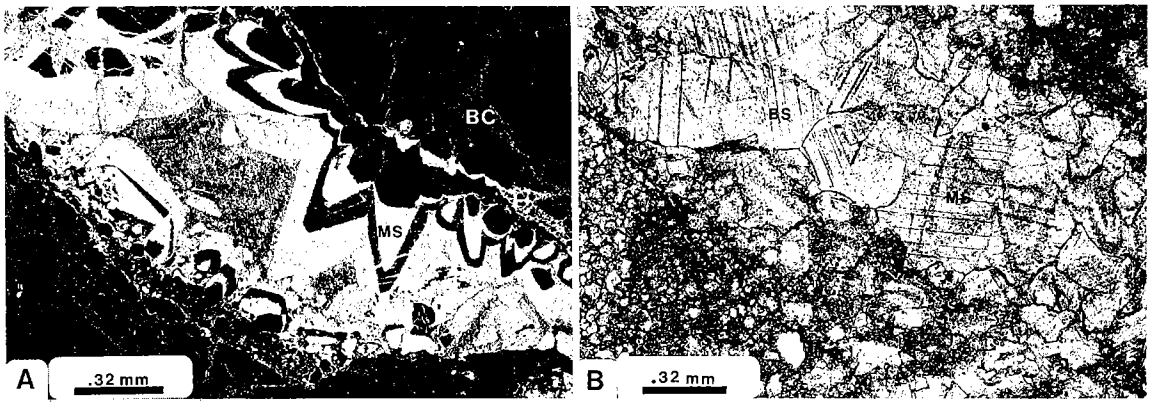


Figure 10. Thin-section photomicrographs of microstalactitic calcite spar. *A*—Cathodoluminescence reveals the delicate spar crystals (MS) that grew downward from the bottom of a breccia clast (BC). *B*—The presence of the microstalactitic spar (MS) is masked in this plain polarized light photomicrograph by later blocky, equant spar (BS). Faint growth zonations are visible internally. (Texaco-Mobil core, –6,305 ft.)

within the environment of deposition or by replacement of lime mud at shallow burial depths. The occurrence of the sucrosic hypidiotopic dolomite within oomoldic porosity and replaced matrix carbonates suggests that it is a product of eogenetic diagenesis. The clay-associated hypidiotopic-rhombic form probably began forming within clay-rich seams subsequent to increasing burial; the concentration of this dolomite along clay seams may reflect incipient stylolite formation. With increasing depth of burial, Arbuckle Group rocks were exposed to elevated formation temperatures and perhaps to heated subsurface brines; at this time the xenotopic dolomite probably began to form. Gregg and Sibley (1984) suggest that xenotopic dolomite precipitates at temperatures >50°C. The idiotopic-rhombic pore-filling dolomite cement may have precipitated from fluid of similar, or slightly cooler, temperature.

The precipitation of columnar and saddle dolomite probably commenced in stages, from fluid heated to >80°C (Radke and Mathis, 1980). This would tend to suggest that this dolomite formed either at depths sufficient to encounter formation temperatures >80°C, or that heated subsurface brines ascended through available conduits such as fractures to dolomitize the rock at shallower depths. Hagni (1976) has shown that Mississippi-Valley-type ore deposits nearly always contain sparry saddle dolomite as the most prevalent gangue mineral, and that the single most common factor among this type of deposit is their occurrence at or near the surface. The ubiquitous presence of growth zonation in this dolomite type suggests that it accreted layer by layer, over an incalculable period of time. Petrographic evidence strongly suggests episodic migration of a fluid capable of periodically dolomitizing and corroding the carbonate host (see Fig. 15).

The absolute timing of the pervasive saddle-type dolomitization is difficult to assess. It is certainly plausible to propose that the extensive fracture systems which developed during Pennsylvanian tectonism could have acted as conduits for ascending, dolomitizing hydrothermal fluids. This premise is substantiated by Kranak (1978), who recognized Pennsylvanian-age Mississippi-Valley-type sphalerite mineralization in the Butterly Dolomite in Murray County, Oklahoma. It is likewise possible that the dolomitization could have occurred earlier by the same general

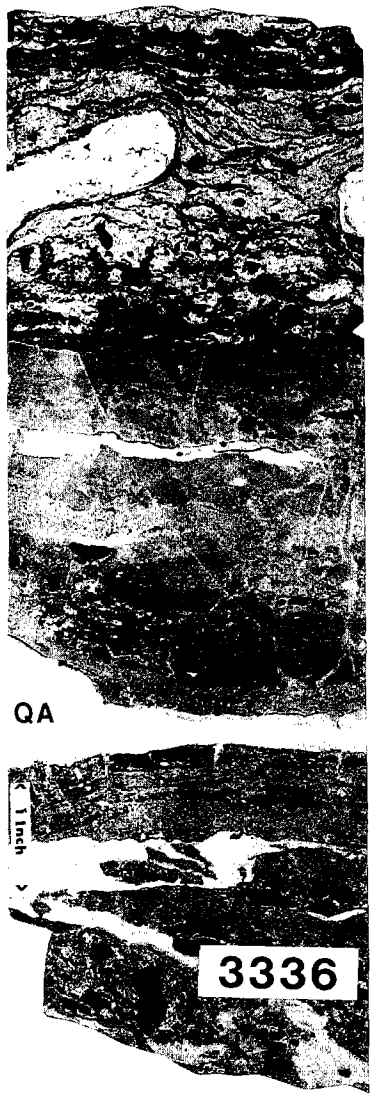


Figure 11. Solution channels filled with quartz-arenite sandstone (QA) of the overlying Burgen Formation (Simpson Group). (Oliphant-Lafortune core, –3,336 ft.)

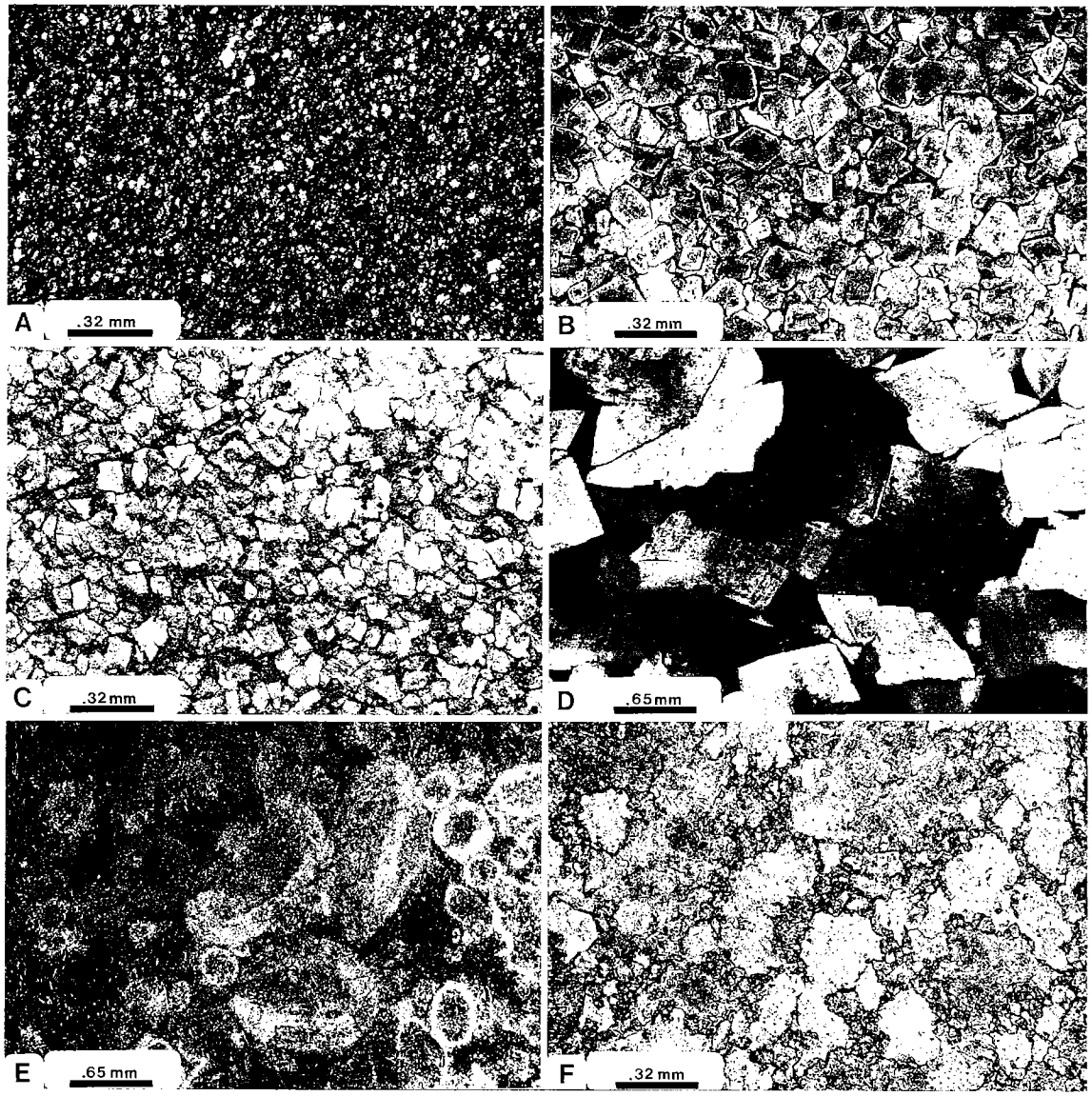


Figure 12. Thin section photomicrographs of host-rock-replacive dolomite types: *A*—host dolomicrospar, *B*—sucrosic dolomite, *C*—clay-associated hypidiotopic-rhombic dolomite, *D*—saddle-rhombic dolomite, *E*—grainstone-replacive xenotopic dolomite, *F*—mudstone-replacive xenotopic dolomite. (All photos taken under plain polarized light.)

process. We suggest that the petrographic and structural data can explain the episodic ascension of dolomitizing hydrothermal fluids, subsequent to the collapse stage of karstification and Pennsylvanian tectonism. Dolomitization was probably a long-ranging process that continued throughout the burial history of the rock.

ARBUCKLE PALEOKARST MODEL AND EVOLUTION

Karst facies in the Arbuckle Group cores of this study are typified by collapse breccias and dissolution features; low-temperature speleothemic cements were not observed in appreciable amounts. The paucity of karstic cements may indicate that Arbuckle paleokarst developed in a semi-arid environment with a low water budget.

The establishment of karst probably began with the dissolution of massive Arbuckle carbonates along open ground-water conduits such as fractures and bedding planes. Solution-enlarged fractures would develop into channel porosity, and perhaps into cavern porosity. Although cavernous porosity was not directly observed in this study, its former presence can be inferred from extant features such as collapse breccias. Certainly, the 20+ ft of heterolithic collapse breccia in the Pan American-State core necessitates a precursor cavity of similar vertical extent, into which the roof rock was able to collapse. The lateral extent of such features is perhaps unknowable, but for comparison purposes it is interesting to note that Curtis (1959) has cataloged present-day Arbuckle caves in Murray County that extend as much as 14,050 ft in total length. Such caves typically exhibit linear trends that may indicate a joint-controlled origin. It has been suggested that karst-facies elements such as collapse breccias may attain thicknesses of 50–100 ft, and may be present hundreds of feet beneath a paleoexposure surface (Kerans, 1988).

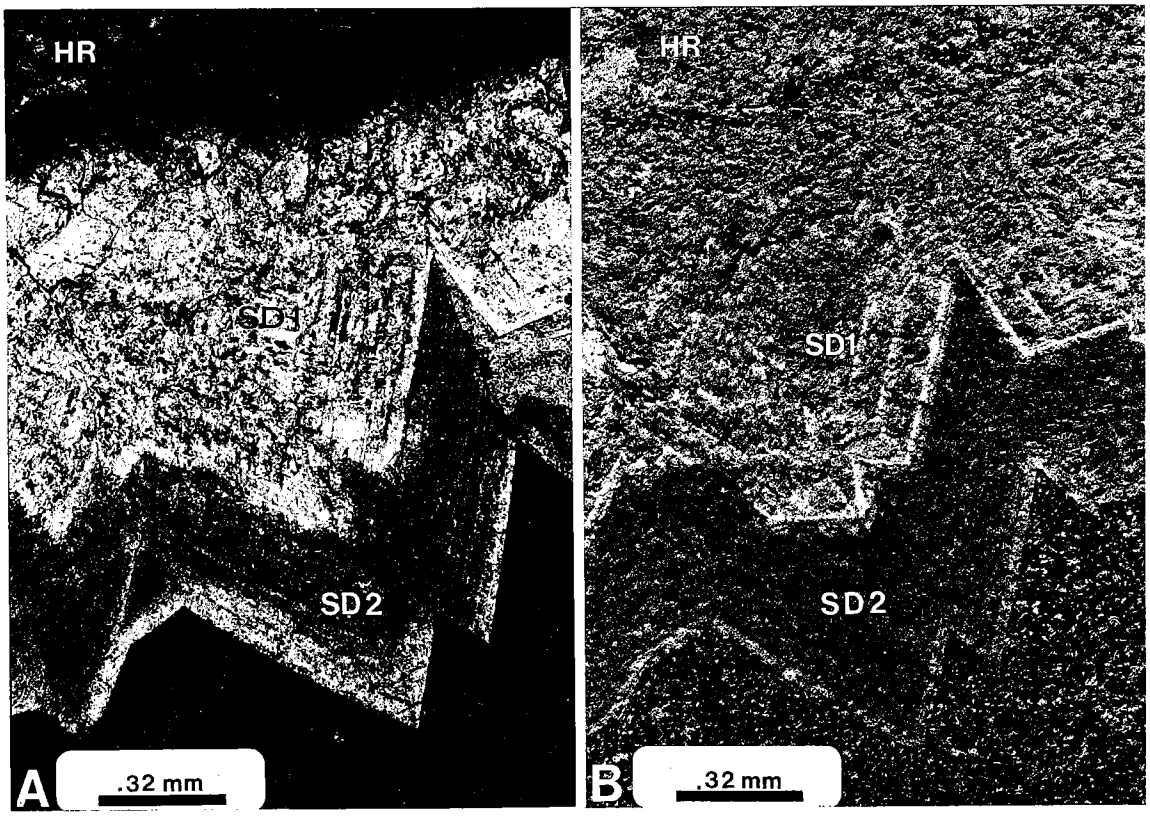


Figure 13. Thin-section photomicrographs of pore-filling saddle dolomite: At least two generations of cement are present and discernible under plain light (*A*) and cathodoluminescence (*B*). First-generation cement (SD1) is adjacent to host rock (HR), is solution pitted and has less-distinct growth zoning, and has alternating bright red and yellow luminescent zones. Second-generation cement (SD2) was precipitated as an overgrowth on the earlier cement. The second-generation dolomite exhibits more-intense growth zoning, and dull red luminescence.

The timing of Arbuckle paleokarstification is less obvious than the features that result from it. Data presented in this and other studies suggest that the paleokarstification of Arbuckle strata may have been an episodic phenomena that occurred (in varying degrees) when Arbuckle rocks were exposed at local or inter-regional unconformities. Numerous authors (i.e., Gore, 1952; Ireland, 1955; Merriam and Atkinson, 1956; Walters, 1958; Kerans, 1988) have documented the presence of paleokarst in Arbuckle and equivalent rocks at the pre-Simpson unconformity in Oklahoma, Texas, and Kansas. Walters (1958) has shown that the porosity present in Arbuckle reservoirs along the central Kansas uplift is directly related to Pennsylvanian karstification that probably modified pre-Simpson paleokarst.

Data presented in this investigation suggest that the establishment of Arbuckle paleokarst may be due to multiple episodes of subaerial exposure and erosion during, and subsequent to, the time of Arbuckle deposition. The presence of similar and biostratigraphically equivalent conodont species (Ritter, personal communication, 1989) in both the matrix and clasts of cavern-fill parabreccia and collapse breccia, and the complete lack of younger (Simpson, Pennsylvanian, etc.) fauna suggests that karstification occurred during Arbuckle time. An argument for karstification at the pre-Simpson unconformity can be made for the cores from Osage County that contain Simpson-derived sandstone in solution channels and vugs. Note that these cores also exhibit intraformational disconformities and sedimentary breccias that are clearly of Arbuckle age. With the exception of a thin, sandy residual zone at the top of the Getty-Cobb core, no evidence for Pennsylvanian erosion was found in the cores of this study. This in no way negates the possibility of Pennsylvanian karst occurring in other areas where Arbuckle rocks subcrop beneath the pre-Permian unconformity (for example, see Donovan, 1987). Walters (1958) speculated that the entire thickness of the Arbuckle Group in Kansas served as a vast regional aquifer during the Pennsylvanian, much as it does presently in the Tri-State region of Kansas, Missouri, and Oklahoma (Macfarlane and Hathaway, 1987).

Preservation of karst porosity appears fortuitous and uncommon, based on the rocks in this study. Solution-channel porosity is commonly occluded by infill sediment, while the interparticle porosity in collapse breccias is typically cemented or filled with sediment. Data from the Oliphant-Nate core suggest that migration of hydrocarbons into solution channels and vugs effectively arrested dolomite cementation, thereby preserving the open pore network. Much of the effective porosity currently present in these rocks appears to be intimately related to diagenetic modification of the karst profile as it was buried and then structurally modified by later tectonism.

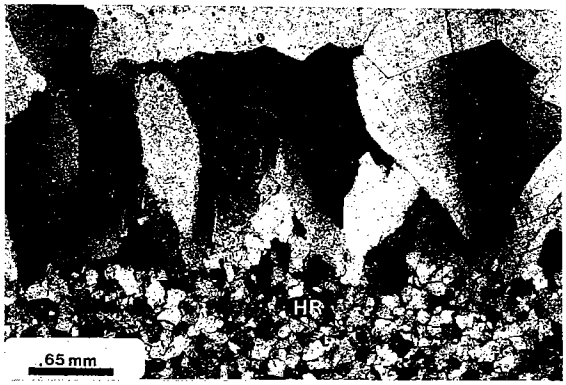


Figure 14. Thin-section photomicrograph of pore-filling columnar dolomite. This cement occurs as drusy, isopachous crusts on laths of host rock (HR) in the zebroid breccia interval, in the Cox-Wesley core. (Cross polarized.)

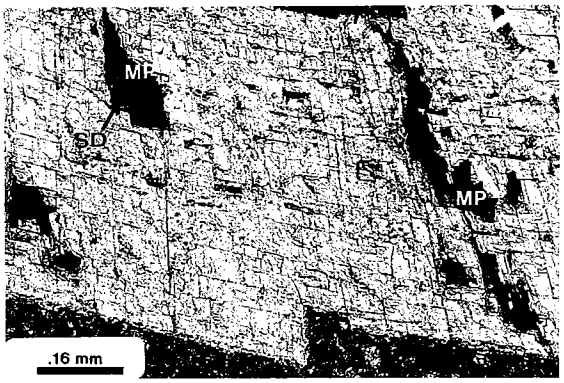


Figure 15. Thin-section photomicrograph of solution-pitted saddle-dolomite cement. Silty dolomite (SD) geopetally infills the solution micro-porosity (MP). (Plain polarized light.)

SUMMARY AND CONCLUSIONS

Paleokarstification of upper Arbuckle Group rocks is evidenced in cores from Oklahoma by (1) breccia facies that form as a result of collapse, subterranean sedimentation, and surficial erosion; (2) vadose cements (infrequently); and (3) dissolution structures, such as enlarged vugular and channel porosity, and solution-enlarged fractures. The presence of Arbuckle-age conodonts in breccia matrix (and the complete lack of younger fauna) suggests that much of the karstification observed may be of Arbuckle age.

A complicated burial-diagenetic history for these rocks is indicated by the variety and paragenesis of matrix and pore-filling dolomite types. Eogenetic, matrix-replacive dolomite types suggest early diagenesis, while coarse-crystalline, xenotopic matrix-replacive varieties indicate burial diagenesis at temperatures >50°C. Pore-filling saddle and columnar dolomites likely precipitated from ascending hydrothermal fluids that may be related to hydrocarbon migration. That these fluids were alternately constructive (precipitating) and destructive (dissolving) is indicated by the presence of compositionally zoned and solution-pitted dolomite cements. Breccia-intergranular porosity (where preserved) and tectonic fractures provided the necessary conduits for fluid migration. Dolomite cementation was apparently long-ranging, but was arrested by the migration of hydrocarbons into pore space.

ACKNOWLEDGMENTS

We extend our appreciation to the University Center of Energy Research (UCER) for supporting this project. This project was partially supported by a research grant awarded to Mark Lynch by the Research Committee of the American Association of Petroleum Geologists.

SELECTED REFERENCES

Adams, A. E.; MacKenzie, W. S.; and Guilford, C., 1984, Atlas of sedimentary rocks under the microscope: John Wiley and Sons, New York, 104 p.

Al-Shaieb, Z.; and Shelton, J. W., 1977, Evaluation of uranium potential in selected Pennsylvanian and Permian units and igneous rocks in southwestern and southern Oklahoma: U.S. Department of Energy Open-File Report GJBX-3S, 248 p.

Arbenz, J. K., 1956, Tectonic map of Oklahoma: Oklahoma Geological Survey Map GM-3, scale 1:750,000.

Bartram, J. G.; Imbt, W. C.; and Shea, E. F., 1950, Oil and gas in Arbuckle and Ellenburger Formations, Mid-Continent region: American Association of Petroleum Geologists Bulletin, v. 34, p. 682–700.

Beales, F. W.; and Hardy, J. L., 1980, Criteria for the recognition of diverse dolomite types with an emphasis on studies on host rocks for Mississippi-Valley-type ore deposits, *in* Zenger, D. H.; Dunham, J. B.; and Ethington, R. L. (eds.), Concepts and models of dolomitization: Society of Economic Paleontologists and Mineralogists Special Publication 28, p. 197–213.

Blount, D. N.; and Moore, C. H., 1969, Depositional and non-depositional carbonate breccias, Chiantla Quadrangle, Guatemala: Geological Society of America Bulletin, v. 80, p. 429–442.

Burgess, W. J., 1964, Stratigraphic dolomitization in Arbuckle rocks in Oklahoma, *in* McHugh, J. W. (ed.), Symposium on the Arbuckle: Tulsa Geological Society Digest, v. 32, p. 45–48.

____1968, Carbonate paleoenvironments in the Arbuckle Group, West Spring Creek Formation, Lower Ordovician, in Oklahoma: Columbia University unpublished Ph.D. dissertation, 91 p.

Chenoweth, P. A., 1968, Early Paleozoic (Arbuckle) overlap, southern Mid-Continent, United States: American Association of Petroleum Geologists Bulletin, v. 52, p. 1670–1688.

Choquette, P. W.; and Pray, L. C., 1970, Geologic nomenclature and classification of porosity in sedimentary carbonates: American Association of Petroleum Geologists Bulletin, v. 54, p. 207–250.

Curtis, N. M., 1959, Caves in the Arbuckle Mountains area, Oklahoma: Oklahoma Geology Notes, v. 19, p. 20–31.

Decker, C. E.; and Merritt, C. A., 1928, Physical characteristics of the Arbuckle limestone: Oklahoma Geological Survey Circular 15, 56 p.

Derby, J. R., 1969, Revision of the Lower Ordovician–Middle Ordovician boundary in western Arbuckle Mountains, Oklahoma, *in* Ham, W. E., Regional geology of the Arbuckle Mountains, Oklahoma: Oklahoma Geological Survey Guidebook 17, p. 35–37.

Donovan, R. N., 1987, The world's smallest oil field?: Oklahoma Geology Notes, v. 47, p. 238, 291.

Donovan, R. N.; Beauchamp, W.; Ferraro, T.; Lajek, C.; McConnell,

D.; Munsil, M.; Ragland, D.; Sweet, B.; and Taylor, D., 1983, Subsidence rates in Oklahoma during the Paleozoic: Shale Shaker Digest, v. 33, p. 86–88.

Esteban, M.; and Klappa, C. F., 1983, Subaerial exposure environment, *in* Scholle, P. A.; Bebout, D. G.; and Moore, C. H. (eds.), Carbonate depositional environments: American Association of Petroleum Geologists Memoir 33, p. 1–54.

Friedman, G. M., 1965, Terminology of crystallization textures and fabrics in sedimentary rocks: Journal of Sedimentary Petrology, v. 35, p. 643–655.

Gatewood, L. E., 1978, Stratigraphic trap possibilities in the Arbuckle Group: general relationships: Shale Shaker Digest, v. 28, p. 219–227.

_____1979, Some Oklahoma Arbuckle production and thoughts on fracturing: Shale Shaker Digest, v. 29, p. 4–11.

Gore, C. E., 1952, The geology of a part of the drainage basins on Spavinaw, Salina and Spring Creeks, northeastern Oklahoma: Tulsa Geological Society Digest, v. 20, p. 144–179.

_____1953, Cave sandstones in Cotter Dolomite, northeastern Oklahoma [abstract]: American Association of Petroleum Geologists Bulletin, v. 37, p. 2186–2188.

Gregg, J. M.; and Sibley, D. F., 1984, Epigenetic dolomitization and the origin of xenotopic dolomite texture: Journal of Sedimentary Petrology, v. 54, p. 908–931.

Hagni, R. D., 1976, Tri-State ore deposits: the character of their host rocks and their genesis, *in* Wolf, K. H. (ed.), Handbook of strata-bound and stratiform ore deposits. II.—Regional studies and specific deposits: Elsevier, New York, p. 457–494.

Ham, W. E., 1955, Origin of dolomite in the Arbuckle Group, Arbuckle Mountains, Oklahoma, *in* Moore, C. A. (ed.), Proceedings of the fourth symposium on subsurface geology, University of Oklahoma, p. 67–74.

_____1969, Regional geology of the Arbuckle Mountains, Oklahoma: Oklahoma Geological Survey Guidebook 17, 52 p.

Ham, W. E.; and Wilson, J. L., 1967, Paleozoic epeirogeny and orogeny in the central United States: American Journal of Science, v. 265, p. 332–407.

Ijirigho, B. T.; and Schreiber, J. F., Jr., 1986, Origin and classification of fractures and related breccia in the Lower Ordovician Ellenburger Group, West Texas: West Texas Geological Society Bulletin, v. 26, p. 9–15.

Ireland, H. A., 1955, Pre-Cambrian surface in northeast Oklahoma and parts of adjacent states: American Association of Petroleum Geologists Bulletin, v. 39, p. 468–483.

Kerans, C., 1988, Karst-controlled reservoir heterogeneity in Ellenburger Group carbonates of West Texas: American Association of Petroleum Geologists Bulletin, v. 72, p. 1160–1183.

Kranak, P. V., 1978, Petrography and geochemistry of the Butterly Dolomite, and associated sphalerite mineralization, Turner Prospect, Arbuckle Mountains, Oklahoma: Oklahoma State University unpublished M.S. thesis, 76 p.

Latham, J. W., 1970, Petroleum geology of the Healdton Field, Carter County, Oklahoma: American Association of Petroleum Geologists Memoir 14, p. 255–276.

Lee, Y. I.; and Friedman, G. M., 1987, Deep-burial dolomitization in the Ordovician Ellenburger Group carbonates, West Texas and southeastern New Mexico: Journal of Sedimentary Petrology, v. 57, p. 544–557.

Lynch, M. T., 1990, Evidence of paleokarstification and burial diagenesis in the Arbuckle Group of Oklahoma: Oklahoma State University unpublished M.S. thesis, 163 p.

Macfarlane, P. A.; and Hathaway, L. R., 1987, The hydrogeology and chemical quality of ground waters from the Lower Paleozoic aquifers in the Tri-State region of Kansas, Missouri, and Oklahoma: Kansas Geological Survey Ground Water Series 9, 37 p.

Merriam, D. F.; and Atkinson, W. R., 1956, Simpson filled sinkholes in eastern Kansas: State Geological Survey of Kansas Bulletin 119, pt. 2, p. 61–80.

Norton, W. H., 1917, A classification of breccias: Journal of Geology, v. 25, p. 160–194.

Pettijohn, F. J., 1975, Sedimentary rocks [third edition]: Harper and Row, New York, 628 p.

Radke, B. M.; and Mathis, R. L., 1980, On the formation and occurrence of saddle dolomite: Journal of Sedimentary Petrology, v. 50, p. 1149–1168.

Ragland, D. A.; and Donovan, R. N., 1985, The Cool Creek Formation (Ordovician) at Turner Falls in the Arbuckle Mountains of southern Oklahoma: Oklahoma Geology Notes, v. 45, p. 132–148.

Reed, B. K., 1957, Geology of the Pre-Atokan unconformity of portions of Love and Carter Counties, Oklahoma: University of Oklahoma unpublished M.S. thesis, 59 p.

Reeder, L. R., 1974, The control of potential Arbuckle hydrocarbon traps in northeastern Oklahoma by Precambrian topography: Shale Shaker Digest, v. 24, p. 84–93.

Ross, R. J.; and others, 1982, The Ordovician System in the United States, correlation chart and explanatory notes: International Union of Geological Sciences Publication 12, 73 p.

Sargent, K. A., 1969, Geology and petrology of selected tectonic dolomite areas in the Arbuckle Group, Arbuckle Mountains, south-central Oklahoma: University of Oklahoma unpublished M.S. thesis, 85 p.

Shelton, J. W.; Stewart, G. F.; and Al-Shaieb, Z., 1987, Depositional environments, diagenesis and porosity development, and petrophysical features of selected Pennsylvanian sandstones in Oklahoma: an examination of outcrop and subsurface data: American Association of Petroleum Geologists, Mid-Continent Section, Field-Trip Guidebook, 30 p.

Shirley, K., 1988, Deeper zone rejuvenates old basin—Oklahoma Arbuckle targeted: American Association of Petroleum Geologists Explorer, v. 9, p. 10–13.

St. John, J. W., Jr.; and Eby, D. E., 1978, Peritidal carbonates and evidence for vanished evaporites in the Lower Ordovician Cool Creek Formation—Arbuckle Mountains, Oklahoma: Gulf Coast Geological Society Transactions, v. 28, p. 589–599.

Tapp, J. B., 1978, Breccias and megabreccias of the Arbuckle Mountains, southern Oklahoma aulacogen, Oklahoma: University of Oklahoma unpublished M.S. thesis, 126 p.

Voss, R. L.; and Hagni, R. D., 1985, The application of cathodoluminescence microscopy to the study of Sparry Dolomite from the Viburnum Trend, south-east Missouri, *in* Hansen, D.; and Kopp, O. C. (eds.), Mineralogy: applications to the minerals industry: American Institute of Mining Engineers, New York, p. 51–68.

Walters, R. F., 1958, Differential entrapment of oil and gas in Arbuckle dolomite of central Kansas: American Association of Petroleum Geologists Bulletin, v. 42, p. 2133–2173.

PART II

CORE DESCRIPTIONS, PETROLOGS, AND PHOTOGRAPHS

The location of each core examined is shown in Figure 1 (Part I). Specific location and other core-interval data are presented in Table 1 (Part I). Each core was slabbed and described on a petrolog form designed specifically for description of both depositional and diagenetic (karstic) features. In addition, photographs of each of the cores described are also included in this part.

Although Part II is focused only on detailed descriptions of the cores involved in this study, the reader is advised to examine Part I of this report to comprehend further the descriptions and interpretations of numerous karstic features in rocks from a wide variety of settings within the State of Oklahoma.

Core: Oliphant 1-A Nate
Location: Sec. 15, T24N, R7E, Osage County, OK
Cored Interval: –2,861 to –2,870 ft
Stratigraphic Interval: Simpson and Arbuckle (Cotter Formation) Groups
Core Description: The following description is given in reference to the core photograph (Fig. 16) and to the petrolog of this core (Pl. 1).

–2,870 to –2,865 ft

This interval consists of interbedded, tan dolomudstones, packstones of rounded algal debris, and minor stromatolitic algal boundstone of middle- to upper-intertidal origin. Numerous subvertical and subhorizontal fractures transect these lithologies; some fractures are healed with ferroan dolomite or calcite cement, and some are open. Solution-enlarged fenestral porosity in the stromatolitic lithology is filled with pyrobitumen and dolomite cement. A 2-in.-thick zone of granule- to pebble-sized sedimentary breccia is present at –2,869.5 ft.

–2,865 to –2,861 ft

This interval is comprised of cherty, dolomitic subtidal mudstones. Disconformity surfaces, dissolution channels, and rubbly breccias are evidence of paleokarstification in these rocks. Channel porosity as much as 0.75 in. in diameter has been partially or entirely occluded by infilling clay, subisopachous dolomite cement, and pyrobitumen.

Arbuckle Group rocks are unconformably overlain by Simpson Group sandstone at –2,861 ft. Solution-enlarged fractures below the unconformity may contain sand derived from the overlying Simpson beds.

Core: Oliphant 1-Lafortune
Location: Sec. 8, T25N, R6E, Osage County, OK
Cored Interval: –3,335.5 to –3,361.5 ft
Stratigraphic Interval: Simpson and Arbuckle (Cotter Formation?) Groups
Core Description: The following description is given in reference to the core photograph (Fig. 17) and to the petrolog of this core (Pl. 2).

–3,361.5 to –3,350 ft

This interval is comprised of dense, dolomitic mudstones, with a thin, silty greenish shale present at –3,355 ft. A faint, clast-supported brecccia of uncertain origin is present at –3,359 to –3,360 ft. A thin, quartz-sand-rich dolomudstone bed at –3,354.9 ft shows the effects of in-place brecciation, perhaps due to foundering instigated by compaction of the underlying shale. An erosional disconformity is present at –3,352 ft; mudstones below the unconformity are crackle-brecciated, while the mudstones above appear to be brecciated by collapse. The dolomudstones of this interval may be of subtidal origin.

–3,350 to –3,335.5 ft

This interval comprises interbedded dolomitic mudstones, packstones, grainstones, and algal laminites of

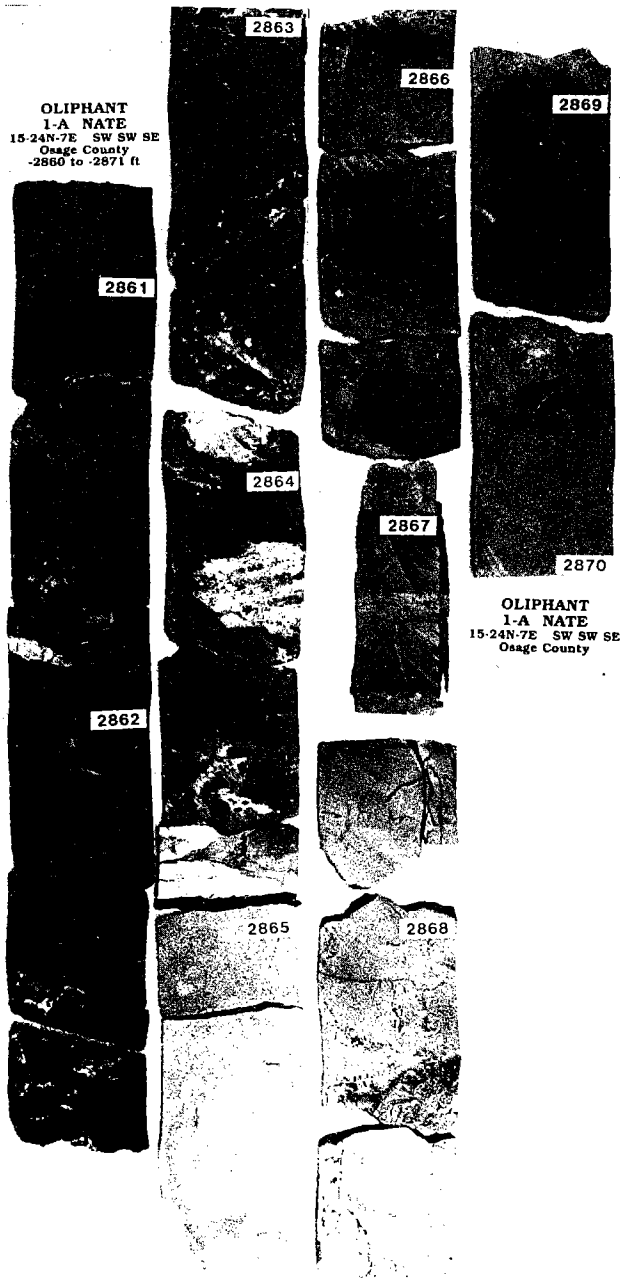


Figure 16. Oliphant 1-A Nate core.

probable intertidal origin. A sedimentary conglomerate containing pebbles of dolomudstone within a quartz-sand-rich dolomicrite matrix occurs at –3,349 to –3,350 ft. Noncontemporaneity between clasts and matrix is suggested by the fact that the clast lithology is entirely devoid of quartz sand. The conglomerate is overlain by 1.5 ft of algal boundstone that has faint stromatolitic structure. The uppermost 7.5 ft of this interval (–3,347.5 to –3,335 ft) contains interbedded dolomudstones and intraclast packstones that appear karstified; the rocks are randomly brecciated and are transected by dissolution channels that are filled with Arbuckle-derived bioclastic and lithoclastic debris and Simpson sand. Shaly sandstone of the Simpson Group (Burgen Formation?) overlies truncated Arbuckle rock in planar unconformity at –3,335.5 ft.

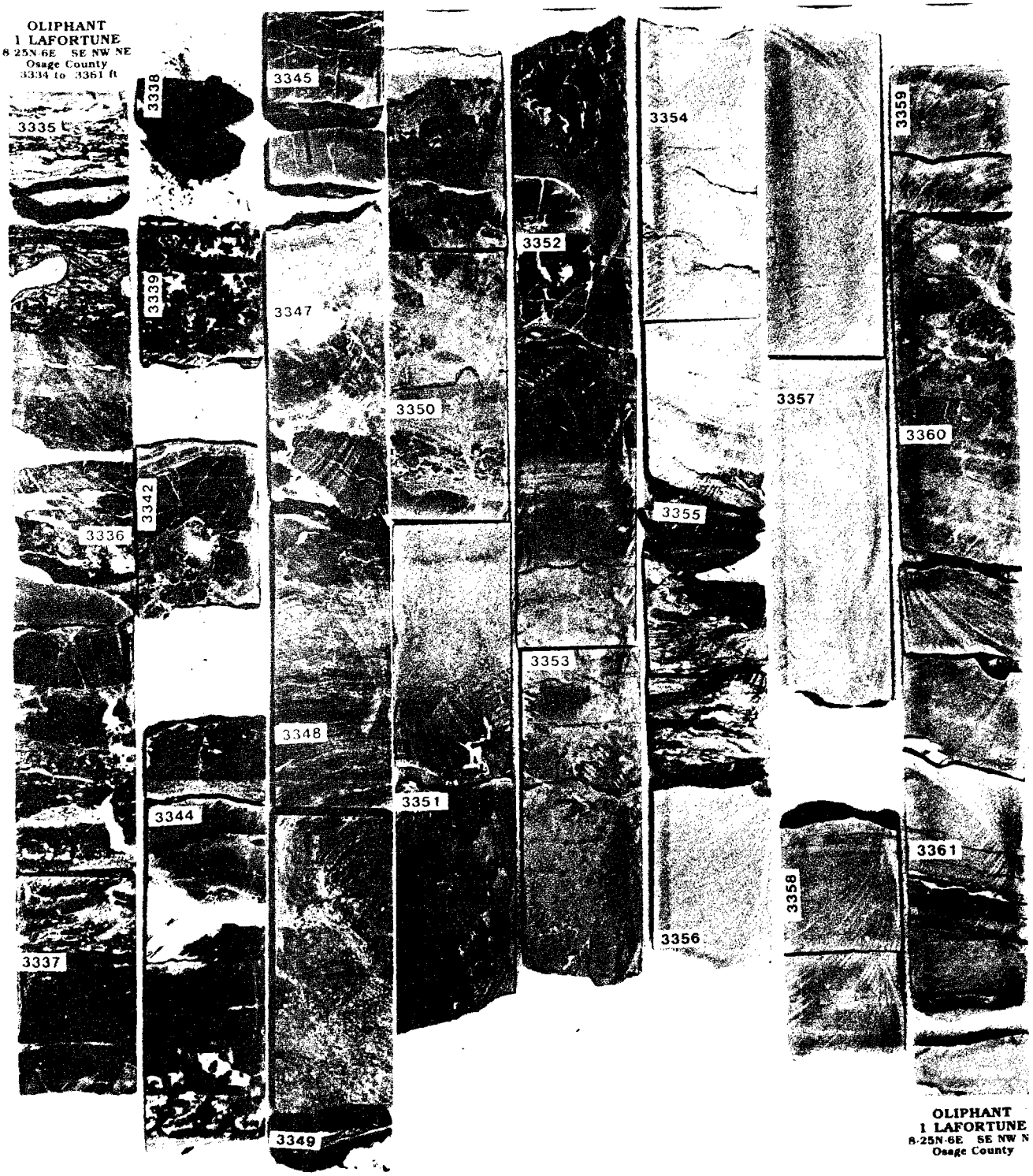


Figure 17. Oliphant 1-Lafortune core.

Core: Getty 6-Cobb
Location: Sec. 3, T17N, R7E, Creek County, OK
Cored Interval: –2,466 to –2,517 ft
Stratigraphic Interval: Arbuckle Group (formation unknown)
Core Description: The following description is given in reference to the core photograph (Fig. 18) and to the petrolog for this core (Pl. 3).

–2,517 to –2,487 ft

This interval is mostly comprised of tan to dark-brown, sucrosic dolomudstones that are probably of subtidal origin. Numerous breccias are present, including collapse breccia from –2,510 to –2,507 ft, –2,503 to –2,498 ft, and also –2,490 to –2,487 ft. The breccia-internal sediment consists of well-rounded detrital quartz and feldspar and dolomudstone. Additionally, a sedimentary breccia is present at –2,506.5 to –2,504 ft. In this breccia, pebble- to cobble-sized clasts of dolomudstone and chert are surrounded by interlaminated green shale and dolomudstone.

–2,482 to –2,466 ft

This interval is comprised of collapse breccia in brown, sucrosic, intertidal dolomudstones and ooid wackestones/packstones. Breccia clasts range from granule- to boulder-size, and considerable rotation of some clasts is evident. The sucrosic dolomite in the ooid wackestone/packstone facies has well-developed oomoldic and intercrystalline porosity. Fine, well-rounded quartz sand is present within the breccia-internal sediment; igneous and metamorphic rock fragments were not observed.

–2,466 to –2,465(?) ft

This thin zone comprises the residual conglomerate at the eroded top of the Arbuckle Group in this core. Pebbles of reworked Arbuckle rock are present within a shaly sandstone matrix in this conglomerate. Conodonts recovered from this conglomerate indicate that it is of Pennsylvanian age.

The Arbuckle rocks in this core are overlain by shales and sandstones of the Pennsylvanian Bartlesville Sandstone (not pictured in the photograph in Fig. 18).

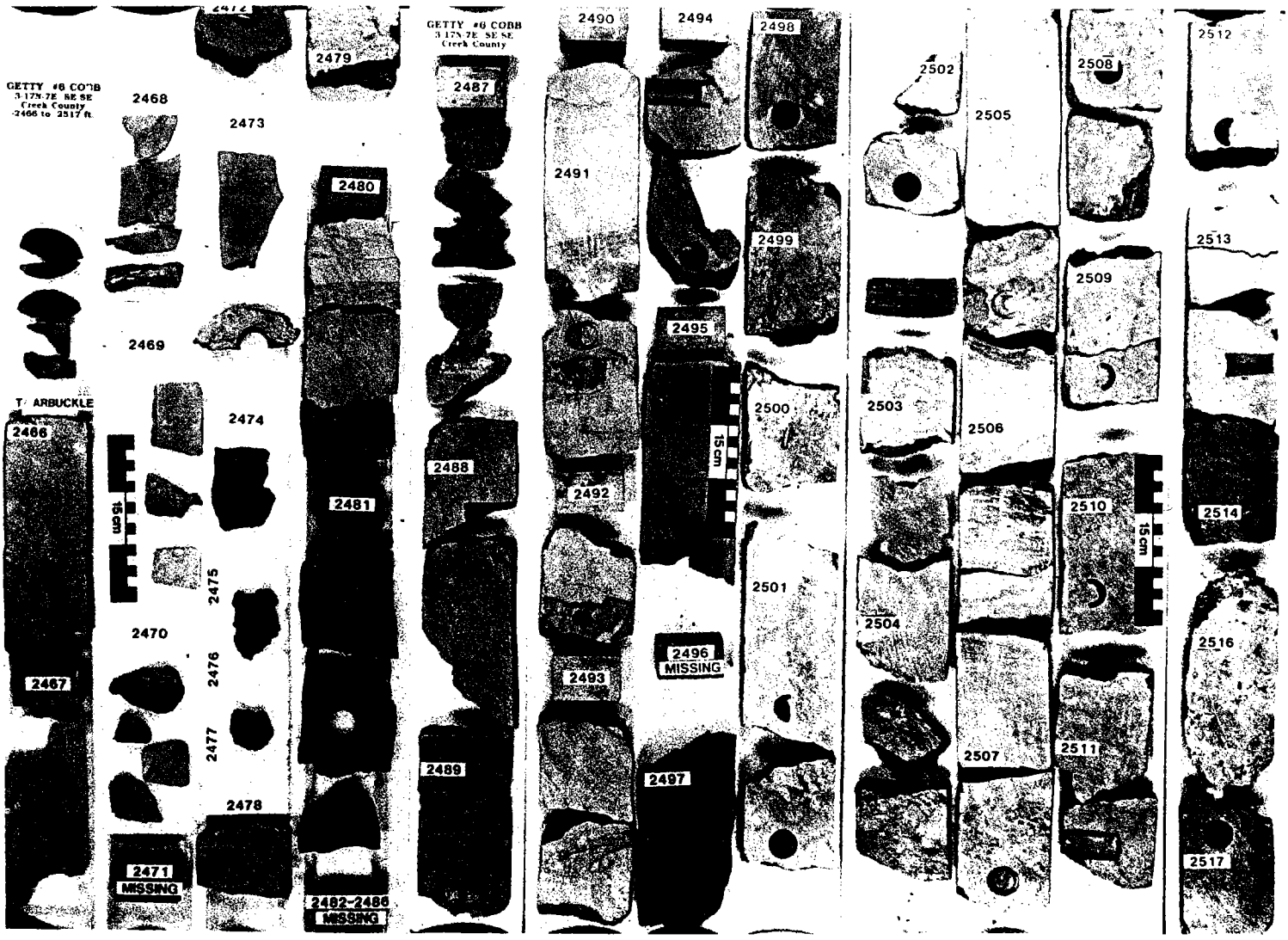


Figure 18. Getty 6-Cobb core.

Core: Cameron 1-Shepherd
Location: Sec. 20, T3S, R4W, Jefferson County, OK
Cored Interval: –6,278 to –6,296 ft
Stratigraphic Interval: Arbuckle Group (formation uncertain)
Core Description: The following description is given in reference to the petrolog for this core (Pl. 4).

The cored "interval" actually consists of a few rubbly pieces of collapse breccia; it may be that the fractured and brecciated nature of the rock prevented recovery during the coring operation.

This monomictic collapse breccia consists of nearly rectangular pebbles of dolomudstone and three lithologies of infill sediment. Geopetal dolomudstone was the first lithology to be deposited, followed by a finely laminated dolosiltite. This lithology was partially lithified, then eroded and redeposited within a matrix of shaly dolomite. Isopachous crusts of saddle dolomite coat the breccia clasts.

Core: Shell 1A-3 Wesley Unit
Location: Sec. 3, T4S, R3W, Carter County, OK
Cored Interval: –3,584 to –3,633 ft
Stratigraphic Interval: Arbuckle Group (Kindblade Formation)
Core Description: The following description is given in reference to the core photographs (Fig. 19) and to the petrolog for this core (Pl. 5).



Figure 19. Shell 1A-3 Wesley Unit core.

–3,633 to –3,603.3

This interval is comprised predominantly of very finely laminated, sometimes hummocky or nodular dolomudstones that may be of subtidal origin. A thin breccia (possibly parabreccia or collapse breccia) is present at –3,625 ft, and is conspicuous due to the thick rind of saddle-dolomite cement present on the breccia clasts. Vugular porosity developed in medium- to coarse-crystalline dolomite is present from –3,624 to –3,620 ft. The primary depositional fabric of this zone has been obliterated by dolomitization. The rocks of this interval are extensively (tectonically) fractured. Thick stylolites in these rocks attest to considerable pressure solution.

–3,603.3 to –3,595 ft

The rocks in this interval have been extensively dolomitized; medium- to coarse-crystalline xenotopic and saddle-rhombic varieties of dolomite are commonly present. Depositional fabric is obscure, but faint wavy laminations reminiscent of algal boundstones are present and suggest an upper-intertidal to lower-supratidal origin. Solution-enlarged, fenestral(?) vugular porosity is present in this lithology. A small, sediment-filled solution channel is present at –3,604.5 ft.

–3,595 to –3,584 ft

This interval is comprised mostly of dense and wavy laminated, tan and gray, clayey dolomudstones. Such lithologies are suggestive of subtidal deposition. The dolomite in this interval is typically microcrystalline or fine crystalline. These rocks are cut by numerous perpendicular and oblique-to-bedding (tectonic) fractures. A small fault(?) or fracture with considerable vertical offset is present at –3,590 to –3,591 ft. Swarms of variable relief, sinuous, and serate stylolites are accentuated by the abundance of terrigenous clays in these rocks.

Core: E. L. Cox 1-Wesley Unit A
Location: Sec. 3, T4S, R3W, Carter County, OK
Cored Interval: –3,806 to –3,983 ft

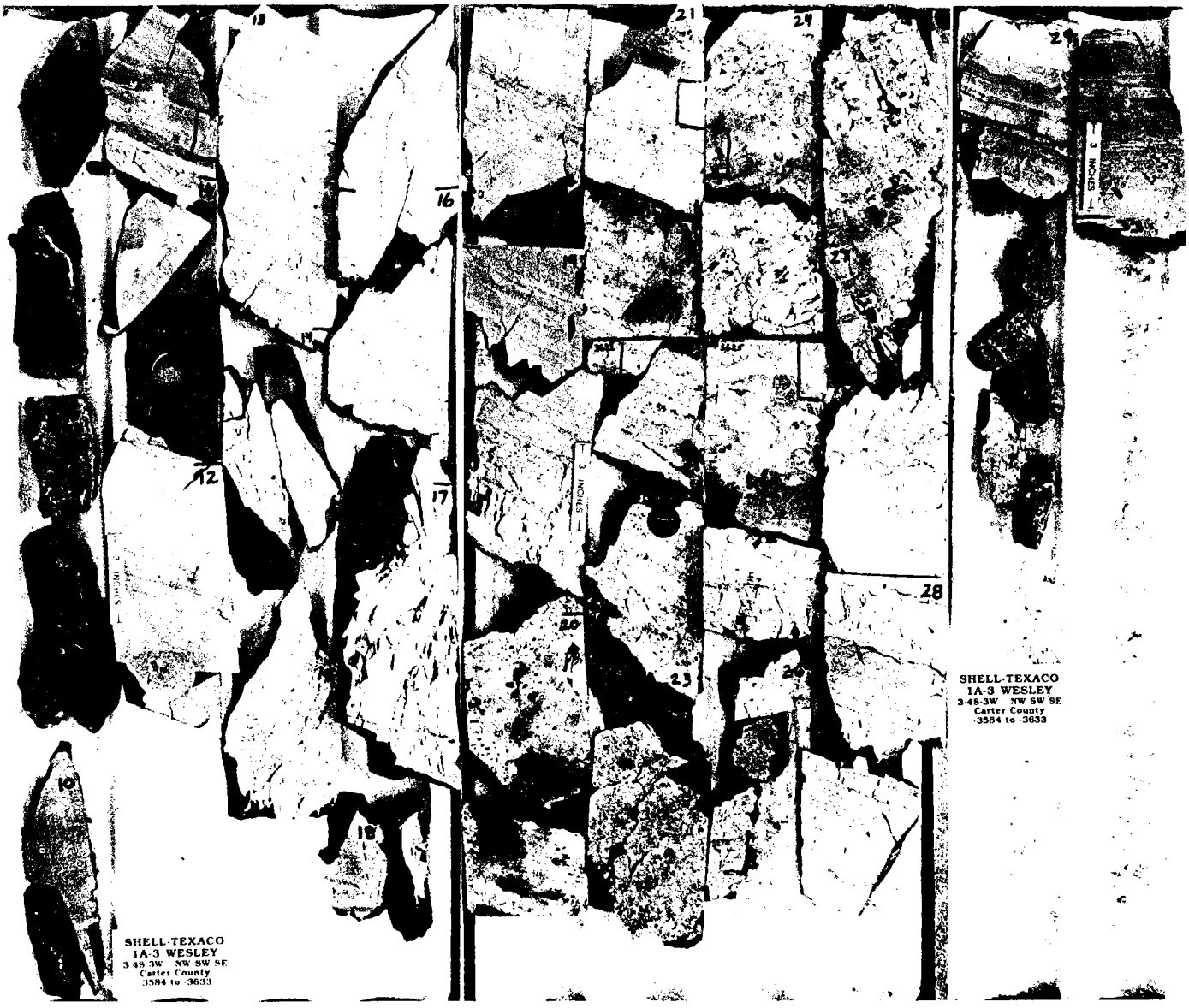


Figure 19. *(continued)*

Stratigraphic Interval: West Spring Creek–Kindblade Formations

Core Description: The following description refers to the core photographs (Fig. 20) and to the petrolog for this core (Pl. 6).

–3,983 to –3,960 ft

This interval is comprised of tan and gray, fine-laminated and massive dolomudstones. Collapse breccias are common, notably occurring at –3,979 to –3,974 ft, and at –3,967 to –3,964 ft. These breccia commonly have light-tan dolomudstone filling the breccia-intergranular porosity. A cavern-fill parabreccia is present at –3,972 to –3,971 ft. The clasts in this breccia are fractured chert, the next closest occurrence of which is at –3,939 ft in the core. Solution-enlarged fractures and vugs occur frequently in these rocks. All breccias and paleokarstic dissolution features are transected by tectonic fractures.

–3,960 to –3,937 ft

This interval is almost entirely made up of "zebroid" collapse breccia—a notable exception is the cavern-fill parabreccia at –3,939 ft. The "zebroid" breccia facies exhibits both random and crackle-breccia fabrics, and is almost entirely cemented by coarse columnar and saddle dolomite. Host rock in this breccia is fine- to medium-crystalline dolomicrite/dolomicrospar and clay-associated rhombic dolomite. Fractures in the crackle-brecciated horizons are predominantly parallel-to-bedding and cemented by dolomite; open tectonic fractures cut all lithologies and paleokarstic features. Extensive dolomitization has obliterated sedimentary structures; the depositional environment of these rocks is therefore uncertain.

–3,937 to –3,890 ft

Tan and gray, massive, fine-crystalline dolomudstones dominate this interval; locally (as at –3,909 ft) faint algal laminations may be present. This interval contains a sequence of intensely fractured, dolomite-cemented rocks that resemble the "zebroid" breccia of the previous interval. However, these rocks appear to have suffered only minor movement along fractures; whereas the previously described breccia showed more obvious signs of collapse.

–3,890 to –3,870 ft

This interval is notable in that it marks the only occurrence of limestone in this core. Slightly fossiliferous, hummocky-bedded, clayey blue-gray subtidal mudstones occur from –3,884 to –3,876 ft; the rocks above and below the limestone beds are either dolomitic limestone or limey dolomite (the latter occurs more frequently away from the limestone beds in either direction). Unlike the dolomitic rocks above and below, this interval is very infrequently cut by open tectonic fractures. Also, fractures in the dolomitic rocks tend to be short, open, and randomly oriented (the rock typically looks shattered); whereas the fractures present in the limestone beds are quite continuous, more singular in occurrence, and tend to be cemented by ferroan calcite.

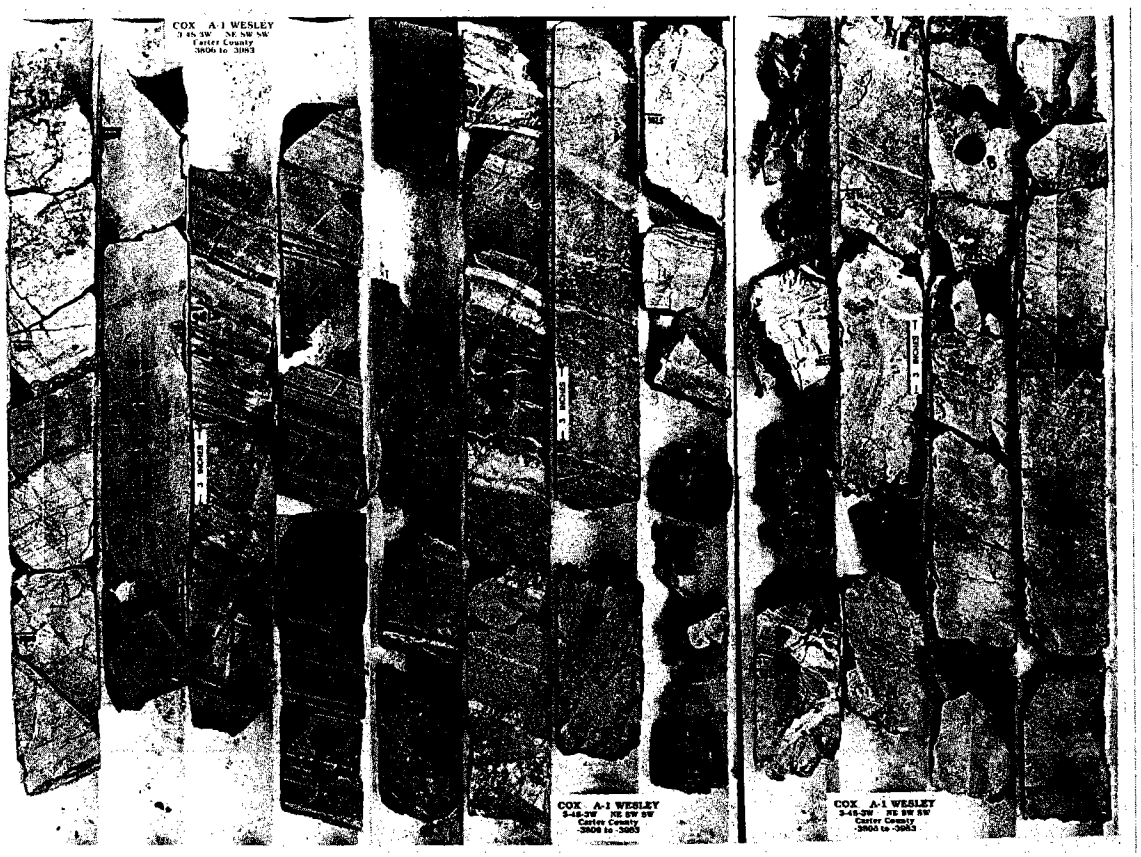


Figure 20. E. L. Cox 1-Wesley Unit A core.

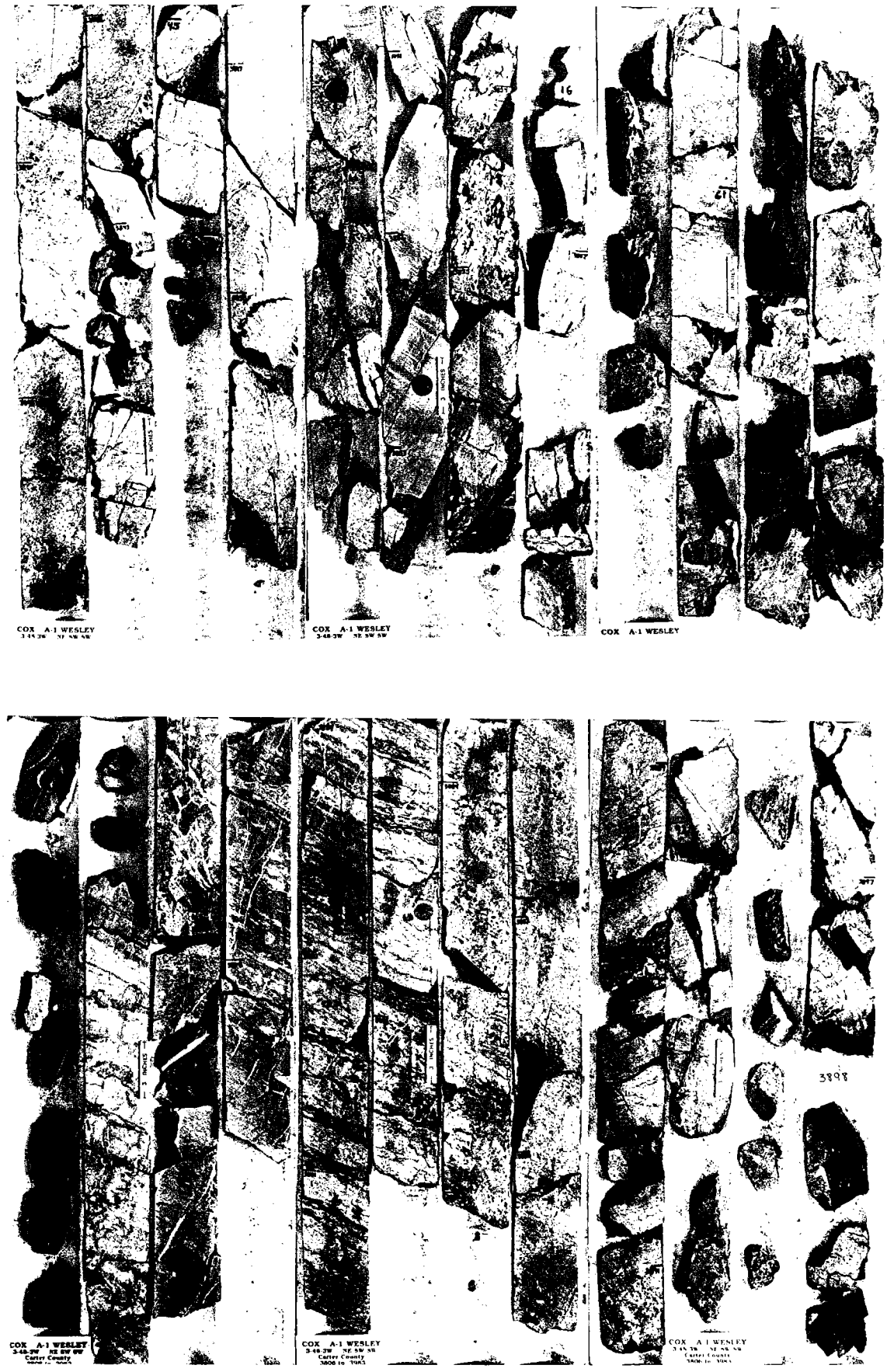


Figure 20. *(continued)*

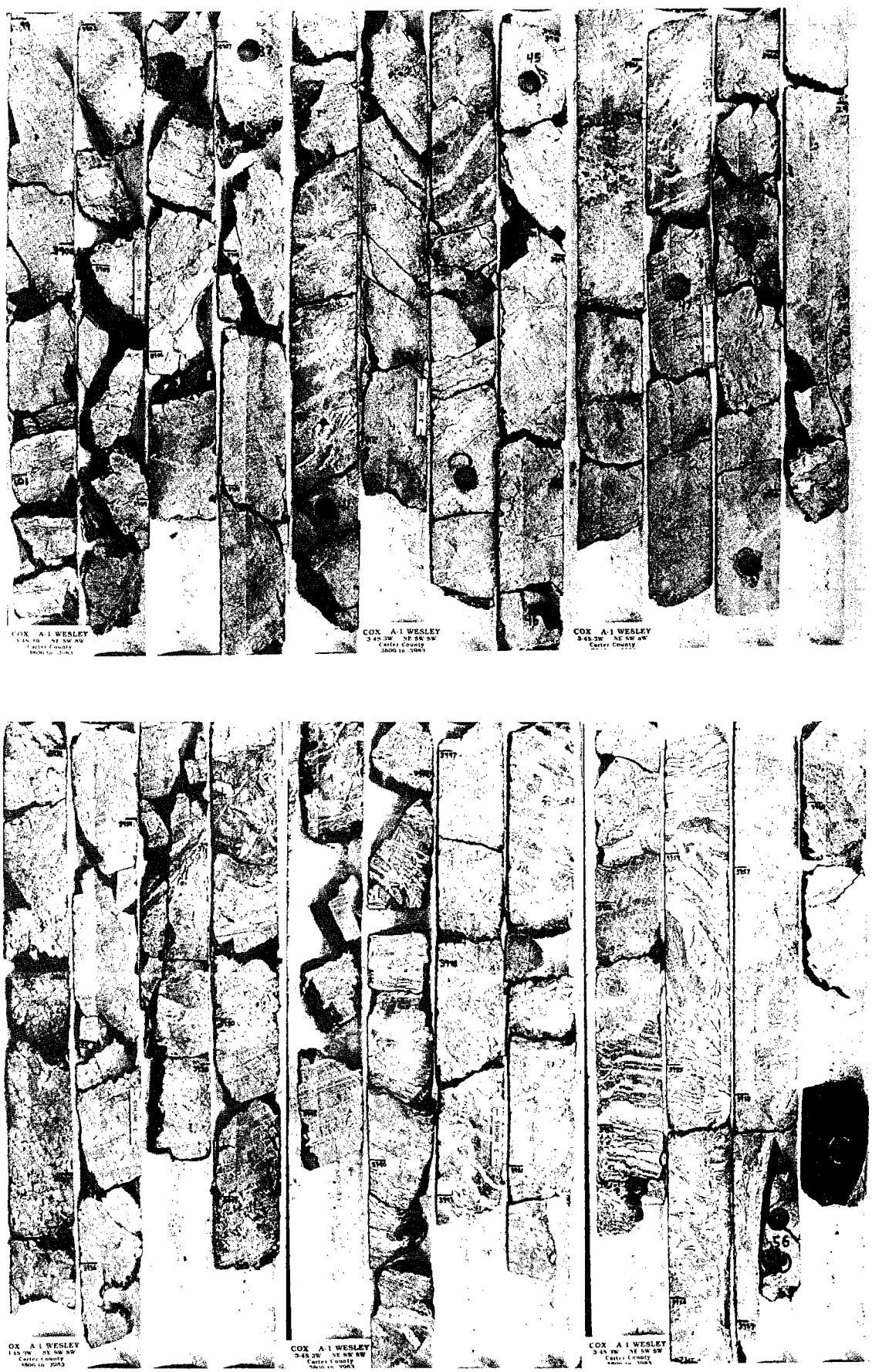


Figure 20. *(continued)*

–3,870 to –3,806 ft

This interval is comprised mostly of tan and gray dolomudstones that exhibit very regular horizontal lamination. An exception to this regularity occurs in a vugular porous zone from –3,842 to –3,831 ft, below what may be an erosional intra-Arbuckle disconformity at –3,831 ft. Vugs as much as 1.5 cm in diameter are present in this zone. Early, parallel- and perpendicular-to-bedding fractures (crackle breccia) are cemented with coarse saddle-dolomite cement. Tectonic fractures are noticeable, though they are not as prevalent here as in some dolomitic zones below.

Core: Texaco 1-Mobil
Location: Sec. 1, T5S, R1W, Carter County, OK
Cored Interval: –6,300 to –6,310 ft (core 1)
–6,519 to –6,534 ft (core 2)
Stratigraphic Interval: West Spring Creek and/or Kindblade Formation

Core Description: The following description is given in reference to the core photographs (Fig. 21) and to the petrolog of this core (Pl. 7).

Core 1

–6,310 to –6,305.7 ft

This interval is comprised of fractured and crackle-brecciated, blue-gray subtidal dolomudstones which may represent the host-rock floor of a paleocavern. The host rock has slightly mottled to massive bedding which dips ~27° from horizontal.

–6,305.7 to –6,300 ft

This interval contains a heterolithic collapse breccia adjacent to what may be the in-place host-rock wall of a paleocavern. The host lithology is the same as that described above. The breccia contains at least two types of dolomudstone: one is fine crystalline and resembles the host rock, while another is coarser crystalline xenotopic dolomite that does not occur in the host rock. Also present



Figure 20. *(continued)*

in the breccia are clasts of calcite cement, shale-rock fragments, and well-rounded quartz sand. A laminar crust of columnar calcite coats the host-rock "wall," separating it from the juxtaposed breccia.

Core 2

–6,534 to –6,526 ft

This interval is comprised of tan and blue-gray, quartz-sand-rich subtidal dolomudstones. Perpendicular-to-bedding fractures (the only effective type of porosity present) are saturated with dead oil.

–6,526 to –6,519 ft

This interval contains ~1.5 ft of rubbly collapse breccia (from –6,522.3 to –6,520.8 ft) bounded above and below by crackle breccia. The host lithology is tan, massive dolomicrospar. Where preserved, breccia-intergranular porosity is filled with dead oil. Vadose, pendant calcite cements are present on the bottoms of some breccia clasts. Vugular porosity is present at –6,519 to –6,520 ft, and seems to be concentrated along bedding planes.

Core: Pan American 1-State C
Location: Sec. 36, T2S, R10W, Cotton County, OK
Cored Interval: –7,475 to –7,500 ft
Stratigraphic Interval: Arbuckle Group (Kindblade Formation)
Core Description: The following description is given in reference to the core photographs (Fig. 22) and to the petrolog of this core (Pl. 8).

–7,500 to –7,475 ft

This core comprises 25 ft of heterolithic collapse breccia. At least seven different lithologies (of host-rock clasts and matrix) are present.

From –7,500 to –7,499 ft the host lithology is a dark-brown, massive dolomudstone. This lithology is extensively fractured and brecciated. Light-brown and tan, fine-laminated, cherty dolomudstones dominate the host rock from –7,499 to –7,491 ft. These beds dip slightly (20–25° from horizontal) and exhibit mosaic- and random-breccia fabric internally.

The dominant host lithology from –7,490 to –7,485.5 ft is brown, hummocky bedded, clayey dolomudstone. This lithology is more steeply dipping than the beds below (~33°) and occurs as cobble- to boulder-sized breccia clasts.

Blue-gray, fine-bedded (or thick-laminated) dolomudstones characterize the host rock from –7,487 to –7,484 ft. This lithology occurs as boulders in a breccia that also contains pebble- to cobble-sized clasts of chert, brown dolomudstone, and silicified ooid grainstone.

The breccia-clast population from –7,484 to –7,475 ft is dominated by cobble- to boulder-sized clasts of dark-brown, hummocky, burrow-mottled dolomudstone. Pebbles of chert, silicified ooid grainstone, and other dolomite types are present in lesser amounts. The breccia-matrix lithology throughout the core is a dark-brown, clayey dolomicrite. Petrographic examination of the matrix revealed the presence of dolomicrite, dolomicrospar, and clay-associated rhombic dolomite types. With the notable exception of the intertidal ooid grainstone, the host-rock lithologies present in this core are most likely of subtidal origin.



Figure 21. Texaco 1-Mobil core.

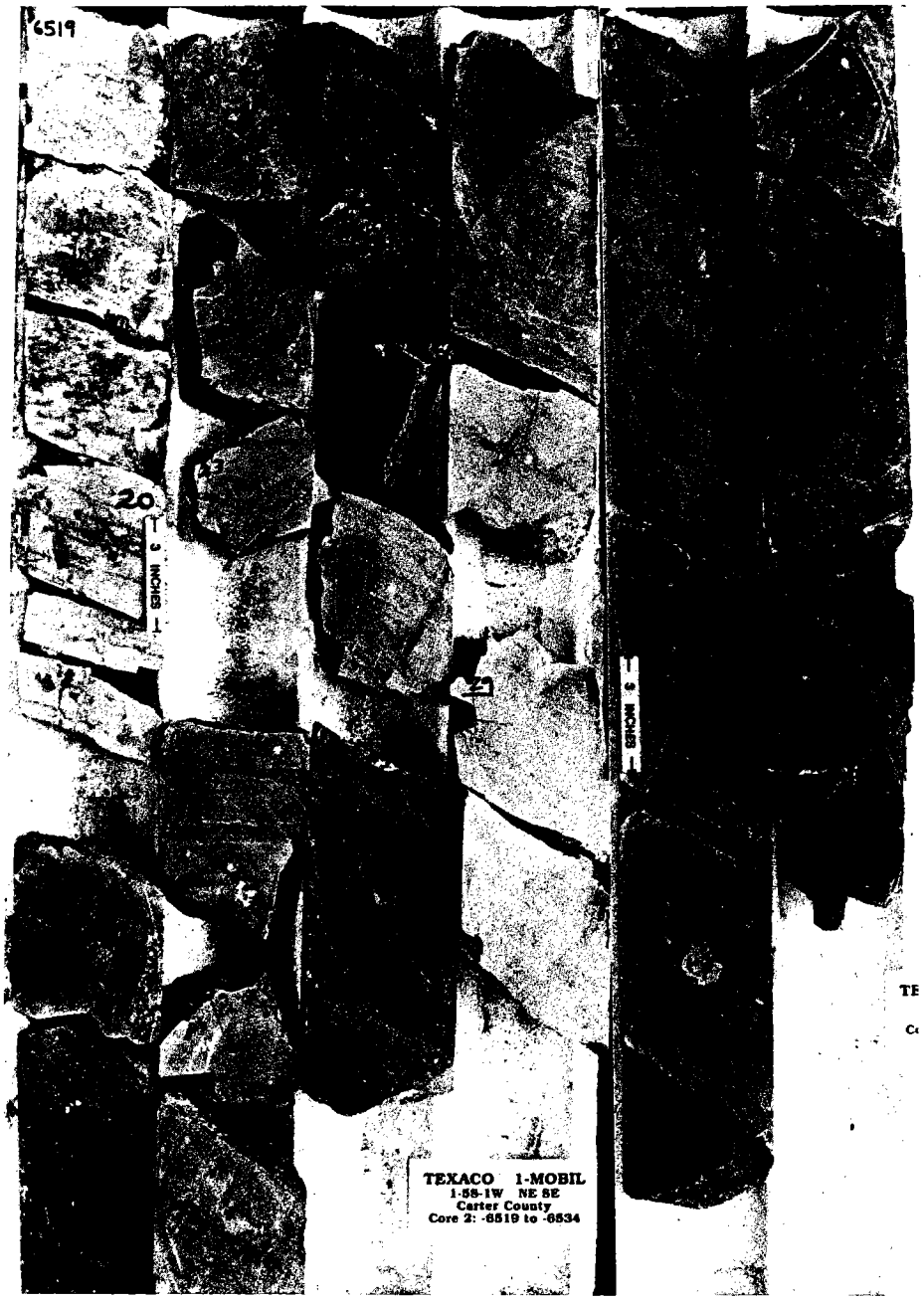


Figure 21. *(continued)*

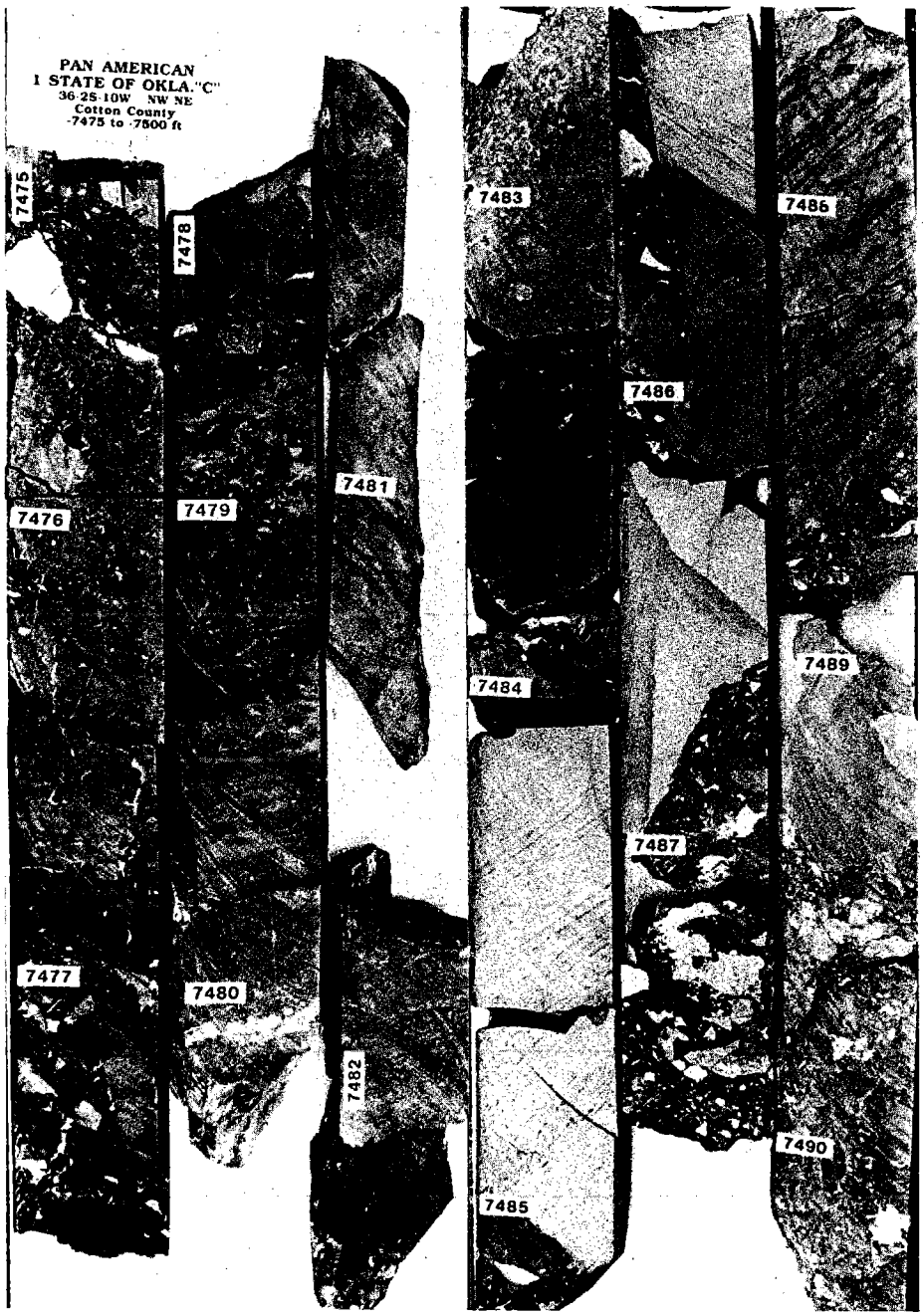


Figure 22. Pan American 1-State C core.

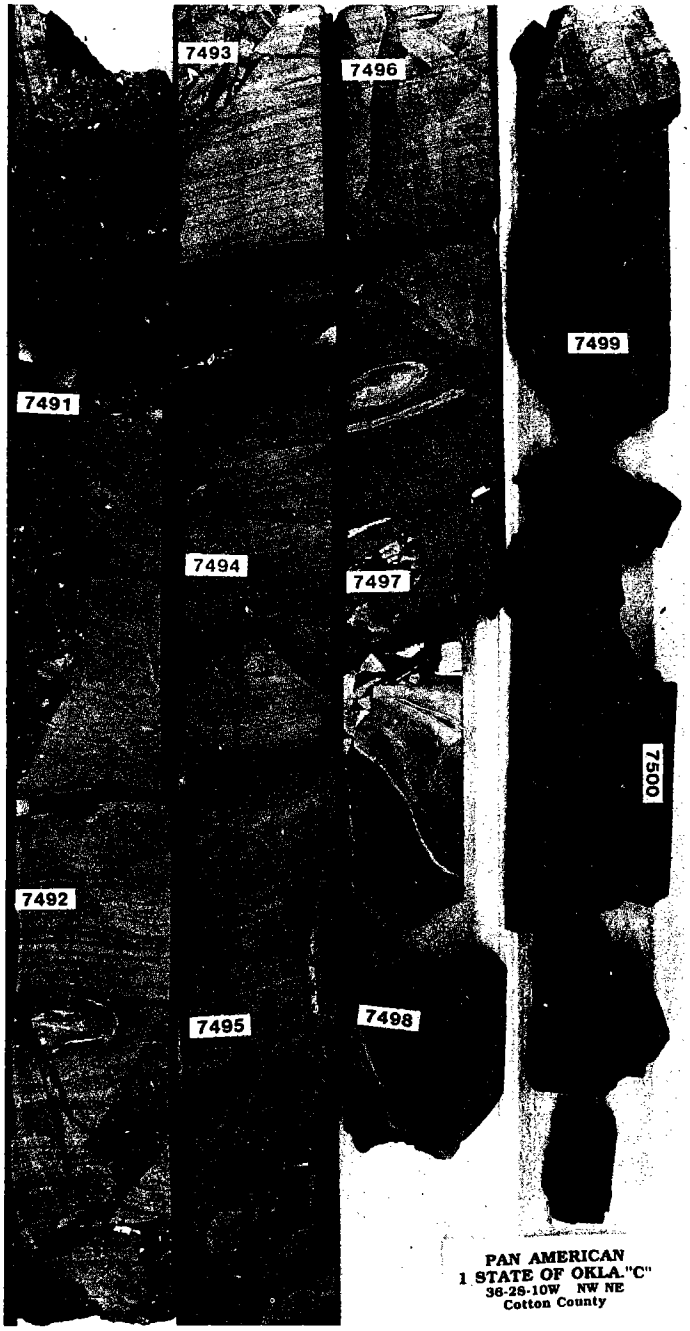


Figure 22. *(continued)*

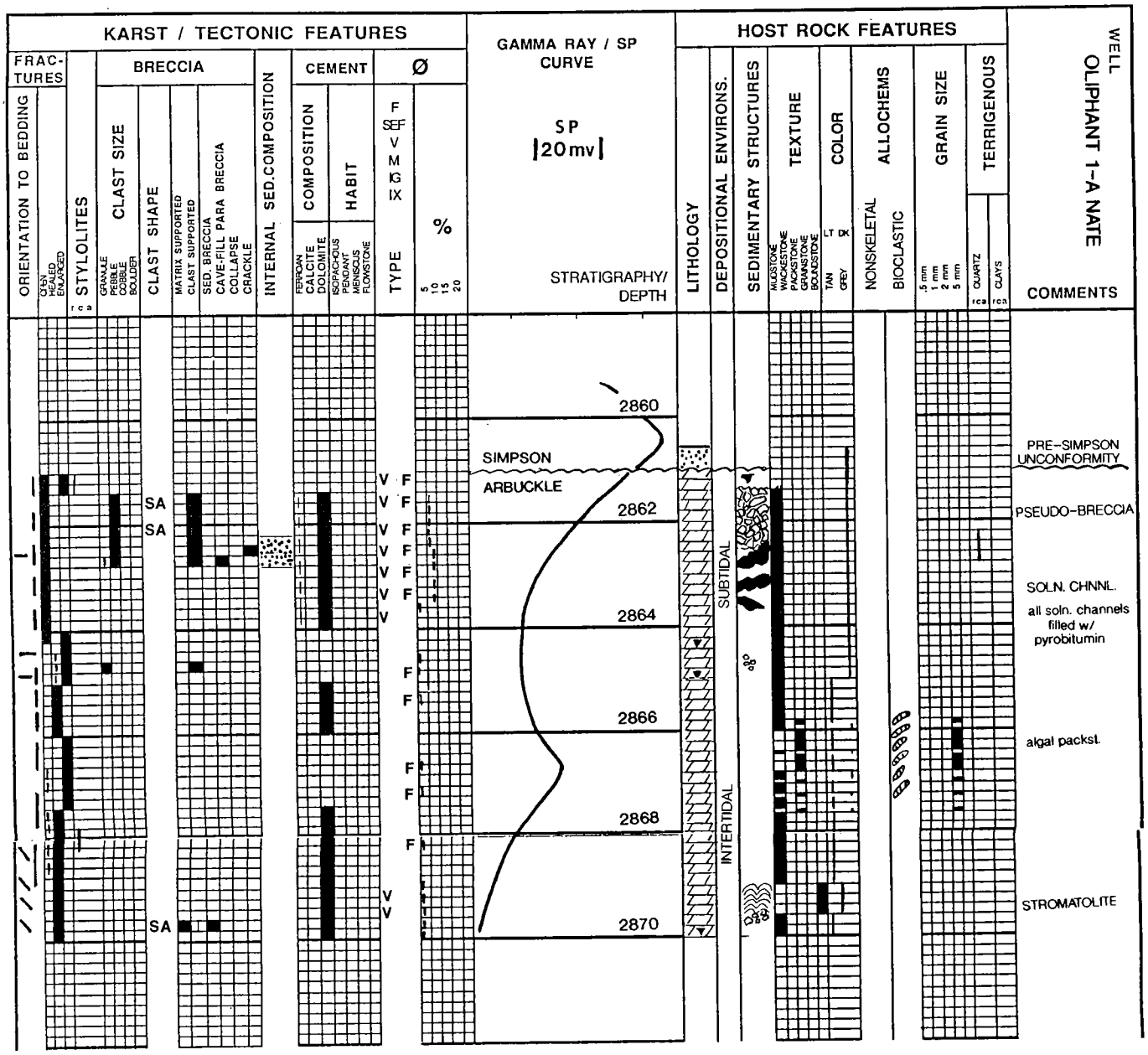


Plate 1. Petrolog of Oliphant 1-A Nate core, sec. 15, T. 24 N., R. 7 E., Osage County, Oklahoma.
Explanation of symbols (shown on Plate 4, p. 63) applies to Plates 1–8.

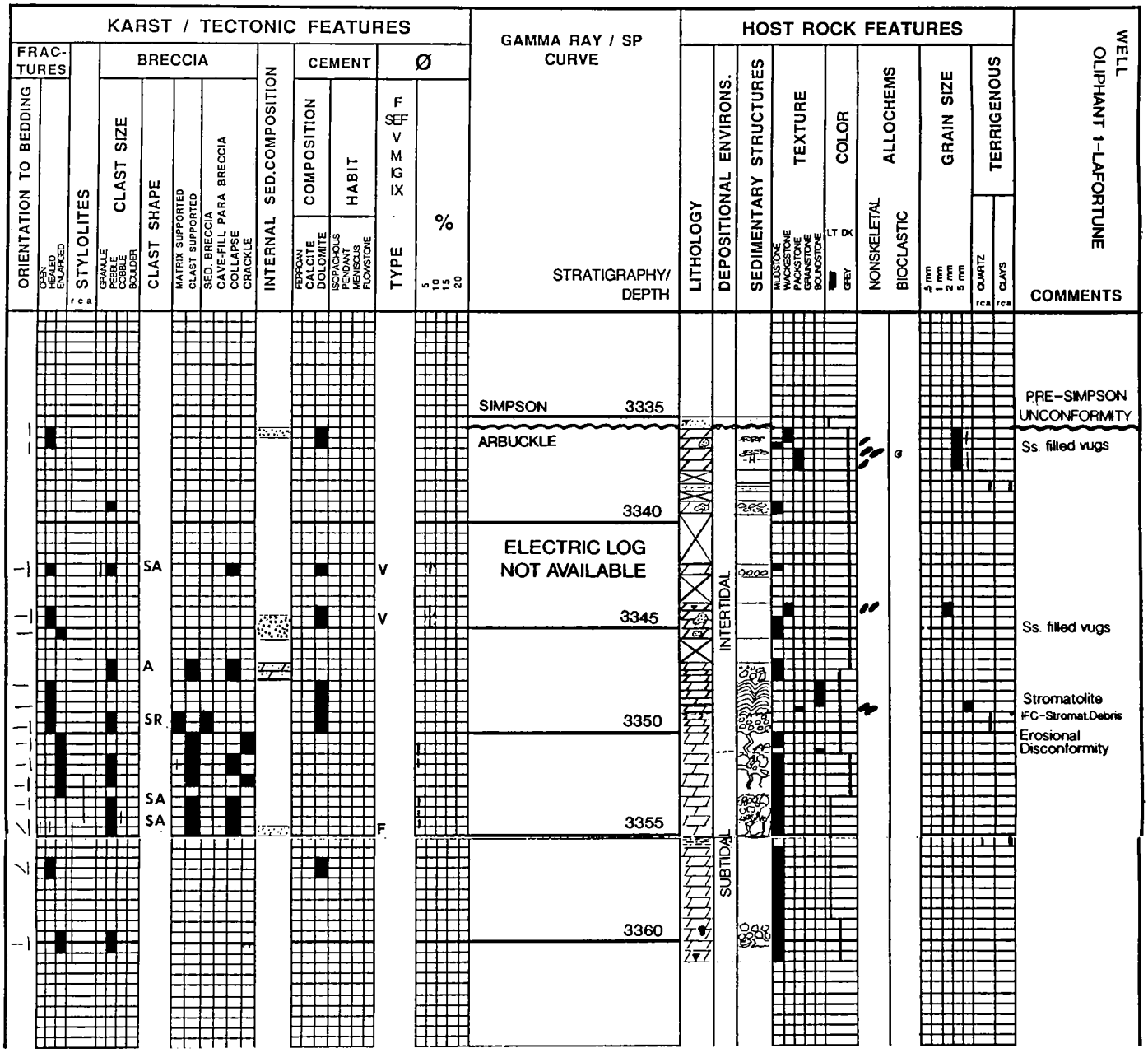


Plate 2. Petrolog of Oliphant 1-Lafortune core, sec. 8, T. 25 N., R. 6 E., Osage County, Oklahoma.

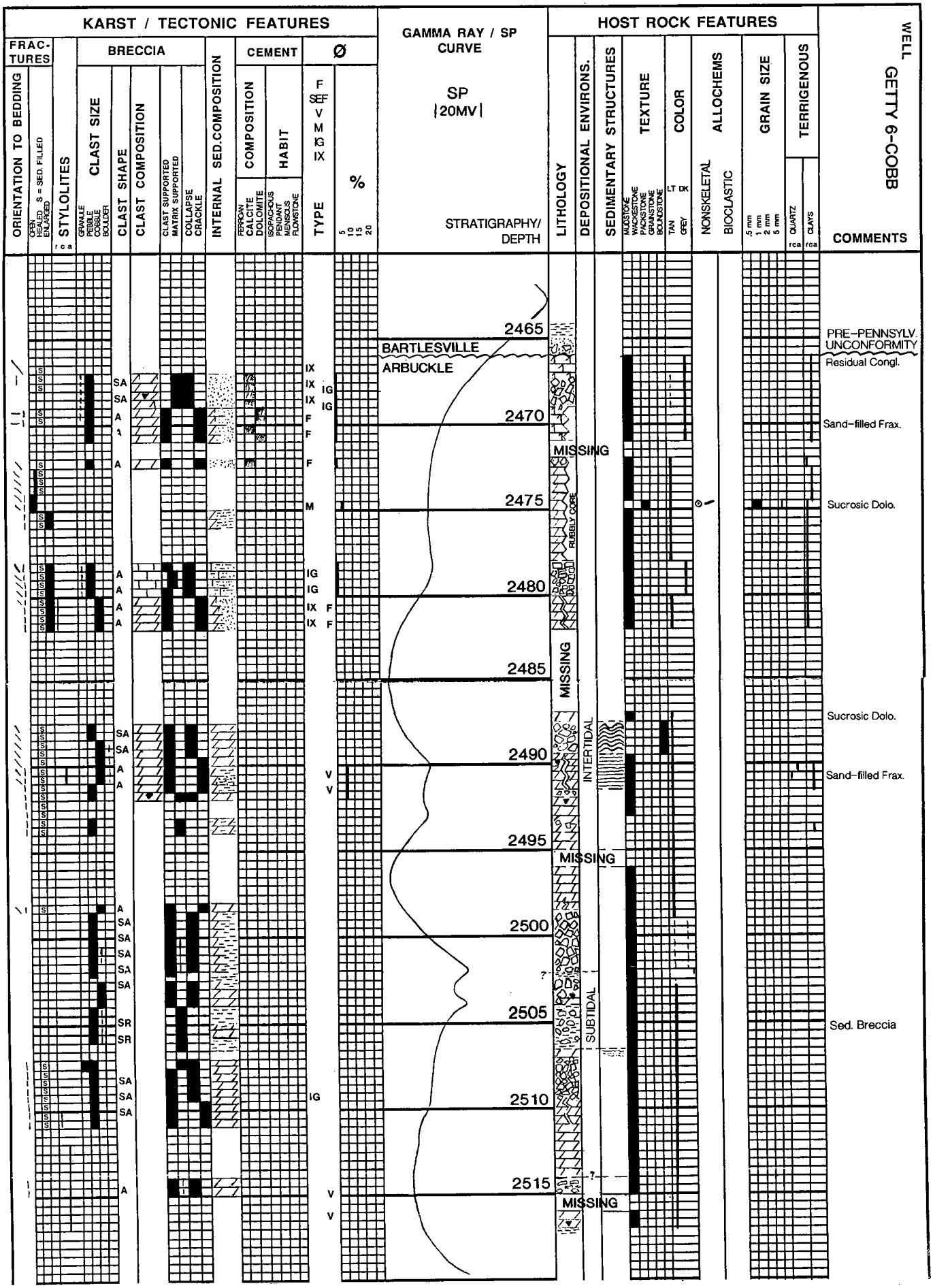
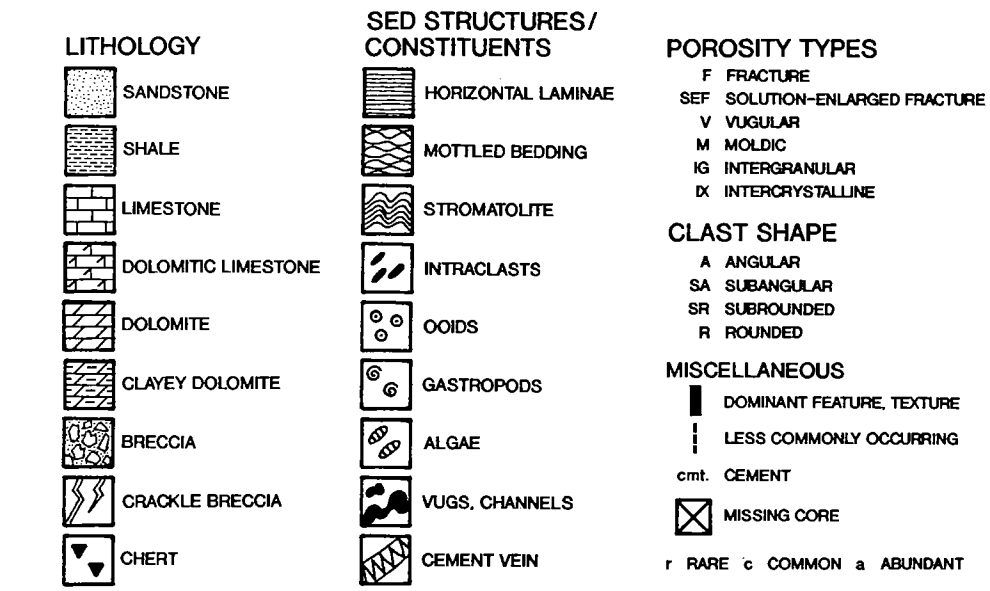


Plate 3. Petrolog of Getty 6-Cobb core, sec. 3, T. 17 N., R. 7 E., Creek County, Oklahoma.



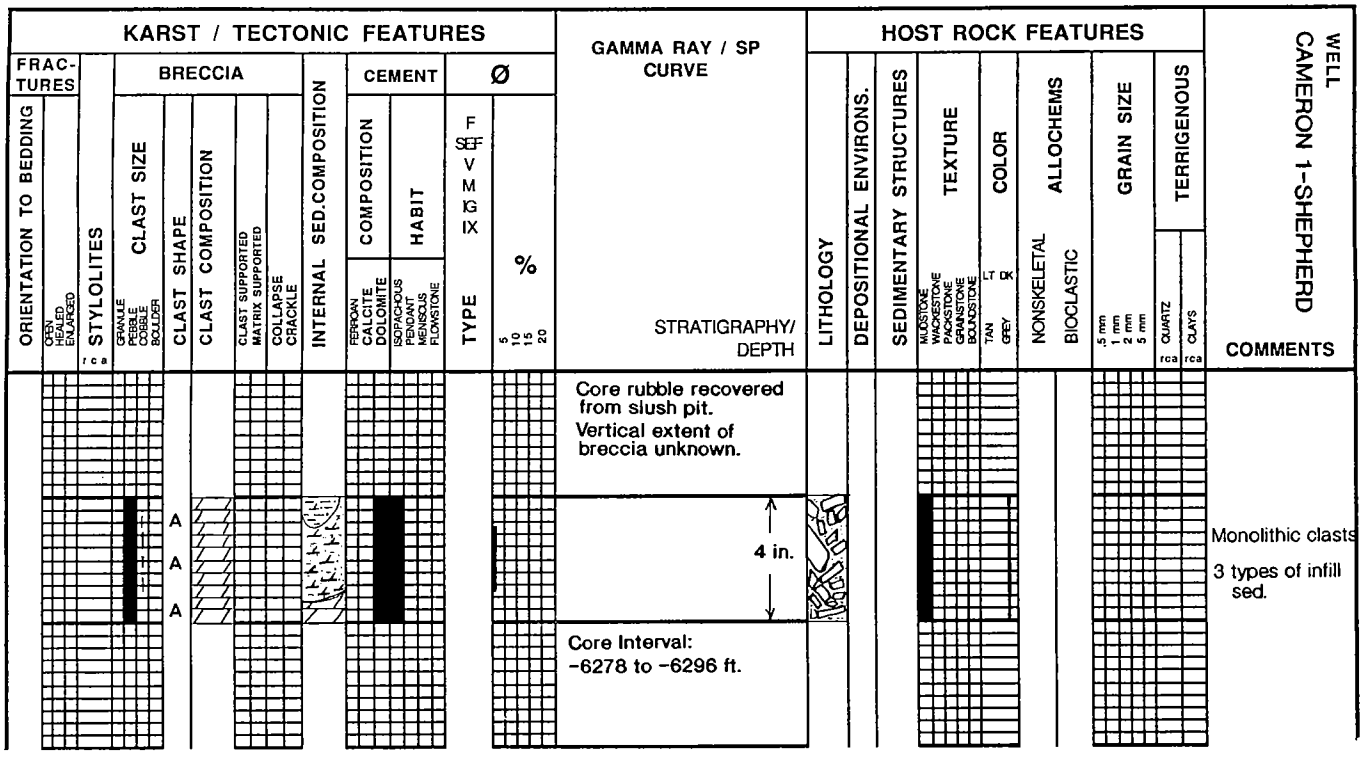


Plate 4. Petrolog of Cameron 1-Shepherd core, sec. 20, T. 3 S., R. 4 W., Jefferson County, Oklahoma.

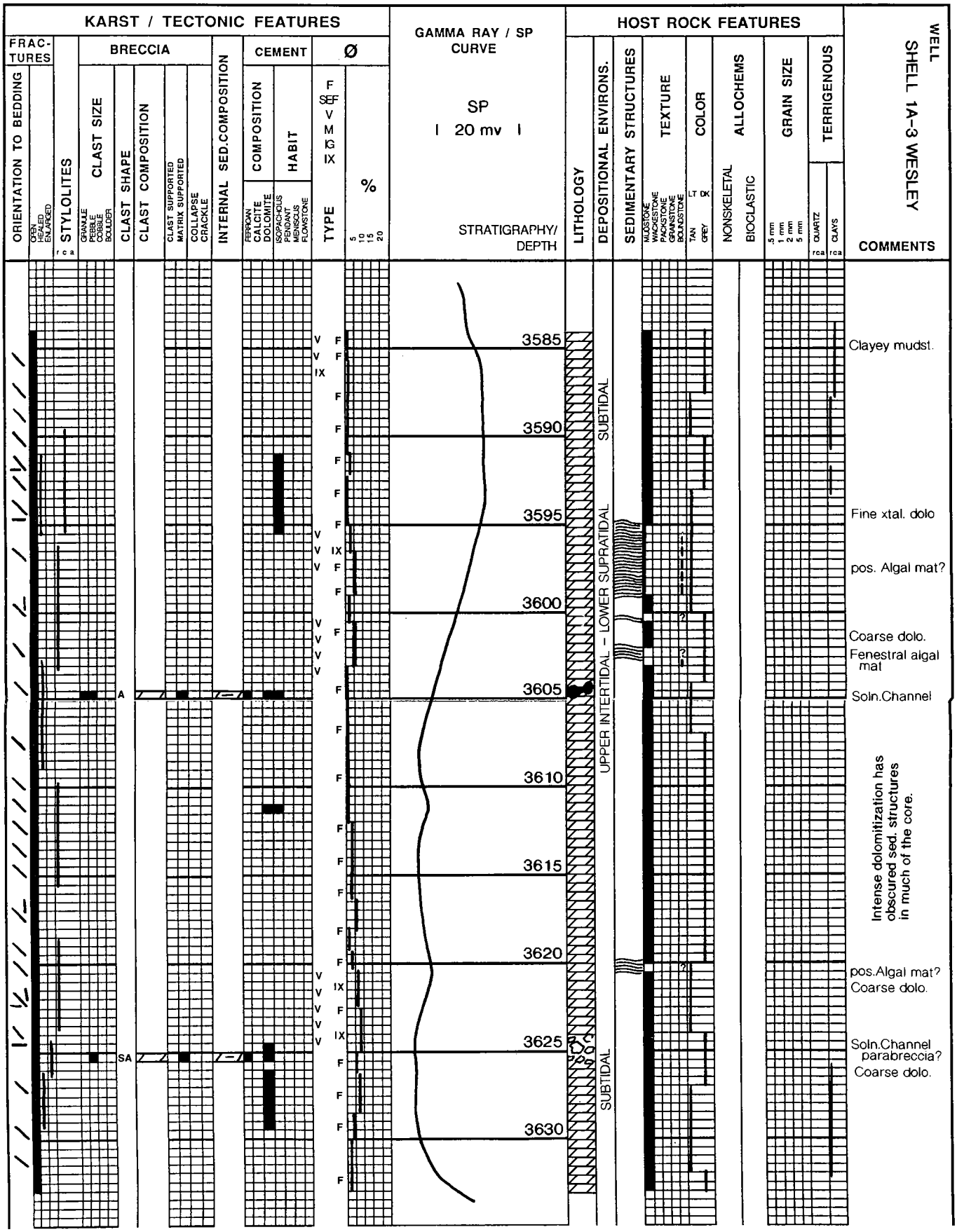
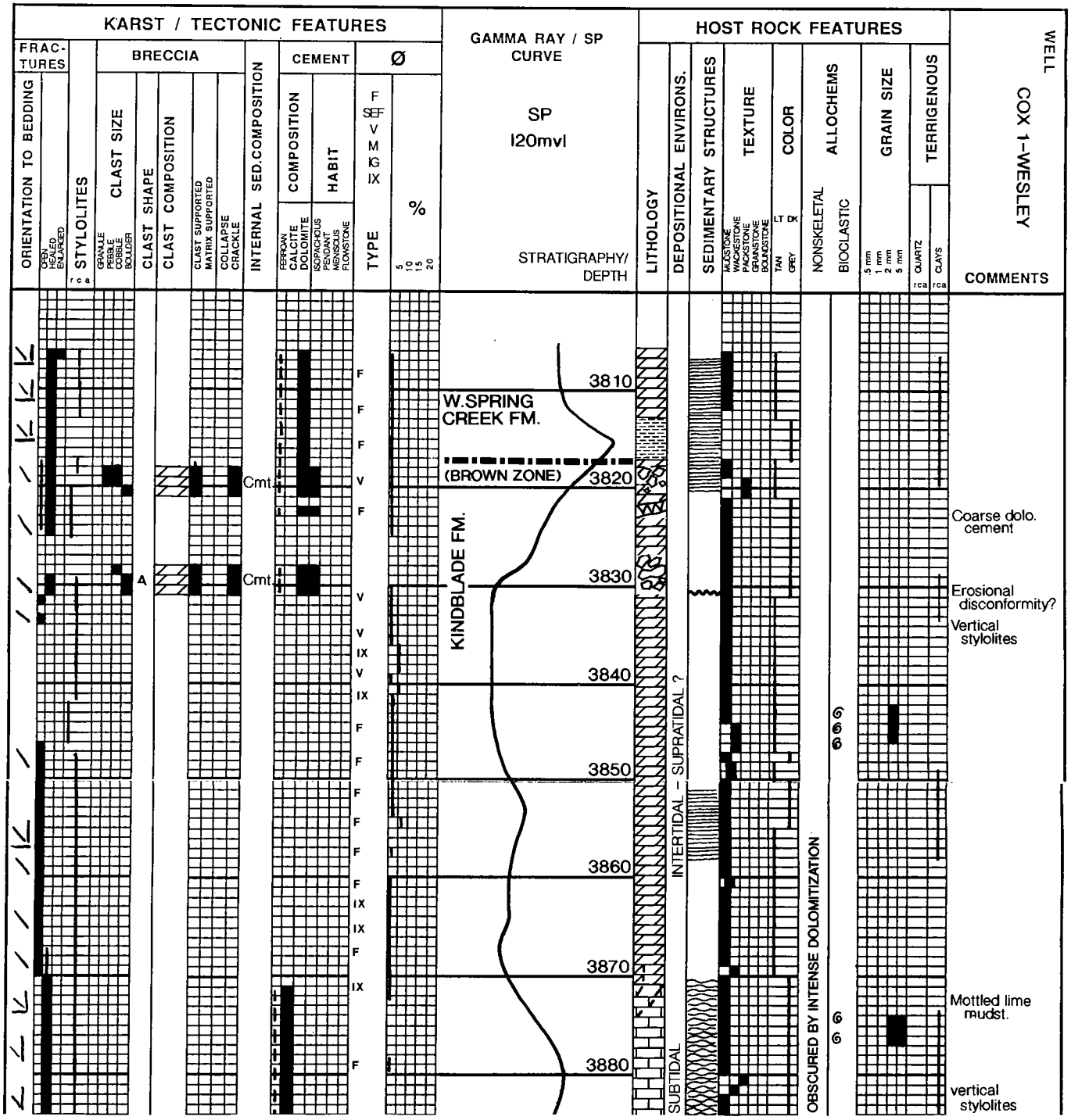


Plate 5. Petrolog of Shell 1A-3 Wesley Unit core, sec. 3, T. 4 S., R. 3 W., Carter County, Oklahoma.



(continued on next page)

Plate 6. Petrolog of E. L. Cox 1-Wesley Unit A core, sec. 3, T. 4 S., R. 3 W., Carter County, Oklahoma.

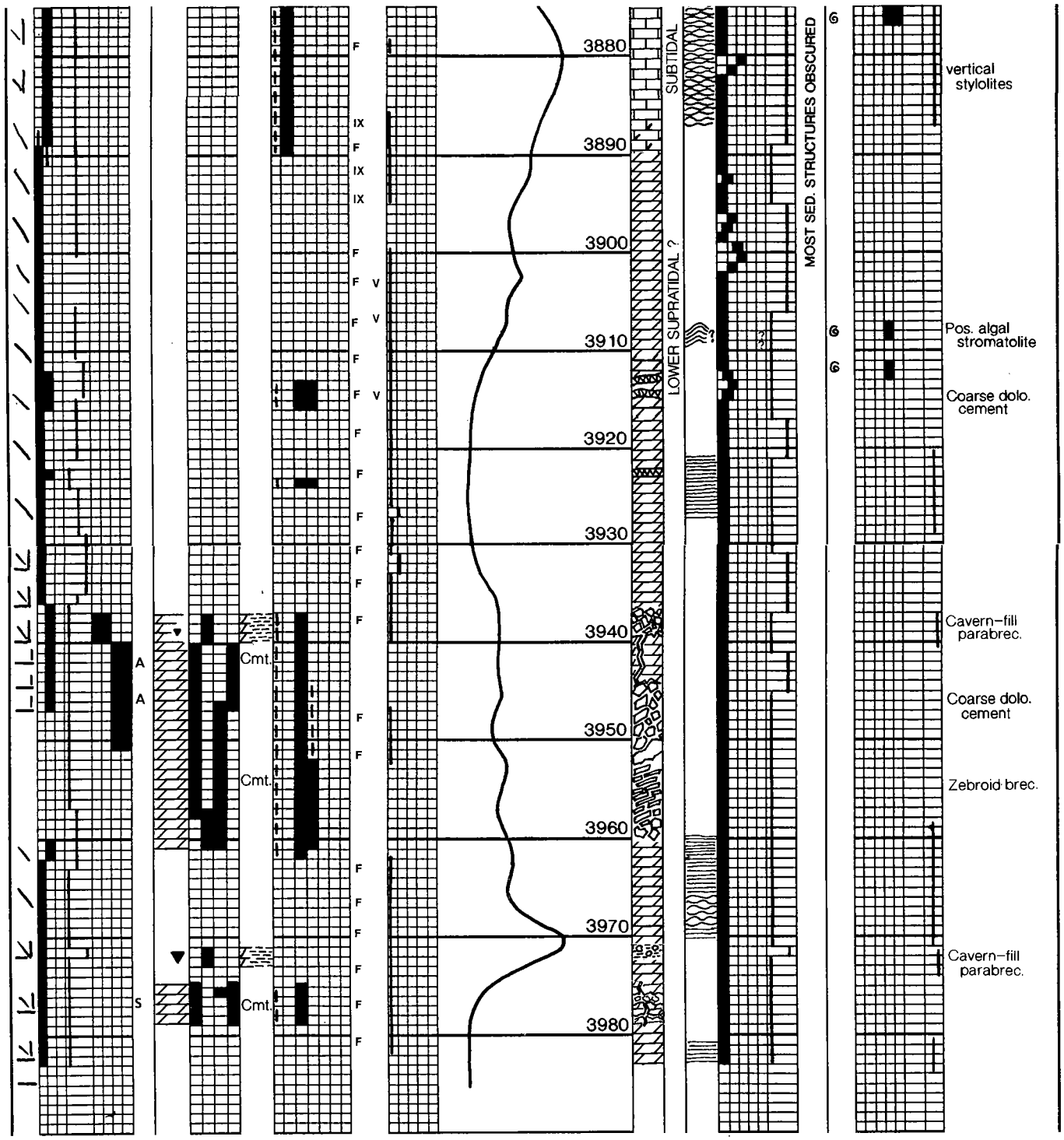


Plate 6. *Continued.*

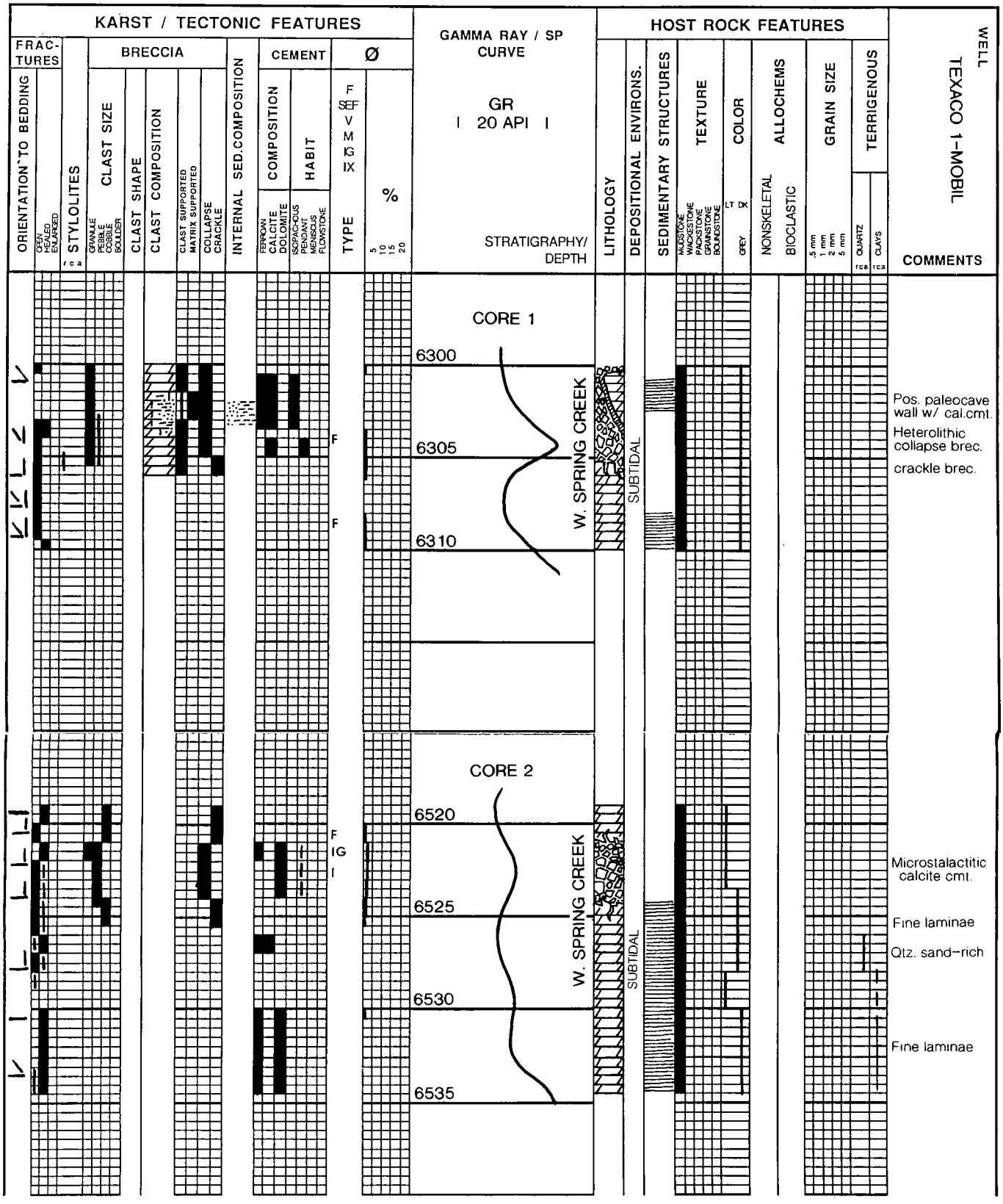


Plate 7. Petrolog of Texaco 1-Mobil core, sec. 1, T. 5 S., R. 1 W., Carter County, Oklahoma.

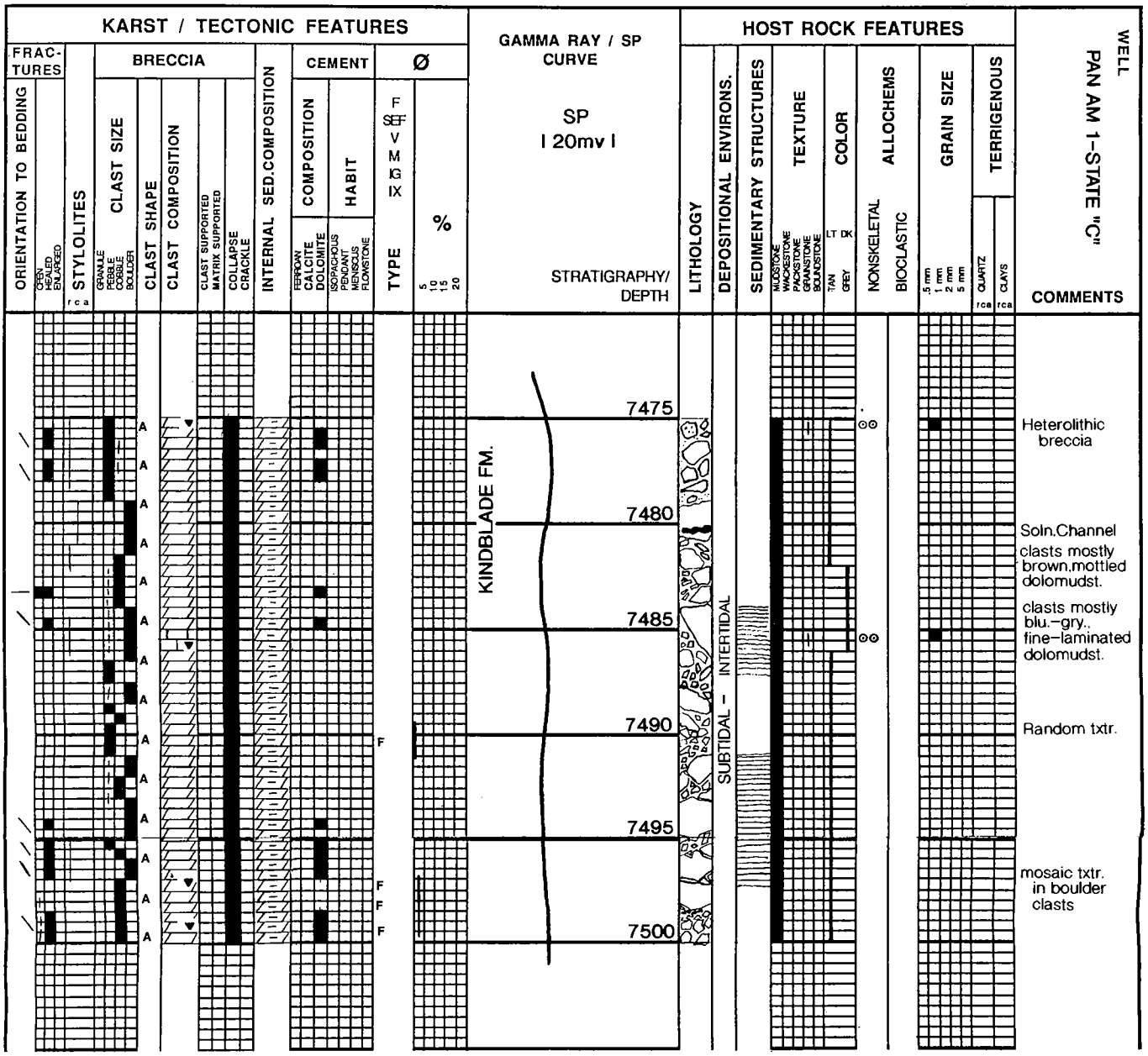


Plate 8. Petrolog of Pan American 1-State C core, sec. 36, T. 2 S., R. 10 W., Cotton County, Oklahoma.

Lithology, Stratigraphy, and Age of the Arbuckle Group in the Amoco SHADS No. 4, a Continuous Core from Grassroots into Basement, Rogers County, Oklahoma

James R. Derby
Consultant, Tulsa, Oklahoma

Henry H. Hinch
Amoco Production Research, Tulsa, Oklahoma

John R. Repetski
U.S. Geological Survey, Reston, Virginia

INTRODUCTION

The Amoco Production Co. SHADS No. 4 was drilled in 1987 at the APC Catoosa Lease in the SE¼SE¼SE¼, sec. 25, T21N, R14E, Rogers County, Oklahoma, to a TD (total depth) of 3,470 ft (458.5 ft into the Precambrian basement). The well was continuously cored, as a 2.5-in.-diameter core, from the surface to the top of the Precambrian, and subsequently cored at 1.7-in. diameter to TD as a test of Amoco's Stratigraphic Highspeed Advanced Drilling System (SHADS). Drilling was performed by Longyear Drilling Co. utilizing their continuous wireline slim-hole coring system. The purposes for drilling the SHADS No. 4 were: (a) to evaluate the quality of core recovered utilizing Longyear's coring system; and (b) to provide core to be used in the development of a mobile, on-site core-processing and evaluation system to be used to evaluate cores from future SHADS wells. Previous SHADS boreholes were also use to evaluate commercially available slim-hole logging tools; however, the SHADS No. 4 was not logged.

The Arbuckle core of the SHADS No. 4 can be compared to the log of the Amoco Drilling Mechanics (DM) No. 1, located ~200 ft southeast, and to the SHADS No. 1, located ~30 ft from the SHADS No. 4. The DM No. 1 is a conventional-diameter (8.5 in.) borehole that penetrated >100 ft in the Precambrian; a full suite of Schlumberger logs is available to TD, and these logs are reproduced herein alongside a graphic, lithologic log of the SHADS No. 4 (Fig. 1). A full suite of logs, run with slim-hole tools by various vendors, are also available for the SHADS No. 1; however, these logs extend only a short distance into the Arbuckle.

Amoco retained J. R. Derby to describe the Mississippian through Arbuckle Group carbonates in the SHADS No. 4, to provide a record of the rocks cored and for comparison to drilling performance data; that description is included in this report (see Appendix). H. H. Hinch had earlier described the SHADS No. 1 core, which reached TD 345 ft into the Arbuckle. Hinch coordinated the work on the SHADS No. 4, facilitated preparation of this report, and prepared the logs for Figure 1. J. R. Repetski completed the heavy-liquid separations, and he picked and identified Arbuckle conodonts from samples selected by Derby and processed at Amoco under the supervision of H. R. Lane.

The core from the Amoco SHADS No. 4 has been released to the Oklahoma Geological Survey and is available for examination at the OGS Core and Sample Library in Norman. This places into the public domain a complete core of the entire stratigraphic section in northeastern Oklahoma, and the fossil data presented here represents the first published biostratigraphic-age determinations for the Arbuckle Group in northeastern Oklahoma. The authors wish to thank Amoco Production Co. both for the release of this core and for their generous support in the preparation of this paper for publication. Specific thanks go to Drs. K. W. Ciriacks, R. Pierce, and J. Baesemann for facilitating release of data and conodont material, and to Ms. Katie Riggs and Janie Hooker for drafting the lithologic and geophysical logs.

Limitations of the Study

The core was described from unslabbed core using a hand lens and low-power binocular microscope. In 1987 a total of 12 days were devoted to the core description of the interval from 1,100 ft (in the basal Pennsylvanian) to TD, of which 4–5 days were devoted to examining the Arbuckle Group. No thin sections or other detailed studies were performed. Significant shaly zones that could be confidently correlated to gamma-ray anomalies on the geophysical logs of nearby wells were noted (Table 1). Porosity types and amounts were visually estimated (Table 2). Fluorescent zones were noted, but are not included in this report. Fossil samples were taken (Table 3), and the majority were selected to be acidized for conodonts. The material was acidized by H. R. Lane of APC in 1988, but no further study was performed at that time.

Conodont identifications recently made by Repetski (Table 4) represent study of only the most productive and best material, and should be considered preliminary. Identification of geologic formations are equally preliminary, and represent Derby's attempt to reconcile the described lithologies and previous correlation in the area by McCracken (1964) and Ireland (1944,1946), with ages determined from the conodonts. This new information, and that of Kurtz and others (1975), may require some modi-

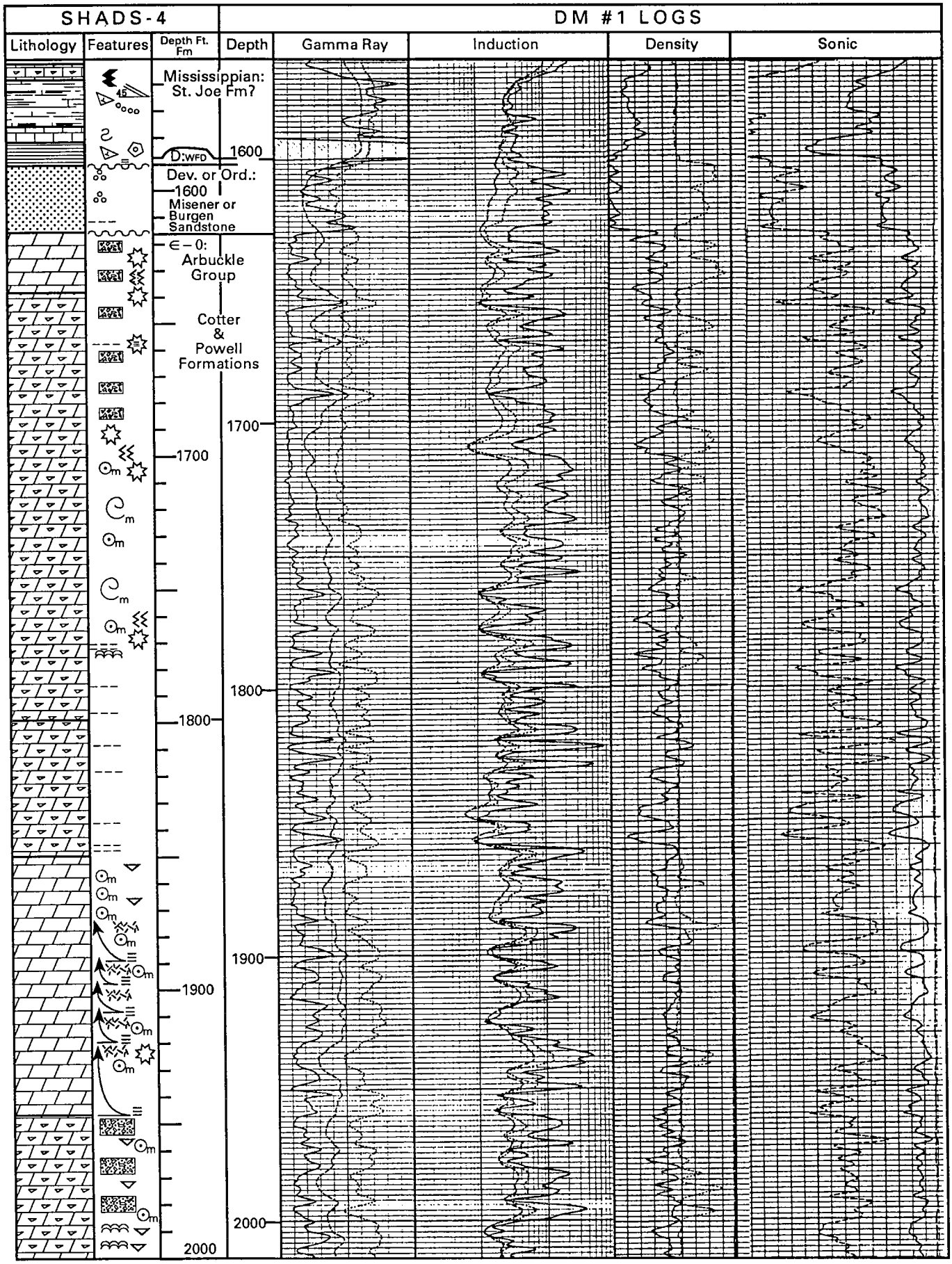


Figure 1 (p. 70–73). Lithologic column of the Amoco SHADS No. 4 core from 1,550 to 3,470 ft, and geophysical logs from the nearby Amoco DM No. 1; both wells are in SE¼, sec. 25, T21N, R14E, Rogers County, Oklahoma.

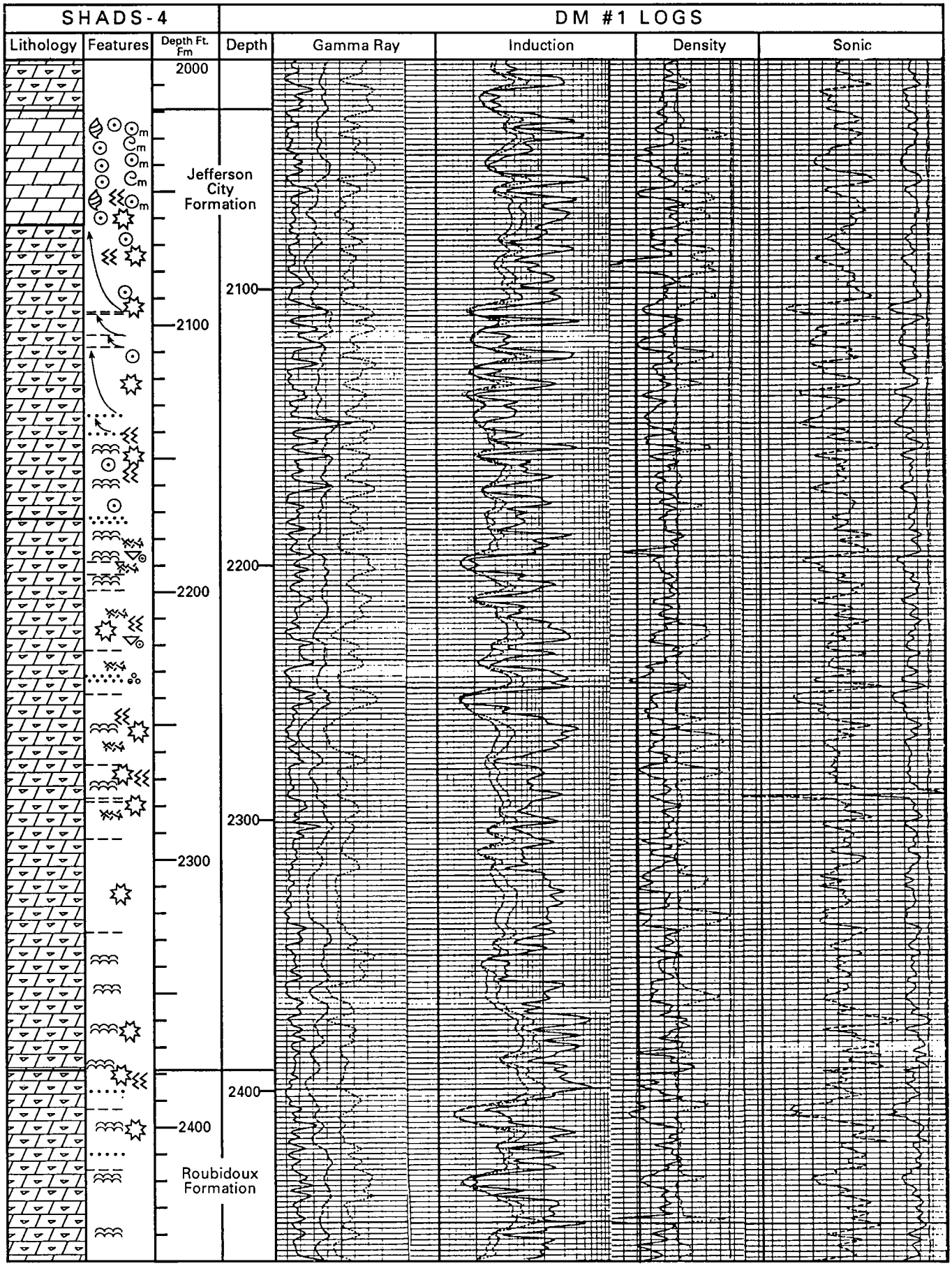


Figure 1. *(continued)*

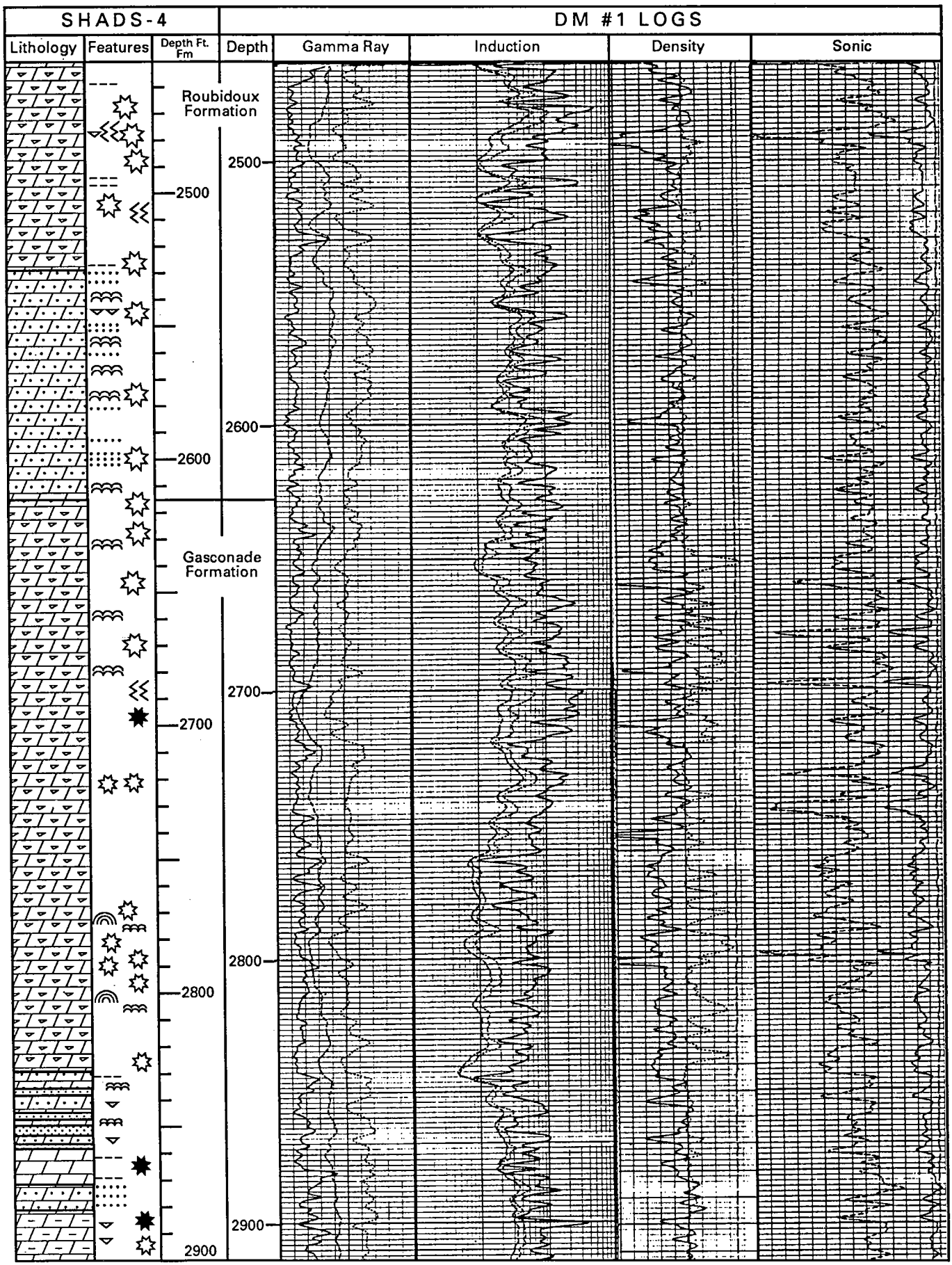


Figure 1. *(continued)*

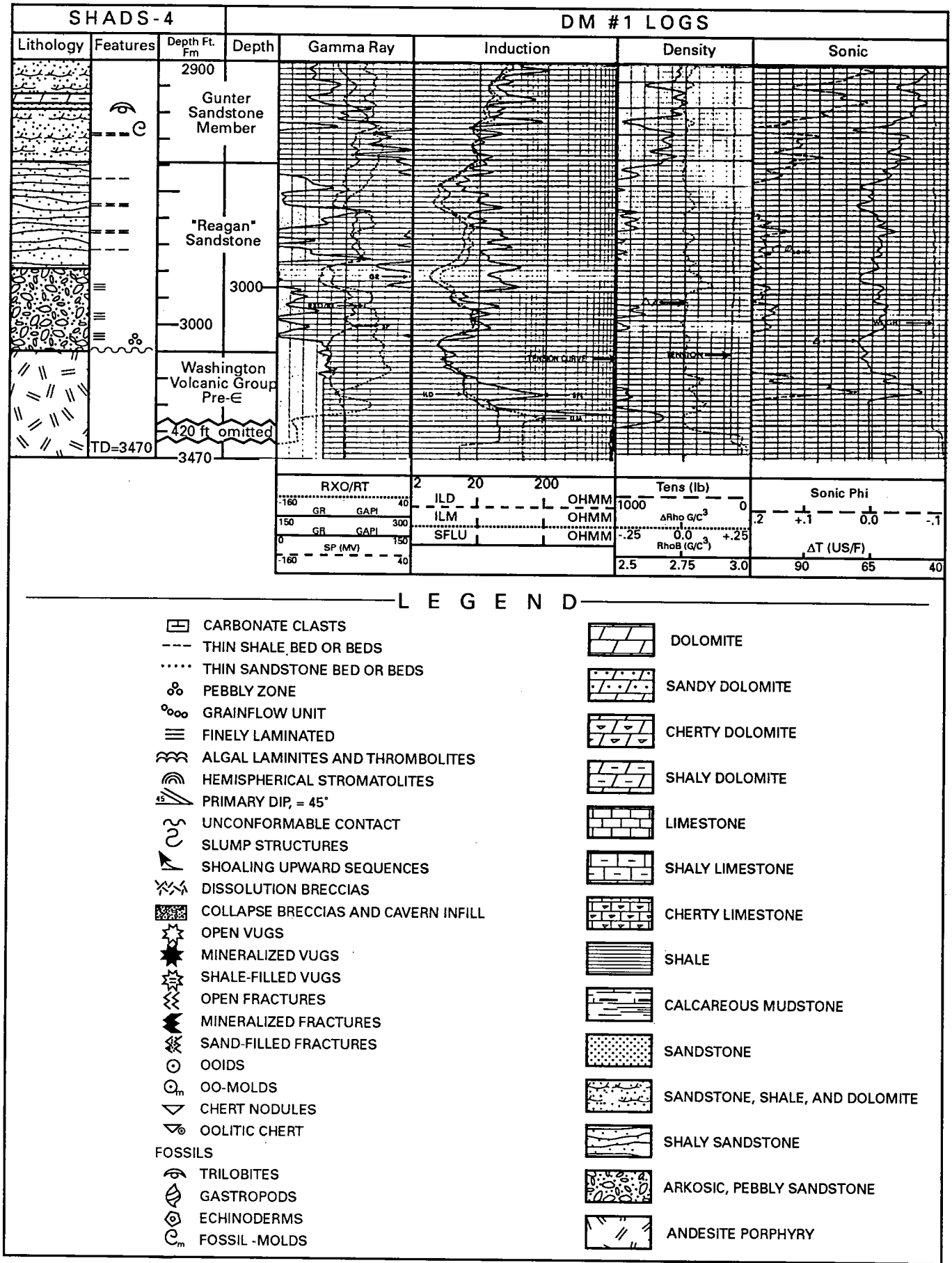


Figure 1. *(continued)*

TABLE 1. — CORRELATION OF SHADS NO. 4 WELL TO DM NO. 1 WELL IN ARBUCKLE GROUP
(Shaly and Other High Gamma Zones)

DM #1 GR-BHC Log depth	SHADS #4 Core depth	Lithology
1638	1628.5-29	Hard light green shale
1653-56	1642-45	Green shale and shaly zone
1668-70	1657.5-.9	Green slaking fissile shale--cavity fill
1688-91	?1679-80.3	Breccia and shaly layers
(1691-1763)	No Shales	Quiet gamma DM#1 and SHADS 1
1763-65	?1750.9	1-cm shale layer
	?1773-74.5	Dk green shaly layer to 0.1 thick
	1806.2-07.5	Shaly layers
1849	?1836-37	Shale
1846-48	?1844-47	Shaly layers
1900	1889	Laminated mudstone at base of cycles
1908	1898	Laminated mudstone at base of cycles
1921	1909	Laminated mudstone at base of cycles
1932	1919	Laminated mudstone at base of cycles
1958	1946	Laminated mudstone at base of cycles

fications of earlier studies which lacked the benefit of biostratigraphic control (e.g., Chenoweth, 1965,1968).

STRATIGRAPHY

Although the Arbuckle Group in northeastern Oklahoma utilizes the group name "Arbuckle," its subdivisions have historically utilized the names of formations which crop out in the Ozark region. Following more recent practice in Missouri and Kansas (Kurtz and others, 1975), the basal sand is termed Reagan. As currently used, the Reagan sand is strongly time-transgressive. In the SHADS No. 4, the Reagan consists of arkosic regolith and shaly arkosic sands overlying an andesite porphyry. This is overlain by a trilobite-bearing marine sand, tentatively identified as the Gunter Member at the base of the Gasconade Formation. The succeeding sequence, Gasconade, Roubidoux, Jefferson City, and Cotter-Powell Formations, are universally dolomites of shoal-water origin, with variable amounts of chert, sandstone, and shale.

The Arbuckle Group in northeastern Oklahoma rests unconformably upon an irregular surface carved into Precambrian granite and volcanics, 1.3 billion years old (Denison, 1981). In the Tulsa–Rogers Counties area, a NE-trending ridge on the Precambrian has local relief of 2,000 ft in 5 mi: the SHADS wells are located on its southeast slope. Only 7 mi to the west, in the Superior Blakemore No. 1 (26-T21N-R13E), Mississippian strata rest on Precambrian; the Arbuckle was never deposited (Ireland, 1944). These exposed islands of volcanic rocks or granite provided a local source for clastic sediments throughout the deposition of the Arbuckle, as well as providing highlands and a source of fresh water under a hydrostatic head.

The entire Arbuckle and Reagan sequence was deposited in shallow-water environments and was subjected to repeated episodes of dissolution and karstification. Dissolution porosity is common throughout the section, with the best-preserved porosity low in the section in the Gasconade, Roubidoux, and lower Jefferson City Formations, as both fabric-selective and non-fabric-selective molds and vugs (Fig. 2; Table 2). In the upper Jefferson City, Powell, and Cotter Formations, dissolution breccias, karstic-collapse breccias, and cavern-infill sediments are common (Fig. 1). The uppermost 76 ft contains fractures, vugs, and collapse breccias containing sand and shale apparently derived from the overlying stratigraphic units.

Abruptly overlying the Arbuckle is a phosphatic, pebbly, medium-grained sandstone 26.4 ft thick (Fig. 3), that is overlain in turn by the Woodford Shale of Late Devonian age. A possible interpretation is to assign the sandstone to the Burgen Sandstone, the basal Middle Ordovician sandstone in easternmost Oklahoma, or to one of the sandstones of the Simpson Group. However, the pebbly, phosphatic nature of this sand suggests that it is more likely Misener (Late Devonian), and is related to the pre-Woodford unconformity. In either case, a profound unconformity either immediately overlies the Arbuckle, or is a short distance above. This period of emergence provides ample time for development of the dissolution features in the underlying Arbuckle carbonates.

The Woodford and overlying St. Joe Formation record an abrupt inundation of the previously exposed shelf, with deep-water basinal to shelf-slope conditions persisting well into the Mississippian.

BIOSTRATIGRAPHY

Conodont faunas identified to date are listed in Table 4; zonal names and their correlation are shown in figures 1 and 2 of Derby and others (1991), which is a review of the Cambrian and Ordovician biostratigraphy of Oklahoma. The three samples from the lower Gasconade (2,897–2,939) have not yet yielded conodonts. Four samples (2,621–2,765) in the upper Gasconade are assignable to the *R. manitouensis* Zone, which is reliably known to occur in the upper McKenzie Hill Formation of the Arbuckle Mountains, and the upper Gasconade of the Ozarks, both of which are well up in the Lower Ordovician. The overlying sandstone therefore cannot be the widespread basal Gasconade Gunter sandstone, which is known to contain conodont Fauna B, within the range of the genus *Cordylodus* (Kurtz, 1981). The overlying sandstones are more likely part of the Roubidoux, and the Gunter immediately overlies the Reagan, if it is present at all. This suggests that no Cambrian strata may be present in the SHADS No. 4. Even if the basal units are correlative with the top of the Eminence dolomite, Kurtz (1981) demonstrated that the top of the Eminence Formation is Ordovician, not Cambrian.

Conodonts recovered from higher samples are somewhat less precise, but confirm the general correctness of the formation assignments. Jefferson City Formation samples from 2,024 to 2,120 yielded faunas assignable to conodont Fauna D or very lowest *O. communis* Zone. This interval is therefore no older than the base of the Roubidoux, as known in Missouri, and indicates correlation to the Roubidoux and Jefferson City Formations. The highest productive sample (1,801) is assignable to highest Fauna D or *O. communis* Zone, indicating correlation to highest Jefferson City through Cotter and Powell Formations, but clearly restricting the age to Early Ordovician. Further study of these samples and processing additional samples will hopefully add precision to the age determinations.

TABLE 2. — SIGNIFICANT ARBUCKLE POROSITY ZONES (≥1 ft thick) IN THE SHADS NO. 4 WELL

Depth, Footage	Visually Estimated Porosity 5-10%	10-20%	>20%
1616.1-23	IC		
1623-25	IC	MV	
1625-27.4	IC	MV	V
1630-38	IC	MV,V, F	(V,1637.6-38)
1647-49.5	V, F, M		
1661.5-63	F, V		
1668-70.5	F, V		
1684.6-89.4	F, V, M		
1692.8-1700		V, M, F, IC	
1706.2-08.2		V, M, F	
1708.2-13.5	F, V, M, IC		
1713.5-26.5	V, F, IC		
1733-34.6	F, V, Breccia		
1742-44	F, V, M		
1751.6-57.6	IC (micro sucrosic)		
1757.6-60	Oomoldic, V		
1761-63	Chalky, MP, Sli M		
1767-71.5	M, V	M, V, F	
1773-79	IC, M, MV		
1785-87	M, V		
1795.8-97.5	OM, IC, MV		
1803-1806.2	F, MV		
1856-1858.8	OM, V, IC		
1863-64	IC, M, V		
1872-74.5	M, IC		
1875.5-78	F, M, IC		
1921.7-1928	OM, F, IC, V	(Very local; Thin Zone V)	
2035-2041.2		M, IC	
2044-2049	IC, F, F		
2053-2054.7	M, V, IC		
2058-59.5		M, V, IC	
2059.5-61	IC		
2070.4-2083		M, F, V, IC	
2091-2093		Discontinuous M, V, IC	
2110.1-2114.5	F, V, IC		
2121.4-2121.5	V, M, F, IC	Discontinuous V, M	
2130.2-2135	Chalky, V		
2144-2148		V, M, F, IC	
2148-2150	F, C		
2157-2170	IC, V, M, F		
2174.9-2177.4	V, M, IC		
2210-2221		F, V, M	
2229-2232	IC, M		
2248-2259.5		IC, V, F	
2266-2270.7		IC, V, F	
2271.3-2277		IC, V	
2294.6-2297.2	IC		
2303-2310		V, IC, F	
2310-2318	V, F, M		
2314.8-2325		V, M, IC	
2365.4-2367		V, IC	
2369-2373	F, V,*		
2377,2379	F, V,*		
2380-2387.5		V, F	
2388.8-2394	IC		
2397-2407		V, IC, F	
2407-2410	F, V		
2423.7-2427		V	
2432.5-2437	V, F		
2439.4-2440.6		V	
2442-2446	IC		
2446-2449	V, F		
2459-2463	V, M, IC		
2465-2467		V, M, IC	
2471-2473	V, F		
2473-2479			F, V, IC Cherty
2480-2484		IC, M, V, (v.c. crystal. dolomite)	
2484.5-2494.6		IC, M, V v.c. crystal. dolomite	
2495-2504.3	IC, V		
2504.3-2510.8		Discontinuous V, F; Cherty	
2510.8-2519		IC, sparse vugs (appears oil stained)	

*Probably very high permeability if vugs are laterally continuous.

TABLE 2. — *Continued*

Depth, Footage	Visually Estimated Porosity 5-10%	10-20%	>20%
2519-2520.5 (2520.6-2520.8)	V, F, Cherty		IC, coarse crystalline dol.
2525-2526		IC, V	
2536-2537.5 (2544.9-2545.1)	IC, M	Thin zone, very large vugs	
2573-2576	IC, M, V		
2576-81 (2586.9)	V, M		1 vug measured 40mm x 28mm x 30mm
2588-2591	V, F		
2601.8-2603.4	IC, IG		
2605.6-2609	V, F, IC (several large vugs)		
2611.5-2615	V		
2616.8-2619		V, F Dol and chert	
2619-2622	IC, V		
2627-2631		Discontinuous zones of open vugs	
2631.4-2634.3		IC, V	
2635-2637		Discontinuous zones of open vugs	
2637.0-2643.0		IC, V	
2645.5-2649.3		Discontinuous zones of open vugs	
2655.3-2657.6	IC, V		
2667-2668		V	
2670-2675	IC		
2675.5-2677.7	IC, V		
2677.7-2683.7	Discontinuous V		
2686-2690	IC (MP), MV		
2690-2700		Discontinuous V, F, M	
2700.2-2704	IC, MV		
2705-2714	Discontinuous F, V		
2714-2718	IC, V		
2720-2721.5		Vuggy rubble and extremely large open vugs. Probably very high perm.	
2725.0-2730	F, V		
2743 - 2758	IC, V (sparse open tabular vugs)		
2759-2768	IC (very local vugs)		
2768-2771		IC, V, M	
2771-2776	IC, V		
2776-2784		IC, V, M	
2784.3-2792.3			Discontinuous 20-50% porosity in large, continuous vugs and channels
2792.3-2798		V, IC, M	
2798-2816	IC, V		
2816-2826		IC, V	
2833.7-2839	IC, IG		
2881-2882	IG, (SS)		
2888-2891		Discontinuous V	
2895-2897.5		Discontinuous V	
2909-2911.3	Discontinuous V		
2916-2918.5	IG (SS)		
2944-2945	IG (SS)		
2957-2959	IG (SS)		
2965.5-2966.5	IG (SS)		
2967.6-2977.5		IG (SS)	
2979.4-2984		IG (SS)	
2984-2990.3 (Tight below 2990.3)	IG (SS)		

Explanations of Porosity Type Codes
(Porosity type codes are listed in order of relative importance.)

IC = Intercrystalline
IG = Intergranular
F = Fracture
C = Chalky
MP = Micropores
V = Vuggy
MV = Microvugs
M = Moldic
OM = Oomoldic
FM = Fossil Moldic

TABLE 3. — FOSSIL SAMPLES COLLECTED FROM THE SHADS NO. 4 WELL

Depth interval	Unit
	Mississippian Slope to Basin facies:
	Slope facies without coarse grainstones
1519.6-1520	Top of second shale, top of transported fossil interval (limestone fine grainstone, mudstone turbidite below)
1532.1-1532.0	Near top of a shaly line mudstone interval
	Slope facies with coarse grainstones
1557.2-57.4	Top of uppermost coarse fossil grainstone
1574.7-75.0	Near top of limestone unit
1587.	Just above Woodford sh.
	Cambrian? and Ordovician Arbuckle Group; Shallow Carbonate Shelf Facies:
	Lithology is fine to medium crystalline dolomite unless otherwise noted. Dunham class described is inferred original limestone lithology
1776.8	Upper Arbuckle, below cavernous zone - Pelletal wackestone and algal/laminites
1801.5-01.9	Burrowed wackestone
1872.5-1873	Oolitic, pelletal, fossil packstone
1901.5-1.9	Burrowed, pelletal wackestone
1925.0-25.8	Conglomerate, fossilferous grainstone, black siliceous layer approximately 1 cm thick along stylolite at top (might be good for chitinozoa)
2006.7-2007.0	Burrowed to laminated mudstone and wackestone
2024.5-25.3	Thin bedded fossiliferous wackestone
2025.1	Megafossil: Helicotoma
2048.8-49.0	Megafossil: Helicotoma
2049.0-9.4	Fossiliferous wackestone
2119.5-2120	Burrowed mudstone
2621.5-22.1	Crystalline dolomite
2672.9-73.5	Crystalline dolomite
2722.8-23.5	Crystalline dolomite
2765.0-.8	Crystalline dolomite
2897.3-0.8	Crystalline dolomite
2921.9-22.7	Crystalline dolomite
2938.7-39.2	Crystalline dolomite

TABLE 4. — PRELIMINARY, PARTIAL LIST OF EARLY ORDOVICIAN CONODONTS FROM THE SHADS NO. 4 WELL

Footage	Selected diagnostic/ characteristic conodonts	Zone or faunal interval assignment
1801.5 - 1801.9	*Diaphorodus delicatus* (Branson & Mehl) *Drepanodus concavus* (Branson & Mehl) *Eucharodus toomeyi* (Ethington & Clark) *Glyptoconus quadraplicatus* (Branson & Mehl)	highest Fauna D or *Oepikodus communis* Zone
1872.5 - 1873.0	cf. *Acodus deltatus* Lindström *Cristodus loxoides* Repetski *Tropodus comptus* (Branson & Mehl)	
1901.5 - 1901.9	*Cristodus loxoides* *Drepanodus arcuatus* Pander *Triangulodus*? cf. *T. brevibasis* (Sergeeva) sensu Repetski (1982) *Ulrichodina abnormalis* (Branson & Mehl) New Genus 2 of Ethington & Clark (1981)	mid-Fauna D to very low *Oepikodus communis* Zone
1925.0 - 1925.8	"*Scolopodus*" aff. *S. rex* Lindström *Triangulodus*? cf. *T. brevibasis* *Ulrichodina wisconsinensis* Furnish	
2006.7 - 2007.0	*Cristodus loxoides* *Oneotodus costatus* Ethington & Brand	
2024.5 - 2025.3	*Glyptoconus quadraplicatus* *Drepanodus concavus*	Fauna D to very low *Oepikodus communis* Zone
2049.0 - 2049.4	aff. *Oneotodus costatus*	
2119.5 - 2120.0	*Drepanodus* aff. *D. concavus* *Glyptoconus quadraplicatus* aff. *Oneotodus costatus*	
2621.5 - 2622.1	*Chosonodina* cf. *C. herfurthi* Müller	
2672.9 - 2673.5	*Rossodus*? n. sp.	*Rossodus manitouensis* Zone
2722.8 - 2723.5	*Clavohamulus densus* Furnish?	
2765.0 - 2765.8	*Oneotodus simplex* (Furnish) *Scolopodus* ? *sulcatus* Furnish	

BASEMENT ROCKS

Rodger E. Denison kindly provided a description of a thin section of the andesite porphyry at 3,159.4–3,159.7, in a memo dated November 1989. The description establishes that the rock is an andesite, not a rhyolite. Part of his description is reproduced below.

Thin section No. Rg-8-1 (Nov. 1989) based upon 1000 points.

Groundmass	49.9%	Sphene	tr
Plagioclase	39.3%	Apatite	0.5%
Chlorite	3.4%	Plagioclase alterations	2.6%
Pyroxene	0.3%	Leucoxene	tr
Iron oxides	2.3%	Zircon	tr
Epidote	1.5%	Actinolite	tr

Fabric: Porphyritic
Grainsize of phenocrysts: 2.5 mm
Name: Andesite porphyry

Phenocrysts of plagioclase, chlorite, pyroxene, and iron oxides are crowded into a reddish groundmass composed of devitrified glass and chloritic micas. The groundmass is probably mostly feldspar. Quartz is probably present but cannot be distinguished in the groundmass.

REFERENCES CITED

Chenoweth, P. A., 1965, A boulder in the Gunter Sandstone, northeastern Oklahoma: Oklahoma Geology Notes, v. 15, p. 3.

_____1968, Early Paleozoic (Arbuckle) overlap, southern Midcontinent, United States: American Association of Petroleum Geologists Bulletin, v. 52, p. 1670–1688.

Denison, R. E., 1981, Basement rocks in northeastern Oklahoma: Oklahoma Geological Survey Circular 84, 84 p.

Derby, J. R.; Bauer, J. A.; Creath, W. B.; Dresbach, R. I.; Ethington, R. L.; Loch, J. D.; Stitt, J. H.; McHargue, T. R.; Miller, J. F.; Miller, M. A.; Repetski, J. E.; Sweet, W. C.; Taylor, J. F.; and Williams, M., 1991, Biostratigraphy of the Timbered Hills, Arbuckle, and Simpson Groups, Cambrian and Ordovician, Oklahoma: a review of correlation tools and techniques available to the explorationist, *in* Johnson, K. S. (ed.), Late Cambrian–Ordovician geology of the southern Midcontinent, 1989 symposium: Oklahoma Geological Survey Circular 92, p. 15–41.

Ireland, H. A., 1944, Correlation and subdivision of subsurface Lower Ordovician and Upper Cambrian rocks in northeastern Oklahoma: U.S. Geological Survey Oil and Gas Investigations Preliminary Chart 5.

_____1946, Maps of northeastern Oklahoma and parts of adjacent states showing the thickness and subsurface distribution of Lower Ordovician and Upper Cambrian rocks below the Simpson Group: U.S. Geological Survey Oil and Gas Investigations Preliminary Map 52.

Kurtz, V. E.,1981, The Cambrian–Ordovician boundary in Missouri as determined by conodonts, *in* Taylor, M. E. (ed.), Short papers for the Second International Symposium on the Cambrian System: U.S. Geological Survey Open-File Report 81-743, p. 115–120.

Kurtz, V. E.; Thacker, J. L.; Anderson, K. H.; and Gerdemann, P. E., 1975, Traverse in Late Cambrian strata from the St. Francois Mountains, Missouri to Delaware County, Oklahoma: Missouri Geological Survey Report of Investigations 55, 112 p.

McCracken, M. H., 1964, The Cambro–Ordovician rocks of northeastern Oklahoma and adjacent areas: Tulsa Geological Society Digest, v. 32, p. 49–75.

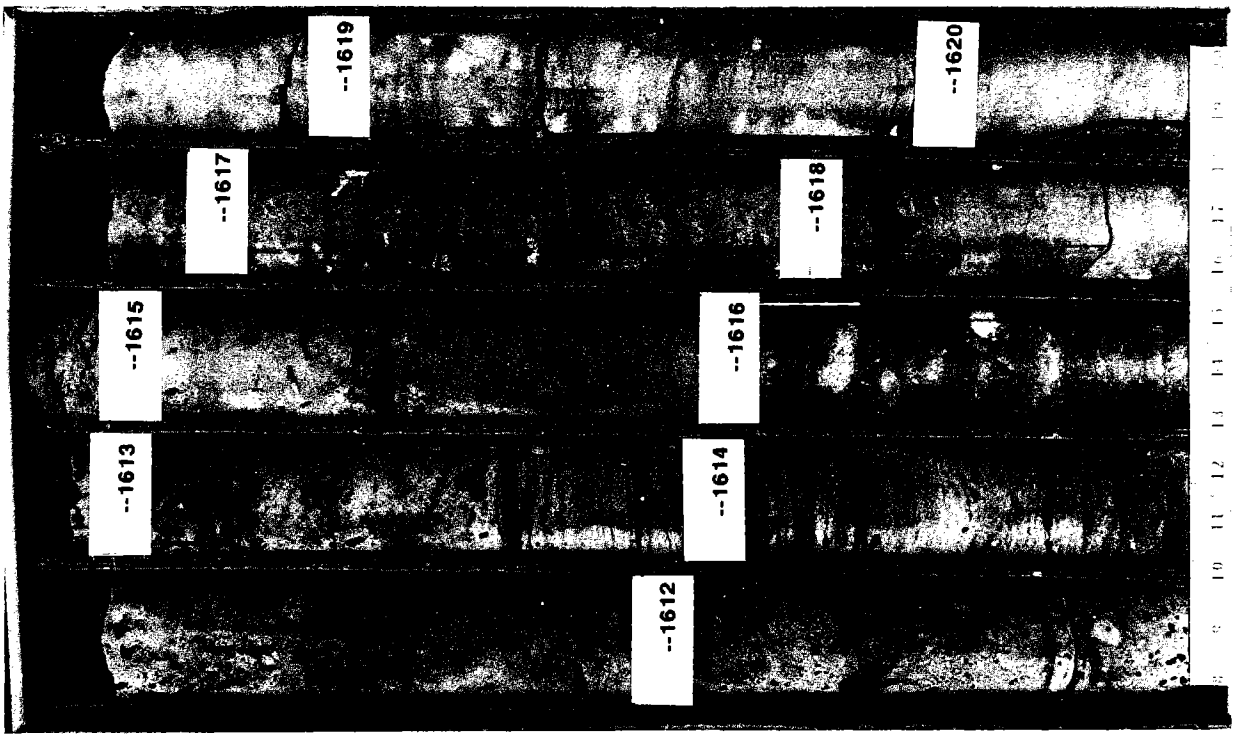


Figure 3. Core photo of the top of the Arbuckle Group and overlying Misener (?) Sandstone in the Amoco SHADS No. 4. Top of Arbuckle dolomite is at 1616.1 ft, just below two dark phosphatic pebbles in the sandstone. Numerous dissolution features are faintly visible in the upper Arbuckle.

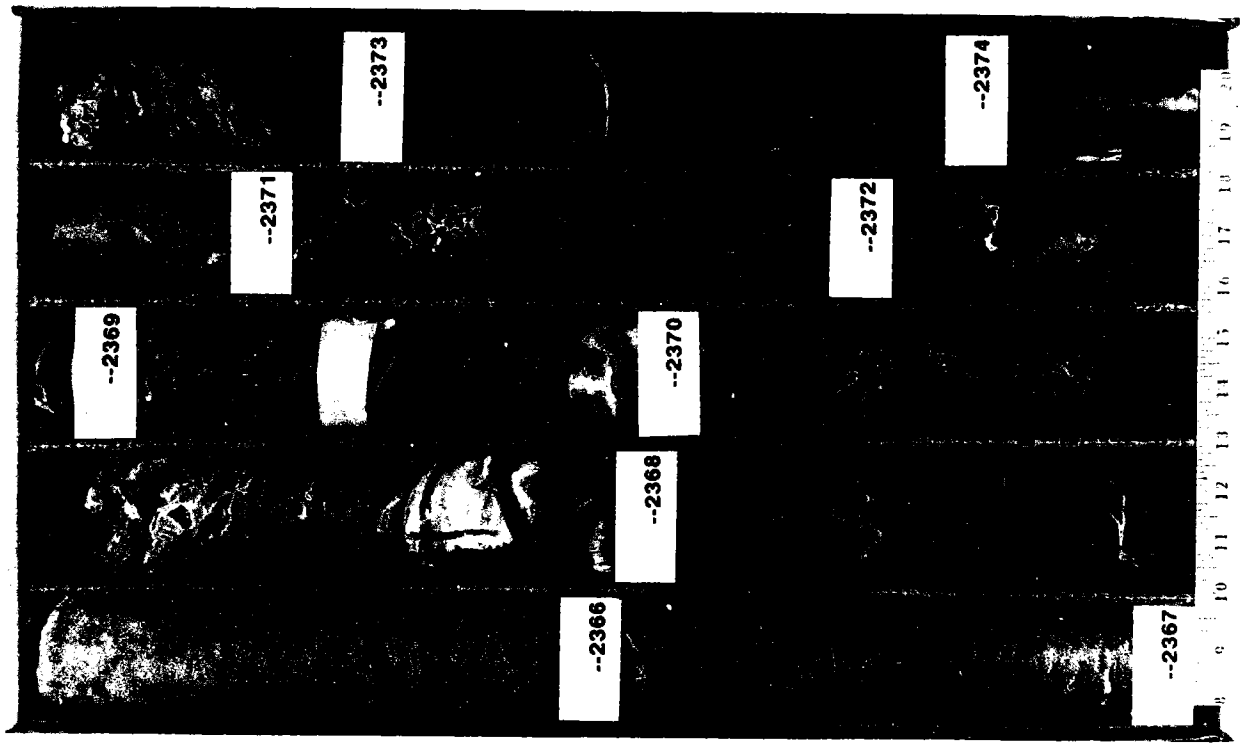


Figure 2. Core photo of the basal Jefferson City Formation in the Amoco SHADS No. 4, 2,365–2,374.5 ft, showing both fabric-selective fenestral porosity, and non-fabric-selective vugs. Fenestral porosity is in planar stromatolites. Cross-cutting vugular porosity may be partly controlled by earlier dissolution brecciation. Vugs are lined with both quartz and dolomite crystals. Scale at base of photo in inches.

APPENDIX: Core Description

Amoco SHADS No. 4; SE¼SE¼SE¼ Sec. 25, T21N, R14E, Rogers County, Oklahoma

Core description by James R. Derby
November and December, 1987

Core depth (top of interval)	Thickness (ft)	Lithologic description
		(EARLY MISSISSIPPIAN)
(1520.25)	(67.1)	(*St. Joe Formation* or possibly *"Cowley" Formation*) (Slope to basinal facies.)
1520.25	0.15	Limestone, argillaceous. Medium brown argillaceous coarse fossiliferous lime packstone. Abrupt contact above; irregular, erosive contact below.
1520.4	10.8	"Shale," limy. Medium to dark brown sparsely fossiliferous slightly calcareous mudstone. (Nonfissile, not shale.) Locally abundant large echinoderms and rarer brachiopods floating in mudstone matrix. Unburrowed, laminated to thin bedded. Abrupt lower contact. Hard.
1531.2	25.8	Limestone, siliceous. Medium to dark gray siliceous lime mudstone, locally large chert nodules to 0.3 ft thick. Locally numerous near vertical fractures, healed. At 1555–57 grades by increasing argillaceous content to unit below. Hard to very hard.
1557	17.5	"Shale," limy, locally conglomeratic. Dark brownish-gray mudstone, nonfissile (not shale), calcareous, with thin clastic zones of coarse to very coarse crinoidal fossil debris and phosphate nodules. One boulder 0.5 ft high. Apparent primary dips in grainflows approach 45°. Slope facies with grainflows, turbidite and slide deposits. Moderately hard. Clastic zones within unit are mostly muddy fossil wackestones, with white fossil grains in mudstone matrix.
1574.5	1.4	Limestone. Light gray coarse fossil grainstone grading down to medium to fine fossil packstone and wackestone. (Possible grainflow deposit.) Hard. (This unit and limestone below are cut by a vertical post-depositional fracture which offsets their abrupt contact.)
		(Disconformity, 1 cm relief.)
1575.9	4.1	Limestone. Light brown to light brownish lime mudstone to wackestone, with small intercalations of distorted brown mudstone and one shaly interval. Many soft-sediment flow structures, many discontinuity surfaces. Sparse cherty fossils and pyrite nodules. Vertical fracture filled with mudstone from 1576.3–.8. Hard.
(1572.2–2.3)	(0.1)	Shale and limestone. Light blue-gray slaking shale interbedded with thin (4 mm) lime mudstone lenses. Hard.
1580	0.9	Limestone to mudstone. Transitional unit: light brown lime mudstone with deformed siliciclastic mud lenses, grading down to slightly calcareous siliciclastic mudstone with sparse fossil fragments. Abrupt but conformable contact below. Hard.
1580.9	1.8	Shale. Medium greenish-gray fissile shale, noncalcareous. Moderately hard.
1582.7	4.65	Shale with carbonate clasts. Black, fissile, slightly silty shale and thick fossil packstones with siliciclastic mud matrix. One phosphate nodule 4 cm long. Grades upward from fine sand clasts at sharp contact with underlying black shale to very coarse fossil fragments (to 1 cm diameter, echinoderms) at 1586.5. Two intervals lack carbonate clasts, top 0.1 ft and 1583.3–3.55. Moderately hard.
		(EARLY MISSISSIPPIAN or LATE DEVONIAN) (*Woodford Shale*) (Deep water; below wave base)
1587.35	2.25	Shale. Black, fissile, brittle shale, highly radioactive. Brittle.
		(?Disconformity? 1.5 cm relief on irregular surface.)
		(*Misener Sandstone*) (Shallow shelf environment?)
1589.6	0.1	Sandstone, muddy. Dark gray to white medium-grained well-rounded quartz sandstone with dark gray mud matrix. Undulating upper and lower surface. 1578.1.
		(?Disconformity? undulatory surface.)
		(*Misener Sandstone*?; possibly MIDDLE ORDOVICIAN *Burgen Sandstone*) (Shallow shelf environment)
1589.7	26.4	Sandstone. White to brown (oil stained) medium-grained well-rounded quartz sandstone. Thin zones of calcite cement throughout. Pebbly, with phosphatic nodule clasts (generally 1 cm, up to 3 cm) in two zones at 1594–95.4, 1609–13.8. Bright fluorescent oil show at 589.9–90.1, but none below. Brown apparent oil stain 1596–1602.6. Phosphatic shaly parting 1613.6–14.7. Generally porous, lower 2 ft tightly cemented. Moderately hard, probably drills soft. Abrupt horizontal lower contact.
		(?Fluvial channel or nearshore transgressive marine shelf sand.) (Unconformity.)
(1616.1)	(1395.4)	(*LOWER ORDOVICIAN* to UPPER CAMBRIAN Arbuckle Group*) (Shallow marine shelf with repeated subaerial exposure.) (Entire unit has dull yellow-green to pinkish-yellow fluorescence.)

*Subdivisions of the Arbuckle Group are indicated with uncertainty. They represent Derby's attempt to identify the rock units previously recognized in northeastern Oklahoma by M. H. McCracken (1964).

(1616.1)	(404.3)	(?*Cotter* and *Powell Fms.*?)
1616.1	6.9	Dolomite. Mostly light gray to buff, medium crystalline, slightly porous; with coarsely crystalline dissolution cavity fillings and pods to tabular units of well-rounded medium-grained quartz sandstone (probably derived from unit above as cavity filling.) Locally brecciated. Sparse green clay lining cavities. Slightly porous, ~8%, no significant vugs.
1623	15.7	Dolomite. Light to medium gray, medium to coarse crystalline, fractured by dissolution brecciation, porous to vuggy. Vugs 3–30 mm across. Short zones of 25% porosity. Tight zone with light blue-gray slaking shale layers 1628.5–29.0.
1638.7	12.9	Dolomite, chert, breccia, shale, sandstone. Dolomite, light gray, finely crystallic, laminated, locally grades to: shale, light greenish-gray. Contains zones of collapse breccia and cave fill, consisting of dolomite, shale, white chalky chert, soft green shale, and white medium-grained quartz sandstone. Local chert nodules. Hard.
1651.6	5.1	Dolomite. Light gray, fine crystalline (microsucrosic). Probably dolomitized lime mudstone. Medium.
1656.7	36.1	Dolomite, chert, and shale. Dolomite, light to medium gray, fine to medium crystalline. Originally laminated and burrow-mottled. Numerous collapse breccias, common vertical and inclined fractures, chert nodules and breccias. Localized green shale cavern fill at 1657.5–.9.
1692.8	7.2	Dolomite. Light gray fine to medium crystalline, highly porous, vuggy, moldic, slight fracture. Thin zones of vuggy porosity >25%. Hard.
1700	73.1	Dolomite and chert. Mostly tight, finely crystalline, originally laminated mudstone, with abundant chert nodules and cherty zones. Numerous partially fractured and vuggy zones with little matrix porosity. Scattered thin zones of oomoldic, fossil(?) moldic porosity.
1773.1	25.7	Dolomite, chert, and shale. Dolomite, light gray, finely crystalline, largely dolomitized algal laminite boundstone grading down to dark brown laminated mudstone. Short intervals of intercrystalline, pelmoldic, and microvuggy porosity near top, moldic and vuggy at base. Thin shales at top, 1774.5, 1789.6, and at base. Siliceous zone throughout; and scattered large white, chalky and light gray, very hard, dense chert nodules throughout. Hard to very hard.
1798.8	11.8	Dolomite, chert, and shale. Dolomite, light brownish-gray, medium crystalline oomoldic packstones(?), with interbeds of medium gray burrow-mottled wackestone. Chertified zones throughout. Dark green shale 1806.3–1807. Very hard.
1810.6	36.4	Dolomite and chert, minor shale. Dolomite light gray to light brown. Tight, finely crystalline laminated mudstone; several thin zones of medium crystalline, slightly porous burrowed wackestone. Chert present in almost every foot in form of nodules, thin layers and indistinct silicified zones up to 0.2 ft thick. Shale is dark greenish-gray, in thin laminae and partings at 1817, 1836, 1844–45. Hard to very hard.
1847.0	27.7	Dolomite, siliceous. Light to medium brownish-gray burrow-mottled dolomite wackestones, mostly finely crystalline. Porous zones of finely crystalline ooid or pellet moldic packstones at 1856–1858.8, 1863–64, 1872–74.5. Very few, small chert nodules, many zones very hard, indistinctly silicified. Very hard with soft porous zones.
1874.7	72.1	Dolomite, siliceous, cyclic. Five distinct shoaling upward cycles as follows: At base is laminated to thin bedded, dark brown to light gray layers of mudstone, finely crystalline. Grades up to burrowed wackestone, fine to medium crystalline, light brownish-gray. Upper unit is fossil and oolitic packstone, may have moldic porosity. Top may have some diagenetic terrane dissolution breccias. Chert distributed throughout as small nodules and vague silicified zones. Bases of cycles as follows: 1946.8, 1919.4, 1908.5, 1897.4, 1889.9. Hard.
1946.8	38.7	Dolomite, cherty. Dolomite, light gray, fine crystalline mudstones and algal laminates, locally with medium to coarse crystalline breccias and cavity fillings. Few zones several feet thick of burrowed wackestones and oomoldic packstone. Prominent white chalky chert nodules to 0.2 ft thick scattered throughout. Local porosity in vugs, molds, and fractures, but no significant porous zones. Grades to unit below. Probably subaerially exposed diagenetic terrane. Very hard.
1985.5	34.9	Dolomites, locally cherty. Light gray to dark brown finely crystalline, tight, mudstones and algal laminates. Thin zones of burrowed wackestones. Sparse small light gray chert nodules. No porosity. Hard.
(2020.4)	(358.6)	(?Top of *Jefferson City Fm.*?)
2020.4	62.6	Dolomite. Light tan to brown, fossiliferous, oolitic, porous packstones, medium crystalline. Insignificant chert. Few thin intervals of brown mudstone. Recognizable large gastropods (*Helicotoma*?) at 2025.1 and 2048.9. Oomoldic and fossil moldic porosity, locally enhanced by fractures and vugs. Hard.

2083	68.2	Dolomite, cherty. Shoaling upward cycles of thin slightly porous fossiliferous pelletal or oolitic packstone(?) at top; light tan to brown, slightly shaly mudstones at base, mudstone 3–5 ft thick, porous intervals 1 or 2 ft. Dark brown, oil stained mudstones in lower two cycles. Cherty or siliceous intervals; 2092–93.3, 2100–2101, 2104.5–2105.4, 2110.7–2112; nodules at 2111.4, 2114.5, 2121.4 (oil shows, leached), 2134.0, 2140–41. Oil stained sandstones, 0.2 ft thick at 2142.2, 2135.1. Shaly zones at 2095.0–2096.1, 2104.4–.5, 2108.6–09.1.
2151.2	21.5	Dolomite, cherty. Light to dark brown, tight mudstones and rubbly thrombolitic slightly porous wackestones; discontinuously cherty throughout. Thin zones of algal laminates appear leached. Vuggy and fracture porosity in wackestone; some coarse crystalline vug fillings. Hard.
2173.7	1.2	Sandstone, dolomitic. White, very fine grained to fine grained, well rounded, well sorted, dolomite cemented, tight. Hard.
2174.9	69.9	Chert and dolomite. Siliceous to chertified cycles of algal laminates to rubbly thrombolitic dolomites, to oolitic, pelletal grainstones. Greater than 50% chert, mostly as replacement of dolomite textures, fewer distinct nodules (see fluorescent list). Chert nodules chalky to light blue-gray and translucent, commonly with moldic porosity. Some cherty zones are agate and silicified ooids. Many zones of dissolution breccias. Generally, tight rock with vuggy and fracture porosity. Locally, distinct stromatolitic structures.
(2232.5–34.5)	(2.0)	Sandstone, white fine grained, poorly sorted and well rounded, pebbly at top with dolomite and phosphatic clasts, dolomite cemented. (Possibly other thin zones of sandstone, difficult to distinguish on unslabbed core from silicified granular dolomite!) Thin (0.1–0.2 ft) dark shale intervals at 2190, 2195, 2199.8, 2221.8, and 2238.8. Extremely hard.
2244.8	109.8	Dolomite, cherty. Medium brown to medium gray porous thrombolitic dolomite, partially silicified, with chert nodules and siliceous zones, and zones of dissolution breccia. Much like unit above but less chert. Thin shaly mudstone zones at 2265, 2278–79, 2287, 2292–94, and 2328. Local vuggy porosity to 30%, vugs to 2 cm across. Sparse very thin quartz sandy zones. Extremely hard in cherty layers to moderately hard in porous dolomite units (see list of porosity zones).
2335.0	44.0	Dolomite, cherty. Medium gray to dark brownish-gray finely crystalline dolomite mudstone, most very tight with 1–2 ft zones of algal laminates, planar stromatolites and thrombolites. Discontinuous vuggy and fracture porosity. Thin (0.1–0.2 ft) zones of very hard, brittle chert, mostly brecciated and adjacent to quartz and dolomite lined vugs. Some vugs extend width of core and 3 cm high. Zone of horizontal fenestral porosity (20%) at 2365.4–2367 in planar stromatolites. Hard to locally extremely hard, much "twisted off" core.
(2379.0)	(236.0)	(?*Roubidoux Fm.*)
2379	150.7	Dolomite, cherty. Light to medium gray, fine to coarse crystalline, interbedded tight and porous. Thrombolitic, stromatolitic, and ?grainstone dolomite. Moderate porosity and permeability at top, increasing to zones of >20% porosity towards base. Thin (0.1–0.2 ft) intervals of light bluish-gray to greenish-gray very dense chert at 2–4 ft intervals throughout. Thicker zones of brecciated white to light bluish-gray chert at 2476.5–2479, 2505.3–2510.8. Porous coarse crystalline dolomites locally partially silicified. Coarsely crystalline slightly porous dolomites strongly resemble sandstones but generally lack quartz sand. Thin (0.1–0.2 ft) dark shaly layers of 2395, 2419.8, 2458, 2494.7, 2497.3, and 2529.7. Thin sandy zones at 2388.6–.7 and 2411.0–.3. Hard to very hard. Extremely hard chert zones at 2402, 2414, 2428, 2447–50, 2457 (breccia), 2509–2511, and 2522–23. Indefinite lower contact.
2529.7	37.8	Dolomite and sandstone. Little to no chert. Dolomite, light gray, medium to coarse crystalline, relatively tight, thrombolitic and stromatolitic. Interbedded sandstone and sandy interval 0.5–1.5 ft thick, white to light brown (oil stained), medium to coarse grained. Mostly fairly tight rock. Sandstone at 2530.8–2531.5, 2533.0–.8, 2534.6–35.5, 2550.6–2552, 2561–2562.6. Highly siliceous below 2552. Thin chert at 2544.8. Hard.
2567.5	47.5	Dolomite, sandy. Dolomite, light gray, interbedded tight fine crystalline mudstone and porous coarse crystalline, vuggy planar stromatolites or recrystallized fenestral mudstones. Thin lenticular sandy dolomite zones throughout, plus thin sandstone beds at 2580.9–81.1, 2593.9–94.2, 2595.0–.2, 2597.5–.8, 2597.4–98.1, 2601.2–.5, and 2602.0–.3. Few thin chert nodules and siliceous zone. Scattered large vugs. Hard.
(2615.0)	(324.3)	(?*Gasconade Fm.*?)
2615.0	62.9	Dolomite, cherty. Dolomite light gray to light brown medium to coarsely crystalline, porous with thin zones of medium bluish-gray very dense chert, typically fractured and/or vuggy. Macro-porosity associated with chert and vugs but thick intervals of good intercrystalline porosity. Highly siliceous chertified dolomite zones throughout. Hard.

2677.9	17.7	Chert, dolomitic. Light gray to brown (oil stained) chertified dolomite algal and thrombolitic mudstone; few white to gray chert nodules. Vuggy and fractured; tight matrix down to 2686, microporous, oil stained 2686 to base.
2695.6	61.4	Cherty, dolomitic. Light to dark bluish- to brownish-gray chertified dolomite mudstone with nodules of white chalky chert and hard dense dark gray chert. White dolomite crystals fill vugs and line cavities. Thin zones of brecciated chert. Vugs to 2 cm high extend across core. Matrix tight to slightly porous (some intervals salt encrusted). Mostly crudely laminated. Gradational to unit below. Very hard.
2757	73.5	Chert and dolomite. Light brownish-gray to medium gray, mostly porous chertified burrowed dolomite mudstones, algal laminates, and hemispherical stromatolites. Nodules of white to dark gray brecciated dense chert. Irregularly interbedded intervals of less siliceous medium to coarse crystalline dolomite. Numerous quartz-crystal-lined vugs, some extending entirely across core and 1–2 cm high. Much intercrystalline microporosity and vuggy macroporosity. Zones of extremely high permeability, cavernous vuggy porosity at 2784.3–.7, 2789.4–90.2, 2791–92.3. Zone of extremely hard dense chert 2785.5–2788.5. Very hard.
(2830.5)	(108.8)	(?*Gunter Sandstone Member* of *Gasconade Fm.*?)
2830.5	33.5	Dolomite, sandstone, and chert. Dolomite, medium brownish-gray, medium to coarsely crystalline, burrow-mottled and algal laminated mudstone; locally siliceous grading to chertified dolomite (no distinct chert nodules). Sand occurs as many thin lenses in dolomite, and thicker beds of white, medium grained, well rounded sand at 2737–38.7, 2846.8–2849.4, 2851.6–2854, 2858.9–2859.8. Transitional contact to unit below. Hard.
2864.0	10.6	Dolomite, siliceous. Medium to dark gray, medium to coarse crystalline laminated to burrow-mottled siliceous mudstone; thin dark shaly zones and sandstone stringers. Generally tight with scattered small vugs, dolomite or chert filled. Hard.
2874.6	9.2	Dolomite and sandstone, interbedded. Dolomite medium to dark gray, medium crystalline tight, siliceous, laminated to slightly burrowed mudstone. Interbeds of white to light gray with brown stringers medium- to coarse-grained quartz sandstone, tight, at 2874.6–75.2, 2878.9–79.1, 2881.0–83.8. Hard.
2883.8	18.3	Dolomite, siliceous to chertified. Medium to dark gray, medium crystalline laminated and burrow-mottled. Tight with mostly isolated open or dolomite-filled vugs. Thin vuggy zones of sulfide mineralization 2885–2897. Dolomite all very hard, siliceous, locally converted to dense chert. Very hard.
2902.1	10.1	Sandstone, dolomite, and shale. Sandstone, white to medium gray, medium to coarse grained, locally pebbly with thin intercalation of dolomite and shale. Dolomite, light brownish-gray, burrow-mottled and medium crystalline mudstone, beds 0.4–1.0 ft thick. Shale dark greenish-gray, thin laminae to units 0.3 ft thick. Hard.
2912.2	3.9	Dolomite and shale, sandy. Dolomite, light brownish-gray, medium crystalline, burrow-mottled mudstone. Shale, light to medium gray laminae to units 0.2 ft thick. Floating quartz sand throughout; few thick sand lenses. Hard.
2916.1	2.4	Sandstone. White to light greenish-gray, medium to coarse grained, locally fine pebbles. Slightly porous (core salt coated). Hard.
2918.5	20.8	Dolomite, shale, and sandstone, interbedded. Dolomite, medium crystalline, light gray to dark brownish-gray, burrow-mottled to laminated mudstone. Thin interbeds of shale or sandstone <0.5 ft thick. Sandstone as above. Shale, light to dark greenish-gray with sparse small fossil fragments. Trilobite fragment at 2919. Pebbly, weathered disconformity zone at 2932–33. Moderate to hard.
(2939.3)	(72.2)	(*Basal Sandstone; "Reagan Fm."*)
2939.3	7.5	Sandstone, locally shaly. White to light brown, fine to very coarse grained, locally with fine pebbles of adjacent lithologies. With thin shaly laminae and shale beds as above <0.2 ft. Moderate to hard.
2946.8	10.2	Sandstone, shale, and mudstone. Fine to very fine-grained sandstone and mudstone, light gray to medium brown with laminae and thin interbeds of greenish-gray shale. Locally burrowed. Transitional contact. Moderate to hard.
2957.0	23.0	Sandstone, locally shaly. White, light brown to medium gray, medium to very coarse grained and fine pebbly, locally highly porous. Brown zones appear oil stained but no cut and no fluorescence. Mostly quartz with pebbles and grains of adjacent lithologies. Shale zones, as above, at 2964.3–.9, 2966.7–67.2, 2973.4–.5. Horizontal bedding. Moderate.
2980	9.0	Sandstone, arkosic. Light to dark brown, fine- to very coarse-grained and pebbly arkosic sandstone, derived from underlying porphyritic andesite with thin fine-grained to slightly shaly layers at 0.5–0.2 ft. Horizontal bedding. Moderately hard.
2989	2.0	Arkosic sandstone. Dark brownish-gray, fine- to coarse-grained, poorly sorted arkosic sandstone with faint dark hori-

		zontal laminae and irregular vertical burrows or root remains. Transitional lower contact. Hard.
2991	20.5	Arkosic sandstone. Light gray to light red-brown grading down to medium to dark reddish-brown; fine to coarse grained with very thin horizontal dark shaly laminae. Increasingly pebbly toward base. From 3010 to 3011.5 are discontinuous layers of pebbles to 2 cm across including white quartzitic sandstone, chert, shale, and andesite. Possibly a volcanic agglomerate. Hard.
(3011.5)	(458.5 to TD)	(PRECAMBRIAN, *Washington Volcanic Group*) (See Denison, 1981.)
3011.5	4.5	Weathered andesite porphyry, medium reddish-brown with dark gray phenocrysts and pale groundmass. Dark shaly material at basal contact. Hard.
3016	454.0	Andesite porphyry, medium reddish-brown, igneous rock with abundant light brown feldspar phenocrysts to 1 cm across, commonly zoned; fine-grained black ferro-magnesium minerals; aphanitic reddish-brown ground mass. Sparse vertical fractures and rare horizontal fracture zones locally altered to bright green epidote. (e.g., 3161: 0.2 ft zone of epidote; 3443: epidote along vertical fracture.) Slight flow banding. Appears identical to TD; core not examined through interval 3173–3442. See thin section description by R. E. Denison, in text.
3470		Total depth

Petrophysical Characteristics (Based on One Core) of the Cambro–Ordovician Arbuckle Dolostone, Arkoma Basin, Wilburton Field, Latimer County, Oklahoma

Liang Chuanmao*
Brooklyn College, City University of New York

Gerald M. Friedman
Northeastern Science Foundation, Troy, New York

ABSTRACT.—The Arbuckle dolostone in the studied core of the Anadarko Petroleum Co. Williams A-3 well can be divided into five distinct facies groups on the basis of megascopic and thin-section examination. These groups are: (A) micro- to very fine-crystalline dolostone, (B) very fine- to fine-crystalline dolostone, (C) unimodal fine- to medium-crystalline dolostone, (D) crystalline dolostone in which original particles are preserved, and (E) terrigenous, sandy dolostone.

The sedimentary facies analysis suggests that these distinct petrofacies groups correspond with three kinds of sedimentary environments. Groups A, B, and C represent a lime-mud supported, low-energy environment of a subtidal shallow-water setting, and group D displays characteristics indicative of a high-energy environment of the intertidal zone. Group E samples, consisting of terrigenous, sandy dolostones, were mostly formed in inferred intertidal to supratidal environments.

The petrophysical characteristics of Arbuckle dolostones analyzed are here related to their facies, and hence will be labeled petrofacies. Groups A, B, and C have the lowest porosity (mean = 0.48%) and recovery efficiency (mean RE = 1.05%) values. Group D has high porosity (mean = 4.14) and medium recovery efficiency (mean RE = 6.86%), and group E is characterized by high recovery efficiency (mean RE = 15.20%) and relatively low porosity (mean = 1.52%).

INTRODUCTION

Upper Cambrian and Lower Ordovician carbonate rocks are widespread throughout North America, comprising the basal transgressive (Sauk) sequence on the craton. The Cambrian to Lower Ordovician rocks in the Oklahoma and Arkansas region are named the Arbuckle Group. The stratigraphic equivalent of the Arbuckle Group in the Texas and New Mexico region is the Ellenburger Group, and in the midwestern and eastern United States, the Knox and Beekmantown Groups. One of us (G. M. Friedman) has studied, with students, the Arbuckle correlatives in Texas and New Mexico (Lee and Friedman, 1987; Amthor and others, 1988; Amthor and Friedman, 1989,1991) and in the midwestern and eastern U.S.A. (Braun and Friedman, 1969; Buyce and Friedman, 1975; Mazzullo and Friedman, 1975,1977; Rubin and Friedman, 1977,1981; Friedman and Radke, 1979; Harris and Friedman, 1982; Dolfi and Friedman, 1983; Conway and Friedman, 1984; Curl and others, 1984). Our study of the Arbuckle Group relates to our experience in the correlative units of other parts of the North American craton.

The Arkoma basin is a structural foredeep basin extending from central Oklahoma to eastern Arkansas, and is bounded by the northeast Oklahoma platform and Ozark uplift on the north, and the Ouachita Mountains on the south (Fig. 1). The Arkoma basin was part of a broad continental shelf along a passive continental margin bounded by the Ouachita trough on the south. Continental convergence began in the middle Mississippian, ultimately resulting in the conversion of the shelf into a foredeep basin in the middle Atokan (Ham, 1969; Houseknecht, 1986; Sutherland, 1988; Vanarsdale and Eugene, 1990). The Arbuckle Group consists almost entirely of carbonates, either limestone or dolostone. Terrigenous material, in the form of distinct beds of quartzose sand-

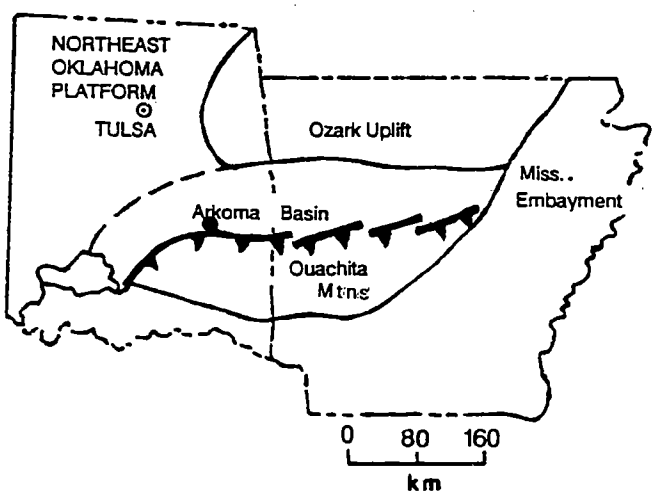


Figure 1. Location map showing Arkoma basin of Oklahoma and Arkansas, and the Anadarko Petroleum Co. Williams A-3 well from which we obtained the cores. The location of the well is indicated by a solid circle; faults are indicated by a heavy line with solid triangles.

*Visiting associate professor from China University of Geosciences, Beijing, China.

stones and thin clay shales, occurs to a very minor degree. In many places, however, the carbonates contain variable amounts of quartz sand grains scattered through the rock. Sporadic occurrences of abundant chert, usually in nodular form, are present (Burgess, 1968).

The potential of the Arbuckle Group as a new carbonate reservoir has recently piqued the interest of petroleum geologists and oil and gas companies (Bertagne and Leising, 1989; Camp and Robter, 1989; Dresbach and Ethington, 1989; Hook, 1990). Lower Paleozoic rocks of Oklahoma and Arkansas are made up of two distinct facies: the Ouachita facies, which is made up of deep-water sediments accumulated in a starved basin south of the southern margin of the North American craton; and the Arbuckle or foreland facies, which is made up of shallow-water clastics and carbonates accumulated in a shelf environment to the north. Rocks of the former facies have since been displaced by northward thrusting to overlie rocks of the latter facies. The Ti Valley fault forms the boundary between the two sedimentary types (Tilford, 1990).

We obtained cores from the Anadarko Petroleum Co. Williams A-3 well in the Wilburton field of the Arkoma basin. The well is located in NW¼ sec. 23, T. 5 N., R. 18 E., Latimer County, Oklahoma, and was drilled in 1989 (Fig. 1).

The total well depth is ~15,000 ft. Core samples were taken from two intervals of the well: from depths in the range 13,562–13,596 ft, and from depths in the range 13,948–13,960 ft. These samples are from the Arbuckle Group and represent a shelf-depositional environment.

Texture and structure of a sedimentary rock are closely related to the rock's sedimentary environment and have an immediate effect on petrophysical characteristics. Studies of petrology and sedimentary environment are necessary for an understanding of the petrophysical characteristics. In this paper, we focus on the relationships between porosity, mercury-recovery efficiency, pore-throat-size distribution, capillary-pressure curve shapes, and lithologic information from petrographic analysis to define petrophysical facies or petrofacies.

MATERIALS AND METHODS

A total of 30 core plugs, with thin sections corresponding to each plug, were made from the Arkoma basin cores. These plugs were analyzed using a Micromeritics Pore Sizer 9305. This instrument is capable of measuring mercury intrusion over a pressure range from 1.5 to 30,000 psia air-Hg (0.01–207 MPa) (conversion factor is psia × 0.006895 = MPa). Some of the sample set were analyzed in duplicate.

The plugs were cleaned before analysis. They were submerged first in a 1:1 toluene-acetone mixture for 48 hours in closed vials, then the mixture was changed to pure toluene for 24 hours (Kopaska-Merkel and others, 1987; Kopaska-Merkel and Friedman, 1989; Ghosh and Friedman, 1989; Friedman and others, 1990). Petrophysical analysis procedures using the Micromeritics Pore Sizer 9305 follow the Micromeritics manual (1983), Kopaska-Merkel and Amthor (1988), Ghosh and Friedman (1989), Kopaska-Merkel and Friedman (1989), Friedman and others (1990), and Melas and Friedman (in press).

TABLE 1. — PETROFACIES OF DOLOSTONE AND NUMBER OF SAMPLES STUDIED

Group	Petrofacies	Number
A	micro- to very fine-crystalline dolostones	10
B	very fine- to fine-crystalline dolostones	9
C	unimodal fine- to medium-crystalline dolostones	5
D	crystalline dolostones in which original particles are preserved	2
E	terrigenous sandy dolostone	4
Total		30

Most samples were exposed to pressures of up to 20,000 psia. For some samples, intrusion continued to increase at pressures above 20,000 psia; these samples were subjected to pressures up to 25,000 or 30,000 psia. Such high pressures cover the full range of porosity in the samples described here.

PETROLOGIC CHARACTERISTICS AND LITHOFACIES

Petrologic Characteristics

The Arbuckle or foreland facies of the Arbuckle Group consists mostly of carbonate sequences. As a result of diagenesis, these carbonates have been changed into relatively pure dolostones. In many cases, the original sedimentary textures and structures cannot be easily recognized, so we employed the classification whereby dolostones are defined on the basis of crystal-size distribution (unimodal or polymodal) and crystal-boundary shape (planar or nonplanar). This classification scheme employs terms introduced by Friedman (1965). The classification is descriptive, but carries genetic implications because size distribution is controlled by both nucleation and growth kinetics, and crystal-boundary shape is controlled by growth kinetics (Sibley and Gregg, 1987).

In this study the classification of dolomite-rock texture is based on the use of the petrographic microscope. For crystal-size distributions, the apparent maximum dimension of the dolomite crystals was measured and estimated, and subdivided using a size scale (Folk, 1962; Friedman, 1965). The following dolostones have been defined (Table 1):

A) Micro- to very fine-crystalline dolostones. These are dense, gray to dark-gray, commonly with developed horizontal laminae, unimodal micro- to very fine-crystalline and locally fine- to medium-crystalline (Fig. 2). In places the micrite texture can be observed, in which pisolites occur as ghosts and terrigenous silt (<5%) may be present. Petrographic characteristics of this dolostone indicate that it was a lime-mud carbonate which accumulated in a relatively low-energy sedimentary environment.

B) Very fine- to fine-crystalline dolostones. These are dense-massive, gray, most of which are composed of very fine to fine, nonplanar, anhedral to subhedral mosaics of

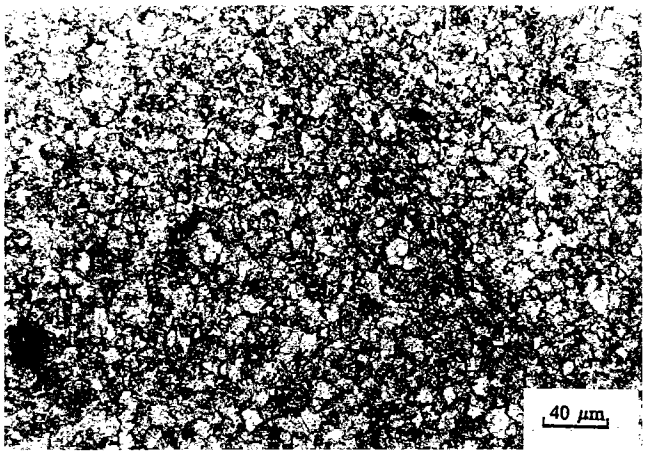


Figure 2. Thin-section photomicrograph of micro- to very fine-, partially crystalline dolostone from group A.

unimodal crystals (Fig. 3). A few samples in this group could be recognized as original micrite. This texture can be observed carefully in the hand samples. Under the petrographic microscope it can be seen that the original grain texture has been completely destroyed as a result of recrystallization. Locally, coarse crystals of dolomite occur in this fabric (Fig. 4).

C) Unimodal fine- to medium-crystalline dolostones. Dense, gray, unimodal fine- to medium-crystalline mosaics of crystals (150–400 μm), with most about 250–300 μm in crystal size; the crystals are planar-subhedral to euhedral (Fig. 5). No pores are observed. This dolostone probably formed at the expense of an original lime mud or micrite.

D) Crystalline dolostones in which original particles are preserved. In these dense, gray dolostones, the particles are mostly intraclasts and ooids, fine to coarse sand, locally fine gravel in size, rounded to subrounded. Intraclasts possess micritic texture. These dolostones underwent recrystallization, but the original texture can be recognized in both hand samples and under the petrographic microscope. Subhedral to euhedral fine-crystalline dolomites occur among the particles as cement, locally developed, with a few vuggy, open pores (Fig. 6B).

E) Terrigenous sandy dolostones. These dolostones are light-gray to gray in color and contain terrigenous sand particles (locally about 40–45%). The terrigenous sand is composed mostly of quartz and some feldspar particles, rounded to subrounded, of medium to coarse texture (Fig. 7A,B,C). In places, carbonate intraclasts and peloids occur. Micrite is polymodal and very finely crystalline. In places, it has enlarged to coarse- to very coarse-crystalline, planar-subhedral to euhedral mosaic texture. Stromatolites are present locally.

Microfractures are developed in places, but were almost totally filled by late-crystallized carbonate minerals. The effect of microfractures on the pore system of the dolostone will be discussed in a later section.

Lithofacies and Sedimentary Environments

Our ability to reconstruct the ancient sedimentary environment is limited because the small number of cores obtained provide insufficient information about macrosedimentary structures, and because diagenetic processes have partially, and in some cases totally, obliterated the original fabric of the rocks.

Three lithofacies have been defined on the basis of studies of hand samples and thin sections. These indicate three shallow-water environments: (1) a subtidal, low-energy, shallow-water, lime-mud dolostone facies; (2) an intertidal, high-energy dolostone facies; and (3) an intertidal to supratidal micritic dolostone facies containing terrigenous particles. These three facies are described as follows:

1) Subtidal, low-energy, shallow-water, lime-mud dolostone facies. This lithofacies includes groups A, B, and C of the petrofacies. They are characterized by original lime-mud carbonates and a few mud-supported dolostones, which are dark-gray, with well-developed horizontal laminae.

2) Intertidal, high-energy dolostone facies. This facies commonly displays intraclasts and ooids and is well sorted; its particles are rounded, and, in places, display cross-bedding. This last is characteristic of an intertidal,

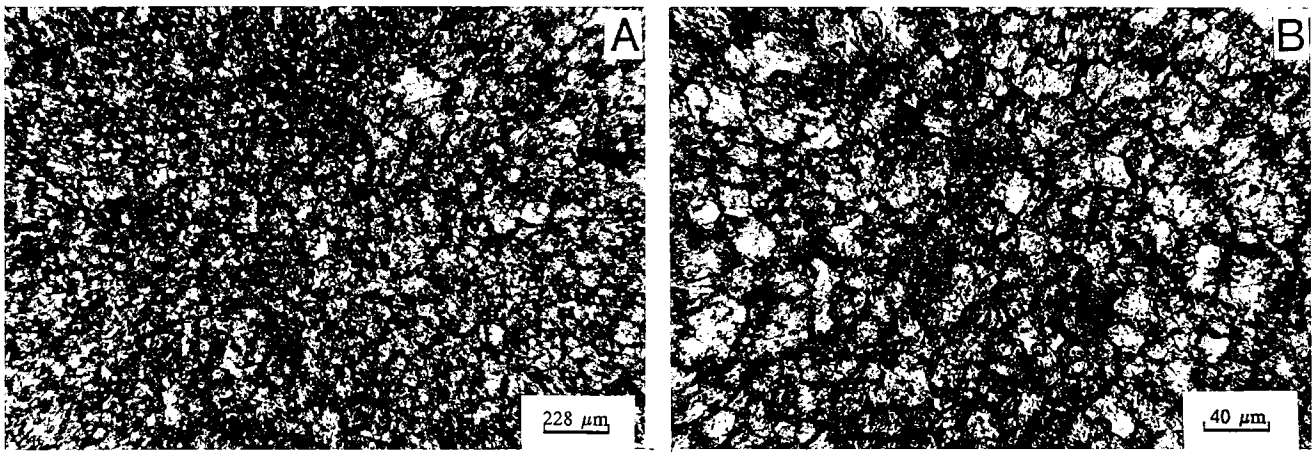


Figure 3. Thin-section photomicrographs of very fine- to fine-crystalline dolostone from group B, showing a unimodal, very fine to fine, nonplanar, anhedral to subhedral mosaic texture.



Figure 4. Thin-section photomicrograph from group B. This sample is a micritic dolostone. The original texture has been completely destroyed. Coarse-crystalline, subhedral to euhedral dolomite occurs locally.

high-energy environment of deposition. Group D is a product of this environment.

3) Intertidal to supratidal micritic dolostone facies containing terrigenous particles. Group E can be regarded as a representative of this lithofacies. It contains terrigenous clasts (5–30%), which are well rounded and well sorted. In places, intraclasts can be recognized, as well as locally developed algal laminae.

The vertical changes of these lithofacies and environments are shown in Figure 8.

PETROPHYSICAL ANALYSIS OF THE ARBUCKLE DOLOSTONES

Petrophysical data obtained from mercury porosimetry indicate that the studied Arbuckle dolostones are characterized by a low-porosity range from 0.17 to 4.34%. Table 2 presents details of their petrophysical characteristics. Five petrophysical groups corresponding to the five petrofacies described above have been defined:

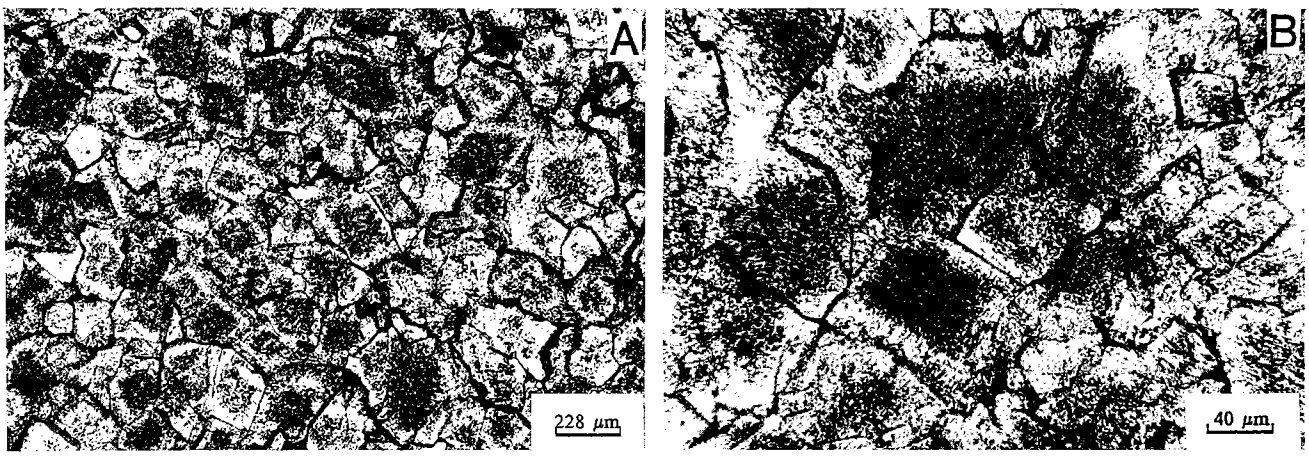


Figure 5. Thin-section photomicrographs from group C, showing a unimodal, fine- to medium-crystalline dolostone with planar-subhedral to euhedral mosaic texture.

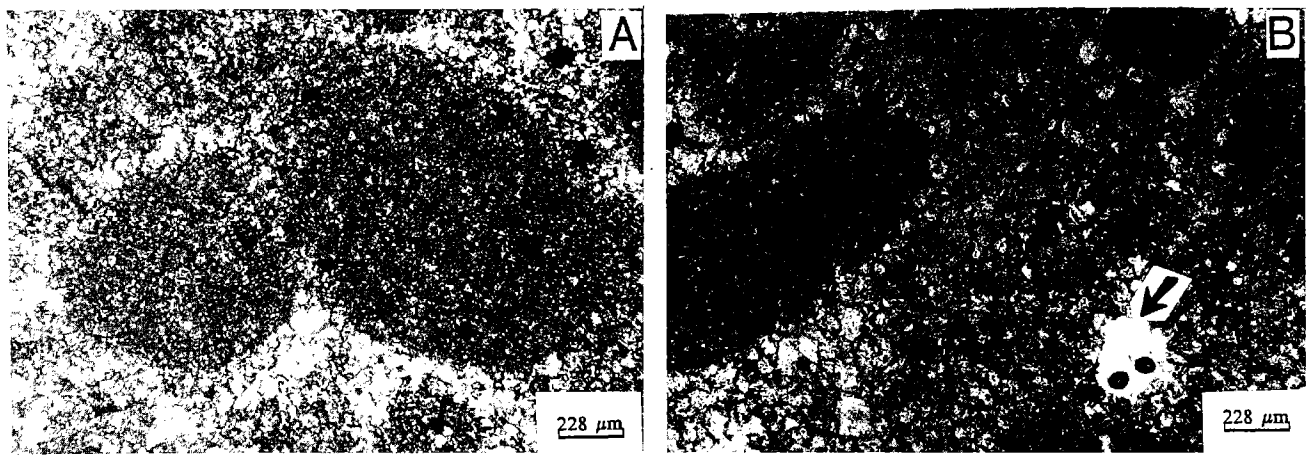


Figure 6. Thin-section photomicrographs of dolostone from group D, showing grain-supported texture, micritic intraclasts, and subhedral to euhedral fine-crystalline dolomites among these intraclasts. A few vuggy pores are present (B, arrow).

Group A—Micro- to very fine-crystalline dolostones. The rocks of this petrofacies are primarily dolomitized, crystalline, mud carbonates. Ten samples belonging to this petrophysical group have been analyzed (Fig. 9). They are characterized by low porosities (mean = 0.48%), large median pore throats (mean = 9.21 μm), relatively small normalized pore throats (mean = 8.90), platykurtic pore-throat size distributions, and very low recovery efficiency (RE). Cumulative intrusion curves are concave. The cumulative extrusion curves, if any, are divergent from the intrusion curves.

Group B—Very fine- to fine-crystalline dolostones. Rocks assigned to this petrophysical group are dolomitized lime-mud carbonates (dolomicrite) and, in part, are mud-supported grainstone. Nine samples belonging to this group have been analyzed. They are mostly composed of very fine dolomite, and locally developed fine to medium, subhedral-euhedral dolomites. Typically, these rocks have convex cumulative intrusion capillary-pressure curves (Fig. 10). A few have gently sloping, incremental intrusion curves, show leptokurtic modes at small pore-throat sizes with minor modes at very large pore-throat sizes; low porosities (mean = 0.99%), low RE values (from 0 to 6.49%, mean = 1.37%), very small median throat sizes (mean = 0.07 μm), and normalized throat-size values are very large (mean = 131.95), resulting from the presence of a substantial coarse tail in the positively

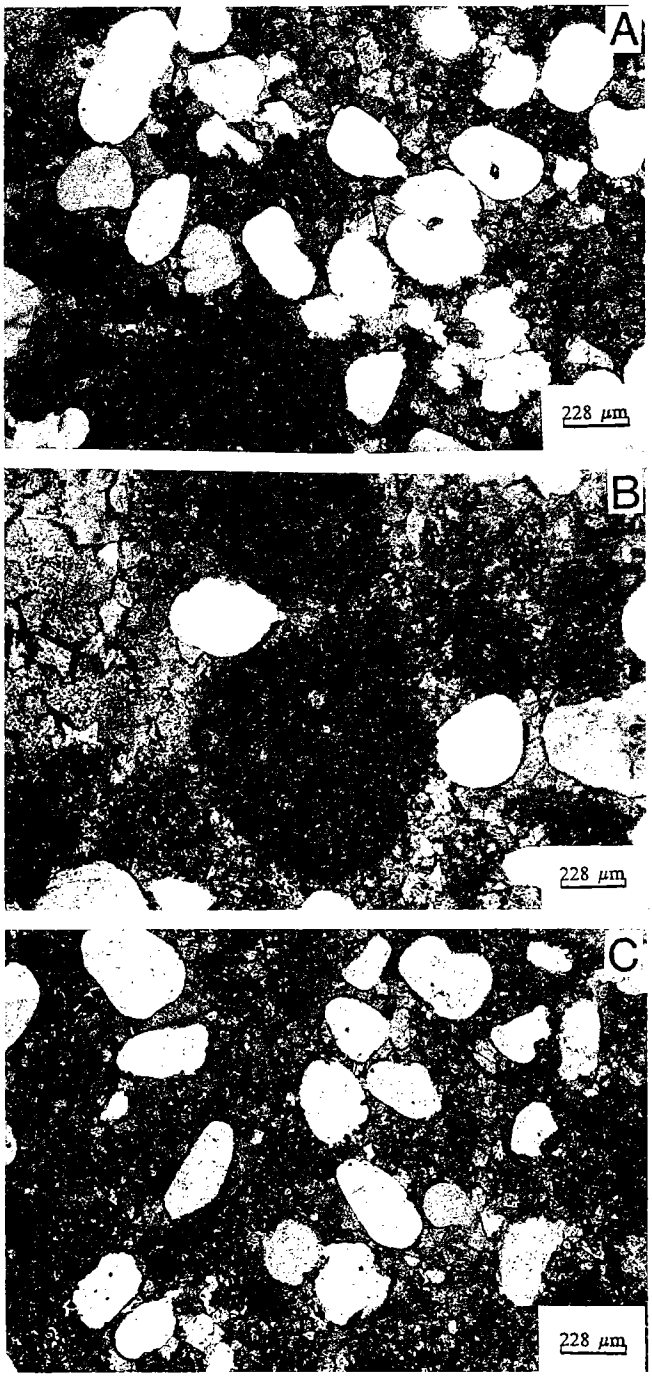


Figure 7. Thin-section photomicrographs of terrigenous sandy dolostones from group E, showing subrounded to rounded terrigenous quartz particles, locally medium- to coarse-crystalline, subhedral to euhedral mosaic texture (*A*), some intraclasts with micrite texture (*B*), and carbonate micrite and peloids (*C*).

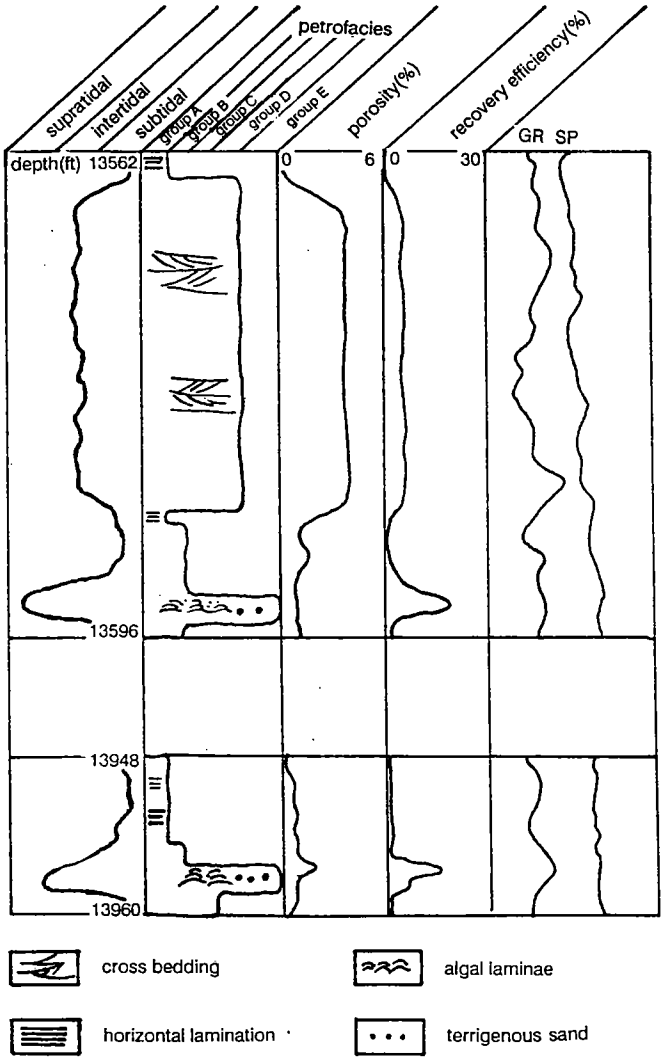


Figure 8. Schematic diagram showing the changes of petrofacies, lithofacies, and petrophysical characteristics.

TABLE 2. — SOME PETROPHYSICAL PARAMETERS OF ARBUCKLE DOLOSTONES STUDIED*

Group**	Porosity (%)	Recovery efficiency (%)	Median throat size (microns)	Normalized throat size	Number of samples
A	0.48 0.17–0.76	1.05 0–10.53	9.23 4.33–19.08	8.90 2.53–28.17	10
B	0.99 0.47–212	1.37 0–6.49	0.07 0.01–0.18	131.95 0.74–669.78	9
C	0.97 0.76–1.17	0.50 0–2.50	0.83 0.51–1.79	28.94 5.19–64.95	5
D	4.14 3.93–4.34	6.86 6.83–6.89	0.42 0.16–0.68	14.38 13.13–15.62	2
E	1.52 0.90–2.36	15.20 8.69–21.87	1.10 0.26–2.09	12.31 6.35–17.76	4

* 0.48 / 0.17–0.76 ----------> average / minimum–maximum

**A—micro- to very fine-crystalline dolostones; B—very fine- to fine-crystalline dolostones; C—unimodal fine- to medium-crystalline dolostones; D—crystalline dolostones in which original particles are preserved; E—terrigenous sandy dolostones.

skewed, pore-throat-size distribution. Many samples have little or no cumulative extrusion. The cumulative extrusion curves, if any, are strongly divergent from the cumulative intrusion curves.

Group C—Unimodal fine- to medium-crystalline dolostones. Five samples belonging to this group have been analyzed. These samples have polymodal, cumulative intrusion capillary-pressure curves (Fig. 11), small median pore-throats (mean = 0.83 μm), low porosities (mean = 0.97%), and low RE values (mean = 0.50%). Normalized pore-throat sizes are relatively high (mean = 28.94). Most samples have no extrusion, and incremental intrusion curves are distinctly polymodal. Groups A, B, and C are all poor reservoir rocks because they have fairly low porosities and low RE values. They were mud carbonates from subtidal, low-energy environments.

Group D—Crystalline dolostones in which original particles are preserved. Two samples have been analyzed from this petrofacies. Despite the small number of samples (two), this is a valid petrofacies because its cores are petrographically very homogeneous. Cumulative intrusion curves for these samples are convex to gently sloping, cumulative extrusion curves are divergent from cumulative intrusion curves, and incremental intrusion curves are bimodal or platykurtic (Fig. 12). They have high RE values (mean = 6.86%), low to median throat sizes (mean = 0.42 μm), and moderate, normalized pore-throat sizes (mean = 14.38). The pores of these rocks are mostly vuggy, open pores formed between the carbonate

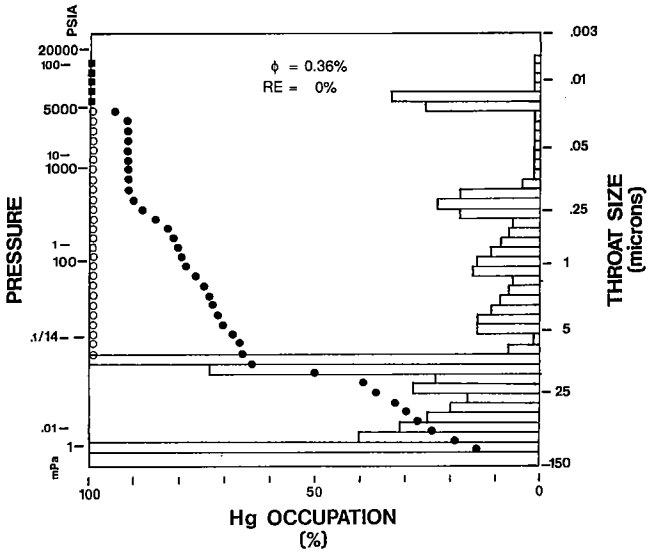


Figure 9. Capillary-pressure curve (CP) of sample from group A (micro- to very fine-crystalline dolostones). CP increase yields cumulative intrusion curve, indicated by filled circles, and cumulative extrusion curve, indicated by open circles. Cumulative intrusion and extrusion curves overlap, as indicated by filled squares, and open bars of histogram show incremental intrusion. The sample shows a platykurtic pore-throat size distribution and the cumulative intrusion curve is concave.

grains (Fig. 6B), with other pores being interparticle and intercrystalline. Mercury intrusion takes place mostly in the vuggy pores.

Group E—Terrigenous sandy dolostones. Analyzed samples come from two intervals of the cores: depths ranging from 13,593 to 13,595.5 ft in the upper interval; and depths ranging from 13,955.8 to 13,958.2 ft in the lower interval. These samples have bimodal cumulative intrusion capillary-pressure curves (Fig. 13), median pore throats (mean = 1.10 μm), low to moderate porosities (mean = 1.52%), high RE values (mean = 15.20%), and low normalized pore-throat sizes (mean = 12.31). Incremental intrusion curves are distinctly bimodal. All cumulative intrusion curves are gently sloping, and most cumulative extrusion curves are convergent from the cumulative intrusion curves. Pores in this petrofacies are mainly interparticle and intercrystalline, which may contribute to the bimodal pore-throat-size distribution.

Groups D and E are the best reservoir rocks found among the samples analyzed, since they have both rela-

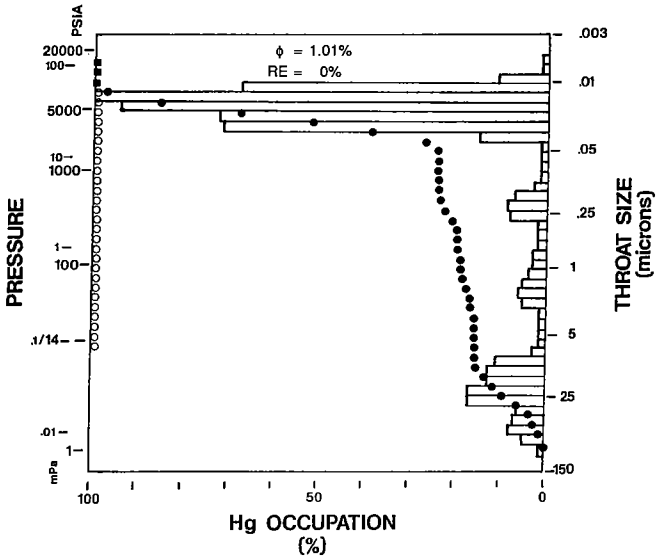


Figure 10. Capillary-pressure curve (CP) of sample from group B (very fine- to fine-crystalline dolostones). Symbols explained in Figure 9. The sample shows a typically convex cumulative intrusion capillary-pressure curve, and leptokurtic modes at small pore-throat sizes with minor modes at large pore-throat sizes.

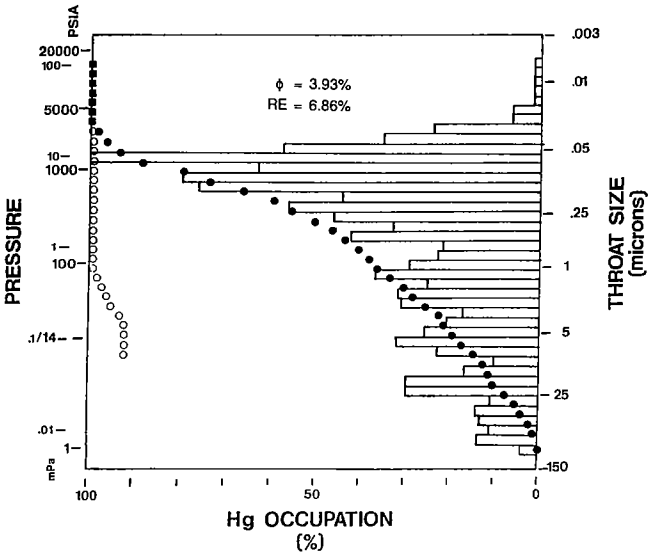


Figure 12. Capillary-pressure (CP) curve of sample from group D (crystalline dolostones in which original particles are preserved). Symbols explained in Figure 9. The sample shows a convex to gently sloping cumulative intrusion curve, and bimodal and platykurtic incremental intrusion curve. Cumulative extrusion curve is divergent from cumulative intrusion curve.

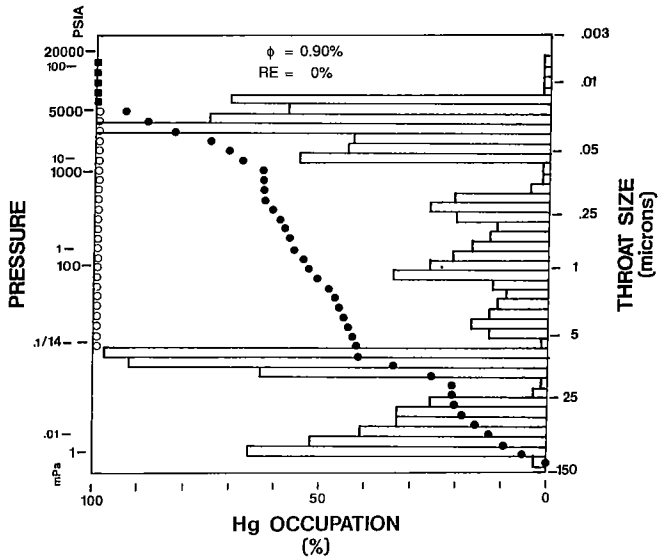


Figure 11. Capillary-pressure curve (CP) of sample from group C (unimodal fine- to medium-crystalline dolostones). Symbols explained in Figure 9. The sample shows a polymodal cumulative intrusion capillary-pressure curve, and distinctly polymodal incremental intrusion curve.

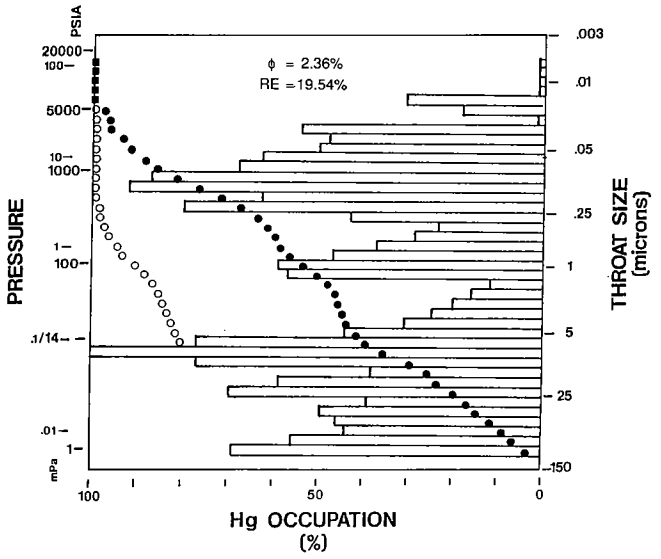


Figure 13. Capillary-pressure curve (CP) of sample from group E (terrigenous sandy dolostones). Symbols explained in Figure 9. The sample has a gently sloping cumulative intrusion curve, and a bimodal cumulative intrusion capillary-pressure curve.

tively high porosity and RE values. These lithofacies were formed mainly in shoals of high-energy zones and terrigenous sandy tidal flats, with stromatolites in intertidal to supratidal zones. Figure 8 shows clearly the relationship between petrophysics and lithofacies, and the relationship between sedimentary environments and changes in the stratigraphic sequences.

RELATIONSHIPS BETWEEN SOME PETROPHYSICAL PARAMETERS

The study of relationships between petrophysical parameters is an important aspect of petrophysical analysis (Wardlaw and Taylor, 1976; Wardlaw, 1979; Friedman and others, 1981; Ruzyla and Friedman, 1982; Etris and others, 1988; Wardlaw and others, 1988). We may predict some petrophysical characteristics of rocks on the basis of petrographic parameters. Of these relationships, RE to porosity, RE to median throat size, RE to normalized throat size, and porosity to median throat size are regarded as most important.

We undertook such a study for all samples. The relationships between some petrophysical parameters are given in Figures 14–16. We use a log scale for the X-axis in Figures 14 and 15, and for both axes in Figure 16, because many petrophysical parameters are so similar (such as porosity) or range so widely (median throat size), that they cannot be indicated using an algebraic scale.

The relationship between RE and porosity is not strong, but a weak positive relationship between them for all samples can be distinguished (Fig. 14). These results suggest that porosity is an important aspect in the relationship between RE and porosity for rocks we studied with very low porosity (commonly <1%), and we can see that most samples in all groups with low porosity (<1%) have no recovery efficiency (Fig. 14). The positive relationship between porosity and RE is different from results of some papers published on petrophysical analysis of dolostones (Amthor and others, 1988; Kopaska-Merkel and Friedman, 1989; Guo and others, 1991). In their papers, an inverse relationship between RE and porosity was shown. However, Wardlaw (1976,1980), found a positive relationship between RE and porosity for two sets of carbonate-rock samples. RE and porosity are also positively related for samples of the Permian San Andres Formation (Ghosh and Friedman, 1989). Wardlaw (1976) attributed this positive relationship to an inferred correlation between pore-system geometry and porosity.

It is difficult to determine the relationship between RE and median throat size for all samples of a group, but samples from groups B, D, and E show a positive relationship between RE and median throat size (Fig. 15). For all samples studied, the relationship between porosity and median throat size is not strong, but the inverse relationship between median throat size and porosity is well defined for groups A, C, D, and E (Fig. 16). Such an inverse relationship is not found in group B (very fine- to fine-crystalline dolostones).

DISCUSSION

Amthor and Friedman (1989) studied petrophysics of the Lower Ordovician Ellenburger dolostones in Stateline field, New Mexico. They defined two petrofacies for the Ellenburger dolostones they studied on the basis of effective porosity, median pore-throat size, pore-throat size at 20% mercury saturation, normalized pore-throat size, recovery efficiency, and the shapes of the capillary-pressure curves. One of the petrofacies is a porous and permeable vuggy dolostone, which is roughly comparable petrophysically to group D of this paper. Another is the tight dolostone. The tight dolostone of Amthor and Friedman is somewhat close to groups A, B, and C of this paper, but with a primary difference in that the tight dolostone of the Ellenburger has a considerable recovery-efficiency value.

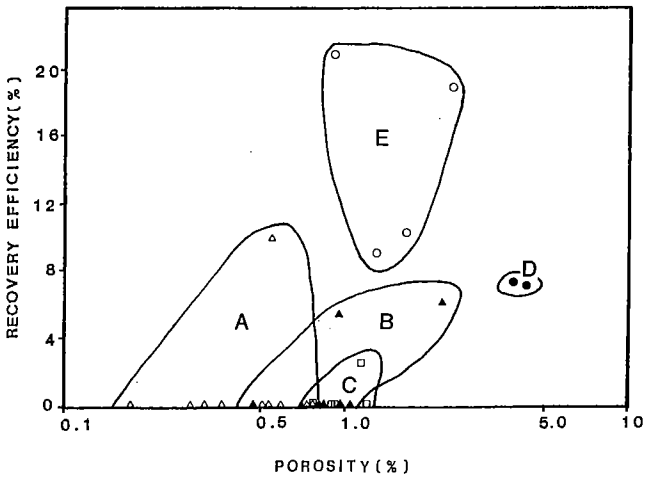


Figure 14. Bivariate plot of recovery efficiency (RE) vs. porosity for all studied samples (note the X-axis indicated by a log-scale), which shows a weak positive relationship between RE and porosity for all samples. Letters A, B, C, D, and E identify the petrofacies groups. Open triangles—micro- to very fine-crystalline dolostones; filled triangles—very fine- to fine-crystalline dolostones; open squares—unimodal, fine- to medium-crystalline dolostones; filled circles—crystalline dolostones in which original particles are preserved; and open circles—terrigenous sandy dolostones.

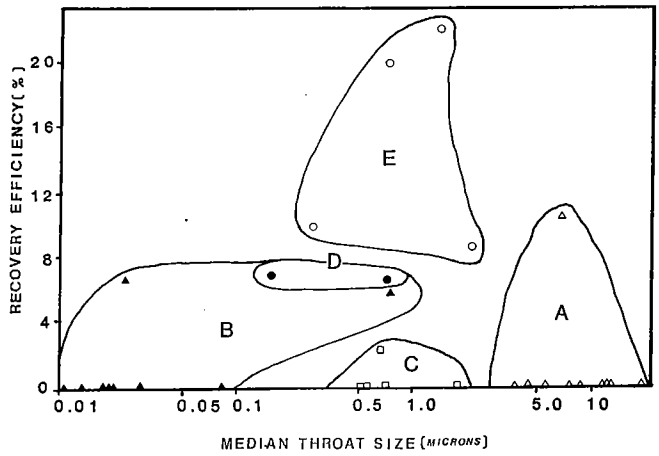


Figure 15. Bivariate plot of recovery efficiency (RE) vs. median pore-throat size for all studied samples (note the X-axis indicated by a log-scale), which shows a weak positive relationship between RE and median throat size for all samples. Letters and symbols explained in Figure 14.

The samples we analyzed are characterized by relatively low porosity. Most have porosities of 1% or less, except group D. The petrographic studies suggest that pores are mainly interparticle and intercrystalline for the groups A, B, C, and E. The porous volume of these rocks is very small because they are almost completely composed of very fine carbonate crystals, which are dense and tightly cemented. Microfractures are observed in these rocks, but are completely filled by late carbonate cement, so the fracture pores cannot contribute to the porosity for these rocks. In group E, the vuggy pores between particles play a key role in porosity. Their original grain-supported fabric may have provided good initial conditions for the formation of pores.

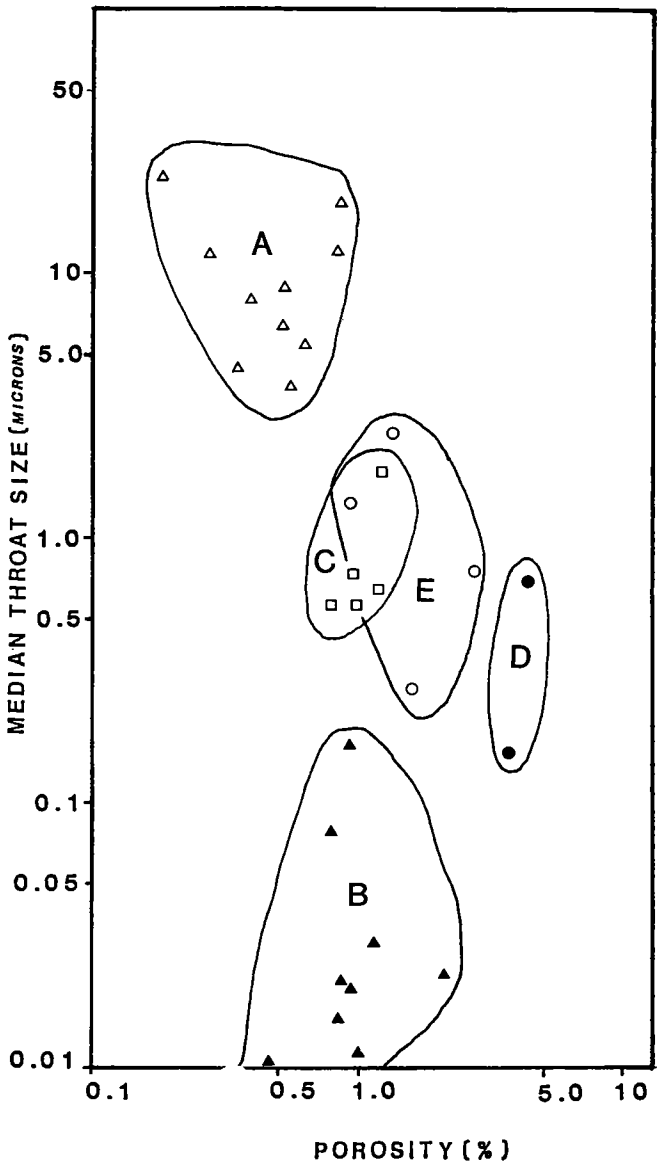


Figure 16. Bivariate plot of median throat size vs. porosity for all samples studied (note both X and Y axes indicated by a log-scale). The relationship between median throat size and porosity is not clear for all samples, but porosity is strongly inversely related to median throat size for samples of groups A, C, and E. Letters and symbols explained in Figure 14.

CONCLUSIONS

The petrophysical classifications of Arbuckle dolostone presented in this paper are based on effective porosity, median pore-throat size, recovery efficiency, and capillary-pressure curve forms. These parameters are directly related to the capacity of the rock to take up, store, and release nonwetting fluids. This capacity can in turn be used to predict and evaluate reservoir characteristics for the Arbuckle dolostones.

The best reservoir candidates among the rocks analyzed in this study are from group D (crystalline dolostones in which original particles are preserved) and from group E (terrigenous sandy dolostone). These rocks are the best potential reservoir rocks because they have both relatively higher porosities and RE values than rocks in the other groups. Groups A, B, and C would be effective hydrocarbon seals.

We determined the relationships between petrofacies and sedimentary lithofacies in order to use the petrophysical classification to predict the distribution of reservoir and seal units, and to pinpoint potential stratigraphic traps on the basis of sedimentary-facies analysis of cores. Generally speaking, the petrofacies and the sedimentary lithofacies are not congruent, but lithofacies located at a certain stratigraphy in the same place may have similar petrophysical characteristics due to the fact that they have undergone the same diagenetic history.

Amthor and Friedman (1989) defined two petrofacies for the Ellenburger dolostones they studies. One of them is a tight petrofacies, which is comparable to the groups A, B, and C in the paper. Another is a porous and permeable petrofacies, which most closely resembles the group D of this paper.

Recent studies of carbonate reservoirs pay more attention to paleokarstification, which greatly influences the petrophysical characteristics of carbonate reservoirs. The vertical and lateral heterogeneities in carbonate reservoirs are thought to result from episodic subaerial exposure and karstification, which creates vuggy, cavernous, solution-channel, moldic, breccia, and fracture porosity (Tobin, 1985; Kerans, 1988a,b). Karstification is absent in the samples we analyzed, and therefore indicates that paleokarstification does not exist in the cores studied; however, we obtained only a small section of core.

ACKNOWLEDGMENTS

We are indebted to the Anadarko Production Co., particularly to John Seitz, Vice President, for providing the cores for study, and to Union Pacific Resources and Stuart C. Strife, Manager of Geology, for financial support. Ken Johnson of the Oklahoma Geological Survey and B. N. Carpenter, Consulting Geologist/Log Analyst, Edmond, Oklahoma, gave us useful information. We would like to thank Steve Buttner of the Northeastern Science Foundation and Helen Tirschwell of Brooklyn College for helpful comments in their reviews of the manuscript.

REFERENCES CITED

Amthor, J. H.; and Friedman, G. M., 1989, Petrophysical character of Ellenburger karst facies: Stateline Ellenburger field, Lea County, southeastern New Mexico, *in* Cunningham, B. K.; and Cromwell, D. W. (eds.), The Lower Paleozoic of west

Texas and southern New Mexico—modern exploration concepts: Society for Economic Paleontologists and Mineralogists, Permian Basin Section, p. 133–144.

_____1991, Dolomite-rock texture and sedimentary porosity development in Ellenburger Group carbonates (Lower Ordovician); west Texas and southeastern New Mexico: Sedimentology, v. 38, p. 343–362.

Amthor, J. E.; Kopaska-Merkel, D. C.; and Friedman, G. M., 1988, Reservoir characterization, porosity, and recovery efficiency of deeply buried Paleozoic carbonates: examples from Oklahoma, Texas, and New Mexico: Carbonates and Evaporites, v. 3, p. 33–52.

Bertagne, A. J.; and Leising, T. C., 1989, Seismic exploration of Ouachita frontal fairway, southeastern Oklahoma [abstract]: American Association of Petroleum Geologists Bulletin, v. 73, p. 1043–1044.

Braun, M.; and Friedman, G. M., 1969, Carbonate lithofacies and environments of the Tribes Hill Formation (Lower Ordovician) of the Mohawk Valley, New York: Journal of Sedimentary Petrology, v. 39, p. 113–135.

Burgess, W. J., 1968, Carbonate paleoenvironments in the Arbuckle Group West Spring Creek Formation, Lower Ordovician, in Oklahoma: Columbia University unpublished Ph.D. dissertation, 165 p.

Buyce, R. M.; and Friedman, G. M., 1975, Significance of authigenic K-feldspar in Cambro–Ordovician carbonate rocks of the proto-Atlantic shelf in North America: Journal of Sedimentary Petrology, v. 45, p. 808–821.

Camp, W. K.; and Robter, A. R., 1989, Balanced cross section through Wilburton gas field, Latimer County, Oklahoma: implications for Ouachita deformation and Arbuckle (Cambro–Ordovician) exploration in Arkoma basin [abstract]: American Association of Petroleum Geologists Bulletin, v. 73, p. 1044.

Conway, S. W.; and Friedman, G. M., 1984, Depositional environments and diagenesis of the Lower Ordovician Gailor Formation, Schenectady County, New York: Northeastern Geology, v. 6, p. 135–150.

Curl, M. W.; Zagorski, T. W.; and Friedman, G. M., 1984, Depositional environments and diagenesis of subsurface Tribes Hill Formation (Lower Ordovician), Mohawk Valley, New York: The Compass of Sigma Gamma Epsilon, v. 61, p. 216–243.

Dolfi, R. U.; and Friedman, G. M., 1983, Regional lithofacies of Lower Ordovician (Canadian age) strata of New York and New England: Northeastern Geology, v. 5, p. 40–53.

Dresbach, R. I.; and Ethington, R. L., 1989, Conodont biostratigraphy of Lower Ordovician rocks, Arbuckle Group, southeastern Oklahoma [abstract]: American Association of Petroleum Geologists Bulletin, v. 73, p. 1045–1046.

Etris, R. J.; Brumfield, D. S.; Ehrlich, R.; and Crabtree, S. J., Jr., 1988, Relations between pores, throats and permeability: a petrographic/physical analysis of some carbonate grainstones and packstones: Carbonates and Evaporites, v. 3, p. 17–32.

Folk, R. L., 1962, Spectral subdivision of limestone types, *in* Ham, W. E. (ed.), Classification of carbonate rocks: American Association of Petroleum Geologists Memoir 1, p. 62–64.

Friedman, G. M., 1965, Terminology of crystallization textures and fabrics in sedimentary rock: Journal of Sedimentary Petrology, v. 35, p. 643–655.

Friedman, G. M.; and Radke, B. M., 1979, Evidence for sabkha overprint and conditions of intermittent emergence in Cambro–Ordovician carbonates of northeastern North America and Queensland, Australia: Northeastern Geology, v. 1, p. 18–42.

Friedman, G. M.; Ruzyla, K.; and Reeckmann, S. A., 1981, Effects of porosity type, pore geometry and diagenetic history on the tertiary recovery of petroleum from carbonate reservoirs: Report No. DOE/MC/11580-5, U.S. Dept. of Energy, National Tech. Info. Service, U.S. Dept. of Commerce, Springfield, Virginia, 217 p.

Friedman, G. M.; Ghosh, S. K.; and Urschel, S., 1990, Petrophysical characteristics related to depositional environments and diagenetic overprint: a case study of San Andres Formation, Mabee field, west Texas, *in* Bebout, D. G.; and Harris, P. M. (eds.), Geologic and engineering approaches in evaluation of San Andres/Grayburg hydrocarbon reservoirs—Permian basin: Bureau of Economic Geology, University of Texas, p. 125–144.

Ghosh, S. K.; and Friedman, G. M., 1989, Petrophysics of a dolostone reservoir; San Andres Formation (Permian), west Texas: Carbonates and Evaporites, v. 4, p. 45–119.

Guo, B.; Sanders, J. E.; and Friedman, G. M., 1991, Petrophysical characteristics of selected formations penetrated by the Finnegan Boring, southern Washington County, New York: Northeastern Geology, v. 13, p. 32–38.

Ham, W. E., 1969, Regional geology of the Arbuckle Mountains, Oklahoma: Oklahoma Geological Survey Guidebook 17, 52 p.

Harris, R. L.; and Friedman, G. M., 1982, Depositional environments of the subsurface Ogdensburg Formation (Lower Ordovician) in northern New York State: Northeastern Geology, v. 4, p. 151–166.

Hook, R. C., 1990, Recent developments at Wilburton field, Latimer County, Oklahoma: American Association of Petroleum Geologists Bulletin, v. 74, p. 677.

Houseknecht, D. W., 1986, Evolution from passive margin to foreland basin, the Atoka Formation of the Arkoma basin, south-central U.S.A., *in* Allen, P. A.; and Homewood, P. (eds.), Foreland basins: International Association of Sedimentologists Special Publication 8, p. 327–345.

Kerans, C., 1988a, Origin of reservoir compartmentalization in Lower Ordovician karstic dolostones, Ellenburger Group, west Texas: American Association of Petroleum Geologists Bulletin, v. 72, p. 25.

_____1988b, Karst-controlled reservoir heterogeneity in Ellenburger Group carbonates of west Texas: American Association of Petroleum Geologists Bulletin, v. 72, p. 1160–1183.

Kopaska-Merkel, D. C.; and Amthor, J. H., 1988, Very high-pressure mercury porosimetry as a tool in reservoir characterization: Carbonates and Evaporites, v. 3, p. 53–64.

Kopaska-Merkel, D. C.; and Friedman, G. M., 1989, Petrophysical analysis of carbonate rocks: example from the lower Paleozoic Hunton Group of Oklahoma and Texas: American Association of Petroleum Geologists Bulletin, v. 73, p. 1289–1306.

Kopaska-Merkel, D. C.; Amthor, J. H.; and Friedman, G. M., 1987, Notes on the use of a mercury porosimeter: Northeastern Science Foundation Technical Report 1, 12 p.

Lee, Y. I.; and Friedman, G. M., 1987, Deep-burial dolomitization in the Ordovician Ellenburger Group carbonates, west Texas and southeastern New Mexico: Journal of Sedimentary Petrology, v. 57, p. 544–557.

Mazzullo, S. J.; and Friedman, G. M., 1975, Conceptual model of tidally influenced deposition on margins of epeiric seas: Lower Ordovician (Canadian) of eastern New York and southwestern Vermont: American Association of Petroleum Geologists Bulletin, v. 59, p. 2123–2141.

_____1977, Competitive algal colonization of peritidal flats in a schizohalin environment: the Lower Ordovician of New York: Journal of Sedimentary Petrology, v. 47, p. 398–410.

Melas, F. F.; and Friedman, G. M. [in press], Petrophysical characteristics of the Jurassic Smackover Formation, Jay field (Conecuh Embayment, Alabama–Florida): American Association of Petroleum Geologists Bulletin.

Micromeritics Manual, 1983, Pore Sizer 9305: Micromeritics Instrument Corp., Norcross, Georgia.

Rubin, D. M.; and Friedman, G. M., 1977, Intermittently emergent shelf carbonates: an example from the Cambro–Ordovician of eastern New York State: Sedimentary Geology, v. 19, p. 81–106.

_____1981, Origin of chert grains and a halite-silcrete bed in the Cambrian and Ordovician Whitehall Formation of eastern New York State: Journal of Sedimentary Petrology, v. 51, p. 69–72.

Ruzyla, K.; and Friedman, G. M., 1982, Geological heterogeneities important to future enhanced recovery in carbonate reservoirs of Upper Ordovician Red River Formation at Cabin Creek field, Montana: Journal of Society of Petroleum Engineers, v. 22, p. 429–444.

Sibley, D. F.; and Gregg, J. M., 1987, Classification of dolomite rock texture: Journal of Sedimentary Petrology, v. 57, p. 967–975.

Sutherland, P. K., 1988, Late Mississippian and Pennsylvanian depositional history in the Arkoma basin area, Oklahoma and Arkansas: Geological Society of America Bulletin, v. 100, p. 1787–1802.

Tilford, M. J., 1990, Geological review of the Ouachita Mountains thrust belt play, western Arkoma basin, Oklahoma, *in* Suneson, N. H.; Campbell, J. A.; and Tilford, M. J. (eds.), Geology and resources of the frontal belt of the western Ouachita Mountains, Oklahoma: Oklahoma Geological Survey Special Publication 90-1, p. 169–196.

Tobin, R. C., 1985, Reservoir development in Ellenburger Group carbonates of west Texas: West Texas Geological Society Bulletin, v. 25, p. 21.

Vanarsdale, B. B.; and Eugene, S. S., 1990, Subsurface structure of the eastern Arkoma basin: American Association of Petroleum Geologists Bulletin, v. 74, p. 1030–1037.

Wardlaw, N. C., 1976, Pore geometry of carbonate rocks as revealed by pore casts and capillary pressure: American Association of Petroleum Geologists Bulletin, v. 60, p. 245–257.

_____1979, Pore geometry in dolomites and its influence on capillary behavior, *in* Symposium on advances in petroleum recovery: American Chemical Society, v. 21, no. 2, p. 231–242.

_____1980, The effects of pore structure on displacement efficiency in reservoir rocks and in glass micromodels: Society of Petroleum Engineers of AIME Preprint SPE 8843, p. 345–352.

Wardlaw, N. C.; and Taylor, R. P., 1976, Mercury capillary pressure curves and the interpretation of pore structure and capillary behavior in reservoir rocks: Bulletin of Canadian Petroleum Geologists, v. 24, p. 225–262.

Wardlaw, N. C.; McKeller, M.; and Yu, L., 1988, Pore and throat size distribution determined by mercury porosimetry and direct observation: Carbonates and Evaporites, v. 3, p. 1–16.

Deformation Characteristics of the Arbuckle Group

Bryan Tapp
University of Tulsa

ABSTRACT.—The deformation characteristics of the Arbuckle Group exercise strong control over the structural styles seen in the region. Data from several field seasons show that the Arbuckle Group deforms largely by a combination of fracturing, cataclasis, and pressure solution. Plastic deformation (formation of e twins in calcite or other dislocation processes) plays only a minor role in the accumulation of strain, and is ancillary to the brittle deformation in the region. As such, the style of structures near and along the Washita Valley fault in the Arbuckle uplift were formed primarily by brittle mechanisms involving cataclasis associated with pressure solution, fracturing, slip along bedding planes, and faulting.

INTRODUCTION

The discussion of deformation of the Arbuckle will be broken into two segments describing (1) the style and occurrence of fractures adjacent to the Washita Valley fault, and (2) cataclastic rocks and associated pressure solution and formation of saddle dolomites in and adjacent to the Washita Valley fault. The fold style and faulting style in the region have been discussed (Tapp, 1991a,b) and are largely due to brittle deformation in a wrench setting. This paper is not intended to provide a complete review of the structural styles preserved in the Arbuckle uplift, but will touch on several aspects of the deformation style that contribute substantively to the preserved structural style. This paper is limited to surface studies of the deformation characteristics of the Arbuckle uplift. Proprietary subsurface reports from productive Arbuckle plays corroborate the discussed deformation mechanisms and styles.

Regional Geologic Setting

The Arbuckle–Wichita trend consists of paired structural basins and uplifts along a NW–SE trend that intersects the Ouachita Mountains at nearly a right angle; it has been termed the southern Oklahoma aulacogen (Hoffman and others, 1974). Aulacogens preserve igneous and sedimentary rocks that record the opening and closure of ocean basins in a complete Wilson Cycle. Rocks in the aulacogen are usually preserved without metamorphism. Nicholi Shatskiy (1946) defined an aulacogen as a long-lived, fault-bounded trough, in an otherwise-stable platform, that intersects a deformed belt or a continental margin at a high angle and contains an abnormally thick, usually undeformed, section of terrestrial and marine sediments. Shatskiy (1946) used the Dnieper–Donets basin of the Russian platform, along with the Wichita system as type aulacogens. Hoffman and others (1974) presented a scenario for the evolution of aulacogens using the Athapuscow aulacogen and the southern Oklahoma aulacogen as examples. The evolution of an aulacogen is divided into three stages: rifting, subsidence, and deformation.

Rifting

The initial rifting stage in an aulacogen is related to continental breakup. Continental rift systems initiate at triple junctions and propagate outward (Burke and Dewey, 1973). In the rifting phase, a regional, positive heat-flow anomaly results in upwarp (doming) by thermal expansion of the lithosphere, forming a system of grabens that radiate away from the center of the uplift (Burke and Dewey, 1973; Hoffman and others, 1974). Axial dike swarms form in the rift systems [examples in the southern Oklahoma aulacogen include: *multiple dike sets in Tishomingo Granite*] that are most likely connected to a mafic intrusive body at depth [*Raggedy Mountain Gabbro and associated mafic intrusives of the Wichita Mountains*]. The materials associated with the earliest history of rifting have mantle affinities and are similar in chemistry to the classic tholeiitic intrusives of the Skaergaard and Stillwater complexes (Burke and Dewey, 1973; Hoffman and others, 1974; Pruatt, 1975; Burke, 1980). In later stages, some melting of crustal material occurs, along with differentiation of the magma source, resulting in bimodal volcanic-rock suites that range from fundamentally basaltic tholeiites, with some differentiated alkalic basalts, to andesitic rhyolites and rhyodacites (Hoffman and others, 1974; Burke, 1980) [*Mount Scott, Quanah, and associated granitic intrusives, and Carlton and Colbert Rhyolite porphyries*].

The rift valley is bounded by normal faults and may contain local horsts. Poorly sorted terrestrial clastics [*Reagan Sandstone*] derived from the elevated walls of the rift may interfinger with the basaltic and rhyolitic lavas erupting in the valley floor. The rift-bounding normal faults may serve as loci for subsidence in the forming aulacogen (Feinstein, 1981), and may also be reactivated (inverted) during deformation of the aulacogen.

Subsidence

Triple-junction related rifts typically propagate on only two of the rift arms of the triple junction, abandoning the third (failed) arm. This failed rift is a zone of weakness in the continental crust. Subsidence, coupled with

sediment-loading-induced flexure, results in the accumulation of marine clastics and carbonates in the failed rift located on a passive, trailing edge margin (the "miogeocline") (Dietz and Holden, 1967; Bott, 1973; Bond and Kominz, 1984).

The failed arm receives the same package of sediments that the continental margin and platform receive. The failed arm subsides along the bounding faults and accumulates an abnormal thickness of sediments relative to the platform (Feinstein, 1981) [*Cambrian Honey Creek Formation through Mississippian Caney Formation*]. Few structures can be associated with the subsidence phase of aulacogen development. If the system continues to subside, there may be local compression in the basal formations due to crowding. There may be cyclic repetition of sedimentary structures and types, if the failed arm subsides in a stick-slip or sporadic nature, resulting in cyclic uplift of source areas by elastic rebound (Tapp, 1978, 1991c).

Deformation

The failed arm is deformed along with the continental margin at the culmination of a Wilson Cycle. The style of deformation is dependent on the angle of convergence and whether the failed arm is on the subducting plate or on the overriding plate. The dominant style of deformation in the Arbuckle region appears to be strike slip (Ham and others, 1964; Tanner, 1967; Booth, 1981; Haas, 1981; Islam and Nielsen, 1984). There may also be reactivation of the bounding faults of the failed arm during closure (Brewer and others, 1981). Deformation by gravity tectonics (Hoffman and others, 1977; Phillips, 1983) or by thrusting, due to transverse compression (Brewer and others, 1983), has also been suggested. The deformation phase generates localized basins and uplifts that can accumulate locally significant conglomerates [*Atokan through Collings Ranch Conglomerates*].

Discussion

The structural and stratigraphic/sedimentologic features preserved in the Arbuckle Group reflect all stages of development of the southern Oklahoma aulacogen. The significant change in thickness of the Arbuckle Group across the Washita Valley fault is controlled by the localization of subsidence-related sedimentation by the initial rifting geometry. Many of the sedimentary features preserved in the Arbuckle Group are related to variations in sea level, caused either by eustatic sea-level changes or by variation in the mechanism and style of subsidence and related sediment accumulation in the aulacogen. The structural features seen in the Arbuckle uplift, while outwardly related to the deformation phase of aulacogen development, are ultimately related to, and in part controlled by, the initial rift geometry and reactivation (inversion) of rift-bounding faults as well as the thickness of accumulated sediments in the aulacogen. The Arbuckle Group represents a thick, mechanical strut that seems to deform as a single mechanical/stratigraphic unit. As such, the depositional characteristics (thickness and type of sediment) of the Arbuckle Group strongly affects the range of rock response that can occur during deformation. The lack of metamorphism in any rocks exposed in the Arbuckle uplift suggests that deformation occurred at low temperature (well below greenschist-grade conditions). Cool temperatures during deformation, coupled with relatively shallow burial during deformation, limited the rock response to pressure-solution dissolution, fracturing, microcracking, and cataclasis with only minor plastic deformation. The structures seen in the area were formed primarily in the brittle field of deformation. As a consequence, the folding in the Arbuckle Group is not ductile (plastic), but is limited primarily to brittle flexural slip accompanied by local faulting and cataclasis. The deformation characters of the Arbuckle Group are discussed separately. In reality, though, all of the features are interrelated. The dominant deformation features in the Arbuckle Group are fractures, fault rocks (cataclasites) and related tectonic dolomites, folds and fold-related faults, and a range of secondary faults.

FRACTURES IN ARBUCKLE ROCKS

Fractures are ubiquitous in the Arbuckle Group. The entire unit is fractured, with a wide range of fracture orientation and spacing. The fracture systems in the Arbuckle Group encompass a complete range of fracture geometries, including open fractures, partially healed fractures, and healed fractures (almost always with calcite). The spacing of fractures in the vicinity of the Washita Valley fault gives some insight into the development of the fault itself, and also into the potential for fractured reservoirs in Arbuckle rocks. Fracture density has been measured on several traverses along the length of the Washita Valley fault. The traverses were perpendicular to the fault trend and extended at least 1 km into the country rock surrounding the fault. Data from one of the traverses is shown in Figure 1 and in Table 1. All of the traverses are not shown, as the variation of lithology across the fault over most of the area does not allow accurate interpretation of the spacing data. The data were originally presented by Ferebee and Tapp (1989). Fracture density was calculated by measuring the number of fracture intersections on circles of known radius on three orthogonal planes cut on oriented samples. The planes were oriented (a) vertical and normal to the Washita Valley fault, (b) vertical and parallel to the fault, and (c) horizontal. The circular grid-counting method results in the lowest standard deviation of the standard counting methods and yields the most accurate measure of actual fracture density (Hillard, 1962,1968; Goodwin, 1979). The program used for data reduction was written by John Cook, who counted some of the early samples. No effort was made to segregate healed vs. open fractures in the samples. Most of the fractures in the Arbuckle are healed. Many of the partially healed fractures indicate late-stage (telogenetic) dissolution of the carbonate healing material.

The data show a significant increase in fracture density in the Washita Valley fault zone and in several small shear zones adjacent to the Washita Valley fault (Fig. 1). The counts within the fault zone and its associated shear zones are underestimated since these rocks are cataclasized and likely have fractures bounding nearly all grains/fragments within the rocks. The data from the fault and associated shear zones were removed in Figure 1B to show the general trend of fracture density. The fracture density, as expected, increases in the Washita Valley

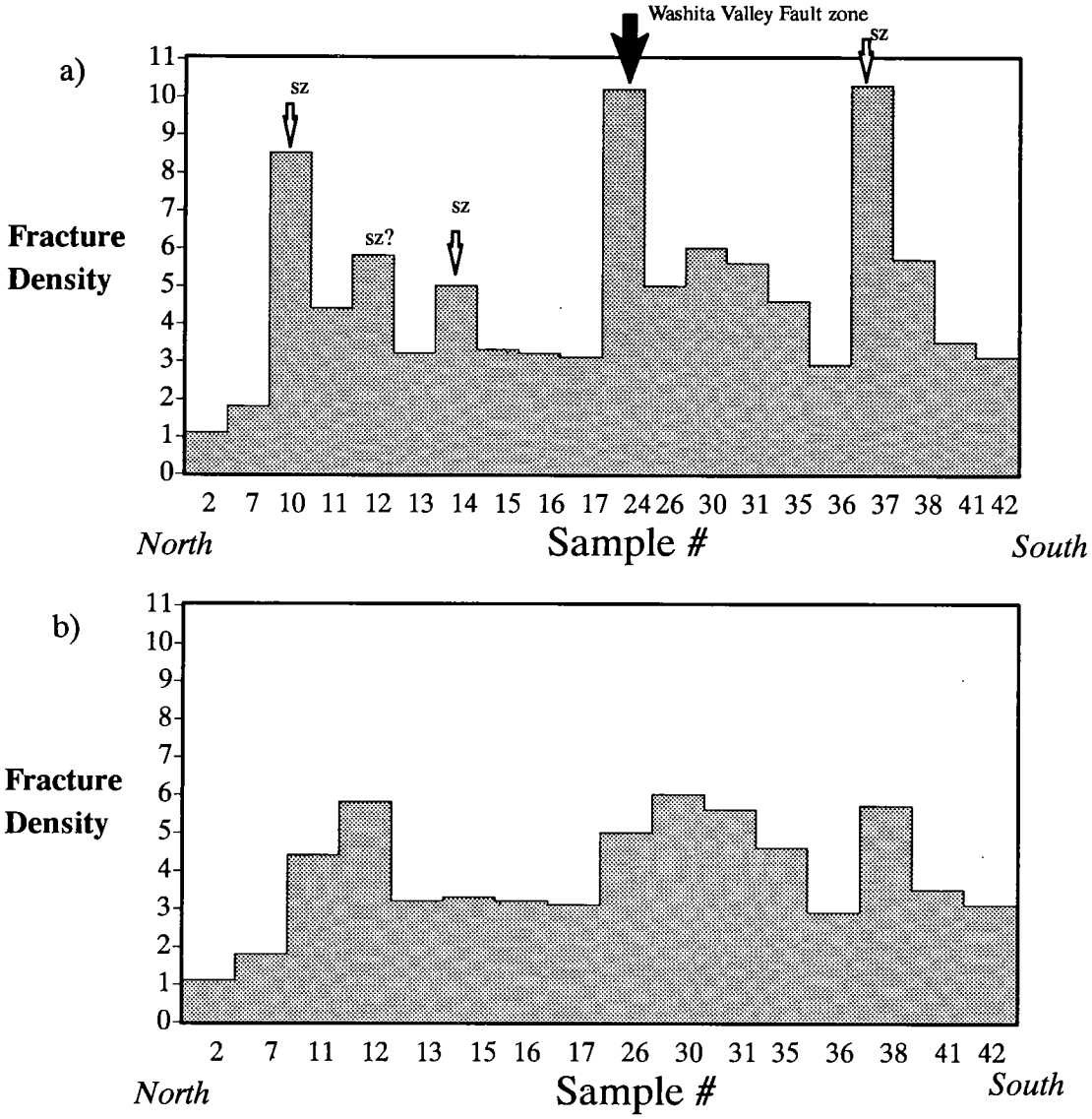


Figure 1. *A*—Plot of fracture density vs. sample number for single traverse across Washita Valley fault (see Table 1 for fracture-density data). Samples 10, 24, and 37 were collected in cataclastic shear zones and have an anomalously high fracture density. *B*—Fracture density, exclusive of shear-zone data, showing a gradual increase of fracture density approaching the Washita Valley fault zone.

fault and associated shear zones. When the data for the shear zones are removed, the fracture-density data do not accurately predict the location of the fault, or of the associated shear zones as is generally expected (Pohl, 1981, 1982). The data do show a general increase in fracture density both from the north and south, approaching the shear zones associated with the Washita Valley fault. This implies that the regions bounded by the shear zones were separated (both to the north and to the south) from the deformation. The shear zones likely acted as distinct slip zones, accumulating most of the strain associated with the fault. The amount of separation on the shear zones decreases away from the fault zone, suggesting that most of the slip, and correspondingly most of the deformation, is limited to the actual fault zone. As such, much of the fracturing seen in the Arbuckle uplift is likely related to the local structural features (folds or secondary faults). Our data suggest that the fractures would make relatively poor reservoirs since they are largely filled and do not form a regional pattern associated with the major strike-slip faults. The fractures within the fault zone are more like cataclastic slip or microcrack surfaces than conjugate shear fractures and would make poor reservoirs. These zones are interesting in that they preserve excellent examples of carbonate cataclasites described below.

FAULT ROCKS IN ARBUCKLE GROUP

Deformation mechanisms observed in Arbuckle Group carbonates include fracturing and microfaulting, cataclasis, pressure solution, dedolomitization, and recrystallization. The predominant deformation mechanism operating to form the fault rocks is brittle fracturing and microfaulting along with cataclastic crushing. Pressure solution and recrystallization also play a role. The interrelationship between pressure solution and cataclasis in grain-size reduction is unclear; however, some obser-

TABLE 1. — FRACTURE DENSITY IN SAMPLES FROM SINGLE TRAVERSE ACROSS WASHITA VALLEY FAULT

Sample Number	Fracture Density (cm)
2	1.1
7	1.8
10	8.5
11	4.4
12	5.8
13	3.2
14	5.0
15	3.3
16	3.2
17	3.1
24	10.2
26	5.0
30	6.0
31	5.6
35	4.6
36	2.9
37	10.3
38	5.7
41	3.5
42	3.1

NOTE: The data are from Ferebee and Tapp (1989). Fracture density was calculated by measuring the number of intersections of fractures on circles of known radius on three orthogonal planes. The planes were oriented (a) vertical and perpendicular to the Washita Valley fault, (b) vertical and parallel to the fault, and (c) horizontal. The circular grid-counting method resulted in the lowest standard deviation of the counting methods tested. The data were collected and reduced using the techniques outlined in Hillard (1962,1968) and Goodwin (1979). The program used for data reduction was written by John Cook.

vations support the idea that they are intimately intertwined, with pressure solution increasing in importance with decreasing grain size. The samples used in this section were again collected on several traverses that crossed the Washita Valley fault and were described using standard and ultra-thin doubly polished thin sections. Many of the samples have been described by McPherson (1989). The evidence for each mechanism contributing to the formation of the fault rocks will be discussed separately.

Cataclasites

All of the rocks in the Washita Valley fault zone can be termed cataclasites and described using the terminology of Sibson (1977). The process of cataclasis involves the brittle breakup of rocks, resulting in grain-size reduction without significant recrystallization, although new crystal growth can occur (Stel, 1981). The formation of cataclasites involves the initial development of crush breccias, followed by progressive grain-size reduction due to microcracking of the breccia grains and frictional sliding (Logan and others,1979) to produce protocataclasites and ultimately cataclasites and utlracataclasites with continued grain-size reduction (Sibson, 1977). The Washita Valley Fault zone proper is not well exposed in the field area; however, there are good exposures of rocks bounding the fault zone that contain well-developed, fine-grained carbonate cataclasites. Cataclasis is important in the formation of fault gouge (common in the field area), and can be recognized optically by the presence of intense fractures and microfractures that cut grains, and the formation of gouge or fine-grained material that may cut individual grains without significant recrystallization.

The formation of cataclasites in the field area includes the formation of crush breccias and protocataclasites (Fig. 2A) with relatively undisturbed fragments of limestone and dolomite separated by bands of fine-grained limestone and/or dolomite cataclasite. Samples from the field area show complex interplay of fractures and microfaults (Fig. 2B) with a variety of crosscutting relationships, both offsetting and being offset by pressure-solution features, and offsetting and being offset by bands of very fine-grained cataclasite. Some of the samples do show twinning and recrystallization. The twin sets observed are narrow, indicating that they were formed under relatively cool conditions, accumulated little strain, and show evidence of brittle disruption with the formation of cataclastic bands across the grains (Fig. 2C). Although the relationships between cataclasis and plastic deformation have been questioned along large-scale shear zones (Shimamoto, 1989; Hadizadeh and others, 1991), the relationships in the samples studied to date show little plastic deformation along the Washita Valley fault, suggesting that the deformation occurred at relatively high strain rates, or at low temperature and shallow depths. Although plastic deformation is limited, and likely of little significance, the role of chemical processes is interesting in the formation of the fault rocks seen in the area.

The interpreted sequence of events in the formation of the fault rocks in the limestones present in the field area is as follows:

1. Formation of fractures.
2. Slip along fractures forming microfaults, isolating fragments of rock along the microfaults.
3. Grinding and crushing of rocks along the microfaults, leading to grain-size reduction and cataclasite zones through the sample.
4. Neomorphic recrystallization within some zones, forming coarsely crystalline calcite replacement along the cataclastic zones. Neomorphism is the formation of new mineral phases during metamorphism or diagenesis (Spry, 1968). Neomorphism in a deforming system results from the destruction of unstable phases, coupled with

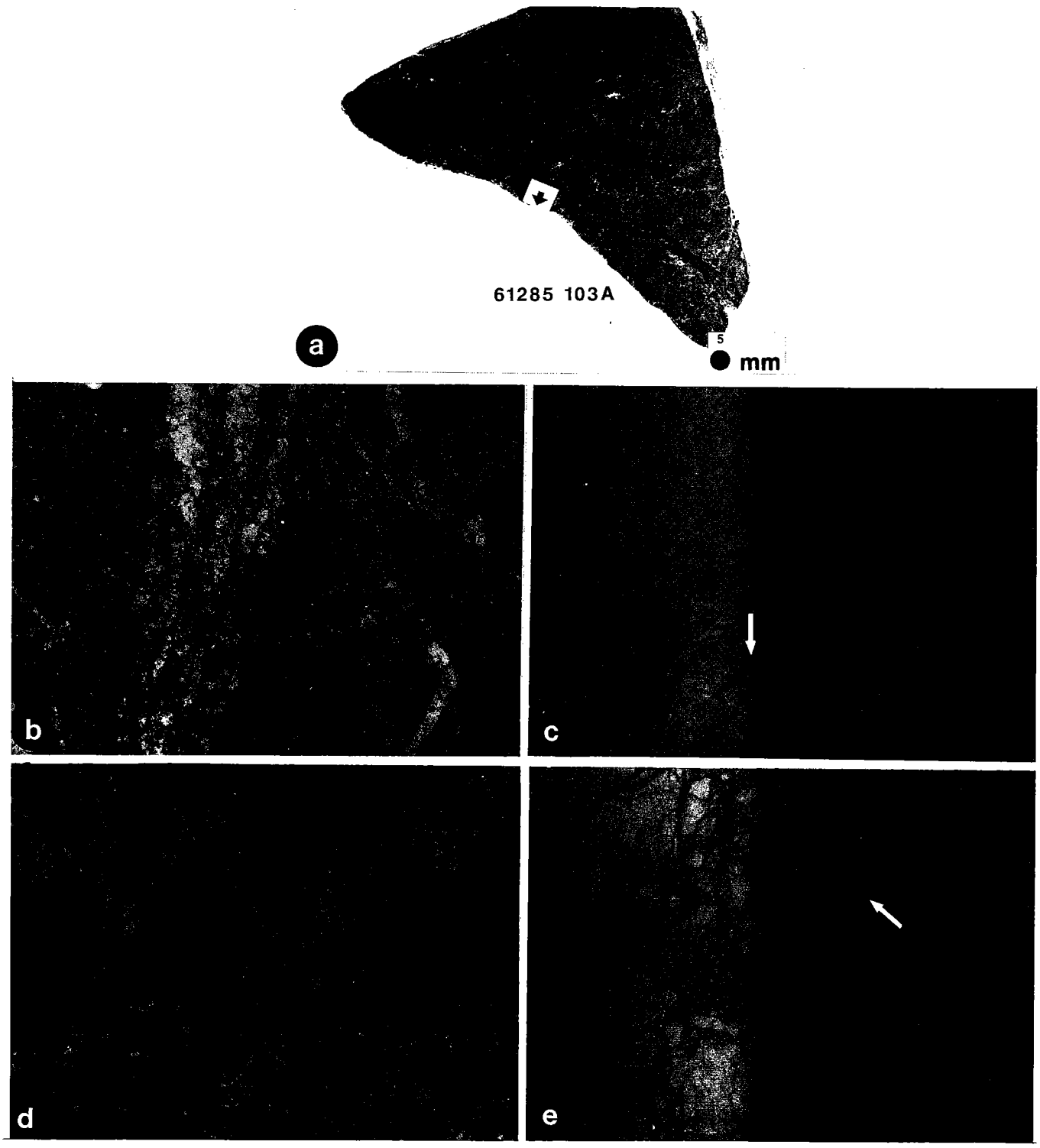


Figure 2. *A*—Polished sample of protocataclasite. *B*—Photomicrograph of multiple fracture and microfault sets in protocataclasite. Field of view is 6 mm wide. *C*—Photomicrograph of cataclastic destruction of neomorphic calcite along curved bands. Field of view is 1.5 mm wide. *D*—Photomicrograph of neomorphic recrystallization of groundmass in limestone cataclasite: note serrate and bulbous crystal boundaries. Field of view is .93 mm wide. *E*—Photomicrograph of pressure solution acting in tandem with cataclasis (arrow) in dolomite cataclasite. Field of view is 6 mm wide.

diffusion and growth of new, stable-mineral constituents.

5. Twinning and cataclasis of newly formed grains.

6. Continued grain-size reduction along with neomorphic recrystallization, apparently maintaining a coherent limestone groundmass (Fig. 2D).

Pressure Solution

Pressure solution is the mass transfer of material from points of high stress to zones of lower stress, in the presence of a fluid (Durney, 1972,1976; Rutter, 1976; de Boer, 1977). Solution surfaces can be recognized by the truncation of fossils and rock particles, and by the presence of accumulated insoluble material on the solution surfaces. Pressure solution is kinetically rapid enough to produce geologically realistic strain rates at low temperatures and low deviatoric stress, and is therefore a significant contributor in the deformation of rocks below metamorphic conditions (Rutter, 1976).

Pressure-solution surfaces in the field area are present both as early bedding-plane stylolites, which are of no significance, and as tectonic-solution surfaces where carbonate materials are being removed during cataclasis. These solution surfaces show accumulation of insoluble materials (Fig. 2E) and offset fracture sets, indicating continued action during or after the onset of brittle deformation. Pressure-solution surfaces can develop grain-size-reduction textures similar to the cataclastic zones in polymineralic materials. Neomorphic recrystallization of calcite during deformation argues that pressure solution is pervasive throughout the cataclasites. Pressure-solution activity depends strongly on grain size, being more significant at smaller grain sizes. This supports the interpretation that pressure solution may be important during cataclasis.

Tectonic Dolomites in the Arbuckle Group

Secondary calcian saddle dolomites are common as a replacement phase adjacent to faults in the field area. The saddle dolomites show the characteristic warped-crystal lattice, resulting in undulatory extinction, curved crystal faces, and commonly they are turbid due to increased inclusion density in the crystals (Zenger, 1983). Saddle dolomites commonly form in late-diagenetic conditions (mesogenetic), and are typically related to fluid migration along fractures or along pressure-solution features (Zenger, 1983). Samples from the shear zone are completely dolomitized and do not show other characteristics of mesogenetic saddle dolomites, such as web structure, zebroid structure, and dolomite tongues (Zenger, 1983). The behavior of dolomites in the system is virtually identical, with the exception of the significance of twinning and neomorphic recrystallization. The tectonic dolomites adjacent to the fault zone have been extensively cataclasized, and they preserve cataclastic texture to extremely small grain size. The lack of twinning is largely due to the behavior of dolomite, which does not twin until at least greenschist-rank temperatures. The cataclasis of the tectonic dolomites shows that the dolomitization is early in the evolution of the fault zone. The saddle dolomites are heavily cataclasized, showing the same evolution as the limestones adjacent to the fault with the exception of twinning and neomorphic recrystallization. The dolomites form both protocataclasites and cataclasites. Evidence of unstable crack growth (crack seal) is seen in several samples, and in a classic outcrop in Mill Creek. Some of the saddle dolomites show development of microporosity that may be due to dedolomitization (McPherson, 1989).

DISCUSSION

The dominant deformation style in the region is brittle—largely fracturing, microfaulting, and cataclasis. This style of deformation pervades the region and strongly affects the style of structures in the area. The structural features seen in the field include folds and faults related to wrench deformation. The faults in the region mimic positive flower structures at most scales of observation. Many of the faults formed small gouge zones, and most of the faults have associated secondary shear zones developed through localization of cataclasite zones.

All of the folding in the region is flexural slip in nature. In many cases the bedding-plane slips die out into thrust faults in the inner arc of the fold hinges. Thrust faults in the hinges of folds can be seen at several locations, including the Hunton anticline at the Hunton quarry just south of Lake of the Arbuckles dam (both in the larger anticline and in the smaller folds in the lower bench of the quarry), the Sycamore Creek anticline and associated smaller-scale folds along the Washita Valley fault, in the small-scale folds at the crest of the Arbuckle anticline, and in the small folds in the Viola Formation on the north flank of the Arbuckle uplift. Thrusting in the hinges of brittle flexural-slip folds formed in thick competent units is common (Ramsay, 1967, p. 401; Ramsay and Huber, 1987, p. 458). The fact that, over the uplift, conjugate thrusts commonly form in the hinge zones of folds, and are seen in all formations, is suggestive that this is the folding mechanism for the Arbuckle anticline (Tapp, 1991a). The folds described also possess fold-related fractures around the outer arc of the folds, and in some cases the hinge zones of the folds preserve cataclastic textures and tectonic pressure-solution surfaces.

The behavior of rocks in the region of the Washita Valley fault is only slightly affected by lithology. The history of development of cataclasites along the fault shows identical paths for both limestone and tectonic dolomites with only minor exceptions. The field data indicate that the dolomitization occurred early in the fault history. Field observations also show that the fractures related to the fault are concentrated in a relatively narrow band, suggesting that the process of cataclasis and the formation of secondary cataclastic shear zones partitioned strain related to the fault. As a consequence, structures directly related to slip along the fault are concentrated within a few kilometers of the fault, and suggest that the larger structures are part of the overall wrench setting.

CONCLUSIONS

The carbonate rocks of the Arbuckle Group were deformed under conditions that strongly favored brittle mechanisms of deformation. Data from traverses across the Washita Valley fault show that:

1. The Washita Valley fault can be thought of as a relatively wide zone that includes several associated cataclastic shear zones that bound relatively undeformed

pods of the Arbuckle and other rock groups.

2. Tectonic dolomitization occurred early during fault movement, and tectonic dolomites are incorporated as cataclasites into the fault zone.

3. Both dolomite and limestone rocks deform primarily by brittle mechanisms, forming protocataclasites and cataclasites in the fault zone. Limestones show some effect of twinning and also show neomorphic recrystallization of the cataclasite groundmass. Dolomites do not twin, and do not show evidence of neomorphic recrystallization.

4. Pressure solution cannot be ruled out, and it is likely that it played a significant role in the grain-size reduction seen in the cataclasites.

5. The brittle-deformation mechanisms strongly affect the styles of structures seen in the field area.

The field area preserved excellent examples of cataclastic textures in both limestone and dolomite rocks. The field area represents a classic site in which to study brittle deformation in carbonates.

ACKNOWLEDGMENTS

I would like to acknowledge three graduate students whose work contributed to the formulation of the ideas presented in this paper. Bruce McPherson worked on several samples from the traverses as part of a non-thesis option report for his M.S. degree. Clive Ferebee performed many of the fracture counts while working toward a M.S. degree at the University of Tulsa. John Cook served as an invaluable field assistant during two field seasons, and also contributed in large part to the implementation of the fracture counts, wrote the program used, and also helped debug the counting method. This paper would not have been complete without their contributions. Any errors in interpretation or omissions, however, are entirely my own.

REFERENCES CITED

Bond, G. C.; and Kominz, M. A., 1984, Construction of tectonic subsidence curves for the early Paleozoic miogeocline, southern Canadian Rockies: implications for subsidence mechanisms, age of breakup and crustal thinning: Geological Society of American Bulletin, v. 95, p. 155–173.

Booth, S. L., 1981, Structural analysis of portions of the Washita Valley fault zone, Arbuckle Mountains, Oklahoma: Shale Shaker, v. 31, p. 107–120.

Bott, M. H. P., 1973, Shelf subsidence in relation to the evolution of young continental margins, *in* Tarling, D. H.; and Runcorn, S. K. (eds.), Implications of continental drift to the earth sciences, Vol. 2: Academic Press, London, p. 675–685.

Brewer, J. A.; Brown, L. D.; Steiner, D.; Oliver, J. E.; Kaufman, S.; and Denison, R. E., 1981, A Proterozoic basin in the southern Midcontinent of the United States revealed by COCORP deep seismic profiling: Geology, v. 9, p. 569–575.

Brewer, J. A.; Good, R.; Oliver, J. E.; Brown, L. D.; and Kaufman, S.,1983, COCORP profiling across the southern Oklahoma aulacogen: overthrusting of the Wichita Mountains and compression within the Anadarko basin: Geology, v. 11, p. 109–114.

Burke, K., 1980, Intracontinental rifts and aulacogens, *in* Continental tectonics: National Academy Press, New York, p. 42–49.

Burke, K.; and Dewey, J. F., 1973, Plume-generated triple junctions: key indicators in applying plate tectonics to old rocks: Journal of Geology, v. 81, p. 406–433.

de Boer, R. B., 1977, On the thermodynamics of pressure solution interaction between chemical and mechanical forces: Geochimica et Cosmochimica Acta, v. 41, p. 249–256.

Deitz, R. S.; and Holden, J. C., 1967, Miogeoclines in space and time: Journal of Geology, v. 65, p. 566–583.

Durney, D. W., 1972, Solution transfer, an important geological deformation mechanism: Nature, v. 235, p. 315–317.

_____1976, Pressure-solution and crystallization deformation: Philosophical Transactions of the Royal Society of London, v. A283, p. 229–240.

Feinstein, S., 1981, Subsidence and thermal history of the southern Oklahoma aulacogen: implications for petroleum exploration: American Association of Petroleum Geologists Bulletin, v. 65, p. 2521–2533.

Ferebee, C.; and Tapp, B., 1989, Fracture density and spacing along the Washita Valley fault, Arbuckle Mountains [abstract]: American Association of Petroleum Geologists, Mid-Continent Section Meeting, Abstracts with Programs.

Goodwin, E. R., 1979, Fracture density in the Rattlesnake Mountain fold, Wyoming: University of Oklahoma unpublished M.S. thesis, 90 p.

Haas, E. A., 1981, Structural analysis of a portion of the Reagan fault zone, Murray County, Oklahoma: Shale Shaker, v. 31, p. 93–104.

Hadizadeh, J.; Babaie, H.; and Babaie, A. A., 1991, Development of interlaced mylonites, cataclasites and breccias, example from the Towaliga fault, south-central Appalachians: Journal of Structural Geology, v. 13, p. 63–70.

Ham, W. E.; Denison, R. E.; and Merritt, C. A., 1964, Basement rocks and structural evolution of southern Oklahoma: Oklahoma Geological Survey Bulletin 95, 302 p.

Hillard, J. E., 1962, Specification and measurement of microstructural anisotropy: Transactions of the Metallurgical Society of AIME, v. 244, p. 1201.

_____1968, Estimation of microstructural properties in the presence of anisotropy, *in* Fulrath, R. M.; and Pask, J. A. (eds.), Ceramic microstructures: their analysis, significance, and production: John Wiley, New York, p. 53–70.

Hoffman, P. F.; Dewey, J. F.; and Burke, K., 1974, Aulacogens and their genetic relations to geosynclines, with a Proterozoic example from Great Slave Lake, Canada, *in* Dott, R. H.; and Shaver, R. H. (eds.), Modern and ancient geosynclinal sedimentation: Society of Economic Paleontologists and Mineralogists Special Publication 19, p. 38–55.

Hoffman, P. F.; Bell, I. R.; Hildebrand, R. S.; and Thorstad, L., 1977, Geology of the Athapuscow aulacogen, East Arm of the Great Slave Lake, District of MacKenzie: Geological Survey of Canada Report of Activities Paper 77-1A, p. 117–129.

Islam, Q.; and Nielsen, K. C., 1984, Detailed fault history in the east and central portions of the Arbuckle Mountains, Oklahoma [abstract]: Geological Society of America Abstracts with Programs, v. 16, no. 3, p. 87.

Logan, J. M.; Friedman, M.; Higgs, N.; Dengo, C.; and Shimamoto, T., 1979, Experimental studies of simulated gouge and their application to studies of natural fault zones, *in* Proceedings of 8th conference on analysis of actual fault zones in bedrock: U.S. Geological Survey Open-File Report 79-1239, p. 305–343.

McPherson, B., 1989, Variations in deformation mechanisms in naturally deformed carbonates by simple shear along the Washita Valley fault, southern Oklahoma: University of Tulsa unpublished Masters report.

Phillips, E. H., 1983, Gravity slide thrusting and folded faults in western Arbuckle Mountains and vicinity, southern Oklahoma: American Association of Petroleum Geologists Bulletin, v. 67, p. 1363–1390.

Pohl, H. A., 1981, Joint spacing as a method of locating faults: Geology, v. 9, p. 258–261.

_____1982, Reply on joint spacing as a method of locating faults: Geology, v. 10, p. 61–62.
Pruatt, M. A., 1975, The southern Oklahoma aulacogen: a geophysical and geological investigation: University of Oklahoma unpublished M.S. thesis, 62 p.
Ramsay, J. G., 1967, Folding and fracturing of rocks: McGraw Hill, New York, 568 p.
Ramsay, J. G.; and Huber, M. I., 1987, The techniques of modern structural geology, Vol. 2: Folds and fractures: Academic Press, New York
Rutter, E. H., 1976, The kinetics of rock deformation by pressure solution: Philosophical Transactions of the Royal Society of London, v. A283, p. 203–219.
Shatskiy, N. S., 1946, Great Donbass and Wichita system: comparative tectonics of old platforms: SSSR Izvestia, Seria Geologie No. 6, p. 57–90.
Shimamoto, T., 1989, The origin of S–C mylonites and a new fault-zone model: Journal of Structural Geology, v. 11, p. 51–64.
Sibson, R. H., 1977, Fault rocks and fault mechanisms: Journal of the Geological Society of London, v. 133, p. 191–213.
Spry, A., 1968, Metamorphic textures: Pergamon Press, Oxford, 350 p.
Stel, H., 1981, Crystal growth in cataclasites: diagnostic microstructures: Tectonophysics, v. 78, p. 585–600.
Tanner, J. H., 1967, Wrench fault movements along Washita Valley fault, Arbuckle Mountain area, Oklahoma: American Association of Petroleum Geologists Bulletin, v. 51, p. 126–141.
Tapp, J. B., 1978, Breccias and megabreccias of the Arbuckle Mountains, southern Oklahoma aulacogen, Oklahoma: University of Oklahoma unpublished M.S. thesis, 126 p.
Tapp, B., 1991a, Folding and thrusting in lower Arbuckle: see Field-Trip Description in this volume.
_____1991b, Flower structure in the lower Arbuckle: see Field-Trip Description in this volume.
_____1991c, Paleokarst origin for bedded breccias in the Cool Creek Formation: see Field-Trip Description in this volume.
Zenger, D. H. 1983, Burial dolomitization in the Lost Burro Formation (Devonian), east-central California, and the significance of late diagenetic dolomitization: Geology, v. 11, p. 519–522.

Diagenetic History of the Arbuckle Group, Slick Hills, Southwestern Oklahoma: A Petrographic and Geochemical Summary, and Comparison with the Ellenburger Group, Texas

Lynton S. Land, Guoqiu Gao, and Julie A. Kupecz*
University of Texas at Austin

ABSTRACT.—The Arbuckle Group in the Slick Hills, southwestern Oklahoma, has been affected by three distinct diagenetic episodes. Early, nearly syndepositional marine diagenesis resulted in the formation of considerable amounts of fine-grained, presumably non-stoichiometric dolomite, as well as opal-CT nodular chert. Early diagenetic dolomite and chert, as well as host limestone, were subsequently modified by meteoric water during the development of subsequent unconformities. Meteoric modification resulted in: (1) light $\delta^{18}O$ values of limestone, early dolomite, and chert; (2) a simultaneous $\delta^{18}O$ decrease and increased dolomite and quartz crystal sizes; and (3) in the case of dolomite, lowered $^{87}Sr/^{86}Sr$ ratios relative to coeval seawater and associated limestone. These two episodes of diagenesis did not affect the $\delta^{13}C$ and $^{87}Sr/^{86}Sr$ of the limestones significantly, and limestones still record primary secular $\delta^{13}C$ and $^{87}Sr/^{86}Sr$ variations.

The formation of minor amounts of late dolomite in the upper Arbuckle Group was the result of late Paleozoic events. Late dolomite, brightly luminescent, is characterized by radiogenic $^{87}Sr/^{86}Sr$ ratios, heavy $\delta^{18}O$ values, and high Fe and Mn concentrations, relative to associated early dolomite and limestone. Upward migration of fluids, derived from the adjacent Anadarko basin during the late Paleozoic, was probably the cause of late dolomitization.

The Ellenburger Group of Texas was affected by similar diagenetic processes, but several differences exist between similar-aged rocks in Oklahoma and Texas. Karst breccias were much more important in focusing both early Paleozoic meteoric water and late Paleozoic basinal fluids in Texas as opposed to Oklahoma. In Texas, early dolomite was more commonly replaced by a late-stage, luminescent, ^{87}Sr-rich dolomite, but the late dolomite is depleted, rather than enriched, in ^{18}O. The most ^{18}O-depleted dolomites are southeast of the Llano uplift. Fluids derived from the Ouachita trough, also capable of dolomitization, were ^{18}O-depleted relative to those derived from the Anadarko basin.

INTRODUCTION

The Slick Hills of southwestern Oklahoma lie between the Wichita Mountains and the Anadarko basin (Fig. 1). Stratigraphically, the Slick Hills consist mostly of the Late Cambrian to Early Ordovician Arbuckle Group, a thick (~1,700 m), shallow-water platform-carbonate sequence which has been subdivided into six formations: in ascending order, the Fort Sill, Signal Mountain, McKenzie Hill, Cool Creek, Kindblade, and West Spring Creek (Donovan, 1986). By the end of the Mississippian, the Fort Sill Formation was buried to a depth of ~4 km, corresponding to a temperature of ~125°C (Donovan, 1986). During the Early Pennsylvanian, the Wichita orogeny caused deformation and uplift of the Arbuckle Group in the Slick Hills, and by Permian time the Arbuckle Group was deformed and uplifted to approximately its present topography (Gilbert and Donovan, 1984; Donovan, 1986). In contrast, the Ellenburger Group has never undergone deformation, and samples which have undergone relatively deep burial can be compared with those outcropping in the Llano area which have never been deeply buried (Kupecz and others, 1988; although see Lee and Friedman, 1987,1988).

Both the Arbuckle Group in the Slick Hills and the Ellenburger Group in Texas have undergone significant dolomitization and silicification, resulting in the formation of massive dolomite units as well as nodular chert (Donovan, 1986). Gao (1990a,b) and Gao and Land (1991a,b) have discussed the diagenetic history of the dolomite and chert in the Slick Hills. We present here a summary of the petrographic and geochemical characteristics of Arbuckle limestone, dolomite, and chert, and relate their diagenetic histories to geologic events that occurred in the southern Midcontinent area, and farther south, in Texas.

METHODS

Samples were collected from various outcrops in the Slick Hills (Gao, 1990b; Fig. 1), and from wells and outcrops in Texas (Kupecz, 1989). Petrographic analysis was performed by polarizing, cathodoluminescent, and scanning-electron microscopy. Sample powders for chemical analysis were examined by X-ray diffraction to ensure mineralogical purity. Elemental concentrations of carbonates were determined by inductively coupled argon-plasma atomic-emission spectroscopy (ICAP-AES) following dissolution of samples in dilute (0.6 N) HCl. Carbonate samples for carbon and oxygen isotope analysis were reacted with anhydrous H_3PO_4, and chert samples

*Current address: ARCO Alaska, Inc., P. O. Box 100360, Anchorage, AK 99510.

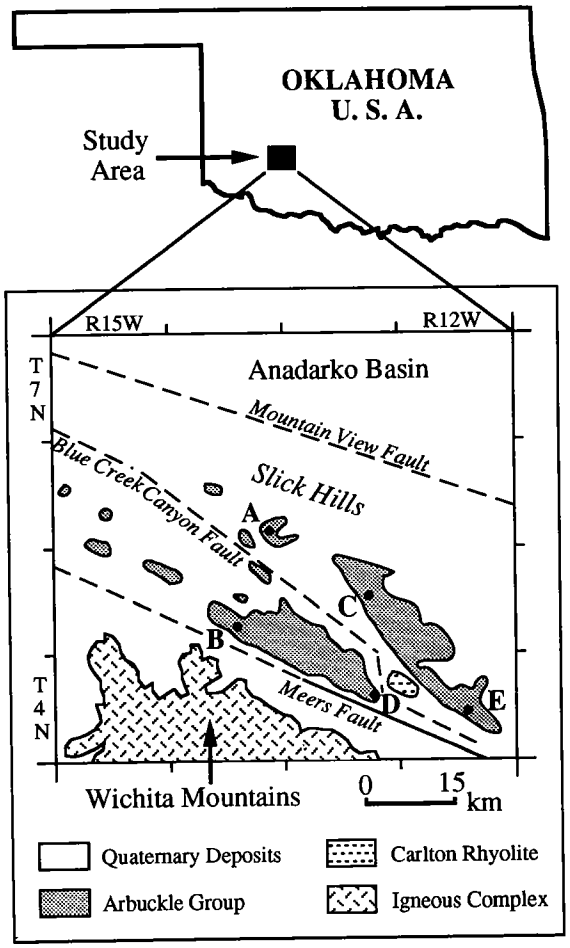


Figure 1. Simplified map of the Slick Hills, showing principal tectonic elements (modified from Donovan, 1982). Samples were collected from Bally Mountain (A), Saddle Mountain (B), Cool Creek Canyon (C), Blue Creek Canyon (D), and East Slick Hills (E).

for oxygen-isotopic analysis were reacted with BrF_5, according to standard techniques (McCrea, 1950; Clayton and Mayeda, 1963). Carbonate samples for Sr-isotopic analysis were cleaned in 0.2 N ammonium acetate and then in ultrapure water. Cleaned samples were dissolved in 1.4 N acetic acid and Sr was isolated and concentrated, using 2 N HCl, through cation-exchange columns. Sr-isotopic analysis was performed by simultaneous multi-collection on a MAT 261 mass spectrometer. Detailed analytical procedures are described in Gao (1990b) and Kupecz (1989).

RESULTS AND INTERPRETATION

Limestone

Isotopic analyses of >200 limestone samples from the Arbuckle Group document stratigraphically correlated changes in chemistry. From Late Cambrian to Early Ordovician, the $\delta^{18}O$ values of limestones increase from −10 to −7‰ (PDB); $\delta^{13}C$ values decrease from 0 to −2‰ (PDB); and $^{87}Sr/^{86}Sr$ ratios decrease from 0.7091 to 0.7088 (Fig. 2).

The $\delta^{18}O$ values of Arbuckle limestones are all lighter than values which have been proposed for presumably unaltered primary sediments of Cambro–Ordovician age, about −5‰ (PDB) (Popp and others, 1986; Veizer and others, 1986; Lohmann and Walker, 1989). Whether or not original Arbuckle sediments were as light as −5‰, it is clear that all Arbuckle limestones have undergone significant diagenetic alteration subsequent to deposition. The gradual $\delta^{18}O$ increase from Late Cambrian to Early Ordovician is most logically explained by increased ^{18}O depletion with increasing burial temperature during alteration. In contrast, the rock-buffered nature of carbon and strontium precludes significant deviation of the $\delta^{13}C$ and $^{87}Sr/^{86}Sr$ of Arbuckle limestones from primary values (Gao and Land, 1991c, fig. 6). The $\delta^{13}C$ and $^{87}Sr/^{86}Sr$ variations of the limestones, in accord with $\delta^{13}C$ and $^{87}Sr/^{86}Sr$ variations in the literature (Gao and Land, 1991c, fig. 8), are interpreted to represent primary secular variations, and the $\delta^{13}C$ values and $^{87}Sr/^{86}Sr$ ratios of early Paleozoic surface seawater seem to have decreased from Late Cambrian to Early Ordovician.

Dolomite

Several massive dolomite units, though not persistent throughout the entire Slick Hills, are present in the Arbuckle Group. These include the Royer Dolomite from the Fort Sill Formation and numerous examples from the Cool Creek, Kindblade, and West Spring Creek Formations (Donovan, 1986). Two separate episodes of dolomitization (the conversion of limestone into dolomite) account for these units in the Arbuckle Group.

Early dolomite, volumetrically dominant, occurs as stratal bodies in the Fort Sill, Cool Creek, Kindblade, and West Spring Creek Formations (Gao, 1990b). Early dolomite is finely to coarsely crystalline, and euhedral to subhedral, with coarsely crystalline, anhedral textures being very common (Fig. 3). Early dolomite samples have $^{87}Sr/^{86}Sr$ ratios similar to, or somewhat lower than, both associated limestone and coeval seawater (Fig. 4). All early dolomite samples are characterized by extremely depleted $\delta^{18}O$ values (Fig. 5), even more ^{18}O-depleted than is characteristic of associated limestones (Fig. 2). The $\delta^{18}O$ values of dolomite decrease with increasing dolomite crystal size, with decreasing Sr concentration, and with lower $^{87}Sr/^{86}Sr$ ratios (Fig. 6). Relative to closely associated limestone samples, some early dolomite samples have lower $^{87}Sr/^{86}Sr$ ratios, and all have lighter $\delta^{18}O$ values (Fig. 2; also see Gao and Land, 1991a, fig.7). The similar $^{87}Sr/^{86}Sr$ ratios of most early dolomite samples to coeval seawater indicate that most dolomite probably formed initially from seawater during early diagenesis. The extremely light $\delta^{18}O$ values, however, demonstrate that the dolomite underwent modification. With increased modification (recrystallization), early dolomite was transformed into coarser-grained crystals having lower Sr concentrations, lighter $\delta^{18}O$ values, and lower $^{87}Sr/^{86}Sr$ ratios (Fig. 6). These simultaneous textural and chemical changes suggest that Sr- and ^{18}O-depleted meteoric water, buffered by Late Ordovician or younger carbonates with $^{87}Sr/^{86}Sr$ ratios lower than Arbuckle carbonates, was most likely responsible for the modification of early dolomite. Preferential circulation of meteoric water through porous, early dolomite "aquifers" resulted in more intensive

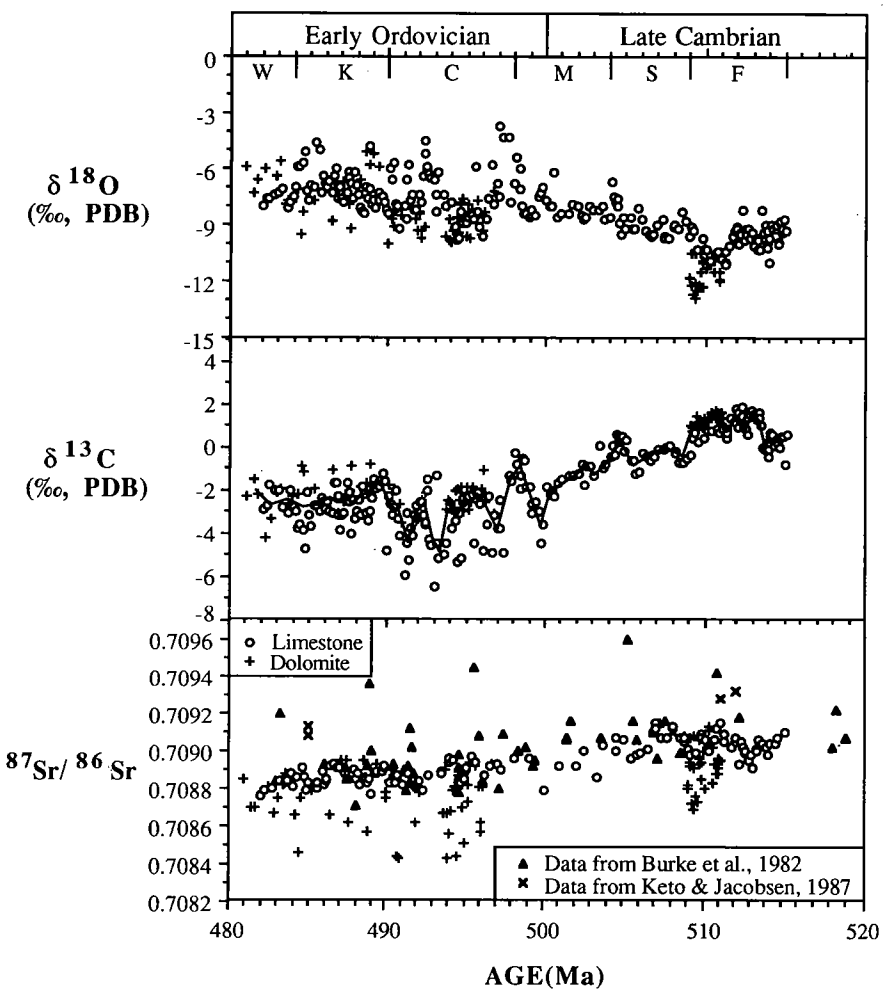


Figure 2. The isotopic compositions of the Arbuckle limestone and early dolomite plotted as a function of age (from Gao and Land, 1991c): F, Fort Sill Fm.; S, Signal Mountain Fm.; M, McKenzie Hill Fm.; C, Cool Creek Fm.; K, Kindblade Fm.; W, West Spring Creek Fm. Note that (1) $\delta^{18}O$ values decrease with increasing age, whereas $\delta^{13}C$ values and $^{87}Sr/^{86}Sr$ ratios increase; and (2) many early dolomite samples have lighter $\delta^{18}O$ values and lower $^{87}Sr/^{86}Sr$ ratios than associated limestone.

modification of dolomite than was true of associated, tighter limestones, accounting for lower $^{87}Sr/^{86}Sr$ ratios and lighter $\delta^{18}O$ values of dolomite relative to associated limestones (Fig. 2; also see Gao and Land, 1991a, fig. 7). Minor saddle dolomite, having a chemistry consistent with modified early dolomite (Figs. 4,6), is also interpreted to have been a byproduct of meteoric alteration of early dolomite, and not the result of basinal processes.

Late dolomite, volumetrically minor, occurs in transition zones laterally and vertically between ^{18}O-depleted early dolomite and limestone in the Kindblade and West Spring Creek Formations at Saddle Mountain (Gao, 1990b; also see Shelby, 1990). Locally, the late, brightly luminescent dolomite also occurs as cements within early dolomite (Fig. 7). Late dolomite displays finely to coarsely crystalline, euhedral to anhedral textures. It is characterized by radiogenic $^{87}Sr/^{86}Sr$ ratios (Fig. 4), unusually heavy $\delta^{18}O$ values (Fig. 5), and high Fe and Mn concentrations relative to associated limestones and previously formed dolomites (Gao, 1990b). Such chemical compositions indicate that the late dolomite originated from fluids enriched in ^{87}Sr, ^{18}O, Fe, and Mn. Fluids derived from the Anadarko basin to the north of the Slick Hills are proposed to have been responsible for the formation of this late dolomite.

Chert

Chert, commonly as nodules of variable size, occurs in the middle and upper Arbuckle Group (Ragland, 1983). In most cases, the distribution of chert nodules is related to initial sediment permeability, mineralogy, and organic-matter content. Specifically, grainstones, burrows, evaporite nodules, stromatolites, and small algal mounds are selectively replaced. Chert nodules are mostly composed of microquartz (<20 μm in size), but fibrous quartz, including quartzine (length-slow) and chalcedony (length-fast), are also present. Most chert nodules display well-preserved textures of precursor sediments and do not show obvious features due to compaction, suggesting an early origin. In samples containing both chert nodules and early dolomite, textures of precursor sediments are

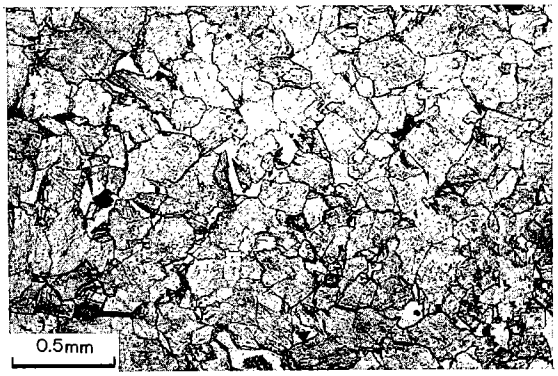


Figure 3. Medium to coarsely crystalline, subhedral to anhedral textures of early dolomite from the Cool Creek Formation. Plane-polarized light. Scale bar is 0.5 mm.

well preserved within chert nodules but not within early dolomite, suggesting that silicification predated early dolomitization (Gao and Land, 1991b). In the upper Arbuckle Group, fractures in some chert nodules are filled by late dolomite, demonstrating that late dolomite precipitation post-dated fracturing of the chert (Gao, 1990b). Sponge spicules, a widely quoted silica source for Paleozoic chert (e.g., Hesse, 1989), are essentially absent in chert nodules, and are rare throughout the entire Arbuckle Group. When etched in HF, many chert nodules display relict lepispheres 8–20 μm in diameter, composed of spherulitic aggregates of nearly equant fine-grained quartz crystals (Fig. 8). The distribution of relict lepispheres, presumably once opal-CT, is correlated with quartz-crystal size. The finer the quartz-crystal size, the more abundant the relict lepispheres. When single quartz crystals in chert nodules are larger than ~5 μm in size, lepispheres are rarely seen. The $\delta^{18}O$ values of chert nodules in the Arbuckle Group range from +21.0 to +28.8‰ (SMOW) (Fig. 9). Most of these values are considerably lighter than Cenozoic and Mesozoic chert formed in the deep sea or from near-surface seawater (Knauth and Epstein, 1976; Karhu and Epstein, 1986), and, as is also true of dolomite, depleted values are associated with coarser-grained quartz crystals (see Gao and Land, 1991b, figs. 4,5). Just as is true of limestone and early dolomite, no chert sample preserves a primary, Ordovician $\delta^{18}O$ signature.

In summary, nodular chert from the Arbuckle Group is interpreted to have formed during early diagenesis by selective replacement of grainstones, burrow fillings, algal structures, and evaporite nodules, constrained by the relative temporal relationships among silicification, burial compaction, and dolomitization. Silica for initial chert nucleation is believed to have been derived from silica-rich Paleozoic seawater and from sponge spicules. Since chert selectively replaced porous grainstones, organic-matter-enriched burrows, and algal structures, chert nucleation appears to have been controlled by the porosity, permeability, and organic-matter content of the precursor sediments. The presence of opal-CT precursor textures in many chert nodules (Fig. 8) suggests that growth of chert probably occurred by a maturation process from opal A(?), through opal-CT, to quartz. Although field and petrographic evidence argues for an early marine origin for chert in the Arbuckle Group, the light $\delta^{18}O$ values are inconsistent with this origin. Diagenetic resetting of the $\delta^{18}O$ values of the chert by meteoric water explains the light $\delta^{18}O$ values, and $\delta^{18}O$ values of chert nodules decrease in parallel with decreasing $\delta^{18}O$ values of host carbonates (Fig. 9). With increasing quartz-crystal size (recrystallization), relict lepisphere textures progressively disappear.

DIAGENETIC HISTORY

Timing of Meteoric Alteration

Nodular chert and most dolomite in the Arbuckle Group formed during early diagenesis. The *present* characteristics, and especially the chemistry, of Arbuckle limestones and associated early dolomite and chert, are very different from the materials which formed in the Ordovician. Both carbonate minerals, and the chert, underwent meteoric modification subsequent to marine deposition. The timing of modification, dependent on meteoric recharge, could have been coincident with the development of regional unconformities corresponding to emergence of the carbonate platform in the southern Midcontinent region. During the latest Early Ordovician, the upper Arbuckle Group was exposed, producing an unconformable contact between the Arbuckle Group and overlying strata (Gilbert and Donovan, 1984). The light $\delta^{18}O$ values of Arbuckle limestone (Gao and Land, 1991c), nodular chert (Gao and Land, 1991b), and early diagenetic dolomite (Gao and Land, 1991a) were at least partly achieved by meteoric alteration at this time. However, many altered early dolomite samples have $^{87}Sr/^{86}Sr$ ratios lower than associated Arbuckle limestone (Figs. 2,4). Since meteoric water buffered by Arbuckle sediments during development of the latest Early Ordovician unconformity would have been characterized by $^{87}Sr/^{86}Sr$ ratios similar to Arbuckle sediments, meteoric water at that time was unable to reset the early dolomite with $^{87}Sr/^{86}Sr$ ratios lower than associated limestone. The resetting of $^{87}Sr/^{86}Sr$ ratios in early dolomite probably occurred during the development of the Late Ordovician unconformity (Johnson and others, 1988), or subsequently, as meteoric water, which infiltrated through Late Ordovician or younger carbonate units, could have achieved $^{87}Sr/^{86}Sr$ ratios lower than Arbuckle limestones (Burke and others, 1982). Locally, especially in Texas, caves developed at times of lowered sea level, leading to formation of karst breccias which then served as important aquifers. Continued meteoric stabilization (alteration) during Late Ordovician burial also explains why the $\delta^{18}O$ values of early dolomites, which also remained aquifers, are depleted relative to associated limestones (Fig. 2). Continued meteoric alteration also affected nodular chert associated with the aquifers because chert nodules from massive early dolomite have significantly lighter $\delta^{18}O$ values and coarser crystal sizes than chert nodules from limestone (Fig. 9; also see Gao and Land, 1991b, figs. 4,5). Early diagenetic chert in the Arbuckle Group has a similar, long-lasting meteoric diagenetic history as does early dolomite.

Late Dolomitization by Basinal Fluids

The ^{87}Sr-, ^{18}O-, Fe-, and Mn-enriched nature of luminescent late dolomite implicates basin-derived fluids. The

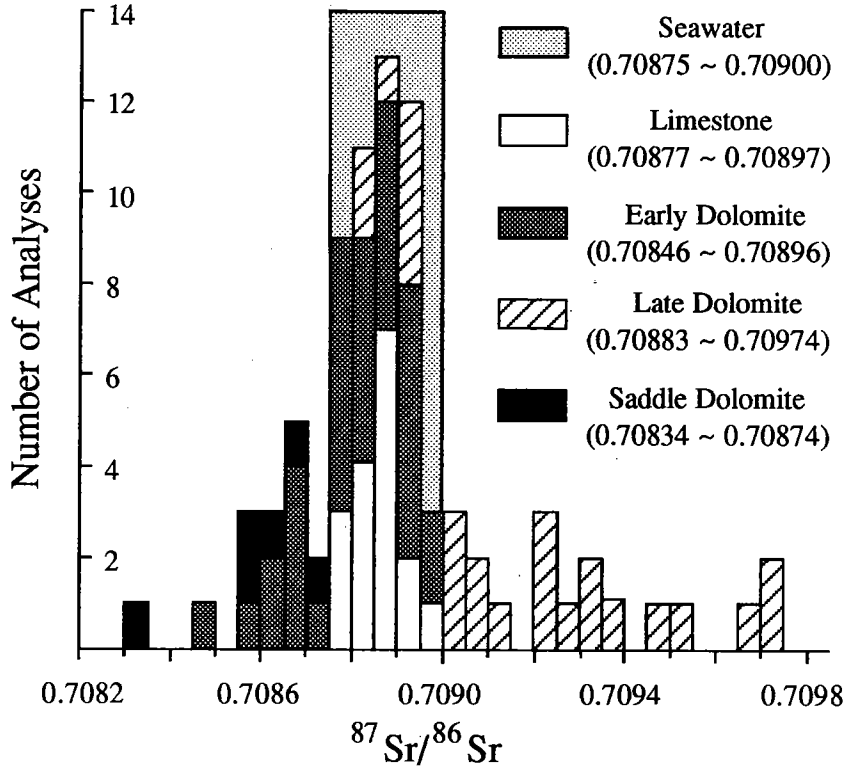


Figure 4. Histograms of the strontium-isotopic compositions of upper Arbuckle limestone, early dolomite, late dolomite, and saddle dolomite (from Gao, 1990b). The age of the upper Arbuckle Group was assigned to be about 478 to 485 Ma (Donovan, 1986), when the $^{87}Sr/^{86}Sr$ ratios of coeval Early Ordovician seawater were between 0.70875 and 0.70900 (Burke and others, 1982). The $^{87}Sr/^{86}Sr$ ratios of all limestone samples and most (70%) early dolomite samples fall in the seawater $^{87}Sr/^{86}Sr$ range, whereas most (75%) late dolomite samples are radiogenic. Saddle dolomite and some early dolomite samples are less radiogenic. Early dolomite from the lower and middle Arbuckle Group displays similar $^{87}Sr/^{86}Sr$ patterns to the early dolomite shown here (see Gao, 1990a; Gao and Land, 1991a).

most likely fluid source was the Anadarko basin immediately to the north of the Slick Hills (Fig. 1). The migration of fluids into the Slick Hills from the Anadarko basin probably occurred post-Early Pennsylvanian, because only after Early Pennsylvanian orogeny did rapid subsidence occur in the Anadarko basin area. Associated faulting and uplift in the Slick Hills area provided conduits, such as faults, in conjunction with the dolomite aquifers, and karst breccias in Texas, which permitted upward fluid migration (Gilbert and Donovan, 1984; Donovan, 1986; Johnson and others, 1988). Paleomagnetic dating of hydrocarbon-related hematite and magnetite from the Arbuckle Group in the Slick Hills also suggests that migration of brines from the Anadarko basin to the Slick Hills occurred during Early Permian time (Elmore and others, 1987). So, at some time between Middle Pennsylvanian and Permian, fluids from the Anadarko basin probably migrated upward, via faults formed during Pennsylvanian orogeny, into pre-existing, porous early dolomite, causing cementation of the dolomite aquifers, and dolomitization of limestones near existing limestone-dolomite contacts. Thus, most late dolomite occurs in transition zones between early dolomite and associated limestones (Gao, 1990b). The magnesium source for late dolo-

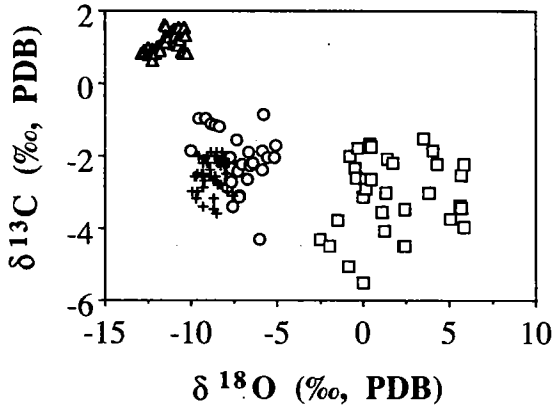


Figure 5. $\delta^{18}O$ versus $\delta^{13}C$ of dolomite (summarized from Gao, 1990a,b; and Gao and Land, 1991a). Late dolomite (squares) from Kindblade and West Spring Creek Formations has heavy $\delta^{18}O$ values (+5.9 to –2.5‰), whereas light $\delta^{18}O$ values (< –5.1‰) characterize early dolomite from the Fort Sill Formation (triangles), the Cool Creek Formation (crosses), and the Kindblade and West Spring Creek Formations (circles). $\delta^{13}C$ variation within early dolomite is due to primary $\delta^{13}C$ secular variations.

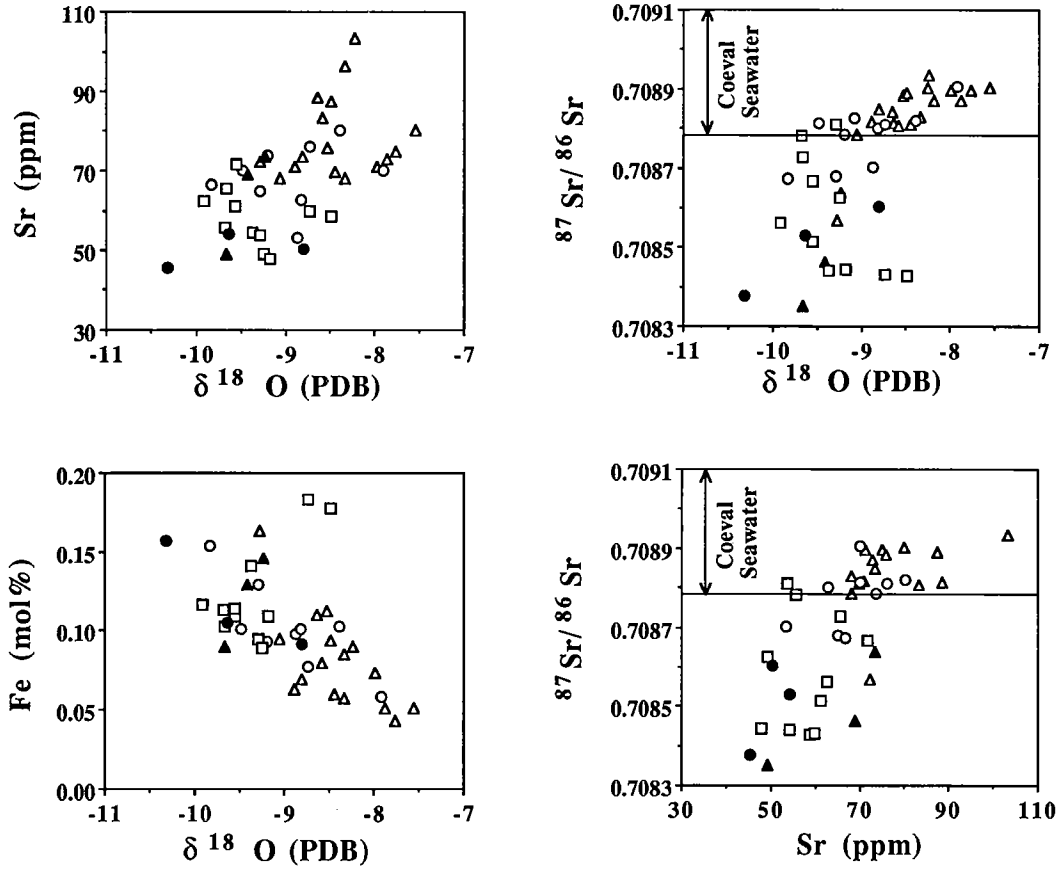


Figure 6. Correlation of geochemical data for early dolomite from the Cool Creek Formation (from Gao and Land, 1991a): fine-crystalline texture (empty triangles), medium-crystalline texture (empty circles), coarse-crystalline texture (empty squares), saddle dolomite cement (filled circles), and nodular saddle dolomite (filled triangles). Progressive decrease in Sr, $\delta^{18}O$ and $^{87}Sr/^{86}Sr$, and increase in Fe and crystal size, is consistent with progressive stabilization (or modification) by ^{18}O- and ^{87}Sr-depleted meteoric water.

mitization was probably from dissolution of both the deeply buried dolomite in the Anadarko basin and dolomite encountered during upward fluid migration.

Comparison with the Ellenburger Group in Texas

The Ellenburger Group in Texas is also extensively dolomitized and composed predominately of early-stage dolomite. Although data from the Ellenburger are dispersed over a much larger area than is true of the Slick Hills, many similarities exist. Most dolomite in the Ellenburger is interpreted to have formed prior to mid-Ordovician karst development (Kupecz, 1989). Early dolomite was recrystallized in a manner similar to that observed in the Slick Hills, where highly permeable pathways, especially grainstones and karst breccias, focused the water responsible for recrystallization. However, due to more extensive late-stage recrystallization, probably due to proximity to the Ouachita trough, early Paleozoic recrystallization event(s) are masked to a much greater degree than is observed in Oklahoma. Modified early dolomite from outcrops in the Llano area is very similar to samples buried to depths of 5 km in the Val Verde basin. Therefore, burial alone is not responsible for the petrography or geochemistry of most of the dolomite which now characterizes the Ellenburger Group (but see Lee and Friedman, 1987,1988; Kupecz and others, 1988).

Late dolomite in Texas is interpreted to have been derived from fluids discharged from the Ouachita trough (Kupecz, 1989). The resulting dolomite, which occurs as both cements and as replacement of both limestones and early-formed dolomites, is similar to that found in the Slick Hills, except that late dolomite from the Ellenburger Group in Texas is much more depleted in ^{18}O (Kupecz and Land, 1991). The most ^{18}O-depleted dolomite is concentrated southeast of the Llano uplift, and was certainly derived from fluids discharged from the Ouachita trough. The difference in the volume of late dolomite and the $\delta^{18}O$ between Texas and Oklahoma is probably the result of large volumes of silicate-buffered fluids (about +6‰ SMOW) being available from the Ouachita trough, whereas in the Anadarko basin, deep fluids were not as abundant, and were buffered to much more ^{18}O-enriched values (about +12‰ SMOW) by Paleozoic carbonates. High fluid-inclusion temperatures in quartz, associated with late dolomite cements from the Llano area, provide

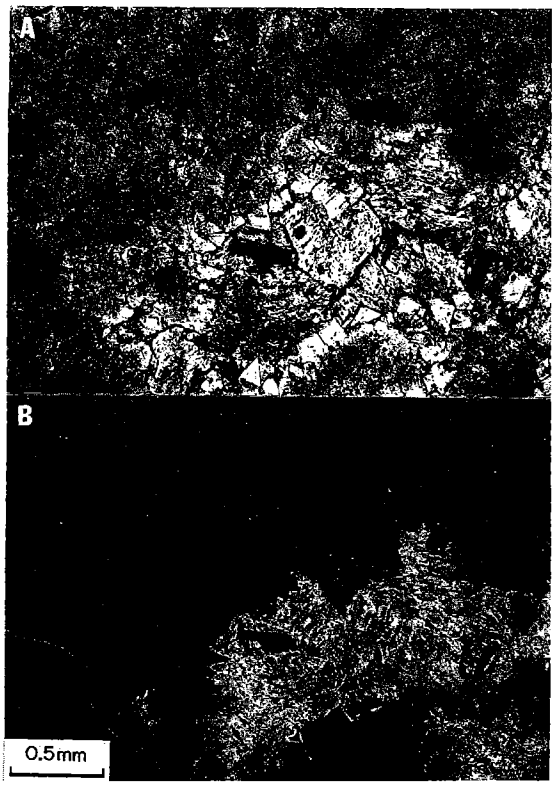


Figure 7. Paragenetic relationship between the two kinds of dolomite from the upper Arbuckle Group (from Gao, 1990b). *A*—plane-polarized light. *B*—cathodoluminescence photo of same area as in *A*. Brightly luminescent late dolomite occurs as pore-filling cements in, and overgrowths on, earlier nonluminescent dolomite. Scale bar is 0.5 mm.

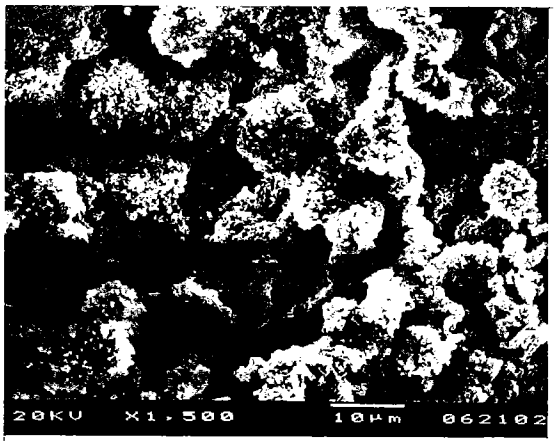


Figure 8. Relict opal-CT lepispheres, now composed of very fine-grained quartz, from an etched chert nodule from the Kindblade Formation.

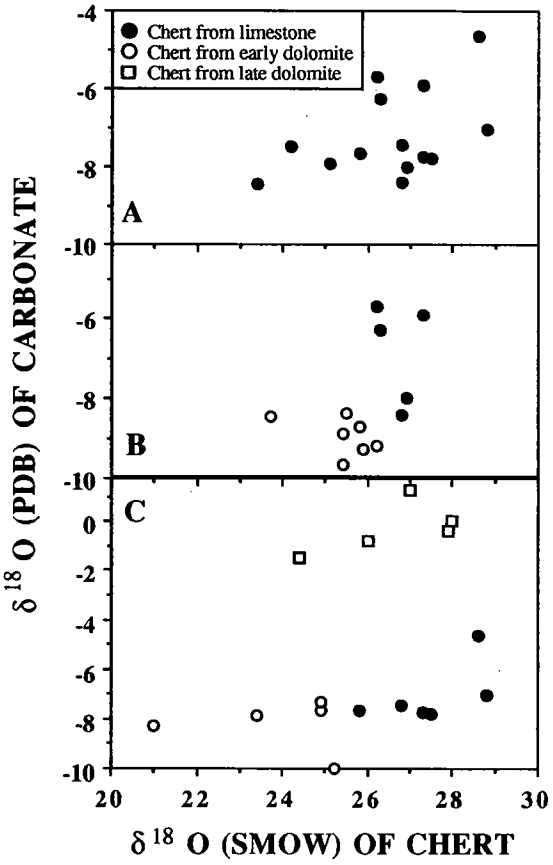


Figure 9. $\delta^{18}O$ plot of chert (SMOW) versus host carbonates (PDB) (from Gao and Land, 1991b). *A*—$\delta^{18}O$ values of chert and limestone from McKenzie Hill, Cool Creek, and Kindblade Formations. Depletion in ^{18}O correlates between limestone and chert. *B*—$\delta^{18}O$ values of chert, limestone, and early dolomite from the Cool Creek Formation. Chert in early dolomite resembles chert in more depleted limestones. *C*—$\delta^{18}O$ values of chert and host limestone, early dolomite, and late dolomite from Kindblade and West Spring Creek Formations. Chert associated with late dolomite was apparently not reset by the basinal fluids.

additional evidence of expulsion of fluids from the Ouachita trough (Kupecz and Land, 1991). Minor occurrences of lead and zinc southeast of the Llano area document similar processes to those which formed the Mississippi Valley-type lead-zinc deposits of the Midcontinent. Basinal fluids, which were spatially variable in composition, seem to have followed the same permeable pathways as those which earlier focused meteoric water, resulting in successive modification of previously emplaced dolomitic strata.

ACKNOWLEDGMENTS

We thank the numerous landowners in the Slick Hills who allowed us access to their land and R. E. Denison, R. N. Donovan, R. D. Elmore, and R. B. Koepnick for help in the field.

REFERENCES CITED

Burke, W. H.; Denison, R. E.; Hetherington, E. A.; Koepnick, R. B.; Nelson, H. F.; and Otto, J. B., 1982, Variation of seawater $^{87}Sr/^{86}Sr$ throughout Phanerozoic time: Geology, v. 10, p. 516–519.

Clayton, R. N.; and Mayeda, T. K., 1963, The use of bromide pentafluoride in the extraction of oxygen from oxides and silicates for oxygen isotopic analysis: Geochimica et Cosmochimica Acta, v. 27, p. 43–52.

Donovan, R. N., 1982, Geology of Blue Creek Canyon, Wichita Mountain area, *in* Gilbert, M. C.; and Donovan, R. N. (eds.), Geology of the eastern Wichita Mountains, southwestern Oklahoma: Oklahoma Geological Survey Guidebook 21, p. 65–77.

_____1986 (ed.), The Slick Hills of southwestern Oklahoma—fragments of an aulacogen?: Oklahoma Geological Survey Guidebook 24, 112 p.

Elmore, R. D.; Engel, M.; Crawford, L. D.; Nick, K. E.; Imbus, S.; and Sofer, Z., 1987, Evidence for relationship between hydrocarbons and authigenic magnetite: Nature, v. 325, p. 428–430.

Gao, G., 1990a, Geochemical and isotopic constraints on the diagenetic history of a massive stratal, Late Cambrian (Royer) dolomite, lower Arbuckle Group, Slick Hills, SW Oklahoma, USA: Geochimica et Cosmochimica Acta, v. 54, p. 1979–1989.

_____1990b, Petrography, geochemistry, and diagenesis of the Cambro–Ordovician Arbuckle Group, Slick Hills, SW Oklahoma: University of Texas, Austin, unpublished Ph.D. dissertation, 162 p.

Gao, G.; and Land, L. S., 1991a, Early Ordovician Cool Creek dolomite, middle Arbuckle Group, Slick Hills, SW Oklahoma, USA: origin and modification: Journal of Sedimentary Petrology, v. 61, p. 161–173.

_____1991b, Nodular chert from the Arbuckle Group, Slick Hills, SW Oklahoma: a combined field, petrographic, and isotopic study: Sedimentology, v. 38 (in press).

_____1991c, Geochemistry of Cambro–Ordovician Arbuckle limestone, SW Oklahoma: implications for diagenetic $\delta^{18}O$ alteration and secular $^{87}Sr/^{86}Sr$ variation: Geochimica et Cosmochimica Acta, v. 55 (in press).

Gilbert, M. C.; and Donovan, R. N., 1984, Recent developments in the Wichita Mountains: Geological Society of America Guidebook for Field Trip 1, South-Central Section, 101 p.

Hesse, R., 1989, Silica diagenesis: origin of inorganic and replacement cherts: Earth Science Reviews, v. 26, p. 253–284.

Johnson, K. S.; Amsden, T. W.; Denison, R. E.; Dutton, S. P.; Goldstein, A. G.; Rascoe, B.; Sutherland, P. K.; and Thompson, D. M., 1988, Southern Midcontinent region, *in* Sloss, L. L. (ed.), Sedimentary cover—North American craton, U.S.: Geological Society of America, The Geology of North America, v. D-2, p. 307–359. [Also published by the Oklahoma Geological Survey as Special Publication 89-2, 53 p.]

Karhu, J.; and Epstein, S., 1986, The implication of the oxygen isotope records in coexisting cherts and phosphates: Geochimica et Cosmochimica Acta, v. 50, p. 1745–1756.

Keto, L. S.; and Jacobsen, S. B., 1987, Nd and Sr isotopic variations of the early Paleozoic oceans: Earth and Planetary Science Letters, v. 84, p. 27–41.

Knauth, L. P.; and Epstein, S., 1976, Hydrogen and oxygen isotope ratios in nodular and bedded cherts: Geochimica et Cosmochimica Acta, v. 40, p. 1095–1108.

Kupecz, J. A., 1989, Petrographic and geochemical characterization of the Lower Ordovician Ellenburger Group, East Texas: University of Texas, Austin, unpublished Ph.D. dissertation, 158 p.

Kupecz, J. A.; and Land, L. S., 1991, Late-stage dolomitization of the Lower Ordovician Ellenburger Group, west Texas: Journal of Sedimentary Petrology, v. 61, p. 551–574.

Kupecz, J. A.; Kerans, C.; and Land, L. S., 1988, Deep-burial dolomitization in the Ordovician Ellenburger Group carbonates, west Texas and southeastern New Mexico; discussion: Journal of Sedimentary Petrology, v. 58, p. 908–910.

Lee, Y. I.; and Friedman, G. M., 1987, Deep-burial dolomitization in the Ordovician Ellenburger Group carbonates, west Texas and southeastern New Mexico: Journal of Sedimentary Petrology, v. 57, p. 544–557.

_____1988, Deep-burial dolomitization in the Ordovician Ellenburger Group carbonates, west Texas and southeastern New Mexico; reply: Journal of Sedimentary Petrology, v. 58, p. 910–913.

Lohmann, K. C.; and Walker, J. C. G., 1989, The $\delta^{18}O$ record of Phanerozoic abiotic marine calcite cements: Geophysical Research Letter, v. 16, p. 319–322.

McCrea, J. M., 1950, On the isotopic chemistry of carbonates and a paleothermometer scale: Journal of Chemical Physics, v. 18, p. 849–857.

Popp, B. N.; Anderson, T. F.; and Sandberg, P. A., 1986; Brachiopods as indicators of original isotopic compositions in some Paleozoic limestones: Geological Society of America Bulletin, v. 97, p. 1262–1269.

Ragland, D. A., 1983, Sedimentary geology of the Ordovician Cool Creek Formation as it is exposed in the Wichita Mountains of southwestern Oklahoma: Oklahoma State University unpublished M.S. thesis, 170 p.

Shelby, D. L., 1990, An occurrence of dolomite in the Lower Ordovician Arbuckle Group in the Slick Hills of southwestern Oklahoma: Texas Christian University unpublished M.S. thesis, 114 p.

Veizer, J.; Fritz, P.; and Jones, B., 1986, Geochemistry of brachiopods: oxygen and carbon isotopic records of Paleozoic oceans: Geochimica et Cosmochimica Acta, v. 50, p. 1679–1696.

Comparison of the Arbuckle Group at Wilburton Field, Latimer County, with N.E. Alden Field, Caddo County, Oklahoma

Bruce N. Carpenter
Consulting Geologist/Log Analyst, Edmond, Oklahoma

Michael C. Evans
Home-Stake Royalty Corp., Tulsa, Oklahoma

ABSTRACT.—Modern logs often enable accurate identification of both lithology and types of porosity. Analysis of modern logs, calibrated by available core data, allow comparison of the Arbuckle between individual wells within a field, and over wide areas from basin to basin. Extensive whole-core data from Wilburton and drilled sidewall cores from N.E. Alden provide excellent confirmation of modern log interpretation.

The Arbuckle Group appears to vary widely in lithology and in the nature of the reservoir. At Wilburton field (Arkoma basin), the upper formations are apparently early dolomites, with a heavy overprint of karst and fracture-related porosity with considerable good quality matrix porosity. At N.E. Alden field (Anadarko basin), the upper Arbuckle alternates between dense limestones, anhydrites, and fractured dolomites. Elsewhere, the West Spring Creek and Cool Creek Formations have anhydrite and apparently are associated with very fine- to coarse-grained intercrystalline porosity, primarily in the argillaceous dolomites. This type of porosity appears to be associated with the evaporites. Fracture porosity also occurs in the lower one-third of the West Spring Creek and in portions of the Cool Creek which are predominantly clean carbonates. Sandy and chert-rich facies appear common to the lower portions of the West Spring Creek and the Cool Creek Formations.

The upper one-third to one-half of the Kindblade Formation is often identified as the Brown zone, after the discovery well for this zone at Healdton field. The Brown zone is an important drilling objective in the Arbuckle. Karst development is more common in the Brown zone, particularly below an intraformational unconformity near its top. Strata-selective dolomitization also appears to be associated with the Brown zone.

At Wilburton, karst development appears to have begun early, perhaps subaerially and soon after dolomitization, and probably reoccurred thereafter at any opportunity. Karst at N.E. Alden appears limited to the Hunton, and perhaps the more anhydrite-free part of the upper Arbuckle. Elsewhere karst appears to be concentrated in what probably was the highest permeability path available at the time to carry surface waters entering from subaerial or erosional exposure or from faults reaching the surface. In deep-burial karst, this permeability path may have originated in fractured limestones. Both dolomitization and karst appear to increase toward surface-water entry points. In many cases, severe karst deveopment results in collapse, cementing, and loss of reservoir quality.

At Wilburton, temperatures in the Arbuckle Group average 260°F at 14,200 ft; temperature gradients exceed 1.3°F/100 ft above the Arbuckle and 2.0°F/100 ft within the Arbuckle. Formation waters are saturated brine, and evidence exists of basinal water activity upward along extensive vertical fracture systems.

At N.E. Alden, temperatures in the Arbuckle barely reach 200°F at this depth; temperature gradients average slightly below 1.0°F/100 ft above the Arbuckle and slightly above 1.0°F/100 ft within the Arbuckle. Fresh formation waters were reported.

In south-central Oklahoma, the Arbuckle appears overpressured (pressure gradients in excess of 0.6 psi/ft), perhaps due to folding and anhydrite seals. Temperature gradients are subnormal to normal above the anhydrites and average 1.36°F/100 ft (some higher) below and within the deep Arbuckle, and formation waters (when recovered) are saturated brines.

Elevated temperature gradients may be related to basinal water circulating upward in extensive, open, vertical fracture systems. These waters are associated with certain dolomites and porosity-destructive sulfide mineralization. Reduced gradients may be related to breach of seal, fresh-water influx and cooling, and possible hydrodynamic components to present hydrocarbon traps. Sharp increases in temperature gradient and brine salinity may indicate anhydrite seals, and overlying shales remain competent enough to contain over-pressured Arbuckle reservoirs below, despite fracturing of limestones and dolomites.

INTRODUCTION

An extensive data base was accumulated on the Arbuckle in and near the Wilburton field (secs. 13–24, 27–30, T5N, R18E, Latimer County, Oklahoma). A large part of the data was provided by participants in Oklahoma Corporation Commission hearings to determine applicability and nature (if any) of field rules for this 400-BCF, prolific gas reservoir.

Modern logs were run, including recently developed borehole-imaging types. One well was extensively cored and four others had significant core coverage. Standard whole-core analysis and descriptions were available, along with color photos, thin sections, and considerable special core analysis. The special core analysis includes extensive fracture analysis on directionally oriented cores, directional permeability with applied effective stress, and CAT scans. These core data were correlated to log characteristics and an excellent understanding of modern log responses were derived for the Arbuckle Group.

This understanding was then applied to log data over uncored intervals in the same well and other wells, along with extensive test and production data, to develop a knowledge of reservoir characteristics, completion and testing pitfalls, and unusual production characteristics.

Modern logs were also run in the more recently discovered N.E. Alden field (secs. 1–2, T6N, R13W, and sec. 8, T6N, R12W, Caddo County, Oklahoma). Here, log responses were compared to petrographic analysis of drilled sidewall cores targeted at selected log features. Core analysis included special XRD, thin-section, and SEM petrographic work. Perforations and stimulation techniques were suggested to test certain conclusions.

OVERVIEW

The volume of data allows touching only the tip of several "icebergs" in this presentation. Some of these "icebergs" include the following:

1) The lithology of the Arbuckle Group is tremendously varied. Original deposition appears to have included clean and argillaceous limestones, evaporites, thin quartz-rich sands, and very organic-rich thin laminae. At Wilburton, no evaporite beds were found. Dolomite appears to predominate in all of the Arbuckle, some 2,262 ft thick, exclusive of the basal Reagan Sandstone. At N.E. Alden, alternating thick intervals of limestones, anhydrites, and dolomites were found and some thin quartz sands. Elsewhere, the West Spring Creek and Cool Creek Formations also have thick evaporite beds, argillaceous to clean limestones, and dolomites. Evaporites appear absent from the Kindblade Formation. An important producing interval, known as the Brown zone, is developed just below an unconformity near its top; it is reported to be as much as 800 ft thick.

2) Diagenesis also varies widely. At Wilburton, early dolomitization is indicated, often developing significant "sucrosic"/matrix porosity and probably progressing to karst development, particularly in the Brown zone equivalent to the top of the Kindblade. Silica, perhaps introduced as sponge spicules, forms cherts and siliceous carbonates. Concentrations of radioactive minerals appear to characterize transitions from gas to water, and vein-filling calcite, quartz, dolomites (some high-temperature), and sulfides appear associated with fracture systems that probably extend down to the basement. At N.E. Alden, only selected thick intervals are dolomitized, apparently because of larger grain size, leaving the wackestones as limestones.

3) Porosity types also vary widely. Significant matrix porosity, reaching as high as 19.9% in the upper Arbuckle (West Spring Creek?) above the Kindblade unconformity, was found in cores and on logs at Wilburton, but this type of porosity was very limited at N.E. Alden. Here, matrix porosity appears restricted to the very clay-free facies and develops in very fine- to fine-crystalline dolomites. Some small vugs were also found in cores and on borehole-imaging logs.

Porosity types at Wilburton are intercrystalline, pinpoint to large vugs, and fracture. The vugs commonly are lined with calcite and/or dolomite crystals and locally they contain quartz crystals. Other dissolution-type porosities appear along fractures. Surprisingly, porosity in the extensively karstic zones characteristic of the Kindblade at Wilburton have little remaining porosity. Pervasive cementing and filling of earlier dissolution features appears to leave only isolated pores and partially open fractures. Even highly brecciated intervals have little reservoir quality.

4) Fracture systems vary from field to field and appear strongly influenced by lithology. At Wilburton, crackle breccia and other fracture systems are characteristic of unsupported roofs of once-open caves below. These fractures have some related porosity in slightly open portions and in dissolution activity along the fractures. Fracturing associated with the karstic intervals appears to be of several generations. Only small segments of perhaps the most recent generation remain uncemented.

An extensive vertical fracture system opens with depth below an argillaceous and siliceous facies which forms a "floor" for the karstic Kindblade (Brown zone) interval at Wilburton. This system appears to carry basinal waters well up into the Arbuckle and possibly explains the presence of minerals characteristic of temperatures that are above normal formation temperatures at this depth. Such a conduit for basinal waters may possibly explain abnormally high temperature gradients within the Arbuckle. Structurally high wells, with hydrocarbon columns extending down into the extensive fracture system, usually cone water if perforated intervals include this system.

In contrast, open fractures contribute much of the reservoir porosity at N.E. Alden. The fracture systems are open and extensive in the dolomites and healed or nonexistent in the limestones, providing some protection from water coning. Elsewhere, limestones have extensive fracture systems which contribute to the reservoir.

5) Arbuckle water salinity is an unexpected variant and may be related to temperature and pressure gradients and seals. At Wilburton, water appears to be saturated brine, as expected. Pressure gradients are near normal. This may be consistent with elevated temperature gradients within the Arbuckle and evidence of basinal water mineralization in an extensive vertical fracture system that probably communicates basinal waters well up into the Arbuckle. However, fresh water is reported north of the field and the major E–W-trending faults. This would indicate a lack of seals and the influx of fresh water down the faults or from surface exposures to the north.

At N.E. Alden, fresh water was reported from tests produced below gas production. A temperature-gradient survey showed subnormal temperature gradients, indicating cooling—perhaps by ongoing fresh-water influx from known faults and outcrops to the north. However, pressure gradients are 0.476 psi/ft, or near normal. Anhydrites are

present to reseal the crest of the fractured structure.

Elsewhere, water production is unknown and hydrocarbon columns perhaps several thousand feet in height appear trapped below thick anhydrites and shales in tightly folded structures bounded by faults. Abnormally high pressure gradients exceeding 0.6 psi/ft are also indicated, confirming a seal and indicating fresh-water influx would be currently hydrostatically impossible. Here, temperature gradients appear normal, indicating a lack of cooling by fresh-water influx or heating by basinal water activity against these pressures.

DATA AT WILBURTON

Extensive coring was conducted in and near Wilburton by ARCO in four wells, and three cores were taken by Anadarko Petroleum in sec. 23 in the middle of the field (see structure map shown as Fig. 1). Conventional core analysis was performed to the extent possible; some cores were unsuitable because of porosity heterogeneity and fractured condition. Most cores were oriented, and oriented permeability and extensive fracture-analysis studies were conducted. Color core photos show many of the reservoir features, such as large open vugs, cemented vugs, breccia, and fractures. Computer Axial Tomography (CAT) scans were used to study the shape of the larger pores and the patterns exhibited by both cemented and uncemented fractures. Only selected examples will be shown here.

Log Data

A wide variety of modern logs were also run both in water and oil-based muds. The most informative logging program proved to be the dual laterolog-micro spherically focused log (DLL-MSFL), spectral gamma ray, multiple calipers, compensated neutron litho-density porosity log combination, some special sonic logs, and borehole-imaging tools.

Water-based mud is recommended, both for more informative logs and minimizing formation damage in this type reservoir. DLL-MSFL logs provided good open vertical fracture identification. The lithology-type porosity combination provided excellent lithology and porosity information, despite some borehole rugosity and some unfortunate use of barite-weighted muds in earlier wells. Digital full-waveform sonic logs also allowed mechanical-property studies. Borehole-imaging logs detail the nature of fractures, pore types, and bedding.

Use of oil-based mud proved too costly in leading to a loss of logging information, to formation damage when whole mud was lost to the large-pore and open-fracture systems, and in some reported difficulty in obtaining good cement isolation.

Despite rumors to the contrary, the preferred logging program provided complex but interpretable data, which was confirmed by core data where available. The neutron log proved to be an effective porosity tool in the less-argillaceous dolomites. Care had to be taken to eliminate argillaceous dolomites which appear porous. Siliceous intervals must also be separately considered. Both may have ineffective microporosity which is filled with bound water and could be misinterpreted as part of a water-wet zone.

Water saturations can be determined where some level above ~2% of true matrix porosity can be validated. Long transition zones from gas to water are typical in low porosity and are found at Wilburton, but water production vs. gas production could be predicted. Test results often reflected communication through open vertical fractures, and, in some cases, loss of cement to extensive fracture systems. Flows from both above and below production perforations were observed.

Data Interpretation

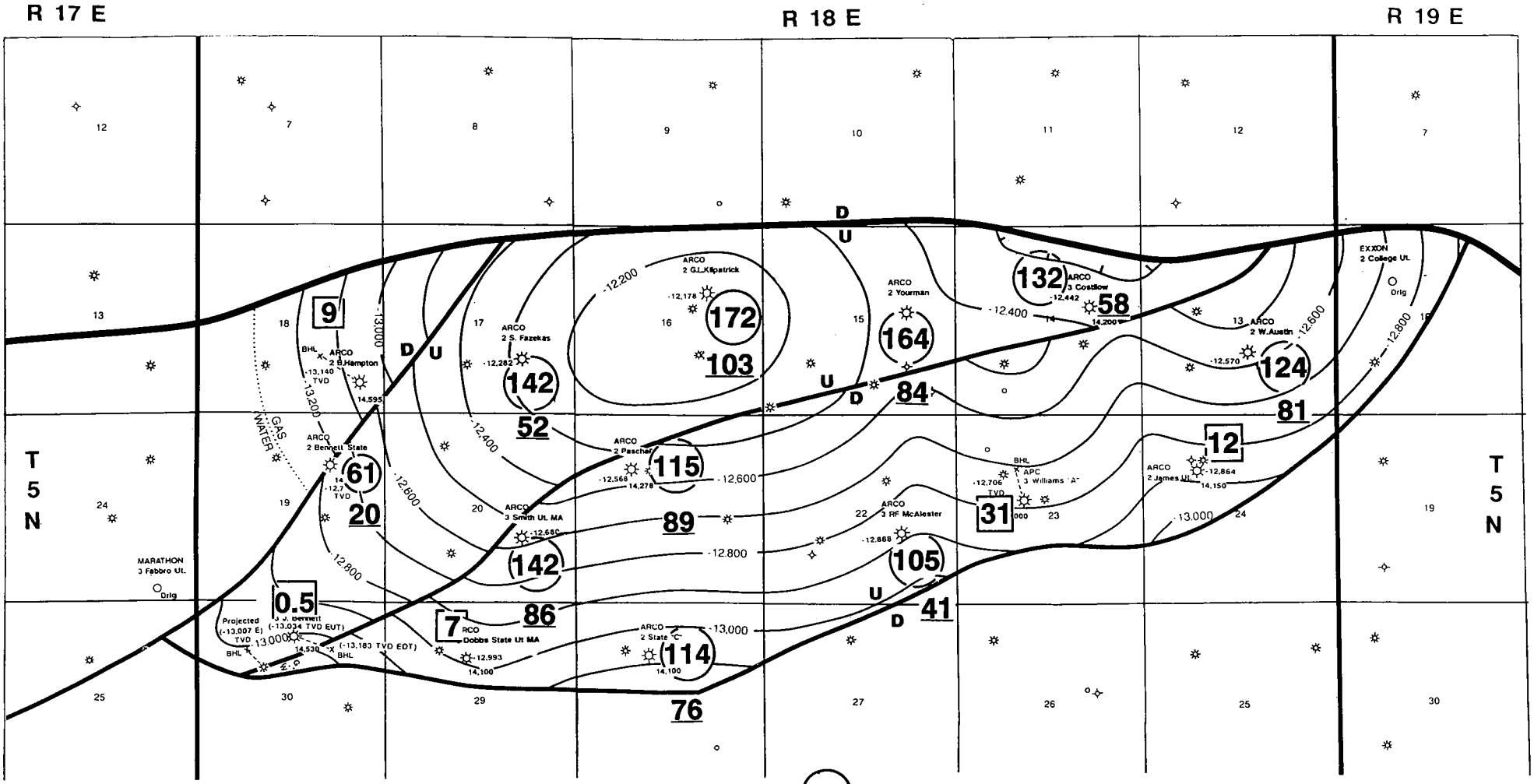
Open fractures were well defined by separation between the DLL curves and separation from these curves and the character of the MSFL curve. Fractures often caused rugosity detectable on calipers and spikes on pad MSFL or ML or skid-derived measurements. The density porosity and correction curves are the most common skid-type measurements. Barite-weighted mud in fractures can also cause spikes on the PEF curve. Borehole-imaging tools, particularly the resistivity type, provided very effective descriptions of both bedding and fracture characteristics and, in many cases, the type of porosity.

Intervals with abundant clay-rich laminae appear to have limited reservoir potential. The laminae restrict flow of dissolving waters and interrupt fracture continuity by providing stress-release surfaces. Intervals which are clay-free have the best reservoir potential, particularly if they are thick and are part of longer trends suggesting shoaling, resulting in cleaner and coarser grainstones. These appear to be predisposed to early dolomitization, probably leading to later karst development in extreme cases (Kerans, 1988). Shoaling would also create high stands subject to subaerial exposure, and would be located in the part of the peritidal setting that would be relatively free of evaporites, but conducive to generation of early-reflux dolomites (Burgess, 1964,1968).

Core Data and Interpretation

Figure 2 shows composite logs over the upper two pay zones at Wilburton field. The DLL-MSFL (with gamma ray and caliper) is on the right and the litho-density/neutron (with gamma ray and caliper) is shown on the left. The Joins sand (Simpson Group) is shown at the top of the log section, just above 12,850 ft. Two matrix-porosity zones are common to the field. The upper matrix porosity zone is between the argillaceous dolomites at 12,915 and 12,946 ft. Porosity exceeds 12%. The lower matrix-porosity zone is between the argillaceous dolomites at 12,960 and 12,990 ft. In this well, the porosity is lower in this more argillaceous dolomite. Both zones show mud cake and smooth MSFL curves, well separated from the DLL curves, which exhibit an RXO<<RT profile. Note that RT exceeds 3,000 ohm-meters in both zones, which would be beyond induction-log range.

These two zones exist throughout the field, except where faulted out in one well. They probably occur in the West Spring Creek and are collectively designated as the "cave roof" in Figure 3, showing the structural view of the field. The cave-roof designation was used by Kerans to place these different pore-type intervals above a large collapsed cave system, here in the zone below 13,000 ft. This cave system is in the Kindblade Formation, as identified by ARCO using conodonts (Mescher and others, 1991). This would place the large karst system in the Brown zone. A system of smaller caves exists below the large system and is "floored" by argillaceous and cherty facies at about 650 ft from the top of the Arbuckle. This floor is shown as the "base of caves" in the structural view shown in Figure 3.



STRUCTURE - TOP ARBUCKLE

(ANADARKO)

(172) INITIAL CALCULATED OPEN FLOW (CAOF) IN MMCF

103 1990 CALCULATED OPEN FLOW (CAOF) IN MMCF

[31] INITIAL PRODUCTION FLOW RATE (IPF IN MMCF

Figure 1. Structure map on top of Arbuckle Group over Wilburton field, Latimer County, Oklahoma. Numbers by wells show initial and 1990 calculated open flow (CAOF) potential in millions of CFGPD (cubic feet of gas per day) for tested wells, and actual initial and subsequent production flows (IPF) for untested wells. Base map is courtesy of Anadarko Petroleum Corp.

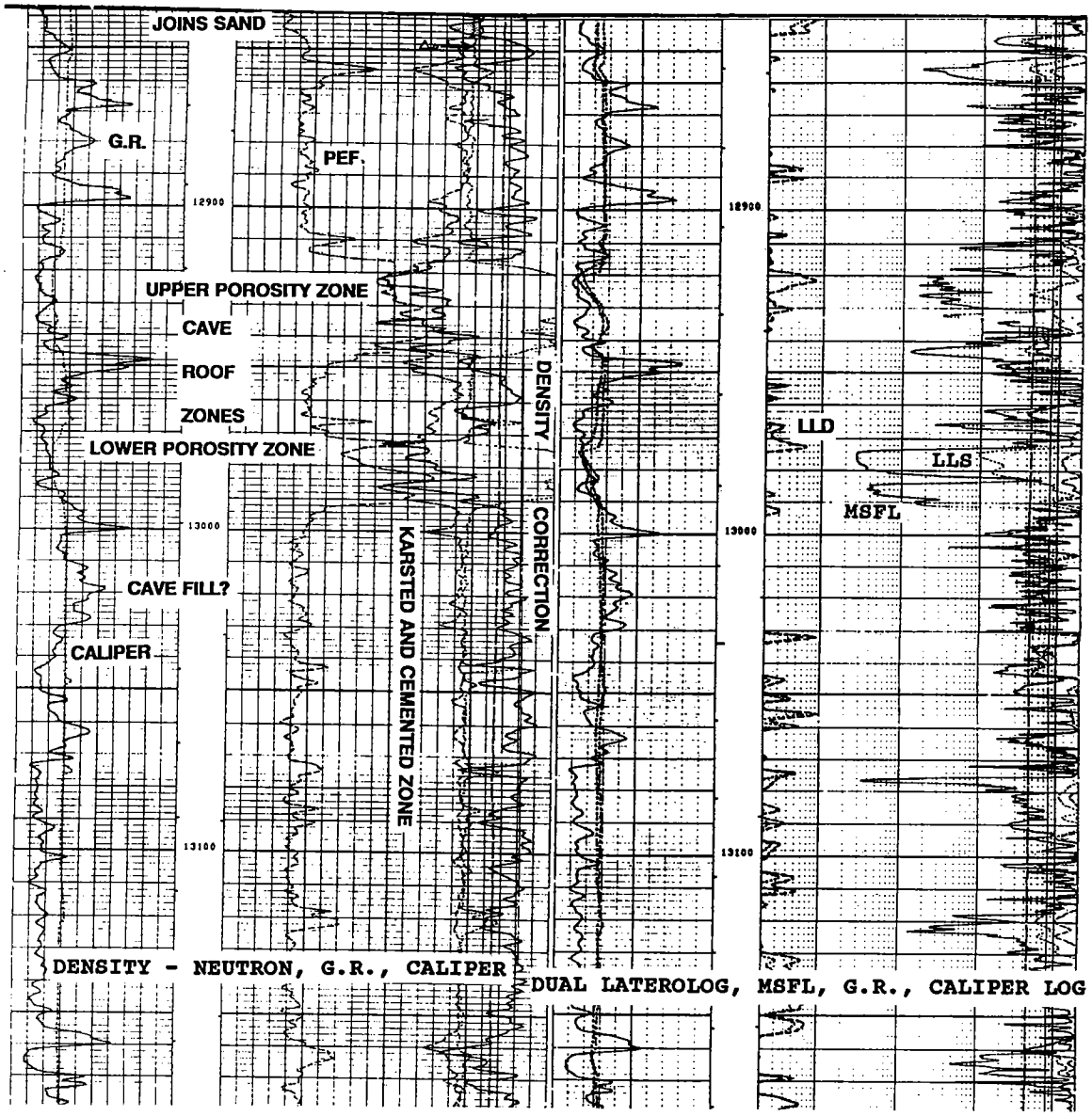


Figure 2. Logs through upper pay zone in the ARCO No. 2-16 Kilpatrick well (sec. 16, T5N, R18E) in Wilburton field showing matrix porosity exceeding 10% in each of two "cave roof" zones centered at 12,923 and 12,973 ft. Note lack of porosity below "floor" at 13,000 ft for lowermost upper pay zone and through karstic but highly cemented zone in the bottom half of figure.

Production perforations, as shown by solid rectangles in Figure 3, are limited to the upper Arbuckle (West Spring Creek and upper Kindblade). An extensive fracture system opens below the facies forming the cave system base or "floor" downward into water. The cave "floor" facies was wisely used as a way to limit upward water coning, as the underlying fracture system usually terminated or closed upward in the highly laminated and argillaceous "floor" facies.

A sample of the core data is provided as Figure 4. The data are a cross-plot of horizontal permeability vs. porosity over 471 ft of core analysis extending from the top of the Arbuckle at 13,244 ft (by core measurements) to 13,744 ft in the sec. 21 well. The cores include well-developed matrix porosity up to 8.5%, typically described as dolomite, medium crystalline, sucrosic, vuggy, with quartz crystals and vertical fractures. Permeability varies accordingly, with measured values approaching 100 mD (millidarcies). Four fractured samples exceeded this value.

Figure 4 also shows the general distribution of both permeability and porosity. Many samples had permeability near or less than 0.01 mD, with associated porosities much less than 1%. However, many porosities near 1% had significant permeability. The average porosity was slightly more than 1%. The average permeability is shown as 0.034 mD. Fractures characterize the scatter of the higher permeability points. This well did not have well-developed matrix porosity in the usually porous upper two pay zones.

The values shown here demonstrate that, in general, the Arbuckle is dominated by extensive intervals of tight dolomite and much thinner intervals with 2–6% porosity and scattered intervals of up to 20% porosity. Only ~250 ft of 2.5% average porosity is needed to store the estimated 400 BCF (billion cubic feet) of gas in place.

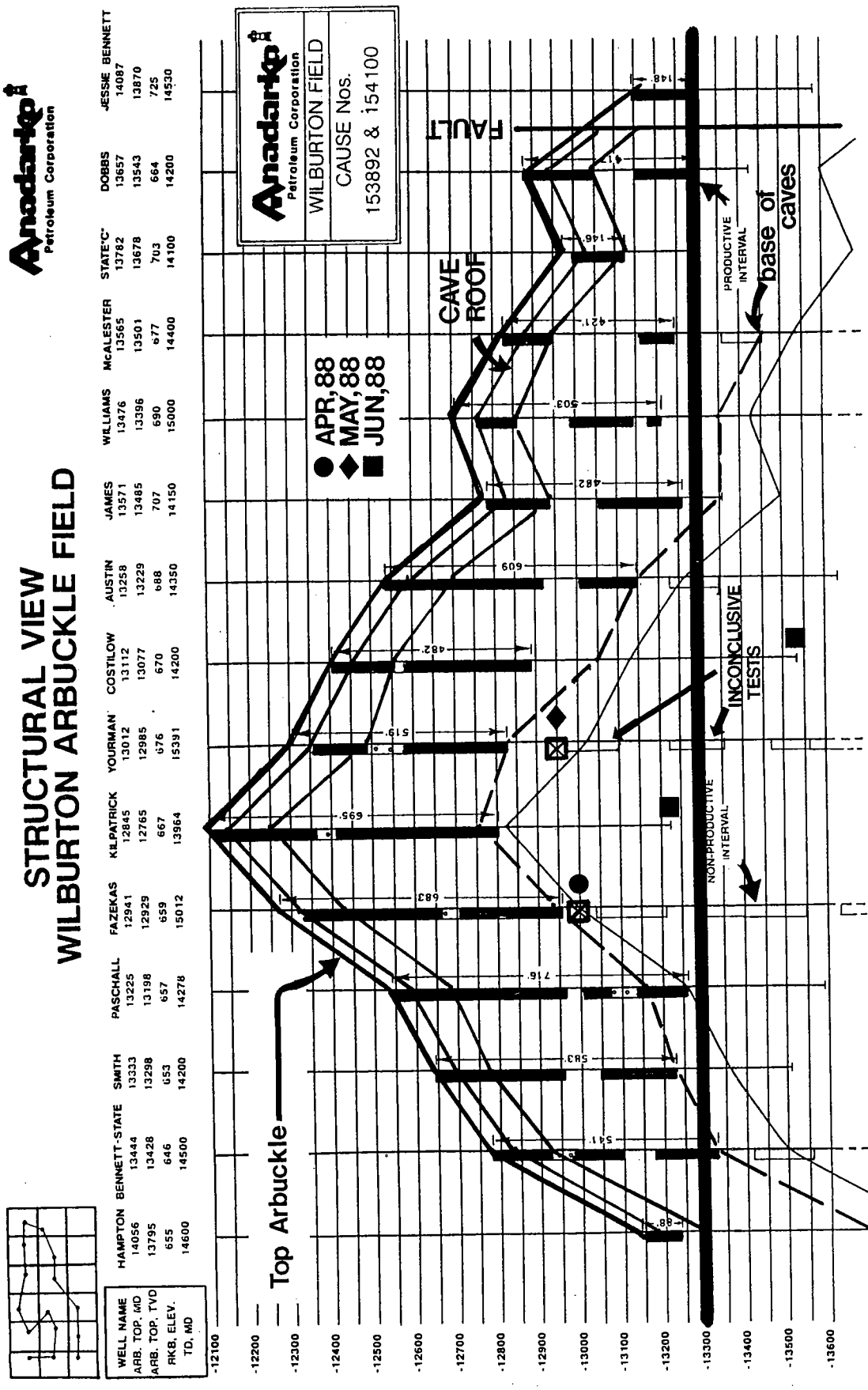


Figure 3. Computer-generated structural view of Wilburton field wells. Arbuckle top is shown, along with production perforations (represented by vertical black rectangles) and feet of pay (88–716 ft). Perforations are zoned to correspondence with matrix-porosity zones shown in "cave roofs" (Fig. 2) and "base of caves" (formed by argillaceous and laminated chert-rich facies). Inconclusive tests and conclusive water tests are shown as open rectangles. Heavy line at –13,300 (subsea) is field-wide top of original transition to water.

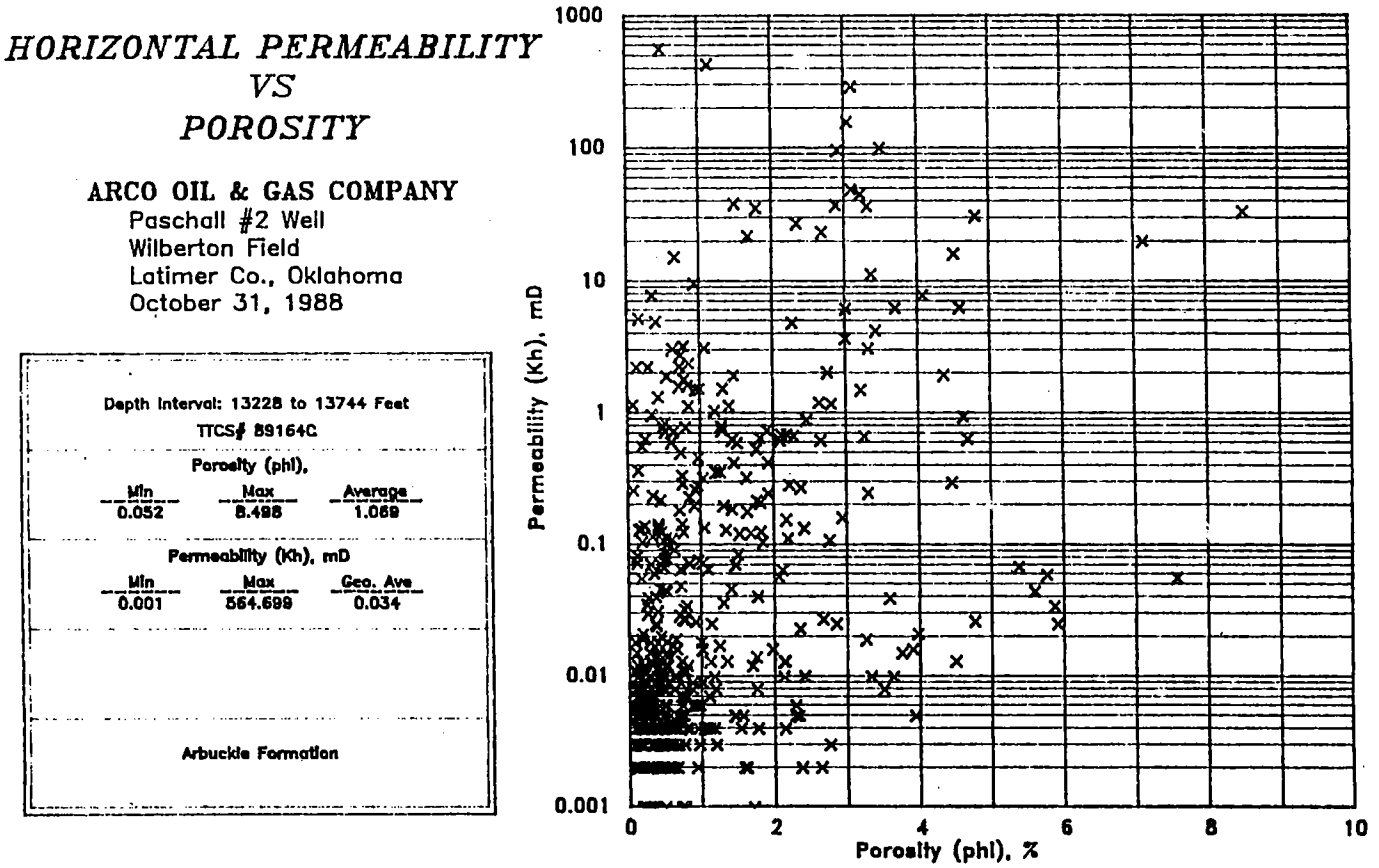


Figure 4. Cross-plot of measured core permeability vs. porosity for 471 samples from ARCO No. 2-16 Kilpatrick well in middle of Wilburton field. Maximum porosity is 8.5% (with permeability of 33 mD); it occurs as intercrystalline porosity and pin-point vugs in very fine- to medium-crystalline sucrosic dolomite.

There is considerable concern about the appropriateness of measurements on fractured cores conducted at ambient conditions. Selected intervals of the above core were subjected to a study of permeability values at four effective-stress levels. Figure 5 shows a typical page from this study. Nearly all samples show permeability reductions of orders of magnitude from the values reported on the standard core analysis.

Figures 6A,B shows selected black-and-white reproductions of CAT scans of the above core. In each figure, three closely spaced scans sequence downward along the axis of this 2.5-in.-diameter core. The images to the left are unenhanced, and those to the right are computer enhanced.

Figure 6A shows CAT scans from an upper pay zone; dark areas are pores. Note the scale and large variety of pore shapes. Figure 6B shows coarse breccia in dolomite from the karst interval. Here fractures have been totally cemented by calcite. Other intervals clearly show both cemented and open spaces that suggest dissolution along fractures.

An extensive fracture analysis was conducted on oriented cores from three Wilburton wells under the direction of an ARCO fracture specialist. One report is nearly 2 in. thick. An independent study was also conducted. Five distinct fracture types were found:

1) Open fractures—totally open and split the core into pieces (some appear induced to open);

2) Incipient fractures—partially open hairline fractures without fill material (some of which may have been induced by coring);

3) Open/incipient fractures—open fractures where the fracture aperture can be measured with a feeler gauge;

4) Filled fractures—containing some type of mineralization, commonly calcite and silica; and

5) Induced fractures—commonly low-angle, penetrative fractures.

Abundant stylolites were also found.

Whole cores were dominated by high-angle incipient and open/incipient fractures with open fractures extending over a few feet. Breccia zones of smaller to larger intervals as much as 8 ft thick were common. One 34-ft core was dominated by breccia zones, but they contained abundant calcite and silica fill.

All types of fractures showed a preferred, generally E–W strike—parallel to both the basement-related normal faults and thrust faults in this area. Fracture strike appeared to be also related to the strike of local bedding planes. Fracture strike appeared to change with local changes in basement fault direction and bedding plane dip. Fractures in breccia showed similar but less-clear trends. Fracture dip varied from 72° to the north to 60° to the south. North and/or south fracture dip would be consistent with the above strike. Some boreholes showed northward deviation. Stylolites formed three different orientation groups.

Fracture intensity generally increased with depth. This trend, and the increasing aperture of the fracture, was also apparent on certain logs. Moderate- to high-angle frac-

Sample No.	Depth (ft)	Effective Stress (psi)	Porosity (%)	Permeability (mD)				
				V	N+0	N+45	N+90	N+135
22	13642.0	2000	3.67	0.8220	0.5857	0.4143	4.506	5.936
		3000		0.6116	0.3543	0.2803	4.302	6.305
		4000		0.4684	0.2775	0.1283	0.1778	4.877
		6650		0.5973	0.0667	0.0573	1.936	4.520
		10000		0.6365	---	---	0.0403	1.411
23	13647.0	2000	3.137	3.569	3.534	4.087	0.5972	1.760
		3000		2.278	2.065	3.275	0.3403	1.553
		4000		2.351	1.579	2.287	0.4437	1.219
		6650		2.322	0.8038	0.8815	0.1080	1.173
		10000		2.169	0.3902	2.675	---	0.8156
24	13689.1	2000	5.482	1.459	36.650	26.025	23.357	26.053
		3000		0.9740	36.102	22.237	20.012	26.074
		4000		0.8819	32.592	26.231	21.438	29.322
		6650		0.8916	36.154	14.159	21.262	23.372
		10000		0.6285	14.582	14.490	8.345	13.904
25	13719.2	2000	1.244	4.626	0.0222	6.107	2.132	0.0258
		3000		3.787	0.0154	6.394	1.457	0.0207
		4000		3.489	0.0120	5.602	0.0794	0.0115
		6650		1.830	0.0056	0.8199	0.1472	0.0072
		10000		1.475	---	0.7659	---	---
26	13736.2	2000	1.36	0.0519	0.0038	0.0170	0.0486	0.0029
		3000		0.0229	0.0027	0.0110	0.0340	0.0024
		4000		0.0180	0.0019	0.0075	0.0178	0.0020
		6650		0.0062	0.0009	0.0038	0.0110	0.0012

Figure 5. Sample data showing changes in directional permeability with increasing effective stress for the ARCO Paschall well. Breaks in trends of decreasing permeability with increasing stress are probably due to shifting of fractured surfaces in generally very fractured dolomite.

tures with calcite, gouge, or silica fill were the most abundant fracture types observed. Brecciated intervals contained abundant filled fractures. In most cases, filled fractures exhibited no visible natural porosity. In one interval believed to correspond to the equivalent of the lower part of the Brown zone, calcite- and silica-filled fractures with vuggy porosity were increasingly abundant. Many fractures exhibited large vugs which contained euhedral quartz crystals. These vugs were large enough to be apparent in core photos and on formation micro scanner (FMS) images. An example is provided in Figures 7 and 8.

The most significant natural porosity and permeability found in the cores is associated with large vugs and vuggy fractures. Logs indicate that there is little pore space of any type in brecciated intervals common to the top of the Kindblade interval. Cores show that cement extensively filled what was previously cavernous porosity. This heavy cementing of karstic intervals has been reported elsewhere (Kerans, 1988; Lynch, 1989; Lynch and Al-Shaieb, 1989).

Open pores were found mostly above this highly cemented interval and well separated by stratigraphically continuous, permeability-restrictive, and possibly mechanically supportive beds. Porosity-log profiles suggest concentrated dissolution-water profiles in permeable dolomites above less permeable (or less soluble) beds or "floors." One interpretation is that these porous intervals were developed separate from, or subsequent to, the main karst development, and therefore did not undergo collapse and cementing. The open vuggy porosity and fractures below the collapsed and cemented intervals are much smaller in scale and also are separated from the large-scale karst features above.

Core-To-Log Comparison

Core-to-log comparison provided an excellent understanding of how various logs respond to features found in the cores. The DLL-MSFL separation gives a reasonably consistent response to continuous open vertical fractures (Fig. 2). The DLL curve separation should be related to the sum of the aperture widths of all open vertical fractures intersecting the borehole at a given depth. The character of the MSFL curve, as compared to the DLL curves, allowed distinction between predominant pore types—i.e., vuggy or sucrosic versus fracture.

Figure 7 shows a small portion of one of the modern imaging type logs—here the FMS. A large vug is shown as a dark area, designated by an arrow. Other vugs aligned along vertical trends suggest that they result from dissolution along fractures. Figure 8 shows the same vug as found in the corresponding core, when depths of core and logs are adjusted.

Porosity values appear to be best represented by the

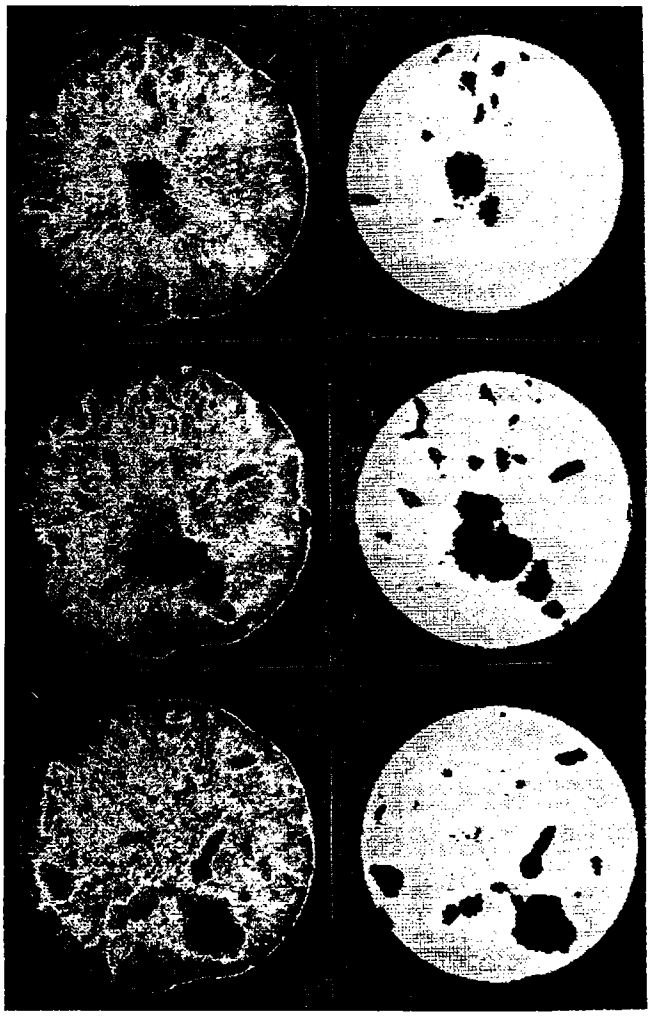


Figure 6A. Black-and-white copies of color photos of adjacent CAT scans along axis of 2.5-in.-diameter core showing shapes of pores (dark areas) changing with depth in "cave roof" portion of reservoir in the ARCO Paschall well. Two top images are at a depth of 13,310.1 ft; middle images are at 13, 310.3 ft; and bottom images are at 13,310.5 ft.

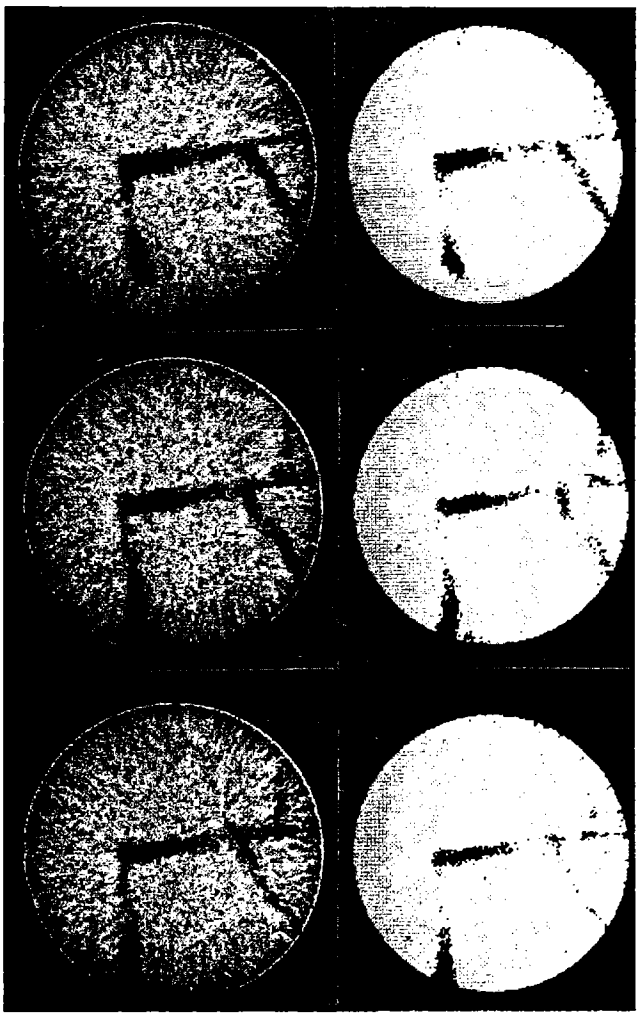


Figure 6B. Black-and-white copies of color photos of adjacent CAT scans along axis of 2.5-in.-diameter core showing healed fracture between breccia in karstic and cemented portion of Arbuckle in the ARCO Paschall well. Top two images are at a depth of 13,371.8 ft; middle images are at 13,372.0 ft; bottom images are at 13,372.2 ft.

neutron log. Figure 9 shows the typical porosity log over a section of the Arbuckle (top at 12,846 ft), believed to be in the West Spring Creek and above the heavily karstic Kindblade interval below 13,000 ft. Whole-core porosity has been plotted using the +30, +20, +10, 0, −10% porosity scale (left to right) of the logs. Both the density and neutron porosity are scaled for limestone. The density is the solid trace and generally is the right-most curve. The neutron is the smoother dashed curve to the left (dolomite porosity profile). Core porosity (unaveraged) is the heavy traced curve. The log-porosity curves tend to enclose the core-porosity trace, but the best fit is given by the neutron.

The separation between the density and neutron curves in the less porous intervals indicates the overall dolomite lithology, as found in cores. Other curves are the gamma ray and caliper to the far left, and the photo electric factor (PEF) curve, generally just to the right of the depth track, which also indicates dolomite (except where barite from 10.2 lb/gal oil-based mud infiltrated the pore system). The density compensation curve (Delta-Rho) also indicates barite. Often, barite in the mud cake or infiltrated into the formation is the most obvious evidence of permeability in oil-based muds. Note the relatively smooth borehole and mud cake. Averages for 107 core measurements were 3.4% porosity and 0.176 mD.

The effectiveness of the matrix porosity, connected by fractures with associated dissolution porosity, is shown by the calculated open flow (CAOF) values shown on the Wilburton structure map (Fig. 1). The above zone was a major contributor to the 172 million CFGPD (cubic feet of gas per day) calculated for this well.

DATA ON N.E. ALDEN FIELD

Only drilled sidewall cores and samples were available for study in this field. Cores were characterized by dolostones, limestones, sandy dolostones, and dolomitic limestones. Only the dolomitic lithologies had matrix porosity

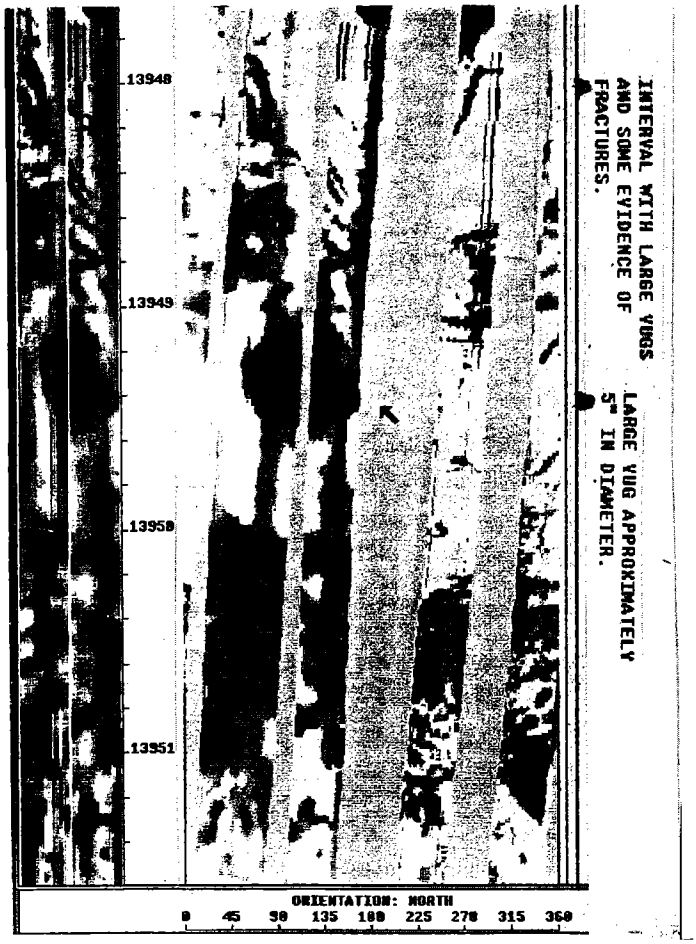


Figure 7. Borehole image from FMS log of well in sec. 23 in Wilburton field showing large vug (in Arbuckle dolomite) denoted by arrow. Vug found in core at corresponding depth is shown in Figure 8; vug measures approximately 2 × 4 in.

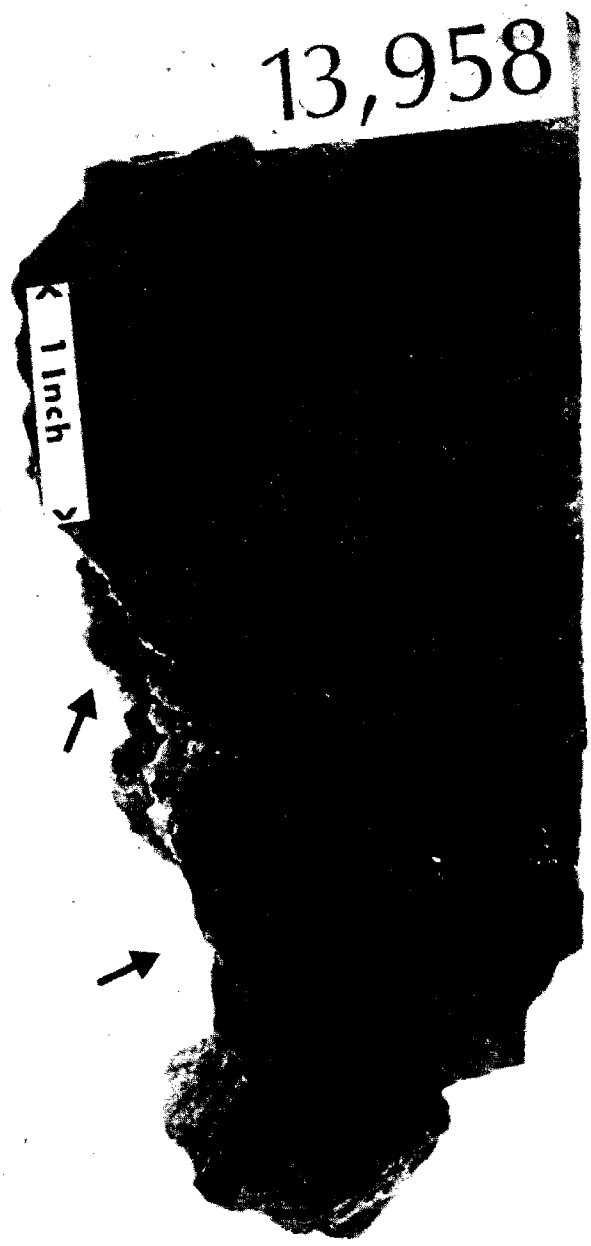


Figure 8. Black-and-white photo of piece of core with approximately 2- × 4-in. open vug, shown at lower left, which was cut during coring and slabbing process. Vug is lined with coarse crystals (arrows). Parallel lines are saw marks; the others are healed fractures. Core is from zone near "base of caves" shown in Figure 2. Borehole image of the vug is shown in Figure 7. Zone had to be abandoned due to excessive water coning. Core is ~9 ft deeper than shown on logs.

as minor intercrystalline and vuggy types. Extensive fracture porosity in the dolomites was also apparent on the logs.

The dolostone samples consisted of ≥90% dolomite or ankerite, an iron-rich dolomite, and minor amounts of detrital quartz and potassium feldspar. The dolomite crystals form a fine to coarsely crystalline matrix with minor amounts of calcite and illite clay. Porosity is generally low, and most open pores are in fractures. A few poorly connected open and vuggy pores are also present.

The limestones are wackestones with poor reservoir quality. The matrix is micrite with calcite fossils. Porosity is very low. Some micropores are associated with matrix fractures formed and healed prior to pressure dissolution. Calcite-filled vugs are also present.

The dolomitic limestones are highly heterogeneous and represent a mix of lithologies. The dolomite is laminated. Intercrystalline pores are small and ineffective. Calcareous portions are micritic. Fractures are common, but most are healed with calcite and dolomite with a few open fractures.

The sandy dolostones also include laminated sandy dolostones and dolomitic sandstones. Quartz is moderately sorted, rounded, and very fine- to medium-grained sand. The dolomite laminae may have been dolomitized micrite, with early dolomitization indicated. Vuggy pores and fractures are apparent under the binocular microscope. Both are filled with dolomite and anhydrite, so the fill postdates their formation. Clays are rare, but illite does coat some dolomite crystals.

Logging programs varied by operator. Muds were salty-water based. Both the DLL-MSFL and DIL-SFL logs defined the open, vertically fractured dolomite intervals, but

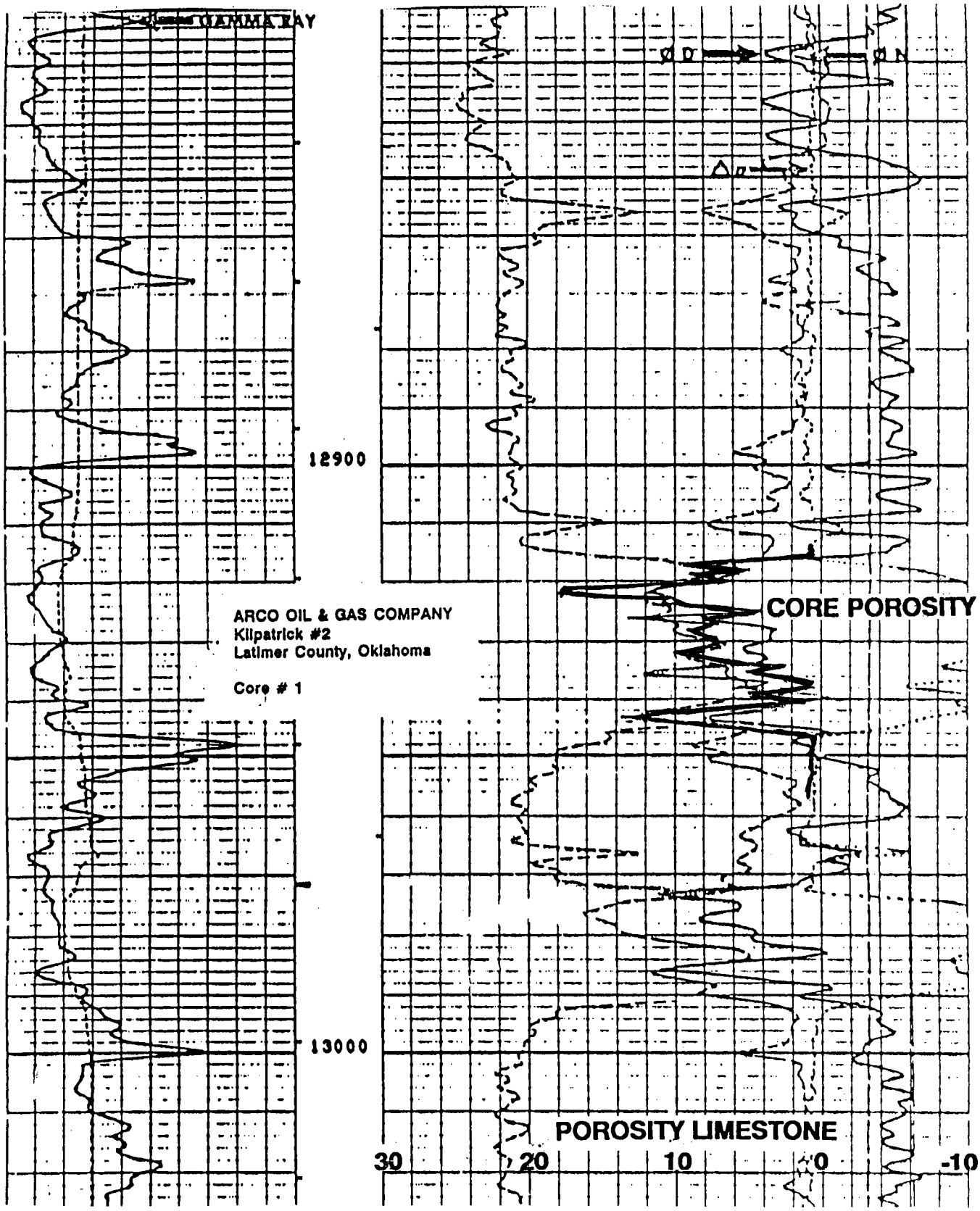


Figure 9. Large-scale porosity logs from well in sec. 16 of Wilburton field (see Fig. 2). Porosity measured from cores (unaveraged) is plotted (dark line) over upper porosity zone at the same scale as the logs. Note good agreement with porosity logs, with the neutron log giving an excellent fit.

the resistivities in the cleaner limestones were too high for induction-log resolution. Litho-density (LDT) and compensated neutron/gamma ray logs indicated massive limestones, dolomites, argillaceous carbonates, and sandy dolomite intervals, consistent with the Arbuckle core descriptions.

Porosity on logs was limited to the dolomites, as indicated by the cores, and is predominantly fracture porosity and some associated vugs. The fractures appear as open vertical systems. The effectiveness of the open fractures is demonstrated by indications of continued invasion between logging runs.

Figure 10 shows the standard logs through the Arbuckle pay zone at N.E. Alden field. The interval is below the Arbuckle top, picked at 11,020 ft, and a considerable thickness of anhydrites and argillaceous carbonates. Some thin anhydrites are also indicated near 11,450 ft. The porosity logs indicate that this interval is essentially dolomite, with some minor matrix porosity indicated in the cleanest portions. The DLL indicates very high resistivities, mostly >5,000 ohm-meters and much of the interval >10,000 ohm-meters. The separation LSS<LLD indicates that the interval is broken into a semi-continuous, open vertical fracture system.

The effectiveness of this system is indicated by three separate tests on different adjacent perforated zones shown on the logs. Each test flowed in excess of 5 million CFGPD, with several hundred bbl oil and some water against small chokes and ~2,000 psi flowing pressures. The well produced in excess of 787 million cubic feet of gas and 46,000 bbl of condensate from July 1989 to the end of 1990.

Three large-scale fracture systems are defined on logs. Each system essentially extends over 100 ft or more of massive dolomite. Each appears to be more open at its top, in contrast to opening with depth at Wilburton. Smaller-scale systems appear in the dolomite/limestone mixed intervals. No open fracture systems were found in the limestones. The DLL and DIL-SFL logs would not indicate the closed and healed fractures found in the cores. The limestones are massive and healed enough to isolate dolomitic fracture systems.

Figure 11 shows conventional logs from the top of the karstic Hunton at 9,362, through a pick for the Bois d'Arc top at 9,434, and a cave centered at 9,462 ft. Porosity and caliper logs show an open-cave interval that extends from 9,460 to 9,466 ft in limestone. The DLL shows, by the separation between the shallow and deep laterolog curves, vertical fractures opening below a shale at 9,441, and extending upward through the cave and closing above the cave at 9,478 ft.

Figure 12 shows another type of borehole-imaging tool, here an acoustic tool. High-frequency pulses are used to scan the circumference of the hole, measuring the reflectivity (center track) and travel time (right track) of the return echo. The type of log shown is denoted as CIBIL for circumferential borehole imaging log. A gamma-ray curve and four-quadrant acoustical calipers are also shown (left track). The cave appears as a black area (no returning echoes). Note the dissolution along fractures in the roof of the cave and irregularity of floor, suggesting collapsed breccia. Also shown above and below the cave are the characteristic sinusoidal patterns created by inclined fractures striking generally to the east–northeast, and dipping down to the south–southeast. A notch worn by the drill pipe appears on the south–southeast side of the hole.

Figure 13A shows the DLL on a 5 in./100 ft depth scale; Figure 13B shows the high-resolution porosity logs in a 10 in./100 ft scale; and Figure 13C shows the acoustic-image log on a 60 in./100 ft scale centered over a highly fractured interval in the Chimney Hill portion of the lower Hunton. The image tool confirms the open vertical fracture system interpretation of the separation between the DLL curves.

Figure 13D is from near the base of the Chimney Hill: it shows a slot or notch worn by drill pipe and tool joints, probably during slow drilling in the Sylvan Shale, the top of which is at 10,257 ft.

Figure 14A is a montage of standard logs over one of few intervals with matrix porosity in Arbuckle dolomite at N.E. Alden. An open vertical fracture system extends through porous zones (14,760 and 14,770 ft), to just below the log breaks at 14,778 ft, as shown by the separation between the dual laterolog curves. The microlog and phasor induction logs included here were not normally used at Wilburton.

The microlog is recommended for areas where matrix porosity is expected, as it assists in distinguishing between ineffective porosity in very fine-grained, intercrystalline, argillaceous dolomites and the effective porosity in coarser grained carbonates. For example, see the mud cake and corresponding resistivity-curve separation in even the low-porosity zone shown in Figure 14A.

The microlog has also proved useful in highly fractured carbonates. Responses similar to those found in permeable sandstones are often observed. Usually these correspond to intervals so intensely fractured that one or more fractures are present, along with associated dissolution porosity, opposite the pad over most of the interval. Often mud cake is not apparent, but it may exist within the formation in the fractures and vugs for the first few inches from the borehole wall.

Another example of this microlog response can be found in the paper by Latham (1970), which shows the type logs for the Brown zone. This "sandstone-like" appearance is a common characteristic of the Brown zone in many areas.

The phasor induction log overcomes the reduction in resistivity caused by conductive mud-filled open vertical fractures on the laterologs, including the LL8 and SFL types. In open vertical fractured intervals, the reduction in resistivity can be so large that the separation between the laterologs makes it apparent that the deep-investigation laterolog departs substantially from true resistivity. The induction logs are much less affected by vertical conductive fractures, and commonly they more accurately approximate true resistivity. However, induction-log accuracy is limited in resistivities above ~200 ohm-meters. The phasor induction appears to improve this accuracy somewhat. If the laterolog and induction logs agree in low resistivities, the cause of this low resistivity is not likely to be open vertical fractures.

Figure 14B shows a CIBIL borehole image of an open vertical fracture that appears to project upward into patterns of small vugs concentrated at the same depths that are indicated to be porous on standard porosity logs in Figure 14A.

Figure 14C continues uphole the CIBIL borehole image of Figure 14B, and indicates that the pore types in the 14,760- and 14,770-ft porous intervals are small vugs, apparently related to the fracture system.

Figure 14D is an enlarged CIBIL borehole image show-

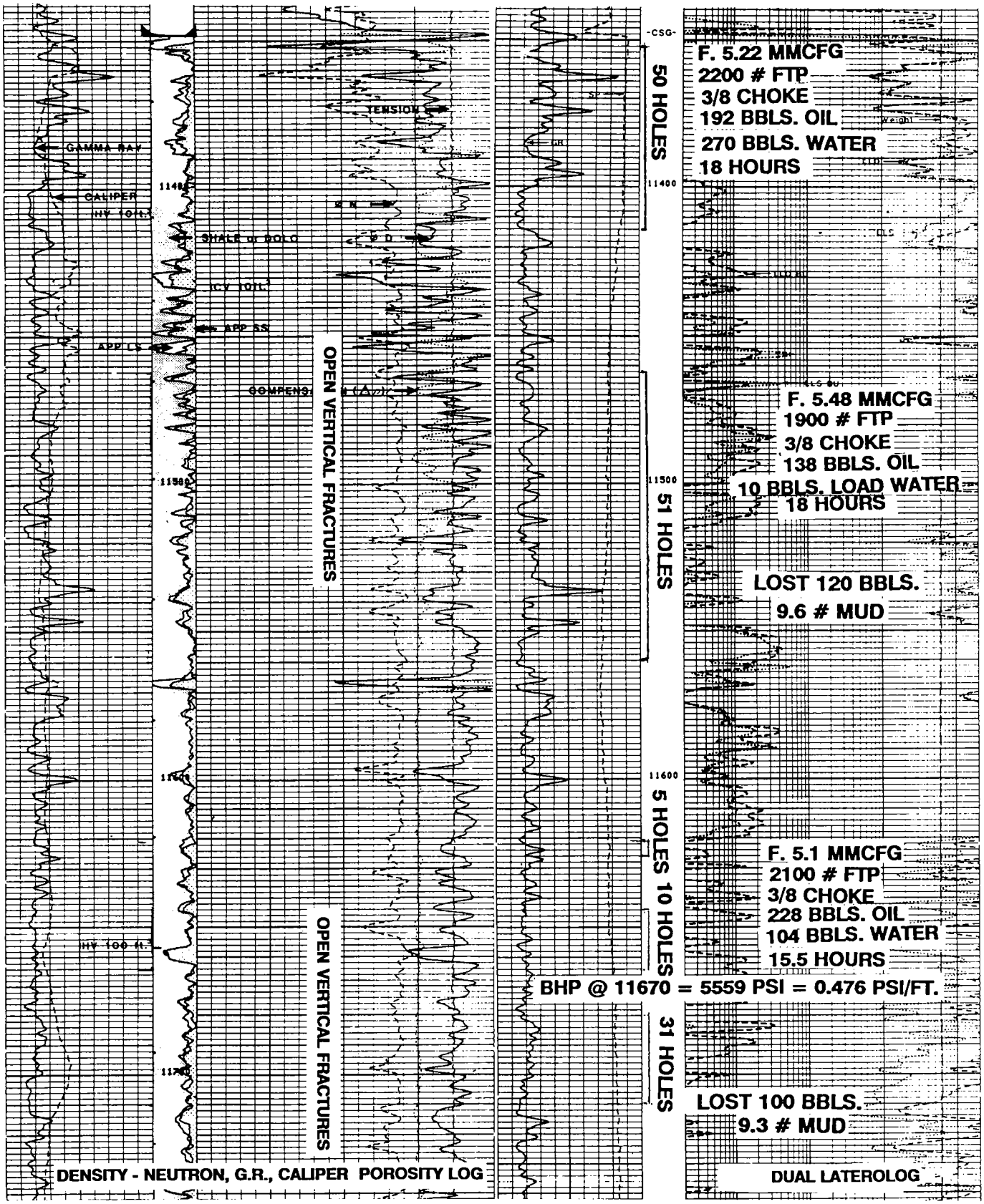


Figure 10. Logs through pay zone in Arbuckle discovery well at N.E. Alden Field, Caddo County, Oklahoma: Home-Stake Royalty No. 1-1 Susie Pi-Hoodle (sec. 1, T6N, R13W). This portion of the Arbuckle is predominantly fractured dolomite, with minor matrix porosity targeted by the lower group of perforations (11,622–11,710 ft). Each of three perforation groups tested in excess of 5 million CFGPD, with several hundred bbl of oil per day and some water.

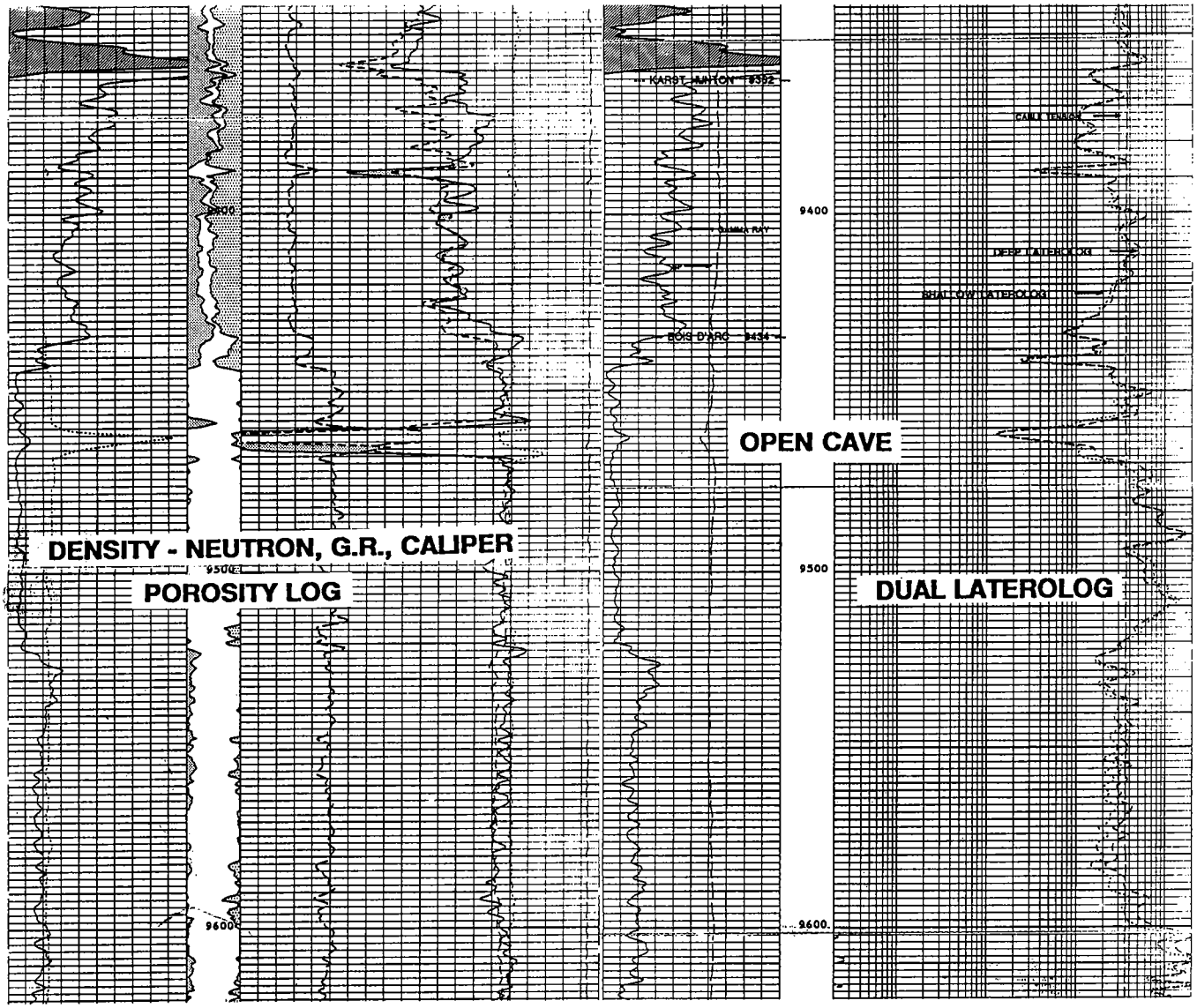


Figure 11. Logs through karstic Hunton interval in the Home-Stake Royalty No. 1-8 Harris Trust, sec. 8, T6N, R12W, Caddo County. Correlation with nearby wells shows variation due to dissolution and collapse. An open cave, centered at 9,462 ft, is indicated by the logs. Figure 12 shows a borehole image of the cave.

ing details of the vuggy porosity along a pattern that parallels the fractures below.

CONCLUSIONS

Extensive core data were used to develop log-interpretation techniques for modern logs which detect open fracture systems and define lithology and pore types.

Cores provide an opportunity to develop a better understanding of log responses, particularly for modern high-resolution and borehole-imaging type logs which approach the detail given by whole cores. With this understanding, modern logs can be applied to larger-scale intervals, wells, fields, and basins, to provide detailed comparisons of a given rock sequence, such as the Arbuckle Group.

The Arbuckle is highly variable. The lithology is pervasively dolomite at Wilburton field, and there are no anhydrite beds. The pay zones are generally found within two well-defined stratigraphic intervals: one interval that is 50–150 ft from the top (West Spring Creek) and has significant matrix porosity; and at scattered intervals, 300–650 ft from the top (Kindblade Brown zone?), which are karstic and fractured with large vugs associated with the fractures. Other karstic intervals are extensively cemented and have little reservoir quality.

Elevated temperature gradients within the Arbuckle Group, accompanied by some mineralization, suggest that warm, basinal waters moved upward through extensive vertical fracture systems which open with depth.

At N.E. Alden field, anhydrite and argillaceous carbonates characterize the upper Arbuckle. Pay zones are scattered well down into the Arbuckle in fractured dolomites with minor matrix porosity. The dolomites are between thick limestones which may be fractured, but are healed.

Elsewhere, pay zones occur ≥1,000 ft down into the Arbuckle, as, for example, in the Brown zone. Many wells were not drilled far enough into the Arbuckle to evaluate this important potential pay.

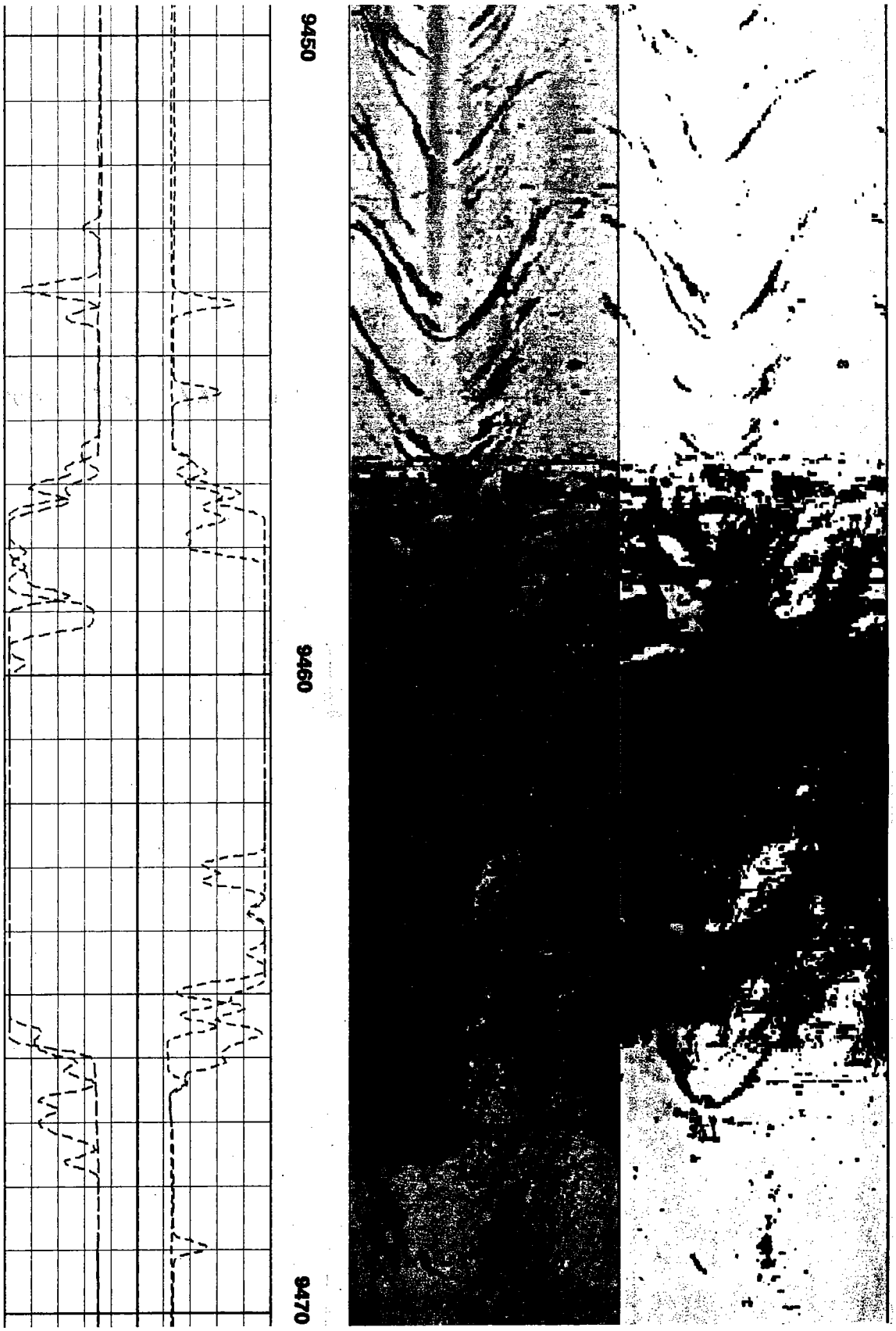


Figure 12. CIBIL borehole image of cave shown on standard logs in Figure 11. Note dissolution along fractures in the roof of the cave and irregularity of floor, suggesting collapsed breccia.

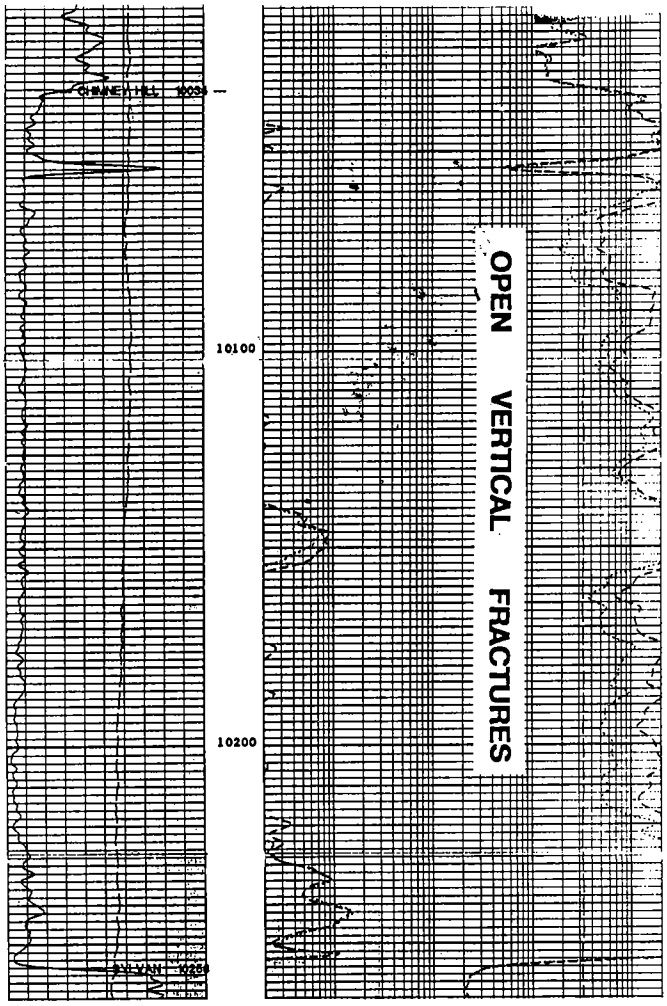


Figure 13A. A DLL log on the standard 5 in./100 ft depth scale showing an open vertical system in the Chimney Hill (Hunton Group) in the Home-Stake Royalty No. 1-8 Harris Trust.

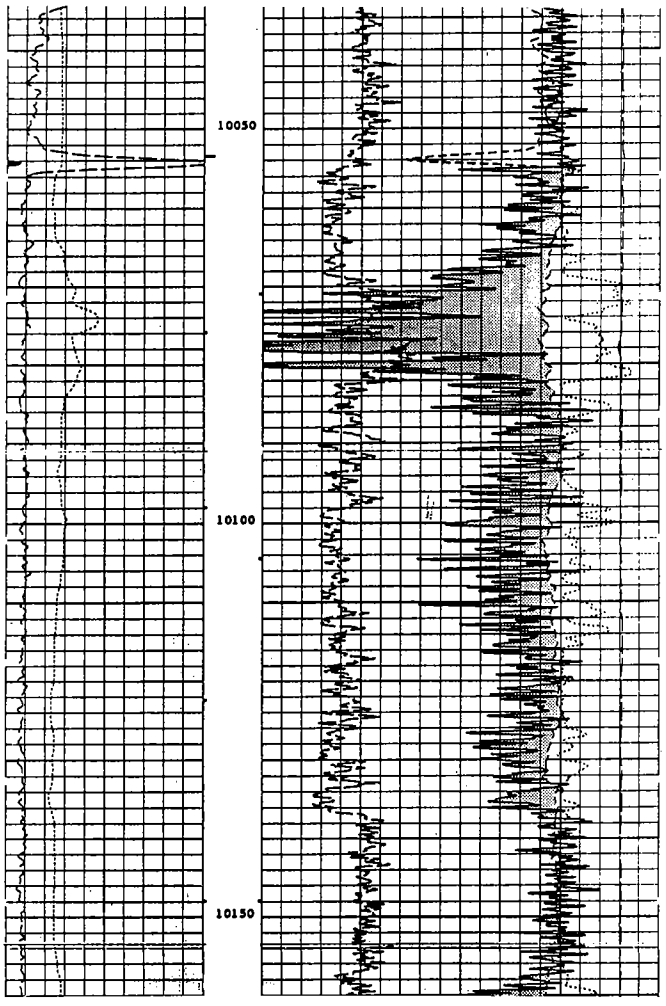


Figure 13B. A high-resolution porosity log on a 10 in./100 ft depth scale over a portion of the fractured interval shown in Figure 13A.

SELECTED REFERENCES

Burgess, W. J., 1964, Stratigraphic dolomitization in Arbuckle rocks in Oklahoma, *in* McHugh, J. W. (ed.), Symposium on the Arbuckle: Tulsa Geological Society Digest, v. 32, p. 45–48.

_____1968, Carbonate paleoenvironments in the Arbuckle Group West Spring Creek Formation, Lower Ordovician, in Oklahoma: Columbia University unpublished Ph.D. thesis, 91 p.

Harrison, W. E.; and Routh, D. L., 1981, Reservoir and fluid characteristics of selected oil fields in Oklahoma: Oklahoma Geological Survey Special Publication 81-1, p. 176–177.

Hook, R. C., 1991, Recent developments at Wilburton field, Latimer County, Oklahoma, *in* Johnson, K. S. (ed.), Late Cambrian–Ordovician geology of the southern Midcontinent, 1989 symposium: Oklahoma Geological Survey Circular 92, p. 65.

Kerans, Charles, 1988, Karst-controlled reservoir heterogeneity in Ellenburger Group carbonates of West Texas: American Association Petroleum Geologists Bulletin, v. 72, p. 1160–1183.

Latham, J. W., 1970, Petroleum geology of the Healdton field, Carter County, Oklahoma: American Association of Petroleum Geologists Memoir 14, p. 255–276. [Also published in American Association of Petroleum Geologists Bulletin, v. 52, p. 3–20.]

Lynch, M. T., 1989, Evidence of paleokarstification and burial diagenesis in the Arbuckle Group of Oklahoma: Oklahoma State University unpublished M.S. thesis, 163 p.

Lynch, M. T.; and Al-Shaieb, Z., 1989, Evidence of paleokarstic phenomena and burial diagenesis in the Ordovician Arbuckle Group of Oklahoma: Transactions of American Association of Petroleum Geologists, Mid-Continent Section Meeting, Oklahoma City Geological Society.

Mescher, P. K.; Schultz, D. J.; Hendrick, S. J.; Ward, M. A.; and Schwarz, J. A., 1991, Geology and reservoir development of the Arbuckle dolomite, Wilburton field, Latimer Co., Oklahoma [abstract]: Oklahoma Geological Survey, Petroleum-reservoir geology in the southern Midcontinent—a workshop, March 26–27, 1991, Norman, p. 29.

Serra, O., 1989, Sedimentary environments from wireline logs [2nd edition]: Schlumberger, p. 199–211.

Waddell, R. T.; Liu, H.; and Forgotson, J. M., Jr., 1991, The influence of depositional facies and karst development on the Arbuckle Brown zone reservoir, Healton field, Carter County, Oklahoma [abstract]: Oklahoma Geological Survey, Petroleum-reservoir geology in the southern Midcontinent—a workshop, March 26–27, 1991, Norman, p. 15, 33.

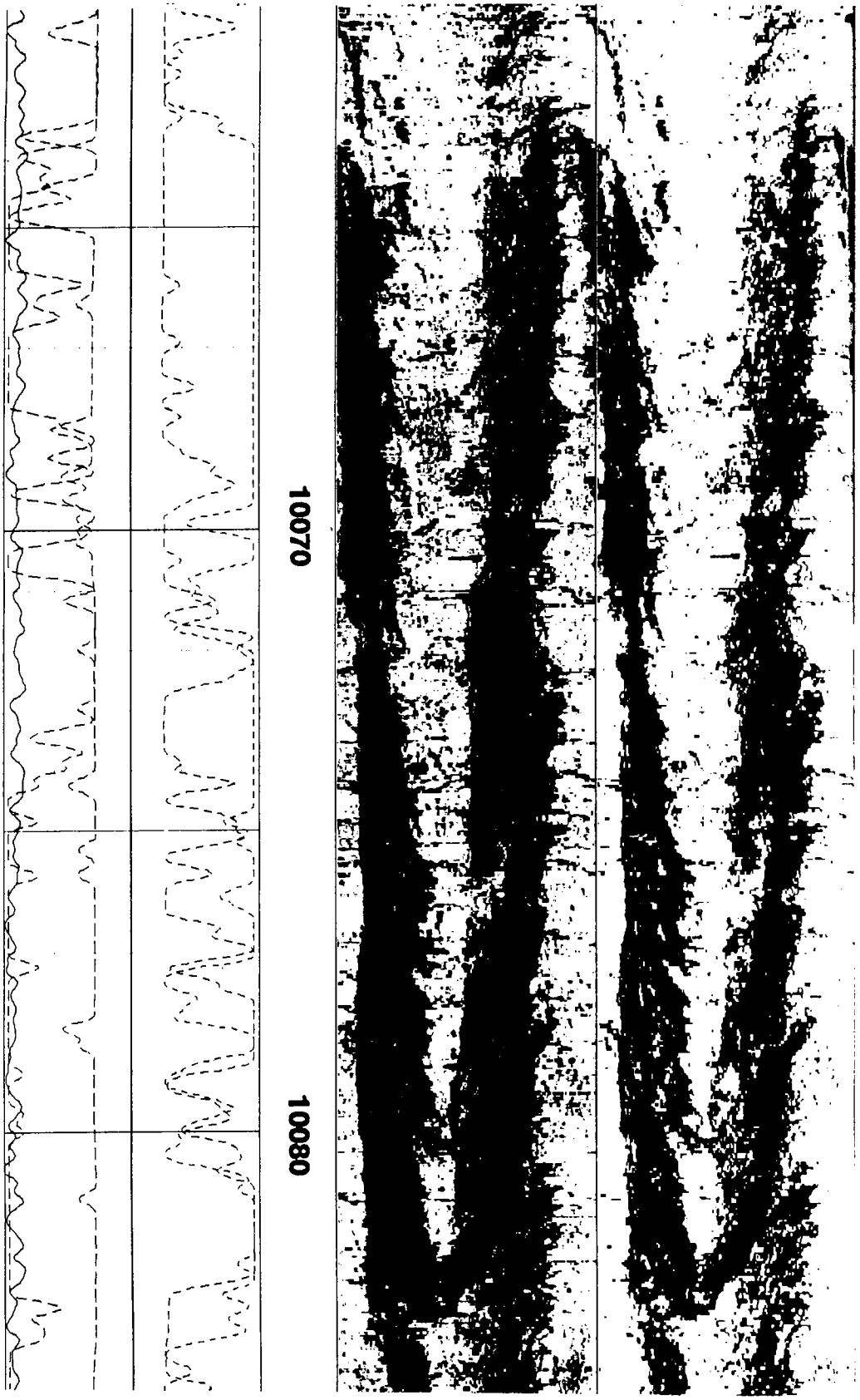


Figure 13C. CIBIL borehole image of fractured interval shown in Figures 13A,B. Facies changes appear to interrupt the continuity of the fractures. Fractures may terminate due to release of stress, or may penetrate (and terminate in) argillaceous laminations.

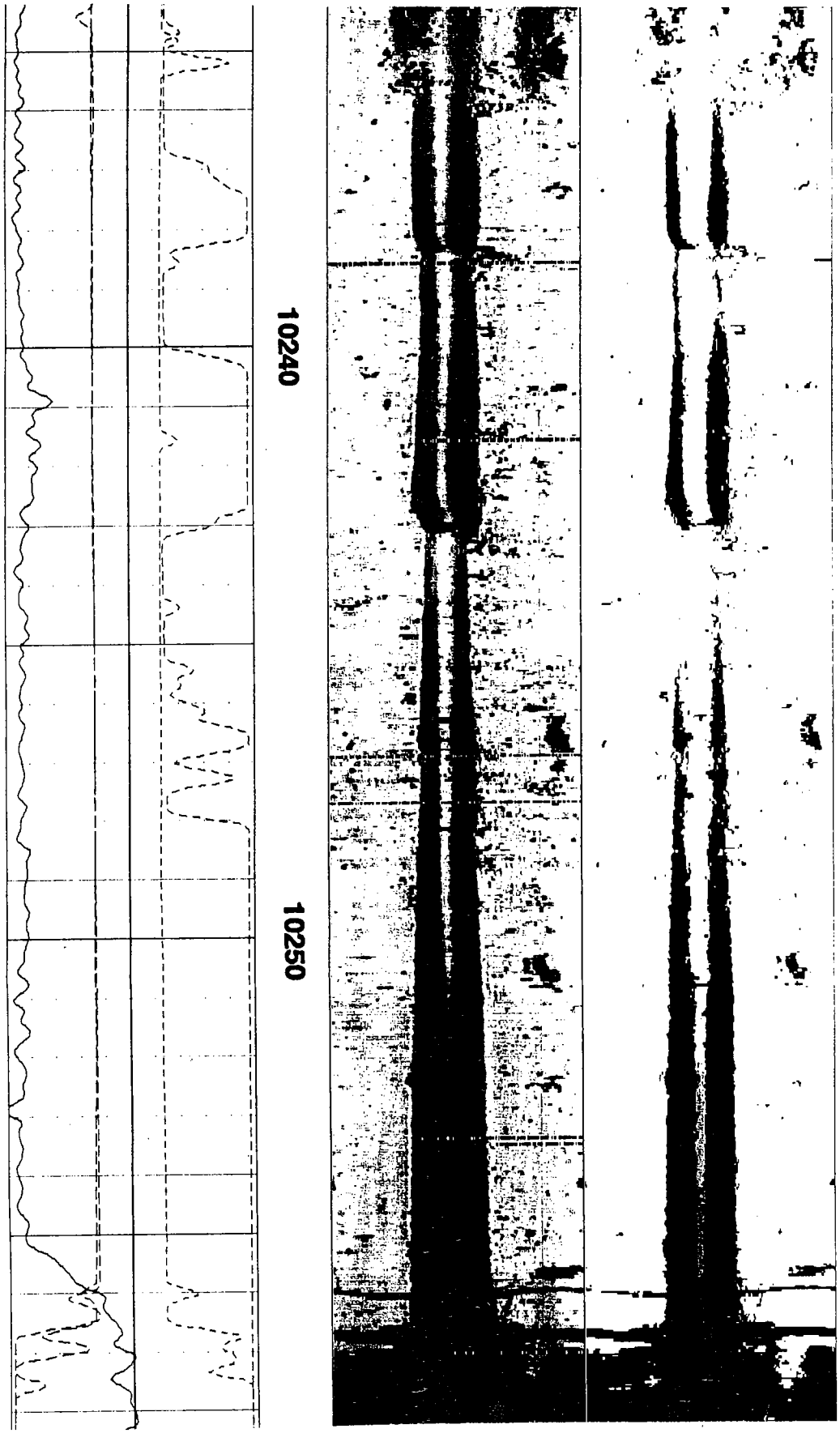


Figure 13D. CIBIL borehole image of Chimney Hill (lower) portion of Hunton shown in Figure 13A. Note notches worn in south side of hole above base of Hunton. Top of Sylvan Shale is at 10,257 ft. Notches near 10,240 ft may have been worn during slow drilling through the Sylvan Shale.

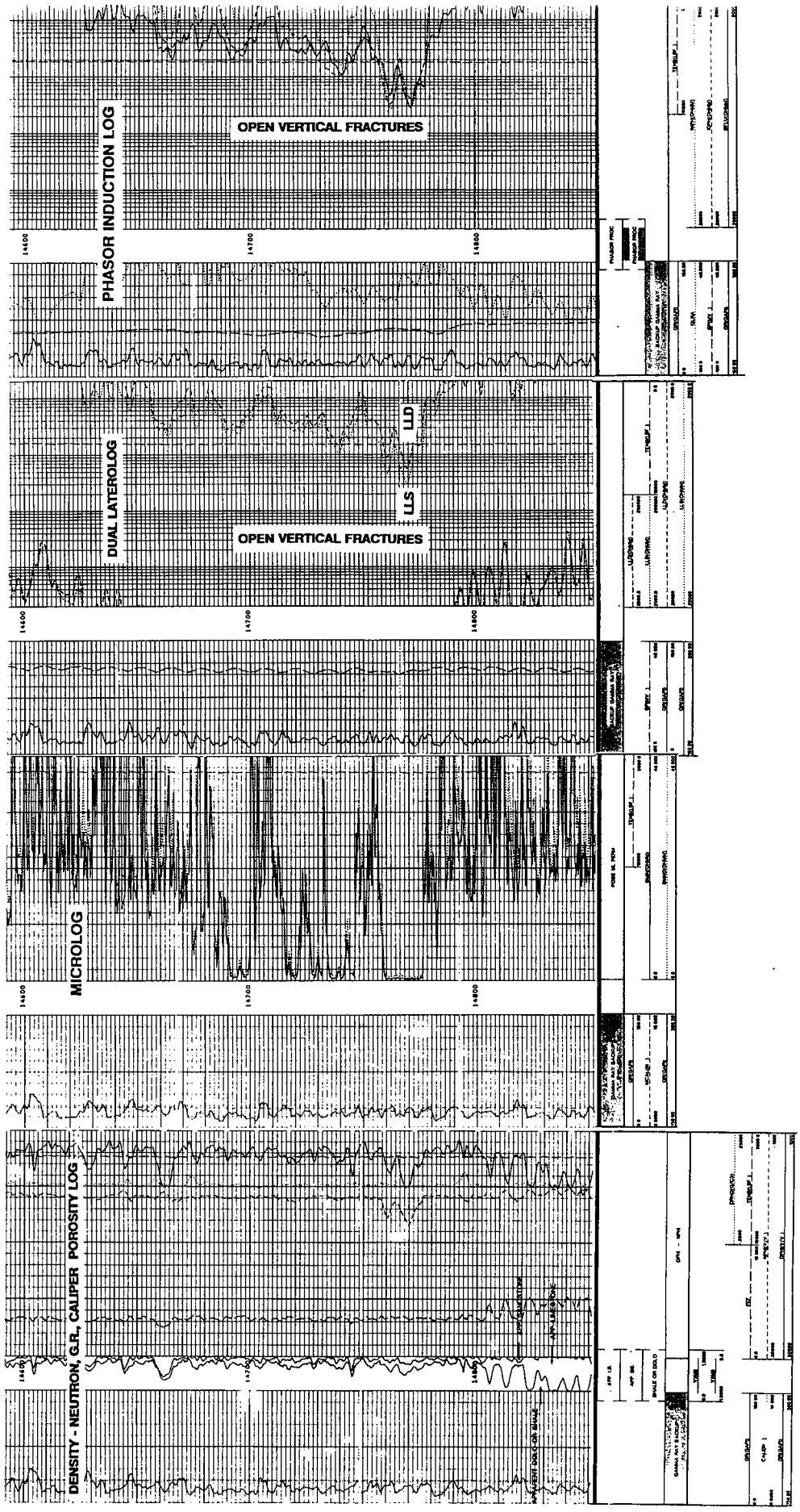


Figure 14A. Montage of standard logs (gamma ray, density-neutron, microlog, dual laterolog, and induction phasor from left to right) over one of few intervals with matrix porosity in dolomite in the Arbuckle at N.E. Alden field; Home-Stake Royalty No. 1-8 Harris Trust, sec. 8, T6N, R12W, Caddo County. Porous intervals are centered at 14,760 and 14,770 ft. An open vertical fracture system extends down through the porous zones to just below the log breaks at 14,778 ft.

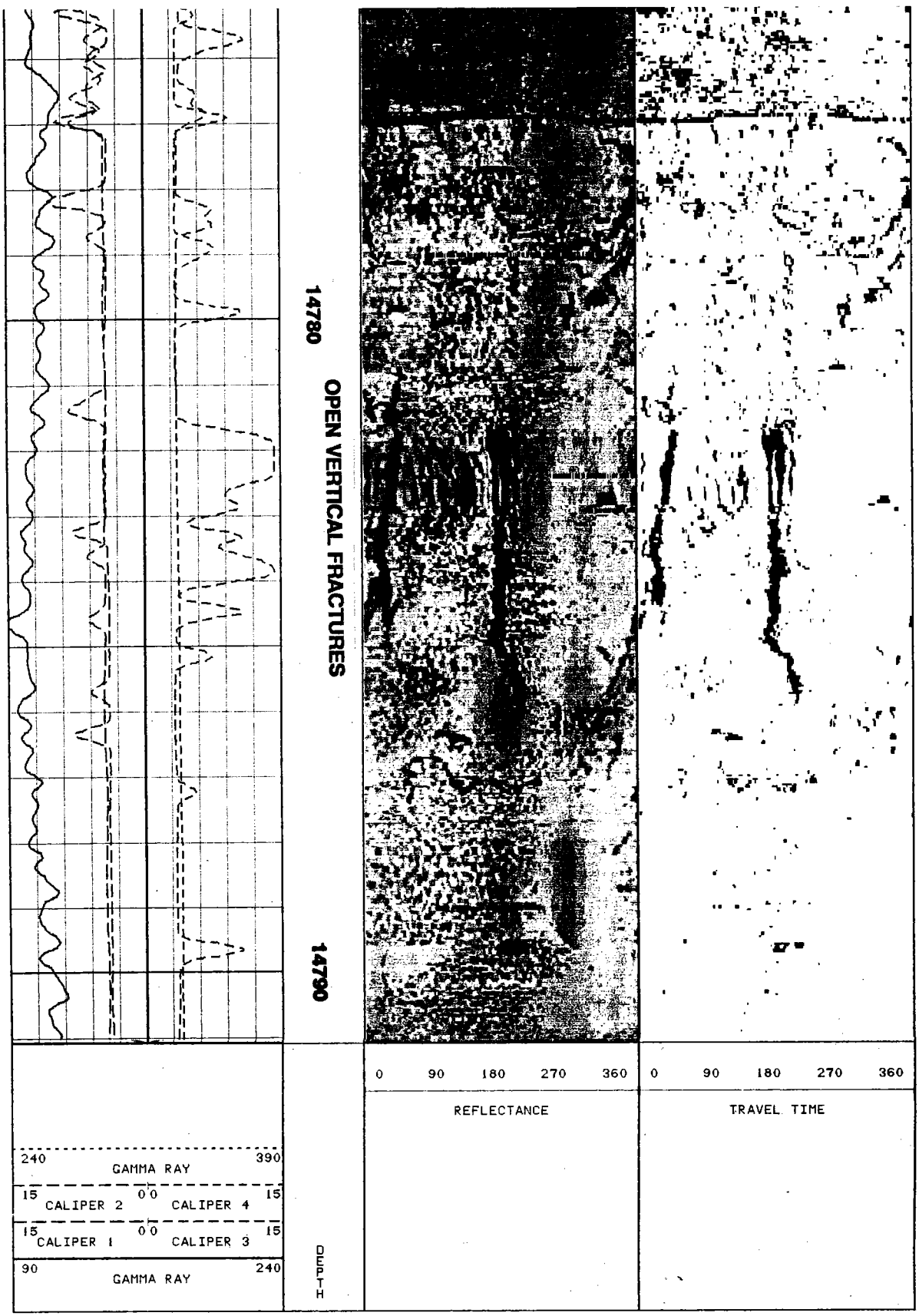


Figure 14B. CIBIL borehole image showing an open vertical fracture that appears to project upward into patterns of small vugs concentrated at the same depths that are indicated to be porous on standard porosity logs in Figure 14A.

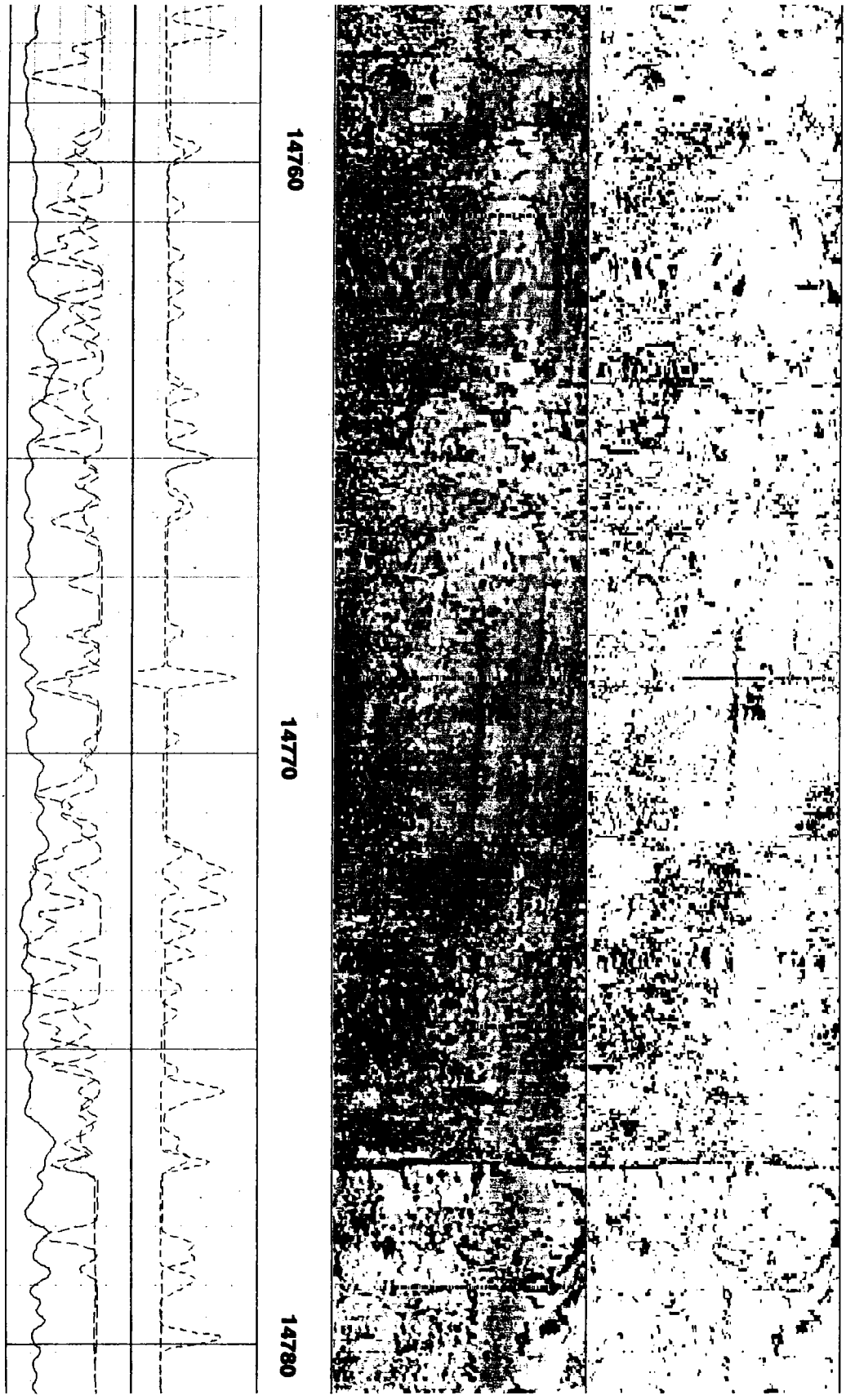


Figure 14C. CIBIL borehole image showing that the pore types in the 14,760- and 14,770-ft porous intervals are small vugs, apparently related to the fracture system; same well as in Figure 14A.

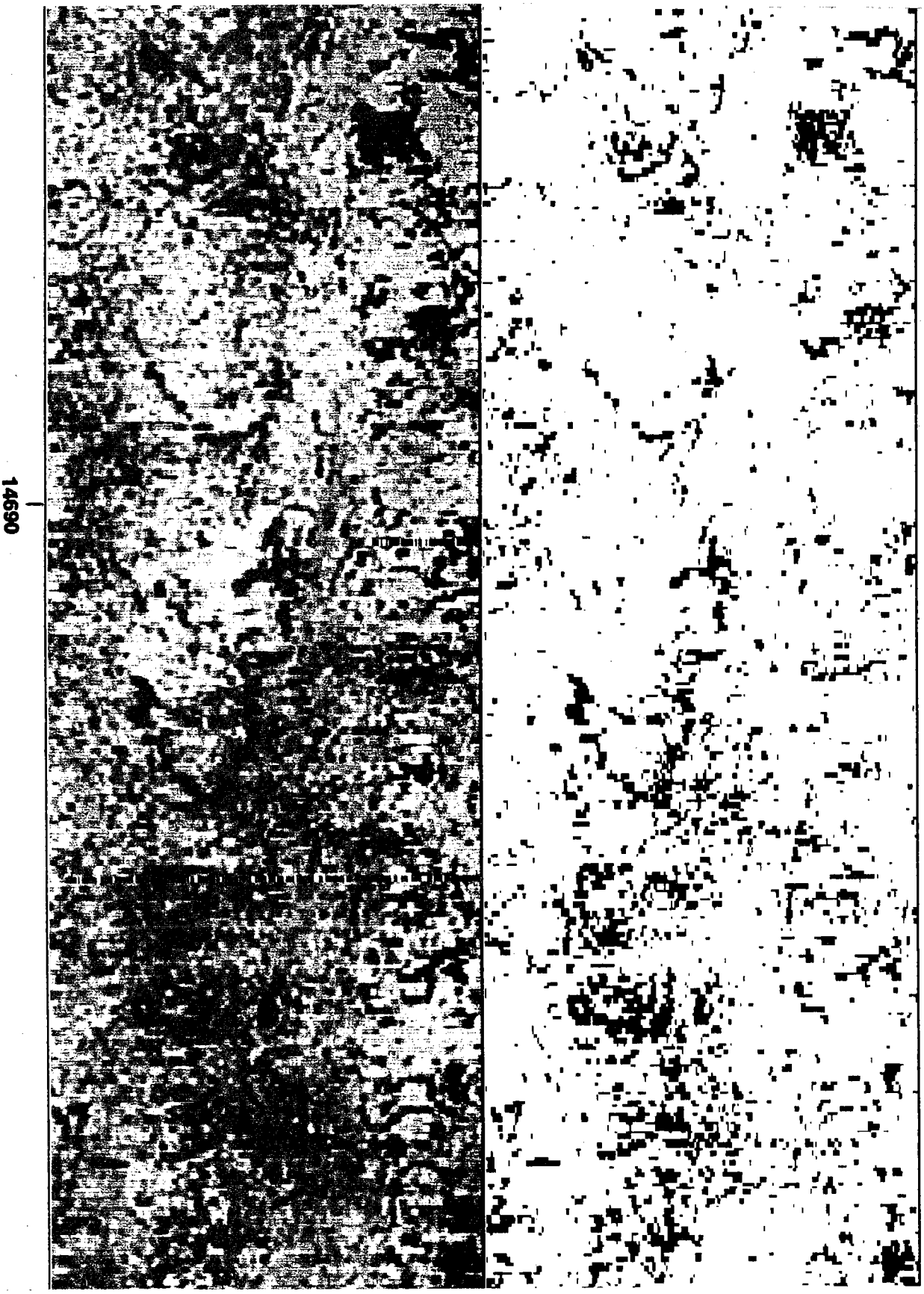


Figure 14D. Enlarged CIBIL borehole image showing details of the vuggy porosity along a pattern that parallels the fractures below; same well as in Figure 14A.

The Arbuckle Group—Relationship of Core and Outcrop Analyses to Cyclic Stratigraphy and Correlation

James Lee Wilson, Richard D. Fritz, and Patrick L. Medlock
MASERA Corp., Tulsa

ABSTRACT.—Correlation of ramp-type carbonates is possible with an understanding of depositional environments and related sequences and boundaries. Hopefully, subtle relationship of facies to log character can be used to develop not only local correlations but regional correlations as well.

Lower Paleozoic carbonates such as the Arbuckle Group, which are dominated by ramp-type peritidal facies, can be subdivided into depositional sequences, and further into parasequences which are commonly in some form of the following upward-shoaling order of facies: open marine—subtidal—intertidal—supratidal. Researchers have usually related these subdivisions to subsidence and eustatic sea-level changes. Episodic tectonic activity has been assumed to be negligible on such broad and stable shelves.

Recognition of carbonate-log response is usually a function of recognizing relatively "clean" and "dirty" facies. In the Arbuckle, the relationship of facies to log response is not always clear, because the facies tend to be restricted to upper subtidal and intertidal environments that do not always show a marked change in clastic input. In many areas, pervasive dolomitization of all facies masks the original textures and the resulting log characters. In general, within the Arbuckle, siliciclastic content is usually greater in the intertidal facies, with concentrated siliciclastic intervals represented by high gamma-ray deflections which are useful in correlation.

Once the relationship of facies to log response is established, parasequences or parasequence sets can be correlated locally, and sequences, bracketed by third-order or eustatic sea-level change, can be correlated regionally. Sequence grouping in the Arbuckle can be effected by use of Fischer diagrams following the lead of other recent studies of Cambro–Ordovician strata in the Appalachians and West Texas.

INTRODUCTION

The Cambro–Ordovician Arbuckle Group was deposited on an extremely broad shallow platform, often referred to as the "Great American Bank," which includes the strata of the Ellenburger Group in the Permian basin, the El Paso Group in extreme southwestern Texas, and the Knox Group in the Appalachian uplift and Black Warrior basin (Fig. 1). These carbonates have recently had a resurgence in exploration activity due to significant oil and gas discoveries in Oklahoma. The enormous thickness of the Arbuckle Group, especially in southern Oklahoma (>8,000 ft) has led to a great many misunderstandings about Arbuckle stratigraphy and reservoir development. The purpose of this paper is to show that, even though structure is a key element in evaluating Arbuckle potential, depositional and stratigraphic relationships must also be understood for exploration and exploitation.

STRATIGRAPHY

The Arbuckle Group can be divided into five primary formations throughout most of Oklahoma and Arkansas. These are, in ascending order, the (1) Fort Sill Limestone, (2) Signal Mountain Formation, (3) McKenzie Hill Formation, (4) Cool Creek Formation, (5) Kindblade Formation, and (6) West Spring Creek Formation (Fig. 2). The Cambro–Ordovician boundary is located in the uppermost part of the Signal Mountain Formation, and the Lower Ordovician–Middle Ordovician boundary is located in the uppermost part of the West Spring Creek Formation (Derby and others, 1991).

In southern Oklahoma, there are several additional zones which are defined and correlated by dolomitization patterns: these are the Royer Dolomite below the Signal Mountain Formation, the Butterly Dolomite below the McKenzie Hill Formation, the Brown zone at the top of the Kindblade Formation, and the Wade and Bray zones within the West Spring Creek Formation. Some sandstones are also important stratigraphic markers, such as the Thatcher Creek Member at the base of the Cool Creek Formation in southern Oklahoma and the Wichita Mountains, and the Gunter Sandstone at the top of the Signal Mountain Formation in the Arkoma basin.

The Arbuckle Group ranges in thickness from <3,000 ft in the Arkoma and Anadarko basins, where it is dominantly dolomite, to >8,000 ft in southern Oklahoma, where it is dominantly limestone.

DEPOSITIONAL SEQUENCES

Deposition of the Arbuckle Group on the platform was dominated by ramp-type peritidal carbonates which can be subdivided into cycles based on facies type and depositional patterns. Researchers have usually related these subdivisions to eustatic sea-level changes, and within the Arbuckle Group there are three types of cycles present (Fig. 3). The building blocks of sequence stratigraphy are parasequences, which are defined as a relatively conformable successions of genetically related, usually upward-shoaling beds that are bounded by marine-flooding surfaces. Parasequences have further been defined as fourth-order and in some cases fifth-order cycles that

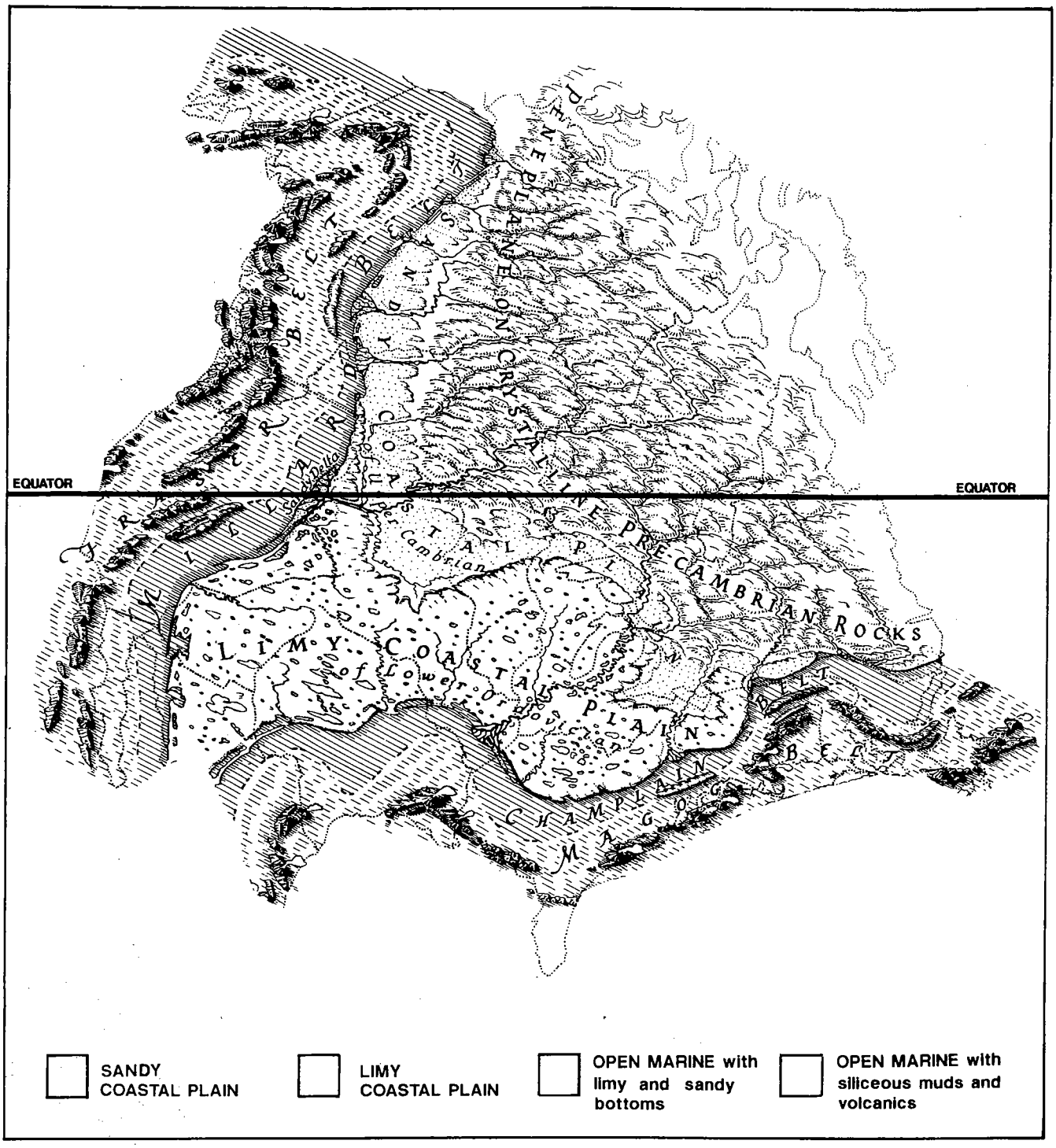


Figure 1. Paleogeography of early Middle Ordovician (modified from Kay, 1951).

have durations of 10–100 ka (thousand years); unless otherwise designated, a parasequence is also herein referred to as a cycle, for simplicity. So-called third-order cycles have durations of 1–10 m.y. (million years), and are thought to be caused by global events such as sea-floor spreading. Parasequences, or a parasequence set (bundling of fourth-order cycles), are thought to be related to Milankovitch orbital perturbations; however, there are numerous events that can also cause sea-level changes, such as tectonic activity, magnitude and frequency of subsidence, sedimentation rate, and depositional processes.

Examination of core and outcrop data in the Arbuckle Group, as well as Knox and Ellenburger carbonates, indicates that parasequences are commonly in some form of the following upward-shoaling order of facies: open marine—subtidal—intertidal—supratidal (Fig. 4). Plates 1–3 are Arbuckle cores (except Plate 1, which also con-

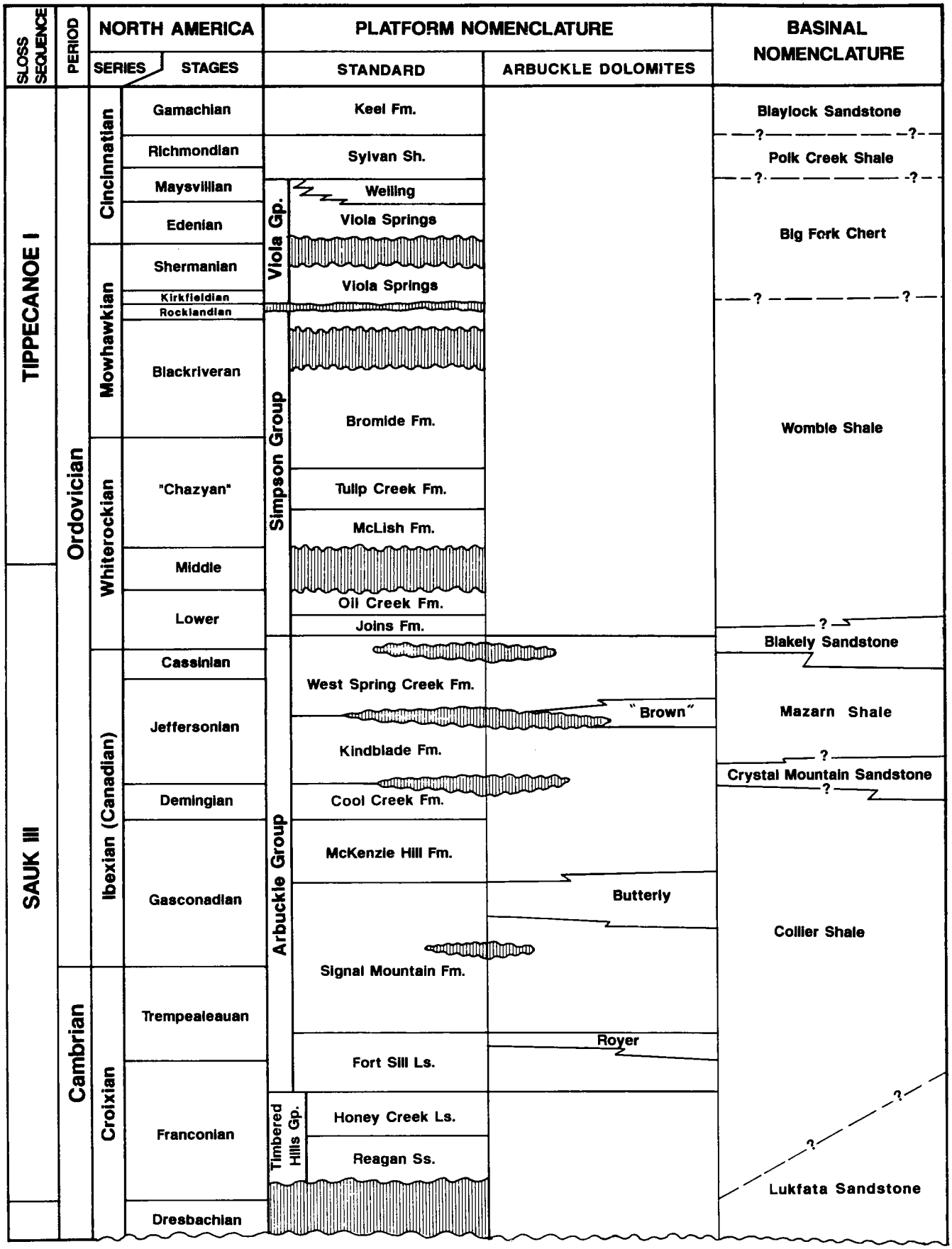


Figure 2. Stratigraphic correlation chart (after Derby and others, 1991).

CYCLE ORDER	TIME SCALE		SEQUENCE STRATIGRAPHY	CYCLE FREQUENCY IN ARBUCKLE GROUP
	Chronostratigraphic	My		
1	ERATHEM SYSTEM	200+ >60	MEGASEQUENCE SUPERSEQUENCE SET (Sloss)	<1
2	SERIES STAGE	30 10-20	SUPERSEQUENCE	<1
3	BIOZONE (GROUPS)	1-10	DEPOSITIONAL SEQUENCE (Vail)	3 1/2 - 4 1/2
4	(FORMATIONS) (MEMBERS)	.1-.01	PARASEQUENCE	>400
5		.01-.001	BED	400X?

Figure 3. Chart showing relationship of cycles to time and stratigraphic sequences.

tains Joins Formation) that illustrate depositional facies, facies boundaries, and parasequence boundaries. Open-marine facies are argillaceous to "marly" limestone; fossil fragments generally are intact. Within the Arbuckle Group, open-marine facies have not been recognized; however, in other Paleozoic carbonates, such as the Hunton Group, this facies is relatively common. Subtidal facies are usually bioturbated, although shoals of bioclastic and oolitic material also are present in the subtidal facies (Fig. 4). Upper subtidal/lower intertidal is a further facies subdivision that can be dolomitized that and preferentially develops porosity. The intertidal facies normally consists of millimeter-scale laminations; within the Arbuckle, stromatolites are common in this facies (Fig. 4). Supratidal facies uncommon to either group occur more frequently in the Arbuckle. Thin laminae of anhydrite, desiccation features, and fenestral features are characteristic of the supratidal facies.

SEQUENCE CORRELATIONS

Correlation of platform and ramp-type carbonates is possible with an understanding of depositional environment and related sequences and boundaries. Usually, correlation of individual parasequences can only be made locally. Bundles of fourth- to fifth-order cycles or parasequence sets can be recognized intra-regionally, using well-log data. Third-order cycles can be correlated regionally and even inter-regionally using logs and Fischer plots.

Recognition of sequence boundaries is crucial in recognition and correlation of cycles. Sequence boundaries are usually associated with subaerial exposure and can be identified by lithologic and/or facies changes, and sometimes by paleokarst. Breccias often form along third-order cycle boundaries, which are represented by disconformities or low-angle angular unconformities. Syndepositional breccias, especially, can be correlated locally, or in some cases sub-regionally along sequence boundaries. An example may be the Brown zone within the Arbuckle Group near the top of the Kindblade Formation (Fig. 5).

Rock vs. Log Response

Subtle relationships of facies to log character can be used to develop gamma-ray and resistivity profiles of a parasequence. For example, most upper subtidal facies are relatively clean, due to the high-energy conditions in which they were deposited, and the resulting log response is often represented by clean gamma ray and high resistivity. Conversely, siliciclastic content is usually greater in the intertidal and supratidal facies, in the form of dispersed windblown clay, silt, and very fine sand which develop relatively dirty gamma-ray and lower resistivity responses than subtidal facies (Fig. 6). Sometimes sand, silt, and clay are concentrated in shallow tidal channels, and these thin clastic intervals cause high gamma-ray deflections which are useful in correlations. However, some thick sands (Thatcher and Gunter) have a "clean" gamma-ray response. Black shaly dolomites,

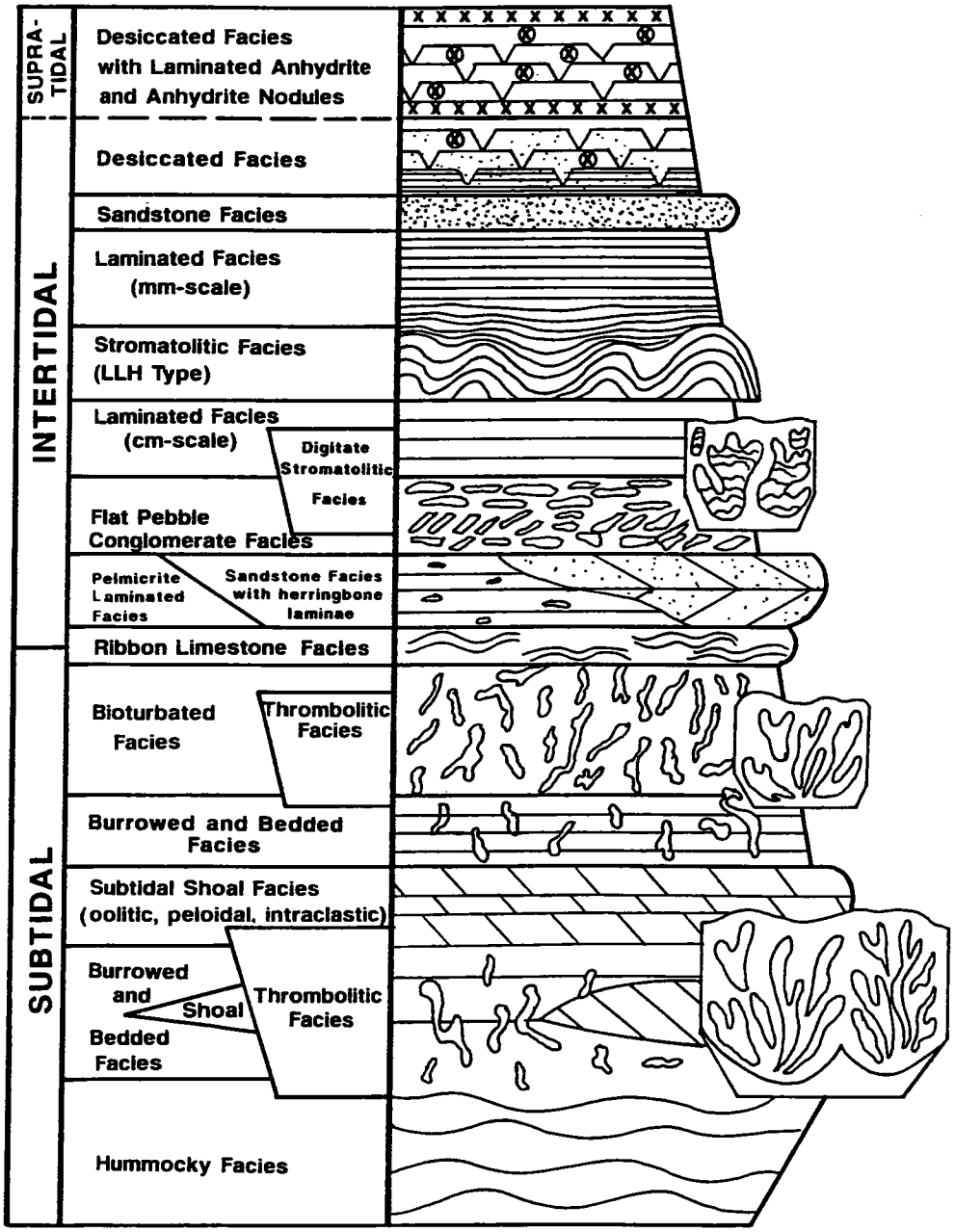


Figure 4. Typical shallowing upward cycle of the Arbuckle Group.

such as those present in the Pan American Tackett core, are important and can be correlated from southern Oklahoma into the Arkoma basin.

The relationship of facies to log response is not always clear, due to the fact that parasequences are not always complete and in some cases there is not a marked change in clastic input between upper subtidal and intertidal environments. Also, in many areas, pervasive dolomitization of all facies masks the original textures and the resulting log characters.

Fischer Plots

Overall transgressive and regressive episodes can be recognized, and sequence boundaries can be further defined by the use of Fischer (accommodation) diagrams (plots of cycle thickness vs. time, assuming linear subsidence). Inter-regional correlations of Arbuckle sequences can then be made by comparison of Fischer diagrams to similar plots made in studies of Cambro–Ordovician strata in the Appalachians and West Texas (Fig. 7).

Within the Arbuckle Group, 3.5 to 4.5 third-order cycles are recognized, based on log analysis and Fischer plots. The total number of parasequences is between 350 and 450. Thickness of individual cycles ranges from 1 ft to >100 ft, which has been confirmed by Lindsay and Koskelin (1991). Average time duration of each cycle is ~40 ka; however, this number can vary significantly, especially between subtidally dominated cycles to intertidally dominated cycles.

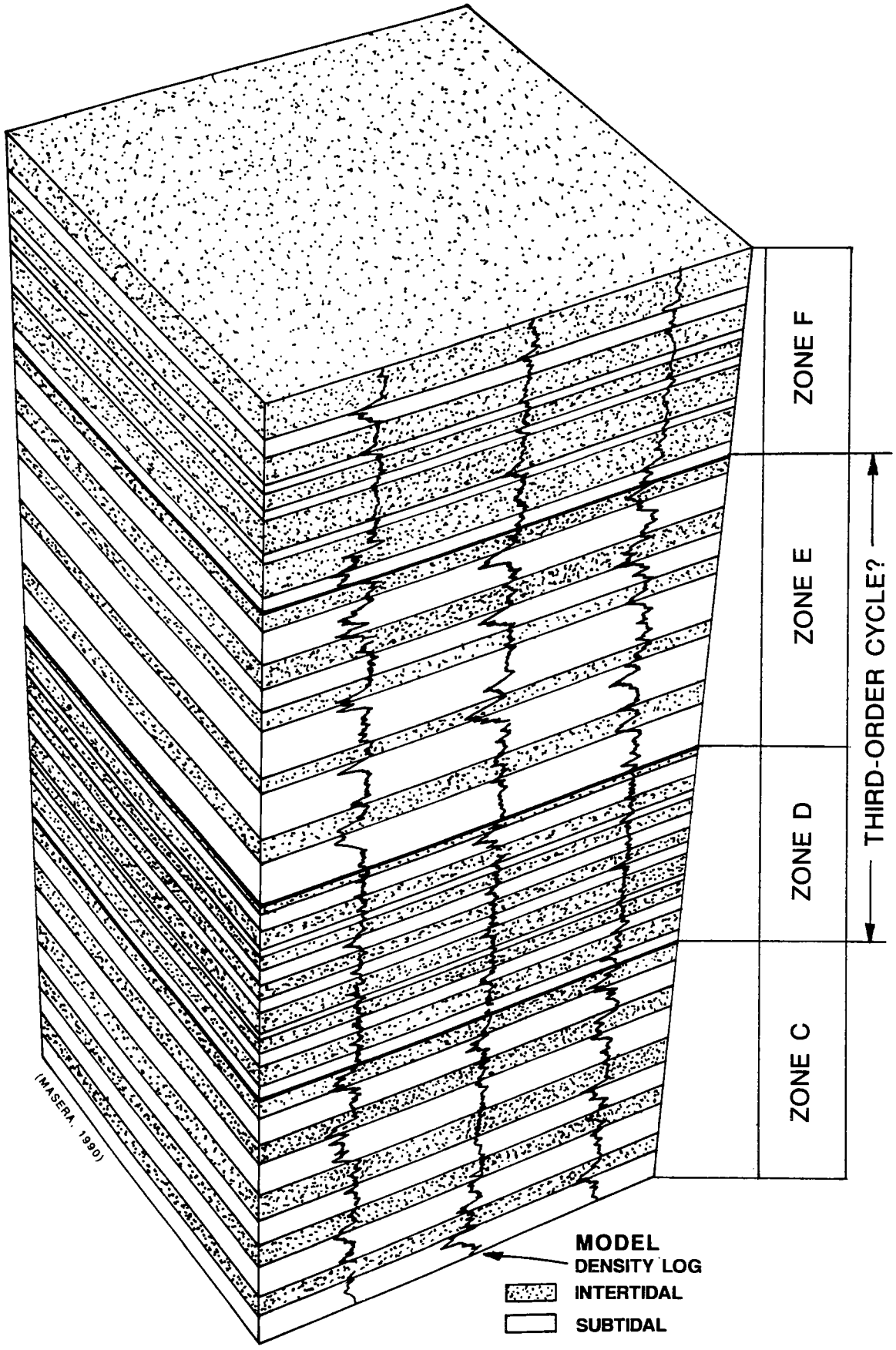


Figure 5. Block model showing typical parasequence types with the Arbuckle Group.

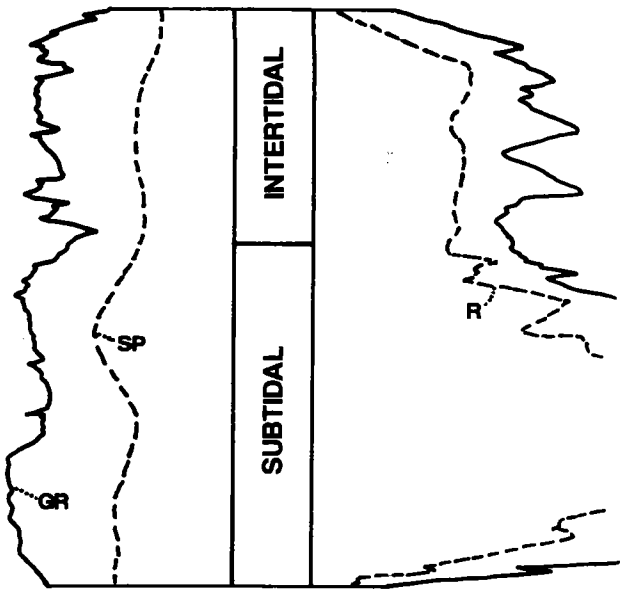


Figure 6. Diagrammatic representation of log response to facies.

EXPLORATION CONSIDERATIONS

Finally, once local and regional correlations are established, production can be compared to core data, log correlations, and Fischer plots to establish the relationship of reservoir development to sequence boundaries and facies type. Reservoir development in the Arbuckle Group usually occurs within upper subtidal to lower intertidal sediments, and is further associated with subtidally dominated parasequence sets. Within the Arbuckle Group, these sets are often located just below sequence boundaries and can be affected by multiple karst episodes.

Although exploration for Arbuckle carbonates primarily involves seismic analysis of tectonic features, stratigraphic factors, especially sequence correlations, should be integrated with structural analyses in order to further define and recognize potential reservoirs.

SELECTED REFERENCES

Derby, J. R., 1969, Revision of Lower Ordovician–Middle Ordovician boundary in western Arbuckle Mountains, Oklahoma, *in* Ham, W. E. (ed.), Regional geology of the Arbuckle Mountains, Oklahoma: Oklahoma Geological Survey Guidebook 17, p. 35–37.

Derby, J. R.; Bauer, J. A.; Creath, W. B.; Dresbach, R. I.; Ethington, R. L.; Loch, J. D.; Stitt, J. H.; McHargue, T. R.; Miller, J. F.; Miller, M. A.; Repetski, J. E.; Sweet, W. C.; Taylor, J. F.; and Williams, Mark, 1991, Biostratigraphy of Timbered Hills, Arbuckle and Simpson Groups, Cambrian and Ordovician, Oklahoma: a review of correlation tools and techniques available to the explorationist, *in* Johnson, K. S. (ed.), Late Cambrian–Ordovician geology of the southern Midcontinent, 1989 symposium: Oklahoma Geological Survey Circular 92, p. 15–41.

Fay, R. O., 1989, Geology of the Arbuckle Mountains along Interstate 35, Carter and Murray Counties, Oklahoma: Oklahoma Geological Survey Guidebook 26, 50 p.

Fischer, A. G., 1964, Lofer cyclotherms of the Alpine Triassic, *in* Merriam, D. F. (ed.), Symposium on cyclic sedimentation: Geological Survey of Kansas Bulletin 169, p. 107–150.

Fischer, A. G.; Premoli Silva, I.; Anderson, R.; Berger, A. L.; Bottjer, D.; Cotillion, P.; Dean, W. E.; de Boer, P. L.; Erba, E.; Foucault, A.; Gardner, J.; Hinnou, L.; Loutre, M. F.; Matthews, M.; Melnyk, H.; Napoleone, G.; Paul, C. R. C.; Ricken, W.; Ripepe, M.; Roth, P. H.; Schwarzacher, W.; Smith, D.; and Strasser, G., 1988, Cyclostratigraphy: CRER (Coherent Cyclostratigraphy of the Cretaceous) Workshop 3, Perugia, Italy, 31 p.

Hardie, L. A.; Dunn, P. A.; and Goldhammer, R. K., 1991, Field and modeling studies of Cambrian carbonate cycles, Virginia Appalachians—discussion: Journal of Sedimentary Petrology, v. 61, p. 636–646.

Kay, G. M., 1951, North American geosynclines: Geological Society of America Memoir 48, 143 p.

Lindsay, R. F.; and Koskelin, K. M., 1991, Arbuckle group depositional parasequences, southern Oklahoma, *in* Johnson, K. S. (ed.), Late Cambrian–Ordovician geology of the southern Midcontinent, 1989 symposium: Oklahoma Geological Survey Circular 92, p. 71–84.

Milankovitch, M., 1941, Kanon der Erbestrahlung and seine Anwendung auf das Eiszeiten Problem: Akad. Royale Serbe 133, 633 p.

Read, J. F., 1989, Use of Fischer plots to define third-order sea level curves in Ordovician peritidal cyclic carbonates, Appalachians: Geology, v. 16, p. 895–899.

Read, J. F.; Grotzinger, J. P.; Bova, J. A.; and Koerschner, W. F., 1986, Models for generation of carbonate cycles: Geology, v. 14, p. 107–110.

Sloss, L. L., 1988, Forty years of sequence stratigraphy: Geological Society of America Bulletin, v. 100, p. 1661–1665.

Vail, P. R.; Mitchum, R. M., Jr.; and Thompson, S., III, 1977, Relative changes of sea level from coastal onlap, *in* Payton, C. E. (ed.), Seismic stratigraphy applications to hydrocarbon exploration: American Association of Petroleum Geologists Memoir 26, p. 63–82.

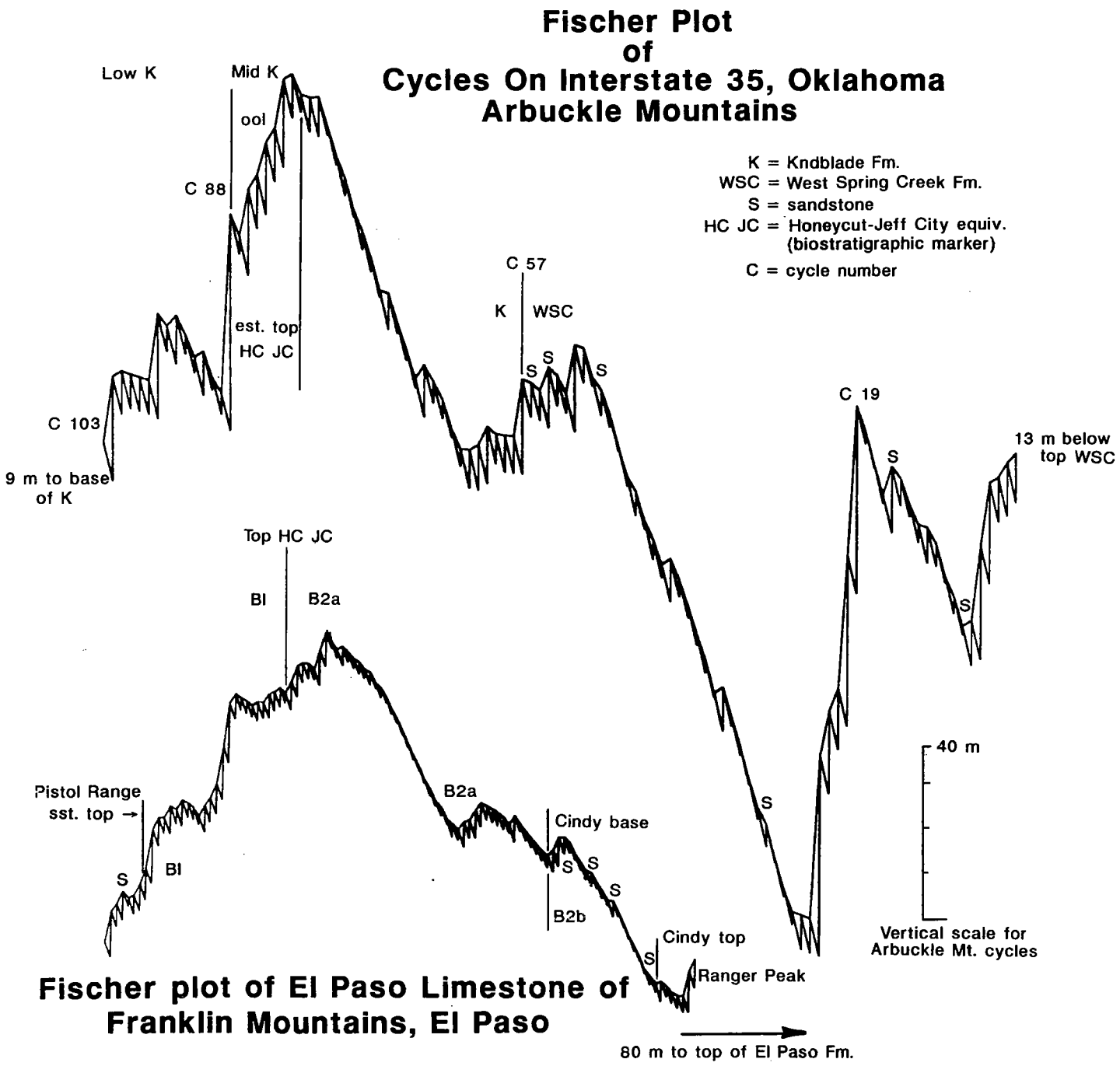


Figure 7. Fischer or accommodation plots of major segments of the Lower Ordovician from the El Paso outcrops and Arbuckle Mountains outcrops along I-35. The major third-order cycle of transgressive and progradation tidal flat and thick subtidal facies during the middle of the Lower Ordovician is obvious (Kindblade–Newala Formations). This is essentially equivalent to cycles with thick and somewhat massive subtidal units, which are widely traceable through the Great American Bank and represent approximately the sponge-algal biofacies of Alberstadt and Repetski as well as the zone of *Ceratopea*.



Plate 1. Union Texas Oil No. 1 Idema, 8,642–8,659 ft.

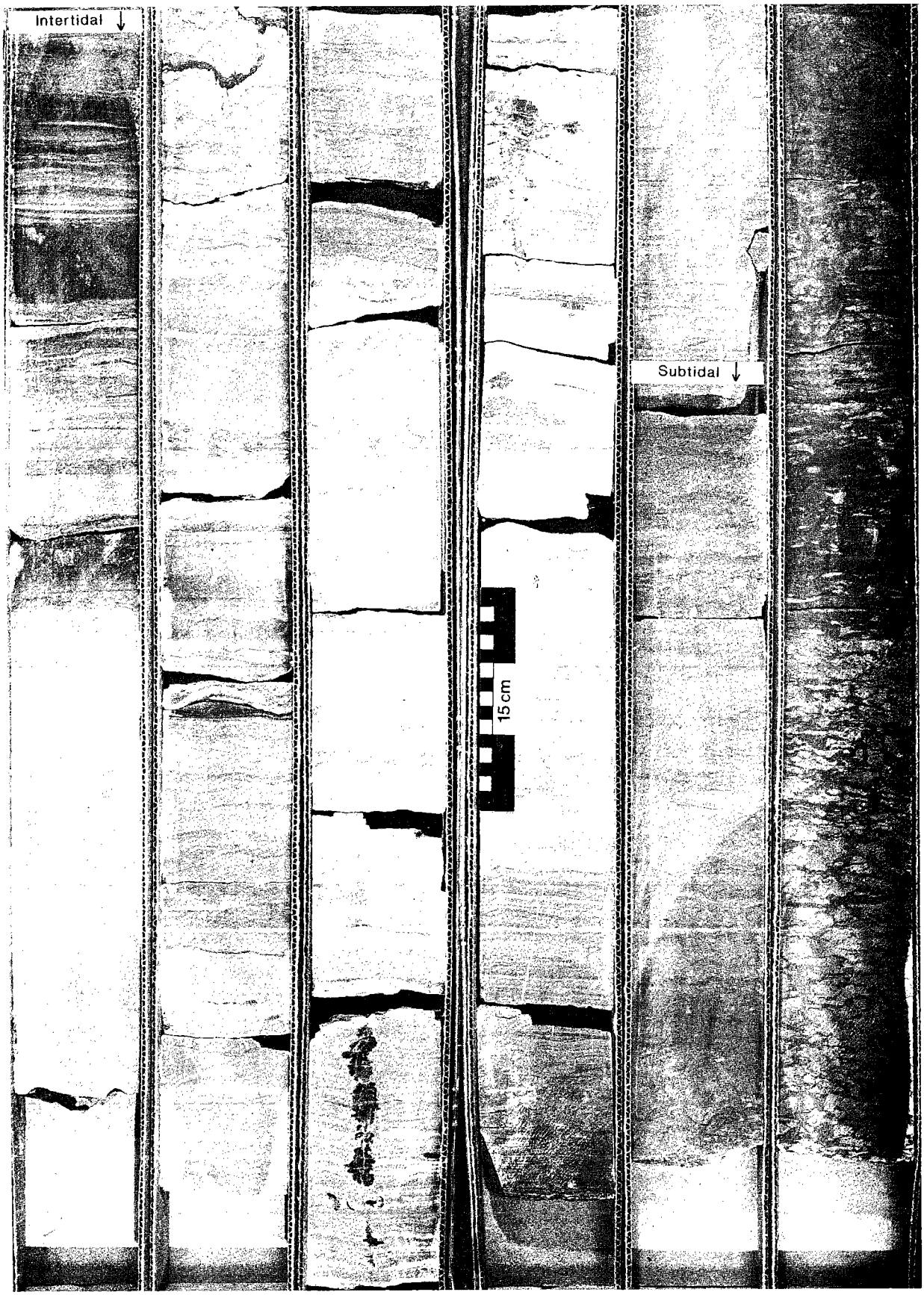


Plate 2. Shell Oil No. 1-28 Chase, 16,423–16,440 ft.



Plate 3. Texaco No. 1 Sanders, 7,687–7,704 ft.

Description and Interpretation of Karst-Related Breccia Fabrics, Ellenburger Group, West Texas

Charles Kerans
Bureau of Economic Geology, Austin, Texas

ABSTRACT.—The Lower Ordovician Ellenburger Group of West Texas is a prolific oil and gas producer in the Permian basin of West Texas. Regional analysis of depositional and diagenetic fabrics within the Ellenburger show reservoir facies to be dominated by a variety of breccia fabrics. A descriptive classification of Ellenburger breccias, including fracture, mosaic, clast-supported chaotic, siliciclastic-matrix-supported chaotic, and carbonate-matrix-supported chaotic types, allows simplified but genetically significant characterization of these highly varied breccia types. Although undoubtedly Ellenburger breccias are of diverse origins, vertical sequences from unbrecciated Ellenburger upward through chaotic, mosaic, and fracture-breccia types in sub-Simpson Group Ellenburger reservoirs are best interpreted in terms of a karst model of cave formation, infill, and collapse. Roof and lower collapse portions of these sequences form the best reservoir intervals with siliciclastic-rich cave-fill sediments commonly acting as baffles to fluid migration.

Core from the Gulf McElroy St. No. 1 well illustrates the characteristic succession of breccia fabrics used to develop the karst model. Karst facies recognized in the McElroy St. No. 1 core are lower collapse, cave-fill, and cave-roof; fracture breccias are not well developed in this core. Additional core material from producing zones in other wells is also displayed to illustrate pore types and breccia fabrics most commonly associated with producing intervals.

INTRODUCTION

The Lower Ordovician Ellenburger Group of West Texas is a prolific reservoir of oil and gas in the Permian basin. In a regional study of Ellenburger reservoir facies, almost one-third of the 15,000 ft of core examined was classified as breccia (Kerans, 1988,1990b). Ellenburger breccias have complex origins, but their classification using a simple descriptive scheme proved highly useful for both documentation of lithologic variability and for genetic interpretation. Emphasis was placed on constructing vertical successions of breccia fabrics to aid interpretation of breccia origin and in prediction of breccia-body geometry. The core material presented here is from the Gulf McElroy St. No. 1, Upton County, situated in the interior of the Lower Ordovician Ellenburger platform of West Texas (Fig. 1). In this area the Ellenburger is directly overlain by the Middle Ordovician Simpson Group. This core is a representative vertical succession through the karst collapse sequence of breccias. Comparison of the breccia fabrics in core with the classification and with the karst model will aid in the understanding of these complex reservoir strata.

STRATIGRAPHIC FRAMEWORK

Ross (1976) discussed three generalized depositional facies in Lower Ordovician carbonates of North America, including restricted-shelf dolostone, open-shelf limestone, and slope/basin carbonate-rich shales (Fig. 2). This three-fold depositional zonation is present in Texas, with most of the Ellenburger reservoirs in the present-day central basin platform and Delaware/Val Verde basin occurring in the restricted-shelf dolostone tract. Eastern shelf Ellenburger reservoirs, Ellenburger Group outcrops in the Llano uplift, and El Paso Group outcrops in the Beach and Franklin Mountains, are characteristic of the open-shelf limestone style. The time-equivalent shale-rich turbidites of the Marathon Group, Marathon area, are of slope/basin affinity (Young, 1968).

Detailed analysis of outcrops of open-shelf strata in the Franklin and Arbuckle Mountains indicates that Ellenburger facies patterns are the result of high-frequency, cyclic deposition during the Early Ordovician (Kerans and Lucia, 1989; Goldhammer and others, 1991). Comparison of Lower Ordovician depositional facies and sequence development in Texas, Oklahoma, and the Appalachian states using data from these open-shelf depositional sys-

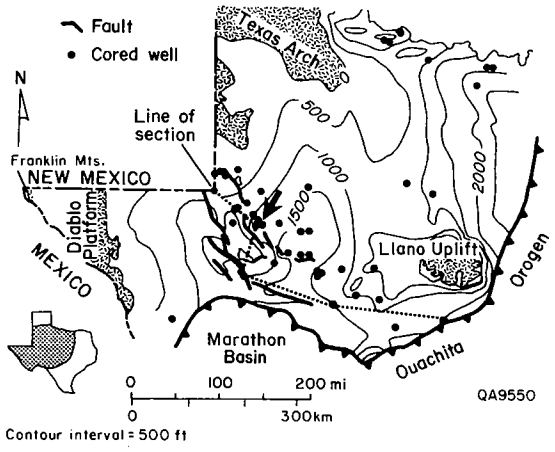


Figure 1. Isopach map of the Ellenburger Group showing the location of the Gulf McElroy St. No. 1 well. Modified from Texas Water Development Board (1972).

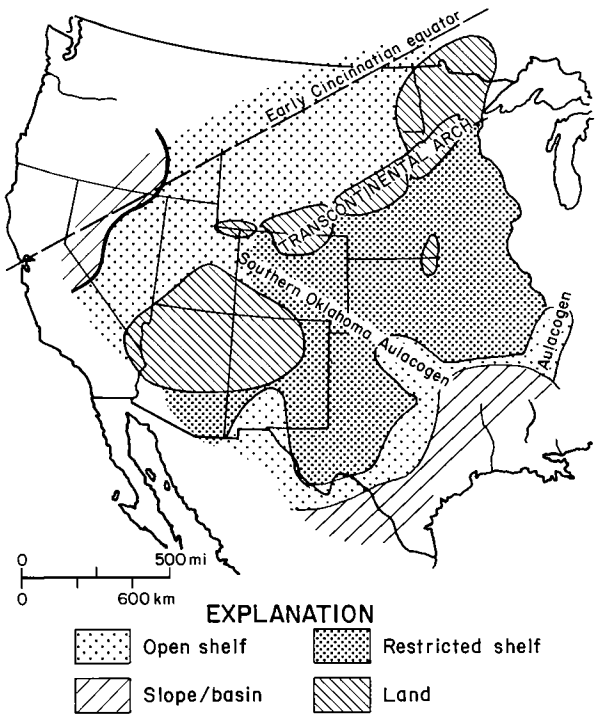


Figure 2. Map showing regional depositional setting during the Early Ordovician. Modified from Ross (1976).

tems suggests many similarities between these geographically widely separated areas. Read and Goldhammer (1988) published Fischer plots (plots that compare changes in accommodation space on the platform vs. time) for the Knox Group of the Virginia Appalachians that compare favorably with those for the El Paso Group of Texas and the Arbuckle Group of Oklahoma (Kerans and Lucia, 1989; Goldhammer and others, 1991; Wilson and others, 1991).

Attempts to recognize these patterns of high-frequency cyclicity in restricted-shelf Ellenburger sequences has met with little success. Apparently, extensive dolomitization of the Ellenburger in the restricted-shelf setting has obscured the high-frequency stratigraphic signature. In place of this framework, a succession of depositional systems has been defined on the basis of lithology, sedimentary structures, and fabrics seen in cores. This depositional-system framework treats only the gross lithostratigraphic elements of the Ellenburger, recognizing that intra-Ellenburger unconformities and high-frequency cyclicity in this region are not resolved (Fig. 3; Table 1) (Kerans, 1990b). These depositional systems and their dominant lithofacies (in parentheses) are:

1) fan delta–marginal marine (litharenite),
2) lower tidal-flat (mixed siliciclastic/carbonate packstone/grainstone),
3) high-energy restricted shelf (ooid and peloid grainstone),
4) low-energy restricted shelf (mottled mudstone),
5) upper tidal flat (laminated mudstone), and
6) open shallow-water shelf (gastropod-intraclast-peloid packstone/grainstone).

The McElroy St. No. 1 core exhibits depositional systems 3 and 4, and the portion selected for this workshop only includes facies from system 4. Further documentation of Ellenburger depositional systems in West Texas can be found in Loucks and Anderson (1980) and Kerans (1988,1990b).

POST-LOWER ORDOVICIAN PALEOKARST

The focus on karst-related breccias in this core display reflects the importance of these fabrics in Ellenburger reservoirs. Karst-modified sequences dominate Ellenburger reservoirs in the Andrews/Crane/Ector/Midland/Upton Counties area of West Texas from which >80% of the total Ellenburger oil production has come (Kerans and others, 1989; Kerans, 1990a). Core data, which are essential for analysis of breccia types and origin, are most abundant in this area. A general classification of breccia fabrics derived from study of these cores is presented below and in Figure 4. This classification is considered generic and should have application to breccias in the Arbuckle Group and other karst-modified units.

Breccia Classification

The abundance and variety of breccia fabrics in the Ellenburger cores examined for this study required development of a breccia classification scheme to be used in both descriptive and interpretive phases of the study. The classification was found useful for both karst-related and fault-related (tectonic) breccias.

Fracture and Mosaic Breccias

Fracture breccias and mosaic breccias, also known as crackle breccias, are intergradational fabrics. Fracture breccias are formed by a dense fracture network that outlines a system of tightly packed, incipient carbonate clasts. Fractures display extensional displacements, with millimeter-wide pore systems that are either open or filled by saddle-dolomite cement (Fig. 5A). Porosity is generally highest in fracture breccias and reaches 15% where dolomite cement is sparse.

Mosaic breccias resemble fracture breccias in that they consist entirely of host dolostone clasts (monomict), but they differ in the greater degree of rotation and relative movement of clasts (Fig. 5B). This relative movement produces a fabric in which open pore spaces developed along fracture planes and between juxtaposed clasts. Clast size in both the fracture and mosaic breccias is similar (generally being 2–8 in. [5–20 cm]), and clasts are highly angular. Void-filling deposits in mosaic breccias include geopetal-carbonate mud, saddle-dolomite cement, and siliciclastic sand and shale (Fig. 5B). Porosity values in the mosaic breccias generally range from 2 to 10%.

Fracture and mosaic breccias commonly occur in close association in zones ranging from 6 in. (15 cm) to several tens of feet thick. Upper and lower contacts of these breccias with host dolostones are gradational. Internal sediment is typically minor in mosaic breccias, but white to pink to gray saddle-dolomite cement is ubiquitous, and megaquartz, coarse-crystalline calcite, and anhydrite cements also occur.

Chaotic Breccias

Chaotic breccias include both clast-supported and matrix-supported varieties, the matrix-supported brec-

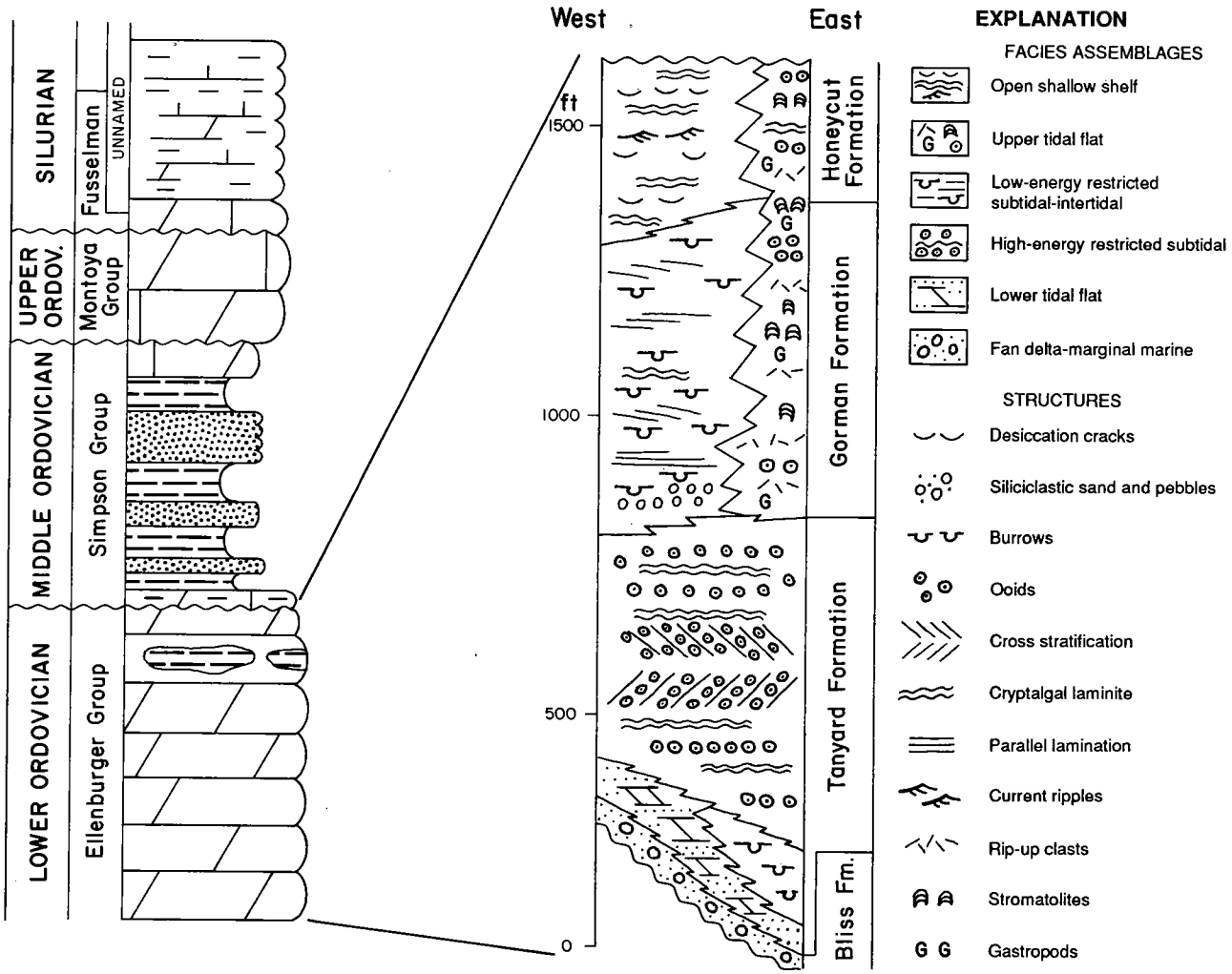


Figure 3. Schematic representation of depositional systems in West Texas compared with formalized Ellenburger stratigraphy in the Llano area. Total thickness of complete section is approximate (from Kerans, 1990b).

cias being further divided into siliciclastic-matrix-supported and carbonate-matrix-supported types. Clast-supported chaotic breccias are highly variable in terms of clast character (composition, shape, size), matrix composition, extent of cementation, and total porosity (Fig. 5C). Clast-supported breccias typically occur as massive, uninterrupted intervals, but locally contain unbrecciated dolostone intervals as much as 10 ft (3 m) thick.

Carbonate clast size varies from a few inches to >3 ft (1 m), averaging 2–6 in. (5–15 cm) (Fig. 5C). Clasts are typically angular, although rounded and embayed surfaces have been observed. Laminations within clasts document their random orientation; many clasts are subvertical. Carbonate clasts are generally locally derived and belong to only one depositional system. However, clasts of burrow-mottled dolostone and cryptalgal laminite are commonly juxtaposed, indicating displacement of depositional units by at least several feet. Pore space in clast-supported chaotic breccias is infilled by a variety of materials, including carbonate mudstone, green to black calcareous shale, and coarse-crystalline white to pink saddle dolomite. Porosity ranges from <1 to 15% locally, depending on the degree of cementation by saddle dolomite.

Siliciclastic-matrix-supported chaotic breccias are associated with intervals of crudely bedded sandstone and shale locally displaying soft-sediment faults and folds (Figs. 6,7C). Clasts compose 5–30% of the siliciclastic-matrix-supported breccias and are a mixture of Ellenburger dolostone clasts and sandstone and shale fragments. These sandstone and shale fragments are identical in lithology to intervals of the overlying Simpson Group. Shale clasts display intense compactional soft-sediment deformation, whereas sandstone fragments are rounded.

Intercalations of bedded sandstone and shale 1–10 ft (0.3–3 m) thick showing delicately graded bedding, thin planar lamination, and climbing-ripple cross-stratification also occur (Fig. 7C). Shales are both green and dark gray, whereas sandstone clasts and quartzose sand within the breccia matrix are white to light gray and texturally and compositionally mature. Disruption of sedimentary structures by soft-sediment deformation is ubiquitous (Fig. 7C). Visually estimated porosity of siliciclastic-matrix-supported breccias is low, generally 1–3%.

TABLE 1. — CHARACTERISTICS OF ELLENBURGER DEPOSITIONAL SYSTEMS

	Fan Delta – Marginal Marine	Lower Tidal-Flat	High-Energy Restricted-Subtidal	Low-Energy Restricted-Shelf	Upper Tidal-Flat	Open Shallow Shelf
Lithology						
Lithic Fragments	A*	—	—	—	—	—
Quartz Sand	C	C	—	R	R	R–C
Chert	R	C	A	C	C	C
Limestone	—	—	R	R	R	A
Dolomite Texture						
> 100 μm (CC)**	C	C	A	R	R	R
10–100 μm (FMC)	C	C	C	A	C	C
1–10 μm (VFC)	R	R	R	R	C	R
Fabrics						
Grainstone	C	C	A	R	R	C
Packstone	C	C	C	C	R	C
Wackestone	C	C	R	C	C	C
Mudstone	R	R	R	A	A	C
Structures						
Cross-Stratified	C	C	A	R	R	R
Current Laminated	C	C	C	A	A	R
Stromatolites	—	R	—	R	R–C	C
Flat Cryptalgal Mat	—	C	C	C	A	C
Bioturbation	—	R	R	A	C	R
Allochems						
Gastropods	—	R	—	R	R	C
Cephalopods	—	—	—	R	—	R
Bivalves	—	—	—	R	—	C
Sponges	—	—	—	—	—	R
Ooids	—	R	A	—	—	C
Peloids	R	C	A	C	R	C

* A = abundant, C = common, R = rare, — = not available.
** CC = coarse crystalline, FMC = fine to medium crystalline, VFC = very fine crystalline.

Carbonate-matrix-supported chaotic breccias are only a minor-component breccia type. These matrix-supported breccias are gradational upward into the siliciclastic-matrix-supported breccias in many breccia sequences. Grading is absent, and bedding is only rarely apparent. Clasts are supported in a matrix of medium-crystalline dolomudstone, the same lithology as that of the component clasts, but the matrix also contains quartz sand and angular, granule-size chert fragments. Clasts range from 2 to 16 in. (5 to 40 cm) long and are rounded to subangular and randomly oriented. The abundance of fine-grained matrix in the carbonate-matrix-supported breccias results in overall low porosity, ranging from 1 to 5%.

Local intense dolomitization of both siliciclastic-matrix-supported and carbonate-matrix-supported chaotic breccias produces a complex fabric. Clast-matrix boundaries are obscured, original depositional fabrics of clasts are obliterated, and much of the original shale matrix of the breccia may be replaced (Fig. 5D). Similar replacement of shale by dolomite in Tertiary strata was reported by Heald and Baker (1977).

Karst Model

Throughout the majority of larger Ellenburger reservoirs that occur beneath the Simpson Group, a repetitive vertical succession of breccia types is observed. This sequence, from clast-supported chaotic breccias at the base through siliciclastic-matrix-supported (and lesser carbonate-matrix-supported) chaotic breccias into upper fracture and mosaic breccias, is well represented in the McElroy St. No. 1 core (Figs. 6,7). The karst model proposed for this vertical succession of breccia types includes: (1) prolonged exposure of the Ellenburger carbonate platform during a major (second-order) sea-level lowstand, (2) dissolution and cave development, (3) enlargement of cavern systems through dissolution and mechanical failure and stoping of portions of cave mar-



FRACTURE BRECCIA
Fabric - dense fracture network defines clasts, no significant rotation of clasts
Clasts - incipient clasts composed of single host dolomite type; highly angular outline
Cements - minor to pervasive saddle dolomite with rare anhydrite and calcite
Internal Sediment - rare geopetal dolomicrite and fine siliciclastics
Porosity - 1-15%



MOSAIC BRECCIA
Fabric - fitted, clast-supported, with discrete clasts displaying minor rotation
Clasts - angular to slightly rounded, monomict breccia of host lithology, size usually 5-10 cm
Cements - common saddle dolomite rim cement, rare anhydrite calcite and quartz
Internal Sediment - geopetal dolomicrite and fine-grained siliciclastics
Porosity - 2-20%



CHAOTIC BRECCIA, SILICICLASTIC-MATRIX-SUPPORTED
Fabric - randomly oriented clasts in massive, upward-fining, or upward-coarsening units 10-200 cm thick
Clasts - angular to rounded dolomite derived from various facies, chert, sandstone, and shale fragments; clast size-1-50 cm
Matrix - mixture of shale, very fine to medium-grained siliciclastic sand and minor dolomicrite and glauconite
Cements - minor dolomite cement in shale matrix
Internal Sediment - none
Porosity - 1-3%



CHAOTIC BRECCIA, CARBONATE-CLAST-SUPPORTED
Fabric - randomly oriented clasts in massive units tens of centimeters to tens of meters thick
Clasts - angular to rounded dolomite and rare chert fragments from a variety of depositional facies; clast size-5-50 cm
Cements - well-developed saddle dolomite rims with rare anhydrite, calcite, quartz, pyrite, marcasite
Internal Sediment - geopetal dolomite with rare fine-grained siliciclastics typically perched on clasts, but can fill intraclast space completely as a sieve-fill matrix
Porosity - 1-15%

Figure 4. Schematic representation of breccia types in Ellenburger paleokarst deposits (from Kerans, 1990b).

gins forming clast-supported chaotic breccias that accumulated on the floors of caves (lower collapse zone), (4) cessation of cave development caused by subsequent (Middle Ordovician) sea-level rise and transgression that resulted in deposition of siliciclastic-matrix-supported breccias filling cavern systems (cave fill), (5) burial of the partially to completely filled cave system, and (6) compaction-driven fracturing of cave-roof material due to increased loading over undercompacted cave-fill material causing formation of cave-roof fracture/mosaic breccias (cave roof) (Fig. 8).

Karst Versus Fault-Related Origin of Ellenburger Breccias

Many of the breccia deposits and fracture systems in the Ellenburger Group have been variously interpreted either as being of karst (Loucks and Anderson, 1985) or tectonic (Ijirigho and Schreiber, 1986) origin. The term tectonic fracture is used here to describe fracturing attributed to fault displacement unrelated to karst collapse. The dominant tectonic event causing fault-related or tectonic fractures in the Ellenburger is the Pennsylvanian-age faulting associated with development of the Marathon–Ouachita orogen.

In this study, fracture systems and associated breccias interpreted to have a tectonic origin were seen to be localized and generally not causally linked to the widespread karst breccias. Most karst-related fractures can be distinguished from tectonic fractures using the criteria of spatial distribution, timing, association with particular breccia fabrics, fracture geometry, and nature of fracture fill. In the case of sub-Simpson Group, pre-Middle Ordovician karst systems, karst-related fractures are generally restricted to the upper 100–300 ft (30–90 m) of the Ellenburger Group. Typically these are developed within a narrow zone immediately above a distinctive siliciclastic-rich chaotic breccia zone (interpreted in this report as a cave-fill deposit). Karst-related fractures are contemporaneous with the main phase of breccia development and do not crosscut breccias. These fractures also predate precipitation of saddle-dolomite cement and are partly to completely filled with this late dolomite. This is an important observation because this dolomite phase can be shown to postdate at least basal Simpson Group strata on the basis of crosscutting relationships (Kerans, 1990b). Besides dolomite cement, geopetal internal sediments of both siliciclastic and carbonate composition occlude karst-associated pore space.

In contrast, a suite of fractures that could be confidently related to tectonic origin had the following characteristics: (1) random occurrence within cored intervals, and (2) crosscutting of all diagenetic phases, including youngest saddle-dolomite cements and karst breccias. Infill deposits include rare megaquartz cement and dark internal sediment. Criteria used to differentiate tectonic from karst-related fractures are given in Table 2.

GULF McELROY ST. NO. 1 CORE: DEPOSITIONAL AND BRECCIA FABRICS

Core from the Gulf McElroy St. No. 1 well in Upton County, Texas, is featured in this presentation (Figs. 1,6,7,9–11). Primary depositional facies are bioturbated peloidal dolomudstones and dolowackestones of the low-energy, restricted subtidal-intertidal depositional system. In terms of breccia fabrics, the core displays a thin cave-roof facies from directly below the Ellenburger/Simpson unconformity (not cored) at 11,600–11,636 ft. This upper 36 ft contains rare fractures that are filled by dolomite cement and dolomudstone internal sediment (Figs. 7A,9). Fracture and mosaic breccias and their associated pore networks are not developed in this uppermost portion of the McElroy St. No. 1 well. Interestingly, this absence of breccia-related porosity is consistent with the drill-stem tests of this interval, which reported low shut-in pressures for this zone. The interval between 11,637 and 11,725 ft that gives the diagnostic high API gamma-ray log response is composed of a complex array of siliciclastic-matrix-supported breccias (Figs. 7B,C,9,10) with a variety of soft-sediment deformation and sediment gravity-flow features. Also important in this unit are dolostone fragments of probable Ellenburger affinity as well as exotic rock fragments, including orthoquartzitic sandstone and shale.

Below this siliciclastic-matrix-supported breccia unit is one composed of clast-supported dolostone chaotic breccia with less common carbonate-matrix-supported chaotic breccias (Figs. 7D,11). In clast-supported zones, breccias are cemented with pervasive saddle-dolomite cement but also retain some inter-clast porosity. This porosity, though not visually impressive, is responsible

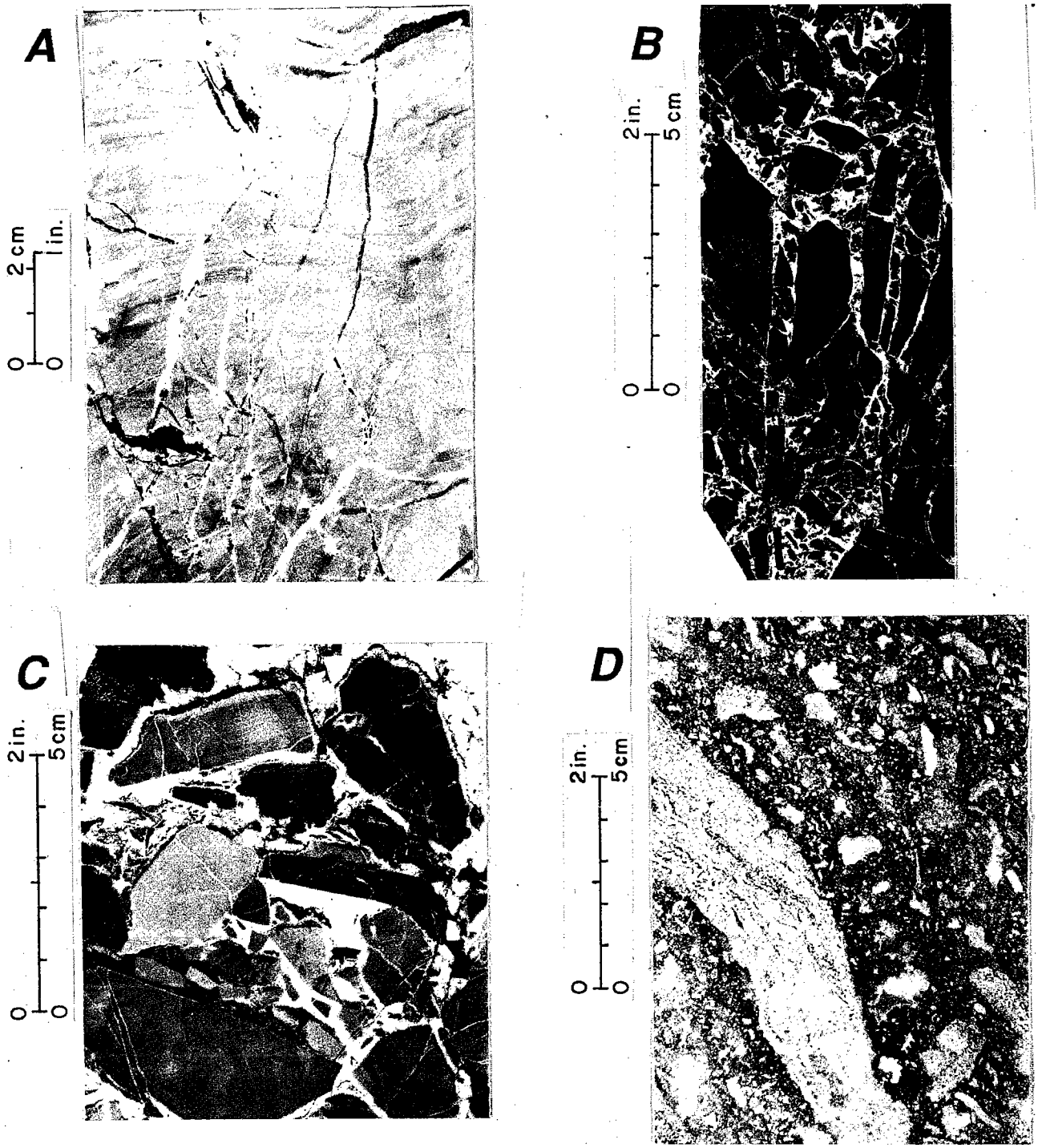


Figure 5. Examples of typical Ellenburger paleokarst breccias. *A*—Fracture breccia showing pervasive network of fractures lined by saddle dolomite and locally filled by internal sediment. Low-energy restricted-shelf depositional system, Texaco Seaboard TXL D-1 well, 13,007 ft. *B*—Mosaic breccia showing slightly rotated clasts and saddle-dolomite cement. Low-energy restricted-shelf depositional system, Cities Service Foster No. 1 well. *C*—Clast-supported chaotic breccia showing mixture of clast types and saddle-dolomite cement. Low-energy restricted-shelf depositional system, Gulf McElroy St. No. 1 well, 11,817 ft. *D*—Siliciclastic-matrix-supported chaotic breccia with large subvertical clast. Both matrix and clasts were extensively recrystallized by pervasive late dolomitization. Low-energy restricted-shelf depositional system, Gulf McElroy St. No. 1 well, 12,035 ft.

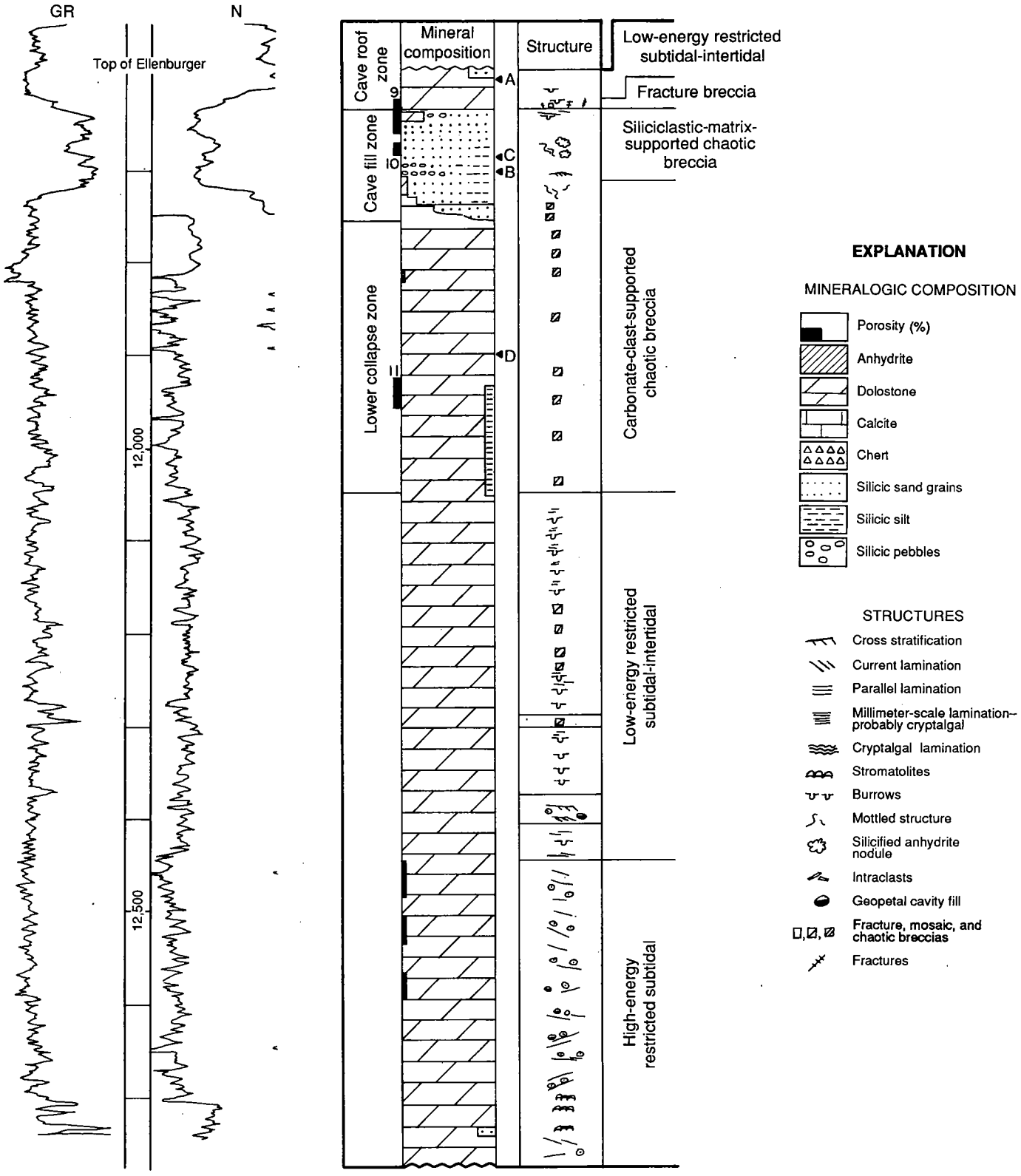


Figure 6. Gamma-ray, neutron, and graphic logs showing distribution of fracture-brecciated roof zone, cave-infill zone, and lower collapse-breccia zone in Gulf McElroy St. No. 1 well, Upton County. The distinctive radioactive zone that occurs in the log 40 ft (12 m) below the unconformity corresponds to the shale-sandstone infill zone. Letters A through D correspond to core photographs in Figure 7, whereas numbered zones 9, 10, and 11 refer to core photographs of Figures 9, 10, and 11.

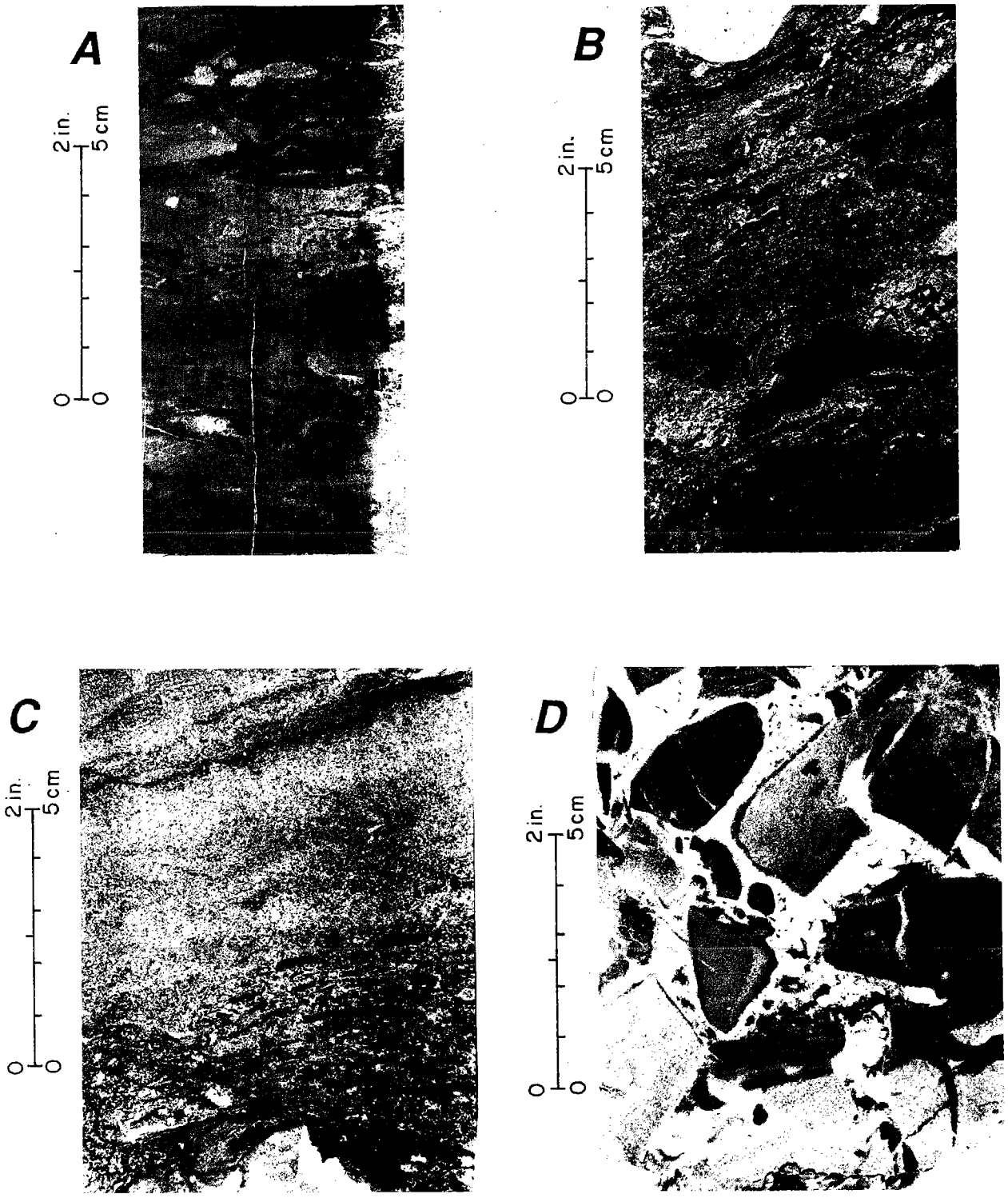


Figure 7. Core photographs, Gulf McElroy St. No. 1 well, Upton County. All scales are in centimeter and inch increments. *A*—Intact carbonate of uppermost Ellenburger (roof zone), 11,601 ft. *B*—Siliciclastic-matrix-supported chaotic-breccia infill sediment containing fragments of sandstone and shale, 11,703 ft. Shale fragments are deformed by soft-sediment compaction. This infill sediment is interpreted to be of Simpson Group derivation. *C*—Graded bedding and soft-sediment deformation in siliciclastic-matrix-supported chaotic-breccia deposit. *D*—Carbonate-clast-supported chaotic breccia showing mixture of clast types and saddle-dolomite cement, 11,909 ft.

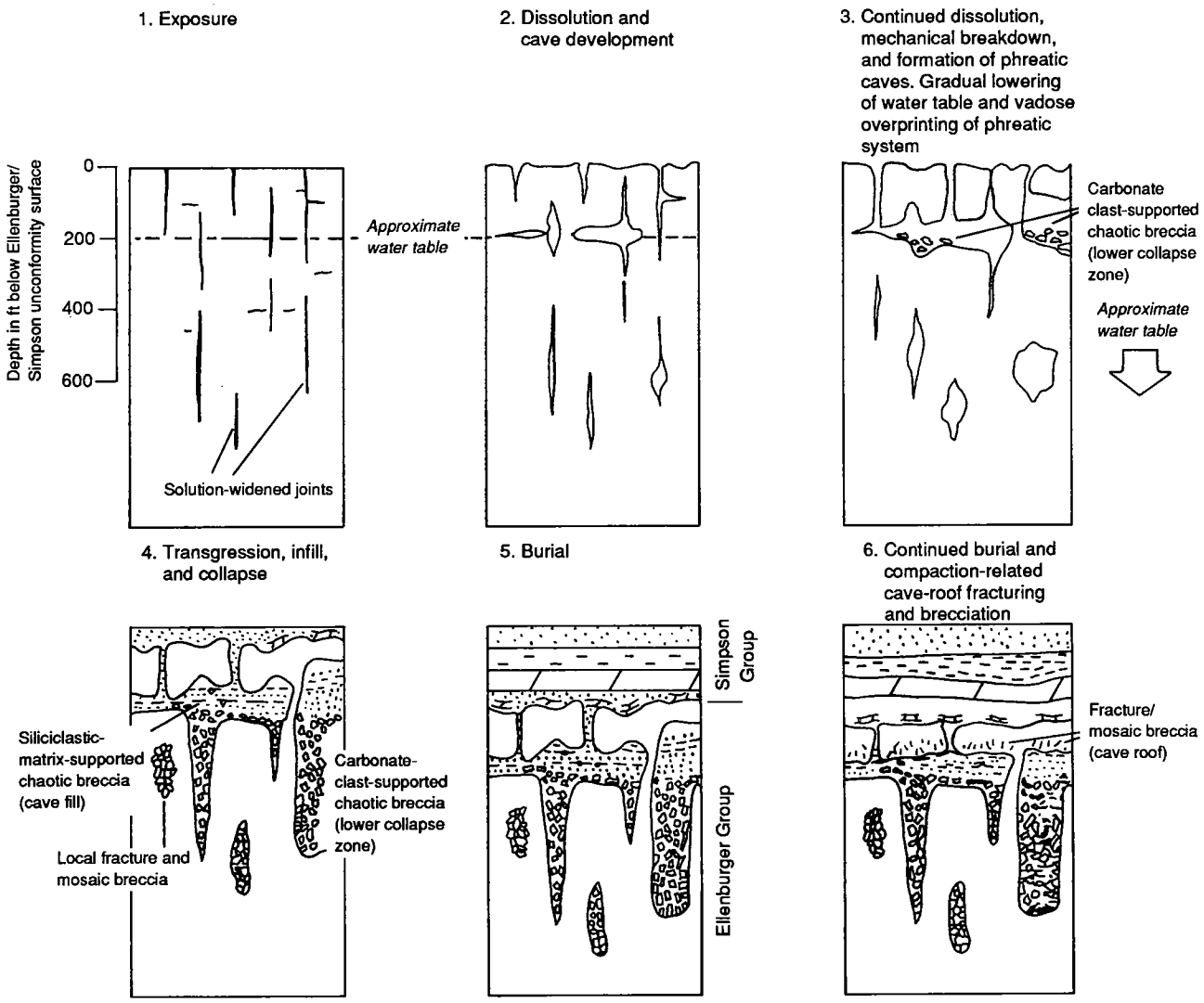


Figure 8. Schematic model of development of Ellenburger paleokarst deposits. Time interval shown is from the end of Ellenburger deposition through at least lower Simpson Group deposition.

for very high drill-stem-test flow rates. Clast types in this lower breccia interval include typical Ellenburger restricted-shelf bioturbated dolomudstones. Rare siliciclastic material has filtered down into this lower breccia unit, forming geopetal perched sediment in inter-clast voids. This sequence, from clast-supported chaotic breccia, through siliciclastic-matrix-supported chaotic breccia, to uppermost intact dolostone with minor fracture breccia, comprises the ideal vertical profile attributed to cave formation, infill, and collapse as discussed above. In terms of this model, the upper unit of the McElroy St. No. 1 core is interpreted as a cave-roof zone (11,601–11,636 ft) (Fig. 9). The middle unit of siliciclastic-matrix-supported breccia would represent cave fill (11,637–11,725 ft) (Figs. 9,10), and the lower carbonate clast-supported chaotic-breccia interval (11,726–12,050 ft) (Fig. 11) is interpreted as lower collapse zone.

SUMMARY

Regional analysis of core material from the Ellenburger of West Texas demonstrates that the majority of the producing reservoirs are developed in facies of the restricted-shelf subdivision of Ross (1976). Extensive dolomitization of these restricted-shelf carbonates prohibits high-frequency cyclostratigraphy to be applied to these strata, but a simplified grouping into depositional systems is possible. These depositional systems include: (1) fan delta–marginal marine, (2) lower tidal-flat, (3) high-energy restricted shelf, (4) low-energy restricted shelf, (5) upper tidal flat, and (6) open shallow-water shelf. Only system 4 will be observed in the core selected for this workshop.

The McElroy St. No.1 core provides an excellent opportunity to observe the different types of breccias commonly associated with karst-modified reservoirs of the Ellenburger Group in the area where the Ellenburger is overlain by Simpson Group strata (Andrews/Crane/Ector/Midland/Upton Counties). A simple, descriptive classification can be applied to these breccias that aids in consistent and potentially genetically significant observation. Major breccia types are fracture, mosaic, clast-supported chaotic, siliciclastic-matrix-supported chaotic,

TABLE 2. — COMPARISON OF FAULT-RELATED AND KARST BRECCIAS

	Fault-Related	Karst
Breccia Fabric	Tightly fitted clasts, interclast areas filled with mechanically disaggregated host rocks and cement	Variable, fracture, mosaic (= fitted), and chaotic breccias all common, both clast-supported and matrix-supported, typically open space between clasts filled with cement or cavity-filling sediment
Clast Morphology	Variable, highly angular to rounded, depending on degree of lateral displacement	Variable, angular to rounded, some clast embayment related to solution
Clast Composition	Monomict, derived from immediately adjacent strata	Either monomict or oligomict, depending on lithologic variability of section involved in collapse
Geometry	Tabular, restricted to area immediately adjacent to fault plane	Tabular upright bodies developed along joint trends and horizontal bodies controlled by selectively dissolved zones

and carbonate-matrix-supported chaotic types. The major karst-breccia facies are lower collapse zone (clast-supported chaotic breccias), cave-fill (siliciclastic-matrix-supported chaotic and lesser carbonate-matrix-supported chaotic breccias), and cave-roof (fracture and mosaic breccias and intact host dolostone).

The consistent and complex stratification of breccia types and their timing relative to late-diagenetic events are considered critical for differentiating these breccias from those of fault-related origin.

REFERENCES CITED

Goldhammer, R. K.; Lehmann, P. J.; and Dunn, P. A., 1991, Third-order sequences and parasequence stacking patterns of Lower Ordovician platform carbonates of the El Paso Group, Franklin Mountains, West Texas [abstract]: American Association of Petroleum Geologists Bulletin, v. 75, p. 582.

Heald, M. T.; and Baker, G. F., 1977, Diagenesis of the Mt. Simon and Rose Run sandstones in western West Virginia and southern Ohio: Journal of Sedimentary Petrology, v. 47, p. 66–77.

Ijirigho, B. T.; and Schreiber, J. F., Jr., 1986, Origin and classification of fractures and related breccia in the Lower Ordovician Ellenburger Group, West Texas: West Texas Geological Society Bulletin, v. 26, p. 9–15.

Kerans, Charles, 1988, Karst-controlled reservoir heterogeneity in Ellenburger Group carbonates of West Texas: American Association of Petroleum Geologists Bulletin, v. 72, p. 1160–1183.

_____1990a, Karst-controlled reservoir heterogeneity in Ellenburger Group carbonates of West Texas: reply: American Association of Petroleum Geologists Bulletin, v. 74, p. 1124–1125.

_____1990b, Depositional systems and karst geology of the Ellenburger Group, (Lower Ordovician), subsurface West Texas: University of Texas at Austin, Bureau of Economic Geology Report of Investigations 193, 63 p.

Kerans, Charles; and Lucia, F. J., 1989, Recognition of second, third, and fourth/fifth order scales of cyclicity in the El Paso Group and their relation to genesis and architecture of Ellenburger reservoirs, *in* Cunningham, B. K.; and Cromwell, D. W. (eds.), The lower Paleozoic of West Texas and southern New Mexico—modern exploration concepts: Permian Basin Section, Society of Economic Paleontologists and Mineralogists Publication No. 89-31, p. 131.

Kerans, Charles; Holtz, M. H.; and Tyler, Noel, 1989, Contrasting styles of reservoir heterogeneity in Ellenburger Group carbonates, West Texas [abstract], *in* Cunningham, B. K.; and Cromwell, D. W. (eds.), The lower Paleozoic of West Texas and southern New Mexico—modern exploration concepts: Permian Basin Section, Society of Economic Paleontologists and Mineralogists Publication No. 89-31, p. 131.

Loucks, R. G.; and Anderson, J. H., 1980, Depositional facies and porosity development in Lower Ordovician Ellenburger dolostone, Puckett field, Pecos County, Texas, *in* Notes for Society of Economic Paleontologists and Mineralogists Core Workshop No. 1, p. 1–31.

_____1985, Depositional facies, diagenetic terranes, and porosity development in Lower Ordovician Ellenburger dolomite, Puckett field, West Texas, *in* Roehl, P. O.; and Choquette, P. W. (eds.), Carbonate petroleum reservoirs: New York, Springer-Verlag, p. 21–37.

Read, J. F.; and Goldhammer, R. K., 1988, Use of Fischer plots to define third-order sea level curves in peritidal cyclic carbonates, Ordovician, Appalachians: Geology, v. 16, p. 895–899.

Ross, R. J., 1976, Ordovician sedimentation in the western United States, *in* Bassett, M. G. (ed.), The Ordovician System: Proceedings of a Paleontological Association symposium, Birmingham, p. 73–105.

Texas Water Development Board, 1972, A survey of the subsurface saline water of Texas: Texas Water Development Board, Austin, v. 1, 113 p.

Wilson, J. L.; Fritz, R. P.; and Medlock, P., 1991, The Arbuckle Group, relations of core and outcrop analysis to cyclic stratigraphy and correlation, *in* Johnson, K. S. (ed.), Late Cambrian–Ordovician geology of the southern Midcontinent, 1989 symposium: Oklahoma Geological Survey Circular 92, p. 61–63.

Young, L. M., 1968, Sedimentary petrology of the Marathon Formation (Lower Ordovician), Trans-Pecos Texas: University of Texas at Austin unpublished Ph. D. dissertation, 234 p.



Figure 9. Core showing the sharp transition from intact cave-roof, low-energy, restricted-subtidal dolomudstones (11,620–11,636 ft) into underlying siliciclastic-matrix-supported breccias of the uppermost cave-fill facies. Lithoclasts in the breccias are of sandstone, shale, and dolomudstone.

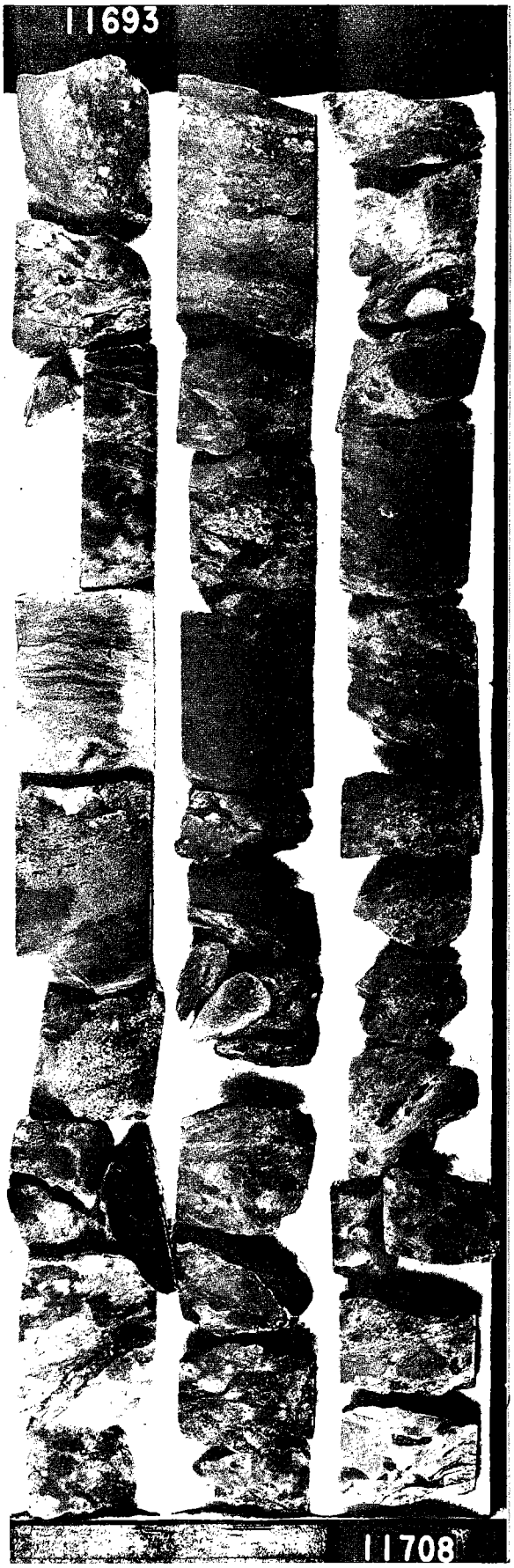


Figure 10. Core of siliciclastic-matrix-supported breccias of the cave-fill facies (11,693–11,708 ft).



Figure 11. Core of carbonate-clast-supported chaotic breccias of the lower collapse facies (11,924–11,947 ft). Clasts are of dolomudstone and laminations within clasts record the rotation of clasts.

Results of a Deep Cambro–Ordovician Drilling Program, Northern Fort Worth Basin, Texas

Joseph R. Whiteside
University of Texas at Dallas

William E. McCommons
McCommons Oil Co., Dallas

ABSTRACT.—Exploration of the Cambro–Ordovician section of north Texas has resulted in more information on the lithologies of the various formations present. Well sites for a deep drilling program were selected based upon the existence of seismically defined structures. Information gained from well data has shown that extensive dolomitization has created several porous zones within the deeper Ellenburger–Arbuckle section, but little evidence indicates indigenous hydrocarbon source rocks in the immediate area. Further investigation of indigenous hydrycarbon source rocks for the Cambro–Ordovician section will probably necessitate the discovery of deeper water marine units in which organic matter was preserved.

INTRODUCTION

In our opinion, if any large oil and gas fields remained to be discovered in the Fort Worth basin, they were most likely to be found in the thick Cambro–Ordovician sections that remained untested. During 1987 and 1988, McCommons Oil Co., Pitts Oil Co., and others formed a joint venture that leased >6,000 acres in the northern portion of the Fort Worth basin in Montague County. The original plan was to drill three deep Cambro–Ordovician tests; however, only two wells were drilled.

Our research of the deep Cambro–Ordovician formations included not only every deep test drilled in the Fort Worth basin and on the Muenster arch, but also of the Arbuckle production in the Healdton field of Carter County, Oklahoma. The following discussion will be limited to the data on deeper strata in the basin in Montague and Clay Counties.

GEOLOGIC SETTING

An examination of Montague and Clay Counties indicates almost every structure with 50 ft or more of closure at the top of the Ellenburger, when tested, is oil productive to the closure limit, or "pour-point," and the quantity of production and reserves generally is porosity dependent (Fig. 1). The deepest Ellenburger production in Montague County, so far, is the Saint Jo, SE Ellenburger field near the eastern county line; this field has ~100 ft of closure on top of the Ellenburger, above a closure limit of –8,025 ft sub-sea. Overlying the Ellenburger are 700 ft of younger Ordovician shales, limestones, and dolomitic limestones of the Simpson Group (Joins shale at base) and Viola Group. Westward across Montague and Clay Counties, the Ellenburger fields and structures become progressively shallower, with each field's structural-closure limit defining either a single oil/water contact or, in some cases, a productivity limit with multiple zones of porosity acting as separate reservoirs.

The Ordovician formations overlying the Ellenburger were progressively eroded in a westward direction across Montague County. In the MPS Ellenburger field of southwestern Montague County, all of the younger Ordovician beds are missing, and the upper portion of the Ellenburger "A" section (see Fig. 2) is absent due to post-Ordovician erosion. This field has a maximum structure of 120 ft above the closure limit of –5,700 ft; this limit was also the original oil/water contact.

At Southeast Dillard field of southeastern Clay County, completions are made near the top of the Ellenburger in zones of fractured porosity in the "B" and "C" sections, where they subcrop against the overlying Barnett Shale. Only a few feet of the "A" section are present in the easternmost portion of the field, and older Ordovician beds subcrop progressively westward.

The presence and location of these and other Ellenburger fields provides evidence that hydrocarbons migrated generally updip from deeper source rocks following horizontal zones of porosity and vertical fractures, ultimately filling every possible trap to its maximum capacity.

In the west-central portion of Montague County, just southwest of the town of Nocona, are the Sanders, Lone Prairie, Woody, and Woody North Ellenburger fields. These fields lie within Fort Worth basin along an uplift just south of the fault system separating the basin from the Nocona arch. Wells in this area have 400–450 ft of younger Ordovician Joins, Simpson, and Viola strata overlying the top of the Ellenburger. The presumably Mississippian Barnett Shale is absent here and is also missing from the entire Red River uplift. This area provides an exception to the "full Ellenburger structure" rule. Although the –6,000-ft sub-sea contour line closes against the fault system on the north, oil production has only been encountered in small, separate closures on the much larger closure that measures as large as 8 mi east to west and 3–4 mi north to south. Within the large struc-

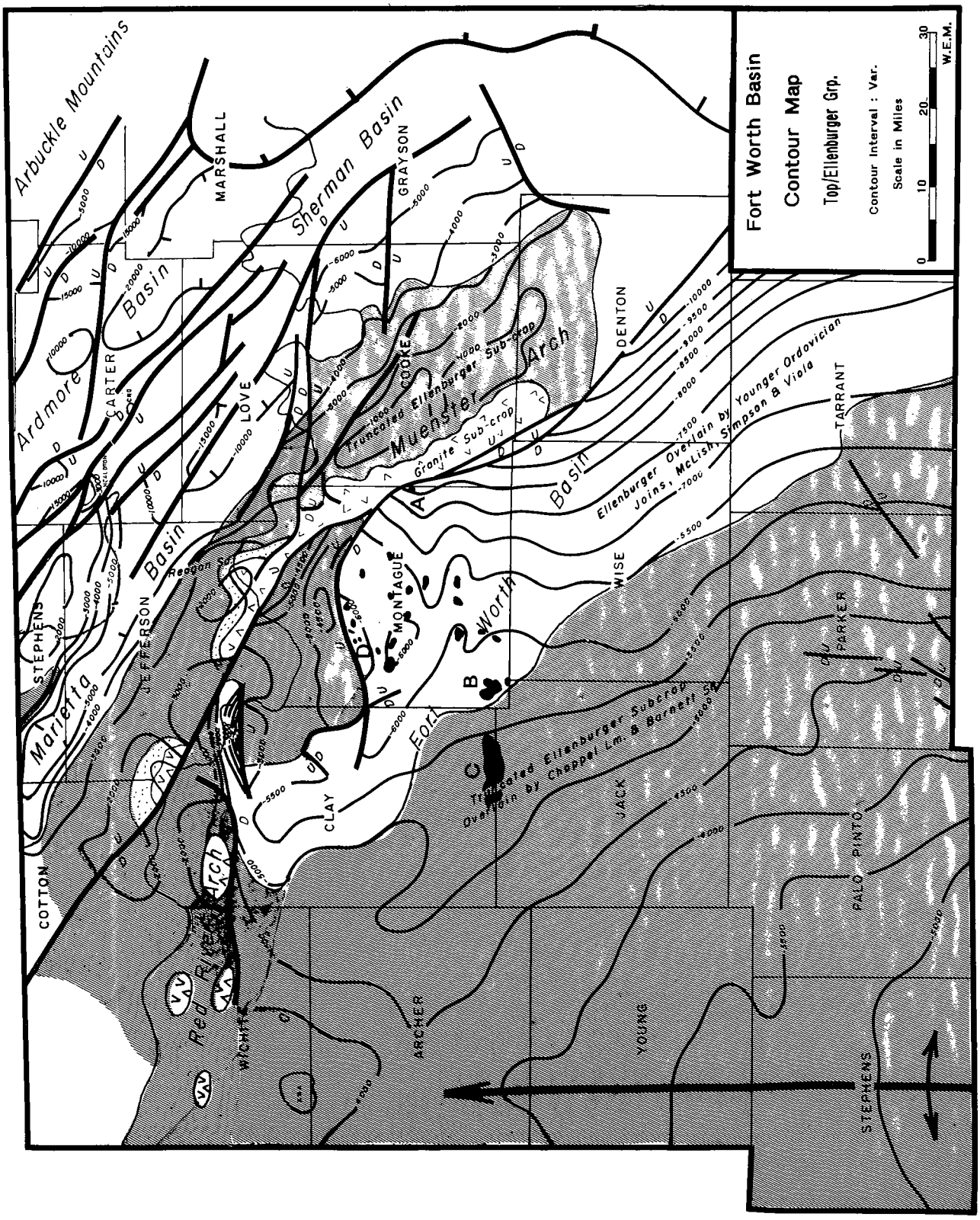


Figure 1. Index map of the Fort Worth basin showing regional contours on the top of the Ellenburger Group. Note the Ellenburger oil fields highlighted in black in Clay and Montague Counties. The following fields (shown on the map) are discussed in the text: (A) Saint Jo, SE Ellenburger; (B) MPS Ellenburger; (C) Southeast Dillard Ellenburger; and (D) Sanders, Lone Prairie, Woody, and Woody North Ellenburger.

tures, good shows of live, although residual, oil are encountered in the Ellenburger to a depth of approximately –6,030 ft sub-sea.

DRILLING PROGRAM

Location Determination

A location for the first deep test, Running High Ranch No. 6, was chosen near the center of the old Chapman-McFarlin field. The Caddo conglomerates between 6,000 and 6,100 ft had provided excellent production in the field, and the Ellenburger at 6,800 ft was productive. A closure limit, that was also the oil/water contact of –6,030 ft sub-sea, was proven for the field, giving the Ellenburger a 200-ft oil column and a productive area of 2,000 acres. However, due to low porosity and permeability, the Ellenburger recoveries have been disappointing. It was believed that this location would be a good test of our theory of carbonate sources and vertical migration. Our extensive seismic data indicated the Precambrian basement here to be –11,000 ft sub-sea, and closure of nearly 1,000 ft at this depth.

The location for the second test, Burns and Stine No. 1, was selected 4 mi to the north of the first test, near the west end of an 8-mi-long structure that parallels the Nocona arch. Our seismic data indicated that this location would not only be on the flank of the structure, but also would be extensively faulted and fractured. The third location, 3 mi east of the Burns and Stine No. 1, was not drilled, although it was expected to be near the crest of the structure and to have thinner formations with some of the sections pinched-out.

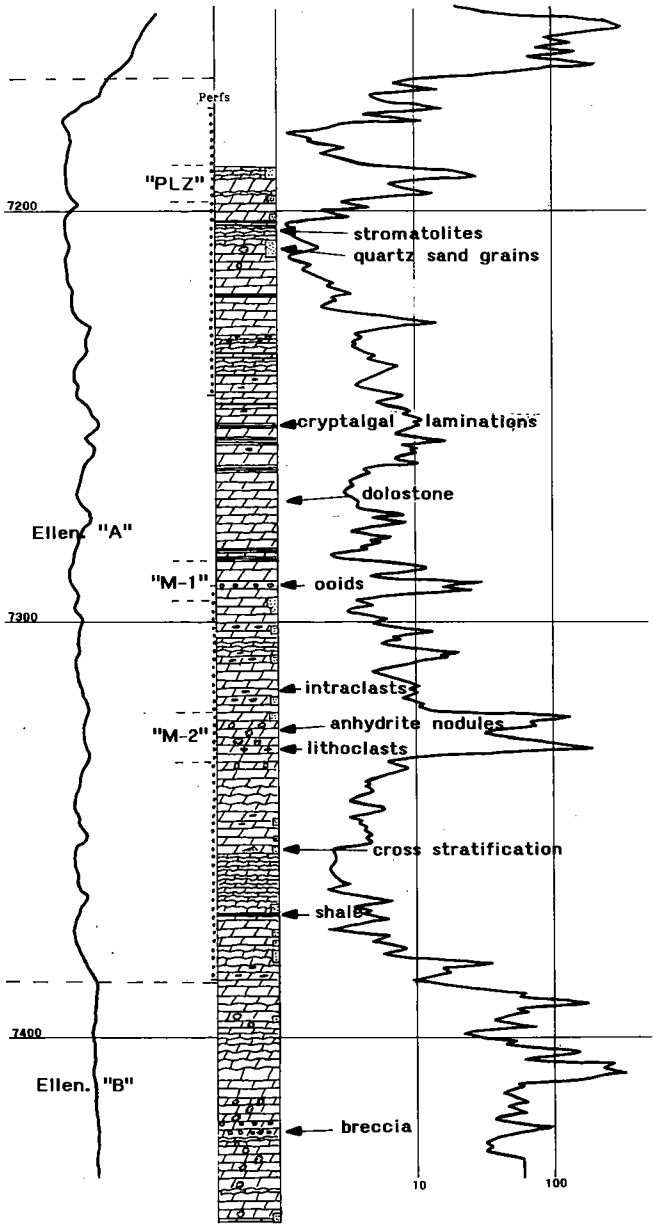


Figure 2. Electric log and core description correlation from the Standard Oil of Texas No. 4 Roberts well of Montague County, Texas. Informal stratigraphic designations are given to some of the more important lithofacies. Note the dominance of stromatolitic dolostones in the section. PLZ, M-1, and M-2 are zones of porosity that are readily identified throughout Montague and Clay Counties.

Drilling Procedures

L. D. Burns Drilling Co. Rig No. 6, rated at 14,000 ft, was selected to drill the first test. This rig utilizes 4½-in. drill pipe, 21 6½-in. drill collars, and has 840-barrel capacity in its steel mud tanks; desilters, desanders, and degassers were also employed. A 14¾-in. surface hole was drilled to 2,100 ft to the top of the Palo–Pinto Lime, and 10¾-in. surface casing was cemented. A 9⅞-in. hole was drilled to the total depth of 10,621 ft. This large hole was a precaution, in case it was necessary to run an intermediate string of 7-in. casing. Initial plans were to reduce to 8¾ in. at 9,000 ft, but this was not necessary.

For the second test, the Burns and Stine No. 1, Felderhoff Drilling Co. Rig No. 2 was used, with a depth capability of 13,000 ft. This rig has 4½-in. drill pipe and 21 6¼-in. drill collars. Steel tanks and mud-control systems similar to the first test were used. A 13¾-in. surface hole was drilled to 1,875 ft and 10¾-in. casing cemented. From here an 8¾-in. hole was drilled to the total depth of 8,595 ft. As no problems had been encountered in drilling the Running High Ranch No. 6, a smaller hole was drilled, reducing some of our requirements and, hopefully, some of the costs. The smaller hole proved to be a poor choice, as it limited our options for setting an intermediate casing string.

CAMBRO–ORDOVICIAN GEOLOGY

Lithologic Characteristics

Correlations of the informal designations for local lithofacies and sections (Fig. 2) of the Ellenburger are used in this portion of the Fort Worth basin. These correlations are defined by electric-log signatures, but correlations to core taken from the Standard Oil of Texas No. 4 Roberts well of Montague County gives some indication of the lithologies. As a result of the limited core availability of lower Paleozoic units, most of the interpretation of lithofacies is left to the discretion of the well-site geologist.

Because few wells have been drilled in this area through the upper portions of the Ellenburger Group, little was known of the lithologic characteristics of these Lower Ordovician and Cambrian strata. Petrographic analysis (Figs. 3,4) of drill cuttings was done in an effort to better understand the gross lithologies and general dia-



Figure 3. Photomicrographs of characteristic grain types that have escaped dolomitization. Dominant grain types include peloids, ooids, and quartz. Bar scale at top of figure is 250 μm and applies to all photomicrographs. All photos were made from cuttings of the Running High Ranch No. 6 well. *A,B*—Peloidal, dolomitic, lime grainstones exhibiting two stages of cementation, rim cement, and pore-filling cement, which were later dolomitized. In *B*, note that dolomitization obliterated more of the original fabric. *C*—Grainstone containing peloids, quartz grains, and few bioclasts. Note that this sample is still composed of calcite. *D*—Photo from oolitic mudstone showing concentric carbonate laminations about a quartz nucleus. The ooids in this interval were probably derived from a higher energy environment, such as a shoal. One of the informal lithofacies of the Ellenburger (Fig. 2) is an oolitic grainstone that is often oil productive. *E*—Lime mudstone specimen that has undergone dissolution of carbonate material at possible grain boundaries.



Figure 4. Photomicrographs of carbonate grains and porosity development within the Arbuckle equivalent lithologies. Bar scale at top of figure is 250 μm and applies to all photomicrographs. All photos were made from cuttings of the Running High Ranch No. 6 well. *A,B*—Dolomite "sand" from the "porous zone" at the base of the Cool Creek section. Note the intercrystalline porosity that develops between the coarse, euhedral dolomite grains. Much of the dolomite in *A* is an overgrowth over a more translucent core. *C*—Fine-grained dolomite with scattered development of intercrystalline porosity. The porosity development within this facies is not of reservoir quality. *D*—Dolomitic lime mudstone that has undergone dedolomitization. Note the apparent dolomite rhombs within the carbonate-mud matrix that have been replaced by calcite. Some porosity develops within this facies as a result of dissolution along the grain boundaries, probably during replacement.

TABLE 1. — LITHOLOGIC DESCRIPTIONS OF CAMBRO–ORDOVICIAN FORMATIONS ENCOUNTERED IN THE RUNNING HIGH RANCH NO. 1 WELL

Formation	Depth (ft)	Description
Ellenburger "A"	6,782–6,944	Dolomite, suc, wh & sdy; s/s/o.
Ellenburger "B"	6,944–7,183	Dolomite, tan, dns.
Ellenburger "C"	7,183–7,937	Dolomite & dol lm, tan, xln; dns w/ sli por sd & sdy dol strks.
Kindblade	7,937–8,650	Dolomite, tan, suc, xln & lm, dk brn, conts olv grn cht. Drlg brk @ 8,527–8,544, drld 2 min/ft.
Cool Creek	8,650–9,150	Dolomite, lt gry & tan, suc, xln, w/est. 10% chert & fn sd. Avg drlg time 3 min/ft. Very por zone 8,851–8,945, drld 1.5 min/ft.
McKenzie Hill	9,150–9,600	Lm, sdy, and dolo lm, suc. Avg drlg time 3 min/ft.
Signal Mountain	9,600–9,730	Lm, dk gry, shly & sh, dk gry to blk. Avg drlg time 6 min/ft.
Fort Sill	9,730–10,040	Lm & sdy lm & dolo, inc sd, fn to crs, w/depth. Avg drlg time 3 min/ft.
Honey Creek	10,040–10,213	Sd, fn to crs, & sdy lm, tan; conts glauc & pyr. Avg drlg time 3 min/ft.
Reagan/Hickory	10,213–10,464	Sd, fn to med, rnd; grad to crs lse qtz xls; V or near base. Good por w/no show.
Precambrian	10,464–10,621	Granite & grt wash or. TD: biotite, blk to dk grn; feld, wh to pnk & lt grn.

NOTE: Correlations of formations below the Ellenburger were made using southern Oklahoma terminology.

genesis of the sediments. The 2,500 ft of rocks encountered in the subsurface below the Ellenburger were correlated to formations of southern Oklahoma (Table 1) using both electric-log response and sample descriptions. Brief sample descriptions and correlations of the formations penetrated in the Running High Ranch No. 6, beginning with the Ellenburger "A" section, are given in Table 1.

Dominant lithologies of the Cambro–Ordovician section are limestones and dolomites which typically exhibit dramatic effects of diagenesis. Limestones in this section are most often dolomitized, and less frequently silicified. Within carbonate particles that have retained some of their original textures (Fig. 4), two early phases of cementation are demonstrated by first-generation, bladed calcite cements and subsequent, blocky, pore-filling calcite cements. Lithologies that retain most of the original depositional textures have lower porosity than those lithologies that have undergone extensive dolomitization. Silicification of limestone particles is minor and probably the result of chert replacing calcite in an early stage of diagenesis (Folk, 1965; Knauth, 1979).

Dolomitization of Cambro–Ordovician carbonates has been extensive throughout the north Texas region, contributing to the porosity and ultimate productivity of these formations. The dolomite fabrics are defined according to three crystal-size classifications: very fine-crystalline dolomite (<10 μm), fine- to medium-crystalline dolomite (10–100 μm), and coarse-crystalline dolomite (100–4,000 μm) (Kerans, 1990). The first two classes of crystal sizes comprise the majority of the dolomites in this area. Very fine- to medium-grained dolomites typically are dense and show little or no intercrystalline porosity in sample cuttings or thin sections. This fabric is interpreted to dominate the facies associated with low-energy restricted-shelf environments, which are thought to have been pervasive in this region (Kerans, 1990). The most important fabric in this area is the coarse-crystalline dolomite, which provides the most effective porosity for oil and gas reservoirs. In our wells drilled, the coarse dolomites acted as poorly cemented carbonate "sands," with well-developed intercrystalline porosity between the large, euhedral crystals.

The formations encountered in the Burns and Stine No. 1 correlate very well with those of the Running High Ranch No. 6. A very porous sandy dolomite section that was encountered at 8,447 ft, with drilling time at 1 min/ft, appears to correlate with the porous section encountered at 8,851 ft in the Running High Ranch No. 6. Complete returns were lost into this zone at 8,520 ft, and after spending five days attempting to restore returns and drilling to 8,595 ft with no returns, the well was abandoned.

Reservoir Quality

In contrast to some of the deep wells drilled in southern Oklahoma and north Texas, the Cambro–Ordovician lithologies encountered in the two wells of our project displayed considerable porosity in most of the samples from around –8,500 ft to the Precambrian, leading to some drilling problems. The principal zone of the Running High Ranch No. 6 well that has excellent potential for an oil and gas reservoir is the "porous zone" (Fig. 4) encountered at 8,851–8,945 ft, a zone considered equivalent to the base of the Cool Creek Formation. This interval was also encountered in the Burns and Stine No. 1 well, and other wells drilled to at least this depth in the county.

Porosity in this interval is probably the result of extensive dolomitization of a preexisting carbonate matrix and the subsequent development of intercrystalline porosity between the coarse, euhedral dolomite crystals. The size and appearance of these fine to coarse crystals often contributes to its reference as "sand" or sandy dolomite in sample descriptions, because of the separate crystal occurrences.

Another porous zone was indicated in the Reagan sand, from 10,213 to 10,464 ft. The nature of porosity development in this interval is not well known from these wells, because petrographic studies have not been conducted on the well cuttings. Further examination should include thin-section analysis to determine the grain-type/porosity relationships.

DEPOSITIONAL INTERPRETATION

The almost total lack of shale and dense limestone deposits leads us to believe that the formations in both of these tests were deposited in environments ranging from low- to high-energy restricted shelf to open-marine shallow shelves. Each of these environments is defined by the texture of the lithologies and the grains contained within. It is interpreted that the Ellenburger was deposited in the low- to high-energy restricted-shelf environment as is evidenced by the oolites, laminations, and burrowed dolostones that were identified in core and thin-section analysis. Most of the remaining formations are interpreted to have been deposited in open-marine to restricted-shelf conditions, due to the variable amounts of dolomite and limestone present. Refined interpretations of the depositional environments for the entire section can only be accomplished through further drilling and core analysis.

CONCLUSIONS

Oil exploration in north Texas has demonstrated that unforeseen drilling problems are possible within the deeper Cambro–Ordovician formations. Correlation of formations below the Ellenburger with Oklahoma stratigraphy are difficult because of the distances involved and the lack of data. High porosities occur in the lower part of the Cool Creek Formation due to extensive dolomitization and intercrystalline porosities. Future deep exploration should be centered on the occurrence of deeper, indigenous hydrocarbon-source rocks that could contribute significant amounts of oil and gas to the porous intervals. Our exploration has contributed to the data on the deeper formations of the Fort Worth basin, but continued investigations of the deeper portions of a mature oil region can often lead to the discovery of previously unknown reservoirs.

REFERENCES CITED

Folk, R. L., 1965, Some aspects of recrystallization in ancient limestones, *in* Pray, L. C.; and Murray, R. C. (eds.), Dolomitization and limestone diagenesis: Society of Economic Paleontologists and Mineralogists Special Publication 13, p. 14–48.

Kerans, Charles, 1990, Depositional systems and karst geology of the Ellenburger Group (Lower Ordovician), subsurface west Texas: University of Texas Bureau of Economic Geology Report of Investigations 193, 59 p.

Knauth, L. P., 1979, A model for the origin of chert in limestones: Geology, v. 7, p. 284–287.

Stratigraphy and Exploration of the Knox Group in the Appalachian Fold and Thrust Belt and Black Warrior Basin of Alabama

Dorothy E. Raymond and W. Edward Osborne
Geological Survey of Alabama

ABSTRACT.—The Cambrian–Ordovician Knox Group in Alabama is a thick cyclic sequence of carbonate rocks present in the outcrop and subsurface of the Appalachian fold-thrust belt, and in the subsurface of the Black Warrior basin and southern flank of the Nashville dome. In the Appalachian fold-thrust belt the Knox Group includes, in ascending order, the Copper Ridge Dolomite, Chepultepec Dolomite, Longview Limestone, Newala Limestone, and the Odenville Limestone. Exposures southeast of the Helena fault generally include the most complete sequences of the Knox Group preserved beneath the regionally developed post-Knox unconformity. Structures northwest of the Helena fault generally include less-complete and laterally variable Knox sequences; locally, only the lower part of the Knox is preserved beneath the post-Knox unconformity.

In the Black Warrior basin, the Knox Group occurs in the subsurface where it is generally undifferentiated. In the southern part of the basin, the post-Knox unconformity, which generally spans 10 million years or more, appears to be absent or of short duration.

The lower Knox consists primarily of cherty dolomite; however, limestone is predominant in the upper part of the Knox in the southern part of the Black Warrior basin and in the Appalachian fold-thrust belt east of the Helena fault. Carbonate cycles seen in core include subtidal to low supratidal sequences. The uppermost unit, the Odenville Limestone, is the deepest water and most open-marine unit of the Knox.

Porosity in the Knox apparently occurs primarily as fractures, subsurface solution features, and vugs in algal units. Drilling in the Knox has recently increased. Most wells are targeting the Knox of the southern Black Warrior basin or Knox in the leading edge of thrust sheets of the subsurface Appalachian fold-thrust belt along the southern margin of the basin beneath the Gulf Coastal Plain. In these thrust sheets, fractured Knox is juxtaposed against potential source rocks of Mississippian and Devonian age.

INTRODUCTION

The Cambrian–Ordovician Knox Group in Alabama is a thick (as much as 4,200 ft) sequence of cyclic carbonate rocks that is present in the outcrop and subsurface of the Appalachian fold-thrust belt and in the subsurface of the Black Warrior basin and southern flank of the Nashville dome (Fig. 1). Our present knowledge of the stratigraphy of the Knox Group in the fold-thrust belt is primarily the result of geologic mapping (Butts, 1910,1927,1940; Osborne, 1990,in press) and detailed stratigraphic studies (Sternbach, 1984; Batchelder, 1984; Hooks, 1985; Shaw, 1987; Roberson, 1988). Studies of the Knox Group in the Black Warrior basin have generally been more regional in scope (Thomas, 1972,1988; Kidd, 1975). The purpose of this paper is to summarize the existing knowledge of the stratigraphy of the Knox Group in the Appalachian fold-thrust belt and Black Warrior basin, and to discuss recent petroleum exploration of the Knox Group in Alabama.

STRATIGRAPHY AND STRUCTURAL SETTING

Appalachian Fold-Thrust Belt

The Appalachian fold-thrust belt consists of Paleozoic sedimentary rocks that were deformed into a series of thrust faults and thrust-related folds during the late Paleozoic Alleghenian orogeny (Fig. 2). In Alabama, the fold-thrust belt is bordered on the northwest by the Black Warrior basin (including the East Warrior platform) and Nashville dome, and on the southeast by metamorphic rocks of the Appalachian Piedmont. In central Alabama, the fold-thrust belt and Black Warrior basin plunge southwest beneath post-orogenic Mesozoic strata of the Gulf Coastal Plain. Subsurface data from wells drilled through the Coastal Plain indicate that the fold-thrust belt trends westward into Mississippi and curves northwestward and is continuous with the exposed Paleozoic Ouachita orogen in Arkansas (Thomas, 1973, 1985).

In the fold-thrust belt the Knox Group crops out in the core of major anticlines and within several large-scale thrust sheets (Fig. 2). The Helena fault in the central part of the thrust belt marks a fundamental change in the stratigraphy of the Knox Group. Exposures southeast of the Helena fault generally include the most complete sequences of the Knox Group. In contrast, structures northwest of the Helena fault include less complete Knox sequences, the upper part of the Knox having been removed by post-Knox erosion (Butts, 1926; Hooks, 1985; Roberson, 1988).

Helena Thrust Sheet

The Knox sequence is best exposed and has been most studied on the Helena thrust sheet in the central part of the fold-thrust belt. On the Helena thrust sheet the Knox

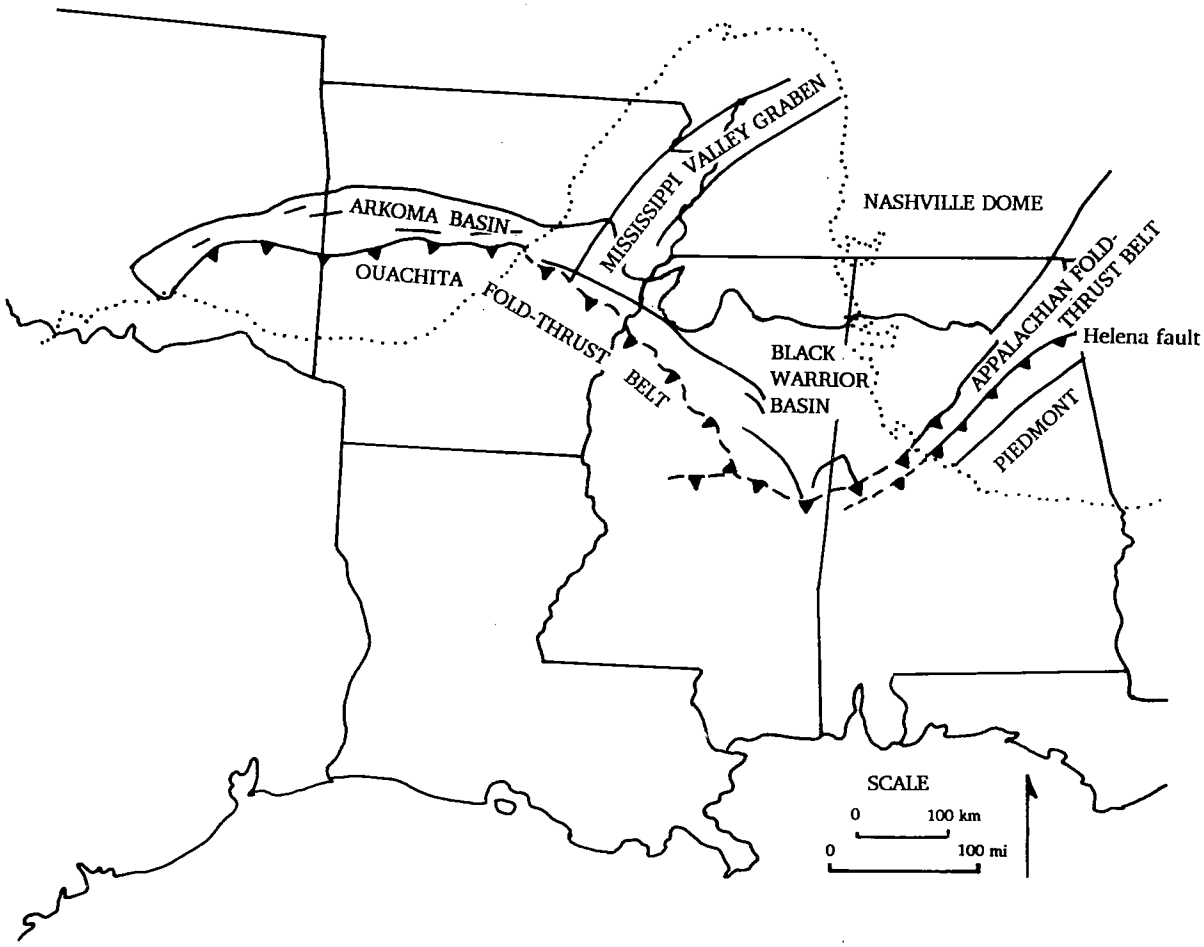


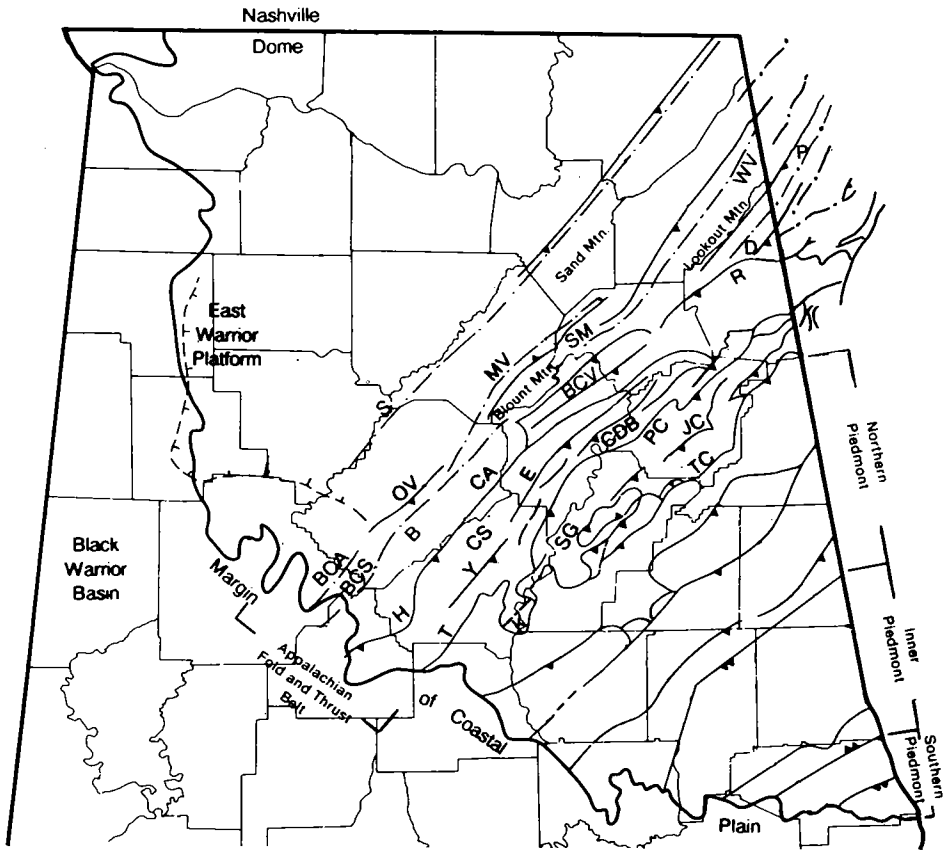
Figure 1. Location of the Appalachian fold-thrust belt and Black Warrior basin and the regional tectonic framework.

Group has been subdivided, in ascending order, into the Copper Ridge Dolomite, Chepultepec Dolomite, Longview Limestone, Newala Limestone, and Odenville Limestone (Fig. 3) (Butts, 1926,1927,1940; Osborne, in press). Although rocks of the Odenville Limestone were included within the Newala Limestone on the recent geologic maps of Alabama (Szabo and others, 1988; Osborne and others, 1989), recent work indicates that the Odenville is lithologically distinct and mappable, and Osborne (in press) has proposed that the Odenville be given formal status as the uppermost formation within the Knox Group.

The Copper Ridge Dolomite is the most poorly exposed unit within the Knox Group in Alabama. Although the Copper Ridge is well known by its abundant dense chert residuum, it is well exposed only along Alligator Creek in Bibb County (Butts, 1926; Batchelder, 1984). At Alligator Creek, the Copper Ridge consists of ~1,150 ft of finely crystalline dolomite (dolomitized mudstone), siliceous dolomite, and bedded stromatolitic chert (Fig. 4) (Batchelder, 1984). Limestone is conspicuously absent in the Copper Ridge. Although the Copper Ridge is best known for its dense stromatolitic chert residuum, cavernous chert similar to that characteristic of the overlying Chepultepec Dolomite is locally present in the Copper Ridge (Osborne, in press). In the central part of the Helena thrust sheet in Shelby County, the Copper Ridge is ~1,475 ft thick (Osborne, in press).

On the Helena thrust sheet the Chepultepec Dolomite is 1,375–1,520 ft thick and consists of a lower limestone-dominated sequence, a middle siliceous dolomite, and an upper thin limestone sequence (Butts, 1926; Batchelder, 1984; Osborne, in press). The limestones are predominantly peloidal and the dolomites are commonly thrombolitic (Batchelder, 1984). The middle part of the Chepultepec locally contains thin lenses and disseminated laminae of quartz sand (Batchelder, 1984). Thin-bedded to shaly limestones have been observed in the middle and upper part of the Chepultepec in the central part of the thrust sheet in Shelby County. Throughout the Helena thrust sheet the Chepultepec is recognized by an abundance of peculiar cavernous chert residuum that Butts (1926) referred to as "worm eaten" (Figs. 5,6). The origin of the cavernous chert is somewhat problematical, but it may represent either preferentially silicified burrows and/or thrombolites. Rounded nodular chert and bedded dense chert are also locally present within the Chepultepec (Osborne, in press).

The Chepultepec is overlain by the Longview Limestone, which ranges from ~200 to 500 ft thick (Butts, 1926; Hooks, 1985; Osborne, in press). The Longview is characterized by abundant peloidal limestone containing inter-



EXPLANATION

SCALE

0 10 20 Miles

Anticline

Thrust fault, teeth on upper plate

Margin of East Warrior Platform

Compound fault or fault with sense of displacement unknown

B	Birmingham anticlinorium	MV	Murphrees Valley anticline
BCA	Blue Creek anticline	OV	Opossum Valley fault
BCS	Blue Creek syncline	P	Peavine anticline
BCV	Big Canoe Valley fault	PC	Pell City fault
CA	Cahaba synclinorium	R	Rome fault
CDB	Coosa deformed belt	S	Sequatchie anticline
CS	Coosa synclinorium	SG	Sleeping Giants klippe
D	Dirtseller Mountain syncline	SM	Straight Mountain fault
E	Eden fault	T	Talladega fault system
H	Helena fault	WV	Wills Valley anticline
JC	Jacksonville fault complex	Y	Yellowleaf fault
K	Kelley Mountain window		

Figure 2. Outline structural geology map of north Alabama showing major structural features in the Appalachian fold-thrust belt (modified from Raymond and others, 1988).

bedded dolomite. Longview Limestone locally contains irregular mottled zones of dolomite. The Longview appears to contain more quartz sand than other units within the Knox Group; quartz sand is commonly present as disseminated grains, thin laminae, and, rarely, in thin beds (Fig. 7) (Hooks, 1985; Osborne, in press). Thin-bedded stromatolitic chert and nodular chert are common in the Longview and typically form abundant dense fragments in the residuum of the unit. Dessication features have been described in the Longview by Hooks (1985) and Osborne (in press). Both the limestone and the chert commonly contain specimens of the gastropod *Lecanospira* sp. (Butts, 1926; Osborne, in press) (Fig. 8).

On the Helena thrust sheet the Longview Limestone is

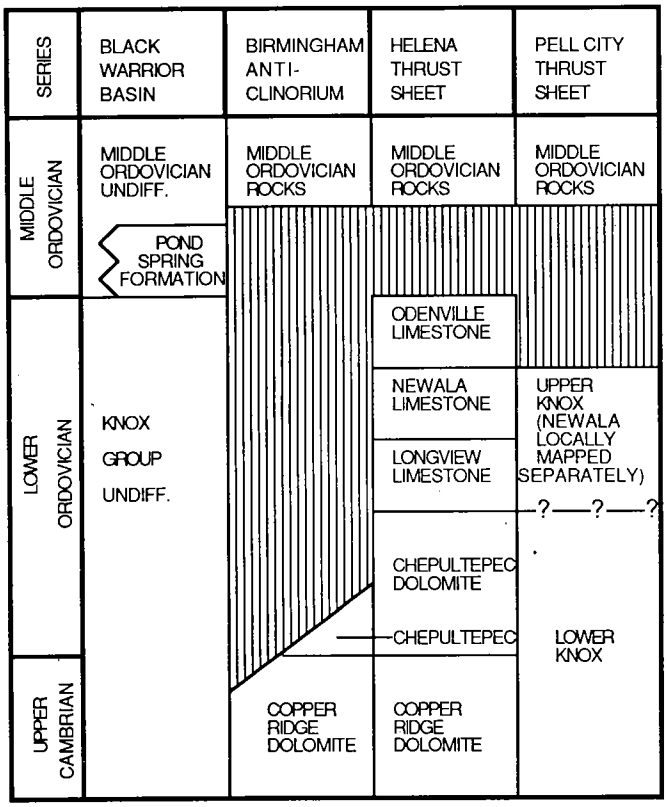


Figure 3. Comparison of the Knox Group stratigraphy in major structures of the Appalachian fold-thrust belt and the Black Warrior basin in Alabama.

overlain by the Newala Limestone. The Newala consists primarily of intraclastic peloidal packstone with intraclasts also composed of peloidal packstone (Puckett and others, 1990). Thin interbeds of laminated dolomite are locally common in the Newala (Fig. 9), and dolomite also occurs as preferentially dolomitized burrow fill in limestone (Puckett and others, 1990; Osborne, in press). Quartz sand is locally present as disseminated grains and thin laminae, and is most common in the lower part of the formation (Osborne, in press). The Newala is generally fossiliferous (Fig. 10), containing a fauna that includes gastropods, ostracods, brachiopods, and cephalopods. Of particular note is the relatively common occurrence of the operculum of the gastropod *Ceratopea* sp. (Butts, 1926; Osborne, in press). In the central part of the Helena thrust sheet the Newala ranges from ~500 to 1,000 ft thick (Osborne, in press). However, between the Helena and Rock Creek School faults at Pratt's Ferry, near the Coastal Plain overlap, the upper Newala is truncated by the post-Knox unconformity and there the Newala is only 200 ft thick (Hooks, 1985).

The Newala Limestone is overlain gradationally by the Odenville Limestone. Following the work of Roberson (1988), the Odenville includes a thin lower unit dominated by burrow-mottled dolomitic limestone and a thicker upper unit consisting of stylonodular fossiliferous limestone. The upper unit locally contains small irregular chert nodules, many of which are silicified sponges. In contrast to the depauperate fauna of the underlying Newala, the Odenville contains a stenohaline fauna that

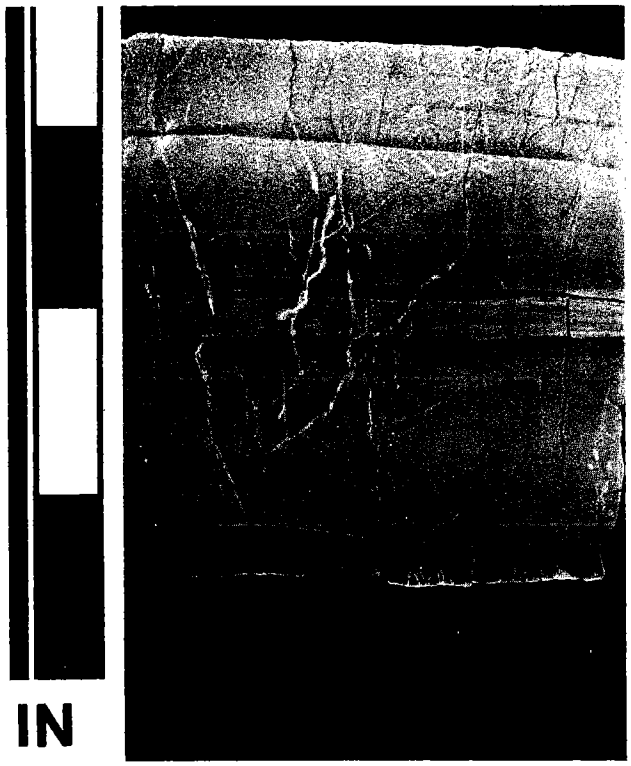


Figure 4. Laminated dolomudstone of the Copper Ridge Dolomite from Alligator Creek, Bibb County, Alabama (Helena thrust sheet).

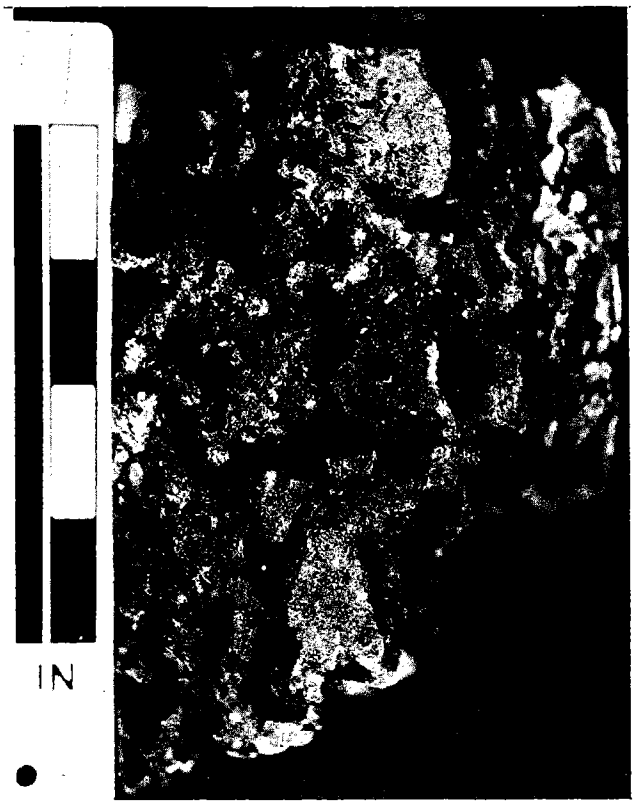


Figure 5. Cavernous chert of the Chepultepec Dolomite from Lake Purdy, Shelby County, Alabama (Helena thrust sheet).

includes lithistid sponges, brachiopods, cephalopods, gastropods, and trilobites (Fig. 11). The Odenville extends along the Helena thrust sheet from some point between Odenville and Fremont Gap, in St. Clair County, southwestward to the Coastal Plain overlap in Chilton County, reaching a maximum thickness of 366 ft (Roberson, 1988). Roberson attributed the thickness variation to variation in the magnitude of the post-Knox unconformity. In the area between the Helena fault and the Rock Creek School fault, in Bibb County, the Odenville is unconformably absent, and Middle Ordovician rocks directly overlie the Newala.

Structures Southeast of the Helena Thrust Sheet

The Knox Group is exposed in several structures southeast of the Helena thrust sheet, including the Coosa deformed belt, Kelley Mountain window area, Pell City thrust sheet, Coosa thrust sheet, and trailing edge of the fold-thrust belt (Fig. 2).

Coosa deformed belt and Coosa thrust sheet.—The Coosa deformed belt consists of numerous imbricate thrust slices of Ordovician through Mississippian rocks (Thomas and Drahovzal, 1974) (Fig. 2). Throughout most of the belt, thrust slices are detached at the stratigraphic level of the Newala Limestone or younger rocks, and the stratigraphy of the pre-Newala Knox is poorly known. The presence of Odenville has not been documented, but the unit could possibly be present within dark-colored stylonodular rocks that are presently mapped as Middle Ordovician. Where the northern part of the Coosa deformed belt trends into the Coosa thrust sheet, Adams and others (1926) mapped undifferentiated Copper Ridge and Chepultepec Dolomites, apparently because of the presence of abundant chert residuum. Cloud (1967) recognized Copper Ridge, Chepultepec, and Longview and Newala Limestones [undifferentiated] in the Coosa thrust sheet, and documented their presence biostratigraphically with collections of fossils that are characteristic of the formations.

Kelley Mountain window.—At the southwest end of the Coosa deformed belt the Knox Group is exposed within and adjacent to the Kelley Mountain window (Fig. 2). In this area Butts (1940) mapped the Copper Ridge Dolomite, Chepultepec Dolomite, and Newala Limestone, and suggested that the Longview Limestone is probably present within the areas mapped as Chepultepec and Newala. Recently, W. E. Osborne and G. M. Guthrie have discovered outcrops of the Odenville Limestone within the window, thus documenting the presence of the entire Knox sequence in this area.



Figure 6. Fresh surface of cavernous cherty dolomite from the Chepultepec Dolomite at Lake Purdy, Shelby County, Alabama (Helena thrust sheet).



Figure 7. Sandy intraclastic limestone near the Newala Limestone–Longview Limestone contact, Pelham, Shelby County, Alabama (Helena thrust sheet).



Figure 8. *Lecanospira* sp. in chert, Longview Limestone at Pelham, Shelby County, Alabama (Helena thrust sheet).

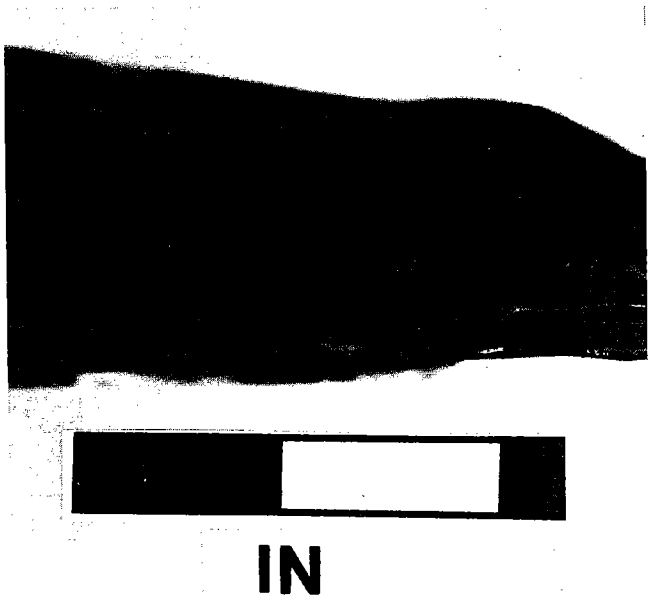


Figure 9. Laminite in the Newala Limestone at Pelham, Shelby County, Alabama (Helena thrust sheet).

Pell City thrust sheet.—The most areally extensive exposure of the Knox Group in Alabama is within the Pell City thrust sheet, a large-scale low-angle thrust sheet in the eastern part of the fold-thrust belt (Fig. 2). The thrust sheet mostly includes the lower cherty part of the Knox Group, and, apparently based on that observation, Butts (1926) suggested that the sequence in the thrust sheet includes the Copper Ridge and Chepultepec Dolomites. However, during recent mapping by Osborne (1990), numerous exposures of fresh rock were discovered, and the details of the stratigraphy do not support Butts' interpretation. The Knox Group in the central part of the thrust sheet is ~3,000 ft thick and can be subdivided into a lower unit, characterized by cherty dolomite and minor interbedded limestone, and an upper unit consisting of less siliceous dolomite and more abundant limestone (Fig. 3) (Osborne, 1990). In addition, massive dense stromatolitic chert typical of the Copper Ridge (Fig. 12) appears to be present at several stratigraphic horizons within the lower Knox in the area. Thus, the occurrence of limestone in the lower Knox and the difference in stratigraphic occurrence of chert indicate that this nomenclature can not be successfully applied in this area. The lower Knox of Osborne (1990) may grossly correspond to the Copper Ridge and Chepultepec Dolomites, whereas the upper Knox may correlate with the Newala and Longview Limestones. The Newala has been mapped separately in the Pell City thrust sheet in the Harpersville area (Thomas and Drahovzal, 1974).

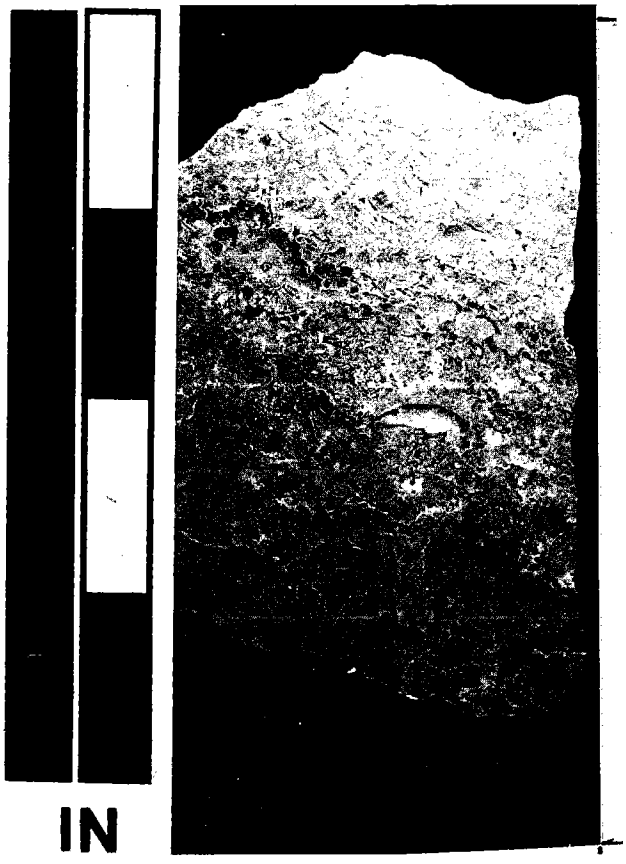


Figure 10. Fossiliferous limestone (primarily gastropods), Newala Limestone at Pelham, Shelby County, Alabama (Helena thrust sheet).

Trailing edge of the fold-thrust belt.—The Knox Group is exposed in the trailing edge of the fold-thrust belt in the footwall of the Talladega fault system (Fig. 2). Adams and others (1926) mapped the areas as "Cambrian or Ordovician dolomite," apparently recognizing that the dolomite-facies equivalents of the upper part of the underlying Conasauga Formation are locally present. Recently, Guthrie (1989) subdivided the Knox Group in this area into two units: the Copper Ridge Dolomite and the upper Knox Group undifferentiated. Guthrie suggested that the upper Knox Group probably includes the Chepultepec Dolomite and Longview Limestone and that the Newala Limestone is not present in the area. The absence of Newala may be due to structural truncation by the Talladega fault.

In addition to the exposures of the Knox Group in the trailing edge of the fold-thrust belt, Knox equivalents are also present within the Sylacauga Marble belt in the hanging wall of the Talladega fault (Tull, 1985). Conodonts collected from the upper part of the marble sequence suggest that the marble belt includes rocks as young as the Newala Limestone (Harris and others, 1984).

Structures Northwest of the Helena Thrust Sheet

Northwest of the Helena thrust sheet the Knox Group is exposed primarily in the cores of large-scale anticlines, including the Birmingham anticlinorium, trailing edge of the Big Canoe Valley thrust sheet, Peavine anticline, Murphrees Valley anticline, Wills Valley anticline, and Sequatchie anticline (Fig. 2). An important charcteristic of the Knox Group northwest of the Helena fault is the lateral variability of Knox units preserved beneath the post-Knox unconformity (Roberson, 1988).

Birmingham anticlinorium.—The Knox is exposed in a number of outcrop belts within the structurally complex Birmingham anticlinorium (Figs. 2,3). Butts (1926) stated that the Chepultepec and younger formations are unconformably absent in the Birmingham area, and indicated that Middle Ordovician rocks directly overlie the Copper Ridge Dolomite. Subsequent geologic mapping in the area (Hooks, 1961; Kidd, 1979; Szabo and others, 1988) generally supported Butts' interpretation, primarily because rocks fitting the few descriptions of Chepultepec and younger Knox rocks had not been seen in the area (in particular the lower limestone sequence in the Chepultepec). Recent workers (Sternbach, 1984; Hooks, 1985) have interpreted the presence of the Chepultepec on the southeast flank of the anticlinorium based on observations from cores drilled by Humble Oil and Refining Co. Rocks interpreted to be Chepultepec include collapse breccias, partly calcareous cherty dolomite, and chert.

Trailing edge of the Big Canoe Valley thrust sheet.—The Knox is exposed along the trailing edge of the Big Canoe Valley thrust sheet on Barker, Canoe Creek, and Hensley Mountains (Fig. 2). In addition to the Copper

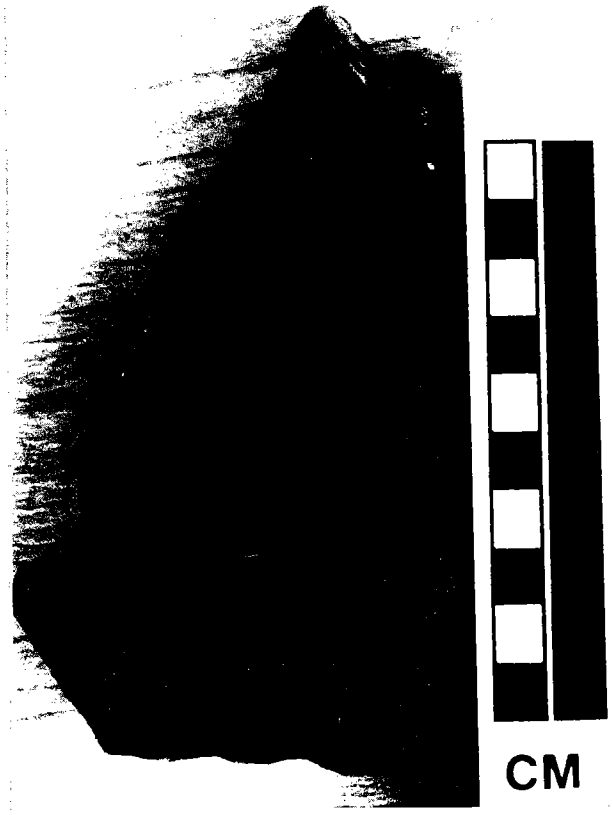


Figure 11. Tabular and cylindrical sponges and trilobites, Odenville Limestone at Shephard Branch, Jefferson County, Alabama (Helena thrust sheet).



Figure 12. Small fragment of stromatolitic chert block similar to Copper Ridge chert, Lincoln, Talladega County, Alabama (Pell City thrust sheet).

Ridge and Chepultepec Dolomites, Neathery (1968) reported that the Longview Limestone is preserved beneath the post-Knox unconformity.

Peavine anticline and adjacent stuctures.—Butts (1926) indicated that in the Broomtown Valley in the core of the Peavine anticline (Fig. 2) only the Copper Ridge is preserved beneath the post-Knox unconformity. Little is known about the Knox sequence in structures southeast of the Peavine anticline in Alabama.

Murphrees Valley anticline.—In the core of the Murprees Valley anticline (Fig. 2) the Knox Group includes the Copper Ridge and Chepultepec Dolomites. The Chepultepec was named for exposures within Murphrees Valley at Chepultepec (Butts, 1926); the community is now called Allgood. Interestingly, rocks presently exposed at Chepultepec bear little resemblance to the Chepultepec in the Helena thrust sheet where Butts (1926) indicated that it is best exposed. The cherty carbonate sequence exposed at Allgood is entirely dolomite and chert (Fig. 13), and very little cavernous chert is present. Apparently Butts (1926, p. 87) defined Chepultepec as the type area of the unit primarily because it was the most fossiliferous locality known to him. The Longview and Newala Limestones have not been observed in the Murphrees Valley anticline, and Middle Ordovician rocks apparently directly overlie the Chepultepec.

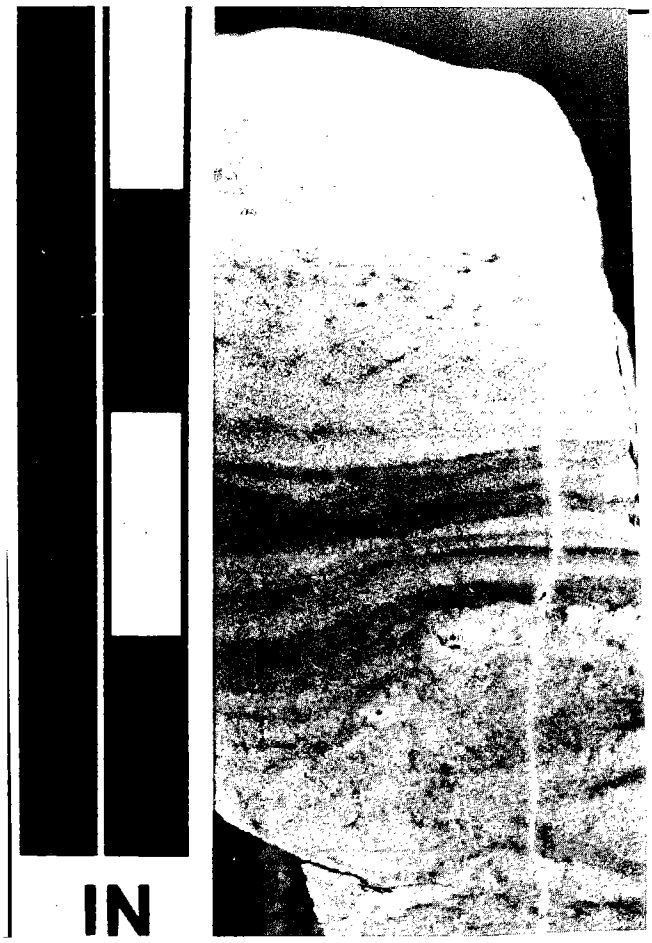


Figure 13. Laminated dolomite of the Chepultepec Dolomite at the type locality, Blount County, Alabama (Murphrees Valley anticline)

Wills Valley anticline.—The stratigraphic sequence of the Knox in the core of the Wills Valley anticline (Fig. 2) is somewhat problematical. In addition to the Copper Ridge and Chepultepec Dolomites, Butts (1926) suggested that dolomite exposed in Big Wills Creek in the core of the Wills Valley anticline may be either Longview or Newala Limestone. Later, Neathery (1968,1988) indicated that the Longview can be recognized at least locally, but suggested that rocks at the approximate stratigraphic level of the Newala more closely resemble the Kingsport and Mascot Formations (upper Knox) at their type locality in Tennessee. Both Thornton Neathery and Berry Tew reported (personal communication to Keith Roberson, 1986) compact "dove-colored" lime mudstone typical of the Newala in the Wills Valley anticline. In Dade County, Georgia, in the extension of the Wills Valley anticline, oil and gas test wells have reportedly penetrated the Newala Limestone (Coleman, 1988).

Sequatchie anticline.—The Sequatchie anticline is the northwesternmost large-scale structure in the fold-thrust belt of Alabama, and the Knox Group in the core of the anticline presumably is similar to the Knox in the subsurface on the southeastern flank of the Nashville dome (Fig. 2). Unfortunately, we know very little about the Knox exposed within the structure. Butts (1926) reported that both the Chepultepec Dolomite and Longview Limestone are exposed in the Sequatchie Valley in Alabama. Structural relief of the anticline in Alabama is apparently not sufficient to expose the lowermost Knox. The Newala has not been reported in the area.

Biostratigraphy

The biostratigraphy of the Knox Group in the fold-thrust belt in Alabama has not been studied in detail. However, enough work has been done to establish a gross biostratigraphic framework (Fig. 3). With the exception of fossil algae, fossils are very rare in the Copper Ridge Dolomite. Butts (1926) noted a few locations in the fold-thrust belt in Alabama where fossil gastropods and trilobites have been collected. In particular, the gastropod *Scaevogyra* sp. has been collected from two locations in Alabama (Butts, 1926), indicating assignment of at least part of the Copper Ridge to the *Scaevogyra* zone of the Upper Cambrian (Resser, 1938).

Fossils are locally common in the Chepultepec. Butts (1926) illustrated several species of gastropods and one cephalopod that are characteristic of the Chepultepec. Although Butts assigned the Chepultepec to Ulrich's proposed "Ozarkian system," Resser (1938) indicated that the faunas of the Chepultepec are equivalent to faunas contained in rocks that overlie the Upper Cambrian in the central and western United States. Consequently, the Chepultepec is assigned to the lower part of the Lower Ordovician.

The Longview is sparingly fossiliferous, and the gastropod *Lecanospira* is by far the most important fossil. Although not particularly abundant at any locality, *Lecanospira* is essentially ubiquitous and has been found at many locations in the fold-thrust belt in Alabama. The *Lecanospira* fauna establishes correlation with numerous

other Lower Ordovician stratigraphic units in the United States (Butts, 1926).

The Newala is commonly fossiliferous, and fossils are locally abundant. Butts (1926) illustrated numerous specimens of gastropods, brachiopods, and cephalopods, and, on the basis of these assemblages, correlated the Newala with rocks of "Beekmantown age" (Lower Ordovician) in the central Appalachians. Of particular interest is the occurrence of the operculum of the gastropod *Ceratopea*. *Ceratopea* is widespread in Lower Ordovician rocks in North America (Yochelson and Bridge, 1957) and is considered to be a guide to the middle and upper part of the Lower Ordovician Series (Twenhofel and others, 1954). *Ceratopea* is relatively common in the Newala in Alabama. Unfortunately, the genus has not been methodically collected and identified. On the basis of all reported faunas, Twenhofel and others (1954) assigned the Newala to the middle part of the Canadian Series of the Ordovician System. More recently, Shaw (1987) assigned the Newala a very latest "medial" Canadian to early late Canadian age based on conodont elements.

On the basis of a brachiopod assemblage found in the residuum of the limestone in the Cahaba Valley (Ulrich and Cooper, 1938, pl. 58), the Odenville has been dated as latest Canadian (late Early Ordovician) (Twenhofel and others, 1954). This is consistent with the late Early Ordovician age assigned to the gastropod *Teiichispira* (Yochelson and Jones, 1968), which is commonly present in the Odenville. Samples from the middle part of the upper Odenville yield a diverse and abundant conodont fauna that belongs to the *Jumodontus gananda* Subzone of the *Oepikodus communis* Zone (upper Fauna E) of very latest Canadian (latest Early Ordovician) age (personal communication from Thomas Shaw, Anita Harris, and John Repetski to Keith E. Roberson, 1985, cited in Roberson, 1988). Samples from the uppermost beds of the Odenville yield an abundant but less diverse conodont fauna that belongs either to the *J. gananda* Subzone of the *O. communis* Zone, or to lower Fauna 1½ of Sweet and others (1971), indicating an age of very latest Canadian (latest Early Ordovician) or earliest Whiterockian (earliest Middle Ordovician) (personal communication from Randal Orndoff and John Repetski to Keith E. Roberson, 1986, cited in Roberson, 1988). Thus, the available biostratigraphic data indicate a very latest Canadian (latest Early Ordovician) age for the bulk of the Odenville, and the uppermost beds may be as young as earliest Whiterockian (earliest Middle Ordovician). As such, the Odenville is the youngest sequence of rocks preserved beneath the post-Knox unconformity in the southern Appalachians.

BLACK WARRIOR BASIN

The Black Warrior basin is a triangular-shaped foreland basin in Alabama and Mississippi that is bounded on the north by the Nashville dome and the Ozark uplift, on the south and east by the Appalachian fold-thrust belt, and on the southwest by the buried Ouachita front (Fig. 1). To the west, the Black Warrior basin is separated from the Arkoma basin by a SW-plunging Paleozoic arch and fault system, the Mississippi Valley graben (Thomas, 1988).

Paleozoic sedimentary rocks of the basin range from Cambrian to Pennsylvanian in age. The Cambrian rocks unconformably overlie Precambrian crystalline basement rocks (Kidd, 1975; Neathery and Copeland, 1983). In the western part of the basin, the Paleozoic rocks are buried beneath Mesozoic and Cenozoic sediments of the Gulf Coastal Plain.

The Black Warrior basin is a SW-dipping homocline (Fig. 14) that is broken by a system of NW-trending normal faults that are generally down to the southwest. The fault system, which may extend westward into the Arkoma basin, displaces rocks as young as earliest Middle Pennsylvanian.

Sediments overlying crystalline basement in the basin include a basal clastic unit of Cambrian age comprised of the Rome and Conasauga Formations, a carbonate sequence of Cambrian to Ordovician age comprised of the Knox Group and overlying Middle and Upper Ordovician carbonates, and a thick mixed clastic and carbonate sequence of Silurian to Pennsylvanian age.

Upper Cambrian and Lower Ordovician carbonate rocks assigned to the Knox Group are generally unconformably overlain by Middle Ordovician limestone. This pre-Middle Ordovician unconformity is present throughout the craton and in the Appalachian fold-thrust belt. In the Plateaus to the north and in the northern part of the Black Warrior basin, the Knox is unconformably overlain by the Pond Spring Formation of the Stones River Group. The contact between the Middle and Lower Ordovician becomes less distinctive to the south and west in the basin, and the position of the boundary between Lower and Middle Ordovician strata is generally uncertain.

Alberstadt and Repetski (1989) studied the subsurface Ordovician of Alabama, Mississippi, and Arkansas and found that sedimentation probably was continuous in the southern Black Warrior basin and Arkoma basin from the Early to Middle Ordovician and that the Whiterockian is represented. Therefore, if there is an unconformity, it was of short duration in this area.

In the subsurface of the Black Warrior basin, the Knox Group is generally undifferentiated, although the Copper Ridge and Chepultepec Dolomites have been tentatively identified in some wells. Upper Cambrian and Lower Ordovician carbonate rocks assigned to the Knox Group in the subsurface of the basin typically consist of light-gray to light-brownish-gray dolomite, dolomitic limestone, and limestone that characteristically contains fine to medium, rounded, frosted quartz sand, ghosts of radial ooids, euhedral quartz, algal stromatolites, and chert (Alberstadt and Repetski, 1989). Much of the Knox shows characteristics of having formed in a restricted hypersaline environment on a carbonate shelf. These carbonate rocks represent a period of maximum transgression of the sea.

In the Black Warrior basin, the top of the Knox has been picked at several different horizons. Throughout the northern part of the basin in Alabama, the top of the Knox is distinct and is picked at the base of the Pond Spring Formation of the Stones River Group. However, to the south, deeper in the basin where the Pond Spring is not recognizable and limestone is interbedded with dolomite, there has been some variation in the horizon chosen as the top of the Knox. In this area there is generally a sequence, going downward, of limestone, dolomite, limestone, and dolomite (Fig. 15). Mellen (1972) and Kidd

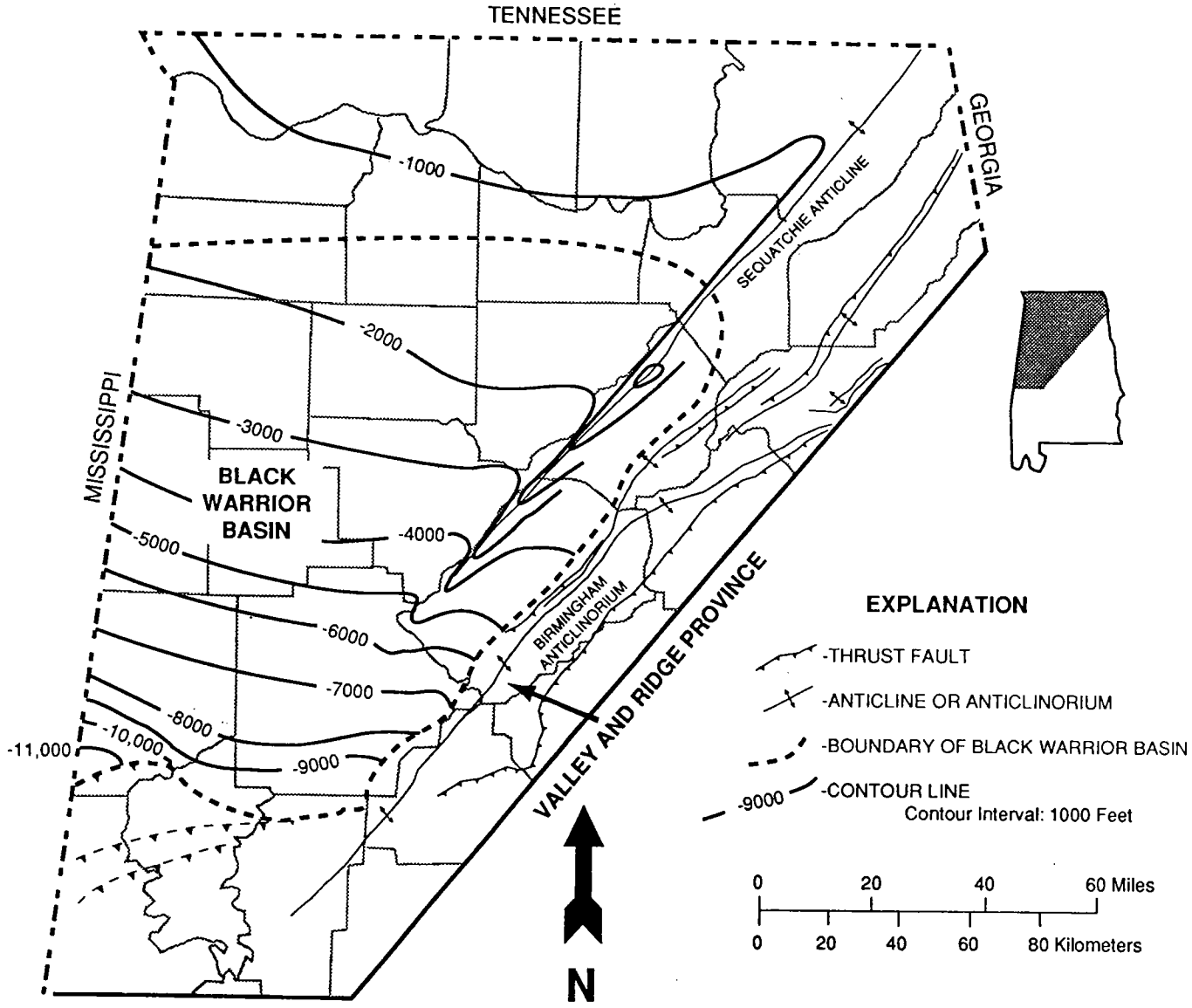


Figure 14. Structure map of top of the Knox Group in the Black Warrior basin (modified from Kidd, 1975).

(1975) placed the Knox at the top of the first or upper dolomite (the "Snow zone"). This pick is commonly used by the petroleum industry. R. W. Harris (*in* Mississippi Geological Society, undated) and Thomas (1972), on the basis of ostracods, placed the top of the Knox in a well in northeast Mississippi at the base of a sandy carbonate unit and at the top of the lower or second dolomite. Alberstadt and Repetski (1989), on the basis of a study of conodonts and Lower Ordovician sponges and algae, determined the top of the Lower Ordovician to be essentially the base of the first dolomite (within the second limestone) in northeastern Mississippi. They found the limestone to contain an Early Ordovician conodont fauna characteristic of the Odenville Limestone.

In the subsurface of the Appalachian Plateaus north of the Black Warrior basin the Knox is predominantly dolomite. Southward into the basin, limestone progressively dominates the section. In the southernmost part of the basin, the Lower Ordovician part of the Knox is dominantly limestone, whereas the Cambrian Copper Ridge is dolomite. The Knox is dominantly dolomite in the eastern part of the basin.

CORE OF THE KNOX GROUP

Most knowledge of the Knox in Alabama has come from the study of outcrops and well cuttings. Because of the highly weathered nature of the Knox, it is rarely well preserved in outcrop. Cuttings also provide a somewhat veiled view of the Knox. Core gives a good look at fresh, unweathered Knox and provides the opportunity for a look at depositional features and cycles.

The Geological Survey of Alabama has core from about a dozen different wells and industrial core tests. Most of these are shallow cores from the Knox in the Appalachian fold-thrust belt in Shelby and Tuscaloosa Counties. Core is also available from deep test wells in Shelby County and Greene County.

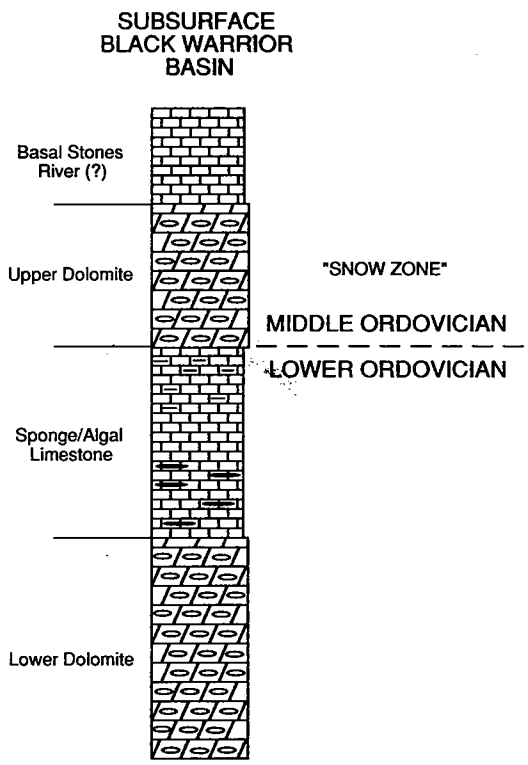


Figure 15. Representative subsurface section illustrating the top of the Lower Ordovician (Knox) in the Black Warrior basin of Alabama and Mississippi (modified from Alberstadt and Repetski, 1989).

Core is not available at present from the Odenville Limestone, the uppermost unit of the Knox. Therefore, a photomicrograph of Odenville from New Hope Church, Shelby County, is shown in Figure 16. The argillaceous and stylonodular nature of the unit is evident. Also, the occurrence of fossiliferous units containing the alga(?) *Nuia*, trilobites, ostracods, echinoderms, and sponges is typical of the formation. The Odenville was deposited in the deepest water and most open-marine environment of all the Knox units. *Nuia*, algae, and sponge spicules have been reported from an equivalent facies in the Black Warrior basin, which serves as a useful marker for the top of the Knox where present and recognizable.

The Newala Limestone is present in several industrial cores from Shelby County. Figure 17 illustrates a peloidal/intraclastic grainstone to packstone from a depth of 55 ft in the Newala in the Vulcan Materials Calera 6011 core in Shelby County. Figure 18 is a photomicrograph of a peloidal/intraclastic packstone from a depth of 118 ft in the same core.

One of the most distinctive features of the Longview Limestone is the presence of sand in the formation. Figure 19 illustrates a sandy intraclastic grainstone from a depth of 7,114 ft in the ARCO/Anschutz Alabama Property Co. 15-11, No. 1, in Shelby County. Well-rounded, medium quartz sand comprises ~15% of the grains in the grainstone illustrated. Silicified mudstone is also characteristic of the Longview, weathering to the typical blocky chert of the formation. A photomicrograph of silicified mudstone from a depth of 7,086 ft in the ARCO/Anschutz



Figure 16. Photomicrograph of the Odenville Limestone from New Hope Church, Shelby County, Alabama (Helena thrust sheet). Note the stylonodular nature of the unit. Fossils include trilobites, ostracods, and *Nuia*. Dolomite rhombs are concentrated in the stylolites. Ordinary light; bar scale is 0.5 mm.

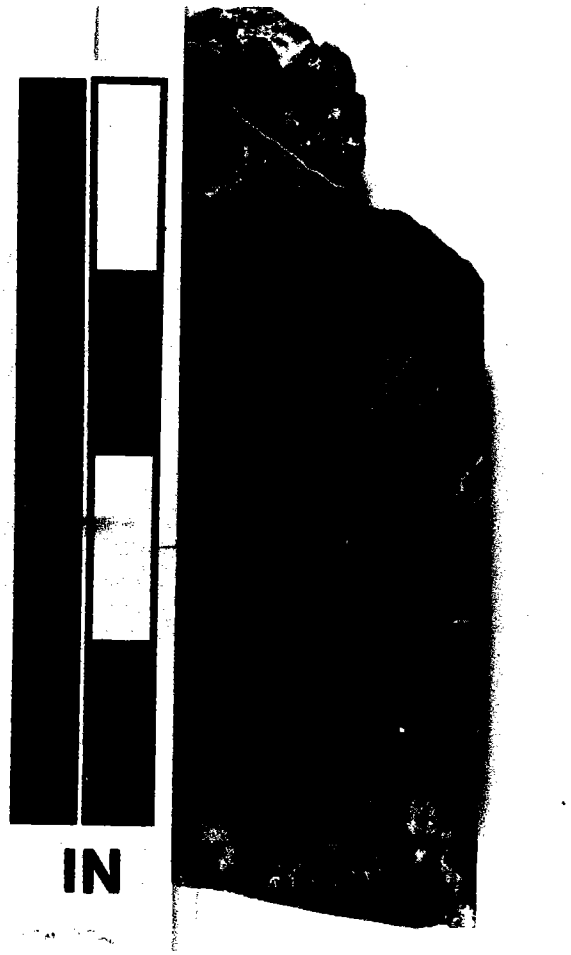


Figure 17. Peloidal/intraclastic grainstone to packstone of the Newala Limestone from a depth of 55 ft in the Vulcan Materials Calera 6011 core in Shelby County, Alabama (Helena thrust sheet). Note the stylolite; stylolites are common in the Newala.

core is shown in Figure 20. Micrite containing scattered quartz silt, calcite, and dolomite inclusions has been replaced by microcrystalline silica (chert). Fractures in the rock are filled with blocky calcite and dolomite.

Figure 21 is a photomicrograph of an intraclastic grainstone from a depth of 7,084 ft in the Longview in the ARCO/Anschutz core. Subrounded intraclasts include mudstone and peloidal packstones. The cement is a mixture of granular and blocky calcite and a small amount of blocky dolomite.

The Chepultepec Dolomite is comprised primarily of intertidal and subtidal facies and also includes low supratidal facies. Figure 22 illustrates a burrow-mottled/thrombolitic(?) unit characteristic of parts of the Chepultepec, especially in outcrop in the Helena thrust sheet. Selective dolomitization and silicification of such units and weathering on exposure may result in the cavernous chert that is typical of the Chepultepec. A photomicrograph of calcareous and dolomitic chert (Fig. 23) from 450 ft in the Humble Southern Cement Core Hole No. 3 illustrates patchy dolomitization and silicification that also may result in the development of porous cavernous chert.

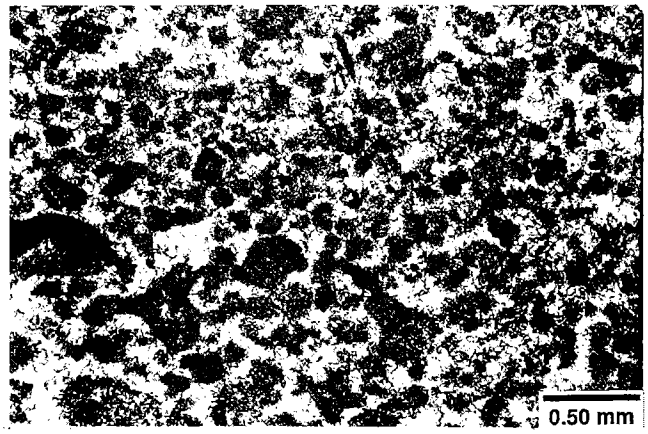


Figure 18. Photomicrograph of peloidal/intraclastic packstone of the Newala Limestone from a depth of 118 ft in the Vulcan Materials Calera 6011 core in Shelby County, Alabama (Helena thrust sheet). Ordinary light; bar scale is 0.5 mm.



Figure 19. Sandy intraclastic grainstone from a depth of 7,114 ft in the ARCO/Anschutz Alabama Property Co. 15-11, No. 1 in Shelby County, Alabama (fold-thrust belt).

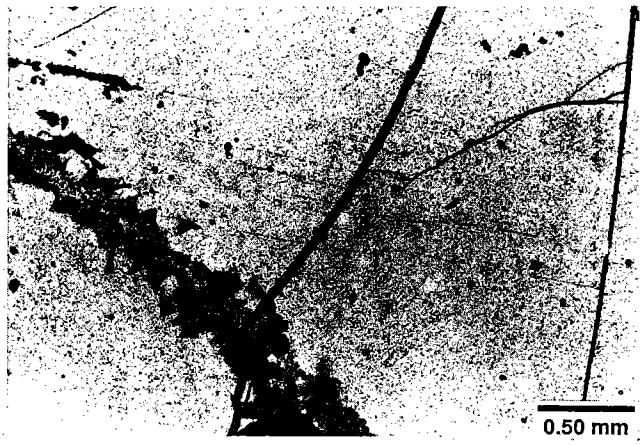


Figure 20. Photomicrograph of silicified mudstone of the Longview Limestone from a depth of 7,086 ft in the ARCO/Anschutz Alabama Property Co. 15-11, No. 1 in Shelby County, Alabama (fold-thrust belt). Fractures are filled with dolomite, and quartz sand (light spots) and dolomite rhombs (dark) are scattered throughout the rock. Ordinary light; bar scale is 0.5 mm.

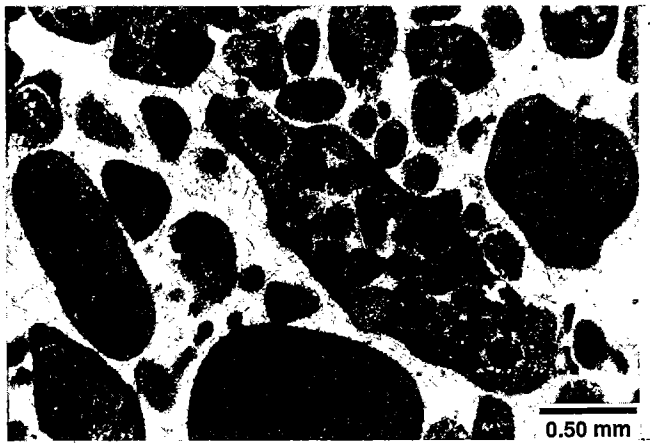


Figure 21. Photomicrograph of an intraclastic grainstone in the Longview Limestone from a depth of 7,084 ft in the ARCO/Anschutz Alabama Property Co. 15-11, No. 1 in Shelby County, Alabama (fold-thrust belt). Ordinary light; bar scale is 0.5 mm.

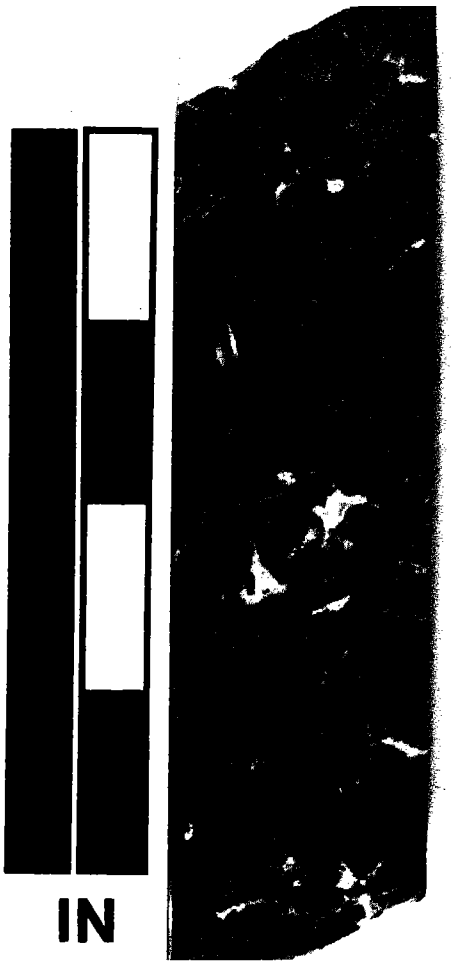


Figure 22. Burrow-mottled/thrombolitic(?) cherty dolomite of the Chepultepec Dolomite from a depth of 480 ft in the Humble Southern Cement Core Hole No. 3 in Shelby County, Alabama (Birmingham anticlinorium).

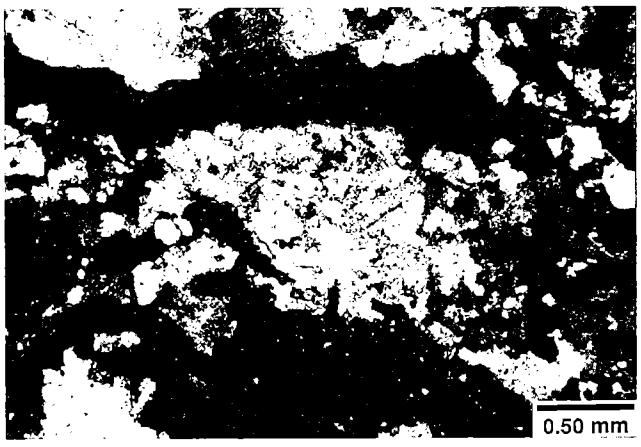


Figure 23. Photomicrograph of calcareous and dolomitic chert of the Chepultepec Limestone from a depth of 450 ft in the Humble Southern Cement Core Hole No. 3 in Shelby County, Alabama (Helena thrust sheet). Crossed nicols; bar scale is 0.5 mm.

Figure 24 shows a fossiliferous packstone/wackestone from the Chepultepec which contains abundant mud-filled low-spired gastropods.

The Copper Ridge Dolomite is primarily comprised of intertidal and low-supratidal facies, although subtidal facies are also present. Figure 25 shows core from an algally laminated unit (high-intertidal) from a depth of 2,170–2,180 ft in the Humble Southern Cement Core Hole No. 3 in Shelby County. A photomicrograph of a similar laminated dolomite at a depth of 2,420 ft in the same core hole is given in Figure 26. "Patterned dolomite" associated with the finely laminated stromatolitic facies is illustrated in Figure 27. This facies is thought to represent low-supratidal deposition. Figure 28 illustrates vuggy porosity in a thrombolitic(?) unit of the Copper Ridge at a depth of 11,019 ft in the ARCO/Amoco et al., No. 1 Ethel M. Koch in Greene County. Such porosity is commonly associated with thrombolitic and stromatolitic units in the Chepultepec and Copper Ridge.

The Copper Ridge is characterized by dense chert in outcrop. In the subsurface in the fold-thrust belt in Shelby County, the presence of megaquartz is a criterion that may be used to help identify the Copper Ridge in well cuttings. Megaquartz in dolomite of the Copper Ridge is illustrated in the photomicrograph of Figure 29. Stern-

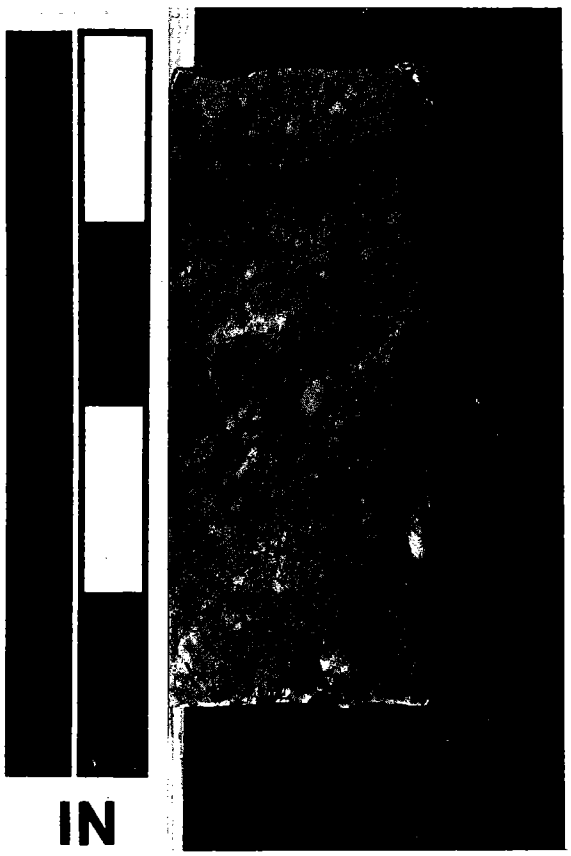


Figure 24. Fossiliferous intraclastic packstone/wackestone from the Chepultepec Dolomite at a depth of 1,010–1,020 ft in the Humble Southern Cement Core Hole No. 3 in Shelby County, Alabama (Helena thrust sheet). Clasts include abundant gastropods filled with carbonate mud and elongated mud intraclasts.

bach (1984) attributes the presence of megaquartz to the replacement of sulfate in the shallow subsurface mixing zone of terrestrial and marine waters.

Figure 30 is a photomicrograph of an intraclastic-oolitic packstone that occurs at a depth of 720 ft in the Humble Claude L. Griffin Core Hole No. 1C in Tuscaloosa County. The highly fractured nature of the rock is typical of the Copper Ridge. Also characteristic of the Copper Ridge are collapse breccias caused by either penecontemporaneous or postdepositional solution development. Figure 31 illustrates a collapse breccia from a depth of 1,170 ft in the Humble Claude L. Griffin Core Hole No. 1C in Tuscaloosa County. Often these breccias may contain a mud matrix filling porosity (Hooks, 1985).

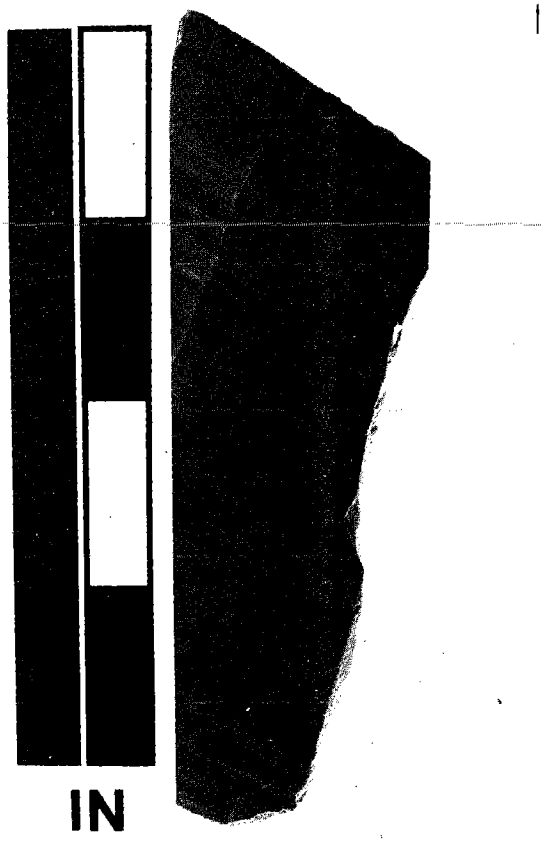


Figure 25. Stromatolitic laminated dolomite of the Copper Ridge Dolomite at a depth of 2,170–2,180 ft in the Humble Southern Cement Core Hole No. 3 in Shelby County, Alabama (Helena thrust sheet).

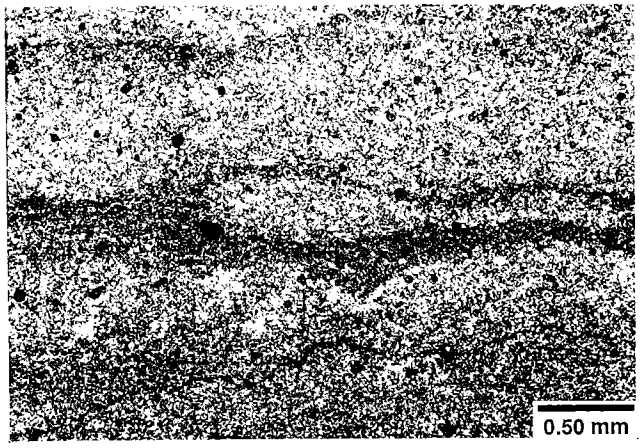


Figure 26. Photomicrograph of algally laminated dolomite of the Copper Ridge Dolomite from a depth of 2,420 ft in the Humble Southern Cement Core Hole No. 3 in Shelby County, Alabama (Helena thrust sheet). Ordinary light; bar scale is 0.5 mm.

PETROLEUM EXPLORATION IN THE KNOX GROUP

Exploration for petroleum in the Alabama Knox Group has been concentrated in the Appalachian fold-thrust belt in the past. Objectives included shallow, upper thrust-sheet traps that could contain low-pressure gas in fractured reservoirs and deep lower traps expected to have high-pressure gas and condensate. In the last 10 years, several unpermitted stratigraphic test holes and a few permitted wells have been drilled in the Appalachian trend in Alabama; however, no wells have yet been completed in the Knox.

Production History

Knox production has been reported from Alabama and adjoining Tennessee and Mississippi. In 1983, gas was discovered in the Amoco-Anschutz No. 1 Reed well in the Knox Group of the Appalachians in Hancock County,

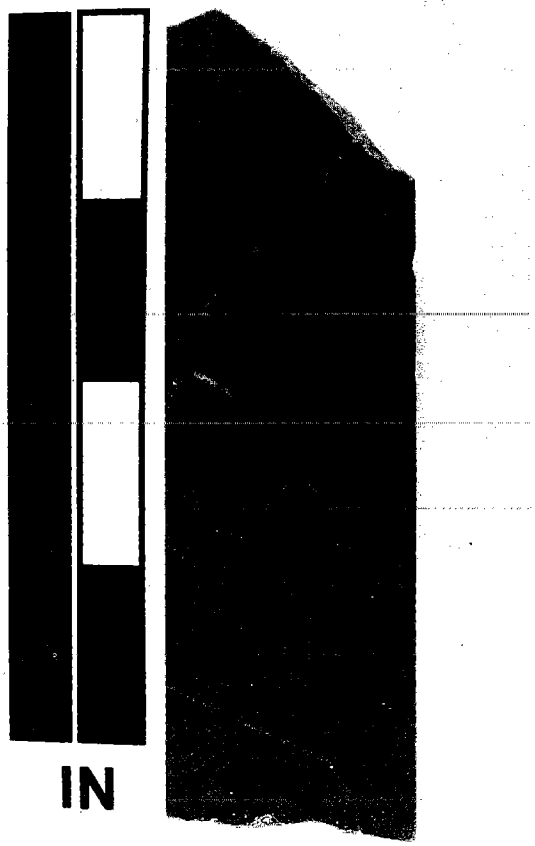


Figure 27. "Patterned dolomite" in the Copper Ridge Dolomite at a depth of 1,360–1,370 ft in the Humble Claude L. Griffin Core Hole No. 1C in Tuscaloosa County, Alabama (Birmingham anticlinorium).



Figure 28. Vuggy porosity in a thrombolitic(?) dolomite of the Copper Ridge Dolomite at a depth of 11,019 ft in the ARCO/Amoco et al., No. 1 Ethel M. Koch in Greene County, Alabama (fold-thrust belt).

Tennessee. Production came from a zone near a major thrust fault. Fractures associated with faulting and solution of carbonate strata near the pre-Middle Ordovician unconformity at the top of the Knox are thought to cause the porosity and permeability in the producing zone (McCaslin, 1983; Oil and Gas Journal, 1983; Sternbach, 1984).

The ARCO-Anschutz No. 1 Alabama Properties well in Shelby County, Alabama, drilled to a depth of 17,005 ft, penetrated two complete repetitons of the Knox section. Gas shows were reported in the Knox at 6,700–6,702 ft in the Newala Limestone and at 6,858–6,870 ft in the Longview Limestone, probably from fractures.

The ARCO/Amoco John Goodson No. 1 drilled in Bibb County, Alabama, had a slight gas show at the base of the Knox above the Helena thrust fault. Underlying Pennsylvanian coal-bearing rocks probably were the source of the gas which was trapped in fractures in the overlying Knox.

Knox production has also been reported from the Black Warrior basin in the Fairview field in Lamar County, Alabama. The S. H. Gilmer No. 4 has produced gas and oil from a depth of 4,352–4,424 ft since 1976. Although initially reported as Knox production, this gas is actually coming from Middle Ordovician carbonates.

Oil and gas production has also been reported from the Knox in the Black Warrior basin in Mississippi. The New Hope field in Monroe County produced oil from a zone of vuggy dolomite called the "Snow zone" after the discovery well (Mellen, 1974). Subsequent drilling indicated the structure to be a low-relief anticline. The well, completed in September 1953, was abandoned in October 1954 after producing 7,813 barrels of oil.

In 1971, the Texaco, Inc., No. 1 Clyde Q. Sheely in Oktibbeha County, Mississippi, produced gas from this same "Snow zone." The well produced 123,752 MCF of gas from September 1971 to June 1973 (Mellen, 1974).

The Magnolia No. 1 Pierce in Monroe County, Mississippi, was an offset to the discovery well in the New Hope

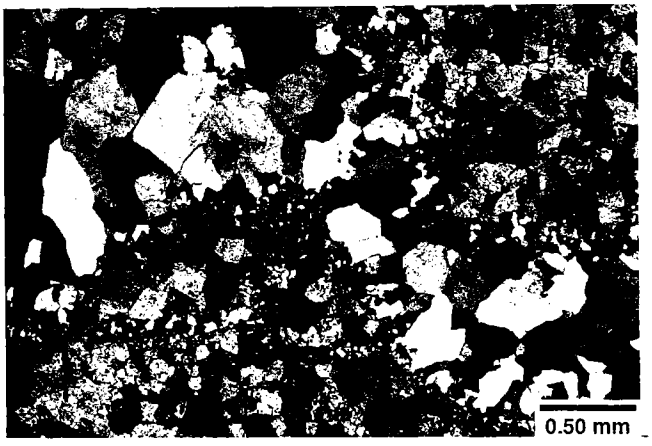


Figure 29. Photomicrograph of megaquartz in dolomite of the Copper Ridge Dolomite from a depth of 1,940 ft in the Humble Southern Cement Core Hole No. 3 in Shelby County, Alabama (Helena thrust sheet). Crossed nicols; bar scale is 0.5 mm.

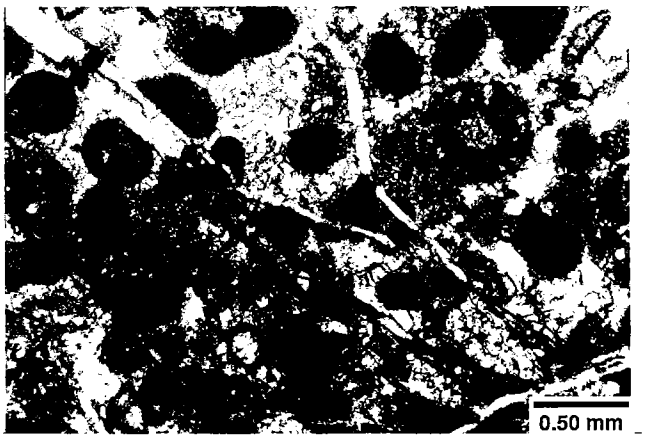


Figure 30. Photomicrograph of a fractured intraclastic-oolitic packstone of the Copper Ridge Dolomite from a depth of 720 ft in the Humble Claude L. Griffin Core Hole No. 1C in Tuscaloosa County, Alabama (Birmingham anticlinorium). Clasts consist of radial ooids and rounded intraclasts of mudstone and peloidal packstone. Ordinary light; bar scale is 0.5 mm.

field. Recent studies of conodonts in this well indicate that the "Snow zone" dolomite is actually Middle Ordovician in age and is, therefore, not the top of the Knox Group, as originally thought (Alberstadt and Repetski, 1989). Mellen (1974) reports another vuggy porous zone at a depth of 7,130 ft in the Knox. Called the "Pierce zone," this zone is fractured vuggy chert, limestone, and dolomite which had shows of oil and gas. This "Pierce zone" is widespread and has been reported from other wells in Monroe County. Originally thought to be in the Copper Ridge, conodont studies (Alberstadt and Repetski, 1989) indicate the strata to probably be equivalent to the Longview Limestone.

Porosity and Permeability

Sternbach (1984) determined porosity and permeability from samples of core from the Copper Ridge in Alabama. Porosity values ranged from 0.8 to 6.6%. Permeability values were 0.01 mD. These values are conservative estimates of rock-matrix porosity and permeability as they do not take into account subsurface fracturing and local solution development. However, surface and subsurface karst development is present in the Knox in Alabama.

Productive porosity in the Arbuckle Group of Oklahoma is related in large part to karstification associated with unconformities and tectonic fracturing. The most significant unconformity associated with the Knox Group in Alabama is the post-Knox unconformity. This unconformity has its greatest magnitude in the Appalachian fold-thrust belt west of the Helena fault, where hundreds of feet of stratigraphic relief developed in the Knox Group (Roberson, 1988). Paleokarst depressions in the Knox surface are locally filled by the Attalla Chert Conglomerate Member of the Chickamauga Limestone of Middle Ordovician age. The magnitude of the unconformity is 30–40 million years. Southeast of the Helena fault, the duration of the unconformity is about 10 million years (Roberson, 1988). To the west, in the southern part of the Black Warrior basin, conodont studies indicate that the post-Knox unconformity is absent or of limited duration (Alberstadt and Repetski, 1989).

Units of the Knox that are recognized to be particularly susceptible to solution-cavity development and sinkhole subsidence in outcrop include the Newala and Longview Limestones and the lower limestone unit of the Chepultepec Dolomite (Warren, 1976). The Newala is especially notorious for sinkhole development. Hooks (1985) reports numerous solution-collapse breccias from the Chepultepec and Copper Ridge Dolomites in cores from the Appalachian fold-thrust belt.

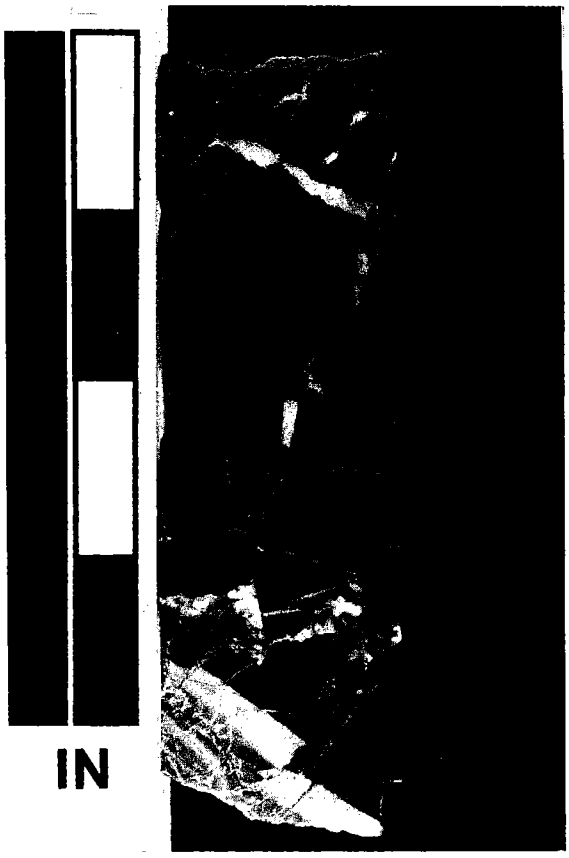


Figure 31. Collapse breccia in the Copper Ridge Dolomite at a depth of 1,170 ft in the Humble Claude L. Griffin Core Hole No. 1C in Tuscaloosa County, Alabama (Birmingham anticlinorium).

Alabama Activity

Recently, there have been several Knox tests permitted in Alabama. Most of these wells have targeted Cambrian–Ordovician carbonates in thrust sheets of the fold and thrust belt buried beneath Coastal Plain sediments. These targets are susceptible to fracturing and are in close proximity to possible source rocks of Devonian, Mississippian, and Pennsylvanian ages. As of June 1991, several more Knox tests had been permitted; some in the Black Warrior basin proper. Results of these tests should help fill the large gaps in our knowledge of the Knox, a potential reservoir which is essentially untested in the Black Warrior basin.

REFERENCES CITED

Adams, G. I.; Butts, Charles; Stephenson, L. W.; and Cooke, C. W., 1926, Geologic map of Alabama, *in* Geology of Alabama: Alabama Geological Survey Special Report 14, 312 p.

Alberstadt, Leonard; and Repetski, J. E., 1989, A Lower Ordovician sponge/algal facies in the southern United States and its counterparts elsewhere in North America: Palaios, v. 4, p. 225–242.

Batchelder, E. C., 1984, Lithofacies, depositional environments, and diagenesis of the Knox Group exposed along Alligator Creek, Bibb County, Alabama: University of Alabama unpublished M.S. thesis, 226 p.

Butts, Charles, 1910, Description of the Birmingham Quadrangle [Alabama]: U.S. Geological Survey Geologic Atlas, Folio 175, 24 p.

_____1926, The Paleozoic rocks, *in* Adams, G. I.; and others (eds.), Geology of Alabama: Alabama Geological Survey Special Report 14, p. 41–230.

_____1927, Description of the Bessemer and Vandiver Quadrangles [Alabama]: U.S. Geological Survey Geologic Atlas, Folio 221, 22 p.

_____1940, Description of the Montevallo and Columbiana Quadrangles [Alabama]: U.S. Geological Survey Geologic Atlas, Folio 226, 20 p.

Cloud, P. E., Jr., 1967, Geology and bauxite deposits of the Rock Run and Goshen Valley areas, northeast Alabama: U.S. Geological Survey Bulletin 1199-N, 74 p.

Coleman, J. L., Jr., 1988, Stratigraphy and structure of the Wills Valley anticline–Lookout Mountain syncline field trip area, *in* Coleman, J. L., Jr.; Groshong, R. H., Jr.; Rheams, K. F.; Neathery, T. L.; and Rheams, L. J. (eds.), Structure of the Wills Valley anticline–Lookout Mountain syncline between the Rising Fawn and Anniston CSD's, northeast Alabama: Alabama Geological Society Guidebook, 25th Annual Field Trip, p. 6–11.

Guthrie, G. M., 1989, Geology and marble resources of the Sylacauga Marble district: Alabama Geological Survey Bulletin 131, 81 p.

Harris, A. G.; Repetski, J. E.; Tull, J. F.; and Bearce, D. N., 1984, Early Paleozoic conodonts from the Talladega slate belt of the Alabama Appalachians—tectonic implications: Geological Society of America Abstracts with Programs, v. 19, p. 88.

Hooks, J. D., 1985, Stratigraphy, depositional environments, and silica diagenesis of the Cambro–Ordovician carbonate sequence, Appalachian Valley and Ridge, Alabama: University of Alabama unpublished M.S. thesis, 199 p.

Hooks, W. G., 1961, The stratigraphy and structure of the Bucksville area, Alabama: University of North Carolina unpublished Ph.D. dissertation, 205 p.

Kidd, J. T., 1975, Pre-Mississippian subsurface stratigraphy of the Warrior basin in Alabama: Gulf Coast Association of Geological Societies Transactions, v. 25, p. 20–39.

_____1979, Areal geology of Jefferson County, Alabama, with a section on lineaments by K. E. Richter: Alabama Geological Survey Atlas Series 15, 89 p.

McCaslin, J. C., 1983, Amoco scores gas discovery in Tennessee: Oil and Gas Journal, January 31, v. 81, no. 5, p. 183–184.

Mellen, F. F., 1972, Regional Paleozoic stratigraphy in Mississippi between Ouachita and Appalachian Mountains: discussion: American Association of Petroleum Geologists Bulletin, v. 56, p. 2457–2458.

_____1974, Possible Ordovician carbonate reservoirs in Mississippi: American Association of Petroleum Geologists Bulletin, v. 58, p. 870–876.

Mississippi Geological Society [no date], Correlation section, Black Warrior basin, pre-Chester.

Neathery, T. L., 1968, Geology of Etowah County, Alabama, *in* Neathery, T. L.; Smith, W. E.; Clarke, O. M., Jr.; and Szabo, M. W. (eds.), Geology and mineral resources of Etowah County, Alabama: Alabama Geological Survey Open-File Report, p. 11–98.

_____1988, Stratigraphy and facies changes of the Paleozoic succession in Wills Valley, Etowah and De Kalb Counties, Alabama, *in* Coleman, J. L., Jr.; Groshong, R. H., Jr.; Rheams, K. F.; Neathery, T. L.; and Rheams, L. J. (eds.), Structure of the Wills Valley anticline–Lookout Mountain syncline between the Rising Fawn and Anniston CSD's: Alabama Geological Society Guidebook, 25th Annual Field Trip, p. 54–68.

Neathery, T. L.; and Copeland, C. W., 1983, New information on the basement and lower Paleozoic stratigraphy of north Alabama [abstract]: Geological Society of America, Southeastern Section, Abstracts with Programs, p. 98.

Oil and Gas Journal, 1983, Upper Knox yields 100 b-d in eastern overthrust belt: Oil and Gas Journal, June 20, v. 81, no. 25, p. 72.

Osborne, W. E., 1990, Stratigraphy and structure of the Jackson Shoals culmination, Appalachian foreland fold and thrust belt, Talladega and Calhoun Counties, Alabama, *in* Guthrie, G. M.; and Osborne, W. E. (eds.), Contrasts in structural styles and mechanisms in a foreland-hinterland transition zone, central Alabama Appalachians: Geological Society of America, Southeastern Section Guidebook, Field Trip 2, Alabama Geological Survey Guidebook Series 3-2, p. 35–44.

_____[in press], Bedrock geology of the Cahaba valley area between Helena and Lake Purdy, Shelby and Jefferson Counties, Alabama: Alabama Geological Survey Bulletin 144.

Osborne, W. E.; Szabo, M. W.; Copeland, C. W., Jr.; and Neathery, T. L., 1989, Geologic map of Alabama: Alabama Geological Survey Special Map 221, scale 1:500,000.

Puckett, T. M.; Roberson, K. E.; and Tew, B. H., 1990, High calcium deposits in the Newala Limestone: Alabama Geological Survey Circular 149, 29 p.

Raymond, D. E.; Osborne, W. E.; Copeland, C. W.; and Neathery, T. L., 1988, Alabama stratigraphy: Alabama Geological Survey Circular 140, 97 p.

Resser, C. E., 1938, Cambrian System (restricted) of the southern Appalachians: Geological Society of America Special Paper 15, 140 p.

Roberson, K. E., 1988, The post-Knox unconformity and its relationship to bounding stratigraphy, Alabama Appalachians: University of Alabama unpublished M.S. thesis, 148 p.

Shaw, T. H., 1987, Stratigraphy and conodont biostratigraphy of the Lower Ordovician Newala Limestone at its type locality, central Alabama: Emory University unpublished M.S. thesis, 550 p.

Sternbach, L. R., 1984, Carbonate facies and diagenesis of the Cambrian–Ordovician shelf and slope margin (the Knox Group and Conasauga Formation), Appalachian fold belt, Alabama: Rensselaer Polytechnic Institute unpublished M. S. thesis, 65 p.

Sweet, W. C.; Ethington, R. L.; and Barnes, C. R., 1971, North American Middle and Upper Ordovician conodont faunas: Geological Society of America Memoir 127, p. 163–193.

Szabo, M. W.; Osborne, W. E.; Copeland, C. W., Jr.; and Neathery, T. L., 1988, Geologic map of Alabama: Alabama Geological Survey Special Map 220, scale 1:250,000.

Thomas, W. A., 1972, Regional Paleozoic stratigraphy in Mississippi between Ouachita and Appalachian Mountains: American Association of Petroleum Geologists Bulletin, v. 56, p. 81–106.

_____1973, Southwestern Appalachian structural system beneath the Gulf Coastal Plain: American Journal of Science, v. 273-A, p. 372–390.

_____1985, The Appalachian–Ouachita connection: Paleozoic orogenic belt at the southern margin of North America: Annual Review of Earth and Planetary Sciences, v. 13, p. 175–199.

_____1988, The Black Warrior basin, *in* Sloss, L. L. (ed.), Sedimentary cover—North American craton, U.S.: Geological Society of America, The Geology of North America, v. D-2, p. 471–492.

Thomas, W. A.; and Drahovzal, J. A., 1974, Geology of the Coosa deformed belt, *in* Thomas, W. A.; and Drahovzal, J. A. (eds.), The Coosa deformed belt in the Alabama Appalachians: Alabama Geological Society Guidebook, 12th Annual Field Trip, p. 45–75.

Twenhofel, W. H. (chairman); and others, 1954, Correlation of the Ordovician formations of North America: Geological Society of America Bulletin, v. 65, p. 247–298.

Tull, J. F., 1985, Stratigraphy of the Sylacauga Marble Group, *in* Tull, J. F.; Bearce, D. N.; and Guthrie, G. M. (eds.), Early evolution of the Appalachian miogeocline: upper Precambrian–lower Paleozoic stratigraphy of the Talladega slate belt: Alabama Geological Society Guidebook, 22nd Annual Field Trip, 92 p.

Ulrich, E. O.; and Cooper, G. A., 1938, Ozarkian and Canadian brachiopods: Geological Society of America Special Paper 13, 323 p.

Warren, W. M., 1976, Sinkhole occurrence in western Shelby County, Alabama: Alabama Geological Survey Circular 101, 45 p.

Yochelson, E. L.; and Bridge, Josiah, 1957, The Lower Ordovician gastropod *Ceratopea*: U.S. Geological Survey Professional Paper 294-H, p. 281–303.

Yochelson, E. L.; and Jones, C. R., 1968, *Teiichispira*, a new Early Ordovician gastropod genus: U.S. Geological Survey Professional Paper 613-B, p. B1–B15.

Hydrocarbon Potential and Subsurface Stratigraphy of the Cambro–Ordovician Sequence, Black Warrior Basin of Mississippi

Kevin S. Henderson and S. Cragin Knox
Mississippi Office of Geology, Jackson

INTRODUCTION

The Black Warrior basin, located in northwest Alabama and northeast Mississippi, is roughly triangular in shape (Fig. 1). This basin is generally defined as being bounded on the southeast by the plunging Appalachian Mountains in Alabama, on the southwest by the buried Ouachitas, and on the north by the Nashville dome (Thomas, 1988).

No outcrops of Cambro–Ordovician sediments occur in Mississippi, and our knowledge of the stratigraphy of the Cambro–Ordovician sequence in the Black Warrior basin is gleaned from the sparse subsurface data. For this reason, a great deal of confusion exists with regard to formational boundaries and ages of this thick sequence of carbonates. A recent study of Alberstadt and Repetski (1989), utilizing conodonts from the Magnolia Petroleum No. 1 Pierce well (Monroe County, Mississippi), affords a much better understanding of the age relationships of the upper part of the sequence than was previously available. Current studies are an effort to differentiate the Cambro–Ordovician strata based on correlation of the lithologic character of the strata with available conodont data. It is hoped that the present report will help clear up much of the conflict and confusion which now exists, and will serve as a usable guide for future study and refinement.

GENERAL STRATIGRAPHY

Although a total of 151 wells have been drilled into Ordovician strata in the Mississippi part of the basin, only two have penetrated the entire Cambro–Ordovician sequence. These two wells are the Exxon No. 1 Fulgham (Oktibbeha County), and the Pruet and Hughes No. 1 Dunlap Brothers (Lafayette County). The sequence, as revealed in the Dunlap well, consists of an apparently "complete" section of 7,950 ft of carbonates with minor amounts of quartzitic sand in the base of the section. The 6,744-ft section of Cambro–Ordovician strata in the Fulgham well is incomplete; much of the Cambrian section is absent, apparently due to nondeposition. The absence of much of the Lower Cambrian strata in the Fulgham well illustrates the high-relief nature of the crystalline Precambrian basement. Although the absence of these strata is interpreted to be due to nondeposition, structural conditions and/or erosion of these missing strata cannot be ruled out. Cambro–Ordovician strata are interpreted to have been deposited on shallow carbonate shelves and banks which remained essentially stable throughout deposition. Very small changes in sea level caused widespread transgressions and regressions on these stable shelves. Regressions led to the formation of repeated and extensive periods of karstification, interpreted to be represented by zones of high porosity in the strata.

CAMBRIAN SYSTEM

As only nine wells have reached the Cambrian, it is difficult to ascertain what constitutes a "normal" section. However, rocks in the subsurface in Mississippi, as far as we now know, are similar to the Cambrian section exposed in the southern Appalachians of Alabama (Fig. 2). The Cambrian System attains a maximum composite thickness of 6,343 ft, and is differentiated into five formations. In ascending order, these are the Weisner Quartzite, Shady Dolostone, Rome Formation, Conasauga Limestone, and Copper Ridge Dolostone. The Weisner Quartzite is a thin zone (maximum thickness of 180 ft) of fine- to very coarse-grained, predominantly quartzitic sandstone resting unconformably on the rugged Precambrian surface. The Shady Dolostone is a relatively pure dolostone, with minor amounts of quartzitic sand and anhydrite, and it attains a maximum known thickness of 1,152 ft. The Rome Formation is of variable lithology, ranging from nearly homogeneous shale to argillaceous dolostone, and is a maximum of 708 ft thick. The Conasauga Limestone reaches a thickness of 1,718 ft and consists of limestone with varying amounts of dolostone. The Copper Ridge is a cherty dolostone which attains a maximum thickness of 2,585 ft and marks the top of the Cambrian System. The Copper Ridge Dolostone is difficult to differentiate from the overlying Knox Dolostone (Ordovician), but the top is picked at a point consistent with a noticeable resistivity decrease on electric logs along with a lithologic increase in the amount of chert.

ORDOVICIAN SYSTEM

The Ordovician System is represented by a maximum composite thickness of 6,778 ft of nearly pure carbonate strata. Only Lower Ordovician and earliest Middle Ordovician (Whiterockian) strata are present, and these sediments are differentiated into four formations based on lithology. In ascending order, these are: Knox Dolostone, Knox Limestone, Stones River Dolostone, and Stones River Limestone. The Knox Dolostone reaches a maximum thickness of 1,906 ft and consists of dolostone with varying amounts of chert and sand. Well-rounded quartz sand grains are characteristic of the Knox Dolostone. Locally, sand is present in sufficient amounts to form what would more properly be described as dolo-

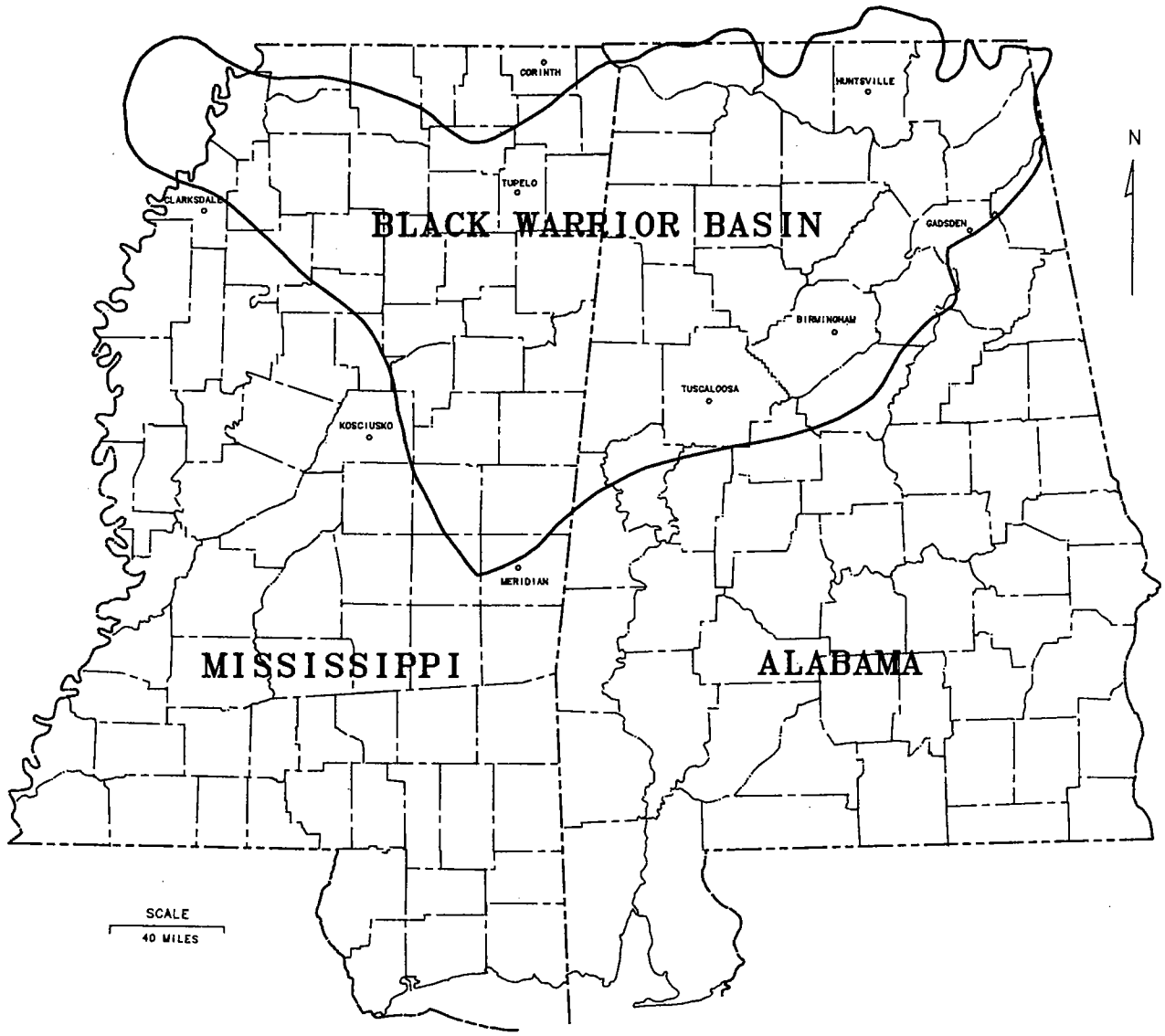


Figure 1. Location of Black Warrior basin in Mississippi and Alabama.

mitic sandstone. These sandstones are thin and discontinuous, but they do seem to be present in roughly equivalent zones of the Knox Dolostone. The Knox Limestone is a thick (maximum of 2,657 ft), largely bioclastic limestone characterized by abundant sponge spicules and algal components. The Stones River Dolostone attains a maximum thickness of 1,535 ft, and it is differentiated from the Knox Dolostone by the general lack of sandy zones and a finer grained texture. The Stones River Limestone is a micritic to finely crystalline limestone which reaches a maximum thickness of 680 ft. A thin graptolitic shale occurs at the top of the unit locally. Graptolites present at the top of the Stones River Limestone, taken from a core in the Florida Exploration No. 1 Morrison (Pontotoc County), have been identified as Middle Ordovician (Mellen, 1982); this further supports the age assignments that have been made, based on conodonts from the Magnolia Petroleum No. 1 Pierce well ~40 miles to the southeast.

As in the underlying Copper Ridge Dolostone, several zones of red and yellow mottling occur within the Knox Dolostone. These zones of oxidized strata are interpreted to represent episodes of subaerial exposure. Karstification of the Knox Dolostone is inferred, and zones of high porosity associated with brecciation are found in the section. One of these zones of porosity was drill-stem tested in the Honolulu No. 2 Davis well (Calhoun County) (Fig. 3) from a depth of 8,134–8,390 ft. This test recovered 3,600 ft of gas and mud-cut salt water in 3 hours, 45 minutes (Mellen, 1974).

HYDROCARBON PRODUCTION

In spite of the fact that only a small amount of oil (7,834 bbls) and gas (850,000 MCF) has been produced from the Cambro–Ordovician section in Mississippi to date, large reservoirs may be present in these strata analogous to the prolific Ellenburger–Arbuckle trend of Texas and Oklahoma. All production to date has occurred from what is informally referred to as the "Snow zone" of the Stones River Dolostone.

The Stones River Dolostone is the only unit in the Cambro–Ordovician succession of Mississippi to produce

ERATHEM	SYSTEM	SERIES	STAGE	GROUP	FORMATION	THICKNESS	LITHOLOGIC DESCRIPTION
PALEOZOIC	ORDOVICIAN	MIDDLE	WHITE-AN	STONES RIVER	STONES RIVER LIMESTONE	214-680'	LIMESTONE, GRAY TO LIGHT TAN, MICRITIC TO FINELY CRYSTALLINE, ARGILLACEOUS IN TOP, THIN DARK GRAY-BLACK SHALES AT TOP LOCALLY, TRACES SANDY IN BASE
					STONES RIVER DOLOSTONE	289-1535'	DOLOSTONE, GRAY TO TAN, GREENISH-GREY, VERY FINE TO FINELY CRYSTALLINE, TRACES SANDY, ARGILLACEOUS IN PART, BRECCIATED ZONES ("SNOW ZONE"), BENTONITES
		LOWER	CANADIAN	KNOX	KNOX LIMESTONE	490-2657'	LIMESTONE, GRAY TO TAN, VERY FINE TO FINELY CRYSTALLINE, BIOCLASTIC IN LARGE % (FOSSILS INCLUDE: SPONGE SPICULES, CONODONTS, CRINOID STEMS, ALGAE)
					KNOX DOLOSTONE	650-1906'	DOLOSTONE, GRAY TO TAN, GREENISH-GRAY, FINE TO MEDIUM CRYSTALLINE, CHERTY, VERY SANDY (VERY FINE TO COARSE, WELL ROUNDED, "FROSTED"), BRECCIATED ZONES OF HIGH POROSITY WITH RED AND YELLOW MOTTLING
	CAMBRIAN	UPPER			COPPER RIDGE DOLOSTONE	795-3200'	DOLOSTONE, GRAYISH-TAN TO DARK BROWN, FINE TO COARSLEY CRYSTALLINE, SANDY, CHERTY (COMMONLY CONTAINS "FLOATING" EUHEDRAL DOLOMITE CRYSTALS) BRECCIATED ZONES WITH RED AND YELLOW MOTTLING
		MIDDLE			CONASAUGA LIMESTONE	0-1187'	LIMESTONE, GRAYISH-TAN, MICRITIC TO FINELY CRYSTALLINE, DOLOMITIC IN PART, THIN DOLOSTONE BEDS, ARGILLACEOUS, MAY CONTAIN THIN DARK GRAY CALCAREOUS SHALE INTERBEDS, VERY SANDY IN BASE-SAND RANGES FROM VERY FINE TO VERY COARSE (UP TO 1/4" IN DIAMETER), CHALKY IN SMALL PART, RARELY GLAUCONITIC NEAR THE BASE OF THE UNIT
		LOWER			ROME FORMATION	0-708'	SHALE/SILTSTONE, DARK GRAY TO LIGHT BROWN, GREEN; LIMESTONE/DOLOSTONE, GRAYISH-TAN, FINELY CRYSTALLINE
					SHADY DOLOSTONE	220-1152'	DOLOSTONE, LIGHT GRAY TO BROWN,"SALT AND PEPPER," FINE TO MEDIUM CRYSTALLINE, SANDY, OOLITIC,
					WEISNER QUARTZITE	0-180'	SANDSTONE, VARICOLORED, FINE TO VERY COARSE GRAINED, QUARTZITIC, FELDSPATHIC IN SM %, GLAUCONITIC IN PART
PRECAMBRIAN BASEMENT							GRANITE AND "GNEISSIC" ROCK

Figure 2. Stratigraphic chart and lithology of Cambro–Ordovician strata in the Mississippi portion of the Black Warrior basin.

hydrocarbons to date. A small amount of oil was produced from the formation at the New Hope field in Monroe County. Approximately 7,834 bbls of 35-gravity oil was produced from the Magnolia Petroleum No. A-1 Snow before abandonment. Completed September 1, 1953, perforations between 4,753 and 4,756 ft flowed at an initial rate of >29 bbls of oil per hour, but production declined rapidly. The well produced an average of ~40 bbls per day for several weeks before finally dying. Shortly after this, the well was placed on pump and produced 224 bbls of oil and 25 bbls of water during the first 24 hours (Oil and Gas Journal, 1953). Unfortunately, this production was short-lived and the well was abandoned October 23, 1954, after going to water. Over the years, several offset wells have been drilled in the New Hope, area but none have been producing completions.

The Stones River Dolostone has also produced gas at the one-well Maben field in Oktibbeha County, ~42 mi southwest and 10,000 ft deeper than the New Hope field. At the Maben field, the Texaco No. 1 Sheely was completed in 1971 from a series of perforations between 14,690 and 15,036 ft ("Snow zone"), flowing 1,959,000 cubic feet of gas per day. The well produced 850,186,000 cubic feet of gas before abandonment in 1989.

The black shales of the Stones River Limestone are inferred to be a possible source rock for hydrocarbons. An analysis of this shale in the Morrison core yielded a total organic-carbon content of 2.02% (Mellen, 1982). This percentage of total organic carbon is considered favorable for the generation of hydrocarbons. Numerous shows of hydrocarbons have been reported from the Stones River Limestone. A small amount of 38°-gravity oil was recov-



Figure 3. Photograph of fractured and vuggy porosity of the Knox Dolostone from the Honolulu Oil Corporation No. 2 Davis, Calhoun County, Mississippi, at the depth of 8,378–8,379 ft.

ered from the Shell No. 1 McCain in Chickasaw County, from a zone 45 ft below the top of the unit. In the Salmon No. 1 Wilson (Pontotoc County), a drill-stem test of the interval 2,940–3,000 ft yielded 525 ft of muddy, gas-cut salt water with fluid entry at the rate of 84 bbls per day (Mellen, 1974). Secondary dolomitization of the dense limestones of the Stones River Limestone could be an attractive reservoir objective.

While drilling the Tipperary No. 1 Harpole-Campbell well in Quitman County, a zone of very high porosity was encountered in the Copper Ridge Dolostone from 7,608 to 7,725 ft. The bit "fell" the first 24 ft of this 117-ft-thick zone and circulation was lost. A drill-stem test was conducted from 7,610 to 7,725 ft and, although the well subsequently loaded up and died, it flowed at an average rate of 12,300 bbls of salt water per day during the first five minutes of the test. This zone of high porosity is interpreted to be a collapse breccia formed during one of many periods of karstification during Cambro–Ordovician time.

CONCLUSIONS

Although only two wells have produced hydrocarbons from Cambro–Ordovician strata in Mississippi, the limited number of wells that have tested the section is not sufficient to condemn the potential of these strata. Only two wells have reached the basement, and just five wells have completely penetrated the Knox Group. The Knox Group is stratigraphically equivalent to all or part of the prolific Ellenburger–Arbuckle strata of Texas and Oklahoma. All hydrocarbon production to date in Mississippi has occurred in the Stones River Group, overlying the Knox Group. As only 37 wells have penetrated the entire Stones River Group, these strata are also essentially untested. Of the 151 wells that have made a penetration of the Cambro–Ordovician section in Mississippi, a large number of these have recorded hydrocarbon shows of some kind.

Potential reservoir rocks of high porosity have been identified throughout the Cambro–Ordovician section in Mississippi. These high-porosity zones are interpreted to be the result of karstification of the carbonates, with subsequent formation of breccias and vuggy porosity. In addition to the breccias, secondary dolomitization and the development of reefs are inferred to have enhanced porosity in parts of the section (Hooks, 1985). Complex structural conditions are also interpreted to have enhanced porosity through faulting and fracturing. Complex thrusting along the southwestern margin of the Black Warrior basin (buried Ouachita trend) has the potential to form numerous hydrocarbon traps. Structural conditions are inferred, whereby the excellent reservoir rocks of the Cambro–Ordovician section are juxtaposed against the high-quality source rocks of the Mississippian and Pennsylvanian strata. With the recent advances in seismic techniques, the discovery of large hydrocarbon reservoirs in the structurally complex Black Warrior basin of Mississippi would seem only a matter of time.

REFERENCES CITED

Alberstadt, L. P.; and Repetski, J. E., 1989, A Lower Ordovician sponge/algal facies in the southern United States and its counterparts elsewhere in North America: Society of Economic Paleontologists and Mineralogists Research Reports, v. 4, p. 679–683.

Hooks, J. D., 1985, Stratigraphy, depositional environments, and silica diagenesis of the Cambro–Ordovician carbonate sequence, Appalachian Valley and Ridge, Alabama: University of Alabama unpublished M.S. thesis, 199 p.

Mellen, F. F., 1974, Possible Ordovician carbonate reservoirs in Mississippi: American Association of Petroleum Geologists Bulletin, v. 58, p. 870–876.

_____1982, Notes on Middle Ordovician, Mississippi and Alabama: Mississippi Geology, v. 3, no. 1, p. 1–5.

Thomas, W. A., 1988, The Black Warrior basin, *in* Sloss, L. L. (ed.), Sedimentary cover—North American craton; U.S.: Geological Society of America, The Geology of North America, v. D-2, p. 471–492.

Karst Breccias of the Wade, Bray, and Brown Zones of the Upper Arbuckle Group in the Healdton Field, Carter County, Oklahoma

R. Todd Waddell
Conoco Inc., Lafayette, Louisiana

Huaibo Liu and J. M. Forgotson
University of Oklahoma

INTRODUCTION

The Healdton field, located in T4S, R3W in Carter County, Oklahoma, produces from the karstic Arbuckle Brown zone reservoir. Cores were examined in the Wade, Bray, and Brown zones of the Cambro–Ordovician upper Arbuckle Group. Thin sections were also examined to observe porosity size, type, and relation to petroleum production. The Brown zone, considered upper Kindblade (Latham, 1968), is by far the most prolific reservoir in the upper Arbuckle Group. Dolomitization and karst development are the controlling factors for reservoir quality. In addition to the vugular dolomitic porosity, the Brown zone has crackle, mosaic, and chaotic breccias and related porosities (including fracture, cavernous, and breccia). In contrast, the Wade and Bray zones are predominantly original depositional fabric with comparatively little diagenesis. Although the Wade and the Bray do produce and have some karst breccias in the Healdton field, their cumulative production is relatively minor compared to the Brown zone.

WADE ZONE

The Wade zone core was taken from the Voorhies No. 1 well (sec. 1, T4S, R3W). The Wade zone is upper West Spring Creek and was deposited in a shallow-water environment (Burgess, 1968; Lindsay and Koskelin, 1991). There are six dominant lithofacies, with some minor variations. Table 1 lists the lithofacies and their descriptions.

These lithofacies are comparable to the depositional facies defined by Lindsay and Koskelin (1991). They had divided the upper West Spring Creek into tidal flats (thick and thin laminated mudstones), beach berms (flat-pebble conglomerates), and bioturbated subtidal (mottled muds). Burgess (1968) had similarly defined these facies as subtidal, intertidal, lagoonal, and supratidal.

The Wade zone lithofacies found in the Voorhies are comparable to the above-mentioned lithofacies. Although there could be possible microkarst locally in the Wade zone, it is primarily depositional fabric and is dominated by lime mudstone and dolomudstone. The Bray zone was also cored in the Voorhies.

The Bray zone was examined in hand sample (a detailed petrographic study was conducted in the Geneva Bray well for the Bray zone). In addition to the lime mudstone and dolomudstone facies, the Bray zone in the Voorhies core contained algal laminites and stromatolites, karst breccia facies, and a more abundant occurrence of the flat-pebble conglomerate facies. The karst development in the Bray zone seems to be related to fault cuts seen in the core and associated with the algal facies (although not all karst development is seen in proximity to the fault cuts). The faults could have acted as conduits for fluid flow and brought karst waters in contact with a porous algal facies. The stromatolite facies, relative to the lime mudstone and dolomudstone facies, would have offered the path of least resistance to flow.

BRAY ZONE

The Bray zone, lower West Spring Creek, core was taken from the Geneva Bray No. 1 well (sec. 2, T4S, R3W). The Bray zone in the Geneva Bray contains >99% depositional fabric. Only 1.5 ft of the 500-ft core shows any presence of karst development, and it is interpreted as a solution pipe. It does not contain the characteristic karst crackle, mosaic, and chaotic sequence of breccias. The majority of the Bray well is composed of carbonate muds, with some dolomudstones, thin-bedded grainstones/

TABLE 1. — WADE ZONE LITHOFACIES AND DESCRIPTION

Lithofacies	Description
A	Gray/green thinly laminated carbonate mud with small fractures, some soft sediment deformation, possible paleocaliche, locally medium bedded, some mottled beds
B	Gray, thinly laminated dolomudstone with some anhydrite nodules/concretions (interbedded with mottled mudstone)
C	Light tan/brown mottled dolomudstone and lime mudstone
D	(2–4 in.) blue-white anhydrite nodules
E	Thin-bedded fossil grainstones, packstones (mostly crinoids, ooids)
F	Flat-pebble conglomerate

TABLE 2. — BRAY ZONE LITHOFACIES AND DESCRIPTION

Lithofacies	Description
A	Dark-gray to gray, brown to light-tan, mottled carbonate mudstone, bioturbated, some chert nodules
B	Fossil packstone and grainstones, thin-bedded, ooids, trilobite, and gastropod fragments
C	Gray to dark-gray/green, thin- to medium-bedded laminated carbonate/dolomudstones
D	Gray/green algal stromatolites (boundstones), dolomitic, stylolites
E	Flat-pebble conglomerates

packstones, stromatolites, and flat-pebble conglomerates. Table 2 contains the major facies observed in the Bray zone in the Geneva Bray well.

The Bray zone is also composed of shallow-water carbonate deposits. However, the Bray zone seems to contain more laminated and mottled mudstones than does the Wade zone (Fig. 1), possibly due to a deeper and quieter water environment. Lindsay and Koskelin (1991) also found more subtidal influence in the lower West Spring Creek.

An interesting observation is the occurrence of stylolites within the algal stromatolites (Fig. 2). The stylolites develop roughly parallel to the bedding plane. Dolomitization occurs along the stylolites and can develop significant porosity. This type of porosity can be further developed through exposure to karst waters. Examples of stylolites and the dolomitic diagenesis can be seen in the Bray zone in the Bray well, and the exposure of this type facies to karst development can be seen in a similar lithofacies found in the Brown zone in the HAU No. 5-3 well (discussed later in the report).

The only significant presence of karst development is found between 3,797.0 and 3,798.5 ft—1.5 ft of karst development out of ~400 ft of core from the Bray zone. We interpreted this type of karst development as a solution pipe (Fig. 3), lacking the sequence crackle, mosaic, and chaotic breccias. The pipe walls seem to remain intact while the interior resembles a dissolved pipe with chaotic breccia and karst fill.

The Bray zone is productive in the Geneva Bray well, but unfortunately the producing interval was not cored. There is a higher SP response, which could indicate a change in lithology from the cores we examined deeper in the well. The Geneva Bray's IP was 190 BOPD and 250 MCFGPD. The cumulative production in the Bray well is 102,447 BOPD.

The lack of karst development in the Bray zone in the Geneva Bray well is due to the preservation of the original depositional fabric. These primarily carbonate-mud-rich strata inhibited the flow of karst waters. In contrast, the Brown zone underwent extensive dolomitization and created a preexisting porosity system for the karst waters. The dolomitization and subsequent karst development in



Figure 1. Photograph of mottled lime mudstone, locally fractured. Core from the Geneva Bray No. 1 well, depth 3,629 ft.

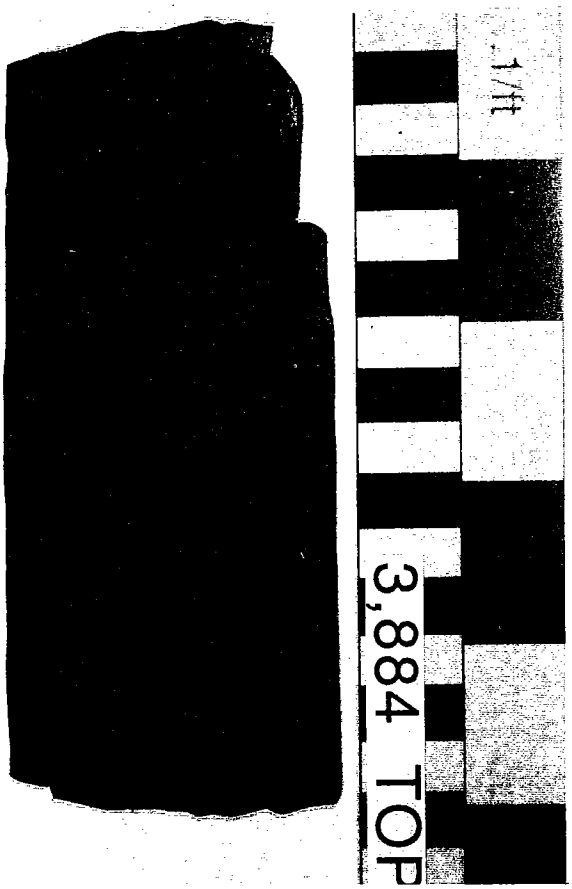


Figure 2. Photograph of stromatolite limestone with stylolites parallel to the algal lamination. Core from the Geneva Bray No. 1 well, depth 3,384 ft.

the Brown zone, which is similar in original environment of deposition, resulted in its prolific production and reservoir quality relative to the overlying Wade and Bray zones.

BROWN ZONE

The Brown zone core was taken from the HAU No. 5-3 well (sec. 4, T4S, R3W). The cored interval covers the lower Bray zone and most of the productive Brown zone. The Brown zone originally contained similar facies found in the Wade and the Bray, but the majority of the strata have been heavily dolomitized and subsequently subjected to karst development. The lower portion of the Bray zone in the HAU No. 5-3 well contains almost 40 ft of crackle, mosaic, and chaotic breccias. Underlying the karstic Bray zone is >280 ft of karst breccias and 60 ft of vuggy dolomudstone. The facies terminology for the Brown zone (Table 3) is partially based on Keran's (1989) study of the West Texas Ellenburger.

In our depositional Arbuckle model, the original depositional facies of the Brown zone were heavily dolomitized and developed into a vuggy dolomite. The vugs evolved into a cavern. The crackle breccia represents the cave floor and cave roof. As the cavern enlarged, rock fell



Figure 3. Photograph of fractured lime mudstone with solution pipe that was filled by breccias and muddy lime sediments. Core from the Geneva Bray No. 1 well, depth 3,797 ft.

TABLE 3. — BROWN ZONE KARST BRECCIAS AND LITHOFACIES DESCRIPTIONS

Lithofacies	Description
Crackle breccia	Network of fractures, strata is still intact, little to no loose clasts
Mosaic breccia	Grid of individual clasts, some partially rotated, heavily fractured
Chaotic breccia	Two types: one that is primarily clast-supported, and one that is breccia clast and fine karst fill (fine silty micrite)
Vuggy dolomudstone	Dolomitized strata that seems not to be fabric selective, porous and permeable
Green karst fill	Green silty micrite, high neutron log response, laminated, soft sediment deformation, a minor facies

from the roof and developed a cone-shaped pile. This lower collapse zone (Kerans, 1989) is recognized by clast-supported chaotic breccia (Fig. 4). The cavern could periodically flood and wash in silts and muds with the upper portion of the chaotic breccia (chaotic breccias and karst fill) (Fig. 5). As the caverns finally collapsed, the roof and upper chaotic breccia clasts become heavily fractured (mosaic breccias) (Fig. 6).

Early dolomitization of the Brown zone created a pre-existing porosity system that provided a conduit for the karst-development waters. Although porosity occurs in the Wade and Bray zones, it is not comparable to that in the Brown zone, thus the Brown zone offered the permeability path of least resistance. The brittle dolomitic Brown zone also had greater susceptibility to fracturing contrasted to that of the overlying limestone units (as reflected in a similar field study by Stearns, 1968). Finally, Morrowan uplift provided further relief and tectonic fractures, which could enhance late karst development, and gave the reservoir the present-day closure of ~1,500 ft (Latham, 1968).

After Morrowan uplift, each of the faults within the field (Latham, 1968), and those bounding the major structure on the north, west, and east sides, could provide a conduit for the waters that produced further karst development in the most porous and permeable zone. The uniform oil/water contact indicates communication between fault blocks, and suggests that the faults were not seals but served as conduits for fluid flow. Karst breccias with baroque dolomite on only one edge of chaotic breccia clasts reveals the history of a karstic cavern or vug wall, also supporting a later episode of karst development.

The rock was first karstic and formed a large vug or cavern wall. The wall was subsequently lined with baroque dolomite. The baroque-lined walls were exposed to dissolving waters again. The cavern walls collapsed and produced chaotic breccia with baroque dolomite lining only one side. This is interpreted as the Brown zone having more than one period of karst development.

The contribution of each episode of karst development to the formation of the Brown zone reservoir is difficult to answer. The Brown zone reservoir probably developed during two major periods of karst development: (1) the Arbuckle intraconformity and/or the Lower Ordovician unconformity, and (2) the pre-Atokan unconformity. Although no cavern infill sediments have been found in the Healdton cores that would undeniably establish Morrowan karst development, the before-mentioned chaotic breccias, with baroque dolomite present on one side only, indicate two major periods of karst development.

In summary, the prolific Brown zone reservoir is distinguished by its dolomitization and subsequent karst development. The vuggy dolomite and mosaic breccia usually have the best porosity. Although the overlying Wade and Bray zones are productive, they usually do not have the dolomitic and karst-related porosity development found in the Brown zone. In contrast to the overlying limestone units, the combination of vugular, dolomitic, fracture, and breccia porosity are responsible for the Brown zone's multi-million barrel reservoir.

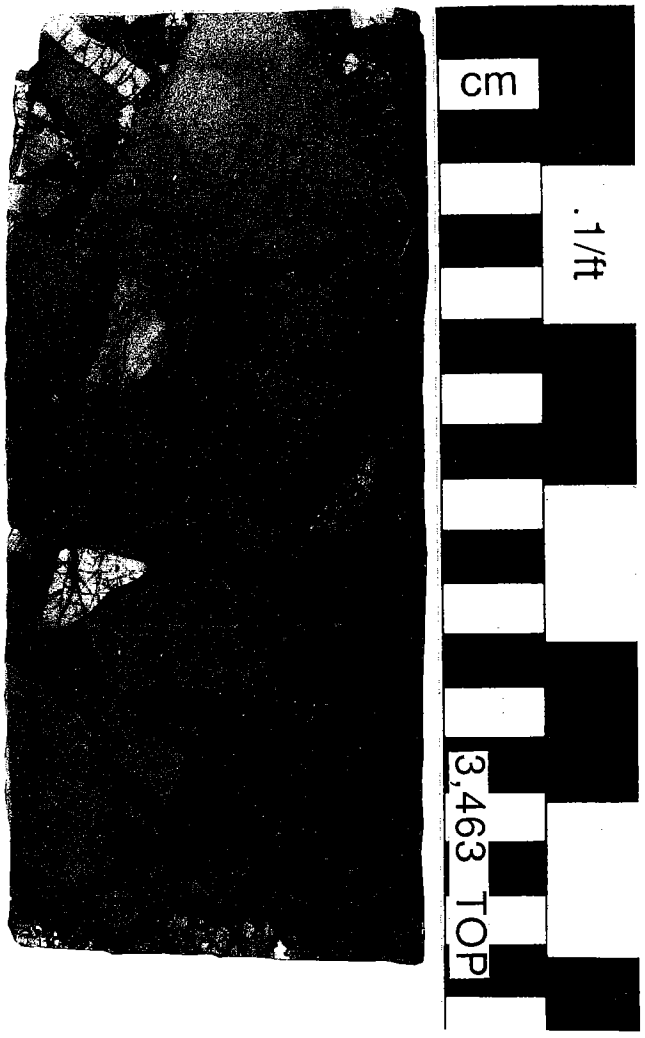


Figure 4. Photograph of clastic-supported chaotic breccias. Note that the breccias consist of mostly dolomudstone and laminated dolomudstone. The breccia pores were filled with hydrocarbon-rich muddy sediments. Core from the HAU No. 5-3 well, depth 3,463 ft.

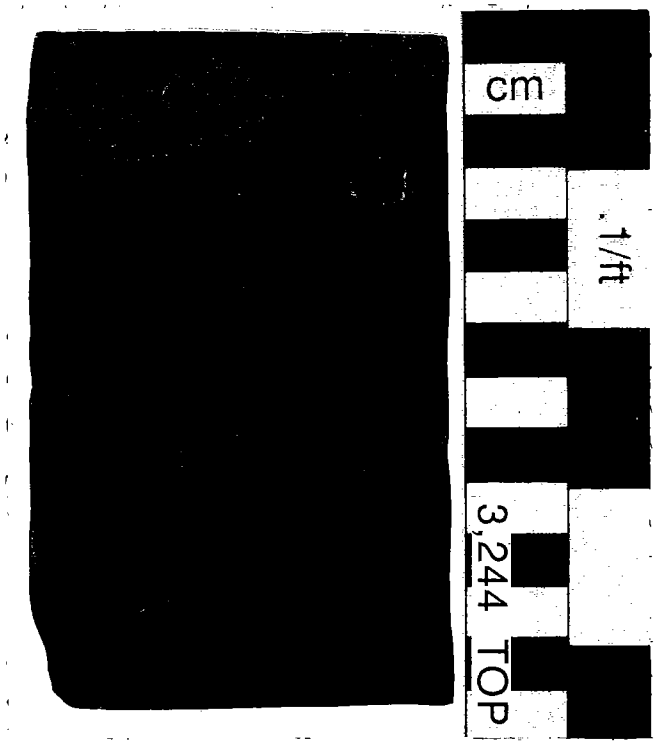


Figure 5. Photograph of chaotic breccias. Note that the breccias were supported by dark matrix (silts and muds). Core from the HAU No. 5-3 well, depth 3,244 ft.

REFERENCES CITED

Burgess, W. J., 1968, Carbonate paleoenvironments in the Arbuckle Group West Spring Creek Formation, Lower Ordovician in Oklahoma: Columbia University unpublished Ph.D. dissertation.

Kerans, Charles, 1989, Karst-controlled reservoir heterogeneity and an example from the Ellenburger Group (Lower Ordovician) of West Texas: Texas Bureau of Economic Geology Report of Investigations No. 168.

Latham, Jack, 1968, Petroleum geology of Arbuckle Group (Ordovician), Healdton field, Carter County, Oklahoma: American Association of Petroleum Geologists Bulletin, v. 52, p. 3–20.

Lindsay, R. F.; and Koskelin, K. M., 1991, Arbuckle Group depositional parasequences, southern Oklahoma, *in* Johnson, K. S. (ed.), Late Cambrian–Ordovician geology of the southern Midcontinent, 1989 symposium: Oklahoma Geological Survey Circular 92, p. 71–84.

Stearns, D. W., 1968, Certain aspects of fracture in naturally deformed rocks, *in* Reicher, R. F. (ed.), NSF advanced science seminar in rock mechanics: Bedford, Massachusetts, Air Force Cambridge Research Laboratory Special Report, p. 97–118.

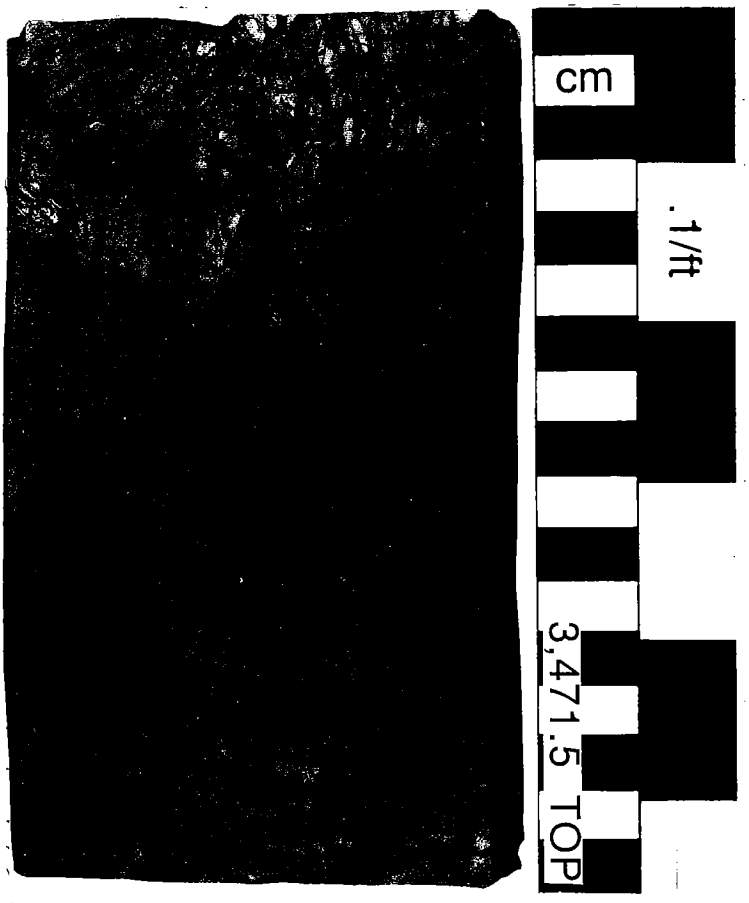


Figure 6. Photograph of mosaic breccias that developed in a laminated (stromatolite) dolostone. The breccias became more chaotic toward the left top. Core from the HAU No. 5-3 well, depth 3,471 ft.

PART 2

Field Trip

Arbuckle Group Workshop

October 1991

Field Trip Guide

FIELD TRIP LEADERS:

R. Nowell Donovan
Texas Christian University

Deborah A. Ragland
Conoco Inc., Ponca City

Bryan Tapp
Tulsa University

INTRODUCTION

Field study is essential to a full appreciation of the challenges offered by the Arbuckle Group. While the basic lithologies can readily be determined by the examination of core in the lab, their complex interrelationships are best seen in a field setting. This is particularly the case where dolomitization and karst are concerned. Similarly, details of the tectonic style of the Arbuckle, such as folding and fracturing, are most clearly understood on the outcrop.

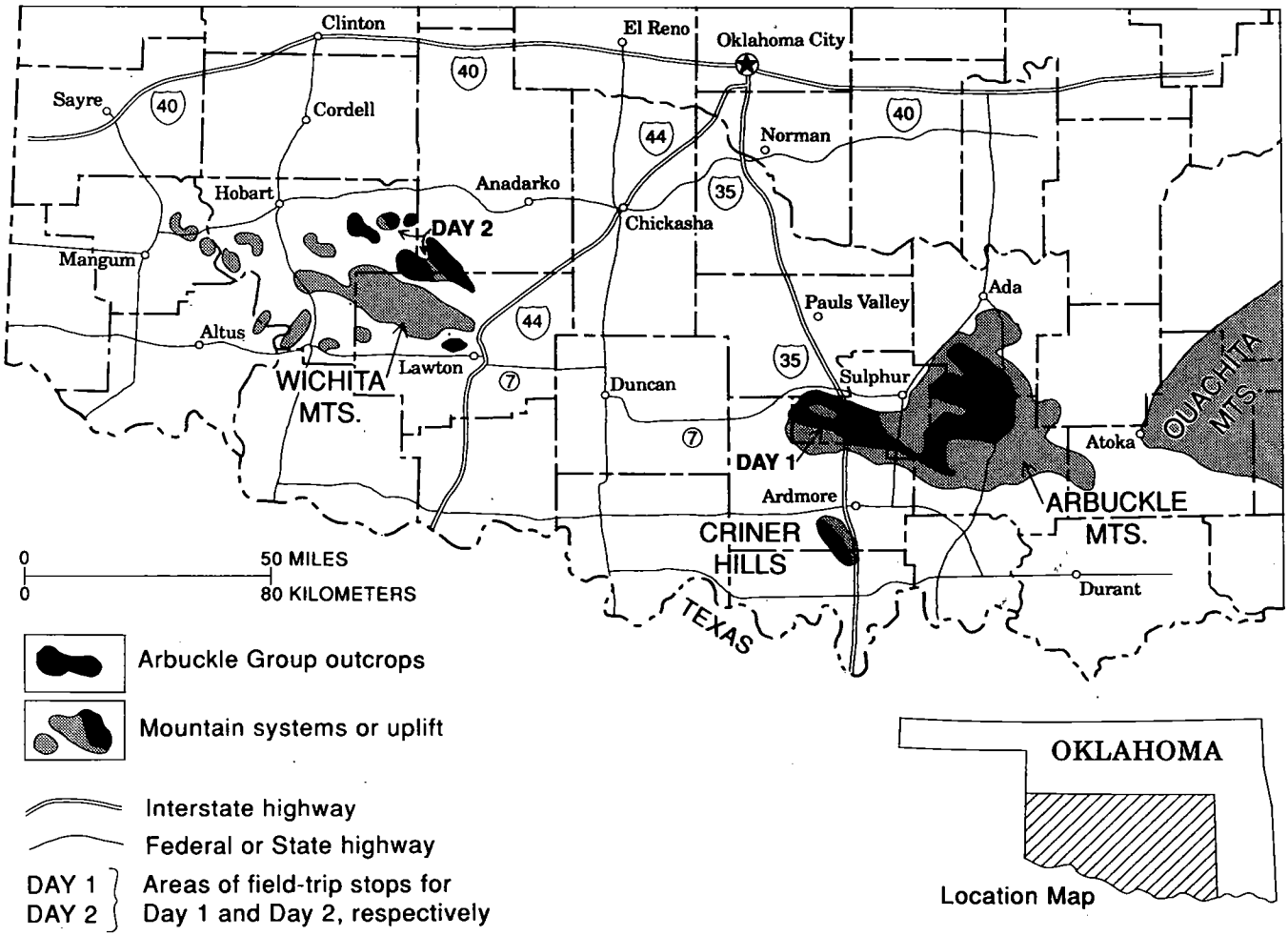


Figure 1. Map of Arbuckle Group outcrops and mountain/uplift areas of southern Oklahoma. Field-trip stops for Day 1 are in the Arbuckle Mountains, and stops for Day 2 are in the Slick Hills part of the Wichita Mountains.

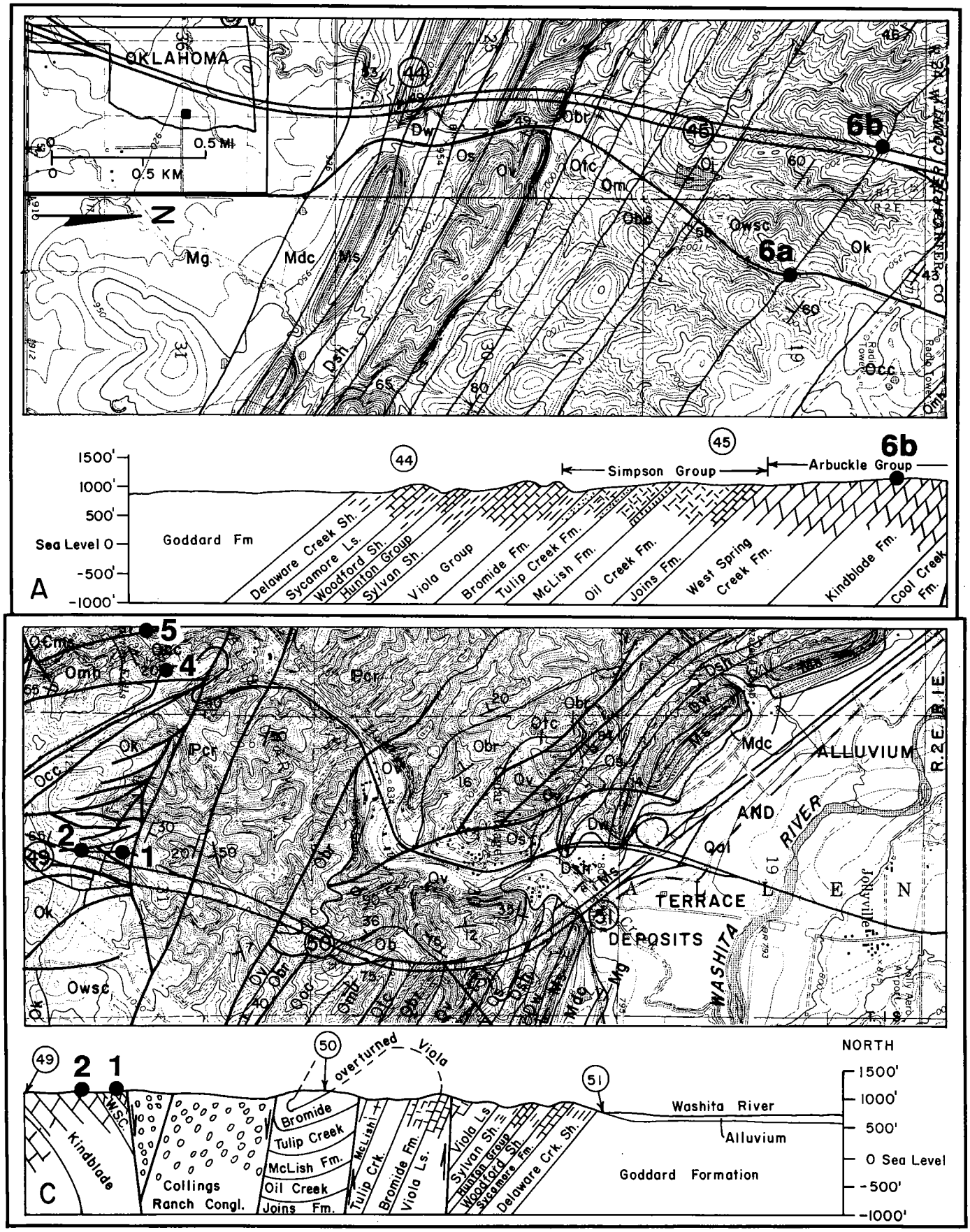


Figure 2. Geologic map and profile of Arbuckle Mountains along Interstate 35 (Fay, 1988). Field-trip stops 1–8 (Day 1) are labeled on the map.

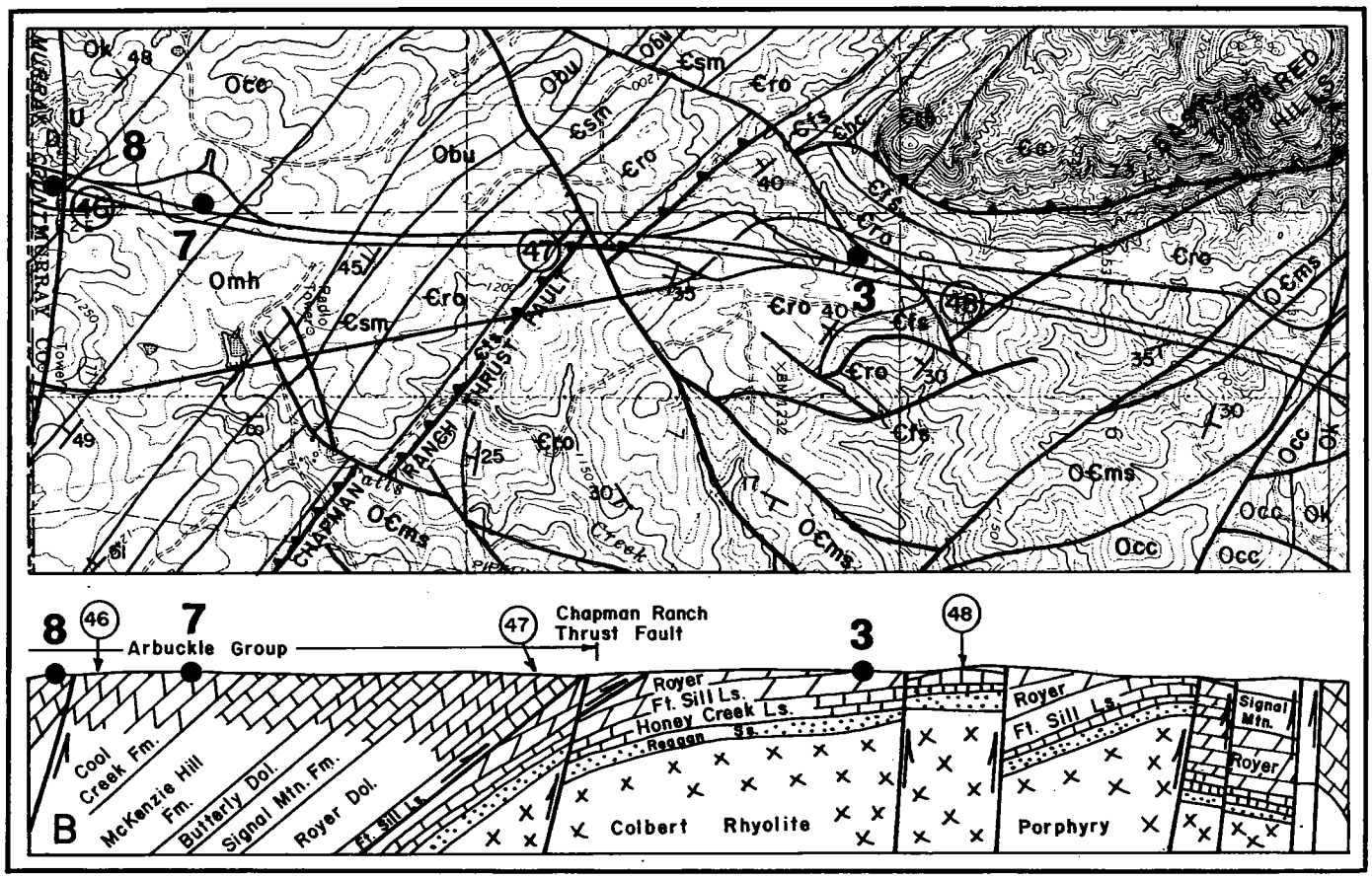


Figure 2. *(continued)*

The two most extensive outcrops of the Arbuckle Group are in the Arbuckle Mountains themselves and in the Slick Hills of southwestern Oklahoma (Fig. 1). Both areas have much to offer the lover of Cambrian–Ordovician carbonates. For example, in terms of sedimentology and stratigraphy, nothing quite equals the magnificent unbroken exposures of the upper Arbuckle Group on I-35 in the Arbuckles. On the other hand, the lower Arbuckle Group is best viewed in the Slick Hills. Both areas beautifully display the structural style that is characteristic of the group. In addition, the Slick Hills display thought-provoking limestone-dolomite contacts as well as a spectacular karst system of Permian age. Field-trip location maps are presented for the Arbuckle Mountains on the first day (Fig. 2) and for the Slick Hills part of the Wichita Mountains on the second day (Fig. 3).

ACKNOWLEDGMENTS

Field work remains the great debating ground of our profession. No one owns an exposure (in the academic sense); we all benefit from the impressions and observations of others on the outcrop, and it is a poor geologist who cannot return to an exposure and come away enriched further. The leaders of this workshop are simply folk who have had the good fortune to visit the outcrops more frequently than the participants—thus, in the nature of things, their level of ignorance is likely to be a little less.

We, the leaders of this field trip, would like to acknowledge firstly the numerous landowners who have so graciously allowed us access to their property. In the Slick Hills we would particularly like to thank Jim Underwood, Stan Kimbell, Charlie Bob Oliver, and Doyle Leatherbury. Secondly, we owe thanks to several of our students who have conducted research on various problems germane to the present context: Debra Shelby-Ross, Kelly Cloyd, Felicia Mathews, Mark Lynch, Judy Khourri, Curtis Ditzell, Randy Hosey, Sherman Smith, Chai, Mary Gide-Rafalowski, Mike Stephenson, and Scott White. Finally it is a pleasure to acknowledge discussions with so many of our peers, notably Tim Denison, J. Markello, L. S. Land, R. B. Koepnich, Bob Folk, D. Elmore, and Guoqiu Gao.

REFERENCE CITED

Fay, R. O., 1988, I-35 road cuts: geology of Paleozoic strata in the Arbuckle Mountains of southern Oklahoma, *in* Hayward, O. T. (ed.), Geological Society of America, South-Central Section, Field Trip Guide, v. 4, p. 183–188.

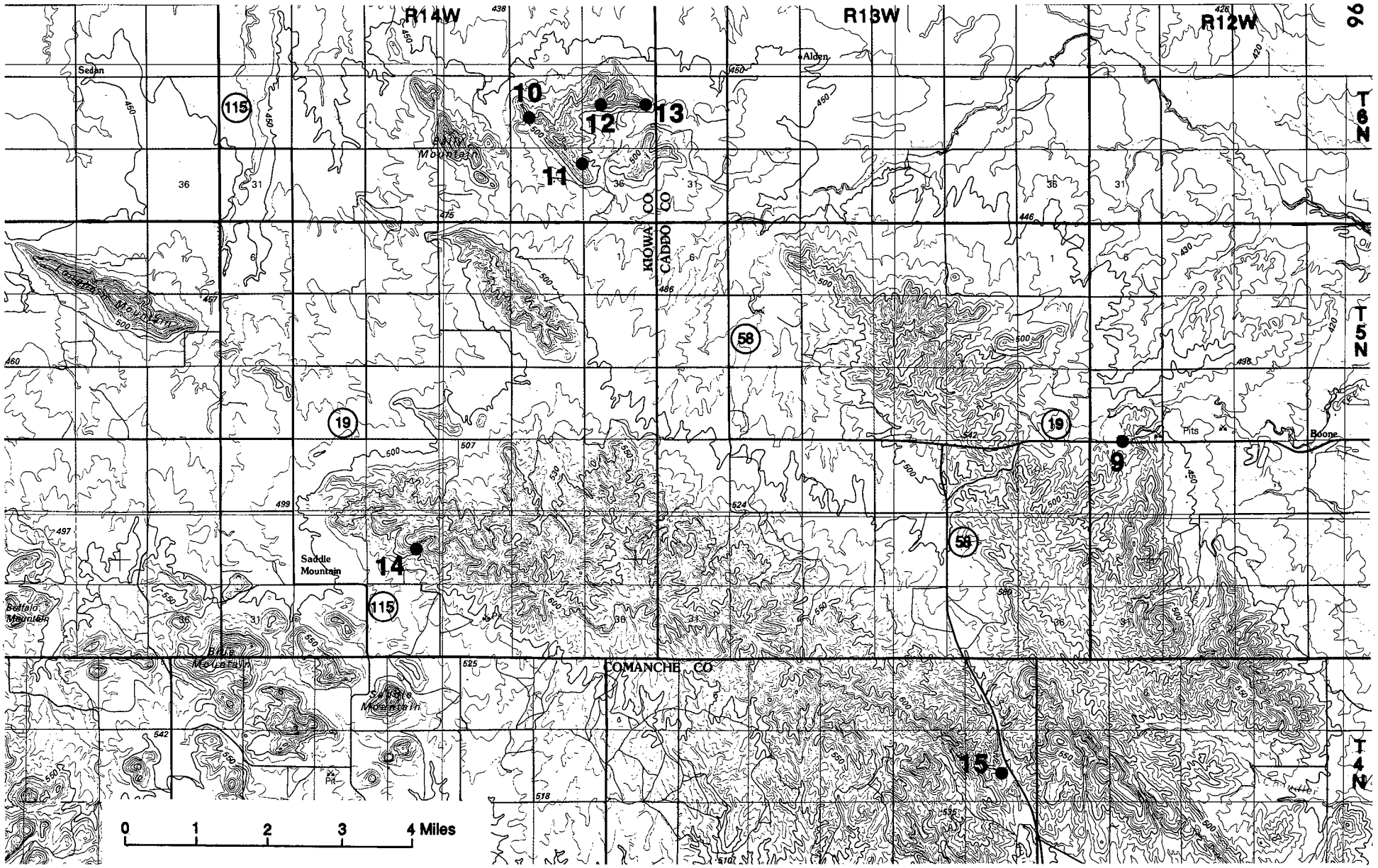


Figure 3. Topographic map of part of the Slick Hills in the Wichita Mountains. Field-trip stops 9–15 (Day 2) are labeled on the map.

ITINERARY

DAY ONE

The Arbuckle Mountains

(see Fig. 2)

STOP 1
Origin of the Kindblade, I-35 Megabreccia

STOP 2
Flower Structure in the Lower Arbuckle

STOP 3
Folding and Thrusting in the Lower Arbuckle

STOP 4
The Cool Creek Formation at Turner Falls Park—A Platform Compendium

STOP 5
Turner Falls: Tufa, Travertine, and Bedding-Parallel Thrusts

STOP 6
Lateral Variations in the Upper Arbuckle Group Rocks—A Comparison Between Sections on I-35 and US 77 in the Arbuckle Mountains

STOP 7
Paleokarst Origin for Bedded Breccias in the Cool Creek Formation

STOP 8
Parallel Folds and Shallowing-Upward Cycles in the Kindblade Formation, I-35

DAY TWO

The Slick Hills

(see Fig. 3)

STOP 9
Permian Karst and Platform Carbonates, Cook Creek Road Cut

STOP 10
The Base of the Arbuckle Group at Bally Mountain

STOP 11
Three Types of Dolomite and the Transition from Fort Sill to Signal Mountain Formation at Raggedy Ridge, Bally Mountain

STOP 12
The Cool Creek Formation and Lower Kindblade Formations on North Bally Mountain

STOP 13
Leatherbury's Quarry—The World's Smallest Oil Field

STOP 14
The Saddle Mountain Dolomite on Maukeen Hill

STOP 15
Parallel Folds and the Thatcher Creek Member in Blue Creek Canyon

The Arbuckle Group—An Aide de Memoire

R. Nowell Donovan
Texas Christian University

INTRODUCTION

On any workshop or field trip it is difficult to judge the general level of knowledge of the participants. In my experience, assumptions can be made that will leave some people floundering in the dark. In an attempt to provide us all with a thorough background to a study of the Arbuckle Group, this paper addresses a number of generalities that will, I hope, put the Arbuckle Group into a regional perspective and highlight problems and unresolved questions.

A few years ago, while I was still at Oklahoma State University, I had the pleasure of teaching a very gifted Chinese graduate student, Jingyao Gong. Whenever we went on a field trip, as soon as it became daylight, he would start to read background materials for the trip. This paper is respectfully dedicated to him.

THE AGE AND SETTING OF THE ARBUCKLE GROUP

The base of the Arbuckle Group is diachronous, as it was deposited over an irregular land surface as part of a major Late Cambrian transgression toward (today's) north and west. In Oklahoma, the initial basal deposits can be assigned to the Franconian subdivision of the Upper Cambrian. Deposition of the Arbuckle Group took place throughout the whole of the Lower Ordovician (Canadian), just extending into the Whiterockian of the Middle Ordovician. Thus, at the most, the period of deposition of the group occupies something like 25–30 million years.

Placed in a regional perspective, the Arbuckle Group was deposited on part of what is arguably the largest carbonate platform ever to have existed (e.g., Ross, 1976). This platform extended from northeast Mexico, across the south-central and eastern parts of the United States, northward into Canada and, making allowances for the opening of the present Atlantic Ocean, into northwest Scotland. The platform developed as a passive margin of the complex Iapetus/Proto-Atlantic Ocean from Cambrian times until closure in the Pennsylvanian, when the final tectonic events, which constitute the Caledonian–Appalachian–Ouachita orogen, took place. Correlatives of the Arbuckle Group include, to the south, the El Paso and Ellenburger of Texas and, to the northeast, the Knox, Beekmantown, Sauk, and Prairie du Chein. Farther still to the north, the Arbuckle correlates with the upper part of the Durness Limestone Group in northwest Scotland.

Generally, isochores on the Arbuckle Group equivalents show a thickening toward the shelf edge (e.g., Johnson and others, 1988; Kerans, 1990). However, in the area of southern Oklahoma, where the weakened basement of the southern Oklahoma aulacogen strikes at a N.60°W. angle into the craton, isopachs parallel this trend and, as a result, the Arbuckle Group is a narrow (~100 mi [160 km]) thickened wedge striking at a high angle into the craton.

During the Late Cambrian–Early Ordovician, southern Oklahoma was located approximately 500–1,000 mi (~800–1,600 km) south of the equator, and was rotated clockwise by approximately 30–45° from its modern position (Ross, 1976; Kerans, 1990). The area formed part of the southwestern edge of the Laurentian plate, the bulk of which straddled the equator. Geographically the shelf/platform boundary would have trended approximately 10–20° north of east–west, while the southern Oklahoma aulacogen was oriented approximately N.15–25°W. (azimuth ~335–345°). Climatically, the area was within the tropics and would have been bathed by the warm waters of the eastward-flowing southern Equatorial current.

THE BASAL UNCONFORMITY OF THE ARBUCKLE GROUP

The Arbuckle Group rests either on the Honey Creek Limestone, top formation of the Timbered Hills Group, or on basement rocks. The latter are either the ancient (~1.3 billion year old) granites and gneisses of the Laurentian craton, or the complex of Cambrian basic and acidic rocks that underpin the southern Oklahoma aulacogen (Fig. 1). Relationships of the latter type are well exposed in the Slick Hills of southwestern Oklahoma, where a hilly land surface formed by the Carlton Rhyolite Group was gradually entombed. The clear evidence of buried relief has given rise to the concept of the southern Oklahoma archipelago (Donovan, 1986; Donovan and Stephenson, 1991). In the Arbuckle Mountains, the same irregular land surface is well exposed near Mill Creek, outside the original boundaries of the southern Oklahoma aulacogen, where hills of Troy Granite rise for ~1,000 ft (~300 m) through the Timbered Hills and lower Arbuckle Group (Ham, 1955). In the subsurface, this irregular land surface can be detected in the neighborhood of Tulsa, where granitic hills project through the Arbuckle Group (Johnson and others, 1988).

FORMATIONS IN THE ARBUCKLE GROUP

Subdivision of the Arbuckle Group has been accomplished by reference to the two principle areas of outcrop. Formations in the lower part of the group (the Fort Sill, Signal Mountain, and McKenzie Hill, plus the Kindblade of the upper Arbuckle) were first recognized in the area of the Wichita uplift, whereas type sections for the Cool Creek and West Spring Creek are in the Arbuckle Mountains (Fig. 2).

The stratigraphic nomenclature of the Arbuckle Group has been confused by the existence of thick, apparently strata-bound dolomite sequences. Thus, in the Arbuckle

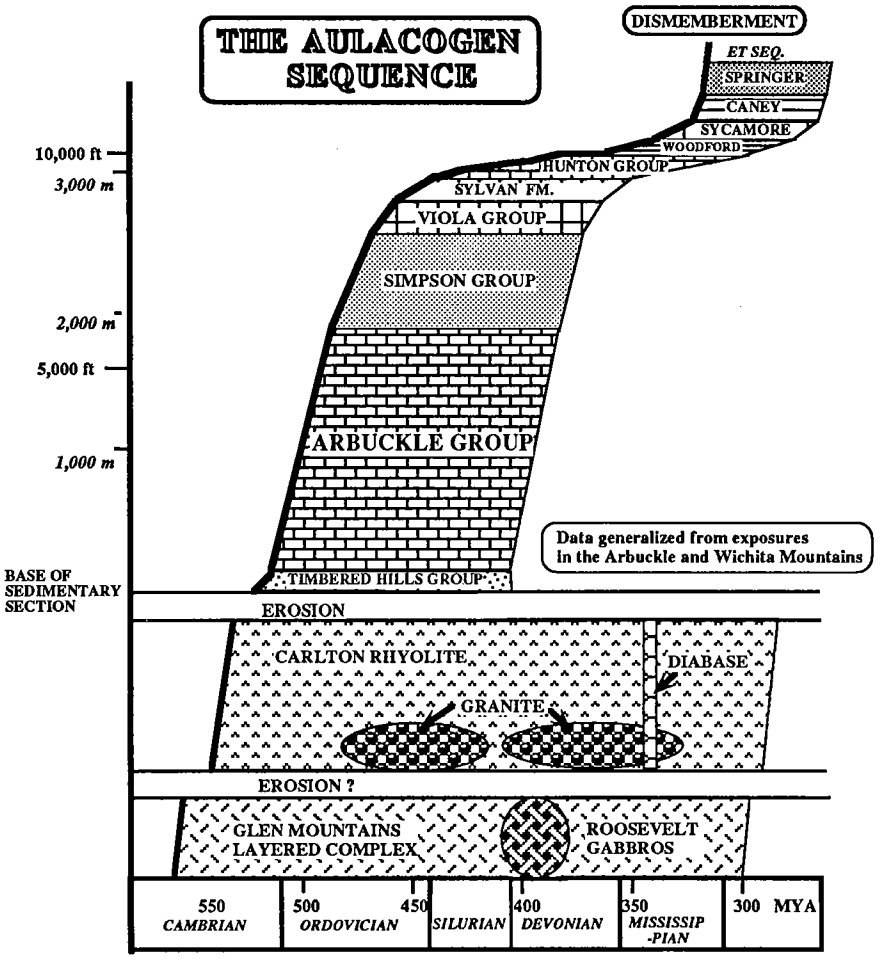


Figure 1. The lower Paleozoic sequence within the southern Oklahoma aulacogen.

Mountains two thick dolomites, the Royer and Butterly have been formally recognized (e.g., Johnson and others, 1988). In the Slick Hills a lower Bally dolomite is approximately equivalent in its stratigraphic position to the Royer (Donovan and Ross, 1991). An upper Saddle Mountain dolomite has no obvious correlatives in the Arbuckle Mountains but occupies the approximate stratigraphic position of the so-called "Brown zone" encountered by subsurface workers. The value of the Slick Hills sections is that in both cases the apparently strata-bound dolomites feather sharply into limestones. Such feathering of carbonate facies must be widespread in the subsurface, for Arbuckle equivalents to the north and south of the aulacogen are dominantly dolomitic whereas, within the confines of the aulacogen, limestones are more commonly seen.

One of the problems in justifying subdivision of the Arbuckle Group is that a combination of lithostratigraphic and biostratigraphic parameters has been used. For example, the contact between the Fort Sill and Signal Mountain, and the McKenzie Hill and Cool Creek is lithostratigraphically defined, whereas the base of the Kindblade Formation is defined on the occurrence of the operculum of the gastropod *Ceratopea*. In the field, this gastropod is only noticeable when it has been silicified. Thus, as in the case of the dolomite units noted above, a diagenetic imprint forms the basis for formational subdivision (Donovan and Ragland, 1986). Such usage reflects the fact that stratigraphic subdivision in the Arbuckle is bedeviled by problems of homotaxy; very few satisfactory marker beds are available to the field geologist. Biostratigraphic zonation using conodonts may well provide the most meaningful basis for detailed stratigraphic work (e.g., Ethington and Dresbach, 1990), although it is clear that precise definition within the group will remain a major problem.

Within the southern Oklahoma aulacogen, the Arbuckle Group is immensely thick, perhaps as much as 7,000 ft (~2,100 m). The group thins to north and south across the boundaries of the aulacogen, and also thins to the northwest, towards the center of the craton. Typical thicknesses of equivalent rocks outside of the aulacogen are on the order of 1,000–4,000 ft (~300–1,200 m). In addition, isochores tend to thin by post-Arbuckle erosion toward the interior of the craton.

The great variation in thickness shown by the Arbuckle Group has led to suggestions that, in the deeper parts of the aulacogen, deeper-water environments existed and that, as a consequence, source-rock potential may exist in this area. If such rocks exist, their most likely stratigraphic position would be as equivalents of the Signal Mountain Formation, which appears to have been deposited in

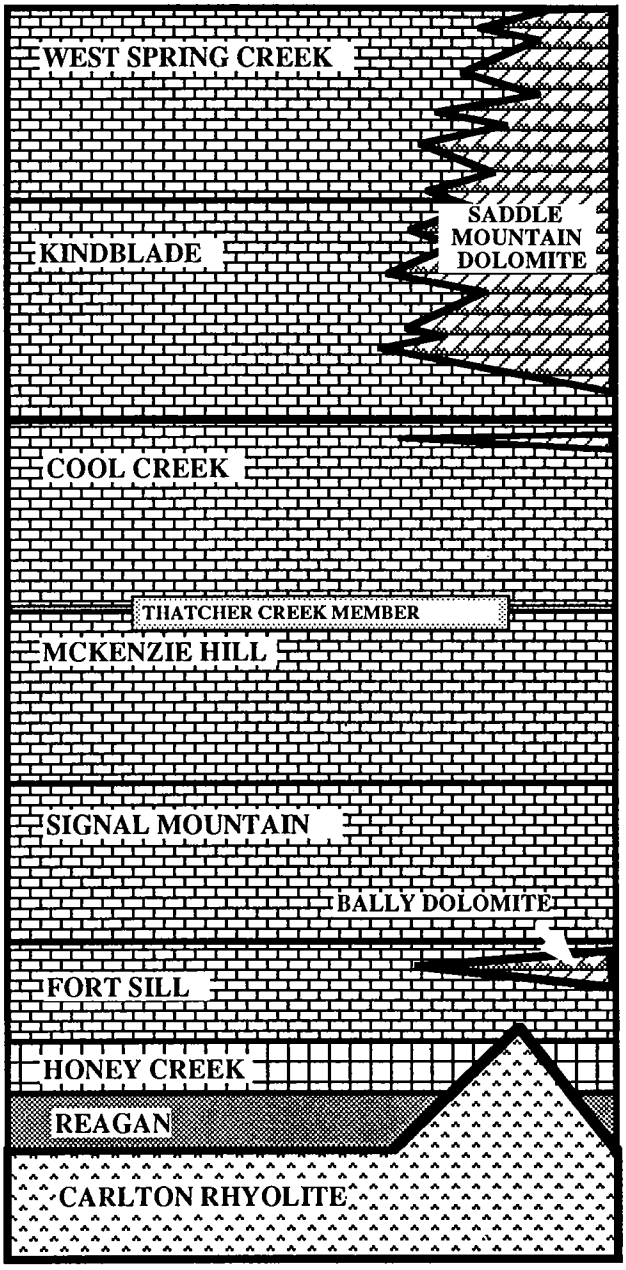


Figure 2. Stratigraphic nomenclature of the Arbuckle and Timbered Hill Groups. Thickness is variable, up to a maximum of 7,000 ft (~2,100 m). Dolomite "formations" found in the Slick Hills are shown. The Thatcher Creek Member is the formally recognized base of the Cool Creek Formation.

slightly deeper water. However, as yet no TOC value much in excess of 0.25% has been recorded (e.g., Ditzell, 1984). It has to be emphasized that the character of sedimentation throughout the Arbuckle Group is that of shallow-water peritidal deposition, characterized by oxidative conditions during sedimentation and early diagenesis. In essence, the carbonate factory that worked on the Laurentian craton at this time produced carbonate sediments more quickly than they could be buried in the passive tectonic setting that existed at this time (Donovan, 1986). Such a situation is not likely to produce widespread anoxia.

CYCLICITY IN THE ARBUCKLE GROUP

Workers in the Arbuckle Group, examining the available sedimentary parameters, have generally concluded that the strata were deposited in warm water of variable, but always shallow, depth. Evidence has been presented to suggest the existence of oolitic-sand shoals, a variety of storm-related deposits, algal boundstones, below-wave-base mudstone accumulation, wave-reworked sedimentation, and hardground precipitation. Other features suggest periods of emergence and "supratidal" sedimentation (e.g., Ham, 1955; St. John and Eby, 1978; Ragland and Donovan, 1985a,b,1986; Donovan, 1986; Ragland, 1990). "Supratidal" is an adjective that must be used with some caution, for the great size of the Arbuckle platform dictates that range and energy of astronomically generated tides must have been greatly damped by comparison with modern environments, particularly toward the landward side of the platform. Calculations (Ragland, 1990) suggest that this was an ultra-microtidal environment, and that our uniformitarian analogies to supra-, intra-, and subtidal may in fact be unnecessarily restricting.

In all likelihood, the greatest input of physical energy into the waters of the platform came in the form of storms. Given the fact that short-term sediment-production rates were so much greater than sediment-entrapment rates (ca. 400 ft [~122 m]/million years, Donovan, 1986), then the frequency of storms affecting the platform can be considered to be a uniformitarian, rather than a catastrophic, control. Consequently, in the long term, each storm can be considered as one element of a constantly applied environmental element applied several times a year, and thus such effects as storm tides and seiche effects would have been a commonly applied sediment modifier. By analogy with modern-day storms, such as the "shamal" of the Persian Gulf, each storm would have been responsible for a track of erosion, resorting, and reworking. However, individual storms, while vectored consistently, according to global-circulation rules, would have followed different tracks. These tracks would have been from east to west with a Coriolis deflection to the southwest, i.e., oblique to the orientation of both platform and aulacogen. Such a direction would constantly have broken up the organization of the platform into the regular shelf-parallel facies belts that are typical of the small carbonate settings of today. Empirically, in most cases individual genetic "events" (e.g., individual intraformational conglomerates, algal boundstones, or hardgrounds) cannot be correlated over distances >1,000 yards (~1 km).

At a coarser level of organization, it has been suggested that the Arbuckle Group is characterized throughout by a cyclic alternation of deep-shallow water conditions (e.g., Lindsay and Koskelin, 1991; Wilson and others, 1991). Each cycle is of the order of 3–15 ft (~1–5 m). Similar shallowing upward "minicycles" have been recognized elsewhere in the lateral equivalents of Arbuckle strata (e.g., Markello and Read, 1982; Koerschner and Read, 1989); they are thought to represent time spans of 20,000–100,000 years and have been attributed to a Milankovitch climatic forcing mechanism.

As noted above, it has been difficult to subdivide the Arbuckle Group into clearly defined formations. At the same time there is no doubt that, for example, a "typical"

sequence of Kindblade does not resemble a "typical" sequence of Cool Creek. The difficulty is in drawing a meaningful stratigraphic boundary between the two. Thus, "typical" Cool Creek will show abundant chert and detrital quartz grains, traces of evaporites, numerous thin beds of "penecontemporaneous" dolomite, mud cracks, and other evidence of emergence. These features are less common in the Kindblade, which is an altogether more fossiliferous formation, dominated by deeper water lithologies. Expressed in terms of the cyclic model, a "typical" Cool Creek cycle displays more shallow-water and emergent facies than does a "typical" Kindblade cycle. Applying the logic developed by Read and his coworkers (e.g., Koerschner and Read, 1989), the differences between the Kindblade and Cool Creek are due to the higher order, longer term type of cyclicity than the hitherto mentioned minicycles (Fig. 3). In the Cool Creek minicycle, development took place during an overall regressive period. On the other hand, Kindblade deposition generally coincided with relatively high rates of long-term sea-level rise.

While it is clear that rises and falls of sea level are a very convenient way to account for many of the features of the Arbuckle Group (including early dolomitization), it may be that the Arbuckle also contains responses to tectonic events. For example, as Donovan (1986) noted, the boundary between the Ft. Sill and Signal Mountain Formations is sharp, involving a change from boundstone-dominated to grainstone-dominated lithologies. Recent work has shown both that there are pronounced facies changes in the Signal Mountain immediately above the contact and that there is relief on the top Ft. Sill surface (Hosey, personal communication). Another indicator of rapid change is the abundance of glauconite in the Signal Mountain. As Feinstein (1981) has shown that subsidence curves in the aulacogen accelerated at this time, it is possible that the changes discussed represent a response to tectonic events.

Another feature that obscures detailed correlation in the Arbuckle Group is the substantial change in thickness that the group shows when traced to north and south from the aulacogen. Do individual minicycles simply thin depositionally when traced away from their maximum thickness, or are there increasingly important disconformities as the sequence thins? Or are we, in fact, dealing with a combination of both effects?

DOLOMITIZATION IN THE ARBUCKLE GROUP

There are several varieties of dolomite within the Arbuckle Group, only some of which are related to hydrocarbon potential (Donovan and Ross, 1991). The earliest are thin dolomicrites that form beds up to a maximum of 10 ft (~3 m) thick. In such beds the amount of dolomite varies from a few percent to an almost complete replacement of the original texture. Much of this type of dolomite is fabric selective (for example, it can be found occupying burrows); it is rarely associated with any significant porosity. Dolomites of this type may or may not be associated with evidence of evaporative conditions. Such beds are perhaps analogous to modern sabkha deposits (Cloyd and others, 1986; Gao and Land, 1991b). However,

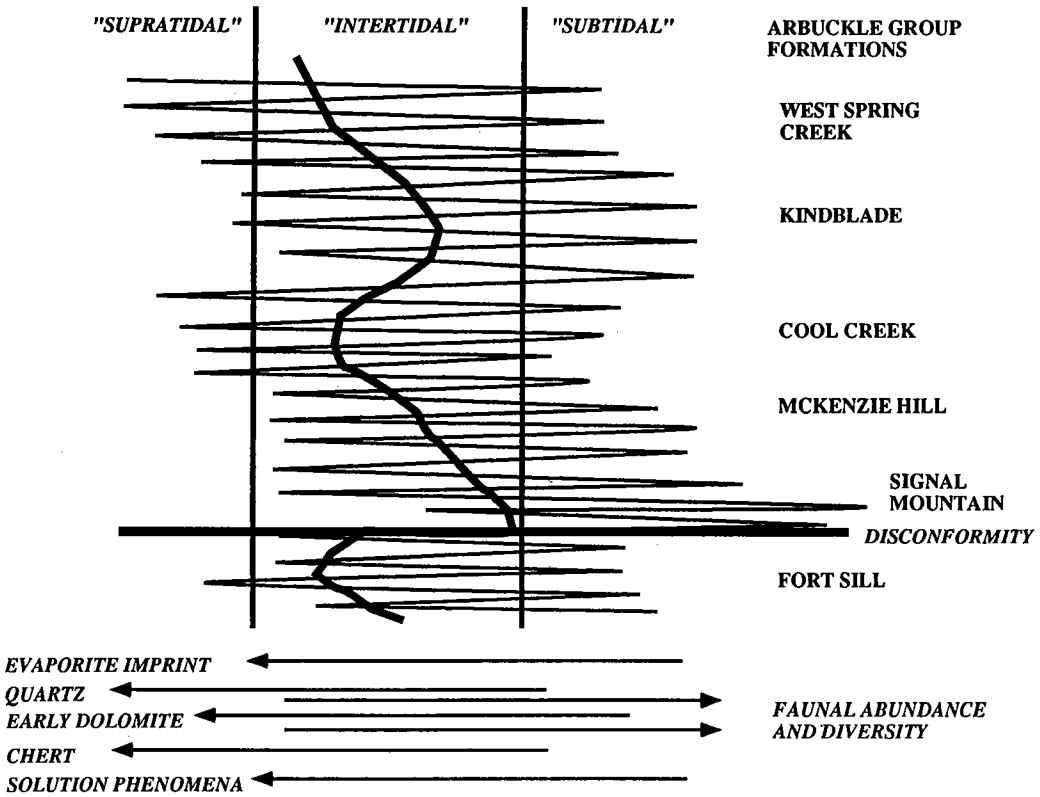


Figure 3. Schematic representation of the basis for lithostratigraphic subdivision of the Arbuckle Group. Note terms involving use of the word "tidal" should be viewed with some circumspection as astronomically generated tides were probably of very feeble magnitude (storm "tides" were a different matter!).

where evaporite indicators are not seen, it is possible that the dolomite is of schizohaline origin.

A second type of dolomite is that usually referred to as "massive" or "stratabound." It is usually a 100% replacement of the original limestone, and shows a variety of medium- to coarse-grained textures ranging from idiotopic to xenotopic. In some cases crystals show zoning, in others they do not. Crystals may show a complex response to cathode luminescence. In the Arbuckle Mountains the principal occurrences of this type of dolomite are the Royer and Butterly Formations. In the Slick Hills, the Bally dolomite, an approximate stratigraphic equivalent to the Royer, is 300 ft (~90 m) thick. A dolomite of this type occurs near the top of the Cool Creek and, in addition, a great thickness (as much as 1,500 ft [~450 m]) is locally developed in the Kindblade and lower West Spring Creek Formations—the Saddle Mountain dolomite of Donovan and Ross (1991) (see also Gao and Land, 1991a). On Maukeen Hill in the western Slick Hills, an approximate thickness of 1,200 ft (~370 m) of Saddle Mountain gives way to ~350 ft (~100 m) of dolomite in a horizontal distance of <400 yards (~370 m). In the field, contacts are knife-edge, passing from 100% limestone to 100% dolomite in a distance of <2 in. (~5 cm).

The origin of this type of dolomite is problematical; it clearly predates Pennsylvanian folding, and it has been suggested (Donovan and Ross, 1991) that the original dolomitization process was one associated with meteoric ground-water mixing, followed by a long period of burial and modification by subsurface brines. Alternatively, Kerans (1990) has suggested that similar dolomites in the Ellenburger of Texas formed as a result of the subtidal evaporative concentration of marine waters on the vast Arbuckle–Ellenburger platform. Field evidence suggests that it is likely that the dolomites originated at an early date, possibly, in the case of the lower stratigraphic levels, during Arbuckle deposition. On the other hand, dolomites at higher stratigraphic levels may well owe their origin to the great regression that took place at the end of Arbuckle Group sedimentation, prior to deposition of the overlying Simpson Group.

Other dolomites are quantitatively insignificant. They appear as small discordant bodies, as vein fills, or as a partial infill of karst features and vuggy pores. Textures are generally coarse and baroque. Zoning is commonly seen and the dolomite is frequently ferroan (Cloyd and others, 1986; Lynch and Al-Shaieb, 1989,1991; Gao and Land, 1991b). In general these dolomites are of late diagenetic origin, and in some cases demonstrably postdate Pennsylvanian tectonism and karst development. The most likely origin for such dolomite is from the circulation of basin brines, either from the deeper parts of the pre-Pennsylvanian aulacogen basin or from one or another of the syntectonic Pennsylvanian basins that developed during the tectonic dismemberment of the aulacogen. In the latter case, the existence of deep zones of abnormal pressure, for example, below 10,000 ft (~3,000 m) in the Anadarko basin (Al-Shaieb and others, 1991), provides a potent driving mechanism for fluid migration. The continuing emergence of barite-precipitating oilfield brines at Zodletone Mountain in the Slick Hills is evidence of the efficacy of this migration (Younger and others, 1986) (Fig. 4).

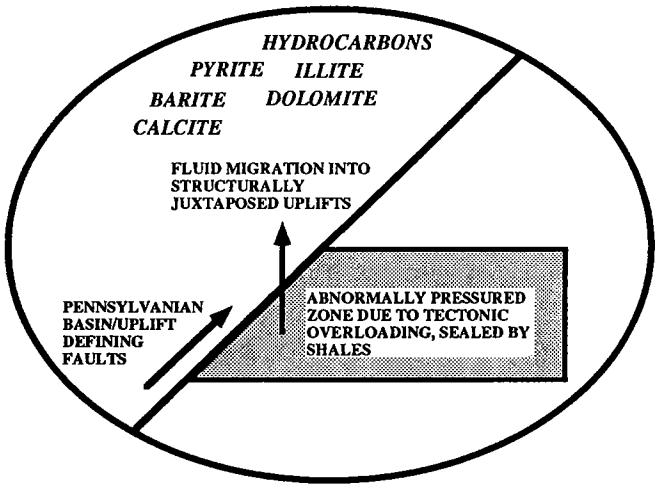


Figure 4. Schematic relationship between deeply buried parts of the southern Oklahoma aulacogen and adjacent uplifts due to overpressuring; diagenetic products, including hydrocarbons, could be precipitated at considerable distances from their source.

Porosity associated with the dolomites is, in order of desirability, cavernous, vugular, and intracrystalline (Lynch and Al-Shaieb, 1989,1991; Kerans, 1990; Read and Richmond, 1991). As noted above, substantial thicknesses of dolomite are seen in the western Slick Hills; however, not all of this dolomite is porous. Only locally are intracrystalline porosities in excess of 10% developed; given the complex paragenesis of this dolomite, it is perhaps not surprising that widespread pore reduction by the addition of later phases of dolomite has taken place.

EVOLUTION OF THE AREA AS A PASSIVE MARGIN

The West Spring Creek Formation appears to have been deposited during a period of gradually falling sea level. Continuing this trend, a major craton-wide regression took place prior to deposition of the overlying Simpson Group. Emergence and karstification to a depth of 600 ft (~200 m) has been documented at this time in the Ellenburger (e.g., Kerans, 1990); similar effects have been noted in northern Oklahoma. Within the confines of the southern Oklahoma aulacogen, the karst surface has not been as well documented; in the Arbuckle Mountains the Joins Formation at the base of the Simpson rests with apparent conformity upon the West Spring Creek (Ham, 1955).

Rocks overlying the Arbuckle Group are assigned to the Simpson Group, Viola Group, Sylvan Shale, Hunton Group, Woodford Shale, and a variety of Mississippian formations. Formations below the Woodford are stratigraphically concordant and burial subsidence curves (e.g., Feinstein, 1981) suggest that the rate of basin development slowed progressively with time (Fig. 1).

At the end of Hunton Group deposition, gentle tectonic warping tilted the area. As a result, the overlying Woodford oversteps all the underlying units down to the Arbuckle with a slight angular unconformity. This rela-

tionship is immensely important, for it juxtaposed a truly magnificent source rock with all underlying potential reservoirs. Following Woodford deposition, which was a craton-wide event, Mississippian deposition was increasingly focused into a series of individual depocenters. This break-up of basin continuity heralded the Pennsylvanian dismemberment of the craton.

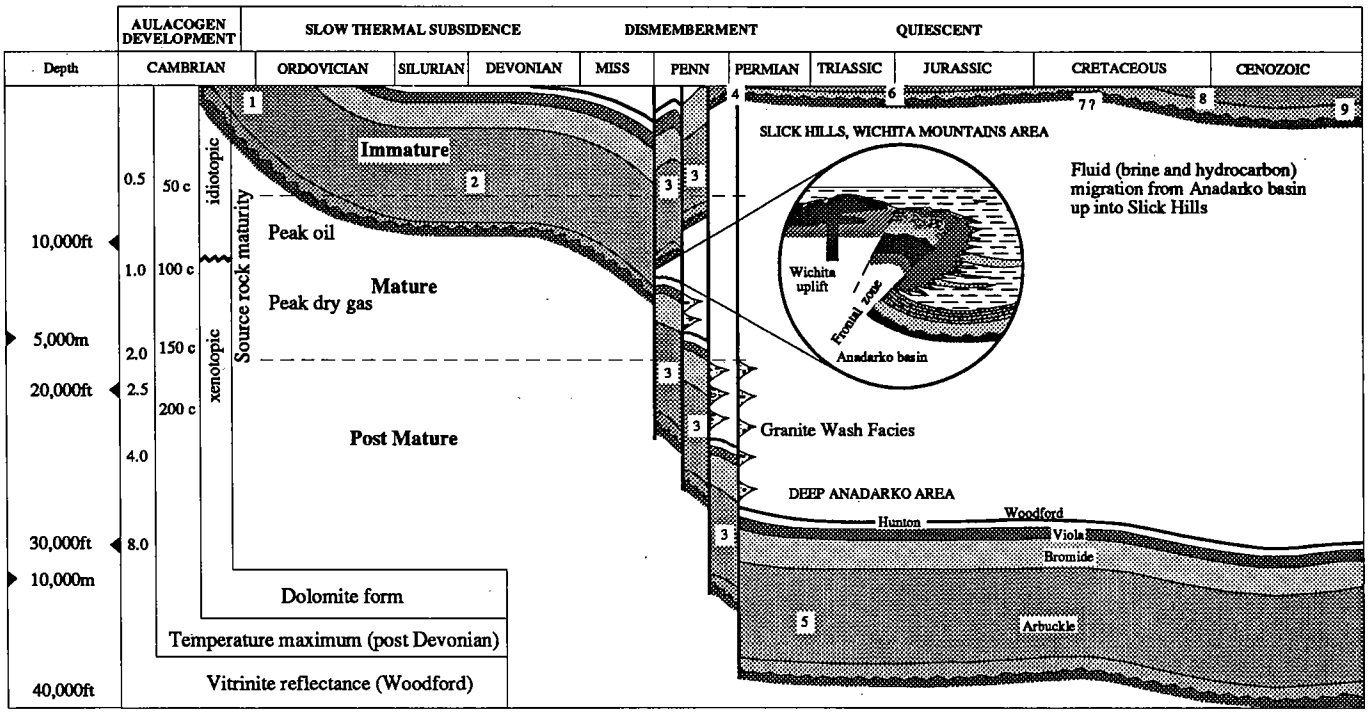
PENNSYLVANIAN DISMEMBERMENT

During the Pennsylvanian the southern Oklahoma aulacogen was dismembered into a series of yoked basins and uplifts (Johnson and others, 1988). While part of the craton was inverted to spectacular elevations (e.g., the Wichita, Criner, and Arbuckle uplifts), part of the craton subsided to produce equally spectacular successor depressions (e.g., the Anadarko, Ardmore, and Marietta basins) (Fig. 5). As a result of this deformation, the Arbuckle Group was emplaced at radically different structural elevations. Thus, there is ample evidence that the Arbuckle cropped out in the Arbuckle Mountains and Slick Hills during Pennsylvanian and Permian times. On the other hand, in the deepest parts of the Anadarko basin the group was emplaced well below 30,000 ft (~10,000 m). Hence, any surface/subsurface comparison of the Arbuckle must recognize the differing diagenetic pathways that have operated during the past 280 million years.

During the Pennsylvanian the Arbuckle Group was subjected to the tectonic deformation that is so obvious a feature of the available outcrops. The group forms approximately 40–50% of the lower Paleozoic section; hence it is clear that an understanding of the style of deformation of this thinly layered, highly anisotropic group is critical to an understanding of the style of deformation in the aulacogen as a whole. This is particularly the case where the basement consists of aulacogen rocks, for it is clear that the Carlton Rhyolite and possibly other layered igneous rocks were involved in folding (Donovan and others, 1989). Outside the boundaries of the aulacogen, deformation was less intense and fold generation took place at higher stratigraphic levels (Fig. 6).

Features characteristic of Arbuckle Group deformation include an abundance of brittle fracturing (joints, shears, broken or collapsed folds) (Fig. 7), parallel folding (accompanied by a great deal of evidence for flexural slip), and pressure solution. Typical folds in Arbuckle strata have sharply defined semi-chevron profiles (Fig. 8). Pressure-solution effects are generally seen as bedding discordant (aka "vertical" or "tectonic") stylolites. In the Slick Hills, in particular, zones of pressure solution are a very common feature.

There are some differences between the Arbuckle Mountains and the Slick Hills. In the Arbuckle Mountains, deformation occurred rather late in the Pennsylvanian; a cross section across the aulacogen at this level (e.g., Denison, 1982) indicates the existence of two uplifts



Diagenetic stage of Arbuckle Group

1. Eodiagenesis
2. Mesodiagenesis (shallow burial submarine)
3. Mesodiagenesis (tectonic)
4. Telodiagenesis (karst)
5. Mesodiagenesis (deep burial submarine)
6. Mesodiagenesis (2nd imprint shallow burial subcontinent)
7. Telodiagenesis (karst?)
8. Mesodiagenesis (2nd imprint shallow burial subcontinent)
9. Telodiagenesis (karst)

Figure 5. Tactical comparison of the histories of the Slick Hills and the Anadarko basin. Hydrocarbon-source maturity is based on the Woodford. Redrawn from Donovan (1986).

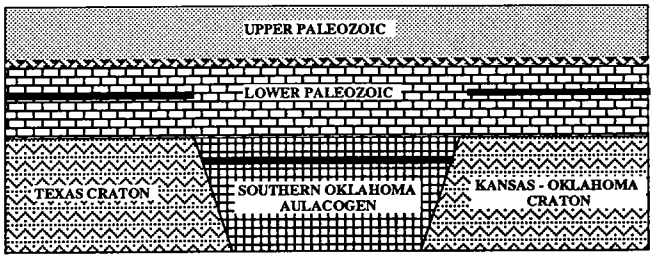


Figure 6. Schematic representation showing how the character of the basement affects the style of tectonic deformation seen in southern Oklahoma. Where the basement consists of layered igneous rocks (e.g., in the southern Oklahoma aulacogen), the lowest level of fold generation is within the basement and, as a result, the Arbuckle Group is intensively folded. However, where the basement consists of rigid granites and gneisses (e.g., in the Tishomingo area, on the Oklahoma craton), fold generation takes place at higher levels within the lower Paleozoic section. Except where it is crushed and flexed adjacent to large faults, the Arbuckle Group conforms to the tilt of underlying basement blocks. Note also that the great lithological difference between the lower Paleozoic section (dominated by carbonates) and the upper Paleozoic (dominated by fine-grained siliciclastics) suggests that the boundary between the two may be a décollement surface.



Figure 7. Aerial view of part of the southern flank of the Arbuckle anticline west of Interstate 35. The strata depicted are mostly in the Cool Creek Formation. Notice the amazing intensity of fracturing and small faults. Such a pattern illustrates the characteristic brittle-deformation style of the Arbuckle Group. It also indicates the large number of potential pathways by which ground-water could be focused during karst development. This terrain could be thought of as a gigantic potential crackle or fracture breccia (Kerans, 1990).

(an early Criner and later Arbuckle) and two contemporary basins (Ardmore and Marietta) in which approximately equal amounts of structural differentiation were achieved by folds and faults. A cross section in the Wichita–Anadarko area, however, shows that only one uplift and two basins (Anadarko and Hardeman) are present and that most of the tectonic differentiation is achieved by fault movements in the frontal fault zone between the Anadarko basin and the Wichita uplift (the exposed part of this fault zone is the Slick Hills; the western Slick Hills are arguably the most comprehensively deformed rocks exposed in the aulacogen). The difference between the two areas may be explained by the widening of the aulacogen to the southeast.

POST PENNSYLVANIAN

Since the Pennsylvanian, there has been almost no tectonic activity in Oklahoma. The Arbuckle Mountains were buried by Pennsylvanian detritus; the Wichita Mountains, in their turn, by Permian detritus. By Late Permian time, both uplifts were entombed (Johnson and others, 1988).

Since the Mesozoic Era, the craton has been essentially stable, and, as a result, no further basin differentiation has taken place in the area. However, during the worldwide Cretaceous transgression, Oklahoma received a thin coat of shallow-marine rocks. Projection of the base of the sub-Cretaceous unconformity makes it clear that the uninspiring flat top to the Arbuckle Mountains is the result of Cretaceous peneplanation. Whether or not this peneplanation affected the Wichitas is a moot point. Cretaceous deposits are known in the Anadarko basin, but there is no direct evidence that the Wichita Mountains were exposed.



Figure 8. Small-scale folding in the McKenzie Hill Formation, Blue Creek Canyon, eastern Slick Hills. Note overall parallel fold style and characteristic sharply defined axis of the anticline.

In more recent time, the area was partially covered by Ogalalla alluvium shed from the Rocky Mountains, and there have been some murmurations on various faults along the old N.60°W. trend; most notable of these has been a slight reactivation of the Meers fault, along the southern boundary of the Slick Hills.

KARST

The term "karst" is widely used to describe the interaction of soluble rock with water that is undersaturated with respect to the minerals with which it is in contact. Common usage involves the dissolution of limestone by meteoric water, although there is an increasing appreciation of the role that acidic brines can play in the subsurface. A spatial distinction is generally made between surface (two-dimensional) and subsurface (three-dimensional) karst, and in the latter between vadose and phreatic settings. Implicit in the development of subsurface karst is the need for a rock geometry that will focus ground-water flow: for example, a fracture system or a contact between soluble and nonsoluble lithologies. In addition, a hydrologically dynamic setting with available relief is required for deep cave development. Clearly a distinction must be made between karstification that is related to withdrawal of seawater and karstification that is related to tectonic uplift. Unless the former is of great magnitude, the latter is more likely to provide deep karst systems.

Caves furnish a wide variety of deposits; sediment transported into the cave from the surface, sediment eroded from within the system, material that has fallen into the cave as a result of roof or wall collapse, as well as a variety of secondarily derived calcite deposits (speleothems). Furthermore, many cave systems show evidence of activity at more than one time.

At several times during the evolution of the Arbuckle Group, there has been a potential for karst development. The earliest of these was contemporary with deposition. For example, Donovan and others (1986) described scalloped surfaces in the Kindblade Formation that they attributed to surface dissolution during low sea-level stands. Similarly, some chert breccias in the Cool Creek Formation appear to be surface-residue deposits that attest periods of limestone dissolution. There is no evidence of subterranean karst development associated with either of these types of surface. Another possibly early development of karst is suggested by collapse breccias where it is thought that evaporite deposits may have been removed by nearly contemporary solution (e.g., Ragland and Donovan, 1985b). In this case it is not necessary to involve meteoric flow, but rather nonevaporative sea water (i.e., submarine karst).

As noted above, at the end Arbuckle deposition, a substantial regression took place across the Laurentian craton. This Whiterockian regression, which was of considerable duration and depth, may well have generated sufficient relief for the development of substantial three-dimensional karst (e.g., Kerans, 1990). In addition, the regression may also have created the environment for a substantial meteoric flushing of the top part of the Arbuckle Group with consequent dolomitization (see above).

Following Simpson Group deposition, it is unlikely that the Arbuckle Group was exposed to surface conditions until the Middle Devonian, immediately preceding deposition of the Woodford Formation. Existing karst may have been reused or new karst developed at this time, particularly in areas of Arbuckle onlap in northern Oklahoma. However, this karst is unlikely to have had any impact on either the Slick Hills or the Arbuckle Mountains, as these areas were both comprehensively buried by lower Paleozoic strata.

According to, perhaps, the most favorable theory, three-dimensional karst development took place during the various tectonic pulses that accompanied the dismemberment. Pennsylvanian karst systems are exposed in the Arbuckle Mountains and fine Permian cave systems are known in the Slick Hills (Donovan, 1982,1986). The characteristic of this type of karst development, because it involves variable amounts of available relief and is developed in tectonically disturbed terrain, is that most of the cave systems are developed as enlarged fissure fractures. At any given site these fractures are generally orthogonal; as a result, a rectangular drainage system developed in the subsurface.

It is worth noting that the available area of uplift as a result of the Pennsylvanian dismemberment was not great. Essentially, southern Oklahoma evolved into a series of rather narrow but long NW–SE-trending hill masses bounded by similarly shaped basins. Depending upon the relief of the uplifts, and given the humid climate that existed during the Pennsylvanian, these cave systems may have developed to quite considerable depths below the existing land surface.

Surface-related cave formation, at least in the Slick Hills, effectively ceased during the Early Permian, both because the uplifts were buried and also because the climate became increasingly arid. It is possible that reactivation occurred during Cretaceous peneplanation and, of course, some caves have been reactivated during the present erosional cycle. Nevertheless, it seems likely that the existing buried karst continued to evolve as basinal brines and hydrocarbons moved through the cave systems (Lynch and Al-Shaieb, 1989,1991).

HYDROCARBON POTENTIAL

1. The Arbuckle Group has yet to yield convincing evidence that it is a potential source rock. If this is the case, given the decreasing crustal mobility suggested by regional sediment-entrapment curves (e.g., Fig. 1), hydrocarbon generation on large scale probably did not take place until the Pennsylvanian dismemberment. It follows that success in exploration is most likely where structure has juxtaposed the Arbuckle Group against a mature source (most likely the Woodford), either as a result of pre-Woodford tilting or as a result of Pennsylvanian tectonism.

2. As a reservoir rock, the Arbuckle suffers from the obvious problem of being at the bottom of what is, in places, an extraordinarily thick sedimentary pile. Simple geothermal considerations suggest that the condition of the group at the bottom of the Anadarko basin must resemble that of a metamorphic marble.

3. At intermediate structural levels, on the margins of late Paleozoic uplifts, the Arbuckle has reservoir potential that is almost all due to the existence of secondary porosity in the following forms: (a) cavernous (i.e., karst), vugular, and intracrystalline porosity associated with dolomitization; this appears to be by far the most productive type of reservoir; (b) karst formation associated with limestone; and (c)fracture potential (as yet largely untested in the context of horizontal drilling).

REFERENCES CITED

Al-Shaieb, Z.; Puckette, J.; Ely, P.; and Abdalla, A., 1991, The upper Morrow fan delta chert conglomerate in Cheyenne and Reydon fields: completely sealed gas-bearing pressure compartments [abstract]: Oklahoma Geological Survey, Petroleum-reservoir geology in the southern Midcontinent—a workshop, Norman, p. 4.

Cloyd, K.; Ragland, D. A.; Jones, L.; and Donovan, R. N., 1986, Dolomite with evaporitic connection in the Ordovician Cool Creek Formation, southwestern Oklahoma, *in* Donovan, R. N. (ed.), The Slick Hills of southwestern Oklahoma—fragments of an aulacogen?: Oklahoma Geological Survey Guidebook 24, p. 29–34.

Denison, R. E., 1982, Geologic cross section from the Arbuckle Mountains to the Muenster arch, southern Oklahoma: Geological Society of America Map and Chart Series MC-28R, 8 p., scale 1:250,000.

Ditzell, C., 1984, The sedimentary geology of the Signal Mountain and McKenzie Hill Formations, as exposed in the Slick Hills of southwestern Oklahoma: Oklahoma State University unpublished M.S. thesis, 165 p.

Donovan, R. N., 1982, Geology of Blue Creek Canyon, Wichita Mountains area, *in* Gilbert, M. C.; and Donovan, R. N. (eds.), Geology of the eastern Wichita Mountains, southwestern Oklahoma: Oklahoma Geological Survey Guidebook 21, p. 65–77.

_____1986, Geology of the Slick Hills, *in* Donovan, R. N. (ed.), The Slick Hills of southwestern Oklahoma—fragments of an aulacogen?: Oklahoma Geological Survey Guidebook 24, p. 1–12.

Donovan, R. N.; and Ragland, D. A., 1986, Paleozoic stratigraphy of the Slick Hills, southwestern Oklahoma, *in* Donovan, R. N. (ed.), The Slick Hills of southwestern Oklahoma—fragments of an aulacogen?: Oklahoma Geological Survey Guidebook 24, p. 13–16.

Donovan, R. N.; and Ross, D. L., 1991, The Saddle Mountain dolomite at Maukeen Hill—a dolomite interface in the upper Arbuckle Group, western Slick Hills, Oklahoma, *in* Johnson, K. S. (ed.), Late Cambrian–Ordovician geology of the southern Midcontinent, 1989 symposium: Oklahoma Geological Survey Circular 92, p. 143–153.

Donovan, R. N.; and Stephenson, M. D., 1991, A new island in the southern Oklahoma archipelago, *in* Johnson, K. S. (ed.), Late Cambrian–Ordovician geology of the southern Midcontinent, 1989 symposium: Oklahoma Geological Survey Circular 92, p. 118–121.

Donovan, R. N.; Ragland, D. A.; and Shaefer, D., 1986, Stop 4: Geology of the Cook Creek road cut, *in* Donovan, R. N. (ed.), The Slick Hills of southwestern Oklahoma—fragments of an aulacogen?: Oklahoma Geological Survey Guidebook 24, p. 100–105.

Donovan, R. N.; Marchini, W. R. D.; McConnell, D. A.; Beauchamp, W.; and Sanderson, D. J., 1989, Structural imprint on the Slick Hills, southern Oklahoma, *in* Johnson, K. S. (ed.), Anadarko basin symposium, 1988: Oklahoma Geological Survey Circular 90, p. 78–84.

Ethington, R. L.; and Dresbach, R. I., 1990, Ordovician conodonts in the Arbuckle Group, southern Arbuckle Mountains, Oklahoma, *in* Ritter, S. M. (ed.), Early to middle Paleozoic conodont biostratigraphy of the Arbuckle Mountains, southern Oklahoma: Oklahoma Geological Survey Guidebook 27, p. 33–37.

Feinstein, S., 1981, Subsidence and thermal history of southern Oklahoma aulacogen: implications for petroleum exploration: American Association of Petroleum Geologists Bulletin, v. 65, p. 2521–2533.

Gao, G.; and Land, L. S., 1991a, Petrography and geochemistry of massive dolomite from the upper Arbuckle Group, Slick Hills, southwestern Oklahoma, *in* Johnson, K. S. (ed.), Late Cambrian–Ordovician geology of the southern Midcontinent, 1989 symposium: Oklahoma Geological Survey Circular 92, p. 64.

_____1991b, Early Ordovician Cool Creek dolomite, middle Arbuckle Group, Slick Hills, SW Oklahoma, U.S.A.: Journal of Sedimentary Petrology, v. 61, p. 161–173.

Ham, W. E., 1955, Field conference on geology of the Arbuckle Mountain region: Oklahoma Geological Survey Guidebook 3, 61 p.

Johnson, K. S.; Amsden, T. W.; Denison, R. E.; Dutton, S. P.; Goldstein, A. G.; Rascoe, B.; Sutherland, P. K.; and Thompson, D. M., 1988, Southern Midcontinent region, *in* Sloss, L. L. (ed.), Sedimentary cover—North American craton; U.S.: Geological Society of America, The Geology of North America, v. D-2, p. 307–359. [Also released in 1989 as Oklahoma Geological Survey Special Publication 89-2, 53 p.]

Kerans, C., 1990, Depositional systems and karst geology of the Ellenburger Group (Lower Ordovician), subsurface West Texas: Texas Bureau of Economic Geology Report of Investigations 193, 63 p.

Koerschner, W. F., III; and Read, J. F., 1989, Field and modelling studies of Cambrian carbonate cycles, Virginia Appalachians: Journal of Sedimentary Petrology, v. 59, p. 654–687.

Lindsay, R. F.; and Koskelin, K. M., 1991, Arbuckle Group depositional parasequences, southern Oklahoma, *in* Johnson, K. S. (ed.), Late Cambrian–Ordovician geology of the southern Midcontinent, 1989 symposium: Oklahoma Geological Survey Circular 92, p. 71–84.

Lynch M.; and Al-Shaeib, Z., 1989, Evidence of paleokarstic phenomena and burial diagenesis in the Ordovician Arbuckle Group of Oklahoma: Transactions of the 1989 American Association of Petroleum Geologists Mid-Continent Section meeting, Oklahoma City, p. 1–55.

_____1991, Evidence of paleokarstic phenomena and burial diagenesis in the Ordovician Arbuckle Group of Oklahoma, *in* Johnson, K. S. (ed.), Late Cambrian–Ordovician geology of the southern Midcontinent, 1989 symposium: Oklahoma Geological Survey Circular 92, p. 42–60.

Markello, J. R.; and Read, J. F., 1982, Upper Cambrian intrashelf basin, Nolichucky Formation, southwest Virginia Appalachians: American Association of Petroleum Geologists Bulletin, v. 66, p. 860–878.

Ragland, D. A., 1990, Sedimentology, paleoenvironmental analysis and diagenesis of upper Arbuckle Limestones in the Slick Hills, southwestern Oklahoma: Oklahoma State University unpublished Ph. D. thesis, 238 p.

Ragland, D. A.; and Donovan, R. N., 1985a, The Thatcher Creek Member: basal unit of the Cool Creek Formation in southern Oklahoma: Oklahoma Geology Notes, v. 45, p. 84–91.

_____1985b, The Cool Creek Formation (Ordovician) at Turner Falls in the Arbuckle Mountains of southern Oklahoma: Oklahoma Geology Notes, v. 45, p. 132–148.

_____1986, An environmental analysis of the Lower Ordovician Cool Creek Formation of southwestern Oklahoma, *in* Donovan, R. N. (ed.), The Slick Hills of southwestern Oklahoma—fragments of an aulacogen?: Oklahoma Geological Survey Guidebook 24, p. 21–28.

Read, D. L.; and Richmond, G. L., 1991, Geology and reservoir characteristics of the Arbuckle Brown zone in the Cottonwood Creek field, Carter County, Oklahoma [abstract]: Oklahoma Geological Survey, Petroleum-reservoir geology in the southern Midcontinent—a workshop, Norman, p. 14.

Ross, R. J., Jr., 1976, Ordovician sedimentation in the western United States, *in* Bassett, M. G. (ed.), The Ordovician System: University of Wales Press, Cardiff, p. 73–105.

St. John, J. W., Jr.; and Eby, D. E., 1978, Peritidal carbonates and evidence for vanished evaporites in the Lower Ordovician Cool Creek Formation, Arbuckle Mountains, Oklahoma: Gulf Coast Association of Geological Societies Transactions, v. 28, p. 589–599.

Wilson, J. L.; Fritz, R. D.; and Medlock, P. L., 1991, The Arbuckle Group—relationship of core and outcrop analyses to cyclic stratigraphy and correlation, *in* Johnson, K. S. (ed.), Late Cambrian–Ordovician geology of the southern Midcontinent, 1989 symposium: Oklahoma Geological Survey Circular 92, p. 61–63.

Younger, P.; Donovan, R. N.; and Hounslow, A. W., 1986, Barite travertine at Zodletone Mountain in the Slick Hills, southwestern Oklahoma, *in* Donovan, R. N. (ed.), The Slick Hills of southwestern Oklahoma—fragments of an aulacogen?: Oklahoma Geological Survey Guidebook 24, p. 75–81.

DAY ONE

STOP 1
Origin of the Kindblade, I-35 Megabreccia

NE¼NE¼SW¼ sec. 31, T1S, R2E; first scenic turnout on I-35, southbound lane, just south of road leading up to scenic sight and geologic sign.

Bryan Tapp
University of Tulsa

BACKGROUND

This stop, and each stop on the field trip, is in the southern Oklahoma aulacogen. All of the rocks and structures observed on the field trip relate back to the development of the aulacogen. Aulacogens preserve the igneous and sedimentary rocks that record the opening and closure of ocean basins. Rocks in the aulacogen are usually preserved without metamorphism, and thus they contain invaluable information about the evolution of continents. Nicholi Shatskiy (1946) defined an aulacogen as a long-lived, fault-bounded trough in an otherwise stable platform that intersects a deformed belt or a continental margin at a high angle and contains an abnormally thick, usually undeformed section of terrestrial and marine sediments. Shatskiy (1946) used the Dnieper–Donets basin of the Russian platform, along with the Wichita system as type aulacogens.

Aulacogens are distinct geotectonic features with a complex history of evolution that are genetically related to "geosynclines" but are not easily explained by "geosynclinal" theory (Shatskiy, 1947,1955). Hoffman and others, (1974) presented a scenario for the evolution of an aulacogen using the Athapuscow aulacogen and the southern Oklahoma aulacogen as examples. The evolution of an



Figure 1. Megabreccia in the Kindblade Formation exposed in the scenic-turnout road cut just south of road leading up to geologic sign. Contact with overlying undisturbed Kindblade strata is on the right. View looking to west.

aulacogen is divided into three stages: rifting, followed by subsidence and infilling of the rift, and finally deformation of the rocks in the ancient rift. The rocks and structures of an aulacogen preserve a relatively undeformed and unmetamorphosed geologic history of a complete Wilson Cycle.

STOP OVERVIEW

The I-35 megabreccia crops out in the scenic overlook on the southbound lane of I-35 near Turner Falls (Figs. 1,2). It is limited to the Kindblade Formation of the lower Arbuckle Group. The outcrop of the megabreccia is roughly rhombohedral in shape, extending no more than 92 m (300 ft) to the west and 308 m (1,000 ft) to the east. The outcrop in the roadcut is small, measuring ~92 m (300 ft) in length at its widest point. The megabreccia can be seen on both the eastern and western wall of the cut. The unit can also be seen on the eastern side of the I-35 southbound lane road cut and on the western and eastern walls of the northbound lanes of I-35. The breccia zone was originally mapped by William E. Ham as a complex zone (notations on original aerial photographs at Oklahoma Geological Survey), and later by Fay (1989) as a fault zone. Both men mapped the outcrop as being fault bounded on all sides. Field relationships support the conclusion that the east and west contacts of the megabreccia zone are fault controlled, where the megabreccia zone terminates sharply against well-bedded Kindblade. The northern and southern contacts are also fault controlled. This fault at the northern end of the megabreccia cuts bedding, truncating ~15 m (50 ft) of Kindblade. The truncation can be accurately measured using a red marker bed in the Kindblade in this area. The southern contact also cuts across bedding and is interpreted as being fault controlled. The megabreccia occurs ~46 m (150 ft) south of the Washita Valley fault, one of the major strike-slip faults in the Arbuckle Mountains.

The megabreccia itself consists of angular limestone boulders set in a variegated clay matrix that shows some layering. The limestone boulders range from cobble size to as large as 3 × 3 m (10 × 10 ft). The limestone boulders are all from the Kindblade Formation, based upon lithology and fossil content. The significant fossils are the pelecypod *Ceratopia* and the brachiopod *Triteoteca*. Gastropods are also visible, but are not diagnostic of the Kindblade.

Orientation Data

The bedding orientation of clasts in the megabreccia unit have only a weakly developed girdle and cluster (Fig. 3), based on 113 bedding plane measurements within the megabreccia (Tapp, 1978). The development of the weak girdle pattern and cluster on the contour diagram of bedding orientation shows that there is no preferred orientation of bedding in the megabreccia.

Clay Mineralogy

Megabreccia Clay Matrix

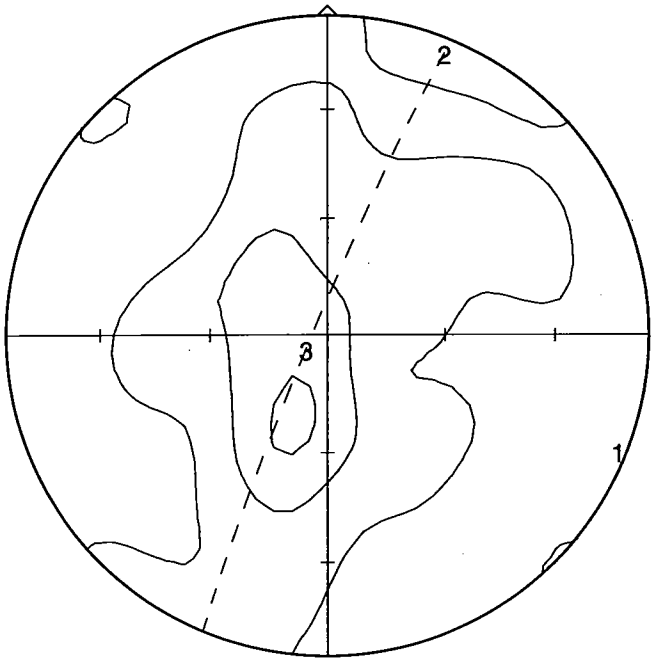
The clay matrix is dominated by illite and kaolinite with only minor montmorillonite. X-ray patterns do not show any marked difference in mineralogy between the upper and lower contacts. The clay samples collected represent small isolated pods of clay that are all bound by limestone in at least the two dimensions of the outcrop face. The similarity in clay mineralogy of such isolated pods of clay suggests that they have (a) shared the same environment of deposition, (b) shared the same diagenetic environment, and (c) that they are secondarily derived from the same parent rock.

Clay Mineralogy of the Megabreccia Boulders

The clay mineralogy of insoluble residue from the megabreccia boulders do not show a marked difference in either the present vertical or horizontal directions. The clay mineral assemblage is dominated by illite and kaolinite with only minor montmorillonite. The X-ray patterns are identical to those obtained for the matrix clays.



Figure 2. View of megabreccia in Kindblade Formation just opposite Figure 1. View looking east.



N = 113 E = 4.17
k = 27.11 Sigma = 1.39
(Peak - E)/Sigma = 4.4
Peak position : 201.8°/ 65.6°

Figure 3. Contour of bedding-pole orientations of 113 bedding planes of clasts in the I-35 megabreccia. The contour shows a weakly developed girdle and cluster. Numbers 1–2–3 on the diagram correspond to numerically determined eigenvectors based on SperiStat® program.

This similarity between the clay mineral assemblages suggests a genetic link between the clay matrix and the insoluble clays in the limestone blocks. The presence of kaolinite in the megabreccia boulders suggests diagenetic alteration. Kaolinite does not accumulate in carbonate depositional environments but can be found in carbonate rocks after diagenetic alteration (Sergonzac, 1970).

Comparison of Megabreccia Clays with Clay Partings in the Kindblade Formation

Four clay seams were found in the Kindblade limestone outcrops along I-35. All four of these seams are located north, or up section from the megabreccia unit. The seams are all present within 15 m (50 ft) stratigraphically of the megabreccia unit. The clay mineral assemblage of the shale partings is dominated by illite and kaolinite with only minor montmorillonite. The X-ray patterns are similar to those of the megabreccia clays and the limestone clast insolubles.

Insoluble Clays in Kindblade Formation

Twenty samples of the Kindblade limestone collected on a linear traverse along the outcrop of that unit on I-35 show a marked change in clay mineralogy away from the megabreccia zone and the Washita Valley fault zone. The mineralogy of the insoluble material stratigrahically above the megabreccia is identical with the clay mineralogy of the clay partings in the area and with both the clay-matrix material of the megabreccia and the insoluble material of the megabreccia clasts. The samples below the megabreccia show increasing montmorillonite content away from the megabreccia and the fault zone.

INTERPRETATION AND DISCUSSION

This unit has been interpreted as a tectonic breccia at the toe of the Chapman Ranch thrust (Fay, 1989), as a deep-seated solution collapse feature along closely spaced tension joints due to percolation of fluids along the Washita Valley fault (Tapp, 1978), as a collapse feature at the unsupported trailing edge of a gravity-glide thrust (Phillips, 1983), as a gravity or tectonically collapsed fold (Hoffman, personal communication), and as a karstic collapse feature (Dennis Prezbindowski, personal communication).

I interpret the megabreccia as a relatively deep-dissolution collapse breccia. As such, the megabreccia preserves rocks associated with the deformation phase of the aulacogen. The model I propose is for the gradual dissolution of the limestone blocks due to percolation of subsurface fluids along tension fractures, where the dissolving blocks slowly rotate and sink inward as the megabreccia develops. The main points to consider in evaluating a model for the formation of the megabreccia are as follows:

1. The megabreccia is not near the toe of a thrust fault, and local thrusting has not been demonstrated. The beds in the surrounding Kindblade are not deformed in a manner that is consistent with compression related to thrusting. The deformation in the Kindblade is limited to local tension fractures rather than compression. The lack of compressional distortion in the surrounding rocks argues against a thrust origin for the megabreccia. This is the only occurrence of a fault-bounded megabreccia in the Arbuckle Mountains. If the megabreccia were related to thrusting, there should be other occurrences of the megabreccia along existing thrusts. The structural setting is unusual. The megabreccia is in the only large releasing bend of the Washita Valley fault (Fig. 4). The orientation of the primary fractures is consistent with extension in the vicinity of a releasing bend.

2. The areal extent of the megabreccia is limited, and all contacts with the Kindblade Formation are faults. The detachment hypothesis is inconsistent with the limited size of the feature. Detachment along a gravity slide (or any relation to a fault escarpment) would produce a feature that is more continuous.

3. The clay mineralogy of the megabreccia matrix is very similar to that of the insoluble clays in the megabreccia blocks and in clay partings of the Kindblade and insoluble clays in the Kindblade near the Washita Valley fault. These similarities are suggestive of a common origin for these clays. The dominance of kaolinite and illite is suggestive of a common diagenetic origin. Away from the fault, the clay mineralogy of the insoluble clays in the Kindblade become montmorillonitic, as expected in marine carbonates. The change in clay mineralogy may be due to structurally controlled diagenesis. The favored environment for montmorillonite is a weakly alkaline system (Sergonzac, 1970). This favors the presence of montmorillonite as a primary clay material in most carbonate environments. Illite is generally believed to

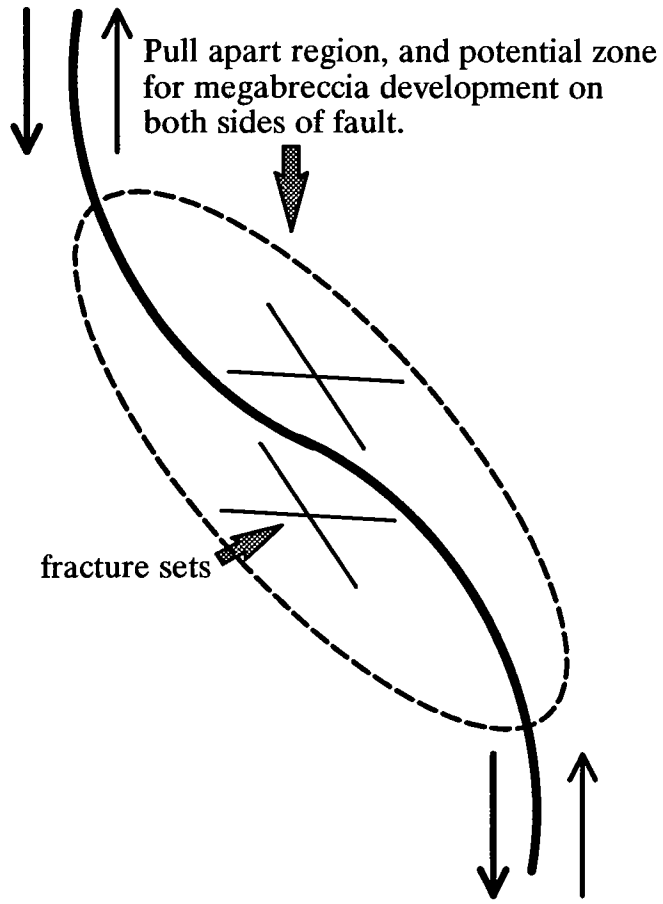


Figure 4. Diagrammatic map view of expected fractures associated with releasing bend in left lateral strike-slip fault.

represent diagenetic alteration of the montmorillonites during burial diagenesis (Sergonzac, 1970; Hower and others, 1976). Kaolinite, on the other hand, forms in arid terrigenous environments as a primary sediment or as a diagenetic product in weakly acidic solutions. Blatt and others (1972) notes that diagenesis of clays may result from exposure to circulating water. He notes that in ancient clastic systems units which have had only restricted water circulation have a composition dominated by montmorillonite, and those that have been subject to a greater water circulation have a composition of kaolinite and degraded illite with chlorite.

4. Travertine has not been identified in any samples from the unit, and the clay material surrounding the blocks is devoid of palynomorphs. This suggests that the feature did not develop as a cave-collapse feature, and did not have water-flow contact with the syntectonic erosional surface. This feature is distinctly different from sinkholes to the south, and within Ordovician units on the Hunton uplift.

5. The bedding orientations in the megabreccia do not show a preferred orientation as would be expected for a collapse fold. There is a weakly developed girdle and cluster to the bedding orientations, but this is statistically insignificant. The clay matrix is folded around the individual blocks, suggesting that at least some deformation occurred after the formation of the megabreccia.

6. The Kindblade is unique in its outcrop appearance and internal characteristics. There are several Pennsylvanian karstic collapse pipes on the Hunton uplift. These pipes are nearly circular in outcrop pattern and contain Pennsylvanian fossils, clearly demonstrating their karst origin.

The two most commonly cited mechanisms for the formation of the Kindblade megabreccia are the deep-dissolution collapse idea and karst. The feature has received significant interest since the discovery of oil in the Cottonwood Creek field. Cottonwood Creek is a karst feature in the releasing bend of a strike-slip flower structure, and the Kindblade megabreccia is the closest analogue available. The primary difference between the Kindblade megabreccia and Cottonwood Creek is that Cottonwood Creek is not infilled with clay. The debate regarding the origin of the feature hinges on whether the feature formed at depth or whether it formed near the surface. It may not be possible to adequately test between these two hypotheses. However, the deep-dissolution model presented here seems to best fit the data. New observations could change the interpretation.

REFERENCES CITED

Blatt, H.; Middleton, G. V.; and Murray, R. C., 1972, Origin of sedimentary rocks: Prentice-Hall Inc., Englewood Cliffs, 634 p.

Fay, R. O., 1989, Geology of the Arbuckle Mountains along Interstate 35, Carter and Murray Counties, Oklahoma: Oklahoma Geological Survey Guidebook 26, 50 p.

Hoffman, P.; Dewey, J. F.; and Burke, K., 1974, Aulacogens and their genetic relation to geosynclines, with a Proterozoic example from Great Slave Lake, Canada, *in* Dott, R. H.; and Shaver, R. H. (eds.), Modern and ancient geosynclinal sedimentation: Society of Economic Paleontologists and Mineralogists Special Publication No. 19, p. 38–55.

Hower, J.; Eslinger, E. V.; Hower, M. E.; and Perry, E. A., 1976, Mechanism of burial metamorphism of argillaceous sediment: 1.—Mineralogical and chemical evidence: Geological Society of America Bulletin, v. 87, p. 725–737.

Phillips, E. H., 1983, Gravity slide thrusting and folded faults in western Arbuckle Mountains and vicinity, southern Oklahoma: American Association of Petroleum Geologists Bulletin, v. 67, p. 1363–1390.

Sergonzac, G. D. de, 1970, The transformation of clay minerals during diagenesis and low-grade metamorphism: a review: Sedimentology, v. 15, p. 281–346.

Shatskiy, N. S., 1946, Great Donbass and Wichita system: comparative tectonics of old platforms: SSSR Izvestia, Seria Geologie No. 6, p. 57–90.

_____1947, Structural correlations of platforms and geosynclinal folded regions: Izvestia Acadamy Sciences U.S.S.R., Seria Geologie No. 5, p. 37–56.

_____1955, On the origin of the Pachelma trough: Byull. Moskvskogo Obshchestva Lyubiteley Prirody, Odt. Geol., v. 5, p. 5–26.

Tapp, J. B., 1978, Breccias and megabreccias of the Arbuckle Mountains, southern Oklahoma aulacogen, Oklahoma: University of Oklahoma unpublished M.S. thesis, 126 p.

STOP 2
Flower Structure in the Lower Arbuckle

NE¼SE¼SW¼ sec. 31, T1S, R2E; along I-35 in the southbound lane between scenic turnout and Turner Falls exit. The exposure is in the west wall of the I-35 road cut.

Bryan Tapp
University of Tulsa

BACKGROUND

The Arbuckle Mountain uplift displays a variety of deformation styles and intensity in a region of roughly 1,000 mi². Interpretation of the surface structures in the Arbuckle Mountains has been problematic. In the field, the structural relations include complicated small thrust complexes, high-angle normal faults, reverse faults, and strike-slip faults. Deformation in the region has been related to wrench tectonics (Wickham and Denison, 1978; Booth, 1981; Haas, 1981; Axtmann, 1983a,b), thrust tectonics (Brown, 1984; Brown and others, 1985), or to distinct phases of both (Islam and Nielsen, 1984). Recent seismic and drilling data suggest that the Arbuckle complex is, at least in part, allochthonous.

There are three prominent structural/tectonic regions in the Arbuckles, each separated by high-angle faults that strike approximately N.60°W. These areas are the Hunton arch, Tishomingo anticline, and Arbuckle anticline. The Hunton arch consists of gently deformed lower Paleozoic carbonates. The Hunton arch is separated from the Tishomingo block by the Mill Creek fault, Mill Creek syncline, and Reagan fault. Studies in the Mill Creek syncline, the Reagan fault, and the Sulphur fault have shown that the style of deformation in this area is consistent with a left-lateral wrench model (Haas, 1981; Islam and Nielsen, 1984).

The Tishomingo anticline, bounded on the north by the Reagan fault and on the south by the Washita Valley fault, has been interpreted as a broad, open fold with a N–S axis. Detailed structural analysis along the Reagan and Washita Valley faults has shown that both have a left-lateral component of offset (Booth, 1981; Haas, 1981). The amount of offset on the Reagan fault has not been determined.

The Arbuckle anticline is bounded on the north by the Washita Valley fault and on the south by the Ardmore basin. The Arbuckle anticline and its associated minor folds have been interpreted as forming in two events: first, the main anticline was formed in middle Virgilian; then, the secondary folds, including the Dougherty anticline, were formed in late Virgilian (Ham, 1969).

The dominant deformation in the Arbuckle Mountain region occurred in Late Pennsylvanian time (Ham, 1969; Axtmann, 1983a,b) although some deformation may have occurred in the Devonian, as shown by local unconformities in the Hunton Group and the presence of a local conglomerate at the base of the Woodford on US 77, and in the Mississippian (Donovan and others, 1983).

The structural style seen in the Arbuckle Mountains is consistent with a left-lateral wrench model. Offset on the Washita Valley fault has been suggested to be from 40 mi, based on offsets in the basal Oil Creek and McLish sands (Tanner, 1967), to 20 mi, based on offset of a Hunton Group thin (Carter, 1979). COCORP data in the Wichita province have indicated that the uplifts are underlain by low-angle thrusts, leading Brewer and others (1983) to suggest that the system has undergone transverse compression.

The structural style of the Arbuckle Mountains has generated significant controversy over the past decade—controversy which can be addressed at the outcrop scale. Structures seen at the outcrop scale can give valuable insight into the structural style at the regional scale.

STOP OVERVIEW

Several subhorizontal to horizontal faults branch from a nearly vertical fault in the outcrop (Fig. 1). The rocks in the immediate vicinity of the faults have been tightly folded and heavily fractured. The rock units to the north and south of the feature are not deformed. I believe the feature serves as a small-scale example of a positive flower structure, where transpression on a strike-slip fault generates low-angle faults and related folds. The narrowness of the deformation zone is undoubtedly related to the relatively small displacement on the fault, but it may also be a function of material character as well as the depth of burial during deformation. The primary deformation mechanism is brittle failure (cataclasis) of the rock material, and pressure solution. The outcrop contains several tectonic stylolites that are subparallel to parallel with local fold-hinge traces in the outcrop face. The outcrop also contains what may be interpreted as a normal fault that has been rotated to its present position. It is unclear whether this "normal" fault is part of the flower structure or is an earlier or later feature.

This pattern of fault orientation and clustering in an apparent positive flower structure repeats itself at several locations in the Arbuckle Mountains. The size of the these flowers changes significantly from outcrop to outcrop, but the overall characteristic does not change appreciably with scale. A somewhat larger flower structure can be seen in the Viola Group to the north of the Collings Ranch Conglomerate along I-35.

The characteristics of these outcrops are highly suggestive of a flower-structure model for the Arbuckle uplift, rather than a thrust origin. Wrench-fault systems can de-

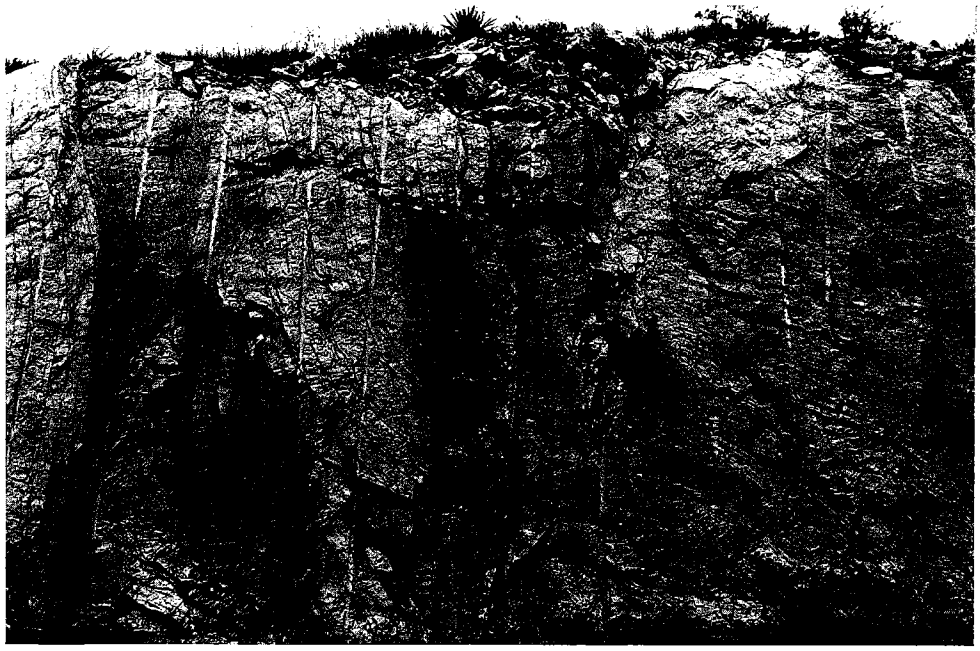


Figure 1. Photograph of flower structure outcrop.

velop a significant range of structures along the length of the fault, and a general discussion may prove useful.

DISCUSSION

Wrench faults are large-scale, strike-slip faults that are generally high angle. Offset on these faults involves all rock units, including basement. The importance of large-scale horizontal movement of the Earth's crust has been recognized for many years, and has led to a great deal of work on wrench faults. Wrench faults can be recognized by a sequence of interrelated features, discussed below.

1. Horizontal offset of lithologies. In a wrench system, the dominant sense of motion on the faults is horizontal. It is common to see lithologic boundaries offset across the fault. This can be recognized in sediments, volcanics, or intrusives that formed prior to faulting, as well as in features formed during fault motion (Moody and Hill, 1956; Wilcox and others, 1973).

2. Braided, anastamosing fault zone near the surface. In most wrench systems a master fault develops late, if at all (Emmons, 1969; Wilcox and others, 1973; Bartlett and others, 1981). The resultant fault pattern is characterized by a series of anastamosing faults, each of which has taken up only a minor part of the total fault offset. These faults fall into two general categories of orientation relative to the master fault: synthetic faults share the same sense of offset as the master fault, and are typically oriented within 10–15° of the orientation of the master fault (Moody and Hill, 1956; Wilcox and others, 1973); antithetic faults have the opposite sense of offset and are oriented at 70–90° to the master fault (Moody and Hill, 1956; Wilcox and others, 1973).

3. En echelon faults and folds. En echelon folds appear to develop early in a wrench system. The hinge traces of these folds are typically oriented at 25–30° to the master fault (Moody and Hill, 1956; Wilcox and others, 1973), and plunge away from the fault zone. These folds are offset by later movement on the fault. In the absence of the master fault, a series of en echelon faults develop at an orientation of 10–15° to the master fault at depth. If the master fault develops, these en echelon faults become synthetic faults (Wilcox, and others, 1973).

4. Horizontal slickensides. The overall horizontal motion of the fault results in a statistically significant population of horizontal slickensides on fault surfaces, where deformation is brittle (Moody and Hill, 1956; Wilcox and others, 1973). With increased depth on the fault, there may be a change from brittle deformation to ductile deformation; however, the overall horizontal fabric would be preserved (Nicholas and others, 1977).

5. Local uplifts and downwarps or pull-apart basins. These features develop in the vicinity of restraining and releasing bends (Crowell, 1974), and as a consequence of localized compression and extension caused by motion on en echelon faults (Groshong and Rodgers, 1978). Thrusts and pop-up features develop in the vicinity of restraining bends (Crowell, 1974) and in the region between en echelon faults (Groshong and Rodgers, 1978). Local downwarps and pull-apart basins develop in the vicinity of releasing bends (Crowell, 1974) and in en echelon systems (Groshong and Rodgers, 1978). These local uplifts and pull-apart basins affect sedimentation in the immediate vicinity of the feature.

6. V-shaped fault zone. The fault zone becomes wider near the syntectonic erosional surface in a wrench system (Bartlett and others, 1981). This increase in the width of the fault zone may be due to changes in confining pressure, or may be related to changes in lithology. Widening of the fault zone may result in the formation of flower structures. Recent investigations have shown that flower structures are common and easily recognized in wrench

systems; however the primary signature is in the seismic expression of the feature (Harding, 1985).

The structural style of the Arbuckle Mountain region uniquely fits these criteria. All of the structural data collected at the surface in the Arbuckle Mountains are compatible with left-lateral, strike-slip deformation in the area. The greatest area of disagreement seems to be whether the major component of deformation has been thrusting, with minor wrench offset, or transpressive wrenching. I suggest that, based on the field observations made over the anticline, the style is best fit by the transpressive wrench model.

REFERENCES CITED

Axtmann, T. C., 1983a, Structural mechanisms and oil accumulation along the Mountain View–Wayne fault, south-central Oklahoma, Part I: Shale Shaker, v. 34, p. 1–12.

_____1983b, Structural mechanisms and oil accumulation along the Mountain View–Wayne fault, south-central Oklahoma, Part II: Shale Shaker, v. 34, p. 13–22.

Bartlett, W. L.; Friedman, M.; and Logan, J. M., 1981, Experimental folding and fracturing of rocks under confining pressure. Part IX.—Wrench faults in limestone layers: Tectonophysics, v. 79, p. 255–277.

Booth, S. L., 1981, Structural analysis of portions of the Washita Valley fault zone, Arbuckle Mountains, Oklahoma: Shale Shaker, v. 31, p. 107–120.

Brewer, J. A.; Good, R.; Oliver, J. E.; Brown, L. D.; and Kaufman, S., 1983, COCORP profiling across the southern Oklahoma aulacogen: overthrusting of the Wichita Mountains and compression within the Anadarko basin: Geology, v. 11, p. 109–114.

Brown, W. G., 1984, Washita Valley fault system: a new look at an old fault, *in* Technical proceedings of the 1981 American Association of Petroleum Geologists Mid-Continent Section regional meeting: Oklahoma City Geological Society, p. 68–80.

Brown, W. G.; Grayson, R. C.; Jamieson, W. H.; and Altum, J. T., 1985, Tectonism and sedimentation in the Arbuckle Mountain region, southern Oklahoma aulacogen: Baylor Geological Society, 44 p.

Carter, D. W., 1979, A study of strike-slip movement along the Washita Valley fault, Arbuckle Mountains, Oklahoma: Shale Shaker, v. 30, p. 80–108.

Crowell, J. D., 1974, Sedimentation along the San Andreas fault, California, *in* Dott, R. H.; and Shaver, R. H. (eds.), Modern and ancient geosynclinal sedimentation: Society of Economic Paleontologists and Mineralogists Special Publication 19, p. 292–303.

Donovan, R. N.; Beachamp, W.; Ferraro, T.; Lajeck, C.; McConnell, D.; Munsil, M.; Ragland, D.; Sweet, B.; and Taylor, D., 1983, Subsidence rates in Oklahoma during the Paleozoic: Shale Shaker, v. 34, p. 86–88.

Emmons, R. C., 1969, Strike-slip rupture patterns in sand models: Tectonophysics, v. 7, p. 71–87.

Groshong, R. H.; and Rodgers, D. A., 1978, Left-lateral strike-slip fault model, *in* Wickham, J. S.; and Denison, R. (eds.), Structural style of the Arbuckle region: Geological Society of America, South-Central Section, Guidebook for Field Trip no. 3, p. 1–7.

Haas, E. A., 1981, Structural analysis of a portion of the Reagan fault zone, Murray County, Oklahoma: Shale Shaker, v. 31, p. 93–104.

Ham, W. E., 1969, Regional geology of the Arbuckle Mountains, Oklahoma: Oklahoma Geological Survey Guidebook 17, 52 p.

Harding, T. P., 1985, Seismic characteristics and identification of negative flower structures, positive flower structures, and positive structural inversion: American Association of Petroleum Geologists Bulletin, v. 69, p. 582–600.

Islam, Q.; and Nielsen, K. C., 1984, Detailed fault history in the east and central portions of the Arbuckle Mountains, Oklahoma [abstract]: Geological Society of America Abstracts with Programs, v. 16, no. 3, p. 87.

Moody, J. D.; and Hill, M. J., 1956, Wrench fault tectonics: Geological Society of America Bulletin, v. 67, p. 1207–1246.

Nicholas, A.; Bouchez, J. L., Blaise, J.; and Poirier, J. P., 1977, Geological aspects of deformation in continental shear zones: Tectonophysics, v. 42, p. 55–73.

Tanner, J. H., 1967, Wrench fault movements along Washita Valley fault, Arbuckle Mountain area, Oklahoma: American Association of Petroleum Geologists Bulletin, v. 51, p. 126–141.

Wickham, J. S.; and Denison, R., 1978, Structural style of the Arbuckle region: Geological Society of America, South-Central Section, Guidebook for Field Trip no. 3, 111 p.

Wilcox, R. E.; Harding, T. P.; and Seely, D. R., 1973, Basic wrench tectonics: American Association of Petroleum Geologists Bulletin, v. 57, p. 74–96.

STOP 3
Folding and Thrusting in the Lower Arbuckle

NW¼NW¼NW¼ sec. 7, T2S, R2E, along I-35 in the southbound lane before the Turner Falls exit. Turner Falls Quadrangle. The exposure is in the west wall.

Bryan Tapp
University of Tulsa

STOP OVERVIEW

This outcrop, perhaps more than any other in the Arbuckle Mountains, has caused more controversy regarding the proposed style of deformation in this region. The two major schools of thought are whether the Arbuckle uplift is due primarily to strike-slip deformation (Wickham and Denison, 1978), or whether the uplift is due primarily to compression (Brown, 1984; Brown and others, 1985). This outcrop has been used as hard evidence that the dominant sense of deformation is thrusting related to compression. The outcrop contains several flexural-slip fold sets in the Fort Sill Formation that have been offset by a series of thrust faults (Fig. 1). The sense of deformation varies across the outcrop, but includes box folds, polyclinal folds, several small-scale folds that developed during thrusting (and whose shapes and attitudes indicate that they are room-accommodation features) (Brown and others, 1985), and a fault-bend fold at a thrust ramp at the north end of the outcrop. The mechanism of folding in the outcrop is bedding-plane slip accompanied by cataclastic failure in the hinge zones of the folds. The apparent sense of transport on the thrust faults is to the north, and the folds show apparent north vergence. There is no question that development of the folds and faults in the outcrop are compressional. The main question is the cause of the compression.

To date, two ideas have been suggested for the cause of the features seen in this outcrop. The outcrop is near the Chapman Ranch thrust, which is exposed under the bridge at the Turner Falls exit. The Chapman Ranch thrust was defined by Fay (1989), who interpreted the feature as a bedding plane thrust that steepens with depth. Work by John Bohon (unfinished M.S. thesis at OU) suggested that the Chapman Ranch fault was vertical at the surface and cut several rock units obliquely. Bohon interpreted the fault as part of a flower structure. This outcrop,



Figure 1. Photograph of north vergent flexural slip fold in Fort Sill Formation. View looking west, with north to the right.



Figure 2. Photograph of flexural-slip thrusting into a fold hinge in hand sample collected from the Viola Formation. The fold hinge is fractured and contains overlapping thrusts that accommodate folding. The thrusting in the hinges is due to flexural-slip folding of competent layers in brittle field, and served to localize the hinge of the folds. This is similar to the folding seen in the Hunton quarry just south of Lake of the Arbuckles dam, both in the large anticline and in parasitic folds in the quarry, and in the hinge zone of the Sycamore Creek anticline.

and others along I-35, have been interpreted as being related to a larger sense of compression that formed the Arbuckle uplift (Brown and others, 1985).

I suggest a third alternative for the origin of these features. The structures present at this outcrop are similar to features seen on folds throughout the Arbuckle uplift. All of the folding in the region is flexural slip in nature. In many cases the bedding-plane slips die out into thrust faults in the hinges of the folds (Fig. 2). Thrust faults can be seen at all scales of observation, from hand-sample to large-scale folds, including the thrusted anticline exposed in the Hunton quarry just south of Lake of the Arbuckles dam. These features commonly form in flexural-slip folding of competent layers (Ramsay, 1967, p. 401; Ramsay and Huber, 1987, p. 458). The fact that conjugate thrusts form in the hinge zones of folds at all scales of observation (Tapp, 1988) is suggestive that this is the causal mechanism for the thrusting in the hinge of the larger Arbuckle anticline. I suggest that the folding and thrusting seen at this outcrop, rather than being part of a larger flower structure, or being related to regional compression, is simply an expression of room accommodation in the hinge zone of a large flexural-slip fold.

REFERENCES CITED

Brown, W. G., 1984, Washita Valley fault system: a new look at an old fault, *in* Technical proceedings of the 1981 American Association of Petroleum Geologists Mid-Continent Section regional meeting: Oklahoma City Geological Society, p. 68–80.

Brown, W. G.; Grayson, R. C.; Jamieson, W. H.; and Altum, J. T., 1985, Tectonism and sedimentation in the Arbuckle Mountain region, southern Oklahoma aulacogen: Baylor Geological Society, 44 p.

Fay, R. O., 1989, Geology of the Arbuckle Mountains along Interstate 35, Carter and Murray Counties, Oklahoma: Oklahoma Geological Survey Guidebook 26, 50 p.

Ramsay, J. G., 1967, Folding and fracturing of rocks: McGraw Hill, New York, 568 p.

Ramsay, J. G.; and Huber, M. I., 1987, The techniques of modern structural geology. Vol. 2—Folds and fractures: Academic Press, New York.

Tapp, J. B., 1988, Structural styles in the Arbuckle Mountains, southern Oklahoma: Geological Society of America, South-Central Section, Centennial Field Guide, v. 4, p. 177–182.

Wickham, J. S.; and Denison, R., 1978, Structural style of the Arbuckle region: Geological Society of America, South-Central Section, Guidebook for Field Trip no. 3, 111 p.

STOP 4
The Cool Creek Formation at Turner Falls Park—A Platform Compendium

On U.S. Highway 77, ~1.5 mi south of I-35 Davis interchange.

Deborah A. Ragland
Conoco Inc., Ponca City

R. Nowell Donovan
Texas Christian University

INTRODUCTION

Turner Falls is arguably the most beautiful spot in the state of Oklahoma. The best known view of the Falls is from the Overview Gift Shop on U.S. Highway 77. Not only is the waterfall a joy to look at, but it is also of great academic interest as a rare example of a waterfall that is presently migrating downstream, rather than receding upstream. This reversal has taken place because the waters of Honey Creek are lime-saturated, and hence they deposit tufa and travertine as they evaporate. The waterfall and its deposits have been interpreted to reveal a complex history of Recent climatic fluctuation (e.g., Emig, 1917; Donovan and others, 1988).

The rocks at the Turner Falls overview have all been assigned to the Cool Creek Formation. Many of the rock surfaces are beautifully weathered to reveal the full range of lithologies characteristic of the formation. These rocks have been described by Ragland and Donovan (1985) and Donovan and others (1988). In this article we reexamine some of the data from these earlier papers and add a short log of a hitherto undescribed section. Unfortunately, the lower part of the steps down to the bottom of the Honey Creek gorge has now been partially barricaded off, thus our first section is somewhat curtailed (Fig. 1). The second section of interest is located immediately opposite the gift shop in a small road cut on the eastern side of US 77 (Figs. 2,3). The third section, newly described here, is located on a somewhat exposed part of the cliff overlooking Turner Falls immediately to the west of the Overview Gift Shop (Fig. 4). In addition, the exposures adjacent to the viewing platform for the waterfall display an eloquent variety of lithologies. In the account that follows, we have condensed our observations from all four locations.

DESCRIPTION OF LITHOLOGIES

The following lithologies can easily be recognized: algal boundstones (Fig. 5), intraformational conglomerates (Fig. 6), a spectrum of intraclast- and bioclast-dominated wackestones and packstones, quartz-rich oolitic grainstones, peloidal limestones, bioturbated lithologies, lime mudrocks, and heterolithic units. Chertification and dolomitization have affected these lithologies to varying degrees. A collapse breccia is present in the lower section (Ragland and Donovan, 1985).

The most common lithologies are varieties of algal boundstone. The external forms present include encrustations, mats, mounds, and reefs. Internal organization into several growth forms of stromatolite and thrombolite (e.g., dendritic, cylindrical columnar, turbinate) is apparent.

About 15% of the sections consists of intraformational conglomerates, forming erosive-based beds as much as 12 in. (30 cm) thick. Most of the clasts are varieties of lime mud, but they also include fragments of encrusting stromatolites. The majority of the fragments of the clasts are disk- or rod-shaped. As a result they have been sorted by storms, currents, and waves into distinctive packing arrangements: random, flat, imbricate, and vertical. Textures observed in the conglomerates vary from mud-supported to open-framework. Sand-sized quartz grains and ooids are commonly observed in most of the conglomerates.

The intraformational conglomerates are the coarse end of a spectrum of detrital limestones which includes grainstones, packstones, wackestones, and mudstones. The principal allochems in the grainstones are ooids and lime-mud intraclasts; less common skeletal fragments include trilobites, brachiopods, echinoids, and (particularly) gastropods. Oval peloids (either fecal pellets or small intraclasts) are the most common allochems in the mud-supported textures. Variable amounts (from none to as much as 50%) of quartz (plus a little microcline) are found, principally in dolomitized heterolithic units and intraformational conglomerates. All of the detrital lithologies are thin bedded, particularly the mud-supported textures (in which many bed boundaries have been stylolitized). Some of the grainstones show evidence of current action in the form of small trough crossbeds (maximum set thickness 3 in. [~8 cm]). Other grainstones are packed around and on top of algal boundstones, suggesting that growth of the latter was terminated when they were overwhelmed by migrating sand shoals. Some of the mud-supported textures are graded; otherwise lamination and bioturbation (including both vertical and horizontal burrows) are the principal sedimentary structures.

The heterolithic units are characterized by varieties of

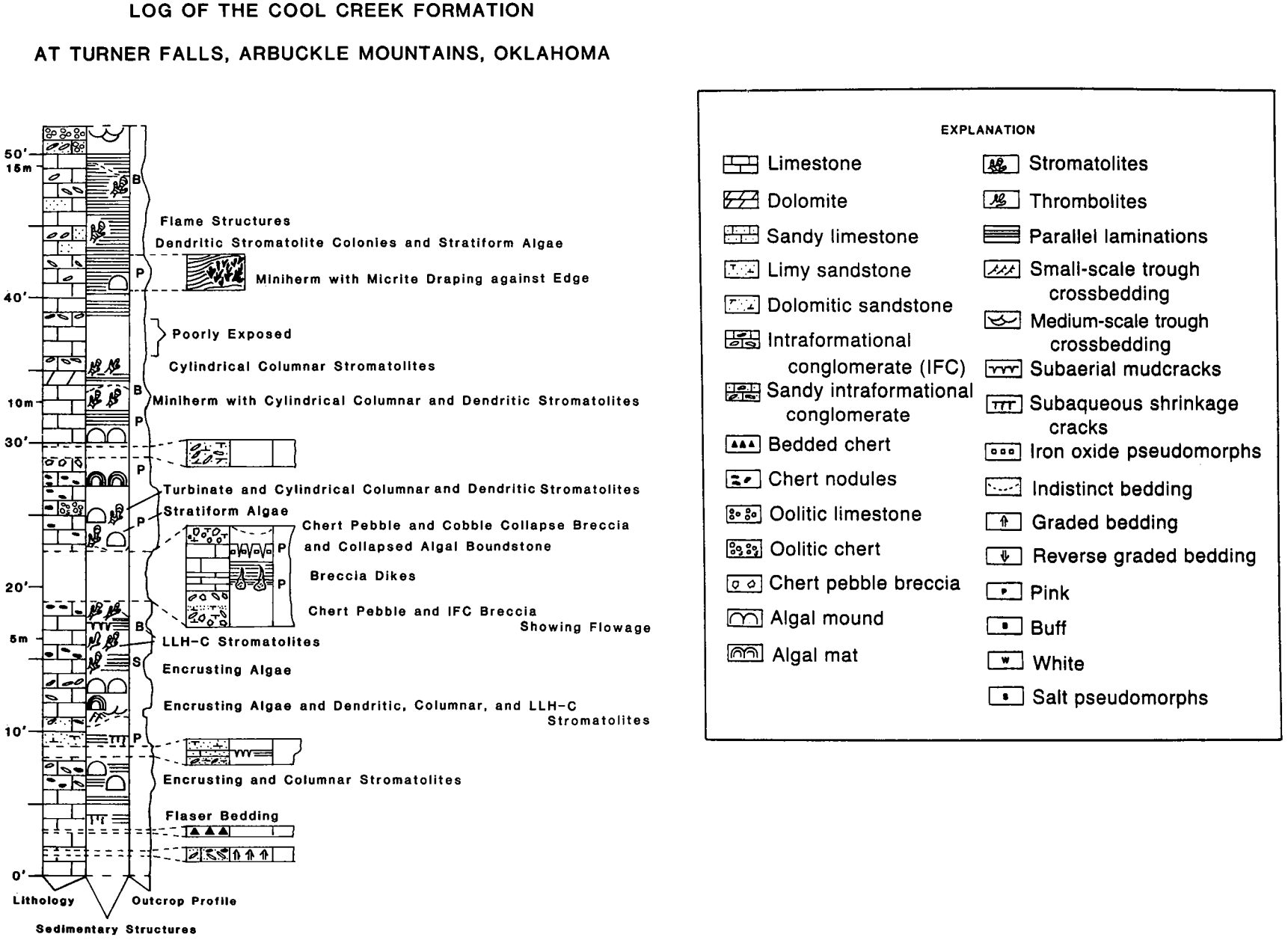


Figure 1. Stratigraphic section of Cool Creek Formation measured on cliff below the gift shop at Turner Falls overview. From Ragland and Donovan (1985).

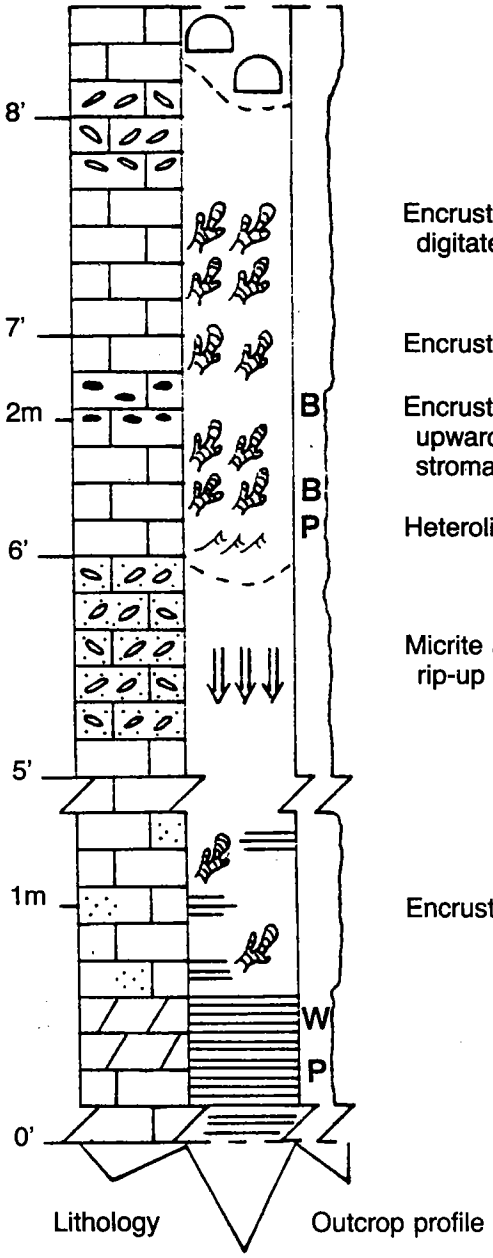


Figure 2. Stratigraphic section of Cool Creek Formation measured along US 77 across from the gift shop at Turner Falls overview. From Ragland and Donovan (1985).

flaser bedding. Alternating layers consist of lime mud and quartz-rich grainstones and siltstones. The latter are characterized by small-scale crossbedding, some of which can be related to both asymmetrical and symmetrical ripple marks. Units of this type are cut by both subaerial and subaqueous mud cracks (Ragland and Donovan,1985); they are also the most likely lithology to have been dolomitized.

Chert is present at several horizons and may have replaced any of the lithologies described above. In addition, some grainstones are partially silicified. A variety of sizes of nodules is found, as much as 3 ft (1 m) in length. Some of the cherts contain molds and pseudomorphs of an



Figure 3. Photograph of part of the section depicted in Figure 2. Base of the unit is marked by an intraformational conglomerate composed of clasts of lime and mud, algal boundstone, and much quartz sand (A). This unit is encrusted by a thin development of algal boundstone (B). Overlying this boundstone is a sequence of thinly bedded micrite, dolomicrite, and quartz silt (C). In turn this unit is encrusted by a growth of digitate stromatolites (D). Next is a relatively homogeneous micrite containing secondary quartz nodules (E), above which is another thin discontinuous boundstone.

evaporite that appears to have been gypsum (Fig. 7). Significantly, SEM studies have confirmed the presence of very small crystals of anhydrite and celestite in the pseudomorph-bearing cherts (Ragland and Donovan, 1986).

The collapse breccia is best exposed by the side of the steps, ~10 yards lower than the terrace noted above, at a point where the cliff slightly overhangs the trail. The breccia consists of angular blocks, up to a meter across, that appear to be the result of gravity-controlled collapse of well-lithified rock (even chert nodules have been fractured). Three zones are present: the lowest shows signs of liquefaction (including the upward injection of clastic dikes), the middle displays listric normal faulting in a heterolithic unit, and the upper comprises an intensively fractured algal boundstone (Figs. 8,9). The fractures have been cemented by sparite. Most fractures and faults have a N–NW trend, and the overall sense of collapse is to the W–SW (Fig. 10). The breccia may be the result of subsurface dissolution of an evaporite-rich layer at a time when (to judge from the upper limit of brecciation) at least 12 ft (~4 m) of lithified sediment was present above the zone (Ragland and Donovan, 1985).

INTERPRETATION

The exceptional exposures of the Cool Creek Formation at Turner Falls elegantly display those features of the formation which have led several authors to reconstruct the environment as a highly productive shallow-marine carbonate platform in an arid or semiarid setting (e.g., Ham, 1973; St. John and Eby, 1978; Donovan, 1982; Ragland and Donovan, 1985). In detail, the exposures show

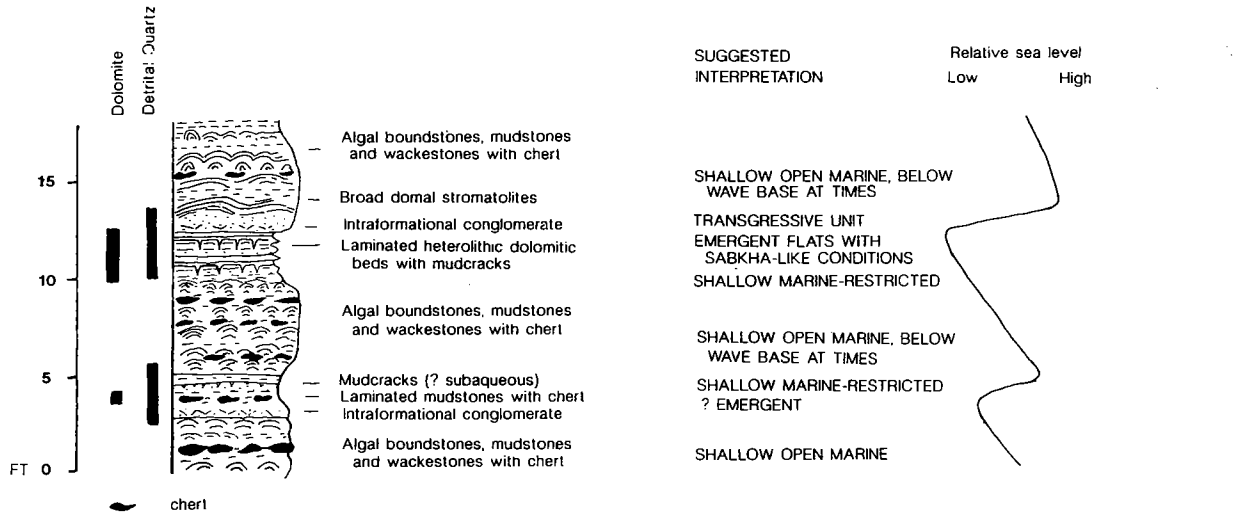


Figure 4. Log of a short section of Cool Creek Formation immediately west of the gift shop at the Turner Falls overview.



Figure 5. Detail of an algal boundstone near the top of the section depicted in Figure 1, showing characteristic digitate growth style evolving from laterally linked stromatolites near the bottom of the boundstone.

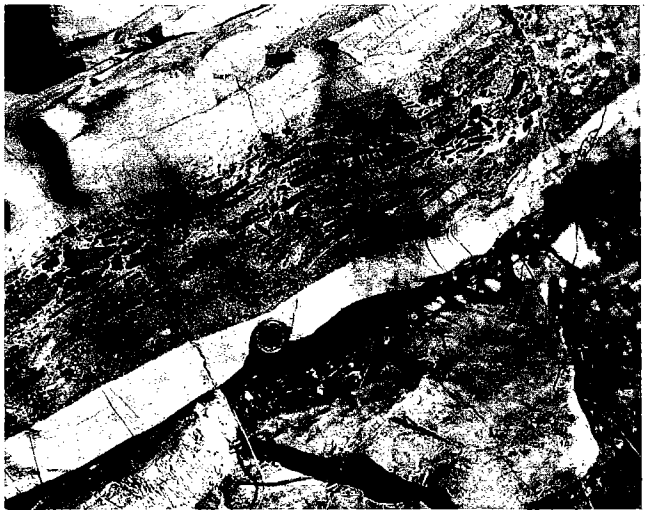


Figure 6. Intraformational conglomerate in section depicted in Figure 1. The conglomerate is composed of flat, packed, lime-mudstone clasts, mixed with abundant quartz grains. It rests with an erosive base on the underlying mudstone and grades upwards into lime mud.

the dominant role of blue-green algae and cyanobacteria in constructing boundstones. The differing forms of boundstone are probably a response to varying water depth. The intraformational-conglomerate pebbles probably owed their origin to storms; some of these deposits were subsequently sorted by waves and tidal currents. Alternatively, they record sea-level rise following temporary low stands. The broad spectrum of detrital-carbonate sandstones seems to indicate an extensive interplay between storms, fair-weather waves, and, possibly,weak tidal currents. The subtle evidence for evaporites, plus the regular occurrence of thin, stratigraphically persistent dolomite, suggest that emergent sabkha-type conditions existed during periods of relatively low sea level. During early diagenesis, ground waters of complex and variable chemistry migrated through the sediments, as is suggested by silica cementation and replacement, sulphate pseudomorphs, and the intraformational breccia.

REFERENCES CITED

Donovan, R. N., 1982, Geology of Blue Creek Canyon, Wichita Mountains area, *in* Gilbert, M. C.; and Donovan, R. N. (eds.), Geology of the eastern Wichita Mountains, southwestern Oklahoma: Oklahoma Geological Survey Guidebook 21, p. 65–77.

Donovan, R. N.; Ragland, D. A.; and Schaefer, D., 1988, Turner Falls Park: Pleistocene tufa and travertine and Ordovician platform carbonates, Arbuckle Mountains, southern Okla-

homa, *in* Hayward, O. T. (ed.), Geological Society of America, South-Central Section, Field Trip Guide, v. 4, p. 153–158.
Emig, W. H., 1917, Travertine deposits of Oklahoma: Oklahoma Geological Survey Bulletin 29, 76 p.
Ham, W. E., 1973, Regional geology of the Arbuckle Mountains, Oklahoma: Oklahoma Geological Survey Special Publication 73-3, p. 1–18.
Ragland, D. A.; and Donovan, R. N., 1985, The Cool Creek Formation (Ordovician) at Turner Falls in the Arbuckle Mountains of southern Oklahoma: Oklahoma Geology Notes, v. 45, p. 132–148.
_____1986, An environmental analysis of the Lower Ordovician Cool Creek Formation in southwestern Oklahoma, *in* Donovan, R. N. (ed.), The Slick Hills of southwestern Oklahoma—fragments of an aulacogen?: Oklahoma Geological Survey Guidebook 24, p. 21–28.
St. John, J. W., Jr.; and Eby, D. E., 1978, Peritidal carbonates and evidence for vanished evaporites in the Lower Ordovician Cool Creek Formation, Arbuckle Mountains, Oklahoma: Gulf Coast Association of Geological Societies Transactions, v. 28, p. 589–599.

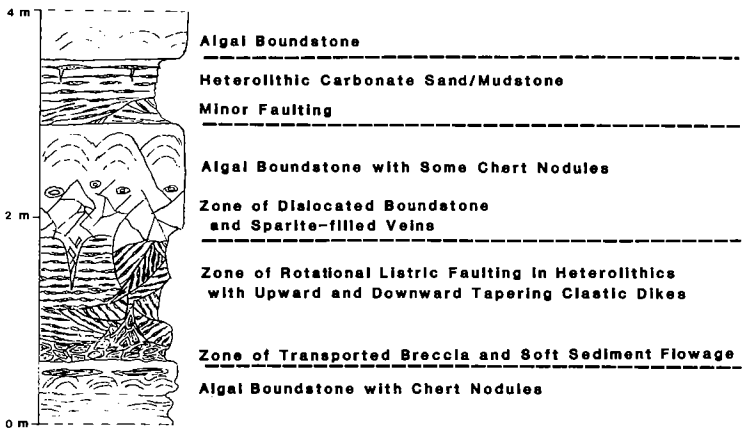


Figure 9. Schematic representation of deformation zones seen in intraformational breccia (from Donovan and others, 1988).



Figure 7. Detail of a silica nodule that has partially replaced an algal boundstone. Clear molds of evaporite crystals, possibly gypsum, are visible below the coin and near the top of the nodule.

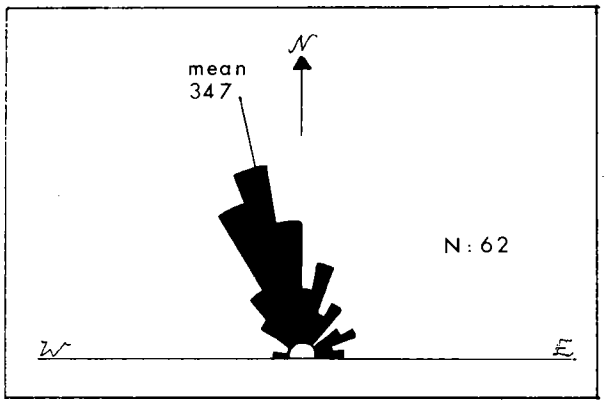


Figure 10. Rose diagram showing orientation of listric normal faults in the lower unit of the collapse breccia.

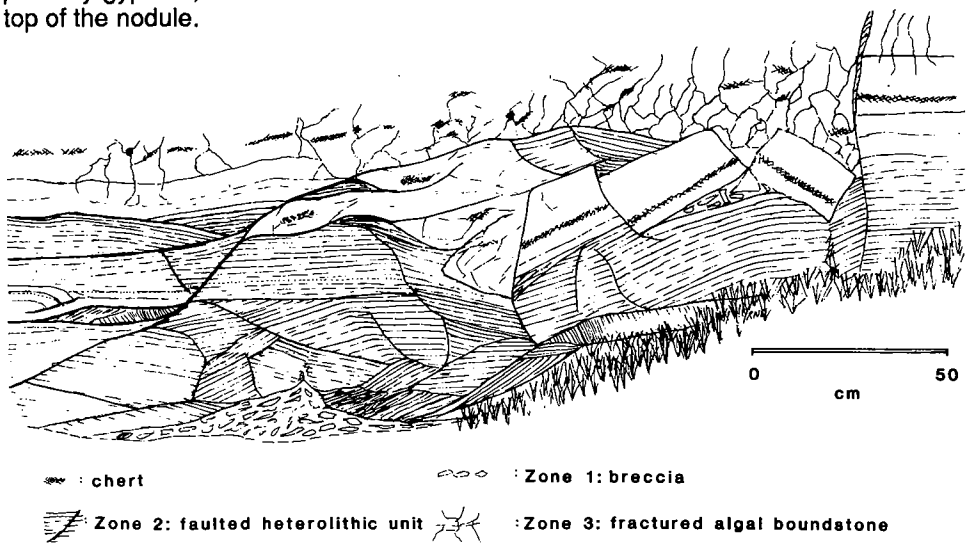


Figure 8. Sketch of intraformational breccia showing style of deformation (from Donovan and others, 1988).

STOP 5
Turner Falls: Tufa, Travertine, and Bedding-Parallel Thrusts

In Turner Falls Park, off U.S. Highway 77.
Entrance to park is ~1 mi south of Davis interchange on I-35.

R. Nowell Donovan
Texas Christian University

Deborah A. Ragland
Conoco Inc., Ponca City

TECTONIC DISTURBANCE EN ROUTE TO THE FALLS

The path from the car park at Turner Falls skirts the northwestern edge of the Honey Creek gorge. As the waterfall comes in view, an interesting section of the Arbuckle Group, displaying several features of tectonic interest, forms the cliff wall on the right-hand (north) side of the path.

Initially the strata are thinly bedded limestones that dip at gentle angles to the north–northeast. The lowest bed exposed at the path level is a thinly laminated dolomitic siltstone that contains abundant quartz grains, especially near the top. Overlying this is a section of relatively thin-bedded limestones that displays several varieties of stromatolite. In essence, this section seems to be continuous with that exposed on the other side of the gorge, a few tens of feet below the Overview point. The presence of quartz suggests that the rocks are in the Cool Creek Formation; indeed it is possible that the laminated unit is the Thatcher Creek Member, lowest unit in the Cool Creek Formation (Ragland and Donovan, 1985). However, as this unit forms the lowest visible beds, this attribution cannot be confirmed.

The principal tectonic feature seen in the thinly laminated beds is a small thrust fault that is almost parallel to bedding. In one or two places, ramps are visible and, for a short section, the thrust develops a small duplex structure. This small-scale fault illustrates how thinly laminated lithologies in the Arbuckle Group may form convenient décollement hosts to low-angle faults. The overall impression of transport shown by the thrust is towards the northeast.

A little farther to the west, i.e., closer to the Falls, the strata suddenly dip towards the northeast at angles varying between 30 and 65°. The beds are more massive limestones and appear to be part of the McKenzie Hill Formation.

In the area where the two Formations abut, several faults cut the section, dipping steeply NE at angles of 60–65° (Fig. 1). The boundary between the Cool Creek and the McKenzie Hill is formed by a near-vertical fault, separating gently dipping Cool Creek from McKenzie Hill beds that have been subject to tight minor folding and low-angle thrusting (Fig. 2).

In essence, the disturbance can be interpreted as the hinge region of a highly asymmetric syncline that plunges

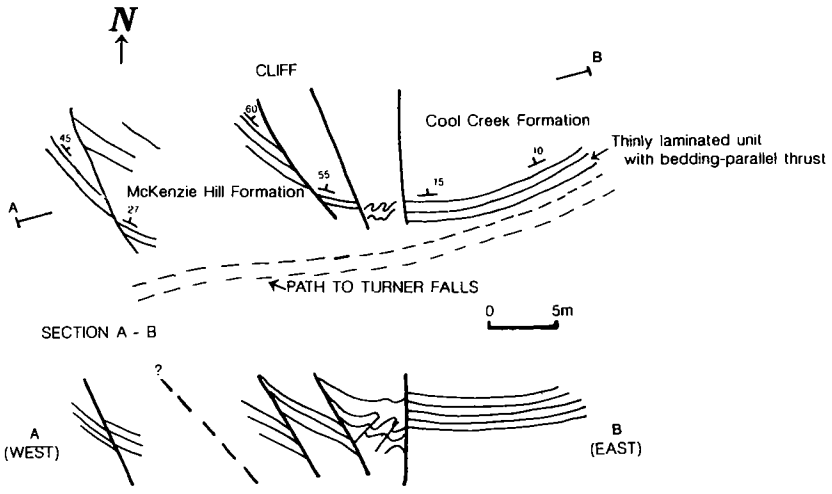


Figure 1. Map (above) and section (below) of part of the northwestern cliff of the Honey Creek gorge. Note that, although bedding traces in the limestone are shown, no correlation has been possible across any of the fault.

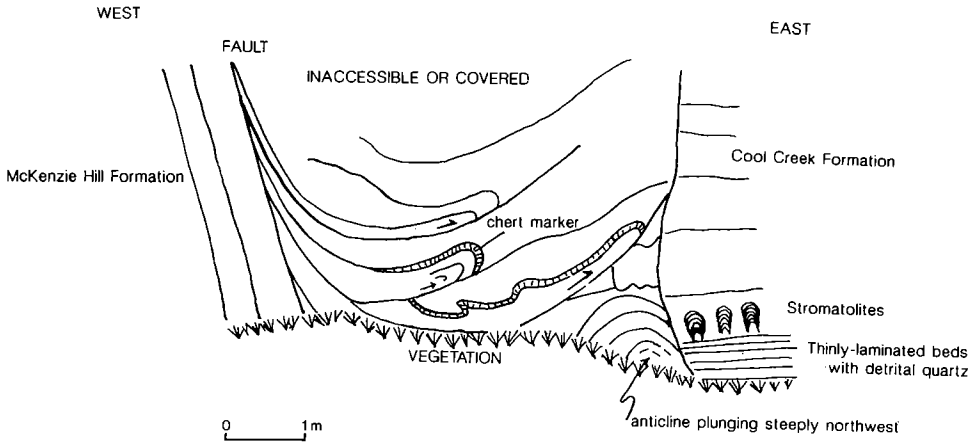


Figure 2. Field sketch of zone of contortion at the contact between the Cool Creek and McKenzie Hill Formations in the northwestern cliff of Honey Creek gorge (see Fig. 1 for location).

gently to the north. Much of the small-scale deformation (including the thrusting in the Cool Creek Formation) appears to be "out of the syncline" movement, caused by crowding in the axis of the fold. The larger faults, west of the zone of disturbance, may also reflect crowding problems in the steeper limb of the fold. These faults have effectively thinned the section displayed by the steep limb.

It is probable that the abrupt change in dip and associated faulting, allied to the contrast between massive and thinly bedded limestone, formed the original relief of Turner Falls.

TUFA AND TRAVERTINE DEPOSITS AT TURNER FALLS

Turner Falls is of unusual geological interest because the tumbling waters of Honey Creek have deposited a complex edifice of calcium carbonate (Ham, 1973); as a result, the waterfall scarp is not receding upstream but has advanced downstream as an impressive cliff of travertine and tufa.

Emig (1917) recognized that the Turner Falls travertine is a complex deposit that records climatic fluctuations. Five distinct stages can be recognized in the evolution of the deposit (Donovan and others, 1988).

1) Initial dissection of the area by vigorous streams with steep gradients. During this phase the Honey Creek valley was first excavated. The long profile of the creek was irregular, reflecting the lithological contrasts, faults, and variations in dip found in the bedrock (see above).

2) Subsequently, the climate became warmer and drier, calcite saturation increased, and as a result a major accumulation of travertine took place. This initial travertine deposit grew downstream until the creek tumbled over a travertine cliff ~100 ft (~30 m) high and 300 ft (~90 m) wide. The base of this deposit has a complicated unconformable relationship with the underlying McKenzie Hill Formation. The unconformity is marked by a discontinuous pebble conglomerate containing clasts of Colbert Rhyolite, Arbuckle Group carbonates, and reworked travertine. The overlying travertine is a complex of banded travertine and moss tufa. Examples of thick travertine tubes, deposited around now-vanished tree logs, are common. The dominant fabric, which emphasizes the downstream progradation of the deposit, is formed by beds of petrified moss that dip downstream at angles of up to 85°. These beds, which vary in thickness from 1 to 4 in. (2 to 10 cm), can persist for as much as 33 ft (~10 m). Within each bed the individual moss-plant casts are horizontal.

3) Subsequently, speleothems developed within the older travertine during a semi-arid stage, when the flow of Honey Creek was diminished and probably intermittent. For example, flowstone and crude stalactites have precipitated on the walls of cavities, and some cave popcorn is present near the base of the deposit.

4) Eventually, the climate became wetter and cooler, carbonate precipitation ceased, and Honey Creek eroded its own deposit, eventually cutting a few feet into the underlying bedrock and forming the steep-sided gorge above the modern waterfall.

5) Finally, the climate became warmer and drier, and Honey Creek re-established its constructive mode. The modern travertine-tufa screen at the Falls is the result.

REFERENCES CITED

Donovan, R. N.; Ragland, D. A.; and Schaefer, D., 1988, Turner Falls Park: Pleistocene tufa and travertine and Ordovician platform carbonates, Arbuckle Mountains, southern Oklahoma, *in* Hayward, O. T. (ed.), Geological Society of America, South-Central Section, Field Trip Guide, v. 4, p. 153–158.

Emig, W. H., 1917, Travertine deposits of Oklahoma: Oklahoma Geological Survey Bulletin 29, 76 p.

Ham, W. E., 1973, Regional geology of the Arbuckle Mountains, Oklahoma: Oklahoma Geological Survey Special Publication 73-3, p. 1–18.

Ragland, D. A.; and Donovan, R. N., 1985, The Cool Creek Formation (Ordovician) at Turner Falls in the Arbuckle Mountains of southern Oklahoma: Oklahoma Geology Notes, v. 45, p. 132–148.

STOP 6
Lateral Variations in the Upper Arbuckle Group Rocks— A Comparison Between Sections on I-35 and U.S. 77 in the Arbuckle Mountains

On U.S. Highway 77, ~2 mi south of the Cattle Pens interchange on I-35. Also at Highway Station 2405 on I-35.

R. Nowell Donovan, Matt Gallagher, Randy Hosey, Chai Phornprapha, Amy Smith, Sherman Smith, and Jeff Templeton
Texas Christian University

INTRODUCTION

Where they cut across the southern limb of the great Arbuckle anticline, the road cuts on Interstate 35 display an almost unbroken section of the upper Arbuckle Group, particularly the Kindblade and West Spring Creek Formations. These road cuts have become a classic reference point for workers who study these rocks. A few hundred yards to the east of the interstate, U.S. Highway 77 meanders through the same rocks, but with rather less spectacular exposures. Nevertheless, this highway does have a few useful road cuts, some of which have weathered to reveal considerable detail. We have selected a road cut that straddles the approximate position of the Kindblade/West Spring Creek Formational boundary, and have tied it in with the equivalent sequence on I-35. Our purpose in doing this is to see which, if any, lithostratigraphic criteria are useful in detailed correlation.

DESCRIPTION OF THE SECTION

Figure 1 is a comparative log of the two sections, comparing 94 ft (~29 m) of section. The log juxtaposes the two sections, and we have suggested a variety of tie points, mostly using the tops of dolomitized sequences. The eight units (cycles) defined in this way show many features in common. While the criteria used in correlation are strictly empirical (and were traced on the ground between the two outcrops), genetically we suggest that we have correlated a sequence in which the dominant motif comprises shallowing-upward cycles. In such cycles, it is convenient to place the initiation of transgressive trends on the tops of dolomite units.

LITHOLOGICAL ASSOCIATIONS

The section displays a variety of lithological associations that are common to all the units (cycles) recognized, although their proportions vary both between units and between the two sections.

Algal Boundstones

Algal boundstones are one of the most common lithological associations found in the Arbuckle Group; the interval that we measured is typical in this respect, displaying a wide variety of different forms. Internal textures include thrombolitic, intermediate, and stromatolitic (the latter are the most common). Branching style stromatolites (i.e., dendritic and digitate) are generally less common than curvilinear boundstones (domes, cylinders, and bulbous). The most common organization of boundstones involves a basal dendritic, multi-branched form that passes upwards into increasingly laterally linked varieties, which, in some cases, are capped by cryptalgal laminite (seen for example at the 3, 12, 58, 77, and 82 ft levels on Fig. 1). This type of arrangement has been invoked to suggest a general shallowing of water depth (e.g., Ragland and Donovan, 1986).

All the cycles that we recognized contain some algal boundstones, although the proportion present varies greatly. Boundstone development may be intense, involving multi-storied, laterally linked boundstone complexes as much as 6.5 ft (~2 m) thick. On the other hand, some cycles display one or two horizons of small stromatolites with widely spaced lateral linkage in which individual colonies may be ≥3 ft apart. It is worth noting that a core has a better than even chance of missing colonies of this sort.

Boundstones in Facies Correlation

Correlation between the two sections suggests that there is considerable lateral variation in the proportions of boundstones in each cycle. As an example, the US 77 exposure displays columnar stromatolites that at 39 in. (~1 m) are the tallest stromatolites that we have yet encountered in the Arbuckle Group (Fig. 2). The same horizon is represented by 9-in.-high stromatolites on I-35. However, these stromatolites have precisely the same form as their larger cousins. This form correlation is one of the most forceful impressions that we gained from

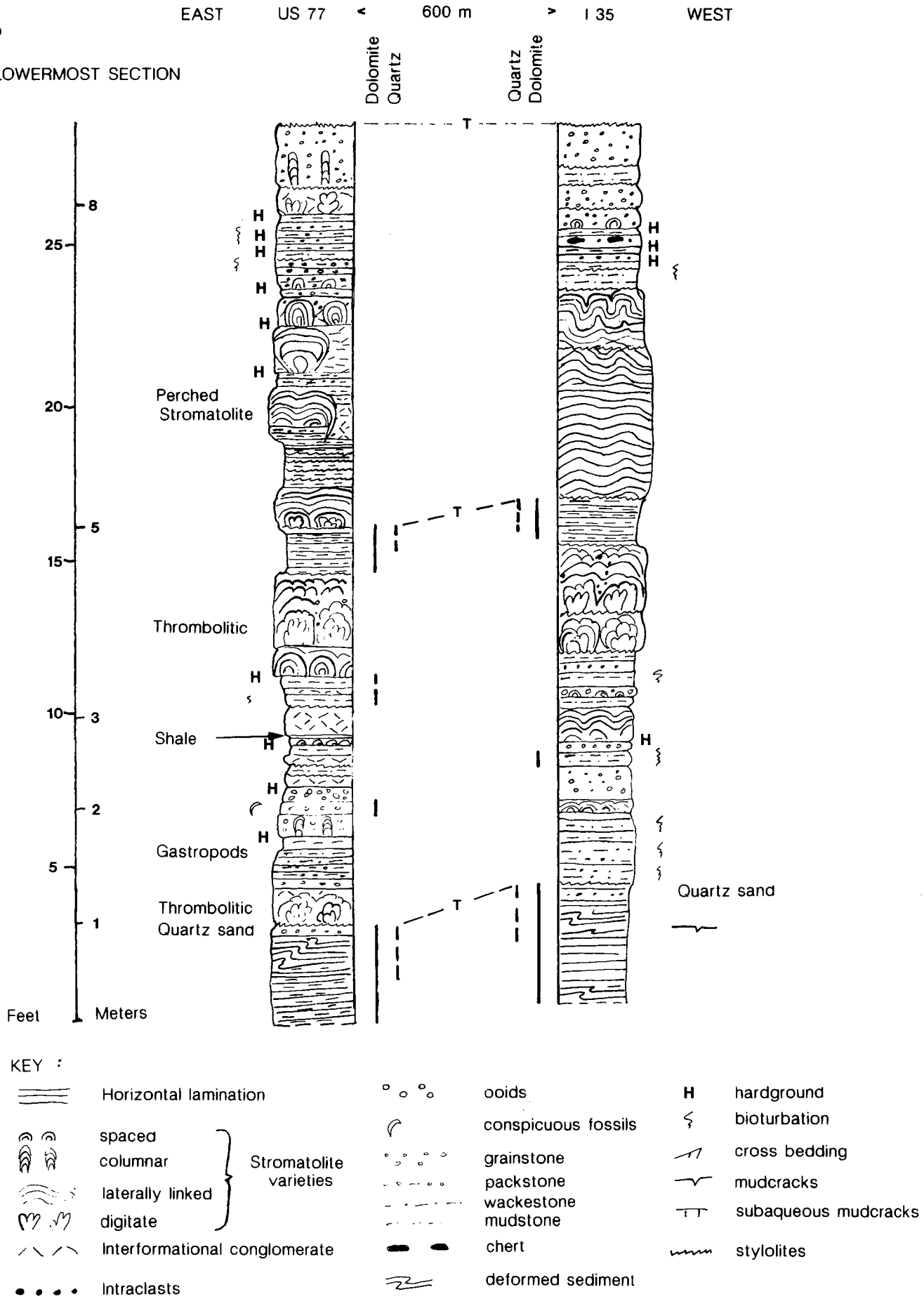


Figure 1 (p. 226–228). Comparative log of the two sections (US 77 on left, I-35 on right) showing attempted correlation based principally upon the top of dolomitized units.

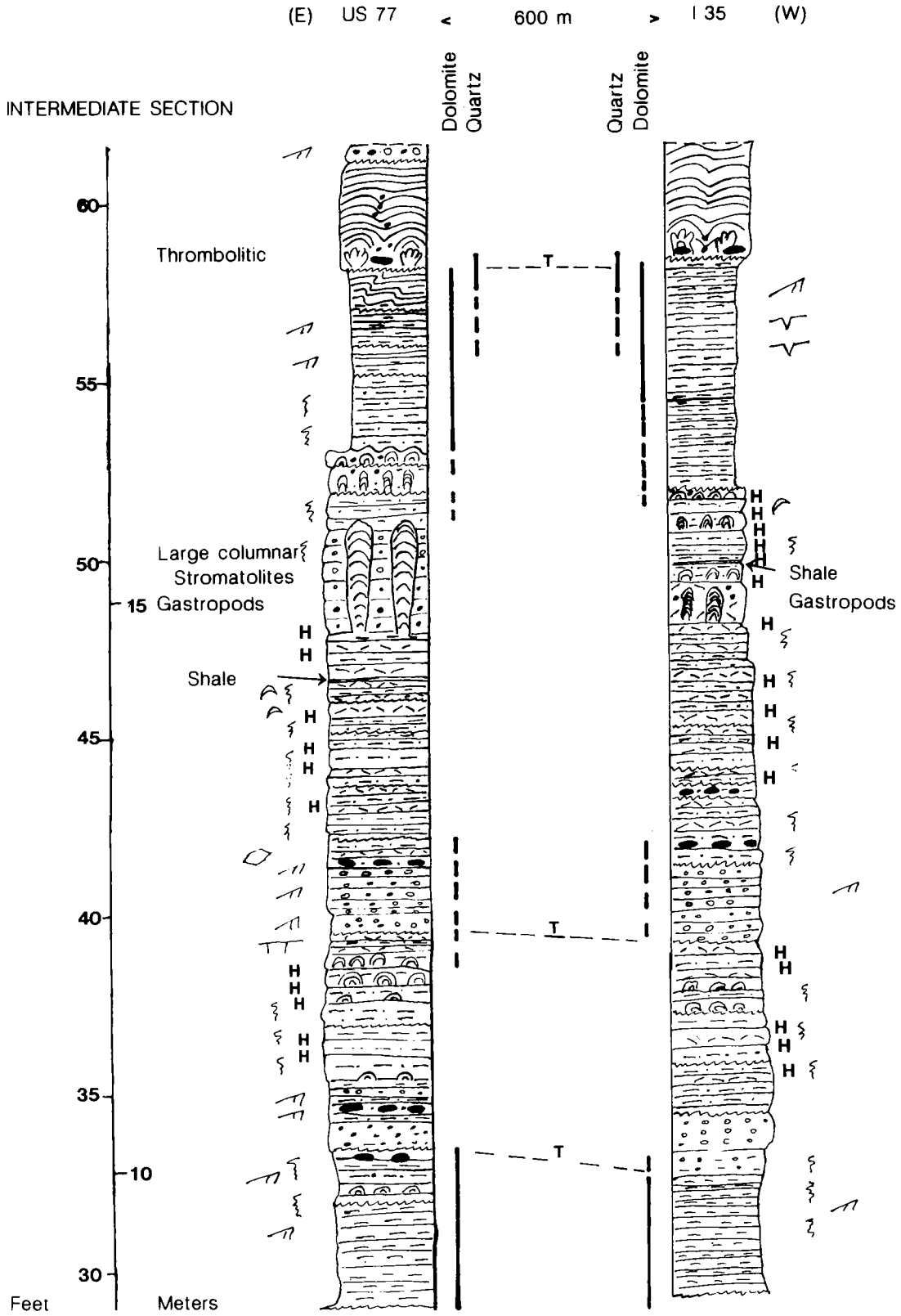


Figure 1. *(continued)*

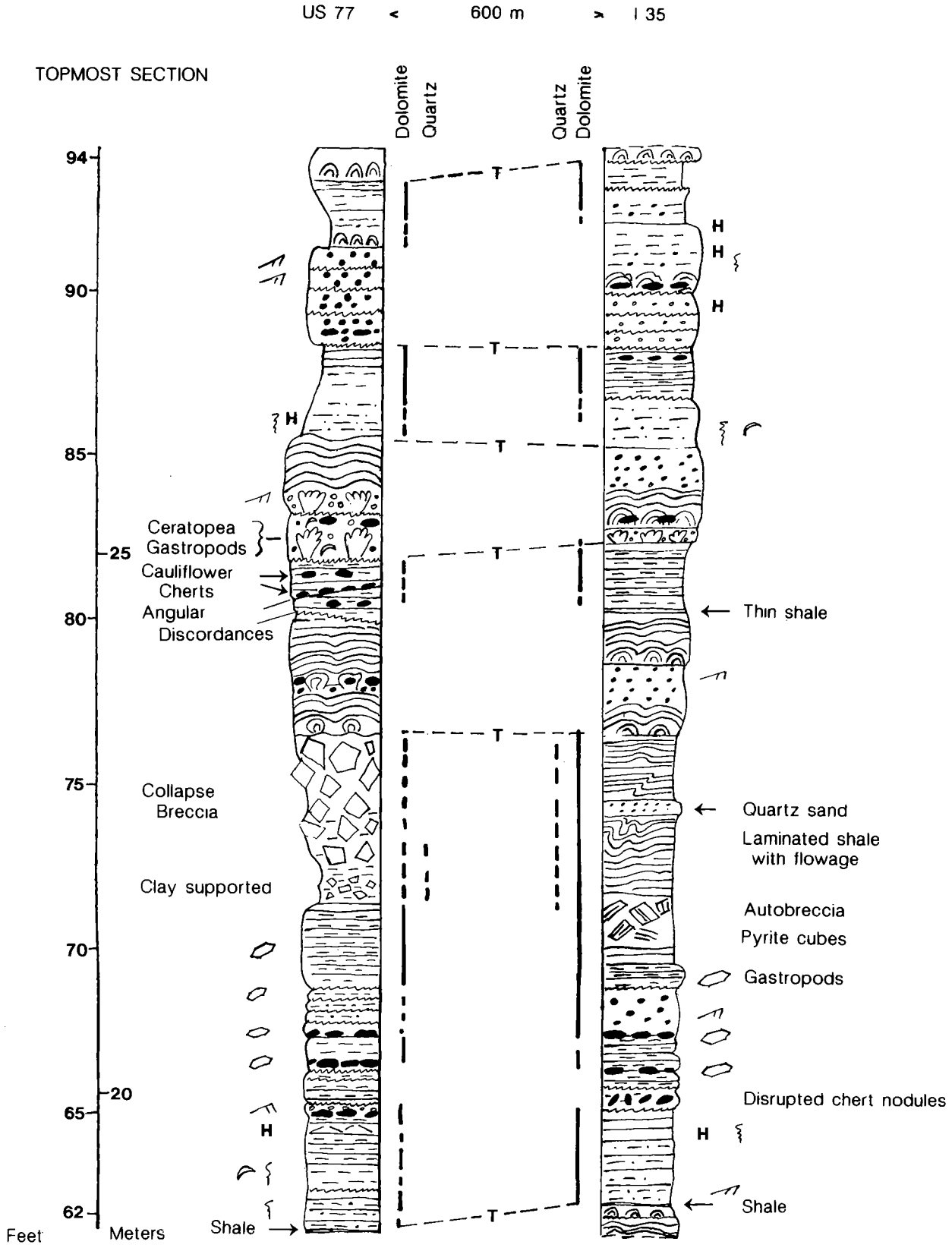


Figure 1. *(continued)*



Figure 2. Tall columnar stromatolites in the US 77 outcrops at the 48 ft level.

comparing the two sections; although the proportion of boundstone varies between the sections, the type of stromatolite is frequently distinctive within individual cycles.

Grainstones and Intraformational Conglomerates

Allochems were noted in the following order of abundance: intraclasts of lime mud, bioclasts, ooids, and peloids. However, peloids are particularly difficult to identify in hand specimen, and we suspect that we have under-represented them in our analysis.

Intraclasts vary in size from silt-sized particles to plate-shaped pebbles up to 6 in. (~15 cm) in length. In general there is a size-related gradation from intraformational conglomerates to intraformational grainstones. Intraclasts are mostly composed of lime mud, but other lithologies are also represented (Fig. 3). They are found throughout the sequence in a variety of settings: as discrete beds, as scattered grains in mud-supported lithologies, and between boundstone colonies. Where the intraclasts are of pebble sizes, they form distinctive packing arrangements; flat lying (gravity settling), imbricate (current-modified), and vertical (wave-modified).

The most commonly seen bioclasts are gastropods, followed by trilobites, brachiopods, cephalopods, and echinoderm fragments. Most of the bioclasts are broken, but in some cases gastropods and cephalopods have been preserved in their entirety. The diversity and abundance of the fauna generally decreases upwards in each of the cycles (except where the base of the cycle is dominated by algal boundstones). Fossils are rarely encountered in dolomitized sequences. However, we noted two gastropod horizons in dolomitic sequences. In both cases, only one species of gastropod is present, and we suspect that populations of this type record ecological stress in waters that were no longer truly open marine.

Ooids can be found scattered throughout most of the grainstones and as small percentages in mud-supported rocks. Three distinctively oolitic grainstone beds were noted (Fig. 4). The most commonly seen ooid fabric involved radial cortexes nucleated about lime-mud nucleii, although a variety of other arrangements have been



Figure 3. Poorly sorted intrasparite cut by bedding-parallel stylolite. Note the complex origin of many of the grains in the deposit, which is interpreted as a polygenetic storm-generated sand. Considerable compaction occurred prior to cementation, as evidenced by the pressure-solution contacts between grains. Ordinary light, field of view is 9 mm across.



Figure 4. Hardground developed between two types of oolitic grainstone. The lower is an oointrasparite of relatively fine grain size. The upper is an oointrasparite in which both the intraclasts and the ooids are considerably larger than those below. Ordinary light, field of view is 9 mm across.

noted (see Ragland, 1990, for a review of Arbuckle Group ooids).

Peloids, similarly, are most often seen scattered throughout varieties of grainstone and mud-supported rocks; however in one or two cases they form relatively unadulterated grain populations. One of the problems encountered in determining the proportions of peloids in the section is that they overlap in terms of size (and, to a lesser degree, shape) with intraclast populations.

Grainstones in the section examined are rarely thicker than 12 in. (~30 cm), although they may form multi-storied deposits as much as 3 ft (~1 m) thick. The most commonly seen sedimentary structures are varieties of cross-bedding (usually small-scale). The grainstones probably record the movement of mobile sand belts across the platform. Intraformational conglomerates, on the other hand, represent storm or transgressive deposits that have either been deposited below fair-weather wave base (in which case they contain various amounts of mud), or are composed of clasts that were too large to be moved during fair weather.

Facies Correlation Using Intraformational Conglomerates and Grainstones

Homotaxy precludes the precise correlation of individual beds composed of these clastic deposits. On the one hand, certain cycles that are grainstone-rich maintain this general character between the two sections (e.g., at the 7–9, 26–29, 34–35, 40–42, and 88–92 ft levels). On the other hand, facies changes by which the grainstones pass laterally either into boundstones (e.g., at the 63–65 ft level) or into mud-supported lithologies (e.g., at the 66–68 ft level), indicate that correlation using multi-storied grainstone/intraformational conglomerates is suspect.

Mud-Supported Rocks

A spectrum of rock types from micrite through wackestone to packstone is seen in both sections. One of the most common lithological associations is an alternation of thin (~1 in. [~2.5 cm]) beds composed of these textures in sequences as much as 4 ft (~1.3 m) thick. Individual bed boundaries are frequently hardgrounds, or stylolites that we suspect are modified hardgrounds. The most common allochems seen are intraclasts (including some of small pebble size), bioclasts, and peloids. Ooids are rare in this lithological association, which we suggest is a record of below wave-base, fair-weather sedimentation and contemporaneous lithification that was frequently interrupted by storms (an example of the "platform triangle" of Donovan, 1986). Sequences of this type are characterized by variable amounts of bioturbation (both vertical and lateral burrows) and small-scale cross-bedding (the latter recording the movement of small, asymmetric "fair-weather" ripples).

Facies Correlation on the Basis of Mud-Supported Sequences

In essence one of the chief distinguishing characteristics of the Arbuckle Group is the amount of lime mud that it contains; not surprisingly, the correlation of mud-dominated sequences of this type is bedeviled by problems of homotaxy. Furthermore, as noted above, they may grade into boundstones. Correlative packages of beds of this type can certainly be recognized in both road cuts (e.g., at the 9, 35, 43, and 64 ft levels), but only on the basis of their relationship to other parameters.

Detrital Quartz

All four occurrences of detrital quartz are found in both road cuts and offer a firm basis for correlation. The quartz is invariably associated with dolomitic deposits; it has been suggested that the quartz was transported across the platform from the exposed craton by wind currents during low-stand periods, and then subsequently reworked into a variety of depositional settings during the next transgressive phase (see Ragland and Donovan, this volume, p. 9). In thin section the quartz is dominantly monocrystalline, representing a mineralogically mature grain population. Where they have maintained their original shape, grains are well rounded; sorting is variable, depending on the final depositional setting of the grains.

Facies Correlation on the Basis of Quartz

On a formational basis, the presence of substantial amounts of quartz has been used to define the base of the Cool Creek Formation (Ragland and Donovan, 1985a) and, in a general sense, can be used to differentiate "typical" Kindblade sections from either the Cool Creek or West Spring Creek. As this section demonstrates, on a more detailed basis the presence of quartz, particularly when tied to dolomite, offers correlative possibilities. If the quartz records low-stand development, as suggested above, then it is clear that it will be widely distributed across the craton at such times. The four occurrences in this section record greater than usual regressive events (or longer than usual progradation). The geography of the southern Oklahoma aulacogen, and its relationship to the craton as a whole, suggest that the amount of quartz in sections will generally increase away from the aulacogen.

Dolomite

As noted, the most common occurrence of quartz is in association with dolomitized horizons that have been used in this study to define the tops of shallowing-upward sequences. The evidences for this interpretation are the intimate association of dolomite with the following: (1) detrital quartz (in four cases); (2) evaporative traces, such as pseudomorphs after gypsum (Fig. 5) and anhydrite (Fig. 6), and cauliflower cherts that contain traces of anhydrite (Fig. 7); (3) an impoverished (stressed) biota (see above); and (4) mud-cracked and ripple-laminated strata in which bioturbation is rare, although not absent.

The dolomite is generally micritic, although it is seen as sparry crystals where pore space allowed the development of cement, as, for example, in fenestrae in mudstones. The amount of replacement varies from very little to complete; visually intermediate amounts of replacement are seen as fabric-selective varieties, such as burrow-filling and leopard-skin textures (Donovan, 1986).

Correlation on the Basis of Dolomite

The dolomitic horizons have been used as the primary basis for correlation between the two sections. Visually



Figure 5. Anhedral, nonferroan calcite-spar pseudomorphs filling evaporite cast, probably after gypsum. Ordinary light, field of view is 9 mm across.



Figure 6. Dolomitic mudstone containing aggregates of evaporite pseudomorphs (probably anhydrite). The pseudomorphing mineral is calcite. Field of view is 9 mm across, ordinary light.

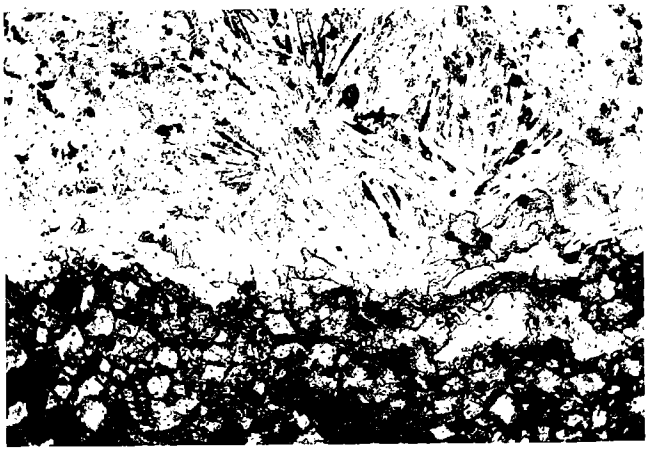


Figure 7. Dolomitic mudstone containing a cauliflower chert. The form of the chert mimics anhydrite laths; this is probably a silicified anhydrite nodule. Field of view 4.5 mm across, ordinary light.

the dolomite is most easily picked out on the basis of its weathering color—tan yellow, as opposed to the gray of the limestones. In cores, staining can achieve similar discrimination. However, the dolomite horizons vary in thickness between the two sections, and, furthermore, assuming that each dolomite does in fact define a similar event in each cycle, cycle thickness varies in some cases by as much as 15% between the two outcrops.

Chert

Chert is reasonably common in both sections and is seen in a variety of forms. For example, chert may occupy a low position in algal boundstone units, in which case the chert tends to be nodular with smooth edges and provides a perfect mimic of the boundstone. Another type of chert is "cauliflower" chert; typically cauliflower cherts show length-slow varieties of chalcedony and leutecite when examined under the microscope. In addition, cherts are found in association with laminated facies where they are seen as smooth oval nodules, characterized by a dense texture of cryptocrystalline silica. Cherts may also locally replace grainstones.

Correlation on the Basis of Chert

Despite their apparently random occurrence and the variety of forms that they exhibit, cherts correlate well between the two sections, although it is unlikely that in and of themselves they are distinctive enough to provide a firm basis for correlation. However, it is interesting to note that one particular chert horizon, in which the nodules contain gypsum pseudomorphs (at the 67 ft level), can be traced between the two outcrops, even though it is only 1 in. (~2.5 cm) thick.

Collapse Breccia

Perhaps the most interesting and noteworthy feature seen in the US 77 road cut is a collapse breccia, ~5 ft (~1.6 m) thick. The lower part of the breccia is mud supported, and contains a variety of clasts of dolomite and some quartz sand in a matrix of laminated illitic clay. Overlying the lower unit is a massive, angular breccia with clasts as much as 18 in. (~45 cm) in diameter. These clasts comprise a mixture of dolomite (often laminated) and limestone blocks.

The attitude of the settling fabrics in the basal part of the breccia suggests that it formed when the beds were horizontal; in other words, the breccia is not a Pennsylvanian karst feature, nor is it likely to be a tectonic structure. A distance of some 5 ft (~1.6 m) above the top of the breccia, two angular unconformities are present in the overlying limestone cycle. We suggest that these two unconformities mark the period of time when the breccia formed and the platform suffered local collapse.

Although strata below the breccia are variably dolomitized, some have been dedolomitized. They also contain abundant pseudomorphs of gypsum and anhydrite (pseudomorphing minerals are calcite and quartz). These features suggest that the collapse breccia may have resulted from the dissolution of an evaporite layer in a sabkha-like sequence, similar to those recorded in the Cool Creek Formation (Ragland and Donovan, 1985b, 1986).

When traced to the I-35 road cut, the collapse breccia disappears; its lateral equivalent is a thinly laminated, quartz-rich dolomitic mudstone that contains a 6 in. (~15 cm) bed of pure quartz sand near the top. Signs of disruption are common in this bed, including local development of autobreccia in the laminite. In addition, the sediments show considerable signs of flowage similar to the distortion features around evaporites in modern Persian Gulf sediments.

In essence the collapse-breccia horizon appears to represent the most substantial low-stand sequence in the interval measured. During this time a sabkha-like setting developed with the precipitation of sulphates. Following the subsequent transgression, flushing by marine waters of normal salinity removed the evaporites, leading to partial collapse of the section.

CORRELATION PARAMETERS

The most useful factors in correlating the two sections are undoubtedly the dolomites, especially when associated with detrital quartz; these seem to mark low stands and are thus reasonably viewed as approximate chronostratigraphic markers. However, even in the case of the dolomite, homotaxy problems abound; hence it is unlikely that any single lithology or diagenetic imprint will, in and of itself, provide a satisfactory basis for correlation. Over a relatively short distance of 600 yards (~600 m) the two sections show enough similarities to suggest that lithostratigraphic correlation on an incremental basis is possible, but not easy, over wider distances.

If the dolomites and quartz provide the chief basis for correlation, then supporting factors may be provided by the type, as well as the general thickness of algal-boundstone colonies, the occurrence of thick grainstone sections (marking the moving of mobile sand belts), and the occurrence of various styles of chert.

REFERENCES CITED

Donovan, R. N., 1986, Geology of the Slick Hills, *in* Donovan, R. N. (ed.), The Slick Hills of southwestern Oklahoma—fragments of an aulacogen?: Oklahoma Geological Survey Guidebook 24, p. 1–12.

Ragland, D. A., 1990, Sedimentology, paleoenvironmental analysis and diagenesis of upper Arbuckle limestones in the Slick Hills, southwestern Oklahoma: Oklahoma State University unpublished Ph.D. thesis, 238 p.

Ragland, D. A.; and Donovan, R. N., 1985a, The Thatcher Creek Member: basal unit of the Cool Creek Formation in southern Oklahoma: Oklahoma Geology Notes, v. 45, p. 84–91.

_____1985b, The Cool Creek Formation (Ordovician) at Turner Falls in the Arbuckle Mountains of southern Oklahoma: Oklahoma Geology Notes, v. 45, p. 132–148.

_____1986, An environmental analysis of the Lower Ordovician Cool Creek Formation of southwestern Oklahoma, *in* Donovan, R. N. (ed.), The Slick Hills of southwestern Oklahoma—fragments of an aulacogen?: Oklahoma Geological Survey Guidebook 24, p. 21–28.

STOP 7
Paleokarst Origin for Bedded Breccias in the Cool Creek Formation

East side NE¼SE¼ sec. 13, T25, R1E, along I-35. Turner Falls Quadrangle. The outcrops are along the west wall of the southbound lane road cut between the exit and entrance for the scenic turnout.

Bryan Tapp
University of Tulsa

STOP OVERVIEW

The outcrops along the road bed show a series of bedded breccia deposits in the Cool Creek Formation. These bedded breccias are continuous around the Arbuckle anticline. Most of the breccias can be traced laterally along strike around the anticline, a distance of roughly 20 km (12.5 mi) along strike. The breccia units vary in thickness from 0, where the horizons pinch out into sandy and cherty limestones, to ~3.1 m (10 ft). Some outcrops display graded bedding, but this is not present throughout the unit. The upper contacts of the breccia beds are irregular, as demonstrated by changes in thickness of the breccia unit. The lower contact does not appear to be irregular. Both contacts appear to be sedimentary in nature. The composition of the breccia varies significantly, depending on location, ranging from nearly pure chert fragments (chert-rubble floatbreccia; terminology of Morrow, 1982) to nearly pure limestone fragments (limestone-rubble packbreccia and limestone-rubble floatbreccia).

The breccias are composed dominantly of chert fragments and limestone fragments with a micrite matrix (Fig. 1). Chert is the dominant rock-fragment type; in some areas the breccias do not contain any limestone fragments and could be described as a chert floatbreccia. The chert-rock fragments vary from dense equigranular chert to porous chert. The chert-rock fragments are dominantly equigranular and angular. The chert fragments range in size from ~31 × 31 cm (1 × 1 ft) to very fine sand. Chalcedony is present, and some of the chert, along with the chalcedony, is a replacement of earlier peloidal and/or pisolitic limestone (Fig. 2). Zebroid, quartzine, and radiating chalcedony are present in chert fragments and as individual clasts floating in the micritic matrix. Many of the chert-rock fragments have a preferred orientation of the long axis and show some imbrication. Many of the chert-rock fragments are fractured. These fractures display two types of vein fill: calcite, both micrite and spar, and quartz. Some of the chert fragments are banded, inherited from the growth of chert in the carbonate rock. Some of the chert-rock fragments have undergone extensive calcification, and some of the cherts contain evaporite casts. Many of the chert fragments replace earlier carbonate structures.

The breccia bed also contains limestone-rock fragments which vary from subround to angular and range in size from 45.7 × 15.2 cm (18 × 6 in.) to medium-sand sized. The larger limestone-rock fragments are identical to the Cool Creek Limestone below the breccia bed and show little or no alteration. Smaller fragments show significant alteration and micritization. The range in size varies with location, and the breccia can be described as a limestone-rubble packbreccia or a limestone-rubble floatbreccia, depending on location. In some areas around the Arbuckle anticline, the limestone-rock fragments are partially rounded and the unit takes on the appearance of a flat-pebble conglomerate. Many of the limestone-rock fragments preserve original bedding, and some show peloidal, algal, and bioturbation structure. Fragments with ooids and pisolites (Fig. 3) are common in the breccia. Some of the limestone-rock fragments contain original depositional quartz sand. Limestone fragments in the chert-rubble floatbreccia are severely altered, and appear as ghosts in the micrite matrix.

The breccia zone also contains minor thin-bedded and cross-bedded sand stringers, with calcite (micrite) cement and intercalations of limestone, and individual sand grains floating in the matrix. The sand is composed largely of rounded polycrystalline and monocrystalline grains with minor microcline and plagioclase feldspar, individual ooids, pisolites and pellets, and chalcedony fragments.

Many of the samples from the breccia are fractured and show formation of stylolite surfaces. Two generations of stylolite formation can be seen in the samples. Several of the limestone-rock fragments contain stylolite surfaces that are marked by hematite stains and accumulated clays. These stylolite surfaces do not cross the rock-fragment boundaries and are contained only in the rock fragments. Late-stage stylolite surfaces are limited to the matrix of the breccia, and they do not cut into any of the rock-fragments but form along the rock-fragment grain boundaries.

The cement in the breccia is mostly unremarkable micrite, but shows evidence of vadose cements (Fig. 4), sparry cements, and clotted and laminated micrite.

DISCUSSION AND CONCLUSIONS

Several hypotheses have been suggested for the origin of the bedded breccias in the Cool Creek Formation. These are as follows:

1. The breccias reflect tidal-flat, upward-shoaling se-



Figure 1. Brecciated bed (lower right) in Cool Creek Formation is overlain by cross-bedded tidal-channel sands. Photograph taken in field away from road cuts.

quences with cyclic changes in water depth controlled by motion on the Washita Valley fault (Smith, 1980).

2. The breccias represent clastic deposits derived from uplift of source areas on an active fault during Cool Creek deposition (Tapp, 1978).

3. The breccias represent collapse breccias formed due to evaporite dissolution during burial or tectonism (Ragland and Donovan, 1985).

I herein suggest an alternative interpretation of the Cool Creek bedded breccias. The model I propose is that of both fault-derived talus for the larger, unaltered limestone blocks (limestone-rubble packbreccia and, possibly, limestone-rubble floatbreccia) and a corresponding paleokarst origin for the chert-rubble floatbreccia. The paleokarst includes the formation of calcrete surfaces, as shown by the presence of clotted micrite, vadose cements, and pisolites forming what may have been a caliche hardpan. The paleokarst also shows the formation of local silcretes, as shown by the formation of zebroid, quartzine, and radiating chalcedony replacing the earlier calcrete pisolites.

The breccias present in the Cool Creek are remarkably similar in style and occurrence with those in the Windermere Formation in the Proterozoic of northern Canada (Mustard and Donaldson, 1990). Much of the model presented here is based on the work of Mustard and Donaldson (1990), and the interpretation presented here is based on the following evidence.

The limestone-rubble packbreccia is limited areally and does not show evidence of alteration. Limestone fragments are found associated with chert fragments, but there is increasing alteration of the limestone with in-



Figure 2. Photomicrograph of chalcedony replacement of pisolitic limestone during silcrete formation in Cool Creek Formation. Field of view is 3.5 mm.



Figure 3. Photomicrograph of pisolitic limestone fragment in Cool Creek breccia. The limestone fragment is larger than the field of view (roughly 2 cm long). The field of view is 3.5 mm.



Figure 4. Photomicrograph of microstalactitic vadose cement underneath chert fragment in Cool Creek breccia. Field of view is 3.5 mm.

creased chert fragments, suggesting significant weathering (Mustard and Donaldson, 1990). The occurrence of pisolites increases with the increase in chert fragments and with the decrease in unaltered limestone fragments, again suggesting the formation of calcrete (Esteban and Klappa, 1983). The pisolites are silicified, showing the formation of three distinct chalcedony types, suggesting the formation of local silcretes which were incorporated into the breccia. The incorporation of these silcretes as fragments in the breccia, along with vadose cements, suggests that the features are surface features rather than being dissolution/collapse features.

The presence of the breccias in the Cool Creek Formation coincides with the most rapid subsidence in the aulacogen (Feinstein, 1981), lending support to the hypothesis that sedimentation of the Cool Creek breccias is related to subsidence of the aulacogen along bounding faults. As proposed, a typical cycle would involve uplift of a source area, caused by elastic rebound of the upthrown side of a fault, followed by regional subaerial exposure forming the characteristic breccia cycles. Downwarping of the aulacogen would be cyclic in nature, with general subsidence interrupted by faulting and rebound when built-up stress on the bounding fault exceeded the strength of the material (Jackson and McKenzie, 1983). The escarpment formed by rebound would serve as the source for carbonate clastics.

The data suggest that the bedded breccias in the Cool Creek Formation are a mix of fault-talus breccias and of paleokarst breccias. The data further suggest that there was significant reworking of original calcretes and silcretes, with fragments of these being incorporated into the breccia. I interpret the presence of angular silcrete and calcrete fragments in the breccia, along with the imbrication of fragments, as showing sedimentary reworking of the calcrete and silcrete horizons during reestablishment of shallow-water marine deposition. The data do not, however, rule out the possibility of collapse. Several lines of evidence point to the presence of evaporites in the Cool Creek. The main question then is whether the evaporites were removed at or near the surface, resulting in a sedimentary breccia, or whether they were removed after burial, resulting in a collapse breccia. The fact that the bedded breccia are continuous along strike, and that they are formed by the intermixed limestone conglomerates and limestone-rubble packbreccias and floatbreccias with chert-rubble floatbreccias, is suggestive of a sedimentary origin rather than a collapse origin. True collapse breccias are somewhat more limited in areal extent, tending to pinch out along strike.

The bedded breccias of the Cool Creek Formation give us a unique opportunity to look at the early subsidence behavior of the southern Oklahoma aulacogen, and to evaluate the interplay between structure and sedimentation where the mode of subsidence (in this case subsidence along faults rather than regional downwarping) significantly affects sediment accumulation.

REFERENCES CITED

Esteban, M.; and Klappa, C. F., 1983, Subaerial exposure environments, *in* Scholle, P. A.; Bebout, D. G.; and Moore, C. H. (eds.), Carbonate depositional environments: American Association of Petroleum Geologists Memoir 33, p. 1–54.

Feinstein, S., 1981, Subsidence and thermal history of the southern Oklahoma aulacogen: implications for petroleum exploration: American Association of Petroleum Geologists Bulletin, v. 65, p. 2521–2533.

Jackson, J.; and McKenzie, D., 1983, The geometrical evolution of normal fault systems: Journal of Structural Geology, v. 5, p. 471–482.

Morrow, D. W., 1982, Descriptive field classification of sedimentary and diagenetic breccia fabrics in carbonate rocks: Bulletin of Canadian Petroleum Geology, v. 30, p. 227–229.

Mustard, P. S.; and Donaldson, J. A., 1990, Paleokarst breccias, calcretes, silcretes and fault talus breccias at the base of Upper Proterozoic "Windermere" strata, northern Canadian Cordillera: Journal of Sedimentary Petrology, v. 60, p. 525–539.

Ragland, D. A.; and Donovan, R. N., 1985, The Cool Creek Formation (Ordovician) at Turner Falls in the Arbuckle Mountains of southern Oklahoma: Oklahoma Geology Notes, v. 45, p. 132–148.

Smith, M. T., 1980, Recurring shoaling-upward sequences of a carbonate tidal flat, Cool Creek Formation (lower Ordovician), Arbuckle Mountains, Oklahoma: University of Wisconsin, Madison, unpublished M.S. thesis, 74 p.

Tapp, J. B., 1978, Breccias and megabreccias of the Arbuckle Mountains, southern Oklahoma aulacogen, Oklahoma: University of Oklahoma unpublished M.S. thesis, 126 p.

STOP 8
Parallel Folds and Shallowing-Upward Cycles in the Kindblade Formation, I-35

I-35 road cut at mile post 46 (Highway Station 2423).

R. Nowell Donovan
Texas Christian University

FOLD STYLES

The I-35 road cuts demonstrate clearly that, for the most part, the southern limb of the great Arbuckle anticline is a homoclinal sequence dipping to the south at 30–40°. However, near the base of the Kindblade Formation the consistency of dip is interrupted by a small pair of folds that plunge to the west–northwest. These structures can be examined both in plan view and in three consecutive road cuts. Given the plunge of the folds, the road cuts display successively higher structural levels when traced from east to west (Fig. 1).

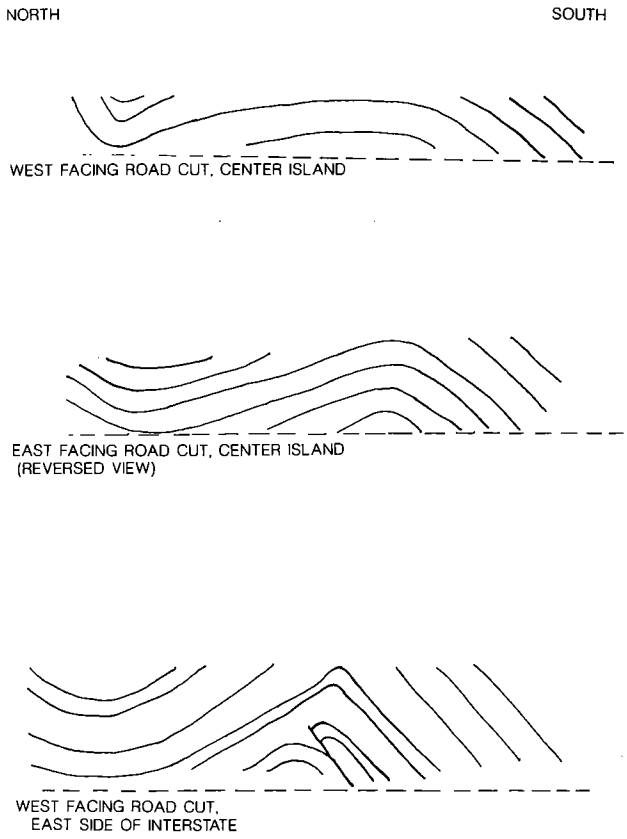


Figure 1. Fold profiles in the three road cuts, adjusted in position to account for the horizontal distance between the exposures, using an averaged plunge of 25° (adapted from Brown, 1990).

Brown (1990) recently described these folds in detail. He noted that the exposures are very instructive because they show the relationships of plunge to map and section views, display abundant evidence of flexural slip along bedding planes, and illustrate fault-propagation folds, out-of-the-syncline reverse faults, and small detached folds. The parallel style of deformation shown by the folds is characteristic of that developed throughout the Arbuckle Group. Because the fold style is parallel, volume adjustments are necessary to compensate for varying amounts of tightness along the axial planes of the folds. In general, the anticlines tighten down-section and the synclines tighten up-section, until an adjustment in the fold form occurs. This can be seen quite clearly in the easternmost road cut (and in plan view on the surface east of the road cut) where the anticline is severed by a bedding-plane slip fold (Fig. 2). In essence the fold is compartmentalized into two sections: a lower, simple anticline, and an upper, more complex section that shows a clear "rabbit ear" profile in plan view. The upper fold compartment shows a different trend and greater plunge than the lower (Fig. 3). Farther to the west, the anticline opens out into what is little more than a structural terrace, while the syncline progressively tightens until, in the end, crowding is so severe that a small syncline-anticline fold pair, plunging to the southeast, is developed in the syncline axis.

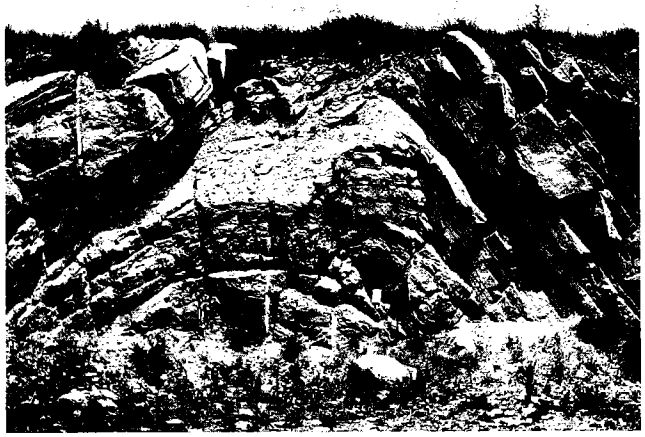


Figure 2. View of the anticline in the easternmost road cut illustrating how a bedding-parallel flexural slip fault effectively compartmentalizes the fold.

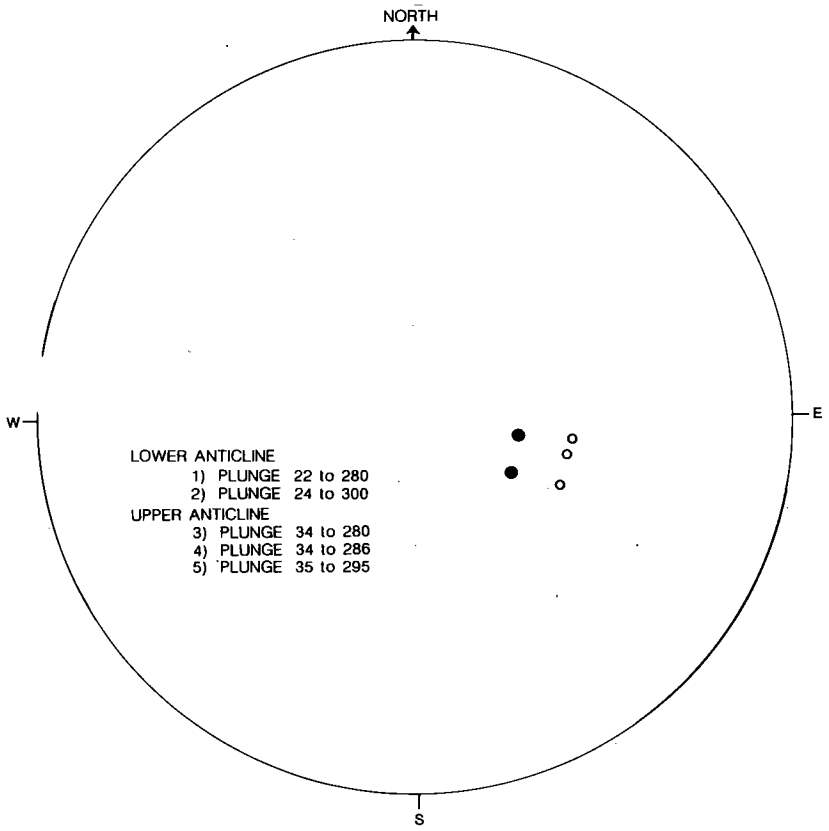


Figure 3. Poles to the plunge of the anticline; all data obtained from the easternmost road cut and the area immediately to the east. Note the great variation in plunge and trend shown by folds in short distances. The two readings that show lower plunge values are from the lower structural level, whereas the other three are from various exposures of the "rabbit ear."

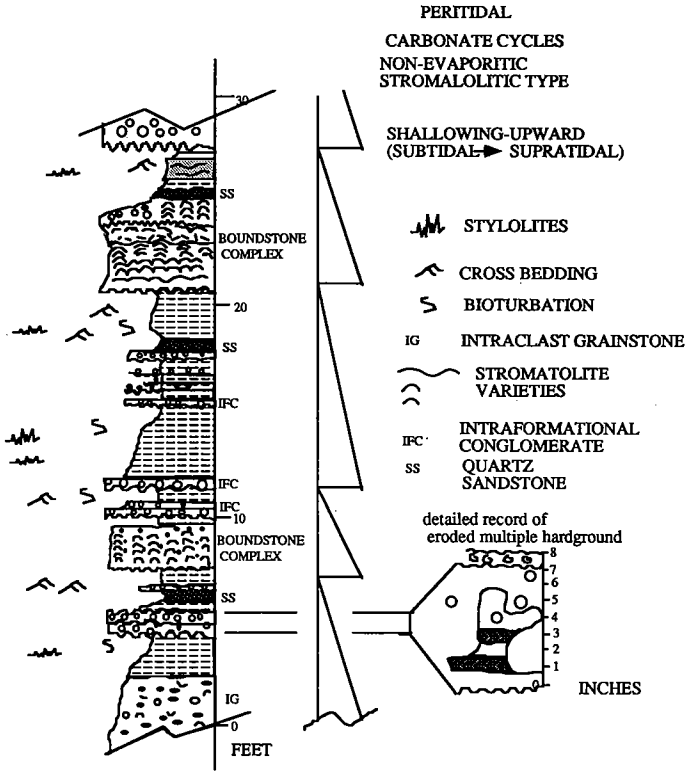


Figure 4. Log of a short section of the Kindblade Formation in the eastern road cut, south of the anticline axis. Log prepared by Jim Markello, Tim Denison, and Nowell Donovan (their permission to publish is gratefully acknowledged).

In a regional context, Brown (1990) noted that the sense of vergence of the small anticline is to the north, which is the same as that shown by the great Arbuckle anticline. He further deduced, from the orientation of vertical (tectonic) stylolites, that when the folds were initiated, sigma one was horizontal and oriented approximately northeast–southwest.

THE KINDBLADE FORMATION

On I-35 the Lower Ordovician Kindblade Formation is ~1,400 ft (~450 m) thick. A small segment of the formation has been logged, immediately to the south of the anticline in the most easterly road cut (Fig. 4). This section displays a sequence of fossiliferous peritidal carbonates, characterized by a variety of algal boundstones, thrombolites and stromatolites, intraformational conglomerates, bioturbated mudstones and ribbon carbonates, hardgrounds (including one spectacular multiple hardground with quite extraordinary relief), oolitic sandstones, and a spectrum of mud-supported lithologies characterized by a variety of allochems. Fossils include gastropods, trilobites, echinoid fragments, brachiopods, *Orthoceras*, and *Renalcis*. Certain horizons, particularly thinly laminated heterolithic beds, contain abundant quartz detritus. By assuming that this laminated facies is an indicator of shallow, relatively low-stand conditions, the sequence can be divided into a number of shallowing-upward "mini" cycles. These cycles show a great deal of individual variety; i.e., it is not possible to describe a "typical" cycle,

except in the most general terms. By comparison with similar shallowing-upward cycles present in the Cool Creek and West Spring Creek Formations, the Kindblade cycles contain less chert, less detrital quartz, and a greater overall thickness of subtidal sediments, including very thick algal boundstones.

REFERENCE CITED

Brown, W. G., 1990, 3-D display of a small fold, *in* Crawford, M. F.; Morgan, K. M.; Donovan, R. N.; and Brown, W. G. (eds.), Remote sensing techniques applied to structural geology and oil exploration in south-central Oklahoma: Geological Society of America Field Trip Guide #4, Dallas, Texas, 105 p.

DAY TWO

STOP 9
Permian Karst and Platform Carbonates, Cook Creek Road Cut

On Highway 19, ~8 mi west of Apache; secs. 18–19, T5N, R12W.

R. Nowell Donovan
Texas Christian University

Deborah A. Ragland
Conoco Inc., Ponca City

INTRODUCTION

Unlike the Arbuckle Mountains, the Slick Hills display few road cuts. One of the most instructive of these is the Cook Creek road cut on State Highway 19, ~10 mi (~16 km) west of Apache, Oklahoma. This road cut has previously been described by Donovan (1982) and Donovan and others (1986). In this communication we review what is known of the exposure, and present petrographic details not heretofore published.

The two principal features of the road cut are: (1) a fissure-controlled paleokarst system; this has been dated as Permian in age on the basis of a single fragment of the reptile *Captorhinus;* and (2) nicely weathered exposures of the Arbuckle Group that can be assigned to approximately the middle of the Kindblade Formation.

PERMIAN PALEOKARST

State Highway 19 cuts through a spur of a hill which forms part of the eastern Slick Hills. The road cut reveals several small cave systems that have developed by the solution of an orthogonal joint set oriented north–south and east–west (Fig. 1). Donovan (1982) suggested that these caves were of Permian age, noting that the hill spur is a Permian landform exhumed from beneath the Post Oak Conglomerate (the latter can be seen at either end of the road cut).

Four types of cave systems can be seen at this outcrop:

1) *Fissures filled with contemporary (Permian) detritus.* These, which are best seen at the eastern edge of the road cut, consist of fissures that have been completely filled with material derived from the overlying land surface. It is in these fissures that the aforementioned bone fragment was found. The infill of these fissures consists of small fragments of limestone and chert, hematite dust, quartz silt, and clay minerals.

2) *Open fissures without wall decoration.* Caves of this type are thin linear fissures that, uncommonly, may open up into man-sized karst pores, but are devoid of any form of speleothemic decoration.

3) *Open fissures, partly filled by calcite speleothem.* A third type of cave system is one in which a variety of speleothems is found. These speleothems mostly consist of cave popcorn and allied vadose deposits that encrust walls of the fissures. In one or two cases the speleothems consist of calcite that is dark brown due to the presence of hydrocarbon inclusions.

4) *Fissures filled with detritus of uncertain age.* Caves of this type contain much unconsolidated red silt and clay, together with limestone and dolomite pebbles, as well as limonite pseudomorphs after pyrite. The latter were probably derived from the Kindblade Formation, for this contains scattered coarse cubic accumulations of pyrite. The age of the detritus is uncertain: it may be Permian or Recent. One cave of this type shows evidence of superadjacent cannibalization. In other words, detrital deposits within the cave include speleothemic deposits that have been worked from higher levels of the cave system than presently exist.

At the present time all the caves are "fossil." The dominant direction of fissure opening recorded is north–south, as might be expected, for the road cut runs approximately east–west. However, east–west karst-opened joints are also present, although fissures are much tighter

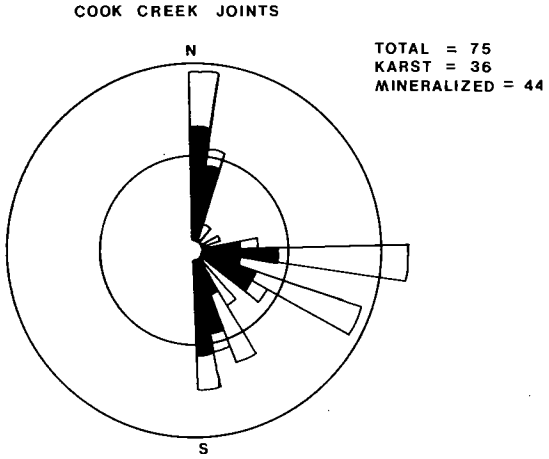


Figure 1. Rose diagram illustrating orientation of vertical joints in the Cook Creek road cut. The largest caves are associated with the north–south joint mode. Karst joints shown in black. From Donovan and others (1986).

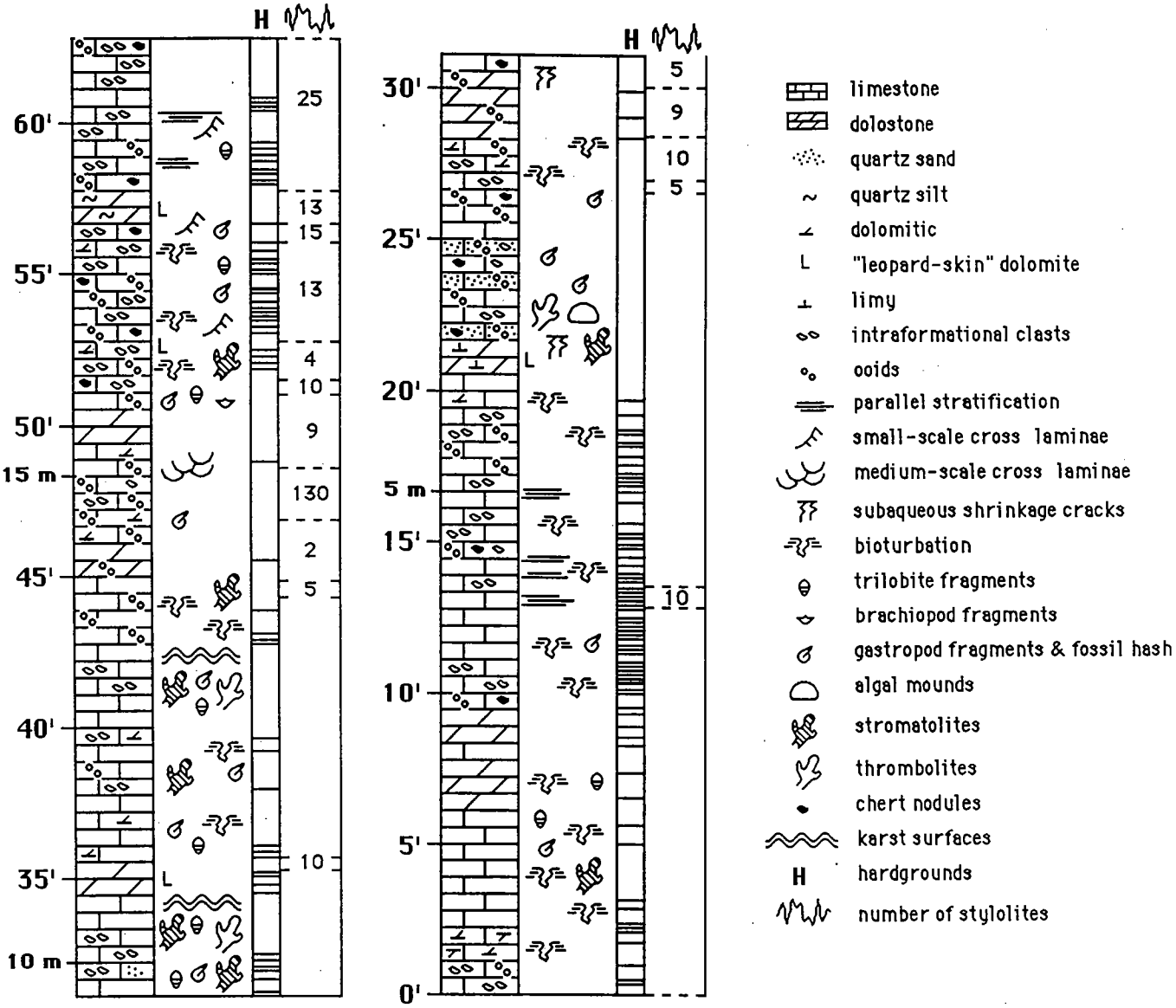


Figure 2. Log of the Kindblade Formation in the Cook Creek road cut.

in this direction. All the fissures are developed on the apex of the Permian hillslope; it is thus difficult to account for their presence unless it is assumed that: (a) their origin had little or nothing to do with modern drainage patterns, and (b) they represent a superimposed drainage pattern lowered onto an originally higher surface of limestone that was subsequently sculptured, in Permian times, into the hillslopes that we see today.

THE KINDBLADE FORMATION

In 1986, Donovan and others logged ~65 ft (~20 m) of section in the road cut. Their log is reproduced here (Fig. 2), as is their quantitative estimate of a variety of sedimentary parameters (Table 1). As they noted at the time, there are some weaknesses in the data. For example, part of the section is dolomitized, to the extent that the original lithology is obscured. Furthermore, exposure in the lower part of the section is not particularly clean: this may have resulted in some misidentification of various sedimentary parameters (for example, hardgrounds are difficult to spot, unless the exposure is excellent). Finally, and this is an important feature of the Arbuckle Group as a whole, a considerable amount of the section has been removed by anastomosing bedding-parallel stylolites (Fig. 3).

Tombstones, Bedding, and Layers

In the field a distinction can be made between empirically defined layers ("tombstones"), that are obvious at outcrop, and genetically defined events (beds) that often can only be observed by close scrutiny of the rocks. In practice, while some tombstone boundaries coincide with bed boundaries, many tombstones are differentiated from each other by bedding-parallel stylolites (Fig. 3). Exceptionally, these stylolites may have maximum wavelength magnitudes of 1 in. (~2.5 cm).

TABLE 1. — SEDIMENTARY PARAMETERS RELATED TO THE COOK CREEK CARBONATE SECTION*

Lithology	No. of beds	Average bed thickness in.	(cm)	Primary lithology (%)
Intraformational conglomerate	43	2.7	(6.9)	14.0
Grainstone	26	3.4	(8.5)	13.5
Oolitic grainstone	37	3.0	(7.8)	17.5
Packstone	44	2.5	(6.4)	17.0
Wackestone	28	2.2	(5.6)	9.5
Mudstone	47	2.5	(6.4)	18.0
Algal boundstones	4	16.5	(42.0)	0.0

*Primary lithology detectable in 88% of sequence; remaining 12% too heavily dolomitized.
Notes: 121 hardground deteced; 2 karst surfaces detected; through 312 in.(792 cm), 306 stylolites were found, with an average maximum amplitude of 0.25 in. (6 mm).

Primary Lithologies

As Donovan and others (1986) noted: "a gradational sequence of lithologies quantitatively dominates the section. This spectrum shows gradual variations of grain size from intraformational conglomerate to mudstone and gradual variations in textural cleanliness from well worked grainstones and intraformational conglomerates to completely mud-supported fabrics. Allochems are variable mixtures of intraclasts, ooids, peloids, and bioclastic grains." Fossils seen in the section commonly include gastropods, brachiopods (some of which may be partially or wholly silicified), echinoid fragments, and rather robust-shelled trilobites (Fig. 4). However, stromatolites and algal mats are underrepresented by comparison with other Kindblade sections.

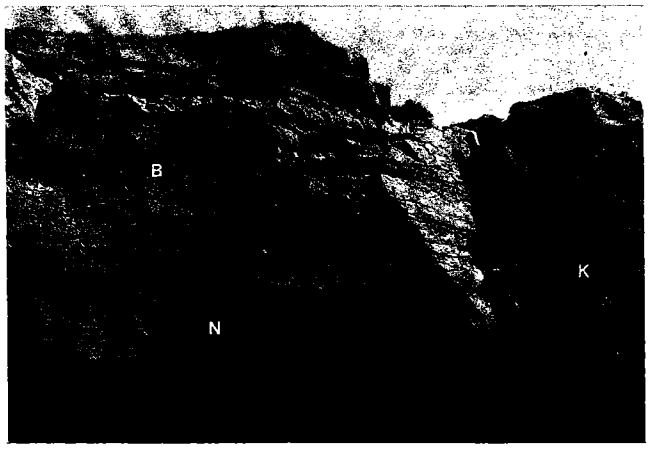


Figure 3. Lime mudstone-wackestone sequence containing multiple stylolites. Note that some bed boundaries (e.g., B) are stylolitized and some are not (N), and that many stylolites do not relate to boundaries. To the right of the pencil is Permian karst fill (K).

Apart from sedimentary layering, the most commonly seen primary sedimentary structure is small-scale cross-bedding; the largest set seen is no more than 3 in. (~8 cm) thick. This particular cross-bedding set occurs in an oolitic grainstone which, at 30 in. (~80 cm), is the thickest genetically homogeneous unit in the entire section. Small-scale cross-bedding is seen in various parts of the section; some of this appears to be due to the migrations of ripple marks. However, for the most part, the section consists of poorly washed, mud-supported lithologies that are devoid of obvious primary sedimentary structures apart from fining-upward grading.

Post-Sedimentation Imprint

Disturbance of the mud-supported textures by bioturbation is commonplace (Fig. 5). For the most part the burrows appear to be due to the actions of a mobile infauna.

As the data in Table 1 show, the section is cut by numerous hardgrounds, some of which are multiple in character (Figs. 6,7). Most of these hardgrounds appear to be submarine in their character and suggest that local pauses in deposition, followed by cementation and erosion, were frequent.

Two scalloped surfaces in the section (Fig. 8) may be related to emergence and the development of low-level karst. These two surfaces display a relief of just a few inches; hollows in the surface are filled by laminated carbonate mud that has clearly onlapped the erosion surface. Neither karst surface is associated with subsurface dissolution; they are simply horizons of surficial corrosion.

The section contains none of the evidences of supratidal sedimentation that are so common in the Cool Creek and West Spring Creek Formations. The closest approach to abnormal salinities is suggested by two or three horizons of subaqueous shrinkage cracks (Donovan and Foster, 1972).

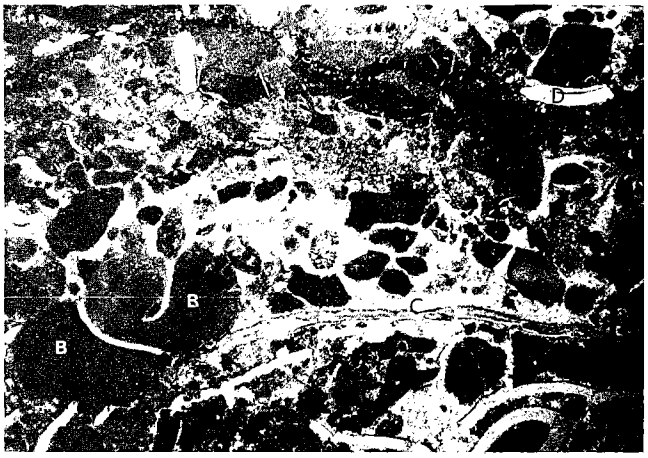


Figure 4. Poorly sorted intrabiosparite; fossils include broken trilobites (A), mud-filled gastropods (B), and partly silicified brachiopods (C). A conodont (D) is also present in this section. Ordinary light; field of view 9 mm across.

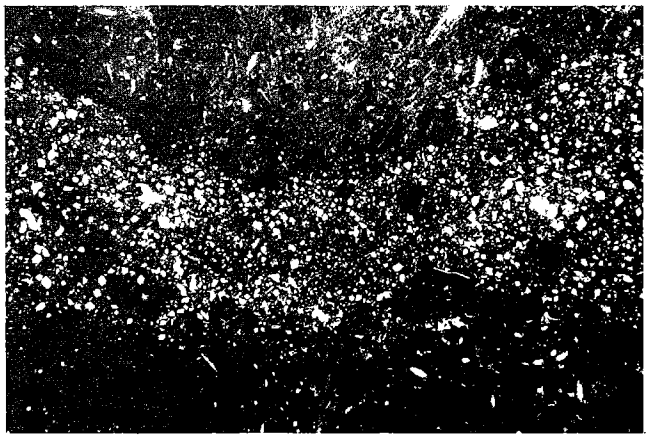


Figure 5. Burrow in biomicrite, showing partial replacement of the burrow fill by tiny idiotopic rhombs of dolomite. Ordinary light; field of view 9 mm across.



Figure 6. Characteristic hardground (H) developed between an oolitic grainstone (O) and a mudstone-wackestone sequence (M) containing several visually less-impressive hardgrounds.

Making allowance for the exceptions noted above, the entire sequence seems to record shallow-water, submarine sedimentation, mostly below wave base. The section has been used by Donovan and others (1986) to illustrate the concept of the platform triangle (Donovan, 1986), whereby "deposition in very shallow water above and below fair weather wave base is followed by rapid cementation and subsequent rip-up by storms (forming the intraclasts that are the commonest allochem in the sequence)."

Dolomite

Thin (up to 4 ft [~1.2 m]) zones of fine-grained, stratigraphically concordant dolomite are distinctive for their tan weathering hues. In the lower parts of the section, these zones are regularly spaced at intervals of 10–12 ft (~3–4 m). Towards the top of the section the spacing of the dolomite is less regular. In thin section, the dolomite is seen to consist of idiotopic micrite rhombs that have partially, but rarely completely, replaced the primary lime-mud textures. Less commonly the dolomite is a void-filling cement in grainstones. In places the dolomite displays a mottled "leopard skin" texture that is characteristic of a great deal of dolomite in the Arbuckle Group (Figs. 9,10). Donovan and others (1986) suggested that this texture reflected variations in permeability in the host limestone. In some places the mottling is clearly concentrated within burrows (Fig. 5), whereas in other areas no such control is evident.

Unlike dolomites found in the Cool Creek and West Spring Creek Formations (Cloyd and others, 1986; Gao and Land, 1991), this dolomite has no obvious relationship to evaporative conditions. However, it does appear to be of penecontemporaneous origin; it predates complete lithification and is stratigraphically concordant (we have traced dolomite horizons of this character for several miles). Donovan and others (1986) suggested that the regular spacing of dolomite zones in the sequence was due to cyclic variations in salinity caused by the mixing of marine and meteoric waters. On the other hand, it is possible that, during periods of relatively low sea level, restricted circulation may have developed, leading to evaporative concentration and the sinking of a submarine dolomitizing brine into surficial sediments.

Platform Carbonate Cannibalization

As Donovan (1986) noted, short-term rates of carbonate production were in excess of long-term rates of preservation on the Arbuckle platform. In other words, the platform could produce sediment faster than it could be trapped by burial. Three lines of evidence show how the problems caused by the super-efficient carbonate factory were resolved. In the first place, multiple intersecting hardgrounds indicate that in the short term the sequence was continuously reworked and redistributed across the platform. Presumably a portion of this reworked detritus was swept off the edge of the platform, leading to seaward progradation. Secondly, karstic weathering during low stands resulted in the removal of carbonate by dissolution. Thirdly, following lithification, large amounts of the section were removed by dissolution along bedding-parallel stylolites. Donovan and others (1986) estimated that as much as 23% of the Cook Creek road cut section had

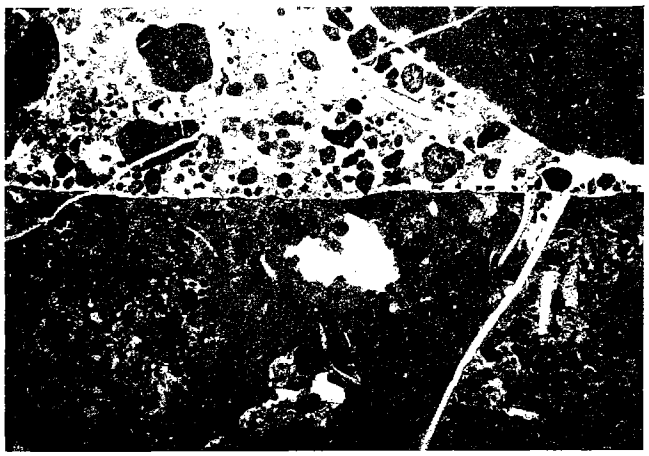


Figure 7. Hardground developed on top of a biopelmicrite. Above the hardground is a rather better-washed intrapelbiosparite. It is difficult to resist the conclusion that the peloids immediately above the hardground were deposited by gastropods moving across the underlying cemented surface. Ordinary light; field of view 9 mm across.

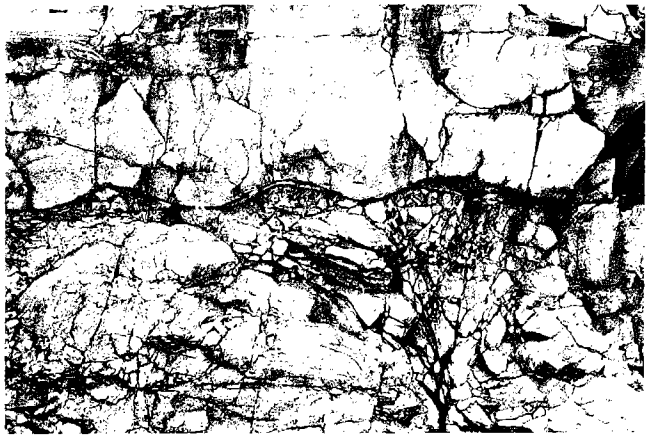


Figure 8. One of two scalloped karstic surfaces (K) occurring in the outcrop. Maximum relief on the surface is 5 in. (13 cm).



Figure 9. Zone of partial dolomitization illustrating typical "leopard skin" dolomite texture (dolomite is lighter than calcite). Note zone of cherts (S) above dolomite.

been removed by solution. Similar figures have been obtained from other sections. It is worth noting that the Cook Creek section is unlikely to have been buried to a depth of more than 5,000–6,000 ft (~1,600–1,900 m). More deeply buried subsurface rocks, entombed since the Cambro–Ordovician, can reasonably be expected to show greater pressure-solution effects.

REFERENCES CITED

Cloyd, K.; Ragland, D. A.; Jones, L.; and Donovan, R. N., 1986, Dolomite with evaporitic connections in the Ordovician Cool Creek Formation, southwestern Oklahoma, *in* Donovan, R. N. (ed.), The Slick Hills of southwestern Oklahoma—fragments of an aulacogen?: Oklahoma Geological Survey Guidebook 24, p. 29–34.

Donovan, R. N., 1982, Geology of Blue Creek Canyon, Wichita Mountains, Oklahoma, *in* Gilbert, M. C.; and Donovan, R. N. (eds.), Geology of the eastern Wichita Mountains, southwestern Oklahoma: Oklahoma Geological Survey Guidebook 21, p. 65–77.

_____1986, Geology of the Slick Hills, *in* Donovan, R. N. (ed.), The Slick Hills of southwestern Oklahoma—fragments of an aulacogen?: Oklahoma Geological Survey Guidebook 24, p. 1–12.

Donovan, R. N.; and Foster, R. J., 1972, Subaqueous shrinkage cracks in the Caithness Flagstones (Middle Devonian) of northeast Scotland: Journal of Sedimentary Petrology, v. 42, p. 309–317.

Donovan, R. N.; Ragland, D. A.; and Shaefer, D., 1986, Stop 4: Geology of the Cook Creek road cut, *in* Donovan, R. N. (ed.), The Slick Hills of southwestern Oklahoma—fragments of an aulacogen?: Oklahoma Geological Survey Guidebook 24, p. 100–105.

Gao, G.; and Land, L. S., 1991, Early Ordovician Cool Creek dolomite, Middle Arbuckle Group, Slick Hills, SW Oklahoma, U.S.A.: Journal of Sedimentary Petrology, v. 61, p. 161–173.



Figure 10. Thin section showing details of typical "leopard skin" dolomite. The dolomite appears light. Ordinary light; field of view 9 mm across.

STOP 10
The Base of the Arbuckle Group at Bally Mountain

On the extreme eastern edge of Kiowa County, ~7 mi north of Comanche County; sec. 26, T6N, R14W.

R. Nowell Donovan
Texas Christian University

Deborah A. Ragland
Conoco Inc., Ponca City

THE BALLY MOUNTAIN RANGE

The Bally Mountain Range is located in eastern Kiowa County in southwestern Oklahoma (T6N, R14W). Bally Mountain itself is the type section of the Carlton Rhyolite, displaying a thickness of 3,600 ft (~1,100 m) of rhyolite lavas and related rocks (Ham and others, 1964). Unconformably overlying the rhyolite are the sandstones and limestones of the Upper Cambrian Timbered Hills Group. In turn, these rocks are overlain by a sequence of Arbuckle Group carbonates that is complete and relatively undisturbed (except for the West Spring Creek Formation, which is overlapped by Permian Post Oak conglomerates). The sedimentary rocks dip to the northeast at angles of 25–40°. Highlights of this range have previously been described by Donovan and others (1986,1988). What follows is an update on selected sites which have been chosen for the insight that they give into the Arbuckle Group. The sites for stops 10, 11, 12, and 13 are located on Figure 1.

THE BASAL UNCONFORMITY

By Late Cambrian time (after an interval of 15 million years, or less), the Carlton Rhyolite, topmost member of the igneous rocks emplaced in the southern Oklahoma aulacogen, had weathered to a range of low hills. This topography was gradually transgressed during Franconian time; initial deposits were the siliciclastics of the Reagan Sandstone (Fig. 2). Subsequently the Honey Creek Limestone heralded the development of the great carbonate platform that would dominate Oklahoma throughout most of the Ordovician (Donovan, 1986). At this later period the higher parts of the rhyolite topography formed an archipelago; one of the islands in the archipelago is well exposed on Bally Mountain. In a distance of 300 yards (~300 m), ~110 ft (~35 m) of Reagan plus an equal amount of the Honey Creek are overlapped (sites A1, B1, and C1 on Fig. 1).

At this location, the Reagan Sandstone consists of a basal breccio-conglomerate of rhyolite clasts. This is overlain by a few feet of tan-colored lithic sandstones that contain increasing amounts of quartz detritus (the latter is not from the rhyolite but is presumed to have come from a source outside of the aulacogen, probably to the north and west). Above these sandstones are poorly exposed shales and lenticular sandstones, followed by the topmost unit of the Reagan, ~30 ft (~10 m) of dark-green glauconitic sandstone (Donovan, 1986). The base of the Honey Creek is marked by orange-weathering stringers of a pelmatozoan-rich grainstone that shows substantial replacement by large rhombs of ankerite (Cloyd and others, 1986). It is the weathering of this ankerite which gives such a distinctive color to the lowest part of the Honey Creek. In a regional context, the transition from Reagan to Honey Creek is gradational and probably diachronous (Donovan, 1986). Petrographically, carbonate grains are added to the existing mix of quartz grains, glauconite pellets, phosphatic brachiopod shells, and rhyolite fragments. All these clastic particles gradually diminish in size and abundance upwards.

Although it is a limestone, the Honey Creek is unlike the Arbuckle Group in that it contains very little lime mud. In essence, the grainstones of which it is built are bimodally cross-bedded bioclastic sands in which the principal fauna consist of broken plates of pelmatozoans, broken fragments of robust-shelled trilobites, and brachiopods. The Honey Creek has been interpreted as a deposit that formed as a stacked series of tidally influenced sandbars (Rafalowski, 1984; Donovan, 1986). The Honey Creek, unlike the Arbuckle, is built of grainstones that contain few intraclasts, peloids, and ooids. Although the contact between the Timbered Hills and Arbuckle Groups is defined on paleontological criteria (Stitt, 1977), it is useful practice in field mapping to take the lowest laterally persistent lime-mud bed as the lowest unit in the Fort Sill Formation. This unit forms a clearly seen ledge (or row of "tombstones").

Both formations of the Timbered Hills Group were deposited in an environment strongly influenced by astronomical tides that ebbed and flowed along northwest–southeast paths around islands of the southern Oklahoma archipelago (Donovan, 1986). These tides helped to mold lenticular sandstones that are characterized by cross beds as much as 4 ft (~1.3 m) thick. It has been suggested that the incoming of carbonate sands into the sequence represents the colonization, by pelmatozoans and other carbonate-producing organisms, of clear-water sites around islands in the archipelago (Donovan, 1986). As the Franconian transgression gradually enveloped the Laurentian (proto-North American) craton, the width of

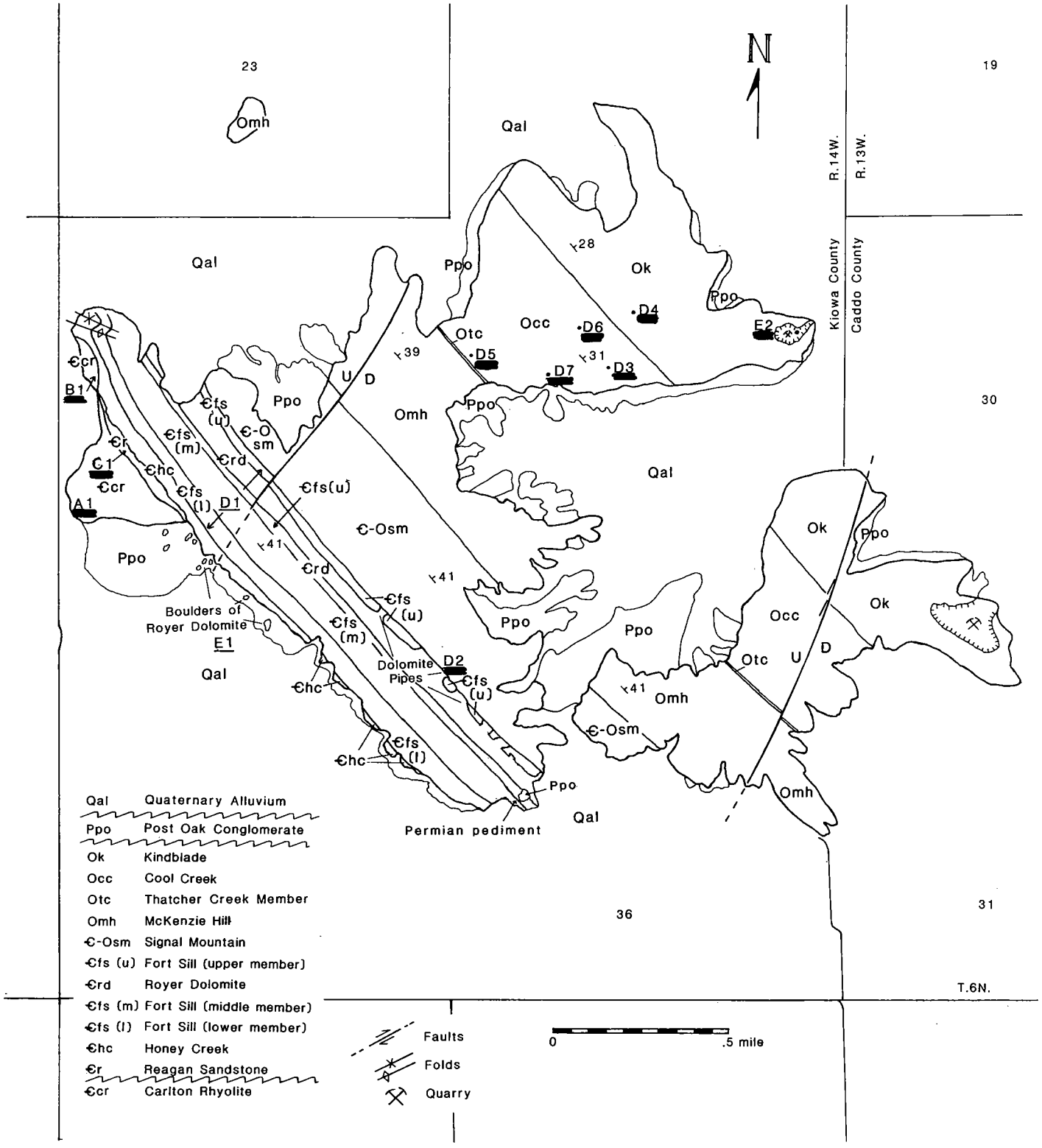


Figure 1. Geological map of the northeast part of the Bally Mountain Range, from Donovan and others (1986). Sites to be visited on this field trip are A1, B1, and C1 (Stop 10), D2 (Stop 11), D3 through D7 (Stop 12), and E2 (Stop 13). Royer Dolomite (in explanation) now called Bally dolomite.

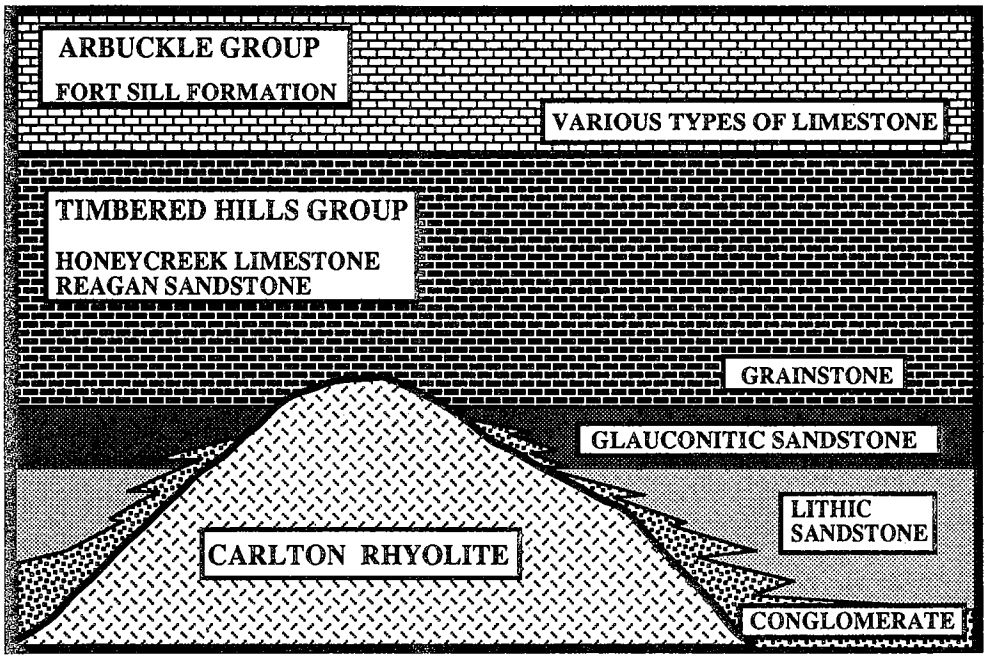


Figure 2. Stratigraphic relationships at the base of the Arbuckle Group, as can be seen at sites A1, B1, and C1.

the inundated shelf margin increased, tidal energy was dampened, and the long-lasting Arbuckle platform evolved.

REFERENCES CITED

Cloyd, K.; Donovan, R. N.; and Rafalowski, M. B., 1986, Ankerite at the contact between the Reagan Sandstone and the Honey Creek Limestone (Timbered Hills Group), *in* Donovan, R. N. (ed.), The Slick Hills of southwestern Oklahoma—fragments of an aulacogen?: Oklahoma Geological Survey Guidebook 24, p. 17–20.

Donovan, R. N., 1986, Geology of the Slick Hills, *in* Donovan, R. N. (ed.), The Slick Hills of southwestern Oklahoma—fragments of an aulacogen?: Oklahoma Geological Survey Guidebook 24, p. 1–12.

Donovan, R. N.; Ragland, D. A.; Cloyd, K.; Bridges, S.; and Denison, R. E., 1986, Stop 2: Geologic highlights of the Bally Mountain area, *in* Donovan, R. N. (ed.), The Slick Hills of southwestern Oklahoma—fragments of an aulacogen?: Oklahoma Geological Survey Guidebook 24, p. 92–95.

_____1988, Carlton Rhyolite and lower Paleozoic sedimentary rocks at Bally Mountain in the Slick Hills of southwestern Oklahoma, *in* Hayward, O. T. (ed.), Geological Society of America, South-Central Section, Centennial Field Guide, v. 4, p. 93–96.

Ham, W. E.; Denison, R. E.; and Merritt, C. A., 1964, Basement rocks and structural evolution of southern Oklahoma: Oklahoma Geological Survey Bulletin 95, 302 p.

Rafalowski, M., 1984, The sedimentary geology of the Honey Creek and Fort Sill Formations as they are exposed in the Slick Hills of southwestern Oklahoma: Oklahoma State University unpublished M.S. thesis, 147 p.

Stitt, J. H., 1977, Late Cambrian and earliest Ordovician trilobites, Wichita Mountains area, Oklahoma: Oklahoma Geological Survey Bulletin 124, 79 p.

STOP 11
Three Types of Dolomite and the Transition from Fort Sill to Signal Mountain Formation at Raggedy Ridge, Bally Mountain

Secs. 35 and 36, T6N, R14W (see Stop 10, Fig. 1, site D2).

R. Nowell Donovan
Texas Christian University

Deborah A. Ragland
Conoco Inc., Ponca City

THREE TYPES OF DOLOMITE

In the eastern part of the Slick Hills, the Fort Sill Formation can be divided informally into three members. These are, from top to bottom: (iii) massive algal boundstones, (ii) alternations of lime mudstones with thinly bedded dolomitic mudstones, and (i) thinly bedded limestones, consisting of alternations of mudstones, oolitic grainstones, packstones, and wackestones, with a few stromatolite and oncolite horizons and some chert.

However, on Bally Mountain and the adjacent Zodletone Mountain, a thick stratabound dolomite, ~120 ft (~35 m) thick, is emplaced in the middle of the upper massive algal-boundstone unit (iii). This unit has been termed the Bally dolomite by Donovan and Ragland (1986) (see also Donovan and others, 1986,1988; Donovan and Ross, 1991). Gao (1990) has described geochemical and isotopic details of this dolomite but names it the "Royer Dolomite," a reference to the fact that a similar dolomite is found at this approximate level in the Arbuckle Mountains. We prefer the term "Bally" for two reasons: in the first place, no lateral continuity has been demonstrated between the two outcrops, and, secondly, the stratigraphic equivalence of the two dolomites is not perfect.

One of the most instructive sites for studying this dolomite is located at the southern end of the Bally Mountain Range (see Stop 10, Fig. 1, site D2, this volume), where three distinct types of dolomite can be recognized in the field.

Dolomite Type 1

The primary lithology of the uppermost Fort Sill (i.e., member iii) consists of relatively thick-bedded algal boundstones and stromatolites (the latter almost always forming closely spaced or laterally linked hemispheroids with a more or less constant diameter of ~3 in. (~8 cm). This lithology can be traced throughout the Slick Hills and, except on Bally and Zodletone Mountains, contains very little dolomite. What little dolomite there is consists of small idiotopic crystals that are preferentially located in the interhemispheroidal areas of the algal boundstones. This suggests that the dolomitization was fabric selective and, by implication, of an early date. Dolomites of this type are seen in the uppermost Fort Sill Formation at Bally Mountain; they are a little unusual in that, because they are ferroan, they weather to an orange color (instead of the usual tan-yellow for this type of dolomite).

Dolomite Type 2

For the most part, the underlying Bally dolomite maintains stratigraphic integrity. However, at the eastern end of its exposure, it is locally discordant; sharply defined beds of Bally dolomite can be found in the uppermost part of the Fort Sill (Fig. 1). This dolomite, which weathers to a brown color, is medium to coarse grained, mostly xenotopic with pressure-dissolved crystal boundaries, contains little porosity, and displays knife-edge contacts with the adjacent limestone (Figs. 2,3).

Following a detailed strontium-, carbon-, and oxygen-isotope study, Gao (1990) concluded that the Bally dolomite "probably formed during early diagenesis from nearly contemporaneous Cambrian seawater." His principal line of evidence to support this interpretation was "the similarity of the $^{87}Sr/^{86}Sr$ ratios of most of his samples to those of coeval late Cambrian seawater and associated limestone." A further conclusion he reached, as a result of light $\delta^{18}O$ values, was that the dolomite was significantly modified after burial by meteoric water. He attributed this modification to subsequent emergence of the carbonate platform.

Dolomite Type 3

The top of the Bally dolomite is associated with a third type of dolomite, characterized by very coarse, baroque crystals (with intracrystalline pores that contain a little green authigenic illite). This dolomite forms a penetrative network that ramifies about the contact between the Bally dolomite and the Fort Sill Limestone (member iii) (Fig. 1), and, in one or two places, penetrates for a very short distance up into the overlying Signal Mountain Formation. Dolomite of this type is some of the coarsest that has yet been found in the Slick Hills; it weathers to a light-tan color, is mildly ferroan, and appears to postdate some tectonic fracturing. Donovan and others (1986) suggested that this dolomite was relatively late in age, possibly Pennsylvanian.

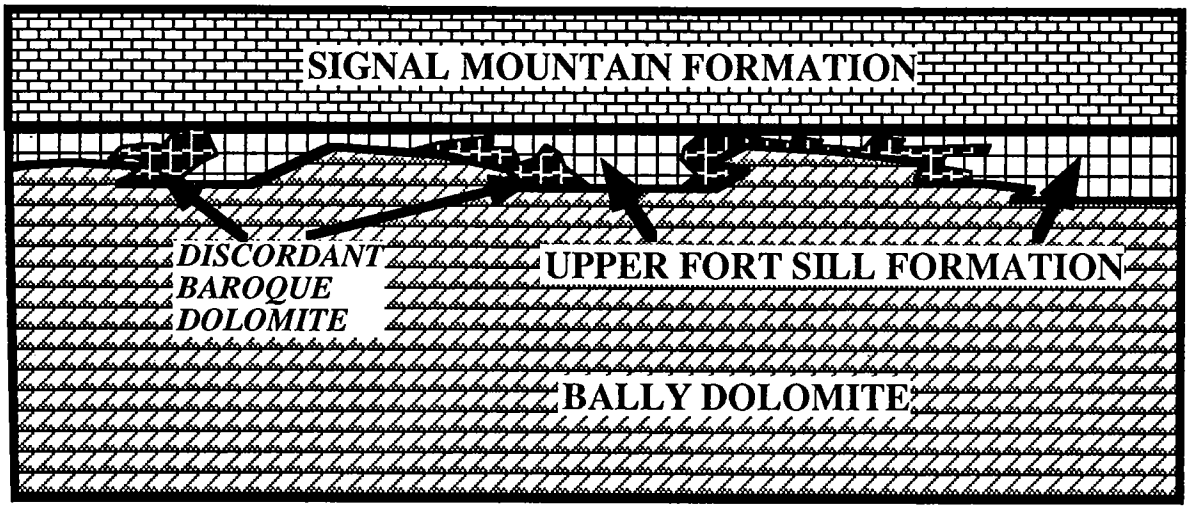


Figure 1. Schematic relationship of the various types of dolomite seen on Raggedy Ridge, Bally Mountain, at site D2 (see Fig. 1 in Day 2, Stop 2, this volume).

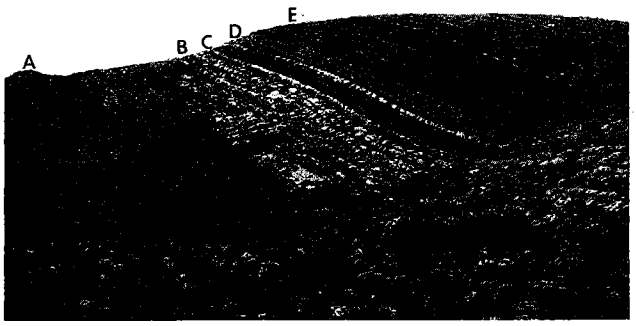


Figure 2. View of part of the eastern end of Raggedy Ridge, Bally Mountain Range, showing the Bally dolomite (A), the uppermost Fort Sill Formation (B), the contact between the Fort Sill and Signal Mountain Formations (C), a single algal boundstone within the Signal Mountain that dies laterally when traced to the west (D), and typical, thinly bedded Signal Mountain lithology (E) (from Donovan, 1986).

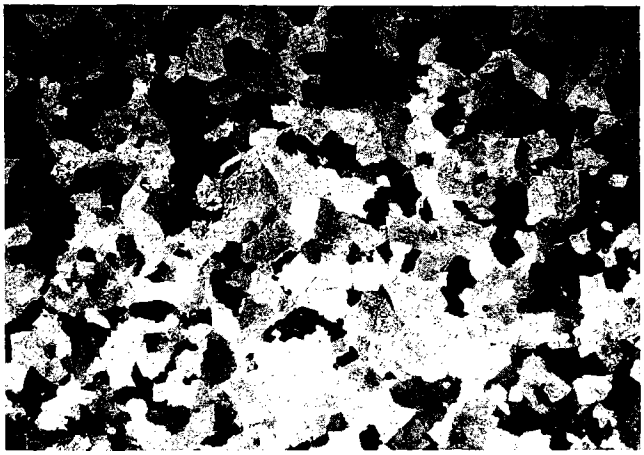


Figure 3. Bally dolomite on Raggedy Ridge, Bally Mountain Range. Most of this dolomite is composed of subidiotopic coarse-medium crystals of equant grain size and porosity of <2%. Polarised light; field of view 9 mm wide.

THE CONTACT BETWEEN THE FORT SILL AND SIGNAL MOUNTAIN FORMATIONS

This contact is perhaps the most convincing formation boundary in the Arbuckle Group; it can be mapped with ease, even on the scale of Landsat data. The most obvious change across the boundary is the disappearance of the algal boundstones that characterize the top of the Fort Sill (member iii). In fact, no similar boundstones are met with until well into the McKenzie Hill Formation, a stratigraphic thickness in excess of 1,000 ft (~330 m). The overall appearance of the Signal Mountain Formation is that of a thinly bedded, dominantly dark-gray limestone, composed of a rapid alternation of intraformational conglomerates, highly fossiliferous grainstones, and bioturbated mud-supported lithologies (Ditzell, 1984).

It has been suggested (Donovan, 1986) that the contact between the two formations is a disconformity marking a tectonically controlled adjustment of the developing aulacogen. Evidence in support of this includes the sudden appearance of as much as 10% glauconite in basal Signal Mountain grainstones (suggesting transgression) and a facies pattern in the basal Signal Mountain which hints that the top Fort Sill surface was emergent to the northwest, along the strike of the aulacogen. The suggestion that the contact marks a tectonic adjustment is in accord with Feinstein's (1981) interpretation of subsidence curves within the aulacogen; he noted that the rate of change of subsidence was at its greatest during Signal Mountain deposition.

The Signal Mountain appears to have been deposited in deeper water than the top of the Fort Sill. Although the richness of fauna in the Signal Mountain is indicative of shallow-water deposition (and the great number of intra-

formational conglomerates indicate that the sea bed was frequently affected by storms), there is less evidence of emergence and restriction than in any other formation of the Arbuckle Group.

If the formation boundary does record a period of emergence followed by relatively rapid sedimentation that could just keep pace with subsidence, then it may well be that the emergent event marks the time during which the Bally dolomite replaced the upper Fort Sill boundstones.

REFERENCES CITED

Ditzell, C., 1984, The sedimentary geology of the Signal Mountain and McKenzie Hill Formations, as exposed in the Slick Hills of southwestern Oklahoma: Oklahoma State University unpublished M.S. thesis, 165 p.

Donovan, R. N., 1986, Geology of the Slick Hills, *in* Donovan, R. N. (ed.), The Slick Hills of southwestern Oklahoma—fragments of an aulacogen?: Oklahoma Geological Survey Guidebook 24, p. 1–12.

Donovan, R. N.; and Ragland, D. A., 1986, Paleozoic stratigraphy of the Slick Hills, southwestern Oklahoma, *in* Donovan, R. N. (ed.), The Slick Hills of southwestern Oklahoma—fragments of an aulacogen?: Oklahoma Geological Survey Guidebook 24, p. 13–16.

Donovan, R. N.; and Ross, D. L., 1991, The Saddle Mountain dolomite at Maukeen Hill—a dolomite interface in the upper Arbuckle Group, western Slick Hills, Oklahoma, *in* Johnson, K. S. (ed.), Late Cambrian–Ordovician geology of the southern Midcontinent, 1989 symposium: Oklahoma Geological Survey Circular 92, p. 143–153.

Donovan, R. N.; Ragland, D. A.; Cloyd, K.; Bridges, S.; and Denison, R. E., 1986, Stop 2: Geologic highlights of the Bally Mountain area, *in* Donovan, R. N. (ed.), The Slick Hills of southwestern Oklahoma—fragments of an aulacogen?: Oklahoma Geological Survey Guidebook 24, p. 92–95.

_____1988, Carlton Rhyolite and lower Paleozoic sedimentary rocks at Bally Mountain in the Slick Hills of southwestern Oklahoma, *in* Hayward, O. T. (ed.), Geological Society of America, South-Central Section, Centennial Field Guide, v. 4, p. 93–96.

Feinstein, S., 1981, Subsidence and thermal history of southern Oklahoma aulacogen; implications for petroleum exploration: American Association of Petroleum Geologists Bulletin, v. 65, p. 2521–2533.

Gao, G., 1990, Geochemical and isotopic constraints on the diagenetic history of a massive stratal, Late Cambrian (Royer) dolomite, lower Arbuckle Group, Slick Hills, SW Oklahoma, USA: Geochemica et Cosmochemica Acta, v. 54, p. 1979–1989.

STOP 12
The Cool Creek and Lower Kindblade Formations on North Bally Mountain

Sec. 25, T6N, R14W (see Stop 10, Fig. 1, sites D3 through D7).

Deborah A. Ragland
Conoco Inc., Ponca City

R. Nowell Donovan
Texas Christian University

INTRODUCTION

One of the more complete outcrops of the upper part of the Arbuckle Group is found on the northern part of the Bally Mountain Range. This hillside displays fine, laterally extensive exposures of the McKenzie Hill, Cool Creek, and Kindblade Formations (Fig. 1). In this account we have utilized previous descriptions by Donovan and others (1986,1988), Cloyd and others (1986), Ragland (1990), Ragland and Donovan (1991), and Gao and Land (1991). The principal justification for visiting this site is that it displays a characteristic sequence of the entire Cool Creek Formation where facies variations can be studied easily. In addition, the outcrop includes a number of dolomite horizons in the upper Cool Creek that have been analyzed by Cloyd and others (1986) and Gao and Land (1991). Finally, the lower part of the overlying Kindblade contains a conspicuous, quartz-rich sandstone; this unit has been interpreted as a transgressive, storm- and tide-influenced sandbar (Ragland and Donovan, 1991).

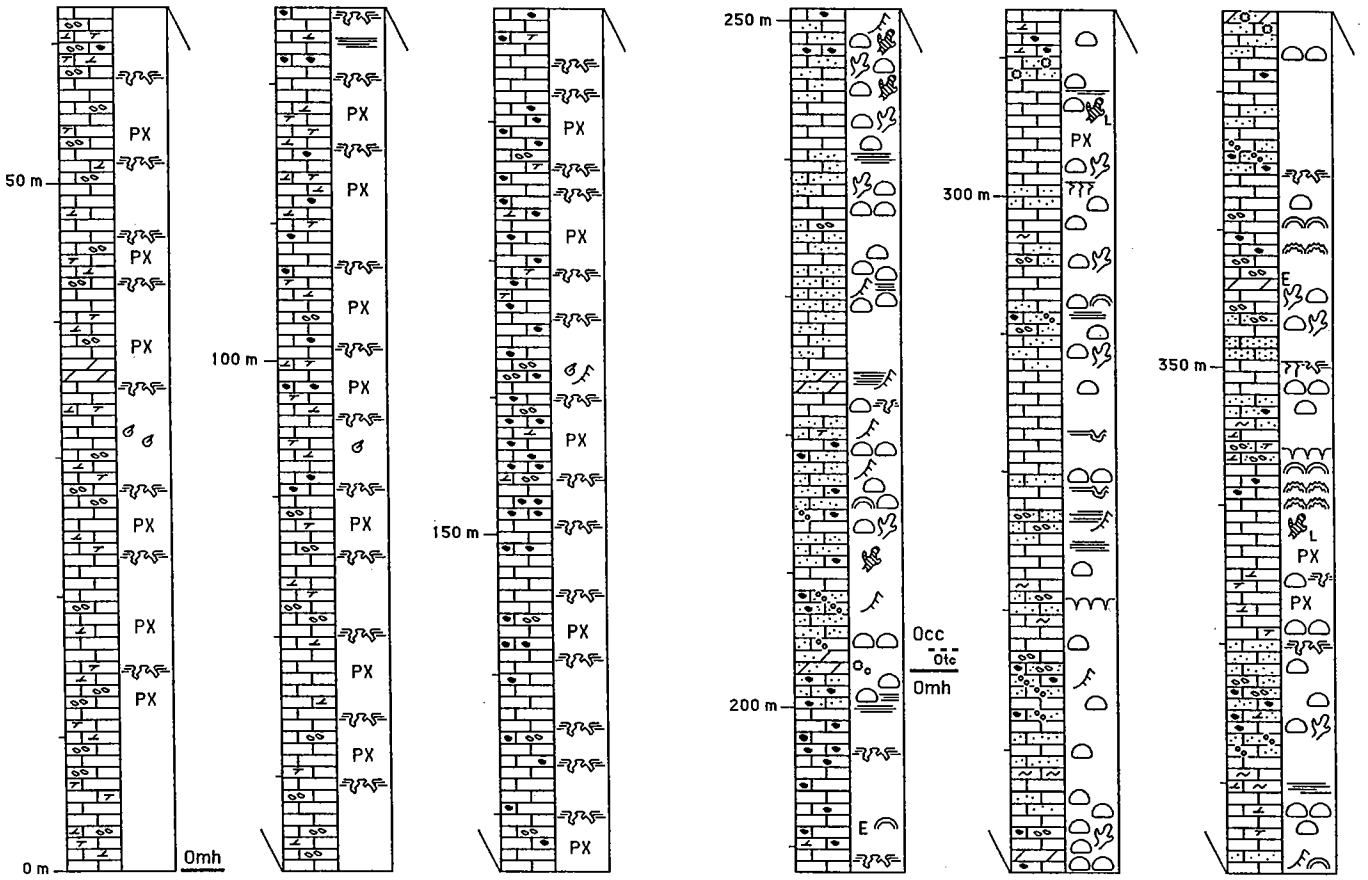


Figure 1. Stratigraphic log of the upper part of the Arbuckle Group on Bally Mountain, showing the McKenzie Hill (Omh), Cool Creek (Occ), and Kindblade (Ok) Formations. The Thatcher Creek (Otc) and Herringbone (Ohb) sandstones were described by Ragland (1990).

LIMESTONE FACIES

The Bally Mountain section contains all the features that are developed elsewhere in the Cool Creek Formation. Algal boundstones are found throughout and, because of the nature of the exposure, they can be examined in three dimensions. Figure 2 shows a typical example in which a well-exposed algal reef is composed of colonies of nonbranching, columnar members that radiate to form a "sunburst" pattern in cross profile (site D3). The internal structure of this unit is intermediate between stromatolite and thrombolite; the well-defined laminations characteristic of true stromatolites are not fully developed, suggesting that the reef grew in the subtidal zone (Ragland and Donovan, 1986). In addition, cross-bedded oolitic-sand shoals (many of which show at least partial silicification) are commonly seen, and intraformational conglomerates are ubiquitous. The latter show a variety of packing arrangements, ranging from flat-packed (due to gravity settling), through imbricate (due to sorting by strong currents), to vertically packed (where the clasts are arranged by waves).

DOLOMITE IN THE SECTION

The Cool Creek Formation at this locality (sites D5 and D7) is constructed of 3–20 ft (~1–6 m) shallowing-upward cycles. Some of these cycles are comparable in their

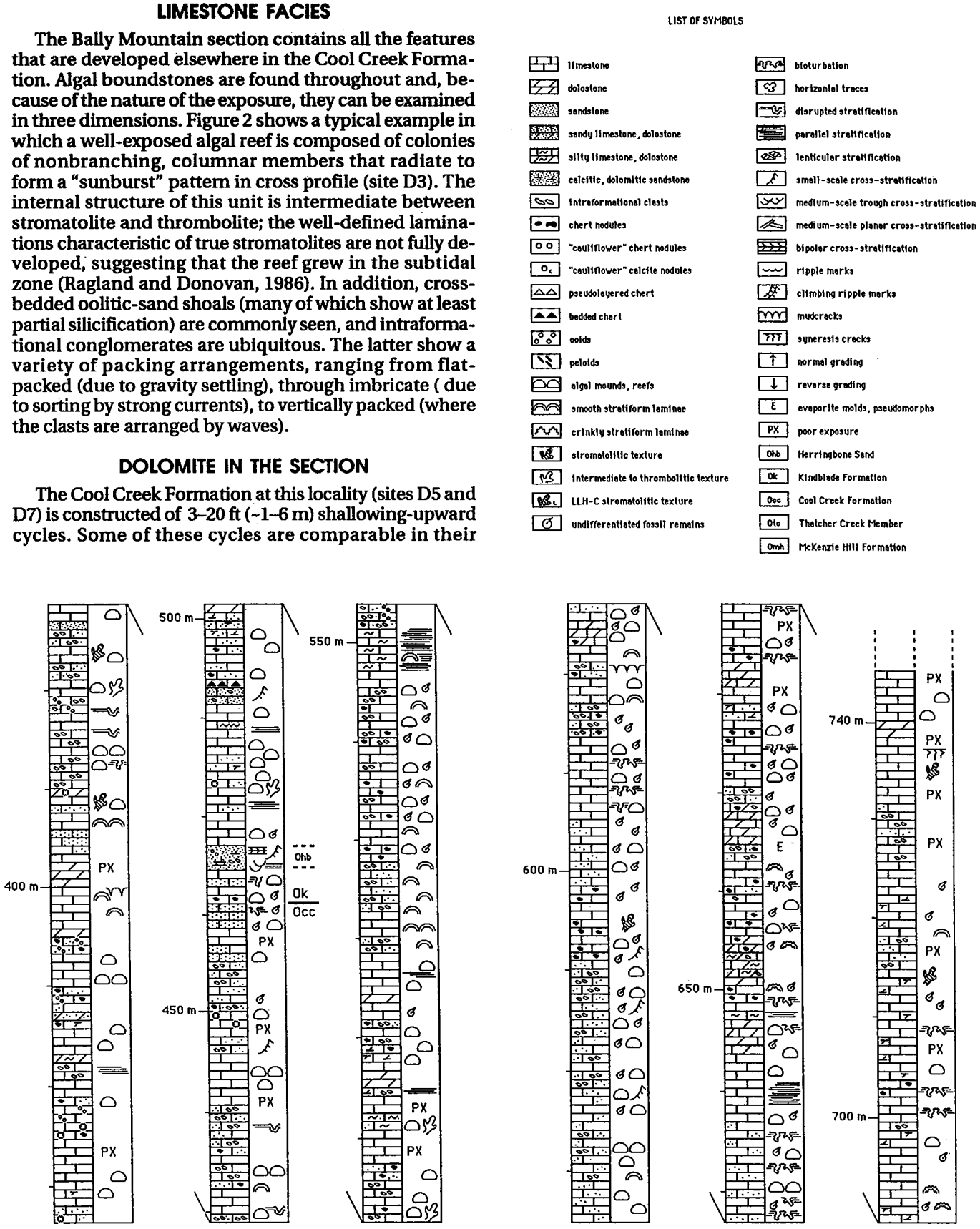


Figure 1. *(continued)*

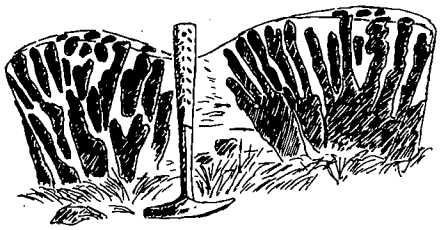


Figure 2. Field sketch of an algal reef in the Cool Creek Formation. Laterally continuous unit composed of dendritic and columnar members. Internal textures are intermediate between stromatolite and thrombolite. Inter-areas are full of ooids (from Donovan and others, 1988).

geometry to the sabkha cycles of the modern Persian Gulf (Cloyd and others, 1986) (Fig. 3). Typically, a Cool Creek cycle comprises a basal oolitic or intraclast grainstone that is overlain by a variety of algal boundstones. The boundstones in turn are overlain by massive mudstones, some of which may be bioturbated. These grade upwards into laminated mudstones that display fenestral fabrics and, more rarely, mudcracks. In the top part of the cycles, massive or laminated dolomitic mudstones are developed. The mudstones contain numerous white, colloform ("cauliflower") chert nodules that mimic the anhydrite nodules found on modern sabkhas. In thin section, some of these cherts display felted fabrics comprising small laths oriented subparallel to bedding; these appear to be pseudomorphs after anhydrite. In some cases, laths of anhydrite and tiny crystals have been trapped during silicification.

Dolomite seen in this section is very fine grained and idiotopic. For the most part it appears to have replaced lime muds; more rarely, replacement of intraclastic grainstones and packstones has occurred. In the latter cases, the dolomite crystals may be somewhat coarser; apparently dolomite-crystal size is, to some extent, a function of primary texture.

On the basis of uniformitarian analogy with modern sabkhas, it has been suggested that this dolomite is penecontemporaneous and was deposited from evaporated sea water of high salinity (Cloyd and others, 1986), either as a result of progradation or as a result of sea-level fall. In this context it is interesting to note that one of the dolomites can be traced laterally into unaltered limestone along strike, suggesting the possibility that sabkha "islands," independent of a prograding shoreline, may have developed from time to time on the platform.

The sabkha analogy has been buttressed by the comprehensive strontium-, carbon-, and oxygen-isotope studies of Gao and Land (1991). These authors concluded that the dolomite formed initially by the replacement of original sediments in an evaporative marine environment. They based this conclusion on the similarity of $^{87}Sr/^{86}Sr$ ratios to those of coeval Lower Ordovician sea water. They noted that light ^{18}O values suggest that the dolomite has undergone significant burial modification, perhaps by contact with ^{18}O-depleted meteoric water that moved through the section during periods when overlying regional unconformities developed.

A second, later type of dolomite is seen in the Bally Mountain sections (Cloyd and others, 1986). This dolomite is coarse grained, discordant, and replaces both limestone and the finer grained dolomite previously described, obliterating all traces of previous texture. Some of this later dolomite is nodular, while some appears to be related to tectonic fractures. Dolomite of this type is quantitatively insignificant and invariably shows the characteristic features of saddle dolomite.

Crystal size and morphology, coupled with an association with tectonic fractures, suggested to Cloyd and others (1986) that the later dolomite formed by migration of warm dolomitizing fluids along Pennsylvanian fracture systems. On the basis of a relatively small number of light oxygen-isotope values, these authors suggested that the fluids originated as pore water that was expelled during compaction of sediments in the Anadarko basin. As Bally Mountain is structurally juxtaposed above the Anadarko basin, they concluded that structural overpressuring of Pennsylvanian pore water was the most likely source of the brines. However, Gao and Land (1991), on the basis of a more extensive isotope and geochemical analysis, con-

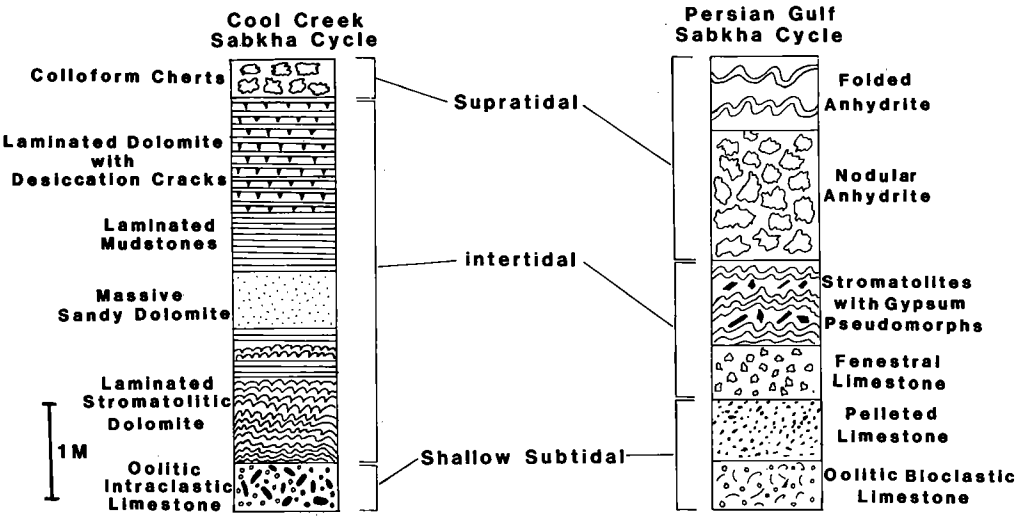


Figure 3. Comparison of a Cool Creek sabkha cycle with a Persian Gulf sabkha cycle (from Cloyd and others, 1986).

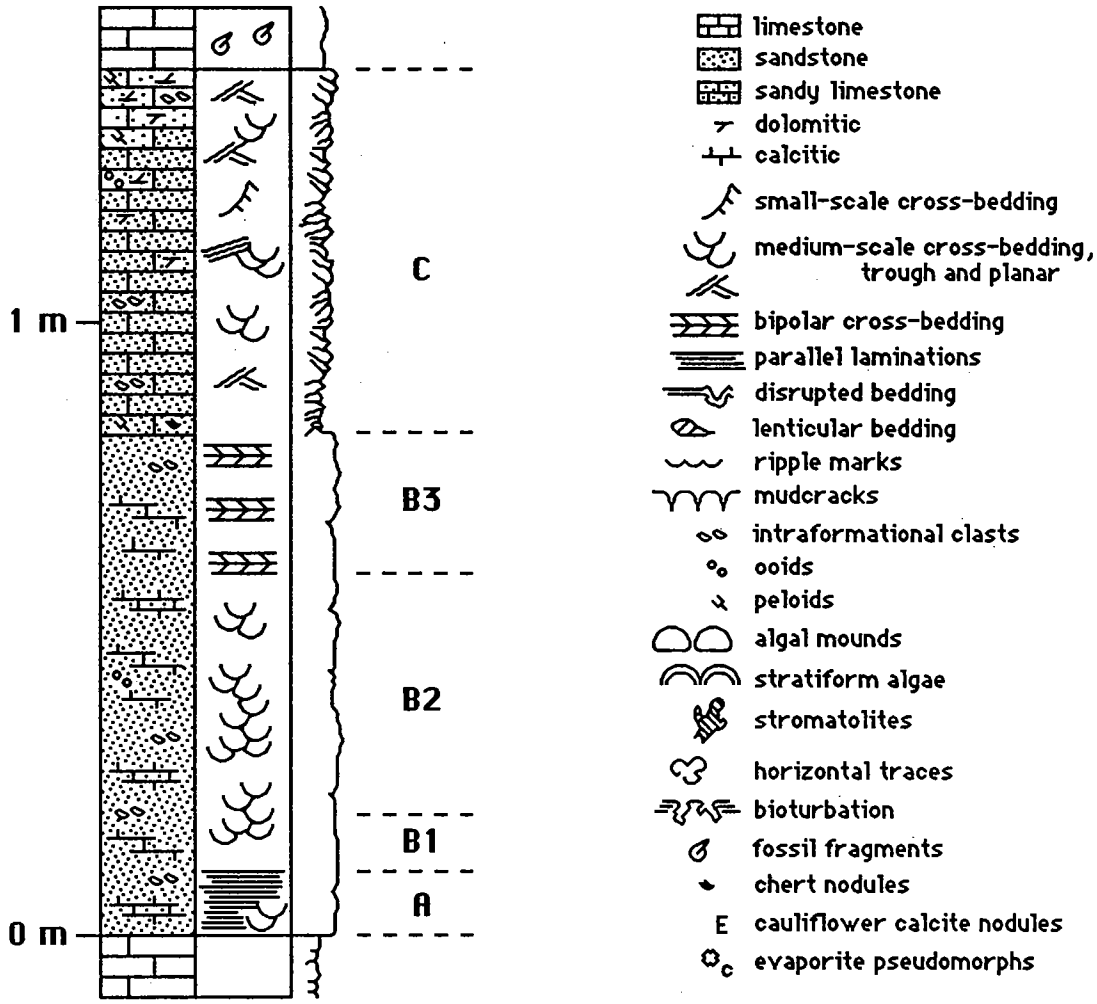


Figure 4. Log of the Herringbone sandstone on the eastern spur of Bally Mountain (from Ragland, 1990).

cluded that the saddle dolomite was deposited by meteoric waters percolating down into the Arbuckle Group from the overlying lower Paleozoic rocks, prior to their removal by Late Pennsylvanian and Permian erosion.

THE HERRINGBONE SANDSTONE MEMBER

About 10 ft (~3 m) above the base of the Kindblade Formation, Ragland and Donovan (1991) informally recognized an unusually thick quartz sandstone unit as the "Herringbone sandstone." On north Bally Mountain they recognized three subunits, based on sedimentary structures (sites D4,D6; Fig. 4). The lowest unit, which rests on a dense, thin-bedded micrite, consists of parallel laminations of quartz sandstone and micrite. The overlying subunit consists of hummocky, cross-bedded quartz sandstones; these are overlain by trough cross-bedded sandstones that pass upwards into bipolar ("herringbone") cross-beds. Although the underlying beds show considerable facies variation, the herringbone facies can be found throughout the Slick Hills. Planar and trough cross-beds form the final subunit in the member; they are overlain by bio- and pelmicrites. The sandstone has been interpreted by Ragland and Donovan (1991) as a linear sandbar that formed after a transgression; the lower hummocky cross-beds record storm reworking of mobile sand sheets in relatively deeper water. As the sand deposit built up into increasingly shallow water, it was increasingly modified by tidal currents.

REFERENCES CITED

Cloyd, K.; Ragland, D. A.; Jones, L.; and Donovan, R. N., 1986, Dolomite with evaporitic connections in the Ordovician Cool Creek Formation, southwestern Oklahoma, *in* Donovan, R. N. (ed.), The Slick Hills of southwestern Oklahoma—fragments of an aulacogen?: Oklahoma Geological Survey Guidebook 24, p. 29–34.

Donovan, R. N.; Ragland, D. A.; Cloyd, K.; Bridges, S.; and Denison, R. E., 1986, Stop 2: Geologic highlights of the Bally Mountain area, *in* Donovan, R. N. (ed.), The Slick Hills of southwestern Oklahoma—fragments of an aulacogen?: Oklahoma Geological Survey Guidebook 24, p. 92–95.

_____1988, Carlton Rhyolite and lower Paleozoic sedimentary rocks at Bally Mountain in the Slick Hills of southwestern Oklahoma, *in* Hayward, O. T. (ed.), Geological Society of America, South-Central Section, Centennial Field Guide, v. 4, p. 93–96.

Gao, G.; and Land, L. S., 1991, Early Ordovician Cool Creek dolomite, middle Arbuckle Group, Slick Hills, SW Oklahoma, U.S.A.: Journal of Sedimentary Petrology, v. 61, p. 161–173.

Ragland, D. A., 1990, Sedimentology, paleoenvironmental analysis and diagenesis of upper Arbuckle limestones in the Slick Hills, southwestern Oklahoma: Oklahoma State University unpublished Ph.D. thesis, 238 p.

Ragland, D. A.; and Donovan, R. N., 1986, An environmental analysis of the Lower Ordovician Cool Creek Formation of southwestern Oklahoma, *in* Donovan, R. N. (ed.), The Slick Hills of southwestern Oklahoma—fragments of an aulacogen?: Oklahoma Geological Survey Guidebook 24, p. 21–28.

_____1991, Silica in the upper Arbuckle Group, Slick Hills, southwestern Oklahoma, *in* Johnson, K. S. (ed.), Late Cambrian–Ordovician geology of the southern Midcontinent, 1989 symposium: Oklahoma Geological Survey Circular 92, p. 127–142.

STOP 13
Leatherbury's Quarry—The World's Smallest Oil Field

Sec. 25, T6N, R14W (see Stop 10, Fig. 1, site E2).

R. Nowell Donovan and Arthur B. Busbey
Texas Christian University

INTRODUCTION

The scenery of the Wichita Mountains and Slick Hills is essentially a Permian inheritance, lightly modified in recent times (Donovan, 1986). In this context, the Bally Mountain Range is an exhumed Permian hill that is slowly being divested of its own detritus (the Lower Permian Post Oak Conglomerate). The exhumation is particularly well seen on the northern part of Bally Mountain, where boulder conglomerates extend well up hill sides carved out of the upper Arbuckle Group. In addition, deposits of the Post Oak at the foot of Raggedy Ridge contain house-sized boulders of dolomite that have clearly tumbled from the outcrop of the Bally dolomite on the hill above. At least two of these giant boulders are imbedded in the calcrete which cements certain horizons in the Post Oak (Fig. 1) (Donovan and others, 1986,1988).

Another interesting feature illustrating the character of Permian geomorphology can be seen at the southeastern end of Raggedy Ridge, where a thin veneer of Post Oak Conglomerate, formed of Bally dolomite clasts, sits on an ancient pediment surface (Fig. 2). In essence, as the climate in the Early Permian became increasingly arid, the rate of landscape evolution became almost static, effectively fossilizing the landscape of the Slick Hills.

KARST DEVELOPMENT ON BALLY MOUNTAIN

Among the most compelling features of the exhumed Permian landscape are the fossil cave systems that perforate the Slick Hills. Although these cave systems are essentially of very modest dimensions (it is rarely possible for a person to crawl into them), they are very common. Quarrying and roadworks in the Slick Hills have exposed several of these cave systems, as, for example, in the quarry at Richard's Spur, in the Cook Creek road cut (Donovan, 1982), and in Leatherbury's quarry on Bally Mountain (Donovan and others, 1986,1988; Donovan, 1987).

The important parameters that influenced the development of caves in Early Permian times were:

1) A general slowdown of tectonic activity that left the Slick Hills structurally emplaced above the Anadarko basin, wherein the Woodford Formation, amongst others, had evolved to become a mature oil source rock;

2) An increasingly arid climate led to a great reduction in the rate of weathering and the preservation of a hilly karsted land surface; and

3) As the Permian Period progressed, this landscape was slowly buried by fine-grained siliciclastic detritus, deposited on alluvial plains.

Typically, cave systems are developed by selective opening of the ubiquitous Pennsylvanian joint systems

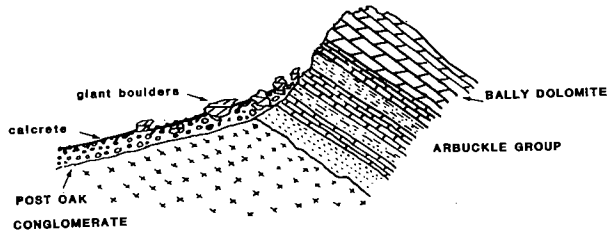


Figure 1. Schematic cross section through Raggedy Ridge on Bally Mountain. The sketch shows the relationship between the Post Oak conglomerate, Carlton Rhyolite, and Arbuckle Group. Giant boulders of the Bally dolomite are cemented in the Post Oak Conglomerate by calcrete. They may have tumbled down the slope either as a result of conventional mass-wasting processes or in response to a seismic disturbance.

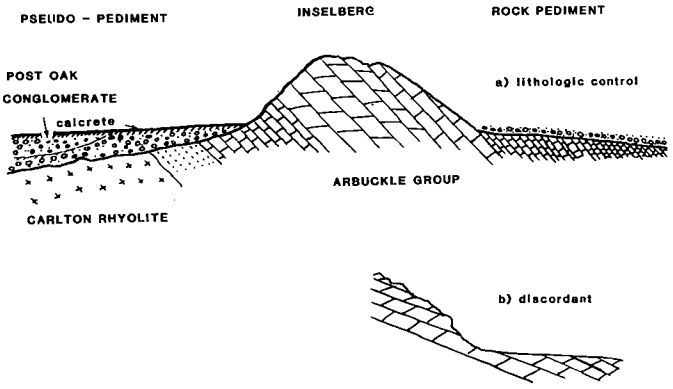


Figure 2. Schematic cross section, based on Raggedy Ridge, showing features of the Permian erosion that are fossilized in the Slick Hills. Essentially two types of rock pediment can be found: (a) where variations in the hardness of the bedrock are a control, and (b) where the bedrock lithology has had no apparent influence on the geomorphology. The rock pediment at the southeast end of the Raggedy Ridge on Bally Mountain is of the latter type. In addition, calcretes (i.e., fossil soils) may encircle the base of many of the Permian hills. In the modern erosion cycle, these have often been exhumed as flat surfaces sloping gently away from the hills and resemble true pediments.

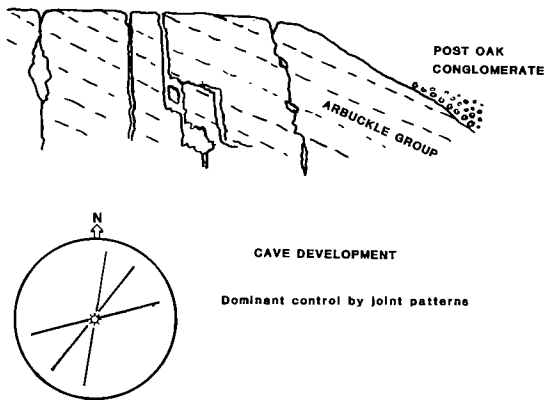


Figure 3. Schematic cross section showing the joint-controlled fissure karst that is widely developed in the Slick Hills.

that cut the Arbuckle Group. As a result the caverns comprise long, narrow fissures and are dominated by vertical shafts; as noted, man-sized chambers are rarely seen (Fig. 3).

In Leatherbury's quarry, the host rock is part of the upper Kindblade Formation. The lithology resembles that seen in the Cook Creek road cut (Donovan and others, 1986,1988; and this volume) in that it consists of peritidal carbonate sequences that show little evidence of emergence. The trend of the karst fissures follows the upper Paleozoic joint pattern, being preferentially developed along two orthogonal directions, ENE and NNW (Fig. 4).

The cave systems in Leatherbury's quarry are securely dated by a rather extensive Permian reptile and vertebrate fauna. This fauna is currently under investigation; ~100,000 fragments of bone have been collected from several fissures in the quarry. The most distinctive and common beast is the reptile *Captorhinus*. Our preliminary investigations show quite clearly that at least four new species of vertebrate animals are present.

None of the fossils seem to represent animals that actually lived in the caves, but rather individuals that died and were washed into them. Some, for example the edaphosaurid pelycosaur *Edaphosaurus*, were quite large and could not have used the surface openings of the cave for protection. The smaller *Captorhinus aguti* was ~12 in. (~30 cm) long and probably used the surface openings of the fissures as dens or hiding places. Plentiful *Captorhinus aguti* remains in the cave fill demonstrate varying degrees of water transport, with some specimens undamaged and others well rounded and abraded. Currently, no articulated specimens have been recovered.

A preliminary faunal list from the Leatherbury quarry is included in Table 1.

The Leatherbury quarry cave fauna may be given a tentative age assignment of Leonardian (Artinskian) age

TABLE 1. — PRELIMINARY FAUNAL LIST, LEATHERBURY QUARRY

Osteichthyes
Indeterminate paleoniscoid teeth
Amphibia
Indeterminate labyrinthodont skull and jaw fragments
cf. *Euryodus primus*, microsaur
Reptilia
Indeterminate reptiles with laterally compressed, strongly recurved teeth, similar to Bolt's (1969) "reptile X"
Captorhinus aguti
cf. *Captorhinikos* sp.
New caseid pelycosaur
cf. *Mycterosaurus* sp., a varanopseid pelycosaur
Thrausmosaurus sp., possibly a varanopseid pelycosaur
Delorhynchus priscus, possibly a varanopseid pelycosaur
Edaphosaurus sp., an edaphosaurid pelycosaur

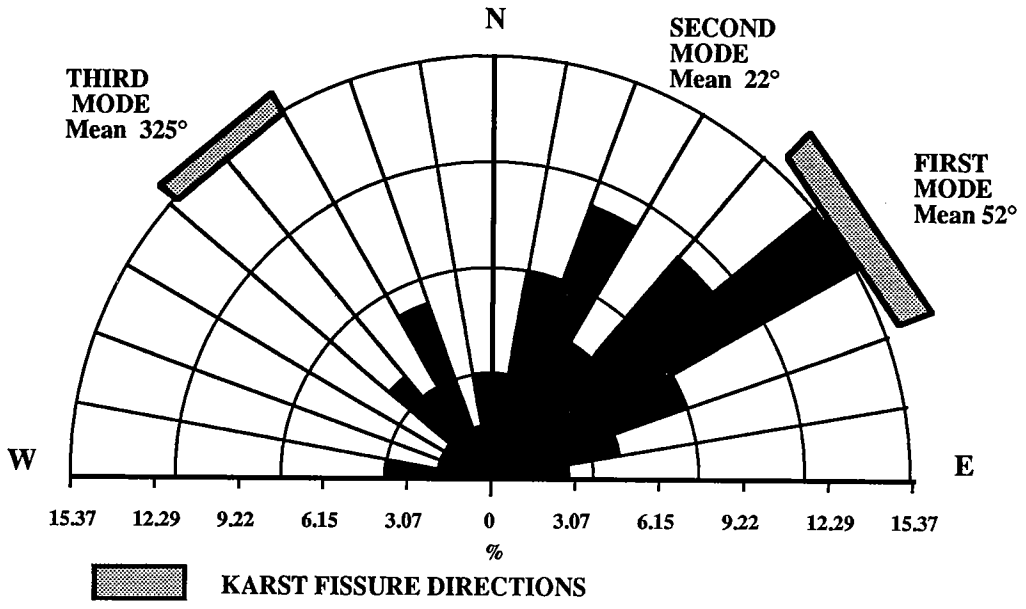


Figure 4. A joint and fissure analysis conducted in Leatherbury's quarry shows that the two principal karst-fissure directions correspond with an orthogonal joint set.

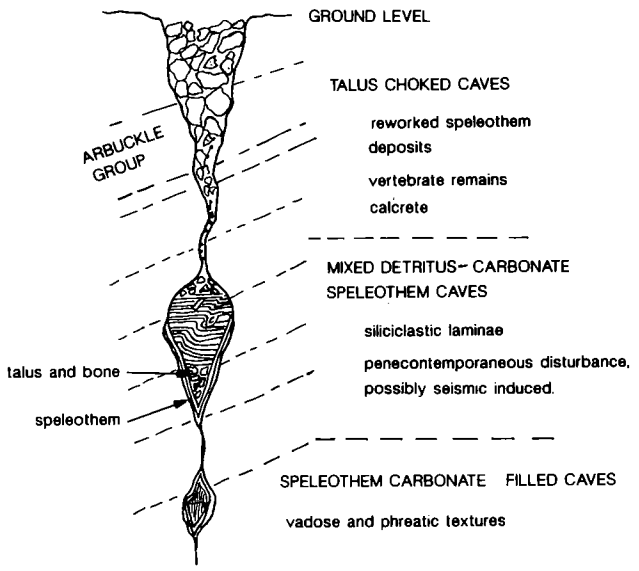


Figure 5. Schematic representation of the deposits found in the fissure fills in Leatherbury's quarry. Within mid-level caves, spatial relationships clearly suggest that surface-derived talus, including vertebrate bones, arrived prior to final infill by laminated clays that are, for the most part, devoid of fossil remains, either vertebrates or spores.

based on Heaton (1979) who views all occurrences of *Captorhinus aguti* in Oklahoma as being of Leonardian age. The possible presence of a more derived caseid pelycosaur in the fauna may represent a slightly later time or possible faunal mixing and reworking. Continued recovery of material will permit a more detailed comparison with other Oklahoma material and that of the Permian of northern Texas.

The geology of the cave systems is remarkably complex, for they are filled by a variety of deposits. Nevertheless, in several places the original water-corroded walls of the caverns exhibit scalloped surfaces and horizontal rim lines which indicate that development of the cave system postdated tectonic tilting of the Arbuckle Group to the northwest at angles of ~20°.

The character of the deposits in the cave varies, according to the level examined (Fig. 5). In general the following sequence of events seems to have occurred:

1) Opening of the fissures by meteoric dissolution.

2) Coating of the fissures by vadose flowstone.

3) Phreatic infill of the fissures in the lower part of the system. In some places phreatic speleothems completely closed the fissures.

4) As the overlying surface was lowered by denudation, the tops of the fissures were partially filled by detritus derived from the overlying land surface. As this detritus includes fragments of speleothems, it must be assumed that the cave systems themselves were being cannibalized by surface erosion on a continuing basis until the landscape was fossilized in the Early Permian. At any given level, the input of abundant clastics effectively terminated speleothem formation.

5) The final infill of the caves took place after the landscape was buried beneath a cover of Permian alluvium; it consists of finely laminated illitic clays that are devoid of both fossil reptiles and palynomorphs (Fig. 6).

One of the most exciting features of the caves in Leatherbury's quarry (a feature shared by other similar deposits in the Slick Hills) is that throughout the history outlined above, hydrocarbons seeped into the cave system and were incorporated into both speleothems and detrital-clay deposits. In the speleothems, hydrocarbons occur in three forms: (1) as minute three-micron inclusions within calcite crystals, (2) as larger inclusions along cleavage lines within the crystals, and (3) as biodegraded coatings on the surfaces of crystals.

Hydrocarbons also impregnate the delicately laminated illitic clays. In the later case the lamination is a distinctive alteration of dark-brown hydrocarbon-bearing layers with light-green nonhydrocarbon layers.

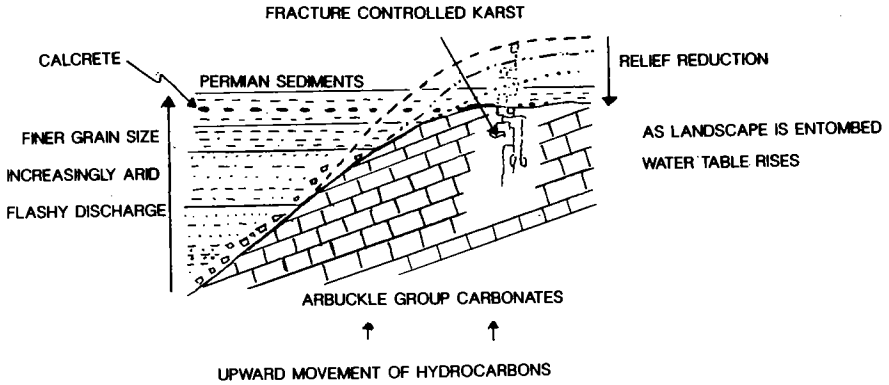


Figure 6. Sketch illustrating the sequence of events that resulted in the entombment of the cave systems beneath Permian alluvium. In essence, entombment of the landscape is recorded by alluviation of the cave fills: i.e., the introduction of increasing amounts of fine-grained siliciclastic detritus. A balance developed between increasingly arid environment (which resulted in falling water tables and fossilization of the karst) and gradual subsidence and burial of the topography, which resulted in rising water tables recorded by the commonly seen passage of vadose textures into phreatic.



Figure 7. The World's smallest oil field, clearly showing a fossilized oil/water contact that is conveniently horizontal.

Speleothem features encountered in the cave include flowstone, stalactites, stalagmites, phreatic crystal palisades, and cave popcorn. Hydrocarbons may be found in all varieties of speleothem. As the local rocks are neither a source nor mature, the likely origin of the hydrocarbons involved the upward migration of hydrocarbons from the Anadarko basin through the faults of the frontal fault zone into tectonic fractures in the Arbuckle. Escaping from these fractures, the hydrocarbons then mingled with carbonate-saturated waters in the caves before being incorporated into the growing speleothems and clays.

THE WORLD'S SMALLEST OIL FIELD

Perhaps the most tantalizing of the cave conduits is illustrated in Figures 7 and 8. A small fissure displays an initial vadose coating around its circumference. Subsequently this conduit was plugged at a level below the present level of exposure, and, as a result, a perched phreatic tube developed. Large calcite-crystal palisades grew upward into this tube and eventually trapped hydrocarbons into their higher portions, thus: (a) fossilizing the oil/water contact, (b) proving conclusively that oil floated on water in the Permian period, and (c) producing a viable submission to the Guinness Book of Records as the "World's Smallest Oil Field."

REFERENCES CITED

Bolt, J. R., 1969, Lissamphibian origins: possible protolissamphibian from the Lower Permian of Oklahoma: Science, v. 166, p. 888–891.

Donovan, R. N., 1982, Geology of Blue Creek Canyon, Wichita Mountains area, *in* Gilbert, M. C.; and Donovan, R. N. (eds.), Geology of the eastern Wichita Mountains, southwestern Oklahoma: Oklahoma Geological Survey Guidebook 21, p. 65–77.

_____1986, Geology of the Slick Hills, *in* Donovan, R. N. (ed.), The Slick Hills of southwestern Oklahoma—fragments of an aulacogen?: Oklahoma Geological Survey Guidebook 24, p. 1–12.

_____1987, The World's smallest oil field?: Oklahoma Geology Notes, v. 47, p. 238, 291.

Donovan, R. N.; Ragland, D. A.; Cloyd, K.; Bridges, S.; and Denison, R. E., 1986, Stop 2: Geologic highlights of the Bally Mountain area, *in* Donovan, R. N. (ed.), The Slick Hills of southwestern Oklahoma—fragments of an aulacogen?: Oklahoma Geological Survey Guidebook 24, p. 92–95.

_____1988, Carlton Rhyolite and lower Paleozoic sedimentary rocks at Bally Mountain in the Slick Hills of southwestern Oklahoma, *in* Hayward, O. T. (ed.), Geological Society of America, South-Central Section, Centennial Field Guide, v. 4, p. 93–96.

Heaton, M. J., 1979, Cranial anatomy of primitive captorhinid reptiles from the Late Pennsylvanian and Early Permian, Oklahoma and Texas: Oklahoma Geological Survey Bulletin 127, 84 p.

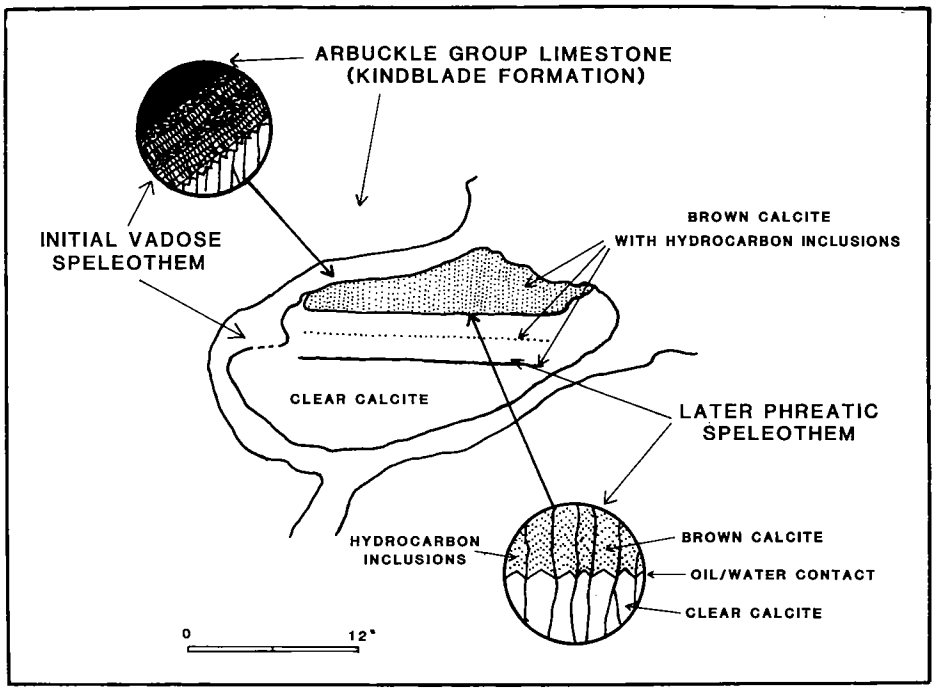


Figure 8. A sketch of the relationships seen in Figure 7.

STOP 14
The Saddle Mountain Dolomite on Maukeen Hill

Maukeen Hill is 0.25 mi north of Saddle Mountain Indian Mission in southern Kiowa County, sec. 28, T4N, R14W.

R. Nowell Donovan and Debra L. Ross
Texas Christian University

INTRODUCTION

Most exposures of the upper Arbuckle Group in both the Slick Hills and the Arbuckle Mountains display sequences that are dominated by limestones. Although dolomites are present, typically they are thin—no more than 30 ft (~10 m) thick (and usually much less). Dolomites of this type are usually predictably developed at the top of small, shallowing-upward sequences. Many, though not all, display characteristics which suggest that they may have developed through the evaporative concentration of sea water. However, in the western part of the western Slick Hills (near Saddle Mountain, and on Longhorn and Unap Mountains), a thick section of the upper Arbuckle Group has been comprehensively dolomitized (Fig. 1). This dolomitization is singular in scale and comprehensiveness. Donovan and Ross (1991) have referred to this dolomite as the "Saddle Mountain dolomite" and noted that the dolomitized interval includes the topmost part of the Cool Creek, most of the Kindblade, and part of the West Spring Creek Formations (the top of the latter is not seen in the Slick Hills). The Saddle Mountain appears to be an approximate equivalent to the elusive Brown zone dolomite, a notable hydrocarbon reservoir in the subsurface. In addition to the work of Donovan and Ross (1991), the Saddle Mountain has also been the subject of an extensive isotopic and geochemical study by Gao and Land (1991).

MAUKEEN HILL

Perhaps the most instructive exposures of the Saddle Mountain dolomite are encountered on Maukeen Hill (Fig. 1), where complex contacts between unaltered Kindblade and the dolomite are dramatically displayed. Over a horizontal distance of ~440 yards (~400 m) the thickness of the Saddle Mountain dolomite is reduced from ~1,000 ft (~320 m) to <400 ft (~125 m). On the hillside the contact between Kindblade and the dolomite is a labyrinthine interdigitation (Fig. 2), although, in the small scale, individual contacts between limestone and dolomite are knife sharp. At most sites the horizontal transition from pure limestone to pure dolomite takes place in <1 in. (~25 mm).

The undolomitized Kindblade on Maukeen Hill can be considered typical of the formation as developed elsewhere in the Slick Hills and Arbuckle Mountains. It consists of an arrangement of small, shallowing-upward sequences that display a rich variety of peritidal limestones. Some of the shallowing-upward cycles are capped by thin dolomites that may or may not display direct evidence of an evaporative connection. Typically, such evidence is provided by: (1) pseudomorphs after gypsum, anhydrite, and/or (rarely) halite (Ragland and Donovan, 1991); (2) relict crystals of anhydrite and celestite in cherts; (3) colloform ("cauliflower") cherts with lutecite, chalcedonite, and flamboyant megaquartz; (4) collapse breccias that may record the near-surface dissolution of evaporites (Donovan and others, 1988); and (5) independent evidence of emergence, such as mudcracks.

Where evidence of this sort is present it is probable that an evaporite "sabkha" model of dolomitization is applicable. However, where such evidence is lacking, it is possible that dolomitization has been associated with meteoric flushing during low stands, or, alternatively, that restricted circulation on the great Laurentian platform allowed high ionic concentrations to build up in deeper water than is the case on the modern sabkhas of the Persian Gulf.

Typically, the style of dolomite developed in these early, penecontemporaneous dolomites is fabric selective (and hence partial), being composed of small idiotopic dolomite crystals. By way of contrast, for the most part, the Saddle Mountain Dolomite is composed of coarse or medium crystals. To some extent, variations in crystal size are inherited from the precursor calcite-crystal size. Thus, for example, dolomitized algal boundstones, in which the precursor calcite is micrite, are typically finer grained than dolomitized grainstones. Crystal fabrics in the Saddle Mountain dolomite replace earlier fabrics, and generally destroy the original texture of the rock; only rarely are ghost textures seen (Fig. 3). Texturally the dolomites are complex, varying from anhedral through subhedral to euhedral. The two most commonly seen textures are idiotopic-S and xenotopic-A (Gregg and Sibley, 1984). It is not clear how much the development of xenotopic texture is due to heat (as suggested by Gregg and Sibley), and how much the crystal shapes have been modified by pressure solution during burial. Cathodeluminescence studies confirm the complexity of the mixtures seen in the dolomite. Both dull and bright luminescent varieties of dolomite are present; in general, though not ubiquitously, the brighter luminescent variety postdates the duller luminescent dolomite. Quantitatively insignificant late-stage veins and vugs cut the dolomite and frequently are lined with coarse, zoned, saddle-dolomite crystals (Fig. 4).

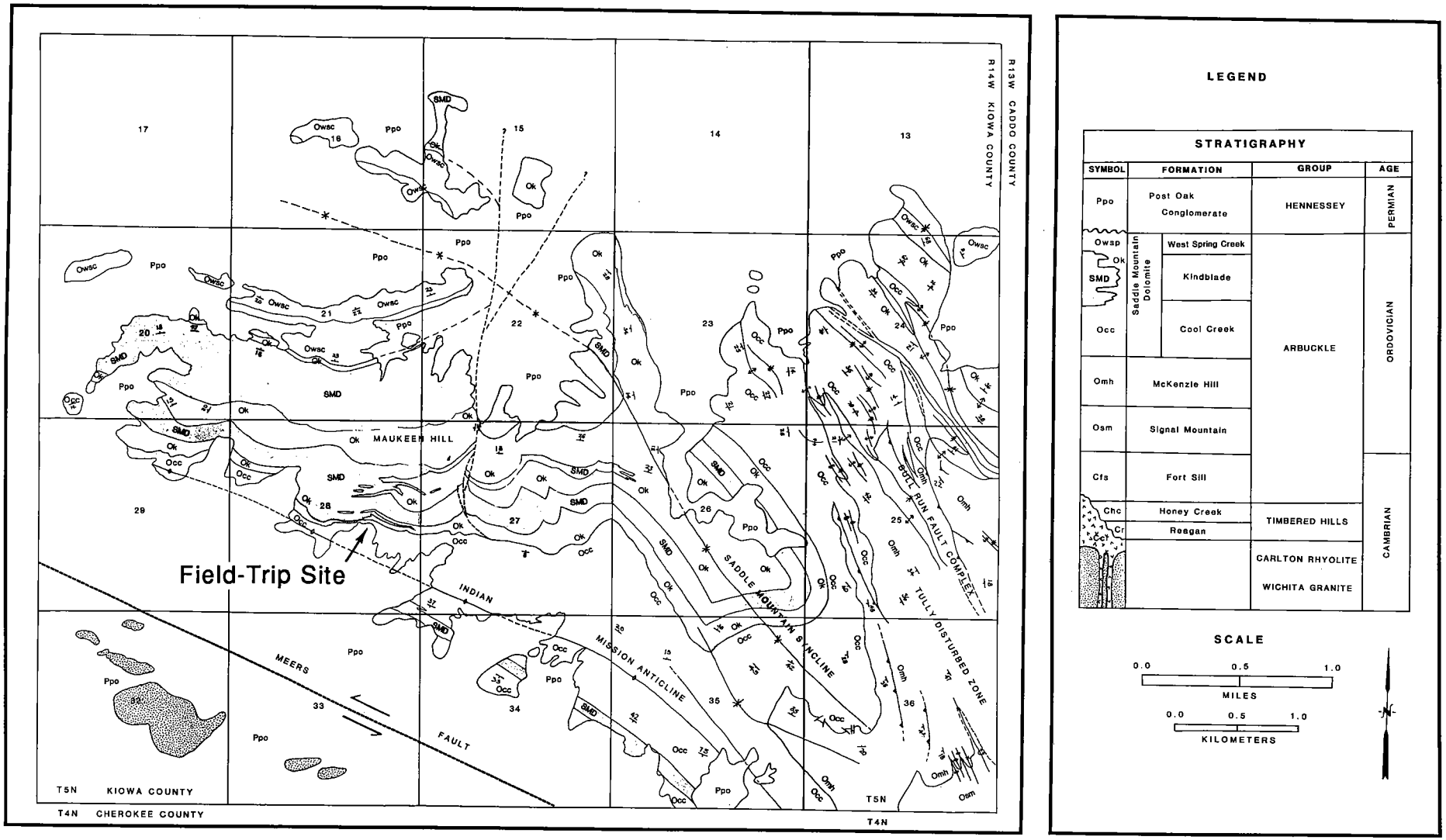


Figure 1. Map of the western part of the western Slick Hills showing outcrop of the Saddle Mountain dolomite and location of field-trip site. From Donovan and Ross (1991).

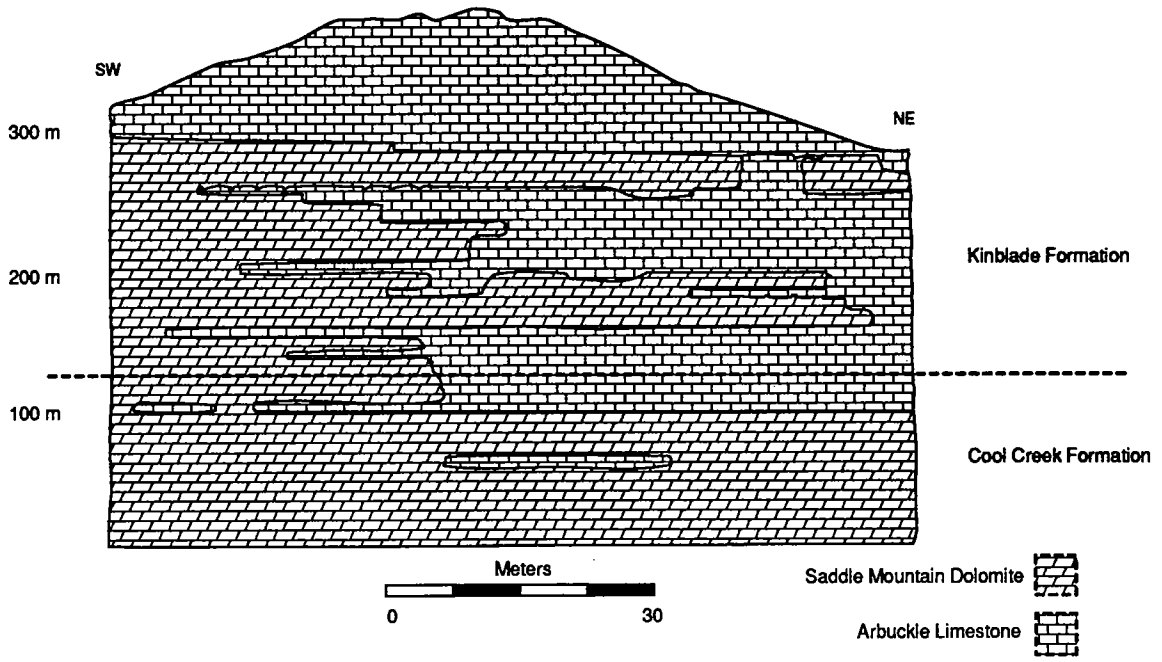


Figure 2. Schematic representation of the limestone-dolomite contacts seen on Maukeen Hill. From Donovan and Ross (1991).

In their study of the Saddle Mountain Dolomite, Gao and Land (1991) reported a clear spatial differentiation of textural types within the dolomite. They found the middle part of the sequence to be composed of medium- to coarse-grained subhedral to anhedral dolomite that exhibits dull luminescence, while the upper and lower parts of the dolomite are composed of dolomite with essentially similar textures but which fluoresces bright red. This latter variety of dolomite contains hydrocarbon inclusions, as well as biodegraded hydrocarbons in pores.

Typically, porosity is variable, ranging from 0% to as much as 15% of intracrystalline or enlarged intracrystalline porosity. In the latter case, at least some of the pore enlargement appears to be related to the overlying Permian unconformity, for pore size decreases away from the surface, beneath the Post Oak Conglomerate that mantles the sides of Maukeen Hill.

The timing of dolomite formation is given a convincing *terminus ad quem* by pebbles of texturally identical dolomite (including vein-fills) that are found in the Post Oak Conglomerate. In addition, the Saddle Mountain area was subjected to fairly intensive late Paleozoic folding; the dolomite clearly predates the folding (Fig. 1). Gao and Land (1991) noted that the $^{87}Sr/^{86}Sr$ ratios of the earlier of the two types of dolomite which they recognized are indicative of precipitation from Early Ordovician sea water, and they suggested that the dolomite formed very shortly after deposition. Subsequent to its initial formation, they considered that the dolomite was modified by meteoric waters during early burial, following which it was more comprehensively modified by the migration of brines from the underlying Anadarko basin through the Slick Hills. This later, additive dolomitizing event produced ferroan crystals characterized by bright luminescence and containing hydrocarbon inclusions.

In his study of the laterally equivalent Ellenburger, Kerans (1990) noted that several mechanisms could have been responsible for the widespread dolomitization that he found, including reflux, ground-water mixing, and subtidal dolomitization, as proposed by Harris (1973). Kerans preferred the latter mechanism for dolomitiza-

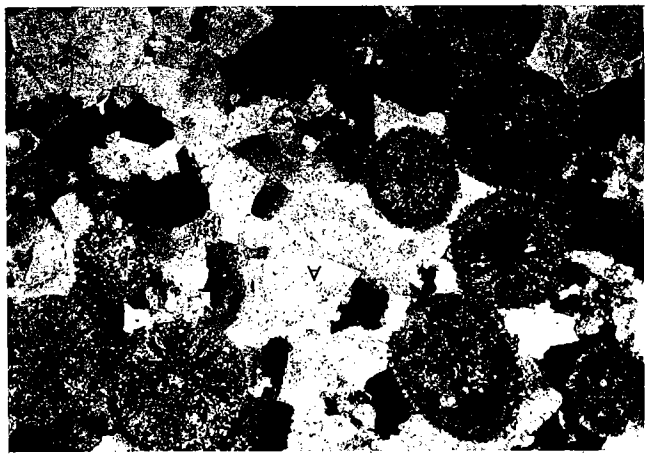


Figure 3. A dolomitized oosparite in Saddle Mountain dolomite; upper Cool Creek equivalent section. Initially this rock was a well-sorted deposit of radial ooids. Some of these were partly silicified prior to comprehensive dolomitization of the remaining limestone. The replacing dolomite is coarse grained and shows slightly undulose extinction. It is most conveniently classified as idiotopic, but modified by pressure solution due to burial. In this view, ghosts of the ooids are just visible in the dolomite (A); they are more convincing where the ooids have been silicified (B). Polarized light; field of view is 4.5 mm wide.

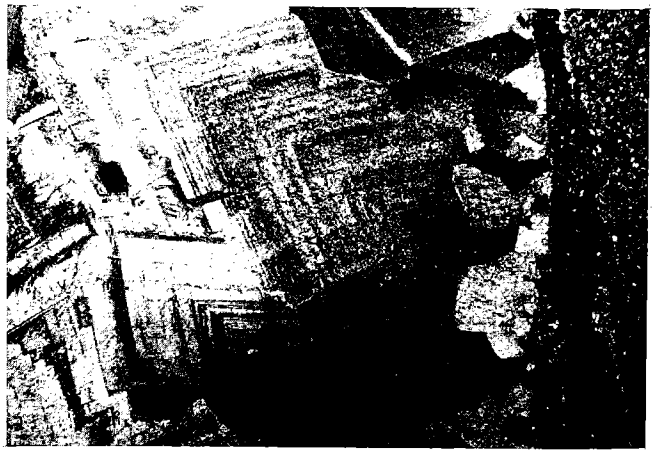


Figure 4. Saddle Mountain dolomite (Kindblade equivalent section), Maukeen Hill. Late vein-filling, drusy-style saddle dolomite showing impurity-defined zonation and undulose extinction. Polarized light; field of view is 9 mm wide.

tion; his conclusion would appear to coincide with the interpretation of the early phase of dolomite in the Saddle Mountain suggested by Gao and Land (1991). However, Donovan and Ross (1991) preferred utilizing the substantial pre-Simpson regression that occurred at the end of Arbuckle Group times. They suggested that much of the dolomitization could have been achieved by flushing of the top part of the Arbuckle Group by meteoric waters at this time. In order to explain the undoubted complexity of the dolomite that resulted, they favored lower Paleozoic modification during extensive pre-Pennsylvanian burial, followed by a phase of Early Pennsylvanian flushing by brines from the Anadarko basin as the dismemberment of the southern Oklahoma aulacogen commenced.

AN ANALOG FOR THE BROWN ZONE?

The Brown zone, a dolomitic reservoir located at or near the top of the Arbuckle Group in the subsurface, remains a very elusive hydrocarbon target in southern Oklahoma. It is possible that the Saddle Mountain dolomite represents an exposure of this reservoir. The complex, remarkably discordant, contacts displayed on Maukeen Hill may explain the elusiveness of the Brown zone.

Models of dolomitization of the Arbuckle Group suggest that the dolomitized equivalents of the group (e.g., the Ellenburger) feather into limestones near the margins of the southern Oklahoma aulacogen (Johnson and others, 1988). If this is correct, then the Brown zone is likely to be best developed at or near the margins of the aulacogen. A similar argument can be used to explain the facies changes shown by the Royer, Butterly, and Bally dolomites.

However, the aulacogen has suffered a great deal of structural dislocation as a result of Pennsylvanian tectonism. If, as consensus suggests, the tectonism has involved a component of left-lateral, strike-slip dislocation along major reactivated aulacogen-bounding faults, then it is clear that another wrench is thrown into the search for the Brown zone!

Finally, it is pertinent to note that the subsurface part of the Arbuckle Group has been buried to considerable depths for ~280 million years longer than the exposures on Saddle Mountain. Hence it is entirely possible that the deeper parts of the Arbuckle have been subjected to very different diagenetic processes than the exposures seen in both the Slick Hills and the Arbuckle Mountains.

REFERENCES CITED

Donovan, R. N.; Ragland, D. A.; Cloyd, K.; Bridges, S.; and Denison, R. E., 1988, Carlton Rhyolite and lower Paleozoic sedimentary rocks at Bally Mountain in the Slick Hills of southwestern Oklahoma, *in* Hayward, O. T. (ed.), Geological Society of America, South-Central Section, Centennial Field Guide, v. 4, p. 93–96.

Donovan, R. N.; and Ross, D. L., 1991, The Saddle Mountain dolomite at Maukeen Hill—a dolomite interface in the upper Arbuckle Group, western Slick Hills, Oklahoma, *in* Johnson, K. S. (ed.), Late Cambrian–Ordovician geology of the southern Midcontinent, 1989 symposium: Oklahoma Geological Survey Circular 92, p. 143–153.

Gao, G.; and Land, L. S., 1991, Petrography and geochemistry of massive dolomite from the upper Arbuckle Group, Slick Hills, southwestern Oklahoma, *in* Johnson, K. S. (ed.), Late Cambrian–Ordovician geology of the southern Midcontinent, 1989 symposium: Oklahoma Geological Survey Circular 92, p. 64.

Gregg, J. M.; and Sibley, D. F., 1984, Epigenetic dolomitization and the origin of xenotopic dolomite texture: Journal of Sedimentary Petrology, v. 56, p. 908–931.

Harris, L. D., 1973, Dolomitization model for Upper Cambrian and Lower Ordovician carbonate rocks in the eastern United States: U.S. Geological Survey Journal of Research, v. 1, p. 63–78.

Johnson, K. S.; Amsden, T. W.; Denison, R. E.; Dutton, S. P.; Goldstein, A. G.; Rascoe, B.; Sutherland, P. K.; and Thompson, D. M., 1988, Southern Midcontinent, *in* Sloss, L. L. (ed.), Sedimentary cover—North American craton; U.S.: Geological Society of America, The Geology of North America, v. D-2, p. 307–359. [Also released as Oklahoma Geological Survey Special Publication 89-2, 53 p.]

Kerans, C., 1990, Depositional systems and karst geology of the Ellenburger Group (Lower Ordovician), subsurface West Texas: Texas Bureau of Economic Geology Report of Investigations 193, 63 p.

Ragland, D. A.; and Donovan, R. N., 1991, Silica in the upper Arbuckle Group, Slick Hills, southwestern Oklahoma, *in* Johnson, K. S. (ed.), Late Cambrian–Ordovician geology of the southern Midcontinent, 1989 symposium: Oklahoma Geological Survey Circular 92, p. 127–142.

STOP 15
Parallel Folds and the Thatcher Creek Member in Blue Creek Canyon

Blue Creek Canyon is situated in northern Comanche County, sec. 11, T4N, R13W.

Deborah A. Ragland
Conoco Inc., Ponca City

Sherman S. Smith and R. Nowell Donovan
Texas Christian University

INTRODUCTION

Blue Creek Canyon is ~15 mi north–northwest of Lawton in southwestern Oklahoma (T4N, R13W). This area has been the subject of extensive study (Donovan, 1982; Donovan and others, 1986,1988,1989), for the Canyon is occupied by the Blue Creek Canyon fault, a major member of the complex of faults in the frontal fault zone between the Wichita uplift to the south and the Anadarko basin. Geographically, the canyon separates the eastern and western Slick Hills.

In this contribution we concentrate on two aspects of the geology of the Blue Creek Canyon area: (1) the base of the Cool Creek Formation; and (2) the style of folding developed in the Arbuckle limestones, as exemplified by the Paradox anticline, one of four principal folds that are found in the canyon area.

THE THATCHER CREEK MEMBER, BASE OF THE COOL CREEK FORMATION

When he recognized the Cool Creek Formation in 1933, Ulrich took the lower boundary to be the change from the heavier (*sic*) beds of limestone at the top of McKenzie Hill Formation to the more easily eroded beds of the Cool Creek. Subsequently, Ham (1956) recognized that the base of the Cool Creek Formation was rich in quartz detritus. In 1985, Ragland and Donovan formally recognized the first obviously quartz-rich sequence above the "heavier" beds of the McKenzie Hill as the base of the Cool Creek Formation. As the sequence has a "tough gritty limey" character, they named it the "Thatcher Creek Member." Subsequently, this member has been traced on the outcrop for >100 mi through the Slick Hills, and has also been detected in the Arbuckle Mountains. It has recently been the subject of a detailed facies analysis (Ragland and Donovan, 1991).

The type section of the Thatcher Creek Member is located on Thatcher Creek, a tributary of Blue Creek, where the member is 12–16 ft (~3.5–5 m) thick and has weathered to form a conspicuous gully. The member is a multistoried bed composed of limestone that contains variable amounts of detrital quartz. This characteristic has been confirmed at a large number of sites within the Slick Hills (Ragland and Donovan, 1991). Typically, exposures of the Thatcher Creek Member contain 5–40% quartz-sand grains in generally thin-bedded units. Associated sedimentary structures, often visually highlighted by the quartz sand, include parallel lamination, symmetrical ripple marks, and medium- and small-scale trough cross-

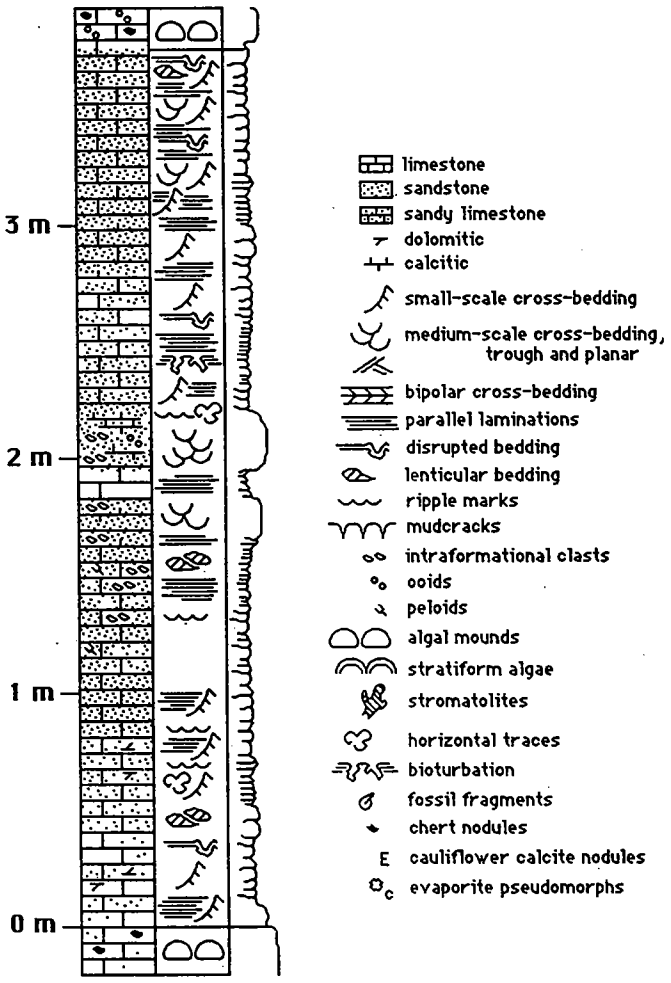


Figure 1. Measured section of the Thatcher Creek Member at its type locality in Blue Creek Canyon. From Ragland and Donovan (1991).

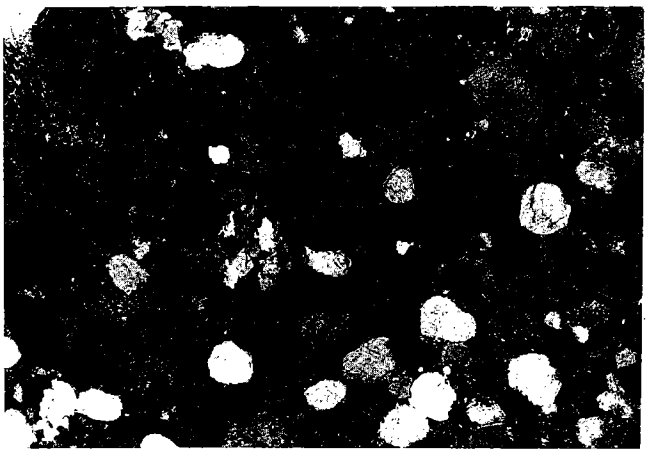


Figure 2. Thin section showing a typical development of Thatcher Creek lithology. In this specimen ~30% of the grains are monocrystalline quartz. There is one conspicuous polycrystalline grain in the middle of the view. Some grains show corroded edges, while others show syntaxial overgrowths. Polarized light; field of view is 9 mm across.

bedding. Disrupted bedding, vertical burrowing, and horizontal trace fossils are commonly seen (Fig. 1). In addition, mud cracks are developed at some sites. Grains associated with the quartz detritus include intraclasts, ooids, and, more rarely, bioclasts. The quartz-grain population is generally unstrained; polycrystalline grains are rare; some grains show linear inclusions (Fig. 2). Feldspar may form as much as 10% of the grain population and is usually fresh microcline or orthoclase. Grain size ranges from coarse silt to coarse sand, while sorting varies considerably, from poorly sorted to moderately well sorted. Many individual grains are well rounded, others are angular, while some have been corroded during diagenesis. On the other hand, other grains show significant syntaxial overgrowths. Clearly, waters percolating through the Thatcher Creek Member were capable of either dissolving or precipitating quartz.

It has been suggested by Ragland and Donovan (1991) that the Thatcher Creek Member is tangible evidence of a gradual fall in sea level (or a slowed rate of subsidence) that began in the aulacogen during the time of deposition of the uppermost McKenzie Hill Formation. Supporting evidence for this interpretation is found in the uppermost 100 ft (~30 m) of the McKenzie Hill, which is composed of laterally interweaving algal boundstones and micrites that display such shallow-water features as mud cracks and evaporite pseudomorphs. Dispersed fine-grained quartz sand is found in the McKenzie Hill throughout this upper interval; what makes the Thatcher Creek Member so distinctive is that it is a facies that has concentrated quartz in sufficient amounts that it has greatly influenced facies recognition and delineation. The Thatcher Creek Member is the ultimate product of an influx of quartz sand that was associated with the shallowing of marine waters across the aulacogen. As quartz sand was introduced into the aulacogen via eolian processes, tides, waves, and storms reworked the detritus into a variety of shallow-water settings.

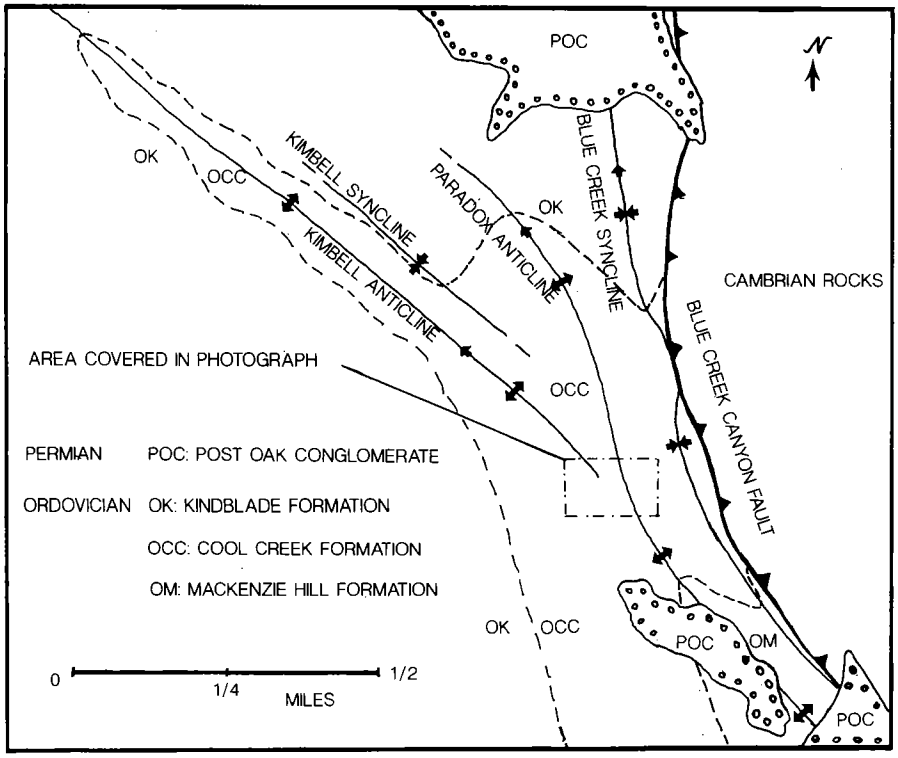


Figure 3. Simplified map of the Blue Creek Canyon area showing the distribution of the principal folds. "Area covered in photograph" is shown in Figure 4. From Donovan (1990).

PARALLEL FOLD STYLES IN BLUE CREEK CANYON

The Thatcher Creek Member is important in that it is a distinctive unit that functions as a punctuation-mark bed in the interpretation of Arbuckle Group stratigraphy. Because it is so conspicuous, it also functions as a very valuable marker bed in structural interpretation (Donovan and others, 1989).

In terms of its response to tectonic stress, the Arbuckle Group is an immensely thick unit of beds with similar mechanical properties that have an ubiquitous built-in anisotropy in the form of relatively thin layering. It is thus an ideal unit in which to study the development of parallel fold styles. Other strain responses are the brittle character of the rock and the ease with which the carbonates will dissolve when stressed.

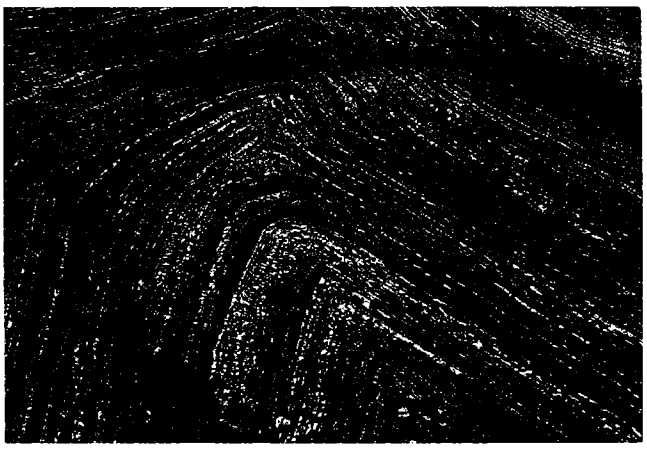


Figure 4. Aerial photograph showing a bifurcation point in the Paradox anticline. Area covered in photograph is shown on map in Figure 3. From Donovan (1990).

Fold styles developed in the Slick Hills exhibit a parallel form in which profile adjustments are achieved by frequent horizons of layer-parallel faulting. Usually these adjustments can only be detected where they become discordant in the hinge area of the folds. Most folds developed in the Arbuckle Group have semi-chevron profiles with sharply defined hinge areas and planar limbs.

The folds in Blue Creek Canyon are spectacular even by Arbuckle Group standards in that, because they plunge consistently to the north at an angle of 20–30°, they show a structural relief in excess of 2,700 ft (~850 m).

Donovan (1990) described the parallel fold relationships in the Paradox anticline in Blue Creek Canyon (Fig. 3). His study focused on a bifurcation point where this anticline diverges upwards into three folds, the Kimbell anticline, the Kimbell syncline, and the upward continuation of the Paradox anticline (Figs. 4,5). More recently, Smith (1991) expanded Donovan's study to include an analysis of the entire Paradox anticline and the related Blue Creek syncline. He noted that parallel fold style is retained throughout both folds and that, in essence, the pattern seen is the established one by which geometrically consistent packages of beds are separated from each other by décollement surfaces. Above each décollement in the anticline, and below each décollement in the syncline, beds generally tighten and in some cases break (Fig. 6). In this way, each décollement compensates for the space problems that are generated when bed thicknesses are held constant.

A total of 24 fold décollement-bounded segments have been recognized in the Paradox anticline and 14 in the adjacent Blue Creek syncline (the smaller number in the

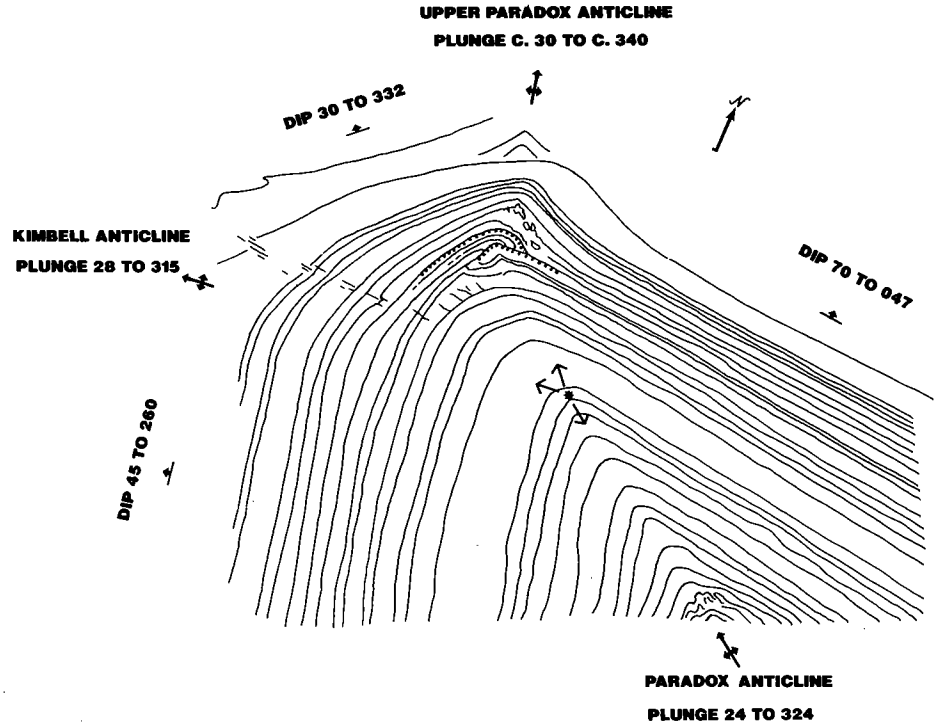


Figure 5. An outline sketch of geometric relationships seen in Figure 4.



Figure 6. A view of hinge crowding in the axis of the Kimbell syncline. The view is toward the northwest; to the left is the Kimbell anticline (see Fig. 3). Notice how the zone of crowding in the hinge of the syncline passes upwards into a broad open synclinal structure; a décollement surface marks the top of the "crowded zone."

syncline reflects the fact that this fold is partly overridden by the Blue Creek Canyon fault). The tightness of these structures ranges from tight folds of chevron type to broad open folds. The thickness of segments increases from 10 to 20 ft (~3–6 m) near the base of the fold to >100 ft (~30 m) near the top. This increase in segment thickness relates to two factors:

1) The plunge of the fold decreases to the north (toward the higher structural levels); and

2) Toward the north the folds, especially the anticline, are broader and more open; i.e., they have a greater wave length with more gentle limb dips. In other words, the folds are more tightly constrained at lower structural levels in the south of the area.

The different fold segments show quite considerable variations in orientation and plunge. In other words, analysis of folds of this type requires complex three-dimensional balancing. Thus it is necessary to consider not only movement of material perpendicular to the fold axis (the conventional cross-section approach), but also movement parallel to the axis. Unfortunately, the limestones of the Arbuckle Group are not amenable to detailed balancing, because of an absence of finely tuned biostratigraphic control and the general homotaxy of the lithologies.

While much of the space problem resulting from the parallel form of the folds is accommodated by décollement surfaces, some strain was taken up by pressure solution, which is seen as axial-plane cleavage wherein pressure-solution stylolites transect bedding. This cleavage is particularly well developed in the hinge areas of tight fold segments.

REFERENCES CITED

Donovan, R. N., 1982, Stop 10—Blue Creek Canyon, *in* Gilbert, M. C.; and Donovan, R. N. (eds.), Geology of the eastern Wichita Mountains, southwestern Oklahoma: Oklahoma Geological Survey Guidebook 21, p. 148–153.

_____1990, Fold bifurcation in the Slick Hills, southwestern Oklahoma: Oklahoma Geology Notes, v. 50, p. 1–2, 34–35.

Donovan, R. N.; Ragland, D. A.; Rafalowski, M. B.; Collins, K.; Tsegay, T.; McConnell, D.; Marchini, D.; Beauchamp, W.; and Sanderson, D. J., 1986, Stop 1: Geologic highlights of the Blue Creek Canyon area, *in* Donovan, R. N. (ed.), The Slick Hills of southwestern Oklahoma—fragments of an aulacogen?: Oklahoma Geological Survey Guidebook 24, p. 84–91.

Donovan, R. N.; Ragland, D. A.; Rafalowski, M. B.; McConnell, D.; Beauchamp, W.; Marchini, D.; and Sanderson, D. J., 1988, Pennsylvanian deformation and Cambro–Ordovician sedimentation in the Blue Creek Canyon, Slick Hills, southwestern Oklahoma, *in* Hayward, O. T. (ed.), Geological Society of America, South-Central Section, Centennial Field Guide v. 4, p. 127–145.

Donovan, R. N.; Marchini, W. R. D.; McConnell, D. A.; Beauchamp, W.; and Sanderson, D. J., 1989, Structural imprint on the Slick Hills, southern Oklahoma, *in* Johnson, K. S. (ed.), Anadarko basin symposium, 1988: Oklahoma Geological Survey Circular 90, p. 78–84.

Ham, W. E., 1956, Resume of the geology of the Wichita Mountains, Oklahoma, *in* Chase, G. W.; Fredrickson, W. E.; and Ham, W. E. (eds.), Petroleum geology of southern Oklahoma: American Association of Petroleum Geologists Guidebook, p. 36–55.

Ragland, D. A.; and Donovan, R. N., 1985, The Thatcher Creek Member, basal unit of the Cool Creek Formation in southern Oklahoma: Oklahoma Geology Notes, v. 45, p. 84–91.

_____ 1991, Silica in the upper Arbuckle Group, Slick Hills, southwestern Oklahoma, *in* Johnson, K. S. (ed.), Late Cambrian–Ordovician geology of the southern Midcontinent, 1989 symposium: Oklahoma Geological Survey Circular 92, p. 127–142.

Smith, S. S., 1991, Parallel fold styles in the Blue Creek Canyon area of the Slick Hills, southwestern Oklahoma: Texas Christian University unpublished M.S. thesis, 96 p.

Ulrich, E. O., 1933, Simpson Group of Oklahoma: Geological Society of America Bulletin, v. 44, p. 105–106.